Massachusetts Water Resources Authority
Boston, Massachusetts

A WATER QUALITY MODEL FOR MASSACHUSETTS AND CAPE COD BAYS: CALIBRATION OF THE BAYS EUTROPHICATION MODEL (BEM)

Job Number: NAIC0103

Prepared by:

HydroQual, Inc.
1 Lethbridge Plaza
Mahwah, New Jersey 07430

and

Normandeau Associates, Inc.
25 Nashua Road
Bedford, New Hampshire 03102

June 1995

Massachusetts Water Resources Authority
Boston, Massachusetts

A WATER QUALITY MODEL FOR
MASSACHUSETTS AND
CAPE COD BAYS:
CALIBRATION OF THE BAYS
EUTROPHICATION MODEL (BEM)

Job Number : NAIC0103

Prepared by:

HydroQual, Inc.
1 Lethbridge Plaza
Mahwah, New Jersey 07430

and

Normandeau Associates, Inc.
25 Nashua Road
Bedford, New Hampshire 03102

June 1995

ABSTRACT

This report documents the development, calibration, and application of a water quality model of Massachusetts and Cape Cod Bays. The report summarizes the evaluation of existing data; describes the development of a time-variable eutrophication model of the Bays system and its calibration to existing water quality data; and analyzes the results of model projections made for various Massachusetts Water Resources Authority (MWRA) wastewater treatment alternatives using the calibrated model.

The water quality model uses the results of a three-dimensional time-variable hydrodynamic model of the Bays system, developed for MWRA by the United States Geological Survey. The hydrodynamic model was used to develop realistic circulation patterns for the water quality model calibration periods of October 1989 through April 1991 and January through December 1992. As judged by model versus observed data comparisons, the water quality model provides a realistic representation of the physical, chemical, and biological processes that determine eutrophication within the study area. The water quality model has been used to investigate and define the relationships between bay circulation, nutrient loadings, primary productivity, and dissolved oxygen in Massachusetts and Cape Cod Bays.

Sensitivity analyses have been performed to investigate the relative impact of anthropogenic nutrient inputs, the influx of nutrients from the Gulf of Maine, and atmospheric sources on primary production within the Bays system. The calibrated water quality model has also been used to project future water quality conditions to be expected when the new MWRA wastewater treatment facilities have been completed and the effluent wastewaters are discharged to Massachusetts Bay. The results of these projection runs indicate: the upgrade to secondary treatment and outfall relocation will provide significant improvement to water quality within Boston Harbor; the outfall will have localized impacts on water quality within the immediate vicinity of the outfall, but will not result in serious deterioration of present water quality; the relocation of the outfall will have almost imperceptible affects on water quality in Cape Cod Bay and Stellwagen Basin.

ACKNOWLEDGEMENTS

CONTENTS

CONTENTS
(continued)

CONTENTS
(continued)

CONTENTS
(continued)

FIGURES

TABLES

SUMMARY

Introduction

The City of Boston and Boston Harbor are located in the northwest portion of Massachusetts Bay. Together Massachusetts Bay and Cape Cod Bay combine to form a roughly 100 X 50 km semi-enclosed basin in the western Gulf of Maine. Serving a population of over two million people in the Greater Boston Metropolitan Area, the waters of Boston Harbor and nearshore Massachusetts Bay provide an important recreational as well as commercial resource. The waters of Boston Harbor have also served as a recipient of the region's sewage. Historically, the input of this sewage had an adverse impact on the water quality of Boston Harbor. Significant efforts to improve the water quality of the Harbor were begun in 1952 when a primary sewage treatment plant was built on Nut Island. This facility treated at least a portion of the sewage that had been previously discharged untreated into the Harbor. In 1968, construction of a much larger facility on Deer Island was completed. The completion of these two facilities permitted the major portion of the region's sewage to receive disinfection, thus reducing the input of disease-causing microorganisms to the Harbor's waters.

However, the discharge of other wastewater constituents, such as solids, oxygen-consuming organic material, and nutrients, still presented a problem to the water quality of the Harbor. After a series of lawsuits were filed in the early 1980's against the City of Boston and the Metropolitan District Commission (the agency then responsible for the sewage system), the Massachusetts Water Resources Authority (MWRA) was created and charged with a mandatory schedule for meeting the secondary treatment standards of the Clean Water Act, and hence improving the water quality of Boston Harbor. To date, as part of this clean up effort, the MWRA has ceased the discharge of scum and sludge associated with wastewater and wastewater treatment and completed construction of a new primary treatment facility.

Also on the federally court mandated schedule is the construction of a new secondary treatment facility on Deer Island and a new outfall tunnel to carry the treated

effluent out to the deeper waters of Massachusetts Bay. It is expected that these improvements in wastewater treatment and effluent outfall relocation will provide improvements to water quality within Boston Harbor. Concerns have been raised, however, about the effect that the outfall relocation will have on water quality within Massachusetts and Cape Cod Bays. While previous modeling efforts suggest that the discharge of effluent organic carbon and nutrients to northwest Massachusetts Bay will have little effect on the environment of the Bays, these studies used relatively simple frameworks for their analyses and are therefore subject to some uncertainty.

In an effort to develop a more rigorous and detailed understanding of the potential impact of the outfall relocation on the water quality of Massachusetts and Cape Cod Bays, the MWRA has funded a number of studies within Boston Harbor and Massachusetts Bay. Included in these efforts have been a number of hydrographic and water quality surveys of the Bay. Also included is funding to support the development of time-variable three-dimensional hydrodynamic and water quality models of the Bay. The hydrodynamic model is being developed by the U.S. Geological Survey (USGS) under a cooperative agreement with the MWRA.

This work is directed primarily towards the development of a mathematical model of the eutrophication processes of Boston Harbor and Massachusetts and Cape Cod Bays. The resulting water quality model can then be used as a management tool to address questions concerning the water quality impacts in Boston Harbor and Massachusetts and Cape Cod Bays resulting from the outfall relocation. The purpose of the Bays Eutrophication Model (BEM) is twofold: (1) to obtain further understanding of the processes relating eutrophication, nutrients, and dissolved oxygen within the Bays system, and (2) to use the resulting modeling framework as an aid in understanding the potential impacts of wastewater treatment and outfall relocation. The BEM is developed herein on the basis of (a) incorporation of known relationships of phytoplankton growth and nutrients, and (b) calibration of the model to observed data for the period October 1989 through April 1991 and January through December 1992.

Point and Nonpoint Source Inputs

Other than exchange with the Gulf of Maine, the principal inputs of oxygen demanding material and nutrients entering Boston Harbor and the Bays system are:

1.   Point source discharges from municipal wastewater treatment plants,

2.   Inputs from combined sewer overflows (CSOs),

3.   Loadings associated with the various tributaries draining to Boston Harbor,

4.   Nonpoint source inputs from study area rainfall runoff,

5.   Groundwater loadings, and

6.   Atmospheric inputs impinging directly on the water surface.

Data necessary to make estimates of the various pollutant loadings to the system were obtained from reports prepared by MWRA and by Menzie-Cura and Associates. These data allowed the generation of monthly estimates of the point source inputs associated with the Nut Island and Deer Island facilities and atmospheric inputs. Although these data were not sufficient to generate monthly estimates of pollutant inputs for the other municipal facilities, CSOs, tributaries, rainfall runoff, or groundwater loadings, they were sufficient to provide yearly-average estimates. Figure S-1 provides a comparison of the annually-averaged daily inputs of organic carbon, total nitrogen and total phosphorus delivered to the study area

Figure S-1. LOADING COMPARISONS OF POLLUTANT SOURCES FOR 1990 VERSUS 1992

from each of the aforementioned sources. As can be seen the major sources of these
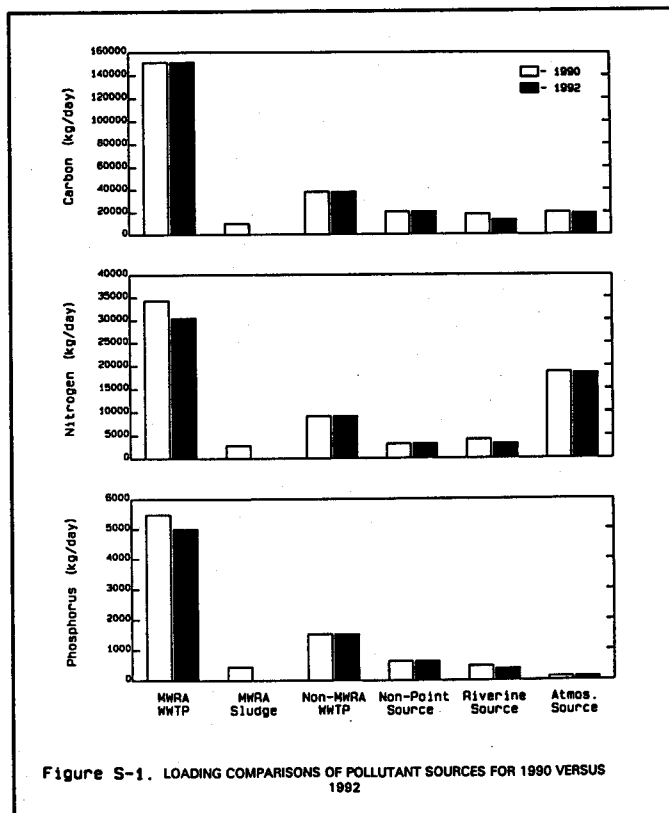
pollutants are the wastewater treatment plants, and the MWRA facilities in particular. With the exception of atmospheric nitrogen, the remaining sources of these inputs are distributed, approximately equally, between non-point sources, riverine sources and atmospheric sources. It should also be noted that in December of 1991, the MWRA ceased discharging sludge into the Harbor, and therefore, this loading input is not included in the organic carbon and nutrient loading estimates for the 1992 period.

Database

The credibility of model calculations are judged, to a large degree, by their agreement with observed data. Besides the obvious constraints that a eutrophication model should behave reasonably well and predict general patterns such as spring-summer phytoplankton growth, comparison of model calculations against observed data is perhaps the only external criterion which is available to determine the validity, and hence the utility, of a complex eutrophication model. The comparison of model computation to actual data indicates whether the assumptions and approximations used in the model adequately represent the "real world."

The principal sources of data for this study were:

1.   For the period October 1989 through April 1991, the Bigelow Laboratory for Ocean Sciences; a joint University of Massachusetts at Boston (UMB)/Woods Hole Oceanographic Institution (WHOI)/University of New Hampshire (UNH) team; the New England Aquarium; and

2.   For the period January through December 1992, the MWRA funded outfall monitoring program conducted by researchers from the Battelle Ocean Sciences, the University of Rhode Island, the University of Massachusetts at Dartmouth and the Marine Biological Laboratory located in Woods Hole, Massachusetts.

Although the purpose and scope of each of the hydrographic and water quality studies conducted by these researchers differed from one another, the data from these efforts provided sufficient coverage with respect to the space and time scale of the water quality model calculation. The spatial coverage of these surveys ranged from 1 to 10 km within the immediate vicinity of Boston Harbor and the proposed outfall location, to 5 to 20 km for the remaining portions of Massachusetts Bay and Cape Cod Bay. The temporal coverage varied considerably between the early Bigelow and UMB/ WHOI/UNH cruises and the MWRA outfall monitoring program. The latter sampling program was conducted on an approximately monthly basis for stations located in the nearfield vicinity of the proposed outfall and on a semi-monthly basis at farfield stations. The MWRA monitoring program also included more measurements of the principal state-variables considered in the water quality model framework, than did the earlier water quality surveys.

Chlorophyll-a -- An important measure of the eutrophication status of the Massachusetts and Cape Cod Bays system is the concentration of chlorophyll-a. Chlorophyll-a is an indirect measure of the overall phytoplankton population, and as such it does not distinguish between desirable phytoplankton groups that are important to the Bays' food chain and nuisance groups such as toxic dinoflagellates. Nevertheless, it is a widely accepted indicator of the standing algal crop.

Within the Boston Harbor and Massachusetts and Cape Cod Bays study area there is marked temporal and spatial variability in chlorophyll-a levels. This variability is due not only to the spatial variability of available nutrients, but is also dependent on the temporal and spatial variability of other environmental parameters. These parameters include water temperature, incident solar radiation, light transparency, and grazing pressure from higher trophic levels. Two of the more important parameters which influence phytoplankton growth, water temperature and solar radiation, have strong annual cycles.

Figure S-2 presents the annual cycle of chlorophyll-a and chlorophyll fluorescence for three stations within the study area. These data are from the 1992 MWRA monitoring program. Panel (a) shows surface (0 to 5 meter depth) chlorophyll-a for a station located

near the entrance to Boston Harbor. As can be seen for this station the annual cycle of chlorophyll-a has its maximum concentrations during the summer months. This is in contrast to panels (b) and (c), which show the annual cycles of chlorophyll-a for stations located in northern Massachusetts Bay and southern Cape Cod Bay. The chlorophyll-a data for the Massachusetts Bay station, panel (b), indicate a small algal bloom in late February; followed by a decline in March and April; low concentrations during the summer months; and, finally a fairly large bloom in early October. Data for the Cape Cod Bay station, panel (c), indicate a similar pattern, except that the February bloom is much larger in Cape Cod Bay than in Massachusetts Bay and the fall bloom is much smaller.
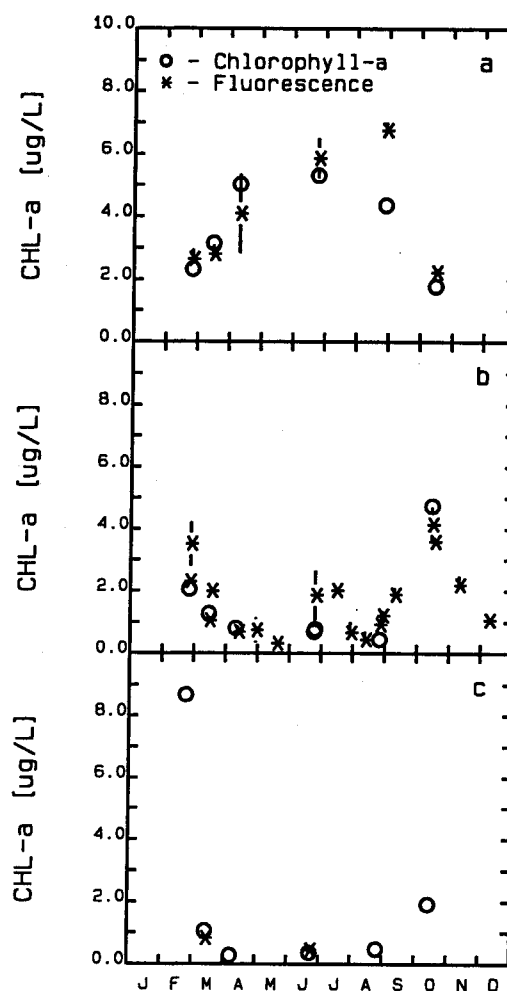
Figure S-2. Annual Cycle of Chlorophyll-a
(a) Boston Harbor
(b) northern Mass. Bay
(c) southern Cape Cod Bay

Nitrogen -- Nitrogen is an important nutrient for phytoplankton growth. In excessive amounts, however, nitrogen can stimulate growth until excessive quantities of algae accumulate. The potential exists for the water column to be depleted of dissolved oxygen when these algae die and decompose. An analysis of the available data within Massachusetts and Cape Cod Bays indicates that nitrogen is the key nutrient limiting phytoplankton growth within these waters. Figure S-3 presents time series plots of surface (0 to 5 meter) dissolved inorganic nitrogen and the ratio of dissolved inorganic nitrogen (DIN) to dissolved inorganic phosphorus (DIP) for two locations within Massachusetts Bay; one station (panels (a) and (b)) is near the entrance to Boston Harbor, while the other station (panels (c) and (d)) is in northern Massachusetts

Bay. The DIN/DIP ratio indicates the potential for either nutrient to limit algal growth. Based on an analysis of phytoplankton cellular composition (the Redfield ratio), DIN/DIP ratios less than or equal to seven, generally indicate that nitrogen is the potentially limiting nutrient; ratios of DIN/DIP greater than seven, indicate phosphorus as the potentially limiting nutrient.

As can be seen in panel (a) for the station near the entrance to Boston Harbor concentrations of DIN are, with the exception of August, above the levels (i.e., 10 μg N/L) that would limit algal growth. Panel (b) indicates that nitrogen is the potentially limiting nutrient with DIN/DIP ratios less than seven. A very low DIN/DIP ratio was observed in June, the period of time corresponding to the near depletion of DIN. The concentrations of DIN observed for the northern Massachusetts Bay station, panel (c), are at or near levels which limit algal growth during the summer months and in October. As can be seen in panel (d) the DIN/DIP ratios are almost always less than three and are less than one during the summer months, indicating a strong nitrogen limitation. Therefore, concerns have been raised about the possible stimulation of phytoplankton growth in Massachusetts Bay
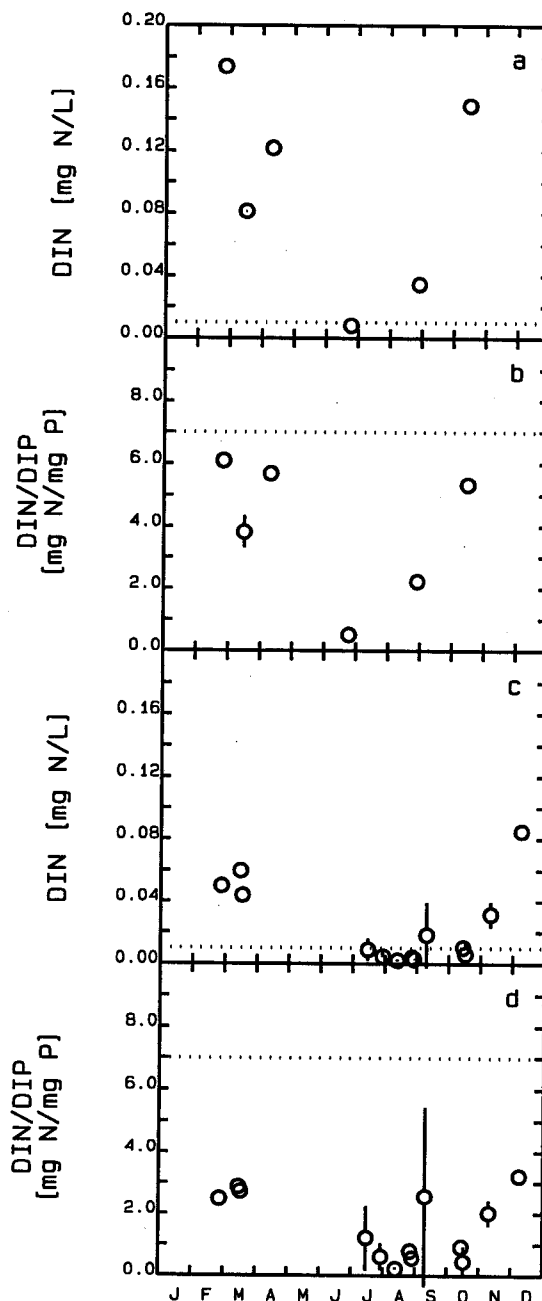
Figure S-3. Surface DIN and Ratio of DIN to DIP

(a), (b) near Boston Harbor entrance
(c), (d) northern Mass. Bay

that may result after the construction of the new outfall is completed and additional nitrogen is introduced into the Bay.

Dissolved Oxygen -- The dissolved oxygen of a water body is one of the more important water quality indicators. The dissolved oxygen reflects the general health of a water body and is a quality variable that indicates the capacity of the water body to support a balanced aquatic habitat. When dissolved oxygen levels are low the propagation of fish and other aquatic life may be impaired and large mortalities may occur. For this reason, states usually set water quality standards for dissolved oxygen (DO) for most water bodies. For most of Boston Harbor the state standard (Class SB) is set to 5 mg/L; for the waters of Massachusetts and Cape Cod Bays the state standard (Class SA) is 6 mg/L. Figure S-4 presents time-series plots of bottom water DO for three water quality monitoring stations. Panel (a) presents DO data for a station located within Boston Harbor for 1990; panel (b) presents 1992 data for a station near the entrance to Boston Harbor; while panel (c) presents 1992 data for a station in northern Massachusetts Bay. Also shown on these plots (as a dotted line) are model estimates of DO saturation. The DO saturation has a strong seasonal cycle, strongly driven by water column temperature. The bottom water DO also tends to follow a similar seasonal cycle, although as can be seen (panel (a)), the concentrations of bottom water DO are well under saturation and occasionally violate the state standard during the
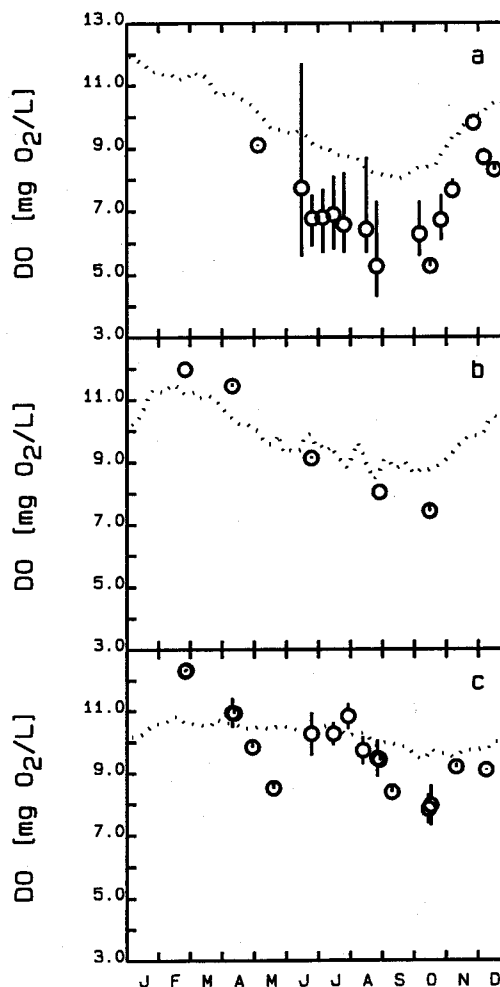
Figure S-4. Bottom Water DO
(a) Boston Harbor 1990
(b) entrance to Harbor 1992
(c) northern Mass. Bay 1992

summer months. As shown in the remaining panels, bottom water DO concentrations are generally near or above saturation for most of the winter and summer months in which data are reported. Minimum DO levels are usually observed to occur during October. These lower levels reflect the oxidation of detrital algal biomass that was generated during the spring and summer months that now has begun to die and decompose in the lower layers of the water column, while the water column is still stratified due to salinity and temperature. This physical stratification limits the exchange of oxygen enriched surface waters with oxygen deficient sub-pycnocline waters. Because the future outfall plume will be trapped below the pycnocline in the summer, concerns have been raised with respect to the impacts that the relocation of the MWRA outfall might have on DO within Massachusetts Bay.

The Massachusetts/Cape Cod Bays Eutrophication Model - BEM

The underlying framework of the analysis detailed in this report is based upon the principle of conservation of mass. Simply stated, the conservation of mass accounts for all of a material entering or leaving a body of water, transport of material within the water body, and physical, chemical and biological transformations of the material. The modeling framework incorporates, then, three components -- external pollutant inputs, transport due to freshwater flow and tidally-induced advection and dispersion, and the kinetic interaction between the water quality variables.

The kinetic equations employed in the BEM framework are designed to simulate the annual cycle of phytoplankton production, its relation to the supply of nutrients, and its effect on dissolved oxygen. The model considers the following twenty-four state-variables, which are space and time dependent:

1. salinity
2. winter functional phytoplankton group
3. summer functional phytoplankton group
4. refractory particulate organic phosphorus (RPOP)

5. labile particulate organic phosphorus (LPOP)

6. refractory dissolved organic phosphorus (RDOP)

7. labile dissolved organic phosphorus (LDOP)

8. dissolved inorganic phosphorus (DIP)

9. refractory particulate organic nitrogen (RPON)

10. labile particulate organic nitrogen (LPON)

11. refractory dissolved organic nitrogen (RDON)

12. labile dissolved organic nitrogen (LDON)

13. ammonia nitrogen (NH_4)

14. nitrite + nitrate nitrogen ($NO_2 + NO_3$)

15. biogenic silica (BSi)

16. dissolved inorganic silica (DSi)

17. refractory particulate organic carbon (RPOC)

18. labile particulate organic carbon (LPOC)

19. refractory dissolved organic carbon (RDOC)

20. labile dissolved organic carbon (LDOC)

21. reactive dissolved organic carbon (ReDOC)

22. algal exudate dissolved organic carbon (ExDOC)

23. aqueous sediment oxygen demand (O_2^*)

24. dissolved oxygen (DO)

The area of interest of the model includes Boston Harbor, Massachusetts Bay, and Cape Cod Bay. The study area is divided into a 20 X 25 grid, ranging in size from approximately 1.5 km^2 to about 15 km^2, as shown in Figure S-5. The model is also vertically segmented using 10 σ-levels.

The circulation and dispersion fields are obtained from a fine-grid hydrodynamic model developed by the U.S. Geological Survey. In order to address the role that the sediments play in the overall nutrient and DO balance, an active sediment layer was included in the modeling framework. This was accomplished by introducing a sediment

segment directly under each bottom layer water column segment. A total of 2,970 active water column segments and 297 active sediment segments are included in the model grid used to calibrate the model.

Figure S-5. Water Quality
Model Grid

Calibration - Once the model inputs (organic carbon and nutrient loadings and exogenous variables such as solar radiation, water column transparency, etc.) were defined, the BEM was then calibrated against the observed water quality and sediment flux data. The calibration procedure consisted of a number of iterative runs wherein adjustments were made to various model inputs and coefficients in such a way as to improve the comparisons between model output and observed data. The initial set of model coefficients were those determined from similiar model calibration analyses for Long Island Sound and Chesapeake Bay. The iterative runs of BEM were continued through adjustments and "tuning" of the model parameters and constants until a satisfactory calibration was achieved.

The final calibration is the result of approximately 100 hydrodynamic and water quality model runs, which were made to obtain a set of model coefficients that are reasonable and consistent across the periods of time for which data sets were available and that reproduce, as well as possible, the observed data for all state-variables considered.

As stated previously, a critical requirement for establishing the credibility of the analysis is a complete calibration which compares the model computation to the available

observations. A few representative comparisons for the water quality model calibration of the water column are presented in Figures S-6, S-7, and S-8. Figure S-6 presents a time series comparison of model computations versus observed 1992 data for a station in northern Massachusetts Bay. Surface data are shown as an open circle; bottom data are represented using a filled circle; and model computations are shown using solid and dashed lines to represent surface and bottom respectively. The model reproduces the observed data fairly well. The salinity and temperature model computations are from the hydrodynamic model. The hydrodynamic model reproduces the annual cycle of surface water heating and stratification. The hydrodynamic model also reproduces the spring freshet associated with the Merrimack River and other northern rivers discharging to the Gulf of Maine. The water quality model provides a reasonable reproduction of the annual cycle of phytoplankton biomass as represented by chlorophyll-a, fluorescence and particulate organic carbon, although it appears to under-estimate the magnitude of the fall bloom in October. The model also reproduces the annual cycle of surface and bottom water nutrients, including the marked stratification between the surface and bottom waters. The model reproduces the near depletion and algal growth limiting concentrations of surface dissolved inorganic nitrogen (DIN) and the non-limiting surface dissolved inorganic phosphorus (DIP) concentrations. The model also reproduces the observed surface dissolved inorganic silica (DSi) concentrations, including the marked decline that occurs between April and late June, followed by the gradually increasing DSi levels throughout the rest of the summer and fall months. Finally, the model provides a reasonable comparison to the observed dissolved oxygen data, reproducing the observed stratification and minimum concentrations that are observed in October and November. The model does not, however, reproduce the decrease in DO levels that occurs between early April and late May.

Figure S-7 provides additional calibration results for a station located in the southwest corner of Cape Cod Bay. Although the data for comparison purposes are not as extensive for the Cape Cod station as for the Massachusetts Bay station, it appears that the BEM also performs reasonably well for this region of the study area. The model is partially able to reproduce the February bloom, although the model bloom is computed a
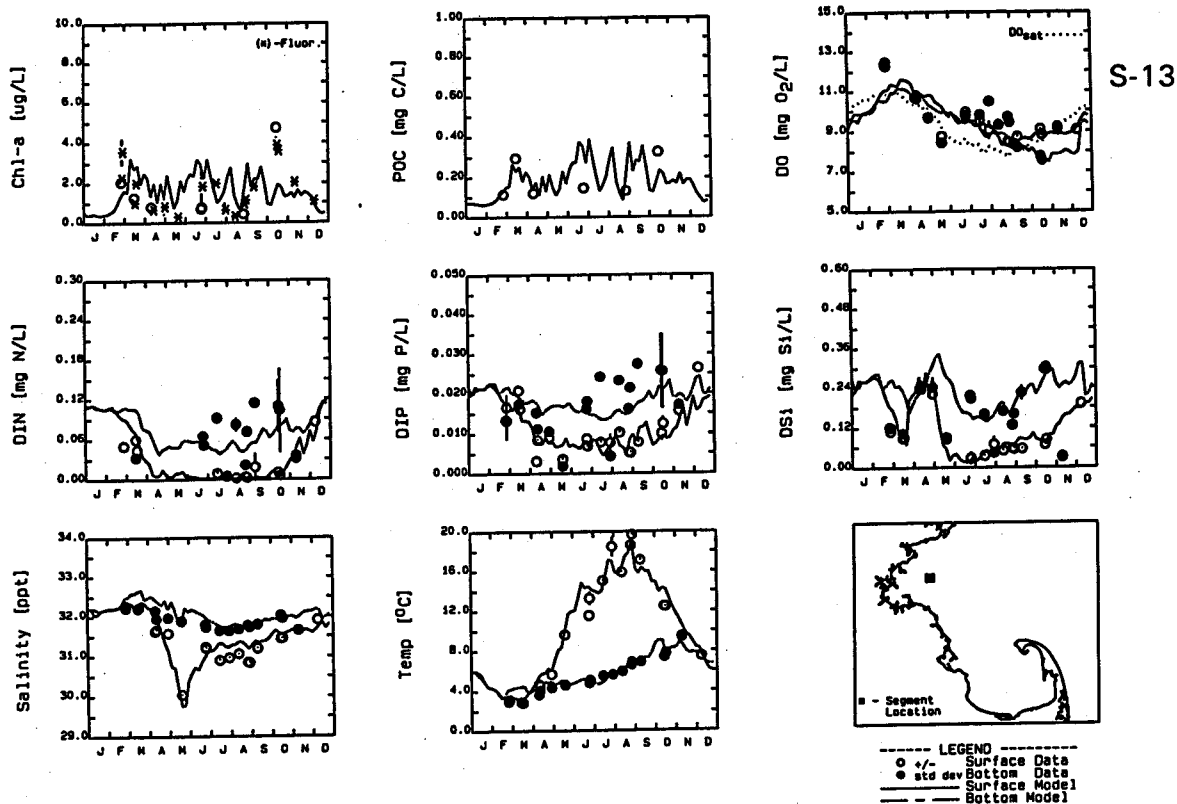
Figure S-6. 1992 Temporal Calibration Results for
Grid Cell (11, 18) Vs Data Station N16P, N17, N21
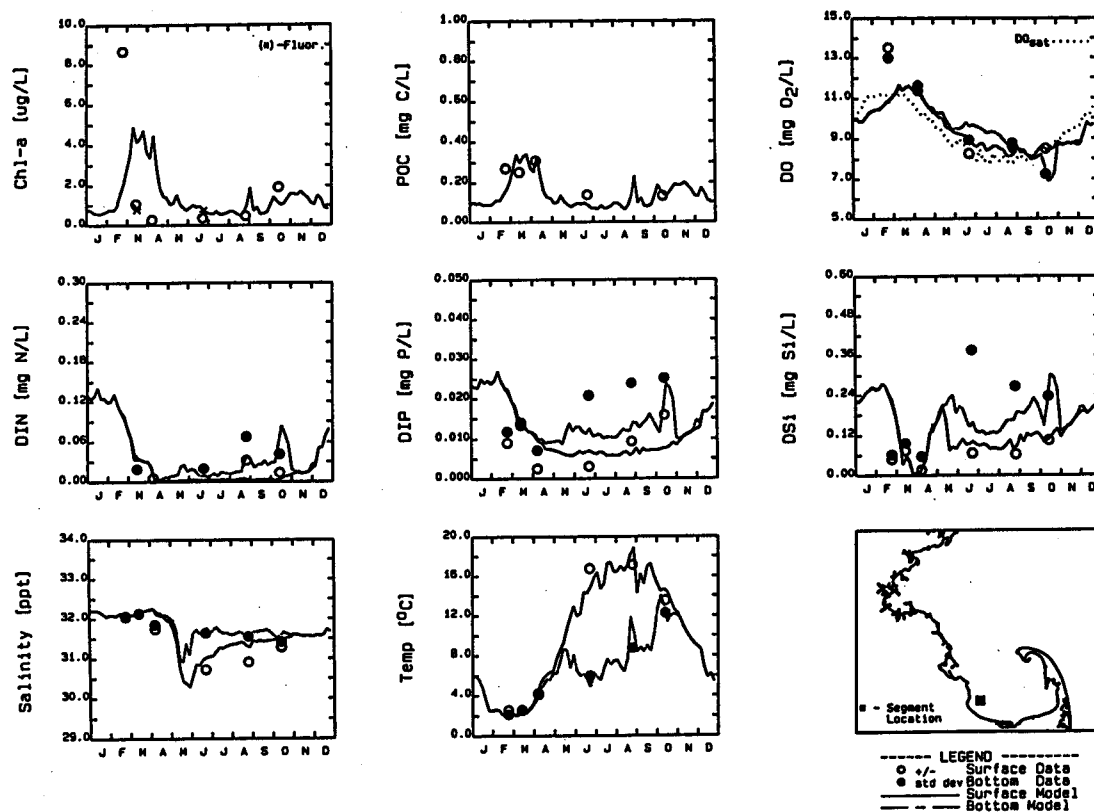
Figure S-7. 1992 Temporal Calibration Results for
Grid Cell (6, 4) Vs Data Station F01P
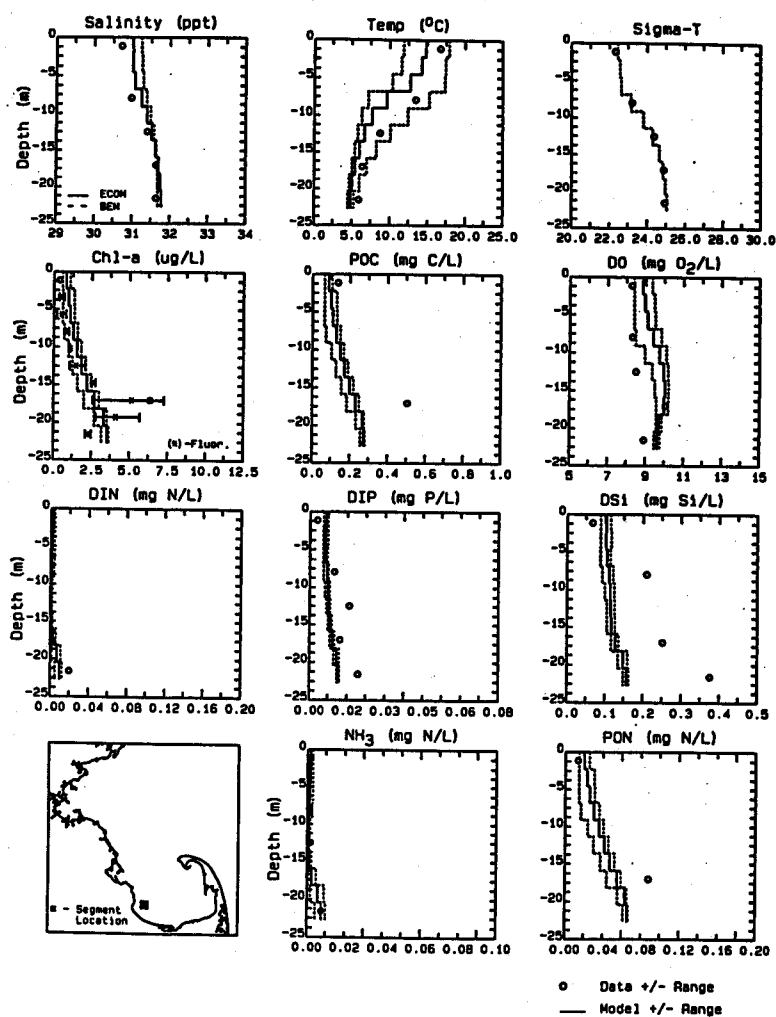
Figure S-8. Calibration Results for Grid Cell (6, 4)
for 06/22/92

1992 Calibration Results for Sediment Flux Submodel
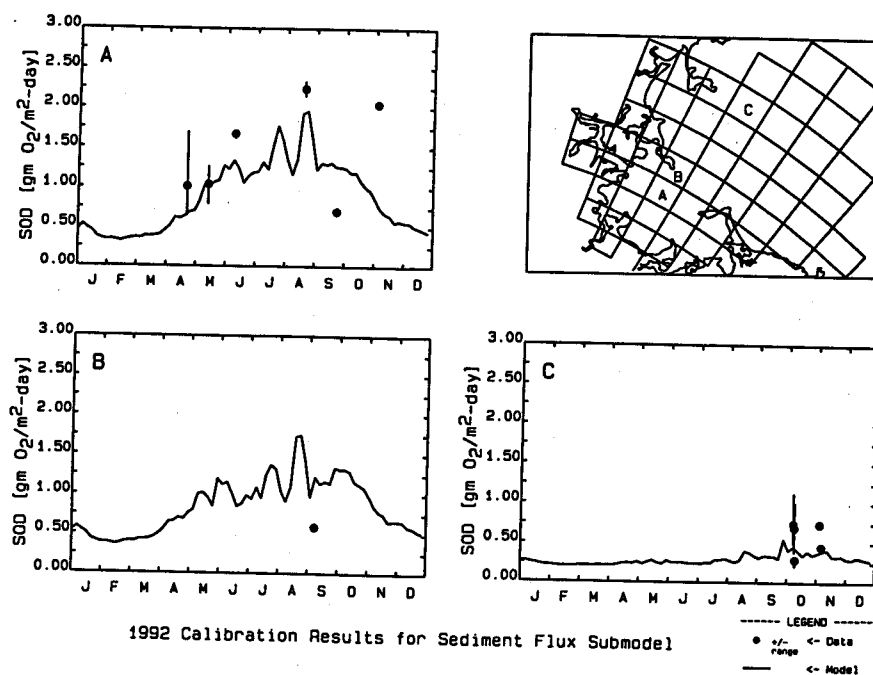
Figure S-9.

little late. The model does, however, compute a bloom in Cape Cod which is larger than that computed in Massachusetts Bay, which is in agreement with the observed data. The model also provides a reasonable calibration to the observed annual cycle of inorganic nutrients. Both the model and data suggest that the winter bloom becomes limited first by DSi depletion, rapidly followed by DIN depletion. The model also reproduces the observed seasonal cycle for DO reasonably well. The model approximately reproduces the fall stratification. However, since the model fails to reproduce the early portion of the winter bloom, it also fails to reproduce the super-saturated DO conditions observed in February.

Figure S-8 presents a depth profile of model computations versus observed data for the same Cape Cod Bay station for late June 1992. This figure illustrates the ability of the hydrodynamic and water quality models to reproduce the observed vertical gradients in water quality. The local depth of the model segment for this location is approximately 23 meters. Since the water quality model uses 10 σ levels, the depth of each vertical cell is approximately 2.3 meters. The observed data have then been binned into 2.3 meter intervals as well. As can be seen the hydrodynamic model computation is quite good for this date, as indicated by favorable comparisons to salinity, temperature and density (sigma-t). The water quality model also reproduces, in part, a number of features of the observed data. These include the generation of a sub-surface chlorophyll-a maximum between 15 and 20 meters. Below-surface phytoplankton productivity is also indicated by higher concentrations of particulate organic carbon and particulate organic nitrogen at depth. The model also reproduces in part the sub-surface DO maximum. Finally, the model approximately reproduces the observed gradients in NH_4, DIP and DSi. Since $NO_2 + NO_3$ data were not available in the surface waters for this period, it was not possible to make a comparison of model versus data for surface DIN.

As has been noted earlier, the water quality model includes a coupled sediment nutrient flux and sediment oxygen demand submodel. Figure S-9 illustrates representative calibration results for the sediment submodel. This figure presents a time-series comparison of computed and observed measurements of sediment oxygen demand (SOD)

for two stations within Boston Harbor and a station located in Massachusetts Bay. As can be seen the model approximately reproduces the annual cycle of SOD, with low values occuring during the winter and early spring, followed by increasing levels during the summer months, followed by diminishing values into the late fall. The model also reproduces the observed spatial gradient in SOD, with high levels of SOD within Boston Harbor as contrasted to very low levels of SOD for the Massachusetts Bay station.

Projections - A number of management scenarios were run using the calibrated version of BEM. These projections considered the following: outfall relocation with upgrade of MWRA facilities to secondary treatment; outfall relocation with no upgrade at the treatment facilities; and, upgrade to secondary treatment but continued discharge at the current discharge sites. A summary of these results is presented in Figure S-10. Each panel presents comparisons between the base calibration run; i.e., primary treatment at the current outfall locations (upper left sub-panel), the future outfall with secondary treatment (upper right sub-panel), current outfalls with secondary treatment (lower left sub-panel) and future outfall with current primary treatment (lower right sub-panel). Panel A illustrates surface dissolved inorganic nitrogen (DIN) averaged over a 5-day period in early March, a period of time during which the spring bloom is occurring. This figure shows that DIN is virtually depleted in Cape Cod Bay. This occurs because the spring bloom usually takes place in Cape Cod Bay before Massachusetts Bay. As can also be seen outfall relocation does not significantly affect the distribution of DIN in either Cape Cod Bay or Massachusetts Bay. The only significant change is a reduction of DIN in Boston Harbor.

Panel B presents a comparison a surface chlorophyll-a for Boston Harbor and northwestern Massachusetts Bay, in the vicinity of the future outfall location. These results represent a 5-day average in mid-August. The results indicate a significant reduction in chlorophyll-a concentrations in Boston Harbor for both scenarios which include outfall relocation. Coincidentally, there is no increase in surface chlorophyll-a near the future outfall for either of these scenarios. This result occurs because the effluent plume

(A)
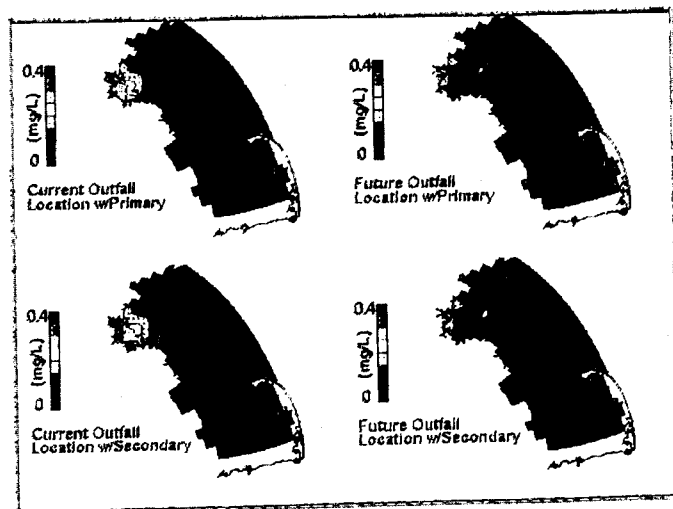
DISSOLVED INORGANIC NITROGEN

(B)
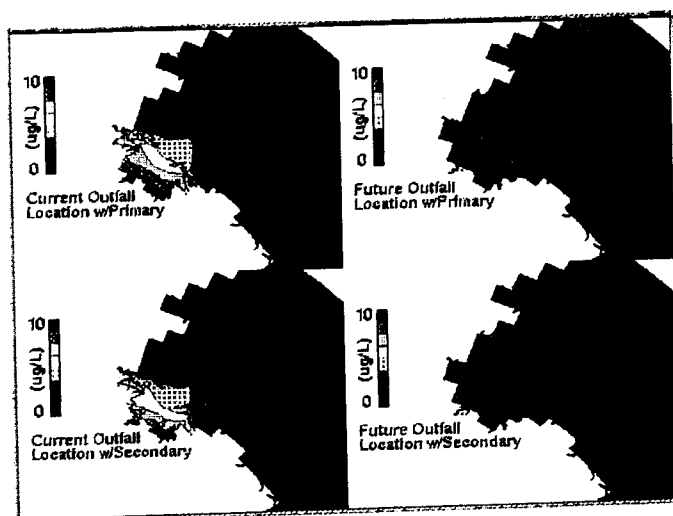
CHLOROPHYLL-A

(C)
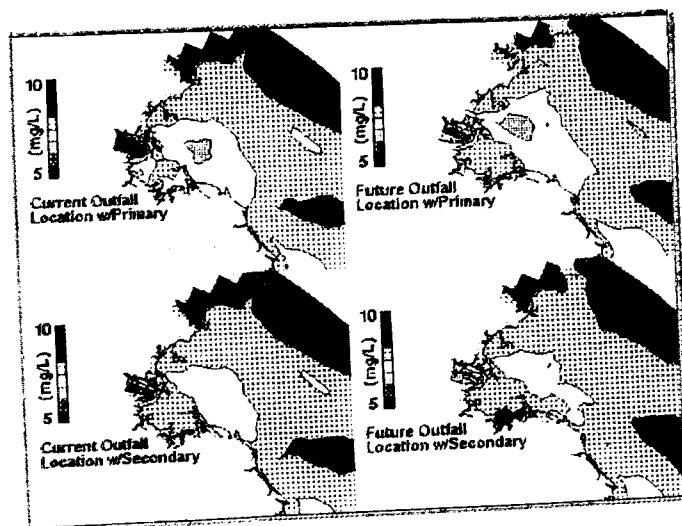
DISSOLVED OXYGEN

S-10. PROJECTION RESULTS

from the future outfall is effectively trapped below the pycnocline, due to water column stratification during the summer months.

Minimum values of bottom water dissolved oxygen in late October are presented in Panel C. The results show that dissolved oxygen concentrations are significantly improved in Boston Harbor for any one of the three management scenarios considered. However, while outfall relocation alone improves dissolved oxygen concentrations in Boston Harbor, it results in a slight degradation in dissolved oxygen in the immediate vicinity of the future outfall. However, it is important to know that even for this scenario State of Massachusetts water quality standards for dissolved oxygen are still met. The slight degradation in dissolved oxygen introduced with the outfall relocation is remediated by upgrading to secondary treatment at the MWRA facilities.

CONCLUSIONS AND RECOMMENDATIONS

A coupled hydrodynamic/water quality model was developed to determine the relationships between nutrient inputs, primary production, and dissolved oxygen in Massachusetts and Cape Cod Bays. The coupled model was also developed to enable water quality managers to project the effects of relocating the effluent from the Massachusetts Water Resources Authority (MWRA) wastewater treatment facilities on water quality in Massachusetts and Cape Cod Bays.

The water quality component of the coupled model represented the physical features of the Bays system using ten vertical layers and a moderately fine scale of 2.8 to 5.7 km in the horizontal plane. Twenty-four state-variables--salinity, phytoplankton, various forms of particulate and dissolved nutrients, and dissolved oxygen--were incorporated in the water quality analysis, for which the circulation and transport were provided by the hydrodynamic model.

The model was calibrated using data from two periods, October 1989 through April 1991 and January through December 1992. Comparisons of the observed and computed values of the relevant variables indicate that both the hydrodynamic and water quality models realistically portray the physical, biological and chemical processes present in the Bay and the spatial distributions of the respective parameters.

CONCLUSIONS

Based on data analysis, model results, and sensitivity analysis, the following conclusions and inferences may be drawn.

Hydrodynamic

1)   Although the details of the hydrodynamic model are presented in a separate analysis, the use of circulation and transport information, provided by the hydrodynamic model, in the water quality model appears to reproduce the observed

temporal, horizontal and vertical gradients of salinity within the Bays system as judged by model versus data comparisons. These comparisons suggest that the hydrodynamic model, representing the state-of-the-practice, can reproduce the time-dependent, three-dimensional stratification, and circulation in Massachusetts and Cape Cod Bays. As with most model applications of this caliber, the major model versus data discrepancies and uncertainties relate to the inability to exactly specify the forcing and boundary conditions for the model simulations.

2) The hydrodynamic model appears to reproduce the plume dynamics of the future outfall when comparisons are made against state-of-the-practice plume models. The plume dynamics produced by the hydrodynamic model are specified directly in the water quality model, at the same spatial scale as the hydrodynamics.

Water Quality

1) The water quality model appears to reproduce or partially reproduce the principal temporal and vertical features of the water quality within the Bays. These features include:

- the onset of the winter/spring phytoplankton bloom earlier in Cape Cod Bay than the rest of the Massachusetts Bay system

- the decrease in phytoplankton biomass, as indicated by chlorophyll-a and fluorescence, in Massachusetts Bay as one moves further away from Boston Harbor

- the limitation of the winter/spring phytoplankton bloom in Cape Cod Bay by silica

- the non-limiting concentrations of inorganic phosphorus, which suggest that the bays are not phosphorus limited

- the limitation of summer primary productivity by inorganic nitrogen

- the observed vertical gradients in the inorganic nutrients with low levels in the surface (due to algal uptake) and higher levels in the bottom waters of the Bays (due to remineralization of detrital algal biomass and less algal uptake)

- the annual cycle of dissolved oxygen, with super-saturated conditions occurring between late winter/early spring and late summer and with minimum levels occurring in late September and October.

- the annual cycle of primary productivity in northwest Massachusetts Bay.

2) The water quality model represents the state-of-the-science in applying time-dependent, multi-dimensional water quality models to primary productivity in estuarine and coastal systems. Because these models are not true depictions of what occurs in natural systems and because there are limitations in the data sets that are available, we have to expect that the model results will not completely reproduce the data. However, the model results do reproduce the major processes that occur in the Bays as judged by model versus data comparisons.

3) The validity of a model can be judged to some extent by the degree that it reproduces the observations to which it is calibrated. A model which can reproduce observations in different estuaries with essentially similar structure and coefficients has a higher level of credibility, since this indicates that it can properly scale between different locations. The Massachusetts Bay model has been successfully applied to Chesapeake Bay, Long Island Sound, and currently New York Harbor with essentially no change in model structure and little change in model coefficients. The degree of calibration for these studies is similar to that achieved in Massachusetts Bay. Therefore, it appears that the model has demonstrated a general level of validity. Based on this feature of the Massachusetts Bay model, as

well as those enumerated above, we believe that the model projections to be described below can be relied on as the best available estimates.

PROJECTIONS

1)   The effect of the new outfall on water quality is predicted to be limited to the nearfield. Nearfield effects include: (1) improved bottom dissolved oxygen, which results from reduced primary productivity, and (2) an increase in particulate organic carbon (POC) flux to the sediment, which results from enhanced solids deposition associated with effluent suspended solids conveyed to the nearfield via the future outfall. The latter, however, remains well below the deleterious effects levels. In addition it was projected that outfall relocation would not reduce dissolved oxygen concentrations in Stellwagen Basin, a region of the Bays system traditionally having the lowest dissolved oxygen concentrations within Massachusetts Bay.

2)   Projections indicate that the combination of secondary treatment and new outfall location meet all water quality standards with respect to oxygen and benthic enrichment. Therefore, it is unlikely that further treatment will necessary. Specifically, the dissolved oxygen standards of 6 mg/l in the Bays and 5 mg/l in Boston Harbor are predicted to be met, and the POC flux is well below the 301(h) level of concern of 1.5 g C/m^2-day.

3)   The water quality in Boston Harbor will greatly improve for any of the projection scenarios. The dissolved oxygen standard should generally be met in the harbor with secondary treatment plus relocation of the outfall, although there may remain localized problems not resolved by this model.

4)   In all of the projection scenarios that were conducted, no adverse changes from present conditions (the 1992 calibration simulation) were predicted for Cape Cod Bay. There were no substantial changes in Cape Cod Bay concentrations of dissolved oxygen, DIN, DIP, or chlorophyll, or in POC flux. Sensitivity analysis

indicates that Cape Cod Bay and most of Massachusetts Bay are relatively unaffected by changes in wastewater inputs into or near Boston Harbor.

RECOMMENDATIONS

1) The water quality model should continue to be applied and refined using water quality data provided by the ongoing Outfall Monitoring Program. As with any water quality model, greater confidence in its predictive capabilities would be provided with calibration to additional water quality data sets which reflect a range of environmental conditions within the Bays system.

2) Additional field data should be obtained which would permit better specification of the open water boundary conditions.

3) Field and laboratory studies should be considered which would permit an assessment of the labile and refractory components of the organic carbon and nutrient inputs to the Bays system, both from landside sources and from advection from the Gulf of Maine.

SECTION 1

INTRODUCTION

1.1   INTRODUCTION

The Massachusetts Water Resources Authority (MWRA) is constructing an ocean outfall, which will divert treated effluent from the Deer Island Wastewater Treatment Plant. The present Deer Island outfall is located at the entrance to Boston Harbor and will be relocated into Massachusetts Bay at a distance approximately 15 km east of Deer Island and at a water depth of 32 meters. The moving of the wastewater discharge from within the confines of Boston Harbor, together with improved sewage treatment and the cessation of sludge discharge to the Harbor, is expected to result in a significant improvement in water and sediment quality within the Boston Harbor area.

Concerns have been raised, however, about the effect that the outfall relocation will have on water quality within Massachusetts and Cape Cod Bays. The offshore outfall discharge will bring organic carbon and nutrients directly into northwest Massachusetts Bay. Previous modeling efforts suggest that these additional organic carbon and nutrients will have little effect on the environment of Massachusetts or Cape Cod Bays (U.S. EPA, 1988, Menzie-Cura, 1991). However, the previous studies used relatively simple frameworks for their analyses and, since coastal eutrophication is a complex process, these initial predictions must be re-evaluated.

In order to develop a more rigorous and detailed understanding of the potential impact of the outfall relocation on the water quality of the Massachusetts Bays system (Boston Harbor, Massachusetts Bay, and Cape Cod Bay) the MWRA has funded or partially funded a number of studies within Boston Harbor and Massachusetts and Cape Cod Bays. Included among these studies are a number of hydrographic and water quality surveys of the Bays. These surveys have collected data on salinity, temperature, phytoplankton, primary productivity, nutrients and dissolved oxygen throughout Massachusetts and Cape Cod Bays. These data represent the most comprehensive data available for the Bays to

date. MWRA has also funded a number of benthic nutrient flux and sediment oxygen demand surveys for stations within Boston Harbor and Massachusetts Bay. Both of these programs have been expanded within an overall water quality monitoring program, the purpose of which is to provide information concerning water and sediment quality before and after the new outfall goes on line. This program is being conducted to evaluate the impact of the discharge of MWRA's effluent on the Bays system and to assist in the evaluation of operational issues.

MWRA has also entered into a cooperative agreement with the U.S. Geological Survey (USGS) to develop a time-variable three-dimensional hydrodynamic model of the Bay. This model encompasses all of Massachusetts and Cape Cod Bays, and extends out, on its eastern and northern boundaries, into the Gulf of Maine. One purpose of this model is to be able to predict the transport of materials discharged from the submerged outfall within the Bays.

Since the eutrophication processes within the Bays system are related to meteorological and climatic forcings, the aforementioned monitoring program would require a number of years of pre- and post-outfall water quality data before statistically significant inferences concerning the impact of the outfall on the water quality of the Bays could be drawn from the observed data. Therefore, MWRA has funded the development and calibration of a time-variable water quality model of the eutrophication processes of the Massachusetts Bay and Cape Cod Bay system. The purpose of the water quality model is to provide another tool to assist in the understanding, evaluation and prediction of water quality response in the Bays subject to changes in the treatment facility's operating parameters, particularly related to the magnitude of organic carbon and nutrient loadings. It is towards this objective that the present study is oriented. In order to place this study in the proper perspective, it is appropriate to briefly review the nature of the study area itself.

1.2   PHYSICAL CHARACTERISTICS

Massachusetts Bay and Cape Cod Bay (Figure 1-1) combine to form a roughly 100x50 km semi-enclosed basin located in the south-western Gulf of Maine. For the purposes of this investigation, the geographical extent of the study area, which includes Boston Harbor, Massachusetts Bay, and Cape Cod Bay, is bounded on the north-east by Cape Ann and on the south and south-east by Cape Cod and the northern tip of Cape Cod at Race Point, respectively. The depth of the study area, from here on in referred to either as Massachusetts Bay or the Bays, varies from as much as 100 m in the deeper sections of Stellwagen Basin to tidal flats that are exposed at low tide and has an average depth of 35 m.

The major sources of freshwater to the Bays are from: municipal and industrial sewage treatment plants located in the City of Boston and other north and south shore communities; the Charles, Mystic and Neponset Rivers; groundwater inflow from along Cape Cod; and waters from the Merrimack River and large rivers in Maine that are entrained in the Gulf of Maine coastal current.

1.3   POPULATION, LAND AND WATER USES

Over 2 million people, nearly half of the State of Massachusetts population, live in some 43 communities surrounding the City of Boston. As reported by Menzie-Cura (1991), utilizing data from the Massachusetts Department of Environmental Protection and the National Oceanic and Atmospheric Administration's National Coastal Pollutant Discharge Inventory (NCPDI), the total drainage area (excluding the Merrimack River) of Massachusetts Bay is approximately 3700 km^2. Approximately 35 percent of the total drainage area can be categorized as urban in use (with nearly 70 percent of the urban area defined as residential and the remaining 30 percent being comprised of commercial, industrial, transportation and mixed urban land use), with the balance of 65 percent being categorized as non-urban.
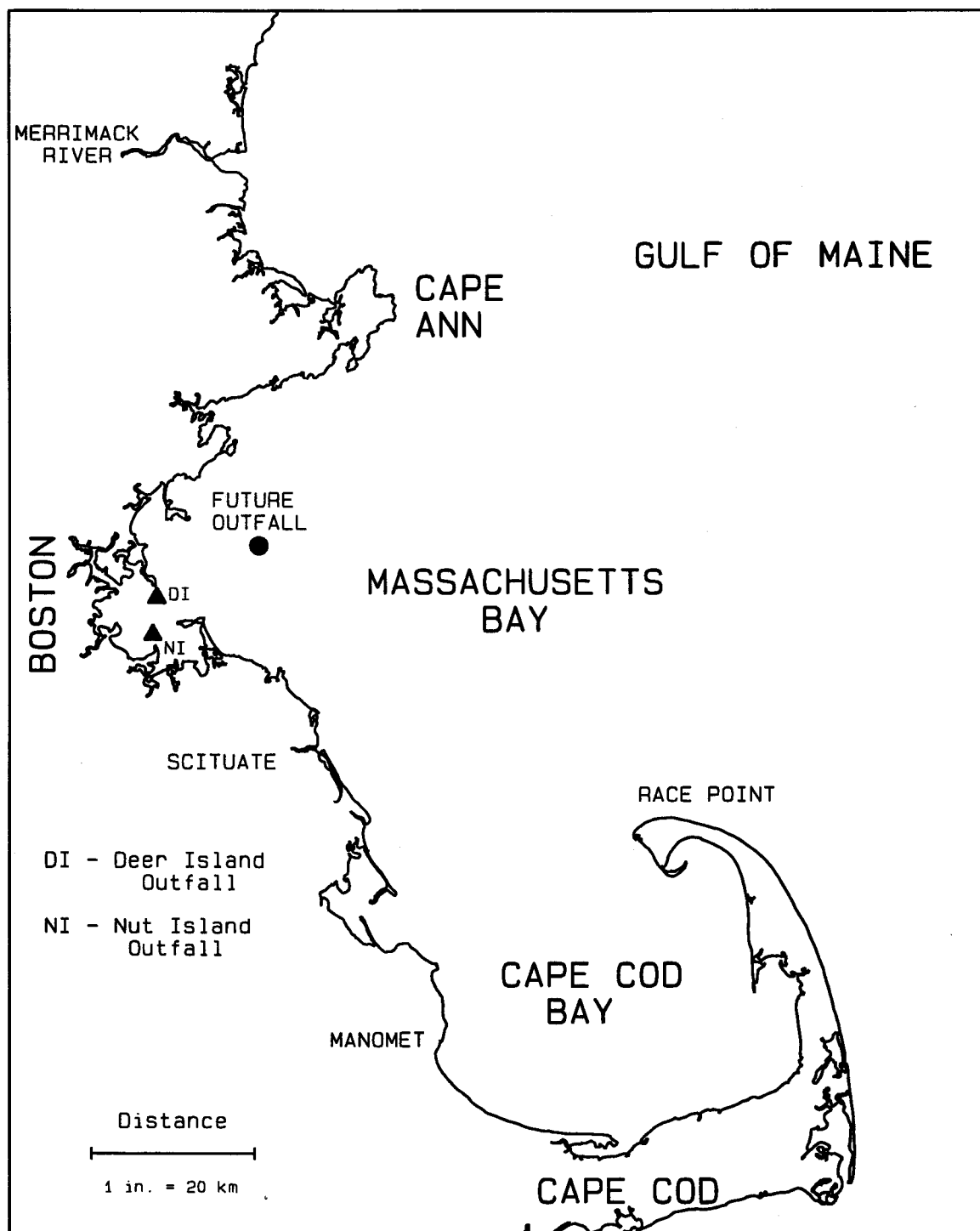
Figure 1-1

Massachusetts Bay Study Area

The principal water uses in the Bays are shipping, transportation, commercial and sport fishing, recreational boating and recreational bathing, as well as receiving waters for wastewater discharges and a depository for dredged sediments.

1.4   POLLUTANT SOURCES

Massachusetts Bay and Boston Harbor in particular are the recipients of domestic and industrial wastewater effluents, combined sewer overflows (CSOs) and runoff from urban and non-urban areas. The system also receives inputs from atmospheric sources (dryfall and wetfall) directly impinging on the water surface of the Bays and Boston Harbor. Presently the major discharge to the system is from metropolitan Boston's Deer Island facility. This facility is currently being upgraded to provide more advanced wastewater treatment as part of an effort to reduce pollutant inputs to Boston Harbor. In an initial phase of this cleanup effort, the discharge of sludge was halted in December 1991. In order to quantify the magnitude of nutrient inputs to the Bay prior to 1992 the U.S. EPA Massachusetts Bays Program funded Menzie-Cura and Associates to develop loading estimates. This work has been completed and a summary report has been submitted to the Bays Program. Additional loading information, specifically related to the MWRA treatment facilities, and CSO and stormwater discharges, has been summarized by Alber and Chan (1994).

1.5   THE EUTROPHICATION ISSUE

Of particular concern to MWRA and other regional water quality managers is how operational changes at the wastewater treatment facilities will affect the eutrophication processes within Massachusetts and Cape Cod Bays. Although phytoplankton production is an essential part of the food-chain for a given water body, excessive phytoplankton biomass resulting from high levels of nutrient enrichment can adversely affect the overall health of the water body. This is in part due to the fact that under certain conditions excessive phytoplankton growth (eutrophication), coupled with extended periods of vertical stratification within the water column, can result in significant loss of dissolved oxygen,

leading to hypoxia (defined as dissolved oxygen concentrations below 3.0 mg/L) or even anoxia (the total absence of dissolved oxygen) in the bottom waters of the system. Although there have been no reported instances of anoxia or even hypoxia reported for Massachusetts Bay (nor did previous studies, which evaluated the MWRA outfall relocation, project this to be the case), dissolved oxygen is still of potential concern to MWRA.

1.6 PURPOSE AND SCOPE OF THIS STUDY

In order to better understand the processes governing eutrophication in Massachusetts Bay and Cape Cod Bay, MWRA is providing funding for field, laboratory and analytical studies and an extensive outfall sediment and water quality monitoring program. In addition, funding has been provided to develop a series of computer models of Massachusetts Bay and Cape Cod Bay circulation and water quality. These studies and computer models will permit water quality managers to better understand the causes of eutrophication and to manage nutrient inputs to assure the health of the living resources of this marine system.

The analysis presented in this report is a follow up to an earlier effort (HydroQual, 1993), which developed a coarse resolution mathematical water quality model of the Bays. This report summarizes work performed leading to the development and application of a fine-grid, three-dimensional, time-variable coupled hydrodynamic/water quality model of the Bays. This study is focused on the issue of conventional eutrophication as related to phytoplankton biomass, nutrients, and dissolved oxygen. It is anticipated that the resulting fine-grid model will provide managers with a tool to make a detailed analysis of facility operations and nutrient inputs as they relate to eutrophication processes and water quality within the Bays.

1.6.1 Nature of a Mathematical Model

A mathematical model of water quality is a representation of the principal components of the environment that influence a given water quality variable. A model does not purport to represent all aspects of the actual environment, rather a model attempts to incorporate only those features of the problem that are most relevant. Thus, for example, a eutrophication model should incorporate such features as estuarine circulation and mixing, the input of point and nonpoint sources, the principal mechanisms of phytoplankton interactions with light, water temperature and nutrients, and the behavior of the various nutrient forms themselves. Similarly, a model of the oxygen balance of Massachusetts Bay should incorporate the same features of estuarine circulation and mixing, point and nonpoint sources of oxygen demanding pollutants, as well as the effects of atmospheric reaeration, photosynthetic oxygen production and algal respiration and sediment oxygen demand (SOD). The knitting together of the various mechanisms affecting circulation and mixing, phytoplankton behavior and dissolved oxygen is accomplished via theoretical equations (the details of which are presented in Section 4 of this report).

The spatial scope of this analysis encompasses Massachusetts Bay and Cape Cod Bay, including Boston Harbor. The eastern boundary of the model is a transect which extends from Cape Ann on the north to Race Point (on the northern tip of Cape Cod) on the south. Figure 1-2 shows the eastern boundary of the model domain. The definition of this boundary location was based in part on hydrodynamic model computations (Blumberg et al., 1993) which showed that the effluent plumes from the current and future outfall locations were confined within Massachusetts and Cape Cod Bays and did not extend into the Gulf of Maine. This boundary was also chosen based upon the spatial and temporal availability of water quality data with which to specify boundary conditions for the water quality model.

The water quality model calculates spatial variations over approximately 1 to 6 km increments. Vertically, the model resolves spatial variations over a range of from 0.3 to
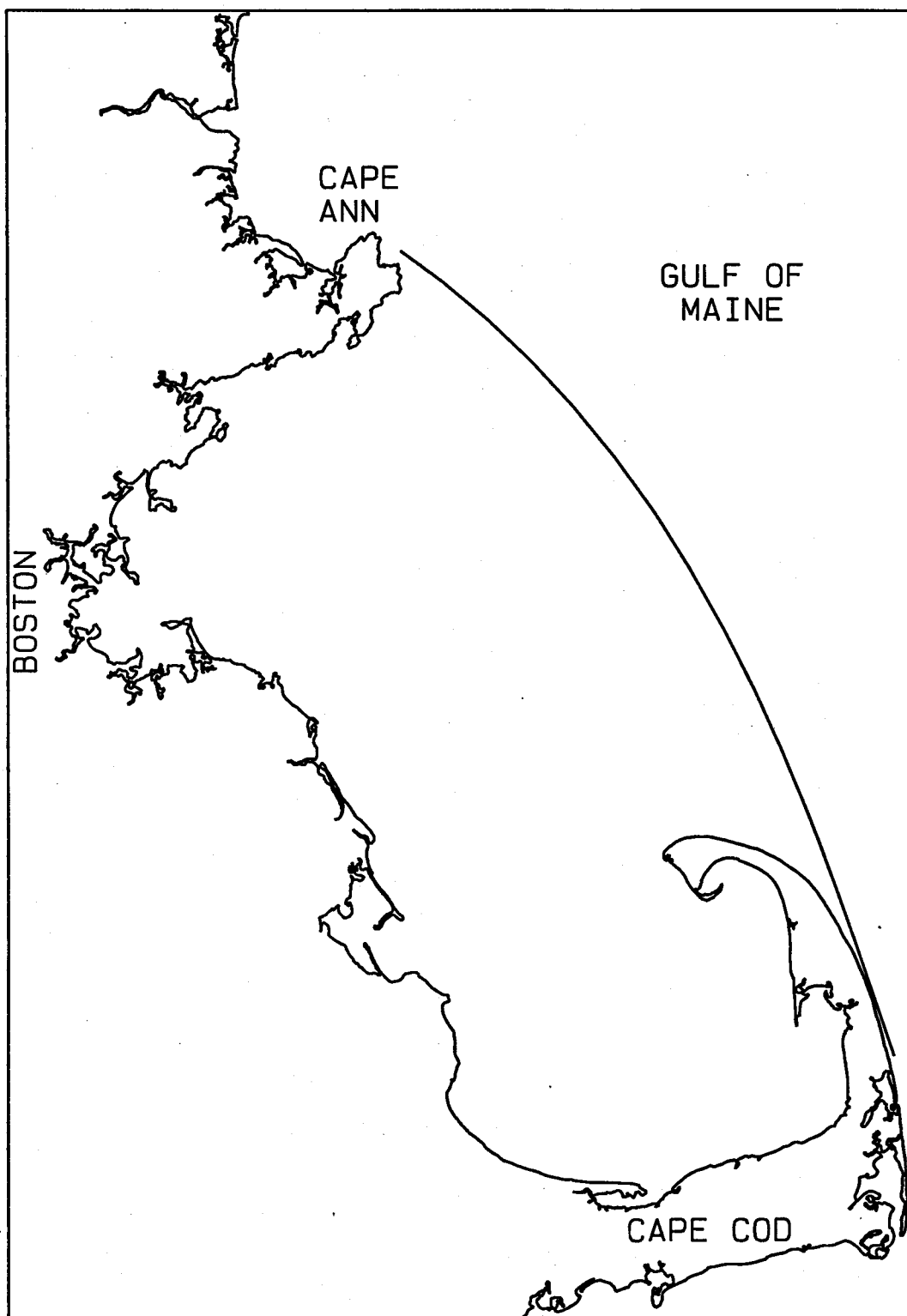
FIGURE 1-2. EASTERN BOUNDARY OF THE WATER QUALITY MODEL FOR BOSTON HARBOR, MASSACHUSETTS BAY, AND CAPE COD BAY

10 m, using 10 sigma-layers in the vertical dimension. Temporally, the model computes the annual cycle of primary productivity, resolving phytoplankton growth dynamics on a daily basis. Information concerning the circulation in the Bay is obtained from an aggregated version of the USGS hydrodynamic model (Signell et al., 1994). The water quality model has been calibrated to data collected over two time periods, October 1989 through April 1991 and January through December 1992. For the purposes of this report the first time period will be referred to as the 1990 data set and the second time period will be referred to as the 1992 data set.

1.7 STRUCTURE OF THE REPORT

Section 2 presents an analysis of the organic carbon and nutrient loadings to Boston Harbor and Massachusetts and Cape Cod Bays from both natural and anthropogenic sources. Section 3 presents the data available for the calibration of the water quality model. Section 4 discusses the theoretical basis for the water quality model. Section 5 describes the calibration of the model. Section 6 discusses the sensitivity analyses from the application of the calibrated model. Finally, projected water quality conditions for the Bays system, generated from the application of the calibrated hydrodynamic and water quality models, for various pollutant load reduction and outfall relocation alternatives are presented in Section 7.

SECTION 2

POLLUTANT LOADINGS

2.1   INTRODUCTION

This section provides a review and summary of the principal inputs of oxygen demanding material and nutrients to Boston Harbor and Massachusetts and Cape Cod Bays. These inputs are comprised of :

- municipal and industrial wastewater treatment plant discharges,
- combined sewer overflow loadings,
- nonpoint source loadings from study area rainfall runoff,
- river loadings,
- groundwater loadings, and
- atmospheric deposition falling directly on the water surface.

A further source of nutrients is via advective and dispersive exchange from the Gulf of Maine. The effect of this latter source has been investigated via sensitivity analysis and is discussed in Section 6.

The loading information used in this analysis was derived from several sources. Information for the area outside of Boston Harbor came almost entirely from the Menzie-Cura & Associates (1991) report to the Massachusetts Bay Program. This report detailed sources and magnitudes of pollutants delivered to Boston Harbor, Massachusetts Bay and Cape Cod Bay including total nitrogen (TN), total phosphorus (TP), and biochemical oxygen demand (BOD). Estimates of total organic carbon (TOC) loadings were derived using the Menzie-Cura estimates of BOD loading and an empirical TOC:BOD relationship (TOC $= 0.7$ BOD$_5$ $+ 18$) developed by HydroQual (1991) for the Long Island Sound Study. Inputs of dissolved silica were estimated using treatment plant data from the Deer Island and Nut Island collected by Battelle Ocean Sciences as part of MWRA's outfall monitoring program.

Menzie-Cura developed pollutant loading estimates for the following sources: municipal and industrial treatment facilities, CSOs, non-CSO storm sewers, non-urban runoff, river discharge, groundwater, and atmospheric deposition. The drainage area of Massachusetts Bays was divided into five basins (Merrimack River, North Shore, Boston Harbor, South Shore, and Cape Cod) and annual loadings were determined for each basin. Loading estimates for the Merrimack River basin and a portion of the North Shore basin were not used because they were outside the model domain. The Menzie-Cura loading estimates for Boston Harbor were not used either because more recent estimates were developed by MWRA.

Loadings for Boston Harbor were obtained from two sources: treatment plant effluent flow and concentration data from the Nut Island and Deer Island facilities, and an MWRA report (Alber and Chan, 1994). The MWRA treatment plant loads were estimated using monthly averaged flows and monthly concentrations for various parameters. The water quality parameters sampled included total Kjeldahl nitrogen (TKN), ammonia (NH_4), nitrate (NO_3), nitrite (NO_2), orthophosphate (PO_4), total phosphorus (TP), BOD and total suspended solids (TSS). The monthly nutrient concentration data were based on a single daily composite for each month. The BOD and TSS concentrations were monthly averages of daily samples. Sludge loading information, for the period during which discharge occurred, included TKN, NH_4, TP, PO_4, and solids. The Alber and Chan report included loading estimates for the Deer and Nut Island facilities' effluent and sludge, CSOs, stormwater, Logan Airport, tributaries, atmospheric deposition, groundwater, and other NPDES dischargers. While the extent of loading information for each source varied, these data were judged sufficient to make reliable estimates of carbonaceous and nutrient loadings to the Harbor. Additional information necessary to compute atmospheric loadings for the model were obtained through Normandeau Associates. This information included precipitation data from Logan Airport.

2.2 POINT SOURCES

2.2.1 Treatment Plants

Effluent flow and concentration data from the major municipal and industrial wastewater treatment plants discharging into the Harbor and Bays were included in the analysis as point source inputs. Point source inputs comprise the largest source of nutrients to the Massachusetts Bay/Cape Cod Bay system. The major point sources of organic carbon, total nitrogen, and total phosphorus to the Harbor and Bays are the MWRA operated Nut Island and Deer Island wastewater treatment plants. Monthly flows and concentrations were available for the 1990 through 1992 period, so loadings were estimated on a monthly basis for model input. Flows and concentrations were averaged to compute the loadings for October through December 1989. Sludge concentrations and volumes were available for 1990 and 1991, after which sludge discharge ceased. The average loadings for the treatment plants are presented in Table 2-1. The Deer and Nut Island treatment plants contributed approximately 17 m^3/s on a daily average basis of freshwater flow to Boston Harbor.

Since for the MWRA treatment plants, TKN, NH_4, TP, and PO_4 data were available, it was possible to estimate the concentrations of total organic nitrogen (TON) and phosphorus (TOP) using Equations (2-1a) and (2-1b).

$$TON = TKN - NH_4 \tag{2-1a}$$

$$TOP = TP - PO_4 \tag{2-1b}$$

Based on information obtained from MWRA, an average dissolved silica (DSi) concentration of 4 mg Si/L was assumed for all plants. Effluent concentrations of particulate silica were assumed to be negligible. An effluent dissolved oxygen concentration of 1.0 mg O_2/L was assumed for all treatment facilities using information from MWRA treatment plant records. This is a conservative estimate, and initial DO deficit is generally a small component of the total oxygen deficit.

TABLE 2-1. DAILY AVERAGE LOADINGS FROM DEER ISLAND AND NUT ISLAND TREATMENT PLANTS (kg/day)			
	1990		1992*
	Deer Island and Nut Island Treatment Plants	Sludge	Deer Island and Nut Island Treatment Plants
Total organic phosphorus (TOP)	2,364	290.3	2,073
PO_4	3,110	128.7	2,930
Total organic nitrogen (TON)	15,932	1,600.0	13,042
NH_4	15,081	1,338.0	16,514
$NO_2 + NO_3$	3,306	0.0	911
Dissolved Silica (DSi)	6,193	0.0	5,614
Total Organic Carbon (TOC)	151,252	9,934.0	150,225
Dissolved Oxygen (DO)	3,095	0.0	2,805
Daily Average Effluent Flow (m^3/sec)	17.7		16.25
*Sludge discharge ended in December 1991			

Loadings for the remaining municipal and industrial treatment plants were estimated on an annual basis using information from Menzie-Cura (1991). Seven municipal facilities, which discharge directly to the Bays, were included as point source inputs. Other facilities which discharge to the tributaries were included in the riverine loadings. Effluent data for carbon, nitrogen and phosphorus were available for only four of the other dischargers. These facilities were the South Essex Sewage District, the towns of Gloucester and Manchester in the North Shore drainage basin and the Hull Wastewater Treatment Plant in the South Shore drainage basin. Five additional facilities which had only carbon data available were the Lynn Water and Sewer facility and Swampscott in the North Shore drainage basin and Plymouth, Rockland, and Marshfield in the South Shore drainage basin. Where estimates of nitrogen and phosphorus were not available, typical municipal treatment plant estimates of 22.0 mg N/L and 4.0 mg P/L were used. Estimates of silica loadings were based on reported effluent flows and an assumption that the effluent silica concentrations of the other facilities were similar to those measured at the MWRA

facilities. The nitrogen and phosphorus loadings, reported by Menzie-Cura, appeared to be in error for the South Essex treatment plant when concentrations were back calculated. These values were replaced by typical South Essex plant values (Camp, Dresser and McKee, 1995). Table 2-2 lists the daily loadings associated with each point source. Figure 2-1 displays the location of each point source with the exception of electric power plants. All of the facilities in this study area with NPDES permits were included in determining pollutant inputs to the Massachusetts Bays system.

2.2.2 River Discharge

Estimates of tributary discharges to Boston Harbor were developed by Alber and Chan (1994). MWRA separated the Boston Harbor drainage area into the North Harbor and South Harbor for analysis. Flows were estimated using USGS gaging station information for water years 1990 through 1992. Total flow was then computed by multiplying the gaged flow by the ratio of the entire drainage basin area to the drainage area above the gage. This was done so as to estimate the flow at the mouth of the river. For the Charles and Mystic Rivers the mouth of the river was considered the site of the Charles River and Amelia Earhart dams, respectively. Concentrations were estimated by MWRA from measurements taken by the Department of Environmental Quality Engineering (DEQE, now Department of Environmental Protection, DEP) and Metcalf and Eddy. Mean loading estimates were used as input to the model. The origins of the silica load in the Charles River are upbasin wastewater treatment plants above the Charles River Dam. The magnitude of the load was based upon STP effluent flows reported in Menzie-Cura and assuming an effluent Si concentration similar to the Deer and Nut Island facilities and also assuming no net loss of silica between the points of effluent discharge and entry to Boston Harbor.

For tributaries outside of Boston Harbor Menzie-Cura estimates were used. To estimate tributary loadings, Menzie-Cura first made estimates of the annual average flow. To do this, a coefficient of 1.7 cfs per square mile (0.0186 m^3/sec per square kilometer)

TABLE 2-2. DAILY LOADINGS FOR TREATMENT PLANTS OUTSIDE BOSTON HARBOR
(kg/day)

	South Essex	Gloucester	Manchester	Hull	Lynn Water & Sewer	Swampscott	Plymouth	Marshfield	Rockland
TOP	95.6	6.2	0.8	4.7	128.8	6.3	5.4	9.6	2.1
PO_4	348.1	35.7	3.8	26.5	730.3	36.2	31.1	53.8	2.4
TON	81.8	76.8	6.6	43.2	945.0	46.8	40.2	69.4	15.8
NH_4	2,457.2	268.5	23.0	151.5	3,307.6	163.9	141.2	243.9	55.1
$NO_2 + NO_3$	351.0	38.4	3.3	21.6	472.5	23.4	20.2	34.8	7.8
DSi	450.4	61.2	11.4	24.9	94.5	23.4	40.3	69.5	15.7
TOC	12,019.5	1,646.1	93.9	187.8	22,376.4	501.3	240.9	445.9	170.9
$Q(m^3/sec)$	1.19	0.136	0.024	0.061	2.49	0.123	0.106	0.183	0.041

1 – Gloucester STP
2 – Manchester STP
3 – South Essex STP
4 – Swampscott STP
5 – Lynn Water and Sewer
6 – Hull STP
7 – Marshfield STP
8 – Rockland STP
9 – Plymouth STP

DI – Deer Island Outfall

NI – Nut Island Outfall

Distance

1 in. = 20 km
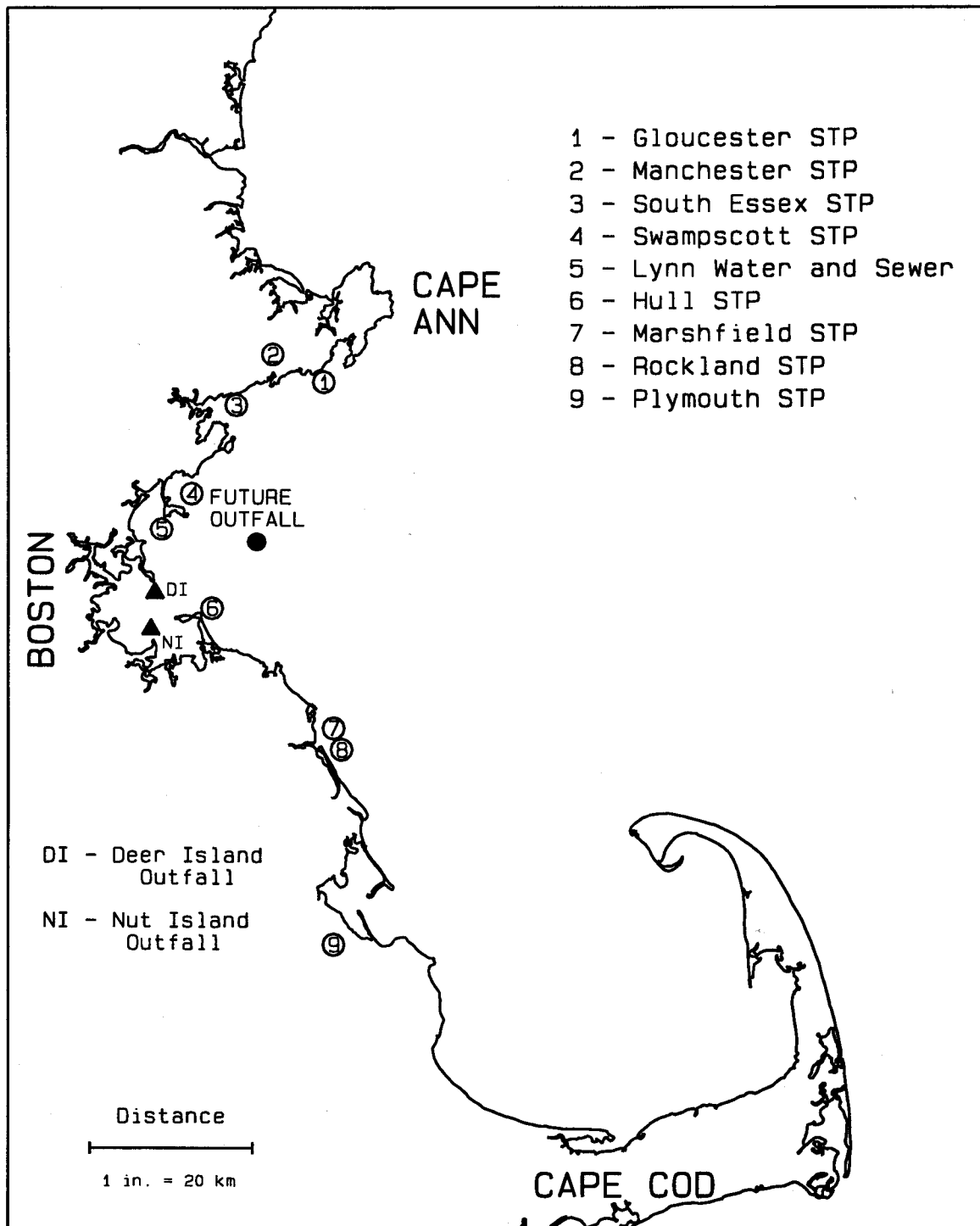
Point Source Locations

Figure 2-1

of drainage area was used. Estimates of pollutant concentrations were developed using historical measurements made by the Massachusetts DEQE.

Tables 2-3 and 2-4 list the flows and loadings used in the model. Since sufficient information was not available to specify riverine loads on a daily or even a monthly basis, all river loads are constant throughout the calibration periods with the exception of the Charles, Mystic, and Neponset Rivers. For these rivers, loadings were weighted according to the monthly average flow from USGS gage data.

TABLE 2-3. ANNUAL AVERAGE RIVER FLOWS	
River	Flow (m³/s)
North Shore	
Annisquam	0.11
Bass	0.07
Danvers	0.59
Crane	0.28
Pines	0.48
Saugus	2.32
Boston Harbor	
Mystic	2.40
Charles	12.30
Neponset	5.30
Weymouth Fore	0.10
Weymouth Back	1.50
Weir	0.10
South Shore	
South	1.15
North	3.90
Green Harbor	0.35
Jones	1.42
Town Brook	0.43
Eel	0.71

River	TOP	PO$_4$	TON	NH$_4$	NO$_2$+NO$_3$	DSi	TOC
Annisquam	0.78	0.50	3.08	0.86	4.76	0.00	28.5
Bass/Danvers/Crane	7.21	4.76	39.64	11.29	62.19	0.00	243.5
Pines/Saugus	21.41	14.29	118.10	33.70	185.43	0.00	724.9
Mystic	16.82	11.20	97.80	27.99	153.77	0.00	724.9
Charles	86.42	57.15	502.58	143.47	789.26	718.50	1,535.0
Neponset	37.06	24.68	216.56	61.69	340.20	0.00	3,388.4
Weymouth Fore	0.75	0.45	4.08	1.18	6.40	0.00	64.0
Weymouth Back	6.32	4.17	36.74	10.48	57.61	0.00	576.0
Weir	0.75	0.45	4.08	1.18	6.40	0.00	64.0
South/North	45.90	30.66	225.34	57.70	316.97	0.00	1,405.5
Green Harbor	2.68	1.77	14.60	4.17	23.04	0.00	90.7
Jones	13.03	8.66	71.68	20.50	112.49	0.00	444.5
Town Brook	2.40	1.59	13.08	3.72	20.50	0.00	80.3
Eel	3.90	2.59	10.75	6.12	33.75	0.00	132.3

TABLE 2-4. DAILY AVERAGE RIVER LOADING (kg/day)

2.2.3 Combined Sewer Overflows

Estimates for CSO loadings were made by both Alber and Chan and Menzie-Cura. The Alber and Chan loading estimates were used for CSOs discharging within Boston Harbor. The Alber and Chan CSO flows were estimated using results from two modeling studies; one based on a Boston Water and Sewer Commission (BWSC) CSO model, and the other from a CSO model developed for MWRA by Metcalf and Eddy (MWRA, 1993). The average of these two estimates was used as input in this modeling effort; CSO flows were estimated to be 0.203 m^3/s. While this estimate is an order of magnitude lower than reported by Menzie-Cura, it reflects the results of a more detailed modeling analysis than was available at the time of the Menzie-Cura analysis. Concentrations for the various water quality constituents were measured by Metcalf and Eddy, BWSC, and MWRA. Pollutant loadings were input into the model by spatially distributing the total CSO loading according to the percentage of the total volume of flow discharged at each location on an annual basis. Small errors associated with this approximation should have only a localized effect on the model computation within Boston Harbor.

North Shore CSO loading estimates were taken from the Menzie-Cura loading report for Massachusetts Bay which are the most up-to-date estimates available. A fraction (75 percent) of the Menzie-Cura loading estimate was used because only a portion of the North Shore drainage basin falls with the water quality model domain. This fraction was determined based on the number of miles of coastline within the model domain. Menzie-Cura's loading estimates were based on flows and concentrations developed by NOAA's National Coastal Pollutant Discharge Inventory (NCPDI). Due to a lack of information concerning the actual CSO locations in this area, the CSO loads were distributed evenly across the entire North Shore. No CSO information was reported for the South Shore and Cape Cod Bay. Daily average CSO loadings for Boston Harbor and the North Shore are presented in Table 2-5.

TABLE 2-5. DAILY AVERAGE CSO LOADINGS (kg/day)		
	Boston Harbor	North Shore
TOP	13.9	70.6
PO_4	10.2	70.7
TON	18.2	120.8
NH_4	39.2	184.4
$NO_2 + NO_3$	5.4	0.0
TOC	1,306.3	9,258.3

2.3   NONPOINT SOURCES

Storm sewers collect runoff and discharge it directly into the Bays. Uncollected stormwater can also flow into the Bays directly via overland flow. Also, stormwater can seep into the ground and eventually enter the Bays as groundwater. Loading estimates were made using measured or estimated flows and concentrations. Estimates of stormwater flow rates were made using drainage basin area, precipitation data and a runoff coefficient based on the imperviousness of the land. The latter was based on land use type. Alber and Chan split non-CSO runoff loadings into stormwater, airport and

groundwater sources. Menzie-Cura computed non-CSO, nonurban, and groundwater sources. Another nonpoint source considered in the model is from atmospheric deposition. This pollutant source includes wet deposition and dry deposition onto the water surface of the Bays.

2.3.1 Stormwater

The following paragraphs discuss the stormwater and airport loads calculated by Alber and Chan and the non-CSO and non-urban loads calculated by Menzie-Cura. MWRA split the Boston Harbor area into the North Harbor, South Harbor, and Logan Airport. For the South Harbor a runoff coefficient of 0.26 was used to estimate the flow of stormwater to the Harbor. For the North Harbor, three runoff coefficients were used ranging from 0.23 to 0.43. Nutrient and BOD concentrations were available from a BWSC sampling program conducted in 1993. The mean calculated loads were used in the water quality model. Flow estimates for Logan Airport were generated from work performed by Rizzo Associates in 1992 (Massport, 1992). The airport was divided into three sections according to land use and runoff characteristics: north outfall, west combination outfall and airfield outfall. Stormwater was measured at these sites during five storms in March, May, and June 1991. Runoff coefficients were then estimated from this information. Pollutant concentrations were also measured by Massport during the sampling events. The mean estimated loadings of nitrogen and phosphorus were used in the water quality model. Carbon loadings were adjusted seasonally to account for the higher winter BODs associated with deicing chemicals. Loadings are presented in Table 2-6.

	North Harbor Storm Sewer	South Harbor Storm Sewer	Airport	North Shore Runoff	South Shore Runoff	Cape Cod Runoff
TOP	9.8	7.7	0.0	149.9	35.5	6.5
PO_4	9.5	7.6	2.4	100.0	22.7	3.8
TON	93.2	70.2	21.0	272.4	132.0	22.8
NH_4	85.7	65.8	9.6	77.6	38.1	5.7
$NO_2 + NO_3$	20.0	15.9	8.5	425.7	208.3	0.0
TOC	953.5	731.4	1,253.2	4,714.2	2,469.0	402.0

TABLE 2-6. DAILY AVERAGE STORM SEWER/RUNOFF LOADINGS (kg/day)

Stormwater loading estimates for the regions outside of Boston Harbor were obtained from the Menzie-Cura Massachusetts Bay loading report. For areas without CSOs, the total annual precipitation was multiplied by a land-use-specific runoff coefficient for each land use type. Loads were calculated using mean urban runoff concentrations for different types of land use compiled for the NCPDI from National Urban Runoff Program (NURP) (USEPA, 1983) and Stenstrom et al. (1984). Nonurban runoff was calculated using the Simulator Model for Water Resources for Urban Basins (SWRRB) which was developed by the U.S. Department of Agriculture's Agricultural Research Service. Runoff estimates from areas that drain directly into coastal waters were calculated by assuming that such runoff occurred from land within 0.5 miles of the shore. The percentage of the total drainage area of this region was calculated and then used to compute the runoff load. Loadings are presented in Table 2-6.

Menzie-Cura also calculated loads for Boston Harbor. These loadings were an order of magnitude higher than MWRA's more recent estimate. The MWRA report (Alber and Chan 1994) attributed the lower loading rates to better model estimates of runoff flow as well as to better estimates of pollutant concentrations.

2.3.2 Groundwater

Loading information associated with groundwater flow was available only for Boston Harbor and Cape Cod. Menzie-Cura provided the loading for Cape Cod and Alber and Chan estimated the loading for Boston Harbor. Groundwater loads for the North Shore and South Shore were estimated by MWRA using the same method as Menzie-Cura (MWRA, 1995). On a bay-wide basis, groundwater contributes only a small portion of the nitrogen loads. However, in the localized Cape Cod region, groundwater is a major contributor of nitrogen. Menzie-Cura provided estimates of groundwater nitrogen loads which were assumed to be composed entirely of $NO_2 + NO_3$. Alber and Chan estimated both NO_3 and PO_4 loads.

The groundwater flow in Boston Harbor was estimated by assuming that half of the rainfall that does not run off via surface flow becomes groundwater. Mean annual loads were used in the model. They were calculated assuming a NO_3 concentration of 2.55 mg N/L and a PO_4 concentration of 0.255 mg P/L based on values reported by Valiela et al (1990). The annual average groundwater flow rate was estimated to be 0.75 m^3/s for the North Harbor and 0.40 m^3/s for the South Harbor. Groundwater loadings for Cape Cod were estimated by assuming a flow equal to the annual recharge in Cape Cod Bay and using NO_3 concentrations from private well samples in Cape Cod. A flow of 4.06 m^3/s and a NO_3 concentration of 2.5 mg N/L were estimated. Daily average groundwater loads are presented in Table 2-7.

TABLE 2-7. DAILY AVERAGE GROUNDWATER LOADING (kg/day)					
	North Harbor	South Harbor	Cape Cod	North Shore	South Shore
PO_4	16.2	8.7	88.9	10.0	10.0
NO_3	165.7	88.5	884.0	100.0	100.0

2.3.3 Atmospheric

Dry deposition and wet deposition of nitrogen, phosphorus and carbon resulting from direct impingement to the surface waters of the study area are included as atmospheric inputs. In this modeling effort, deposition was considered to be spatially constant. Estimates of atmospheric dryfall flux rates for inorganic phosphorus were taken from the Menzie-Cura report, while atmospheric dryfall fluxes of inorganic nitrogen were taken from Zemba (1993). Using this information, together with the surface area of the model domain, dry deposition loadings were estimated. Similarly, for wet deposition loading estimates, observations of inorganic phosphorus and inorganic nitrogen concentrations in precipitation were used together with monthly rainfall data from Logan Airport. To account for atmospheric sources of organic nitrogen, phosphorus, and organic carbon, data from the Long Island Sound Study were used. No estimates of organic

carbon dry deposition were available. The concentrations used to estimate dry deposition and wet deposition loads for each pollutant can be found in Table 2-8. The observed monthly rainfall is shown in Table 2-9. Monthly average loadings are presented in Table 2-10 for the 1990 period and Table 2-11 for the 1992 period.

TABLE 2-8. WET DEPOSITION NUTRIENT CONCENTRATIONS AND AREAL DRY DEPOSITION RATES USED TO ESTIMATE ATMOSPHERIC LOADINGS

Constituent	Wet fall ($\mu g/L$)	Dry fall ($mg/m2-yr$)
NH_4	91.8	145.
NO_3	233.6	710.
TON	116.	42.80
PO_4	3.74	0.66
TOP	3.06	0.54
TOC	1300.	-

TABLE 2-9. MONTHLY RAINFALL AT LOGAN AIRPORT FOR CALIBRATION AND VERIFICATION PERIODS

1990		1992	
Month	Rainfall (in.)	Month	Rainfall (in.)
October 1989	5.70	January 1992	3.10
November	4.14	February	2.28
December	0.81	March	3.59
January 1990	3.78	April	2.34
February	3.61	May	1.40
March	1.71	June	4.62
April	5.94	July	2.67
May	6.54	August	4.25
June	0.69	September	3.45
July	4.09	October	1.61
August	6.57	November	6.15
September	1.59	December	8.25
October	7.35		
November	1.59		
December	3.19		
January 1991	3.26		
February	1.57		
March	4.34		
April	4.83		

TABLE 2-10. ATMOSPHERIC DEPOSITION (1990) (kg/day)						
	TOP	PO_4	TON	NH_4	NO_3	TOC
October 1989	76.4	93.4	3,191	3,999	14,700	29,410
November	59.1	72.2	2,536	3,480	13,380	22,060
December	16.9	20.7	939	2,216	10,160	4,155
January 1990	53.1	64.9	2,307	3,299	12,920	19,500
February	55.7	68.1	2,407	3,379	13,120	20,670
March	27.9	34.0	1,352	2,543	11,000	8,789
April	81.7	99.8	3,391	4,157	15,100	31,640
May	86.5	105.8	3,577	4,304	15,470	33,720
June	15.8	19.3	895	2,182	10,080	3,676
July	56.8	69.5	2,450	3,412	13,200	21,100
August	86.9	106.2	3,591	4,315	15,500	33,880
September	27.1	33.1	1,323	2,521	10,940	8,470
October	96.3	117.7	3,948	4,598	16,220	37,880
November	27.1	33.1	1,323	2,521	10,940	8,470
December	45.9	56.1	2,036	3,085	12,370	16,460
January 1991	46.7	57.0	2,065	3,108	12,430	16,780
February	28.2	34.5	1,366	2,555	11,020	8,949
March	59.8	73.1	2,564	3,503	13,440	22,380
April	67.7	82.8	2,863	3,740	14,040	25,730

TABLE 2-11. ATMOSPHERIC DEPOSITION (1992)
(kg/day)

	TOP	PO_4	TON	NH_4	NO_3	TOC
January 1992	44.8	54.7	1,994	3,051	12,290	15,980
February	36.9	45.1	1,694	2,014	11,680	12,630
March	50.8	62.1	2,222	3,232	12,740	18,540
April	36.5	44.6	1,680	2,803	11,650	12,470
May	24.1	29.4	1,209	2,431	10,710	7,192
June	65.1	79.6	2,764	3,660	13,840	24,610
July	39.5	48.3	1,794	2,893	11,880	13,750
August	58.7	71.7	2,521	3,469	13,350	21,900
September	50.4	61.6	2,208	3,221	12,720	18,380
October	26.7	32.7	1,309	2,510	10,910	8,310
November	84.3	103.3	3,491	4,236	15,300	32,760
December	107.2	131.1	4,361	4,922	17,600	42,510

2.4   LOADING SUMMARY

Figure 2-2 presents a loading summary of the carbon, nitrogen and phosphorus entering the Boston Harbor and Massachusetts and Cape Cod Bays system from various sources and provides a comparison between the 1990 and 1992 periods.   Excluding exchange with the Gulf of Maine, the Deer Island and Nut Island treatment plants contribute the majority of the carbon, nitrogen, and phosphorus to the system.   These plants discharged similar quantities in 1990 and 1992. Cessation of the sludge discharge in December 1990 provided only a minor change in the total loadings to the system. Outside of Boston Harbor, non-MWRA treatment plants contribute the most carbon and phosphorus to the Bays. Atmospheric deposition is the second largest source of nitrogen to the Bays. Non-point and riverine sources contribute similar amounts of carbon, nitrogen and phosphorus to Massachusetts and Cape Cod Bays. In Figure 2-2, non-point sources include storm sewers, CSOs, other runoff, and groundwater.

Figure 2-3 presents a spatial distribution of the total loading from each area within the Massachusetts and Cape Cod Bays system, for the 1990 and 1992 periods. The filled triangles on the figures separate the drainage areas into the North Shore, Boston Harbor, South Shore, and Cape Cod. Atmospheric deposition is shown as a separate category because it impacts all regions. This figure shows that Boston Harbor is the source for the majority of carbon, nitrogen, and phosphorus that enters Massachusetts and Cape Cod Bays from the shore and the atmosphere. The North Shore drainage area and atmospheric deposition also contribute a significant fraction of the loadings to the Bays. The South Shore and Cape Cod drainage basin contribute a minute fraction of carbon, nitrogen, and phosphorus to the Bays. The difference in percentage contribution between the 1990 and 1992 periods results from the cessation of sludge discharge, the inherent variability in treatment plant loads and differences in precipitation.
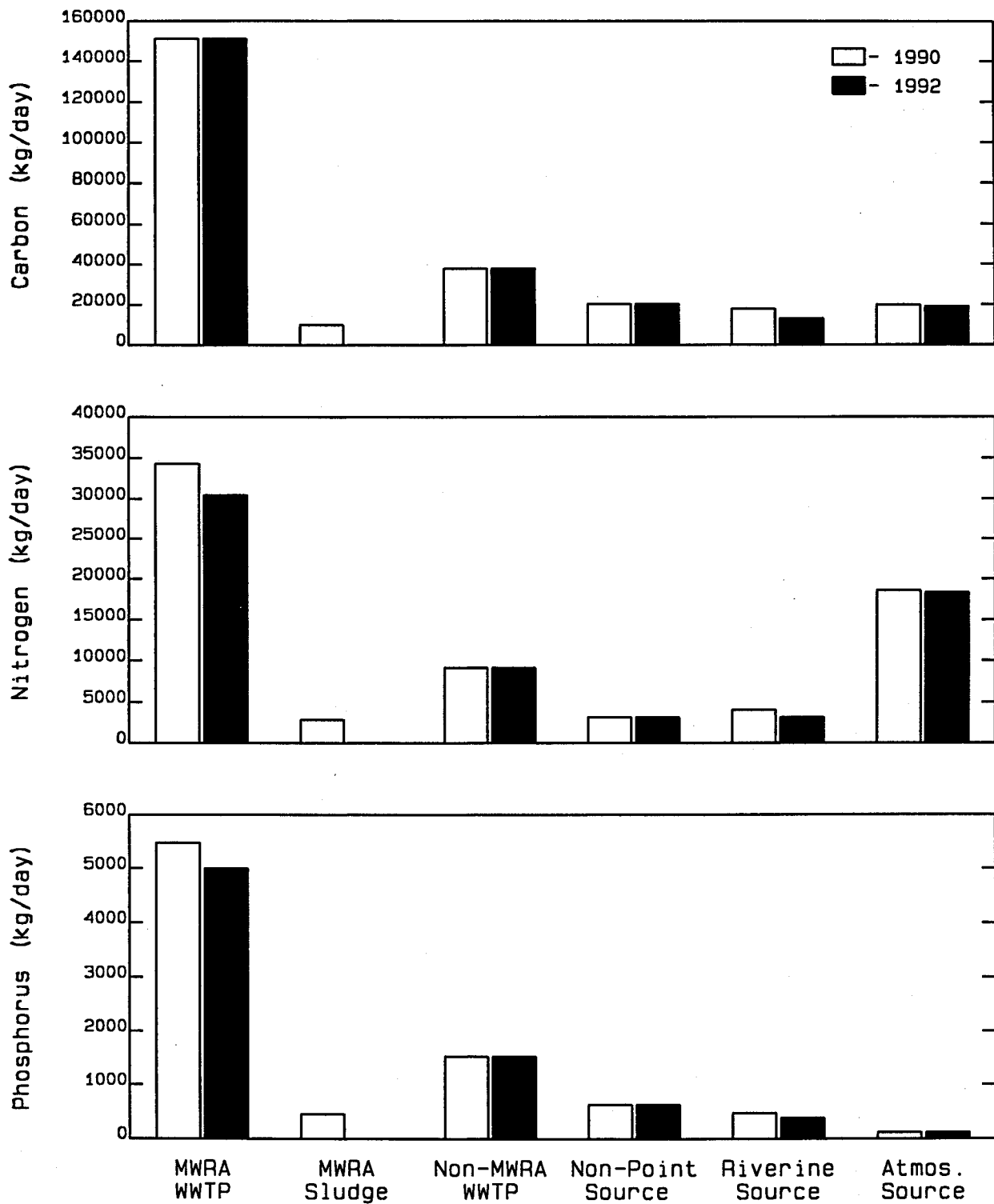
FIGURE 2-2. LOADING COMPARISONS OF POLLUTANT SOURCES FOR 1990 VERSUS 1992
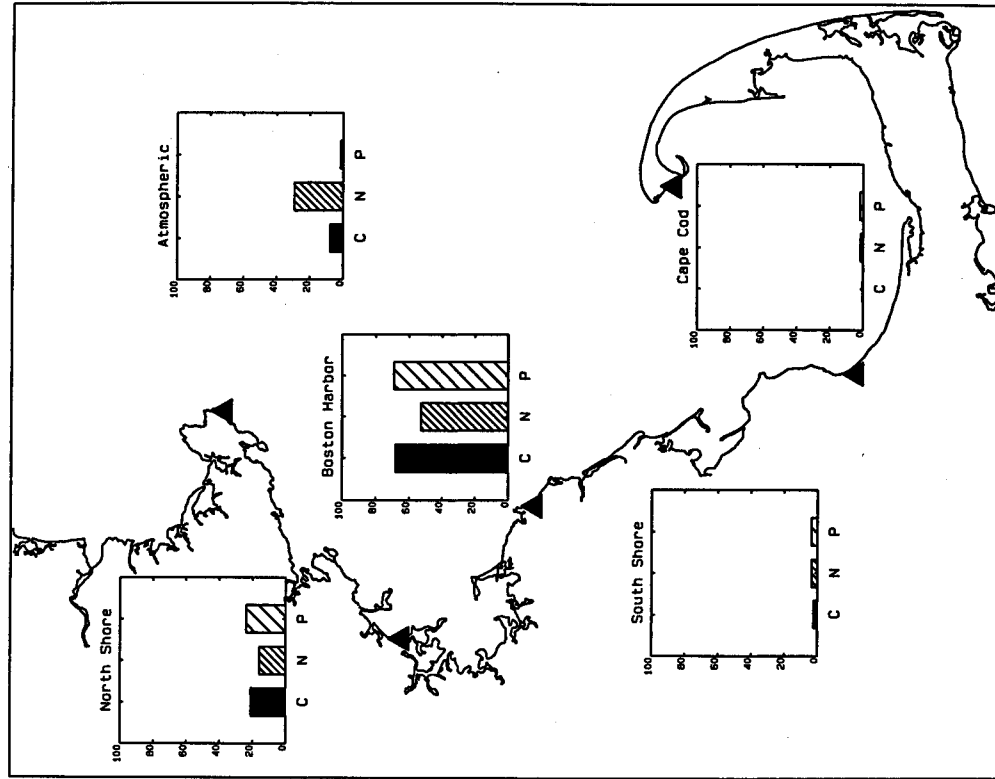
Percent Contribution of C, N, and P Loading by Location - 1992
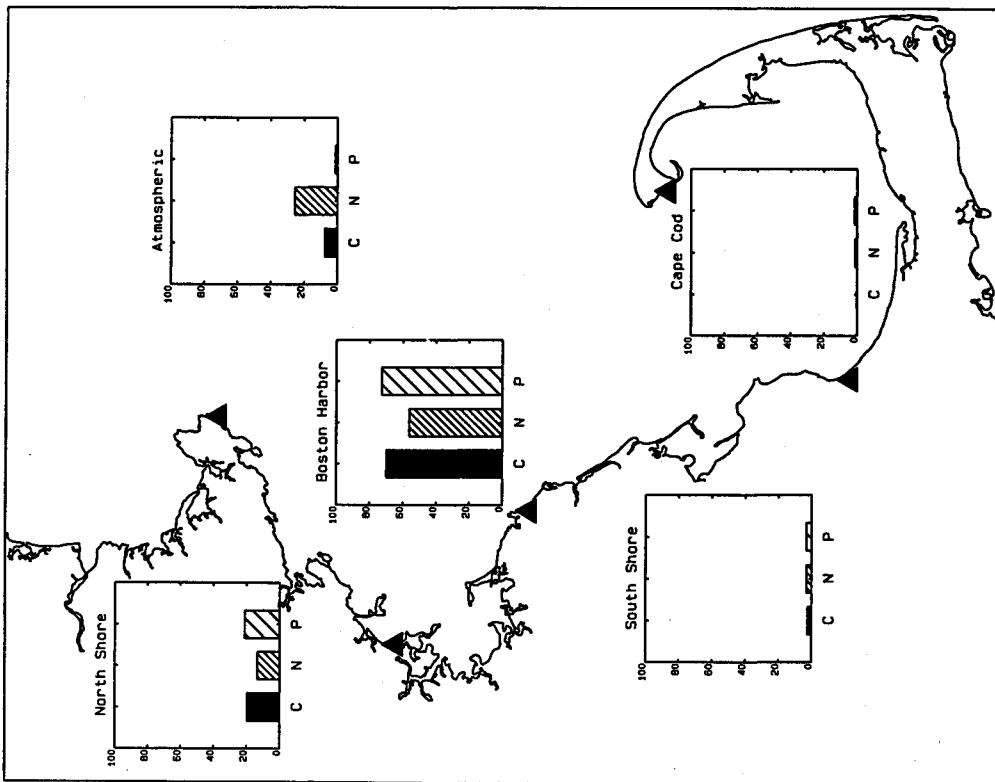
Percent Contribution of C, N, and P Loading by Location - 1990

FIGURE 2-3. COMPARISON OF POLLUTANT LOADING DISTRIBUTIONS - 1990 VERSUS 1992

SECTION 3

WATER QUALITY DATA

3.1 INTRODUCTION

The credibility of model calculations is judged, to a large degree, on the basis of the agreement of the model with observed data. Beyond the constraint that the model must behave reasonably well and conform with general scientific principles, observed data offer perhaps the only external criteria available to assess the validity and, hence the utility of a complex hydrodynamic/water quality model. A properly validated deterministic model is a powerful tool because it represents, as closely as possible, the mechanisms which affect the problem.

The monitoring programs which provided the available data base for model calibration were not designed specifically for use in a water quality model. As a consequence, there are some gaps in the data desired for model calibration. However, the monitoring programs were extensive enough to provide a reasonable data set for calibration purposes. The scope, logistics, and results of the sampling programs used for model calibration are introduced and discussed below.

3.2 1990 DATA SET

The major sources of data used for the initial model calibration were obtained during a series of synoptic cruises extending in time from October 1989 through April 1991. These data were collected by the Bigelow Laboratory for Ocean Sciences (Townsend et al., 1990) and a joint University of Massachusetts at Boston/Woods Hole Oceanographic Institution/University of New Hampshire/United States Geological Survey (UMB/WHOI/UNH/USGS) team (Geyer et al., 1992).

Figure 3-1 shows the station locations for the Bigelow cruises, while Figures 3-2 and 3-3 show the station locations of the two sets of UMB/WHOI/UNH cruises. Note that
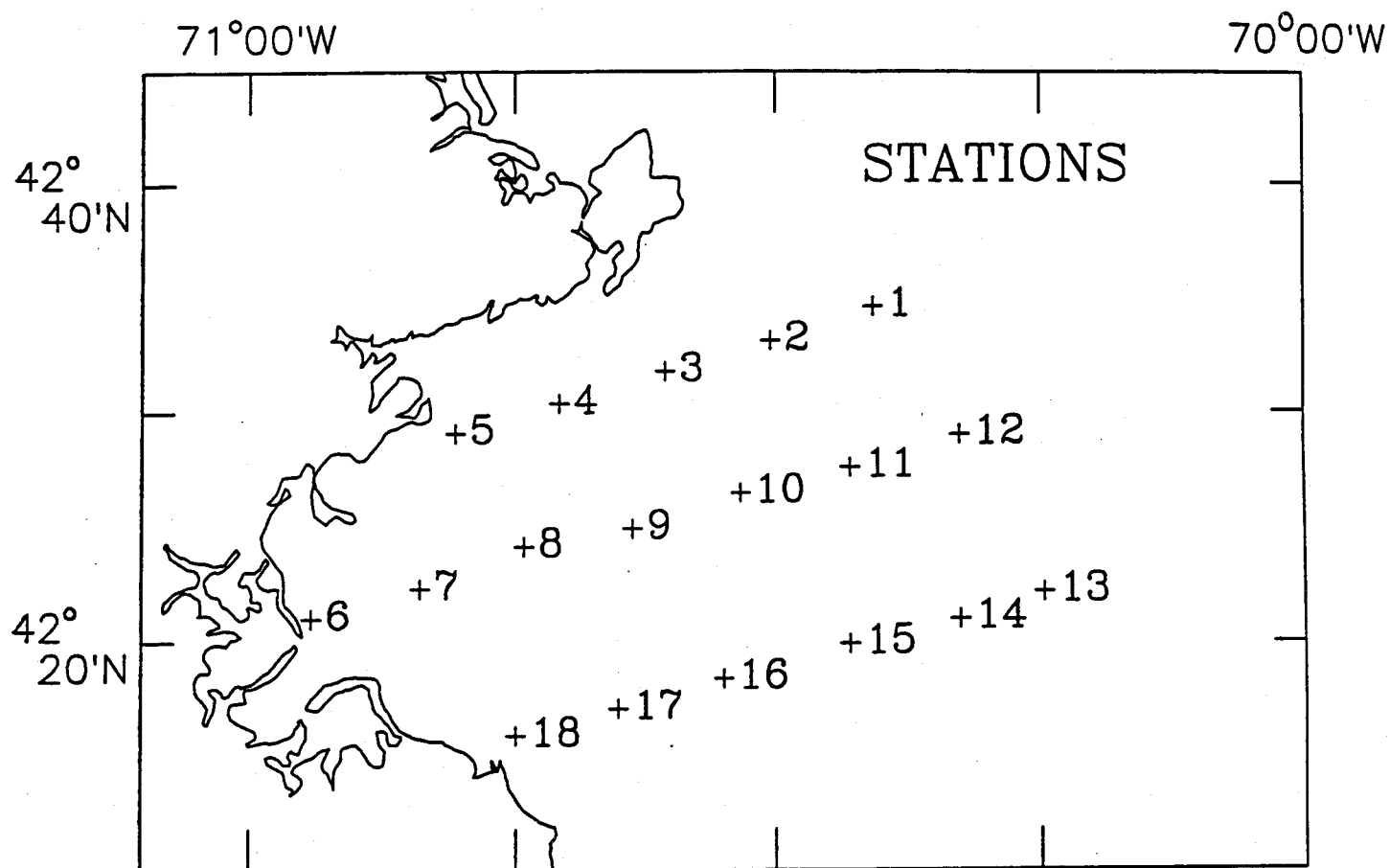
FIGURE 3-1.   STATION LOCATIONS FOR BIGELOW LABORATORY CRUISES
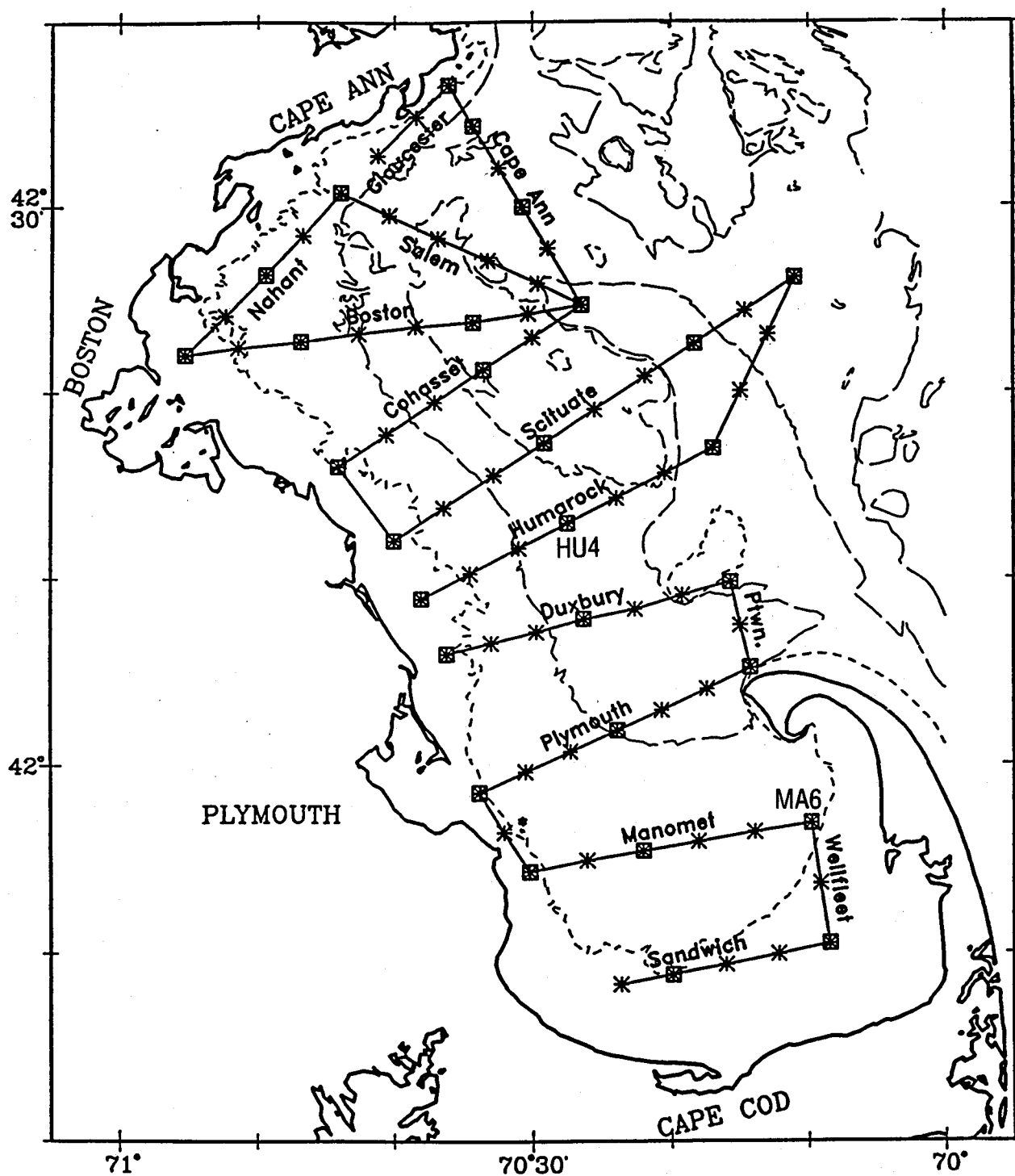
FIGURE 3-2. CRUISE TRACK FOR THE FIRST THREE SEASONAL CRUISES
CONDUCTED BY WHOI/UMB/UNH
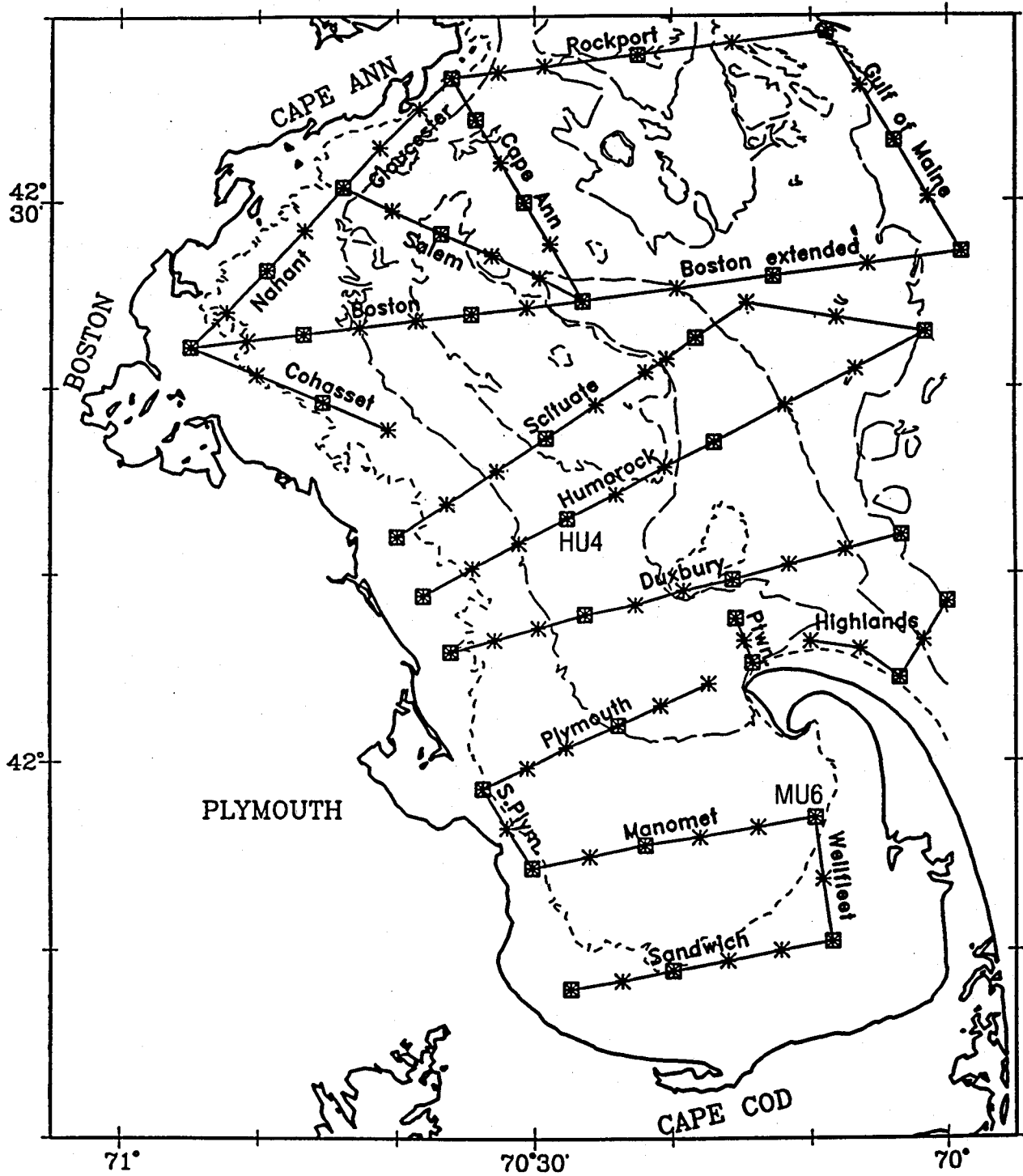
FIGURE 3-3. CRUISE TRACK FOR FINAL THREE SEASONAL CRUISES CONDUCTED BY WHOI/UMB/UNH

the nutrient stations for the UMB/WHOI/UNH cruises are defined with squares around them. A third data set which contains data within Boston Harbor was obtained from the New England Aquarium (Robinson et al., 1990). The station locations for these data are found on Figure 3-4. The final data set is the MWRA combined sewer overflow receiving water quality monitoring data set. This data set contains data within Boston Harbor. The station locations are found on Figure 3-4.

The six Bigelow Laboratory cruises covered 18 stations in the northern portion of Massachusetts Bay. Four of these stations (2, 4, 14, and 16) were hydrographic stations where only salinity, temperature, fluorescence and beam attenuation were measured. Nine stations (1, 3, 5, 9, 11, 13, 15, 17, and 18) were nutrient stations where hydrographic casts were taken as well as discrete bottle samples for $NO_2 + NO_3$, NH_4, DSi, PO_4, dissolved oxygen (DO), spectral absorption, phytoplankton pigments, particulate organic carbon (POC), and particulate organic nitrogen (PON). The remaining five stations (6, 7, 8, 10, and 12) were productivity stations which included all the analyses listed for the nutrient stations plus primary productivity, phytoplankton community structure and zooplankton. Sampling cruises were conducted on October 24, 1989, February 6, March 6, April 10, June 5, and August 14, 1990; weather conditions caused abbreviated sampling for March and April 1990. A detailed account of the data and the methods used for analysis is available in a series of four reports written by the Bigelow Laboratory for MWRA (Townsend et al., 1990a,b,c, 1991).

A team consisting of researchers from WHOI, UMB, UNH, and the USGS conducted 12 hydrographic surveys from April 1990 through June 1991. These data are reported in Geyer et al. (1992). Six of these cruises also included baywide nutrient sampling. All cruises included measurements of temperature, salinity, fluorescence, light transmission and dissolved oxygen. The nutrient sampling cruises measured NH_4, $NO_2 + NO_3$, PO_4, DSi, and suspended solids. These samples were taken at several depths within the water column.
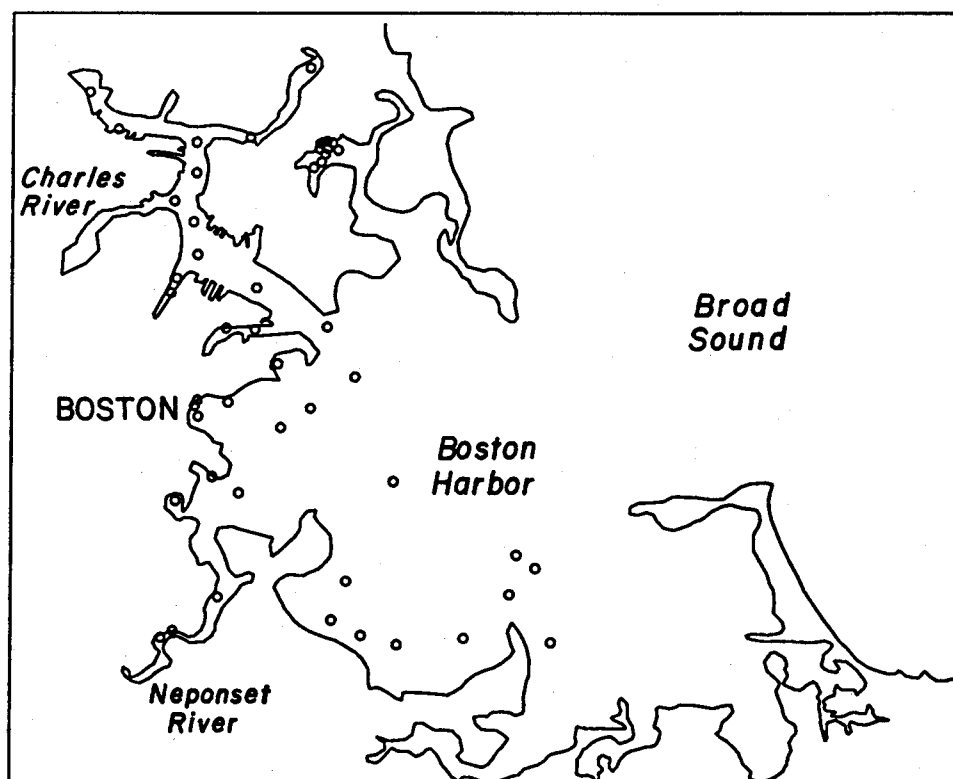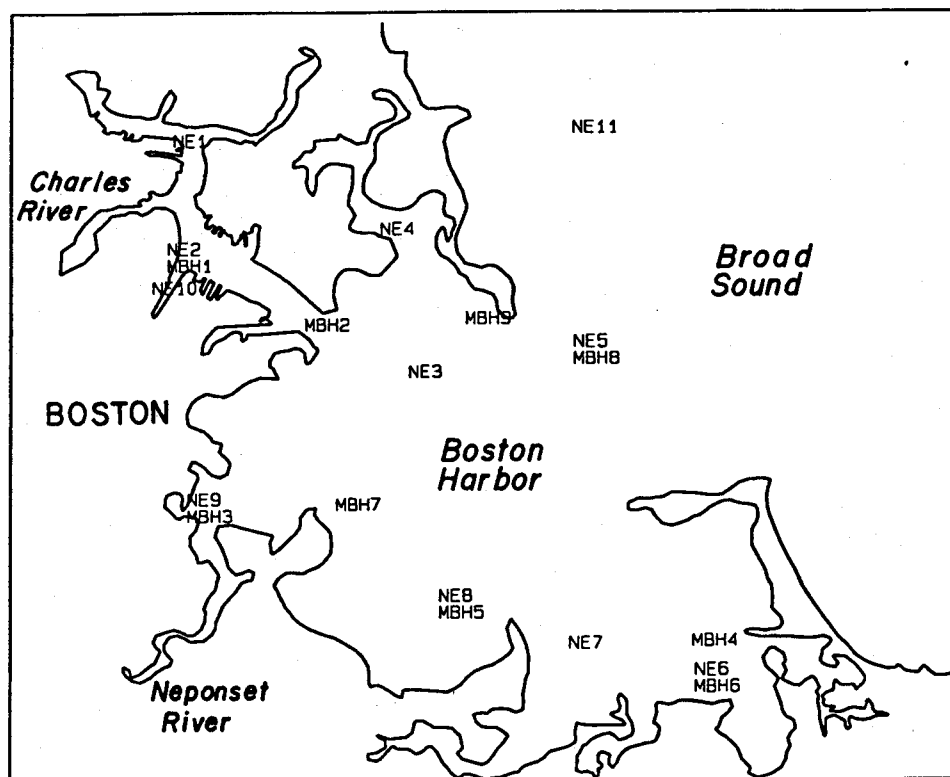
FIGURE 3-4. NEW ENGLAND AQUARIUM SAMPLING STATIONS (TOP PANEL) AND MWRA CSO/HARBOR RECEIVING WATER QUALITY MONITORING STATIONS (BOTTOM PANEL)

The first three WHOI/UMB/UNH water quality surveys were conducted in April, June, and October of 1990. These cruises followed the tracks shown on Figure 3-2. A total of 74 stations were sampled, 29 of which included nutrient measurements (as indicated by a square). The three remaining water quality surveys followed the path indicated on Figure 3-3. These cruises extended farther into the Gulf of Maine and consisted of 96 sampling stations, 39 of which included nutrient measurements. These field studies were conducted in February, March, and April of 1991.

A third data set contains data from the New England Aquarium for Boston Harbor (Robinson et al., 1990). The data set contains surface and bottom samples taken monthly from March 1988 to November 1991 excluding December, January, and February. Eleven stations were sampled for temperature, salinity, density, DO, secchi depth, pH, suspended solids, TKN, PO_4, TP, DSi, chlorophyll-a, and phaeophytin. The data set also includes nine stations which were sampled from August through December 1989. The final data set from MWRA contains data for Boston Harbor from September 1989 through August 1991 (MWRA, 1991; Rex, 1993). This data set contains temperature, salinity, and DO measurements.

3.2.1 Physical Water Quality Parameters

3.2.1.1   Introduction

A number of physical water quality parameters are important to the hydrodynamic, eutrophication, and dissolved oxygen processes that affect the Massachusetts Bays system. Among the more important physical parameters are temperature, salinity, and transparency. Water temperature strongly affects phytoplankton growth rates, nutrient recycle kinetics, and temperature-mediated biological decomposition in the water column and in the sediment. Temperature, and to a lesser degree salinity, influence the solubility of dissolved oxygen in water. Differences in water temperature can create temporal and spatial gradients in dissolved oxygen saturation. Temperature and salinity also affect water column density, an important driving force in estuarine circulation. Density

stratification within the water column can exacerbate the occurrence of hypoxia in the bottom waters because it limits the exchange of surface oxygen-rich water with oxygen-deficient water below the pycnocline. Conversely, density stratification can limit phytoplankton growth by trapping nutrient-rich water below the pycnocline.

Water transparency affects the extent of sunlight penetration into the water column. Reduced water transparency reduces the euphotic zone, the region within the water column where photosynthesis is possible.

The following paragraphs present a portion of the available data in order to gain insight into the processes occurring within the Massachusetts Bays system both spatially and temporally. Five representative stations have been chosen to illustrate the available data. These stations were chosen for their location, quantity of observations, and proximity to stations which were monitored in 1992. Boston Harbor is represented by two stations located near the entrance to the harbor, close to the Deer Island outfall. One station is the Bigelow Station 6 (see Figure 3-1) the other is Station MBH9 from the New England Aquarium data set (Figure 3-4). These stations are plotted together in the first panel of the data figures. The northern portion of Massachusetts Bay is represented using Bigelow Station 8. For the central portion of Massachusetts Bay, UMB/WHOI/UNH station HU4 is used. Finally, eastern Cape Cod Bay is represented using UMB/WHOI/UNH station MA6. The data shown are surface and bottom samples, using open circles and filled circles, respectively. Lines emanating from the circles present the standard deviation of the data if more than one measurement was available for that time. Additional data are available vertically within the water column, but are omitted from the figures in order to make the figures less cluttered. One thing to note during the review of these data is the relative paucity of data in terms of temporal coverage. The paucity of the data makes it very difficult to draw any inferences concerning short-term events within the study area. However, there is, in general, sufficient data with which to determine the seasonal dynamics of primary productivity within the Bays system.

3.2.1.2   Water Column Temperature

Water column temperature is recognized as an important parameter affecting both the hydrodynamic and biological processes that occur in all water bodies. The water column temperature distribution in Massachusetts Bay is a function of both surface heat flux and the transport of water into and out of the system. Figure 3-5 displays 1990 temperature data observed at the stations previously mentioned.

These data show a seasonal cycle of heating and cooling as well as vertical stratification and destratification. Temperatures are lowest in February and March, reported at about 2 to 4°C; surface temperatures peak in August in the low twenties. The Boston Harbor station differs from the other stations in that there is less temperature stratification. This is due to its shallow depth, large tidal range and high tidal current velocities at the narrow mouth of the harbor, all of which act to cause high vertical mixing. Signell and Butman (1992) observed these higher tidal velocities in their modeling analysis of Boston Harbor. Other regions of the Bays are observed to be well mixed during the winter and become thermally stratified during the summer. As the year progresses beyond the summer and into the fall both air and surface water temperatures begin to cool resulting in the fall overturn (which occurs in October or November) wherein the water column becomes well mixed again. During the summer stratification period the difference between surface and bottom water temperature can be as much as 15°C , as can be observed in the data from Cape Cod Bay. The degree of stratification depends a great deal on the depth of the water column. Deep water off-shore locations in central Massachusetts and Cape Cod Bays tend to have greater temperature stratification than do near-shore shallow water locations.

3.2.1.3   Salinity

Massachusetts Bay has a large open boundary with the Gulf of Maine. In addition, Massachusetts and Cape Cod Bays have only a few small tributaries that discharge freshwater. Therefore, most of the water within the Bays is coastal ocean water with a
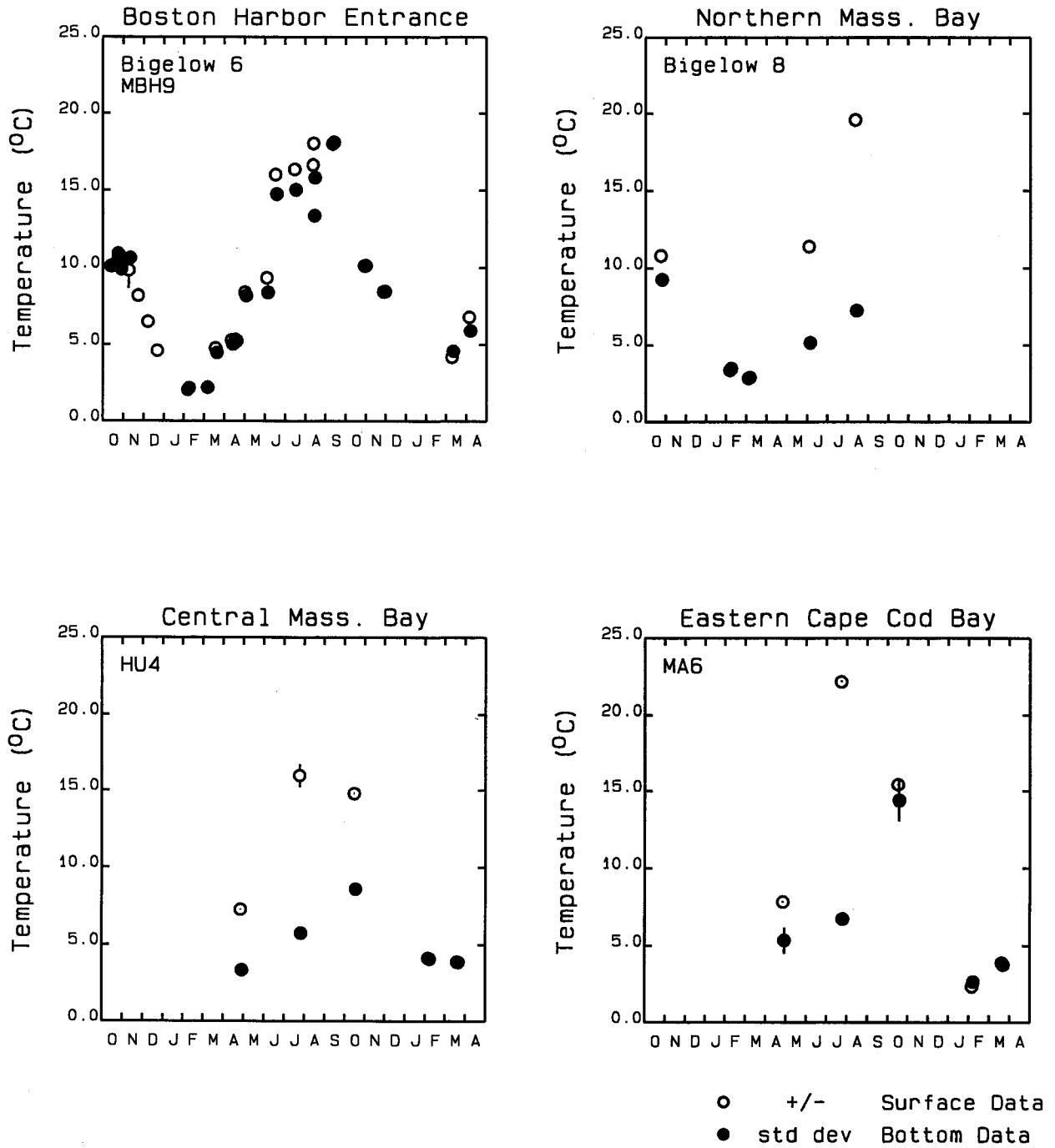
FIGURE 3-5. OBSERVED 1989 THROUGH 1991 TEMPERATURE DATA FOR SELECTED STATIONS

relatively constant salinity. There are occasions, however, when a pulse of freshwater, or freshet, enters the northern portion of the Massachusetts Bay. These freshets originate from the Merrimack River and other northern rivers flowing into the Gulf of Maine. They are transported south along the Maine/Massachusetts coastline by the Gulf of Maine coastal current and enter Massachusetts Bay just south of Cape Ann.

The effect of these events can be observed in the salinity data presented on Figure 3-6. The Boston Harbor entrance is again shown to be well mixed with salinity stratification less than one part per thousand (ppt). With the exception of some low surface salinities observed in December 1989, salinities at this location range from 30 to 32.5 ppt. In the remainder of the system salinity is unstratified during much of the fall, winter, and spring, with surface and bottom salinities between 32 and 33 ppt. During the summer period salinity stratification of approximately one ppt is observed in the central and southern stations shown. The northern station shows more stratification, as much as two ppt in late May/June. This increase in stratification may be due to freshwater entering from the Gulf of Maine, as evidenced by a decrease in surface salinity. Summertime surface salinities across the Bays range from 30.5 to 32 ppt, and bottom waters range from 32 to 33 ppt.

3.2.1.4   Water Transparency and Light Extinction Coefficient

Water transparency plays an important role in the growth of phytoplankton. The extinction coefficient is a measure of the vertical light attenuation through the water column. Light extinction increases markedly with the presence of suspended solids and is a strong function of phytoplankton density. As the concentration of phytoplankton increases, the extinction coefficient increases as well, particularly at photosynthetically active wavelengths. This process is known as self-shading and can have a marked effect on reducing the phytoplankton growth rate.

During the Bigelow Laboratory cruises several optical measurements were collected: particle absorption, dissolved material absorption, vertical profiles of beam attenuation and
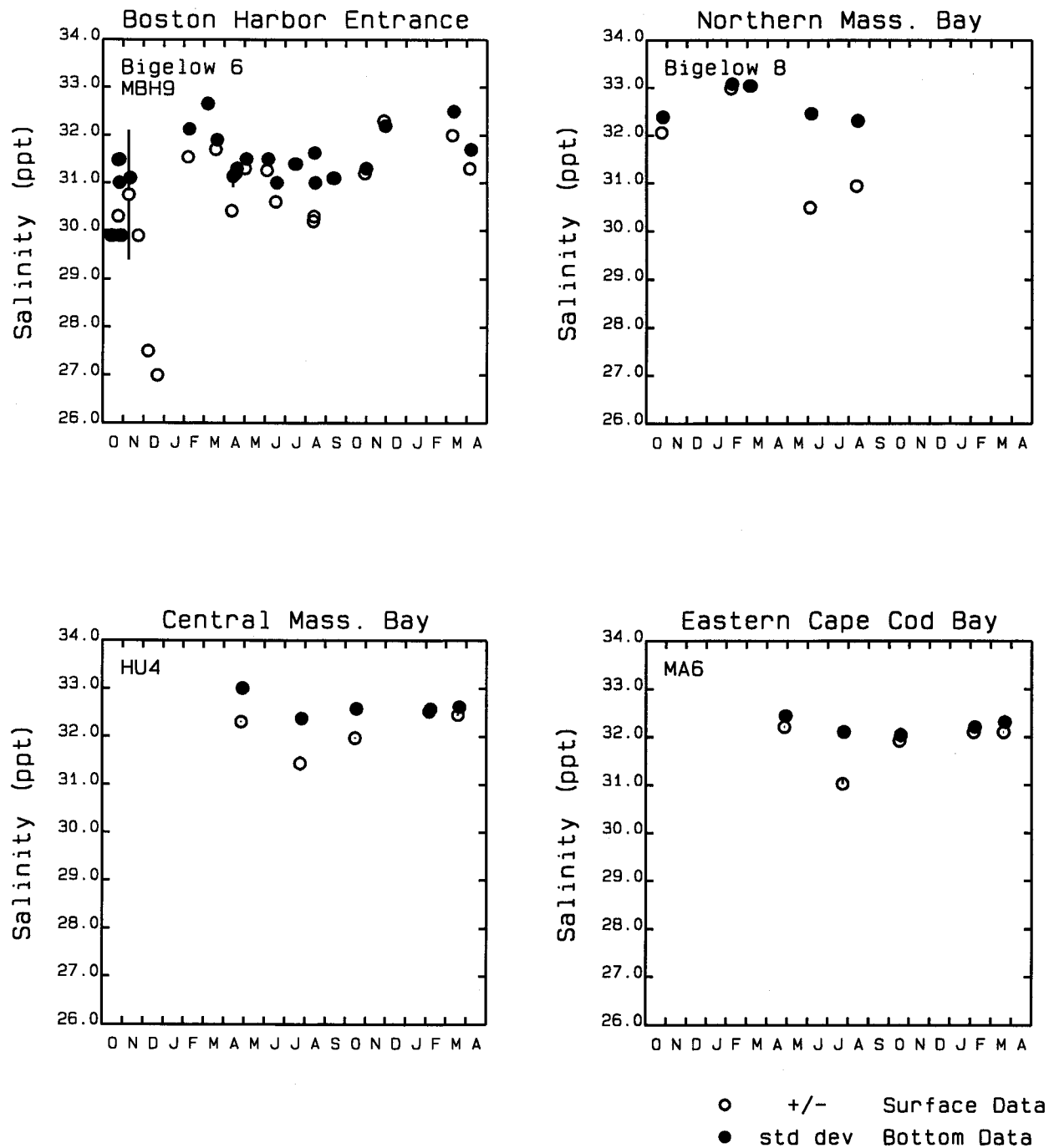
FIGURE 3-6. OBSERVED 1989 THROUGH 1991 SALINITY DATA FOR SELECTED
STATIONS

photosynthetically active radiation, and secchi depth. Secchi depth was measured at only the center transect stations (6 through 12). Secchi depth measurements can be converted to extinction coefficients via the following relationship (Sverdrup et al., 1942; Beeton, 1958):

$$k_e = 1.7 \ / \ SD \tag{3-1}$$

where k_e is the extinction coefficient (m^{-1}) and SD is the secchi depth (m).

During the late winter and early spring period, secchi depths of 4.0 to 6.0 m were measured at the western stations and 10.0 to 16.0 m at the eastern stations yielding extinction coefficients of 0.28 to 0.43 m^{-1} and 0.11 to 0.17 m^{-1}, respectively. In the late spring and summer periods, secchi disc depths of 2.0 to 3.8 m were measured (k_e = 0.44 - 0.85 m^{-1}) at the western stations and from 8.0 to 10.5 m (k_e = 0.16 - 0.21 m^{-1}) at the eastern stations.

3.2.2 Chemical and Biological Water Quality Parameters

3.2.2.1 Introduction

The various programs, which collected data used for this study, analyzed water samples for chemical and biological parameters, as well as physical parameters. These parameters included measurements of algal biomass, various forms of nutrients, and dissolved oxygen. Generally, the observed data showed variation between surface and bottom measurements and, therefore, will be presented in the same manner as the temperature and salinity data.

3.2.2.2 Chlorophyll

A commonly used measure of algal biomass is chlorophyll-a. Both the New England Aquarium and Bigelow Laboratory data sets include chlorophyll-a and these values are plotted in Figure 3-7. The WHOI/UMB/UNH data set includes measurements of chlorophyll
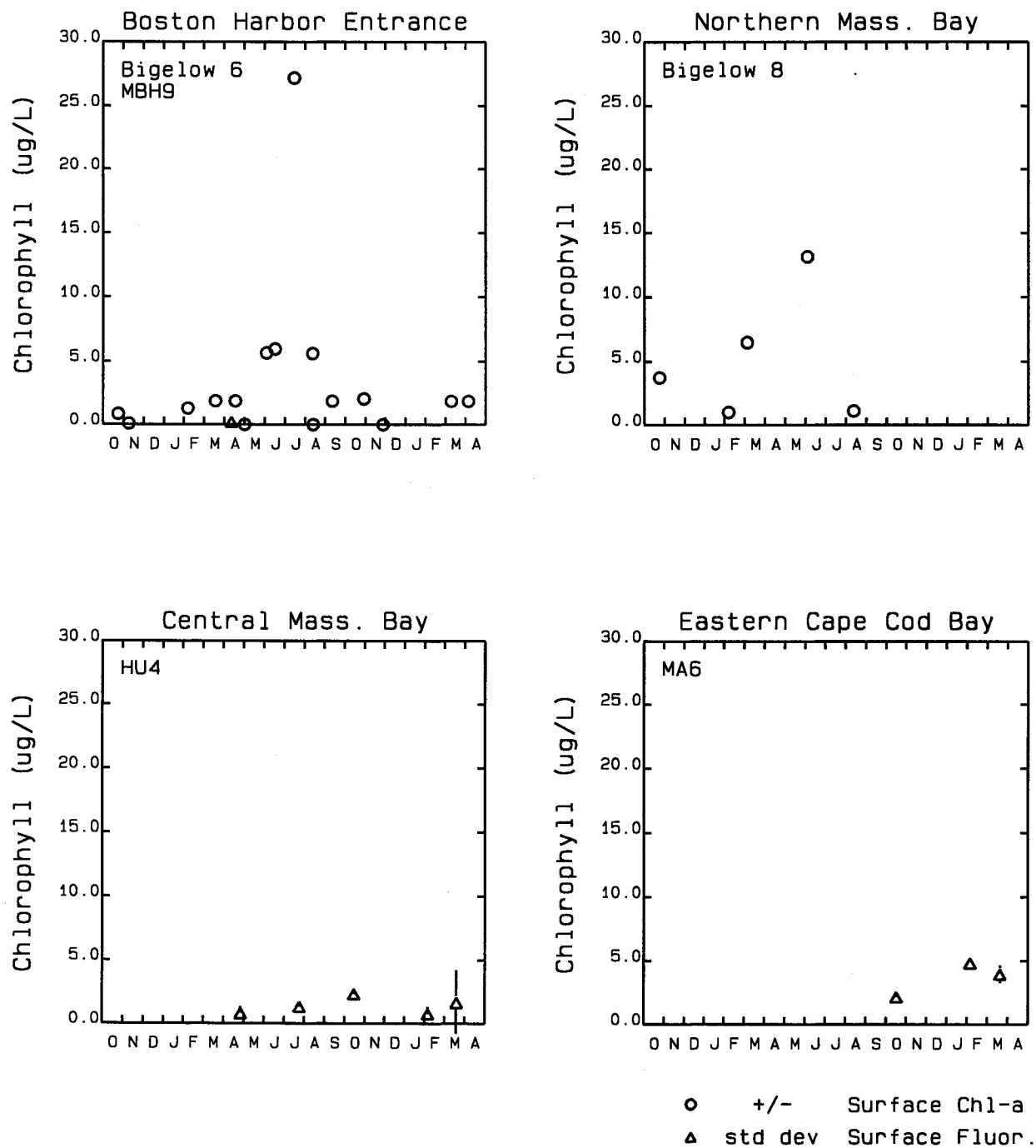
FIGURE 3-7. OBSERVED 1989 THROUGH 1991 CHLOROPHYLL AND FLUORESCENCE
DATA FOR SELECTED STATIONS

fluorescence, as determined via calibration to discrete chlorophyll measurements (Geyer et al, 1992). The Boston Harbor station has low levels of chlorophyll-a at the end of 1989 into early 1990, one μg/L or less. During March chlorophyll concentrations begin increasing, coincident with increasing water column temperature and increasing solar radiation. The chlorophyll-a concentrations peak during June and July with concentrations near 7 μg/L and one value above 25 μg/L. The concentrations then decrease in late summer into the fall and winter.

The northern Massachusetts Bay station shows a similar pattern. Chlorophyll-a concentrations decrease between October 1989 and early February 1990 during the reduced light and colder period of the year. By late February/early March 1990 the spring bloom develops. Chlorophyll levels continue to increase until June when chlorophyll-a reaches a maximum value of approximately 13 μg/L. Concentrations then decrease to less than 1 μg/L by August.

Fluorescence data in central Massachusetts Bay show low levels of algal biomass. Measurements are relatively constant throughout the year. A peak value of 2.5 μg/L is observed in October. In eastern Cape Cod Bay the limited fluorescence data show a peak concentration of 5 μg/L in early February. This peak occurs a few weeks before the bloom begins in northern Massachusetts Bay.

3.2.2.3   Organic Carbon

The New England Aquarium and Bigelow Laboratory data sets contain particulate organic carbon (POC) data. However, none of the 1990 data sets contain measurements of dissolved organic carbon (DOC). Particulate organic carbon can be used as an indicator of algal biomass in regions removed from anthropogenic inputs. Figure 3-8 displays the available surface POC data. These stations show temporal patterns similar to the chlorophyll-a data, with moderate POC concentrations in October decreasing to near zero values by early February. This trend reflects the low population of phytoplankton in the winter. By late February/early March POC levels increase as the phytoplankton bloom
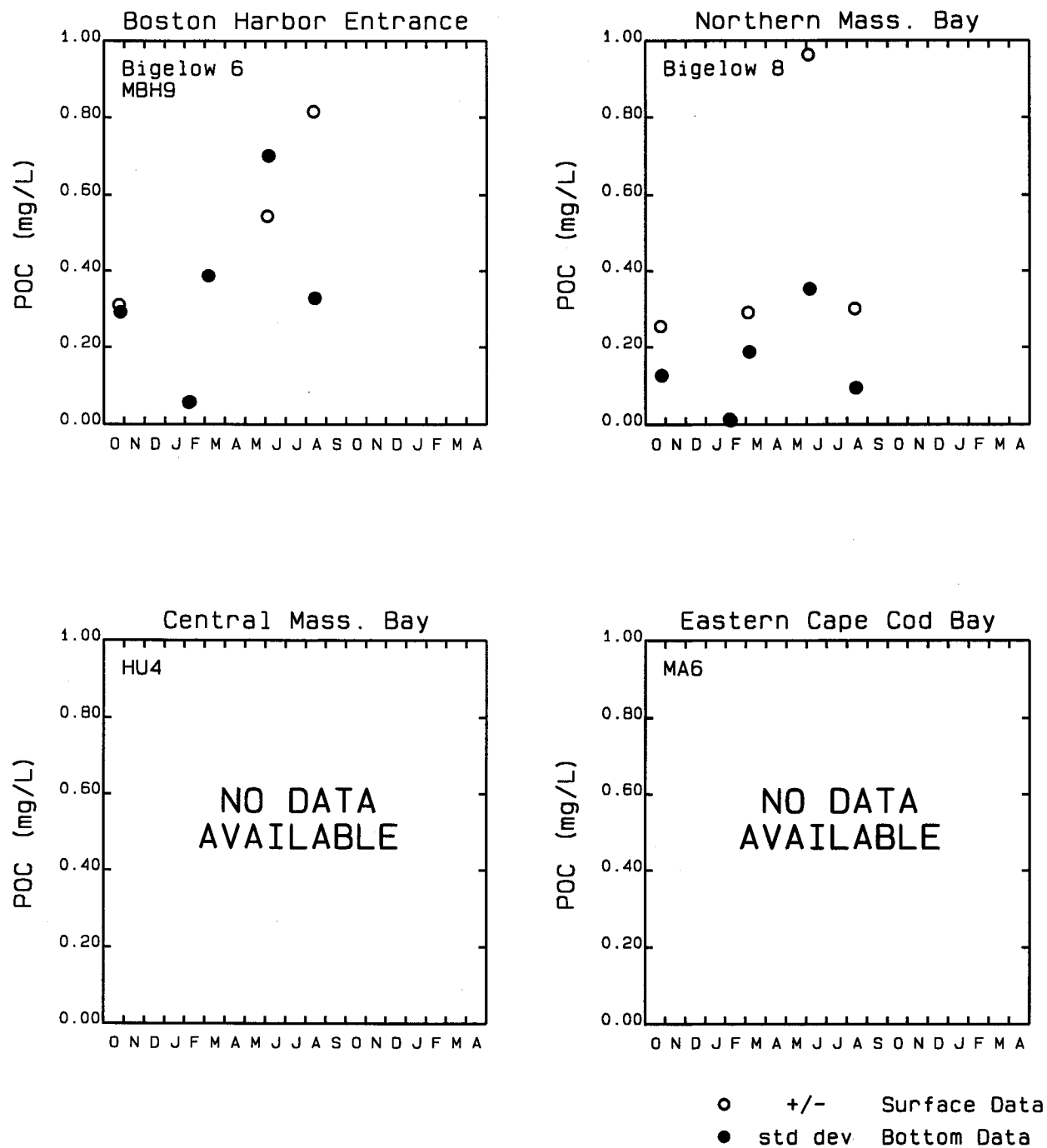
FIGURE 3-8. OBSERVED 1989 THROUGH 1991 POC DATA FOR SELECTED
STATIONS

develops. Concentrations of POC peak in August near 0.8 mg C/L at the Boston Harbor station. In northern Massachusetts Bay the maximum POC concentration of approximately 1 mg C/L, is observed in June. Concentrations of POC at this station then decrease to March levels by early August. It should be noted that some of the POC measured near the Boston Harbor entrance can be attributed to the discharge of wastewater effluent and sludge from the Nut and Deer Island treatment plants.

3.2.2.4   Phosphorus

Measurements of dissolved inorganic phosphorus (reported as orthophosphate, PO_4) were taken in all of the nutrient surveys. However, no total or organic phosphorus measurements are made during the 1990 period. Inorganic phosphorus is an important nutrient for phytoplankton growth. Figure 3-9 presents PO_4 measurements at four locations. The PO_4 data at the Boston Harbor entrance range from 0.02 to 0.10 mg P/L. Maximum concentrations are observed during the summer for this station. The remaining stations show relatively constant bottom concentrations ranging from 0.02 to 0.04 mg P/L. Surface PO_4 concentrations are comparable to bottom water PO_4 concentrations during the winter. However, during the spring and summer months, PO_4 concentrations are found to be significantly lower, ranging from near zero to 0.01 mg P/L. These low surface concentrations are a result of inorganic phosphorus uptake by phytoplankton.

3.2.2.5   Nitrogen

Measurements of nitrogen are available in the forms of NH_4, $NO_2 + NO_3$ and particulate organic nitrogen (PON). Figure 3-10 presents NH_4 data available for the four chosen locations. The Boston Harbor entrance station shows a continuous reduction in NH_4 levels, associated with algal uptake, between October 1989 and July 1990. Ammonium concentrations decrease between 0.08 to 0.16 mg N/L to minimum concentrations of approximately 0.015 mg N/L. Concentrations then increase in the early fall to their previous winter levels. The following April (1991), concentrations again begin to decrease as a consequence of algal uptake. It is interesting to note the considerable
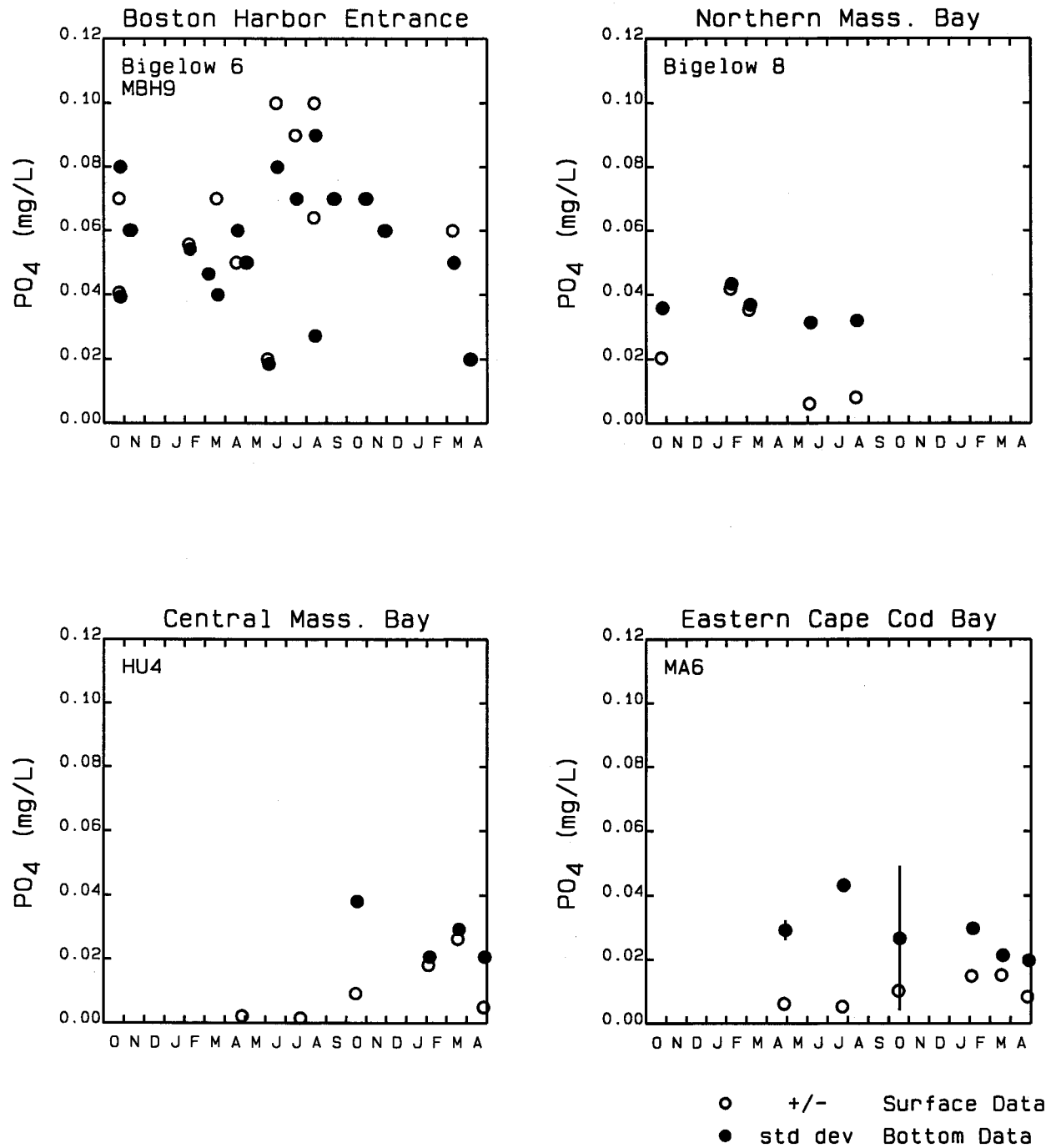
FIGURE 3-9. OBSERVED 1989 THROUGH 1991 PO_4 DATA FOR SELECTED STATIONS
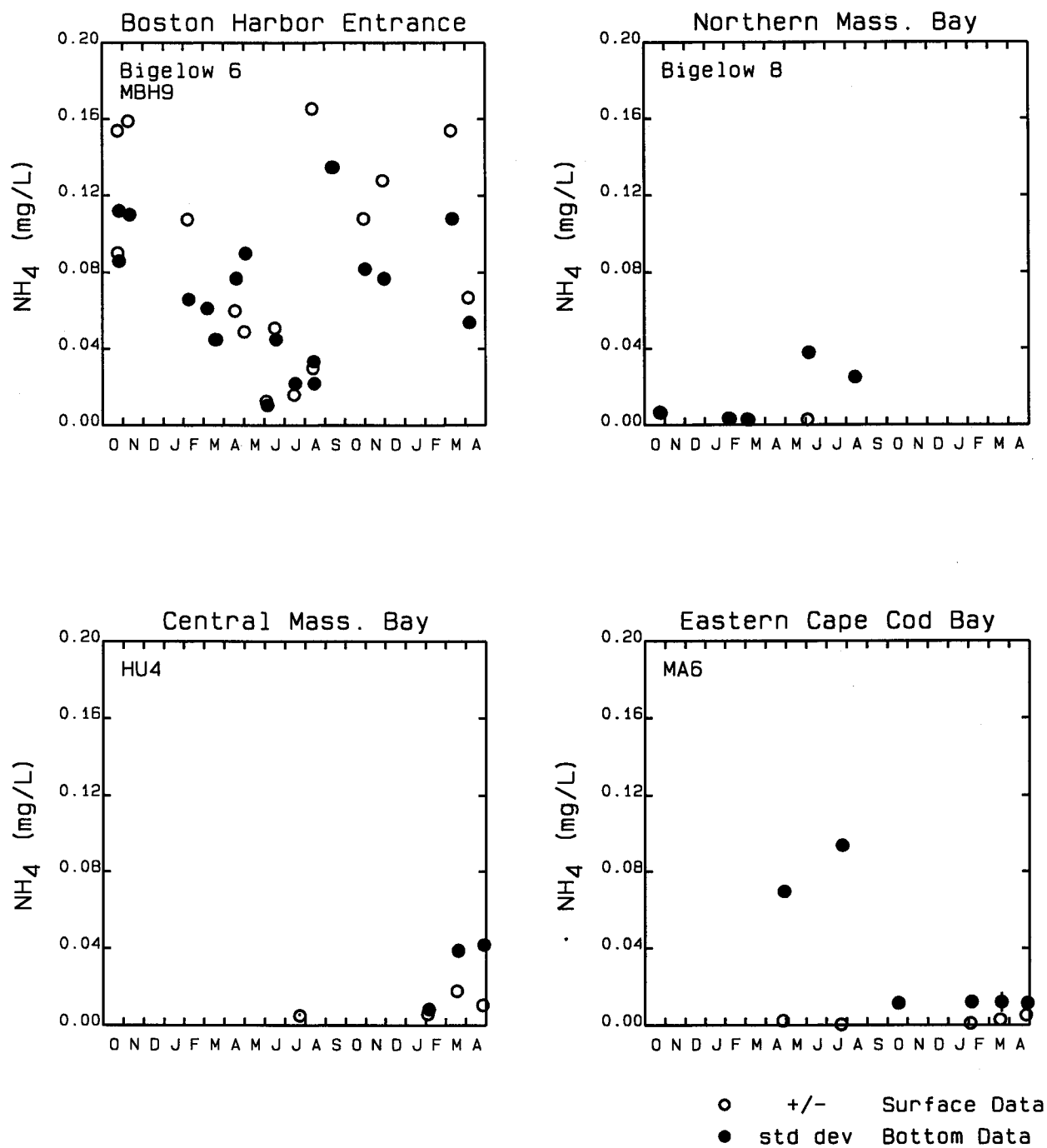
FIGURE 3-10. OBSERVED 1989 THROUGH 1991 NH$_4$ DATA FOR SELECTED
STATIONS

variation in observed concentrations for this station. This may be due to the point of the tidal cycle when the measurements were made. If sampling was performed on an ebb tide NH_4 concentrations would be typical of Boston Harbor and high; if sampled on flood tide concentrations would be more typical of Massachusetts Bay and therefore lower in value.

Data for the remaining stations are somewhat sparse. The available data suggest that surface concentrations remain low for most of the year from near zero during the summer to 0.02 mg N/L. Bottom water concentrations are also lower at these stations than those found near the Boston Harbor entrance at corresponding times of year. Bottom water NH_4 concentrations tend to be higher when the water column is most stratified during the spring and summer.

$NO_2 + NO_3$ concentrations also have a strong seasonal cycle as shown in Figure 3-11. The available data show increasing $NO_2 + NO_3$ concentrations between October 1989 and February 1990. There is then a rapid decrease in surface $NO_2 + NO_3$ concentrations from approximately 0.18 mg N/L to below 0.01 mg N/L by July at the Boston Harbor entrance and to near zero in June and August at the surface in northern Massachusetts Bay. These changes are due to algal uptake. Similar decreases in $NO_2 + NO_3$ are observed in the spring of 1991 at both the central Massachusetts Bay and eastern Cape Cod locations. During the fall, an increase in $NO_2 + NO_3$ levels can be observed for the Boston Harbor entrance and eastern Cape Cod Bay stations, as primary productivity decreases and there is less uptake by phytoplankton.

The seasonal trends observed in NH_4 and $NO_2 + NO_3$ concentrations can be explained by considering the cycle of algal productivity. During the winter when water temperatures are cold and solar radiation is at a minimum, algal productivity is low. As water temperatures and solar radiation increase so does algal productivity and nutrient uptake. Since NH_4 and $NO_2 + NO_3$ are used by photoplankton for growth, NH_4 and $NO_2 + NO_3$ concentrations tend to be inversely correlated to algal productivity, i.e. they are high during periods of low productivity (late fall/early winter); during periods of high
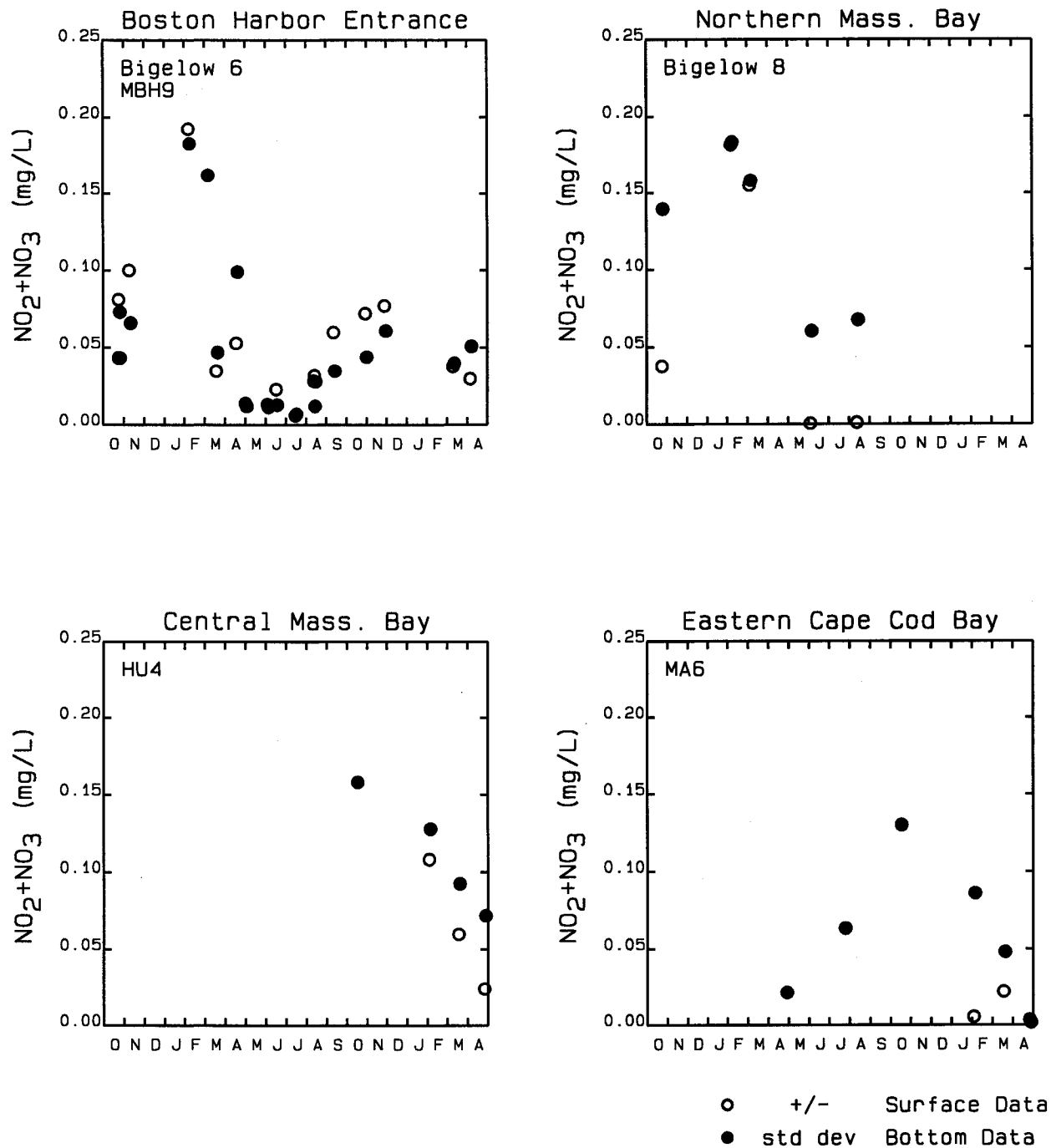
FIGURE 3-11. OBSERVED 1989 THROUGH 1991 NO$_2$+NO$_3$ DATA FOR SELECTED
STATIONS

productivity (late winter, spring and summer) surface concentrations of both NH_4 and $NO_2 + NO_3$ are low.

Figure 3-12 displays PON data for the Boston Harbor entrance and northern Massachusetts Bay location. These data show an inverse cycle to NH_4 and $NO_2 + NO_3$ concentrations. Concentrations of PON are near zero in February when conditions are less favorable to phytoplankton growth. However, during the spring, as the algal population blooms, NH_4 and $NO_2 + NO_3$ are converted to algal biomass and hence PON increases.

3.2.2.6   Silica

Dissolved silica measurements were available at all four locations as shown on Figure 3-13. Dissolved silica is an important nutrient required by diatomaceous phytoplankton. Dissolved silica follows a similar pattern to the other nutrients as dictated by the phytoplankton growth cycle. Higher dissolved silica concentrations are found in the winter while lower concentrations are found in the spring and summer. As the water column becomes stratified, silica rich bottom waters become trapped beneath the pycnocline and surface water concentrations are depleted.

3.2.2.7   Dissolved Oxygen

The dissolved oxygen (DO) of a water body is one of the more important water quality parameters. Since DO is necessary to maintain aquatic life, it reflects the general health level of a water body and indicates the ability of an aquatic ecosystem to support a balanced habitat. When periods of hypoxia occur, the ability of fish and other aquatic life to reproduce may be impaired. Under extreme hypoxia or anoxia, large mortalities of fish may occur.

Figure 3-14 presents temporal profiles of DO at four locations in the study area. Dissolved oxygen concentrations in the water column behave in a seasonal fashion, due to changes in DO saturation as well as due to biological and chemical reactions. As the
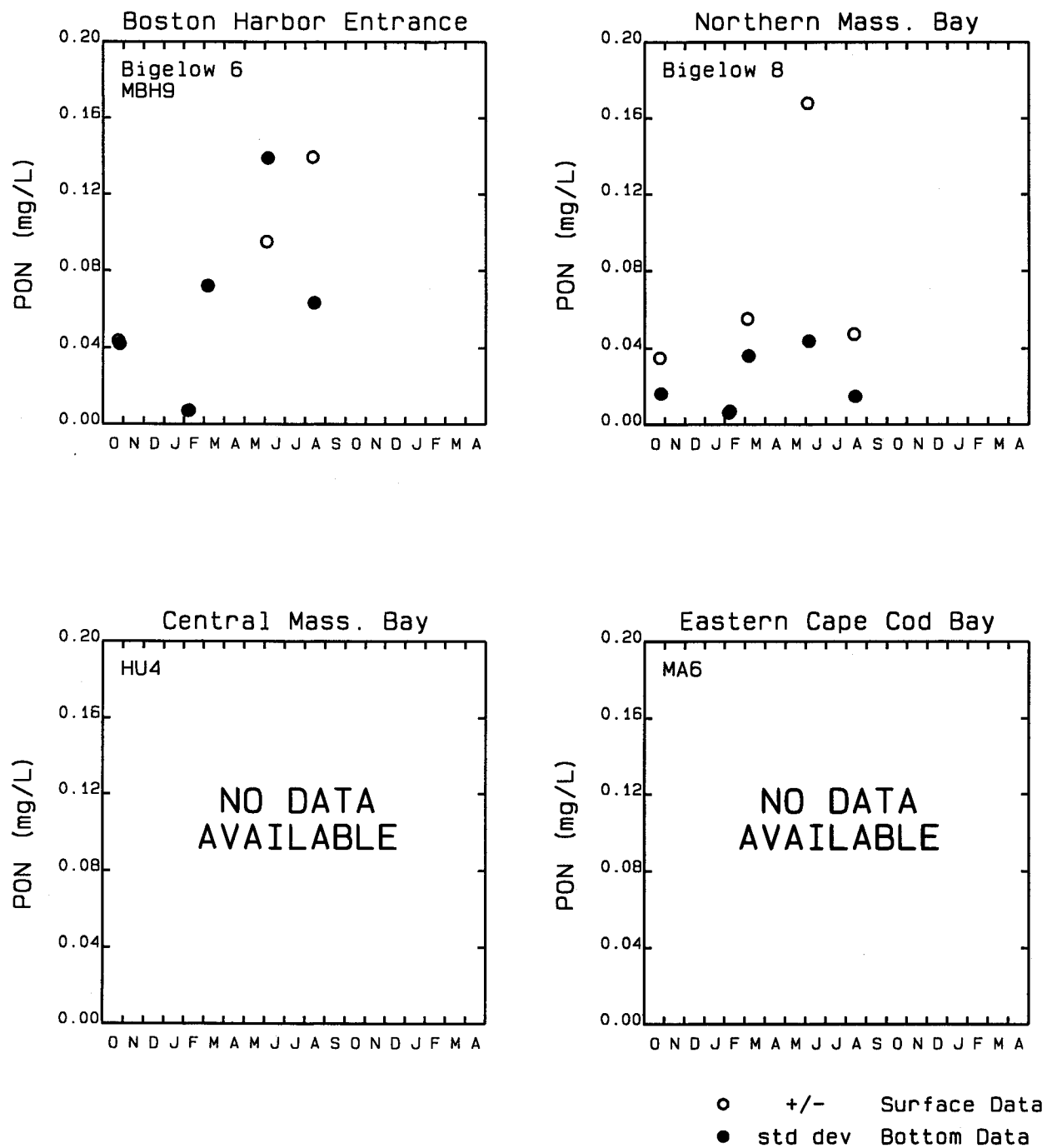
FIGURE 3-12. OBSERVED 1989 THROUGH 1991 PON DATA FOR SELECTED STATIONS
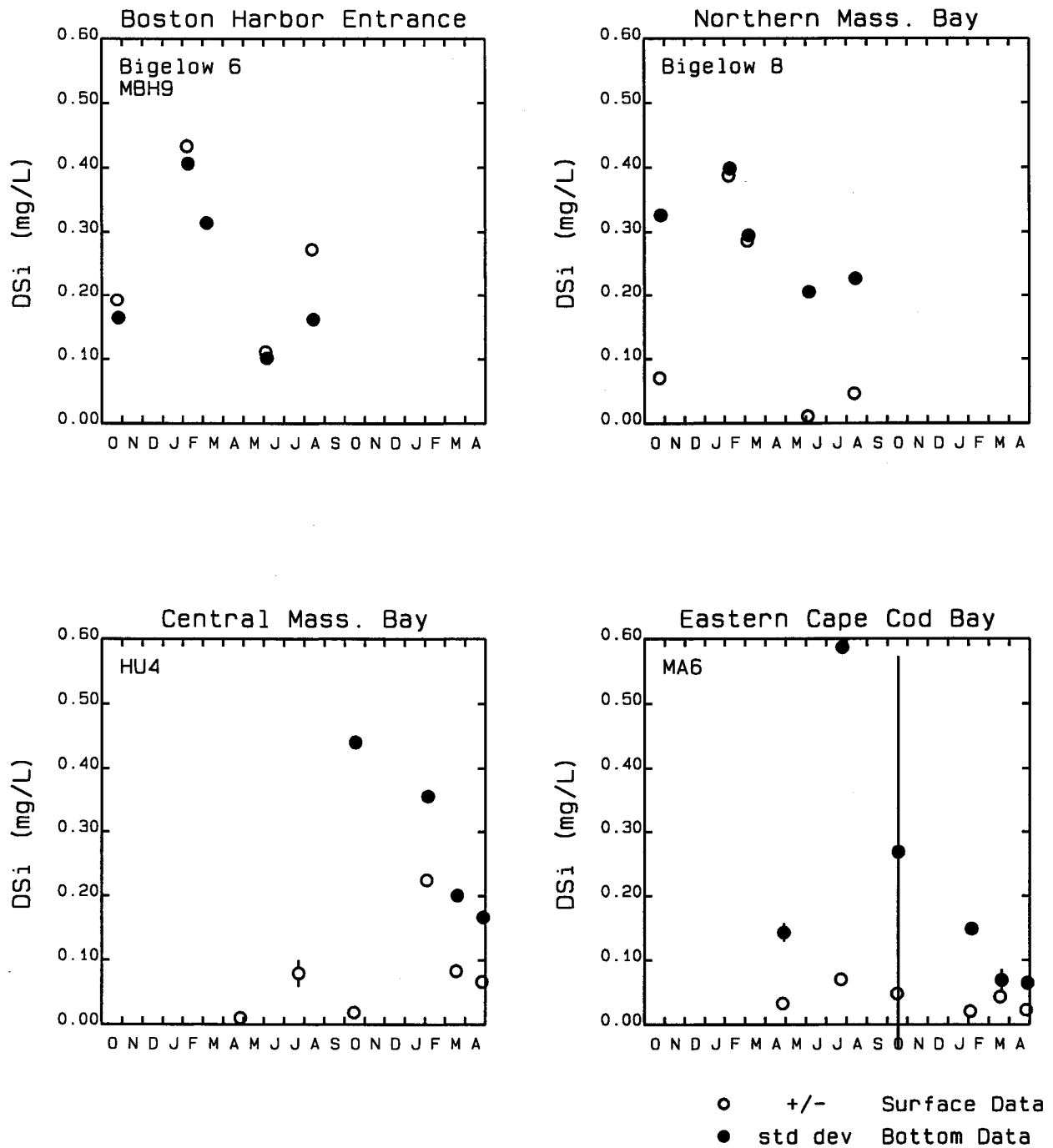
FIGURE 3-13. OBSERVED 1989 THROUGH 1991 DSi DATA FOR SELECTED
STATIONS
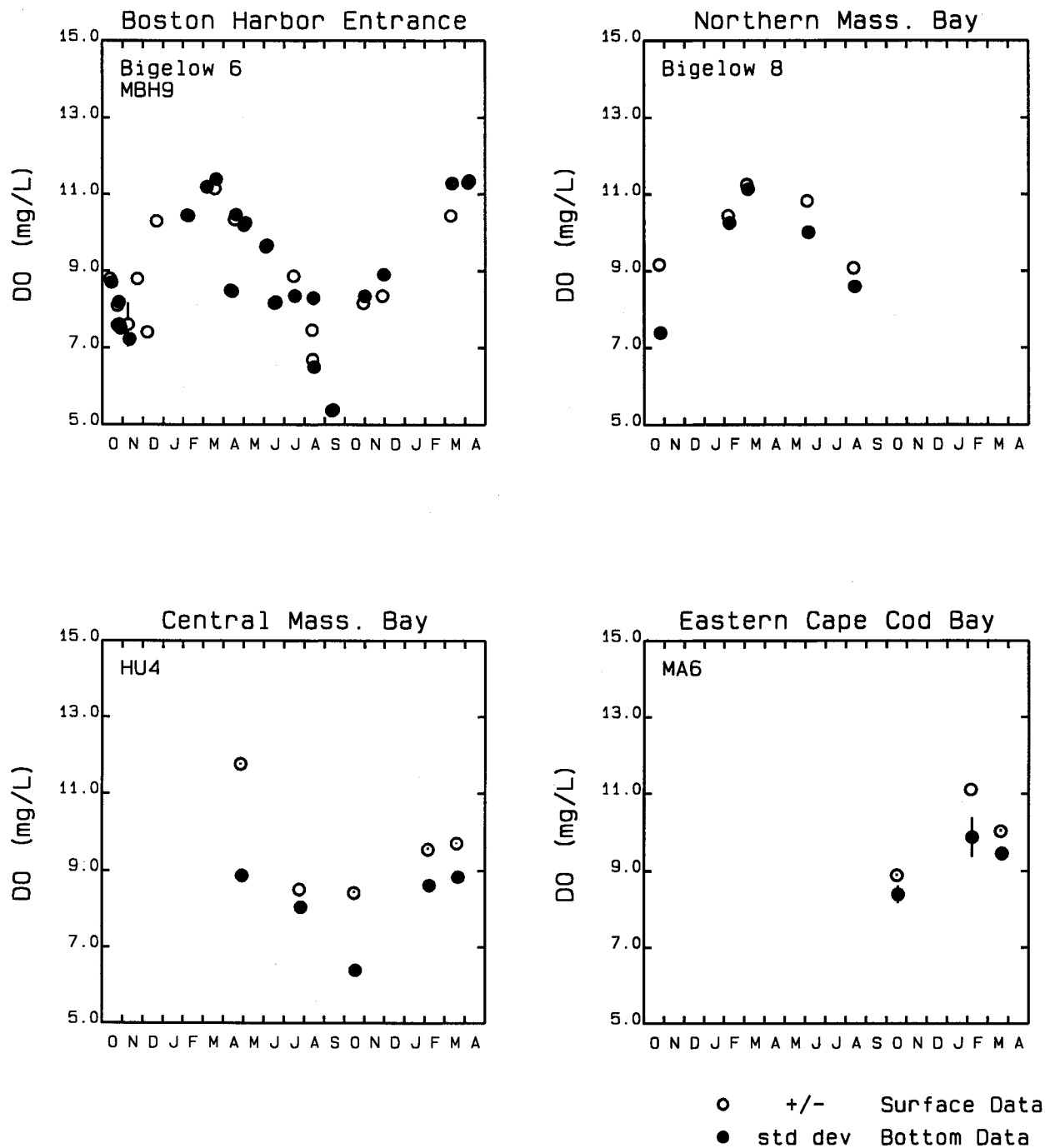
FIGURE 3-14. OBSERVED 1989 THROUGH 1991 DO DATA FOR SELECTED
STATIONS

water temperature decreases, the saturation concentration of dissolved oxygen within the water column increases. The opposite is true for increasing temperature; i.e., DO saturation decreases. In addition, as water temperatures increase, biological activity (i.e., phytoplankton photosynthesis and respiration and biological oxidation of organic carbon) increases. These coinciding factors act to produce the annual cycle of DO observed. The highest DO concentrations are observed in March, near 12 mg O_2/L, when the water column temperature is still low and when phytoplankton have begun to increase their photosynthetic production. As water temperatures increase, DO concentrations decrease, in part due to decreasing DO saturation and degassing to the atmosphere. The decrease is even greater in the bottom waters due to increased biological oxidation of organic carbon and detrital algal biomass. A minimum DO concentration of approximately 5 mg O_2/L is observed in Boston Harbor in September; a minimum of about 6 mg O_2/L is observed in October in central Massachusetts Bay. It should be noted that for some locations in Boston Harbor lower concentrations have been observed. There is considerable variation in the observed DO for the Boston Harbor entrance station. Some of this variation may be due to the point within the tidal cycle at which the data were taken.

An area of concern for possible low concentrations of DO is Stellwagen Basin. During periods of strong stratification and weak horizontal mixing, there is little exchange between the bottom waters of the Basin and the surrounding bottom waters located in the shallower waters of Stellwagen Bank, eastern Massachusetts Bay and northeastern Cape Cod Bay. It is possible that low oxygen levels could result from the settling and oxidation of particulate organic matter generated in the surface waters of the Basin. Figure 3-15 presents DO data for four locations within the Stellwagen Basin. As can be seen these stations do not violate the Massachusetts state standard of 6.0 mg O_2/L at any time during the period of October 1989 through April 1991.
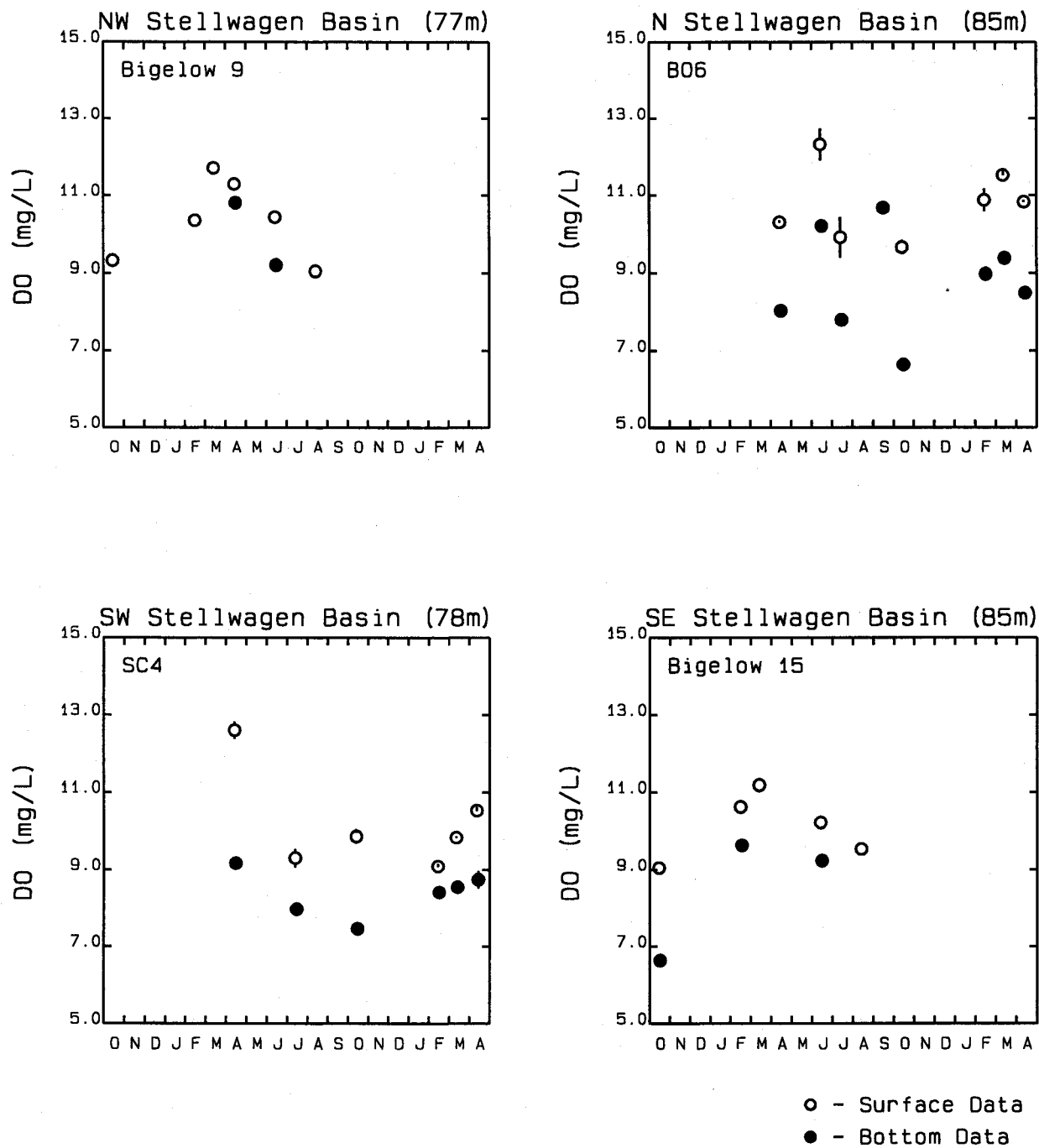
FIGURE 3-15. OBSERVED 1989 THROUGH 1991 DO DATA FOR STELLWAGEN BASIN

planned outfall. These data (Kelly et al., 1993; Kelly and Turner, 1995) afforded the opportunity to calibrate the model against an additional data set. The 1992 monitoring program included 46 stations: 21 nearfield, i.e., in the vicinity of the planned outfall, and 25 farfield. Routine monitoring included measurements of temperature, salinity, dissolved oxygen, fluorescence, dissolved nutrients and light attenuation. Data on biology and primary productivity including chlorophyll-a and particulate nutrients were collected at 10 stations. During the course of the year, from February through December, 15 nearfield surveys were conducted, which measured only hydrography/nutrient data. An additional 6 surveys were conducted, which measured biology/productivity data at 9 nearfield/farfield stations and hydrography/nutrient data at the remaining 21 farfield stations. Figure 3-16 displays the location of the sampling stations. Station names that begin with N are nearfield. Station names that begin with F are farfield. Stations names that end with P are biology/productivity stations.

Routine hydrography/nutrient surveys included measurements of salinity, temperature and dissolved oxygen (CTD casts), dissolved inorganic nutrients (NO_2, NO_3, NH_4, PO_4 and DSi), chlorophyll fluorescence, optical beam transmittance, in situ and surface irradiance. Sampling at biology/productivity stations was more comprehensive. Sampling at these stations included: the same suite of measurements as the hydrography and nutrient surveys; chlorophyll-a and phaeopigments in extracts of filtered water; measurements of total suspended solids (TSS) and DO in discrete water samples; and measurements of organic nutrients including POC, PON, dissolved organic carbon (DOC), dissolved organic nitrogen (DON) and dissolved organic phosphorus (DOP). Phytoplankton and zooplankton species were also identified and enumerated and rates of water-column respiration and production versus irradiance were determined. Sampling at non-biology/productivity farfield stations included measurements of dissolved organic nutrients, chlorophyll-a and phaeopigments in extracts of filtered water for calibrating the fluorometer, oxygen samples for titration and calibrating the DO probe and phytoplankton samples for archival purposes. The nearfield surveys also included high resolution "tow-yo" profiling to sample various physical parameters and phytoplankton fluorescence.
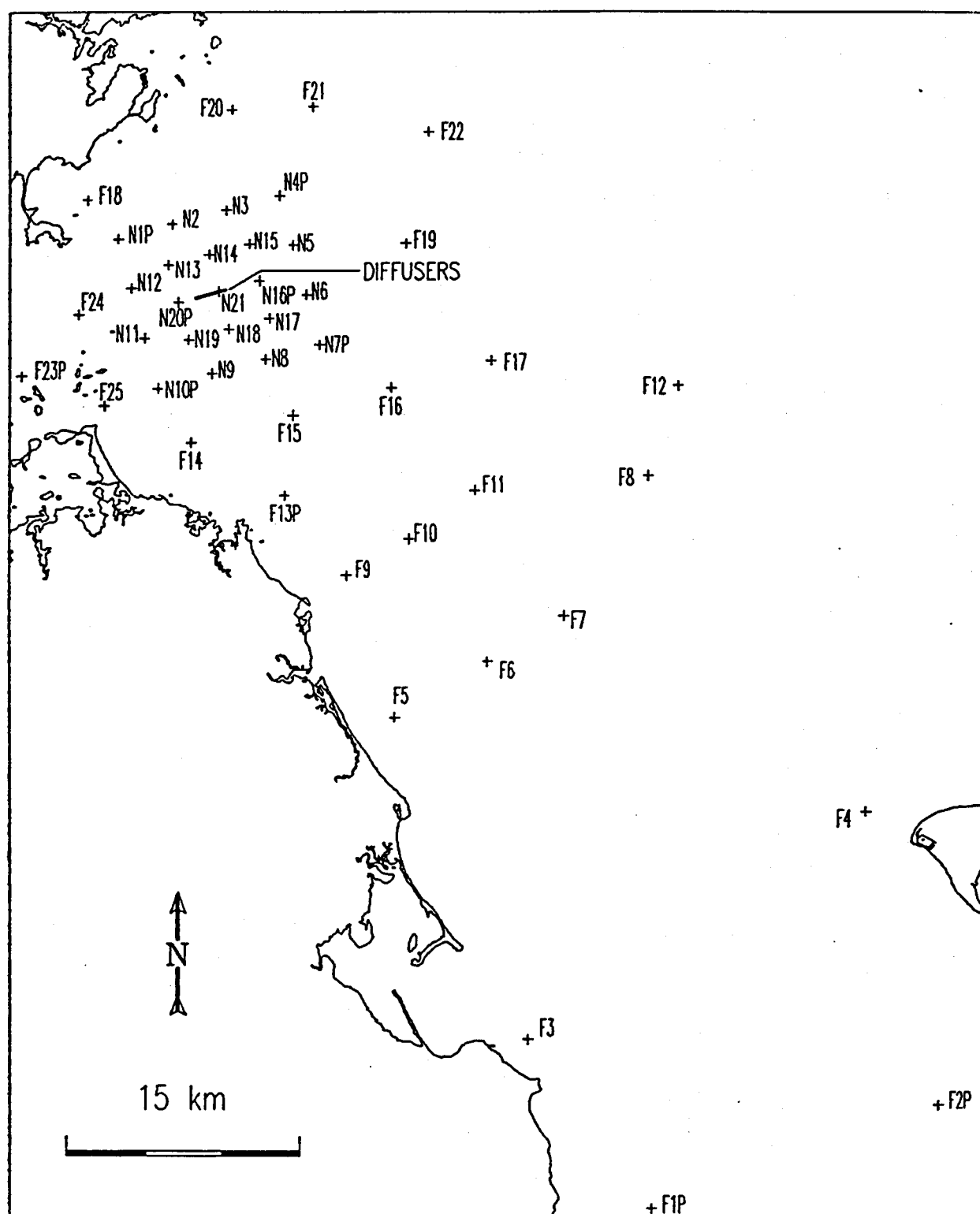
FIGURE 3-16. BATTELLE OCEAN SCIENCES 1992 OUTFALL MONITORING PROGRAM
SAMPLING STATIONS

Six stations were chosen to illustrate typical data for 1992. These stations were chosen to cover the spatial extent of the Bays and for the quantity of data collected. Station F23P is located near the entrance to Boston Harbor. Stations N10P, N04P, N06, and N07P reflect conditions in the nearfield area. Station F13P is located in shallow waters near Scituate. Station F08 in the center of the Massachusetts Bay/Cape Cod system and station F01P is located in southwest Cape Cod Bay. As this project progressed, additional data from the monitoring program became available. Although data from the 1993 surveys were not used for model calibration, they are presented here in comparison to the 1992 data in order to characterize the year to year natural variability of the Massachusetts Bays system. In the figures to follow, open symbols represent surface (roughly the upper 10 percent of the station depth) and approximate mid-depth (12.5 to 17.5m) data, while filled symbols are used for bottom data (roughly the lower 10 percent of the water column depth). Circles represent 1992 data and triangles are used for 1993 data. It was not possible to include comparisons to 1990 data due to the differences in sampling locations.

3.3.1 Physical Water Quality Parameters

3.3.1.1   Temperature

The 1992 and 1993 data sets show similar patterns in the annual cycle of temperature as shown in Figure 3-17. For the Bay stations, the seasonal cycle of stratified and unstratified waters is much more evident than for the Boston Harbor stations. November through April is a period during which the water column is well mixed. Beginning in the spring, as the air temperature and solar radiation increase, water temperatures increase, with the surface warming more quickly than the bottom. Deeper waters in central Massachusetts Bay take longer to warm than shallower bottom waters in Cape Cod and Massachusetts Bay. With the onset of colder weather in the fall, surface water temperature drops. Fall overturn occurs between late October and early November in both 1992 and 1993.

FIGURE 3-17. OBSERVED 1992 AND 1993 TEMPERATURE DATA FOR SELECTED STATIONS
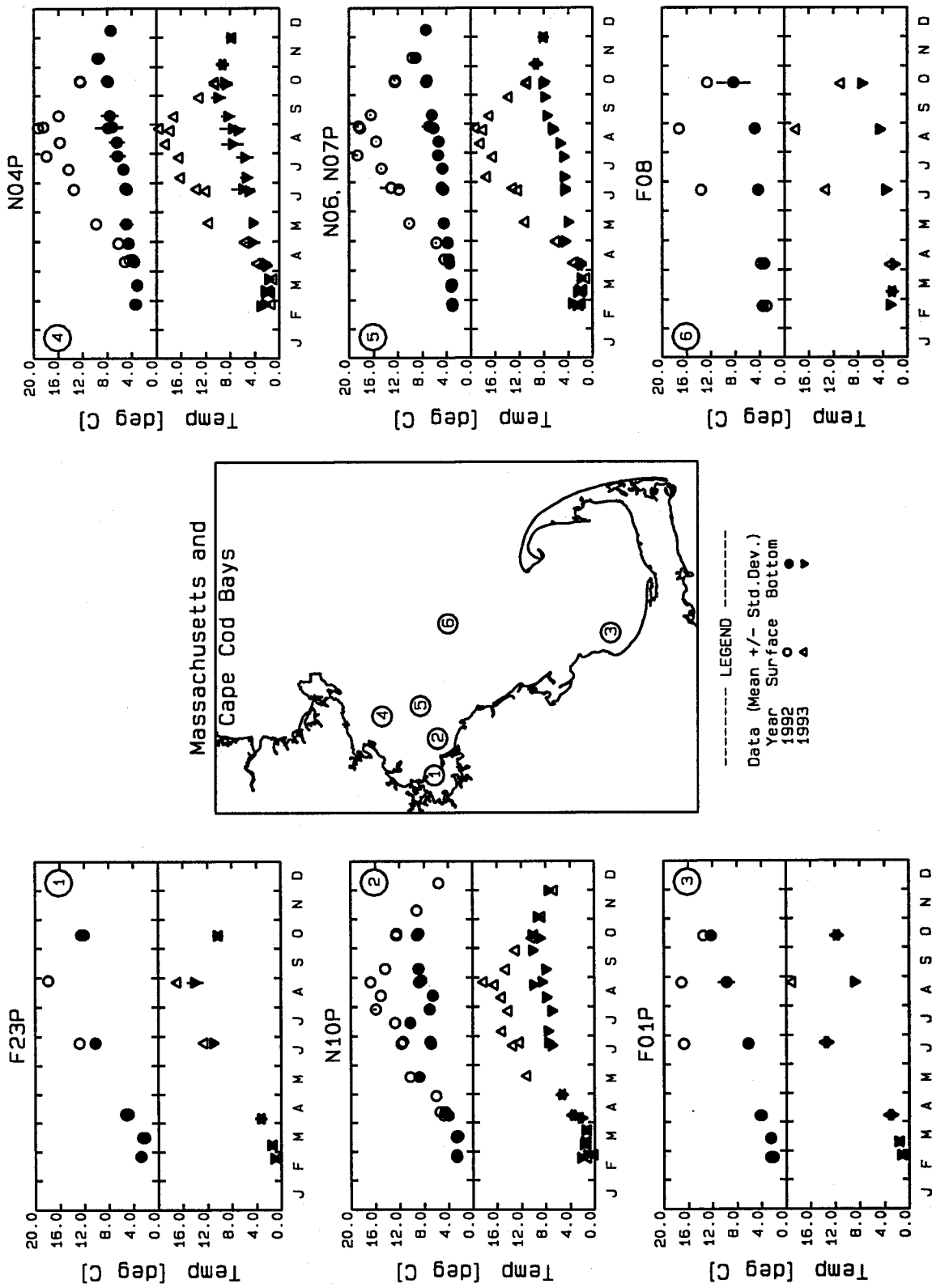
As was observed in the 1990 data set, the 1992 and 1993 temperature data indicate that the Boston Harbor entrance (F23P) is well mixed due to its relatively shallow depth and high tidal velocities. The temperature differences between surface and bottom generally do not exceed 3°C. Temperature stratification is very pronounced at the mid-Massachusetts Bay segment (N06, N07P). Temperature gradients between surface and bottom waters are on the order to 8 to 12°C during June, July and August. Temperature data for 1992 and 1993 are very similar, although some differences can be observed in the winter, with 1993 being 1 or 2°C colder. The 1990 and 1992 temperature data also show similar patterns as can be seen by comparing Figures 3-5 and 3-17. It is also worth noting that the 1992 and 1993 data sets have better temporal coverage than does the 1990 data set.

Figures 3-18 and 3-19 present seasonal and annual probability plots of surface and bottom water temperatures, respectively, for the nearfield and farfield stations. The surface data were taken from the top ten percent of the station depth while the bottom data were taken from the bottom ten percent of the water column. These figures indicate that the winter (i.e. the months of February and March, since no surveys were conducted in the month of January) water temperatures were approximately 1.5°C colder in 1993 relative to 1992. The spring (April, May, and June) surface water temperature distributions are approximately the same in both years, while the nearfield bottom waters appear to have warmed slightly faster in 1993 versus 1992. The nearfield summer (July, August, and September) surface waters appeared to be quite similar for both years with median temperatures of about 17°C and maximum temperatures of approximately 20°C. The data also indicate that the bottom water temperatures were lower in 1992 versus 1993 with 1992 having median summer temperatures of approximately 7°C versus 11°C in 1993. The fall (October, November, and December) surface temperatures were approximately 2°C warmer in 1992 relative to 1993, while bottom water temperatures were about 1°C warmer in 1992. On an annual basis the surface water temperatures are quite similar except for the lower temperature, which represent winter observations. There is more of a contrast between the two years in the bottom waters, with 1993 having both lower temperature (winter values) and higher temperature (representing summer values).
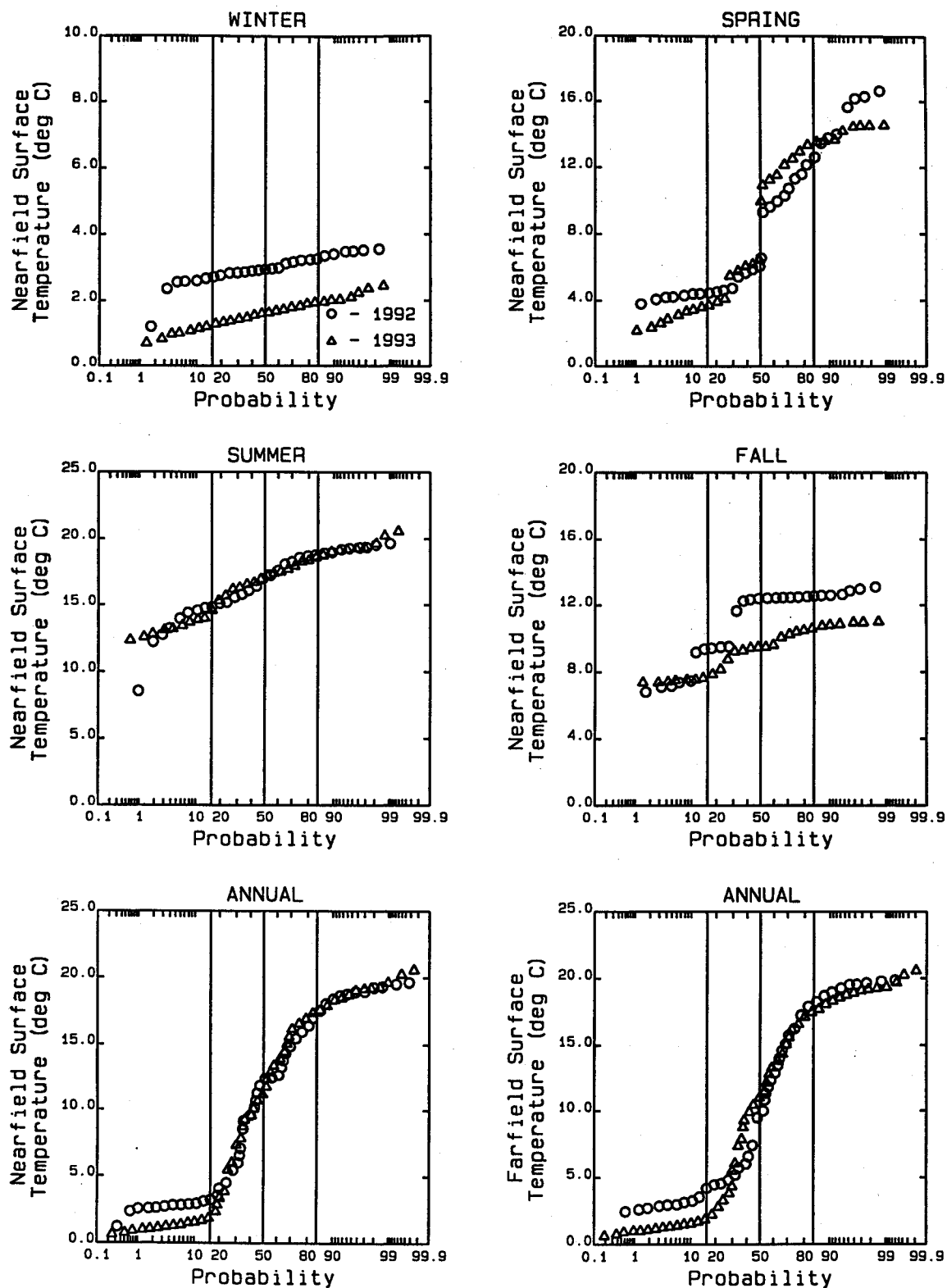
FIGURE 3-18. SEASONAL AND ANNUAL PROBABILITY DISTRIBUTIONS FOR 1992 AND 1993 TEMPERATURE DATA AT NEARFIELD AND FARFIELD STATIONS
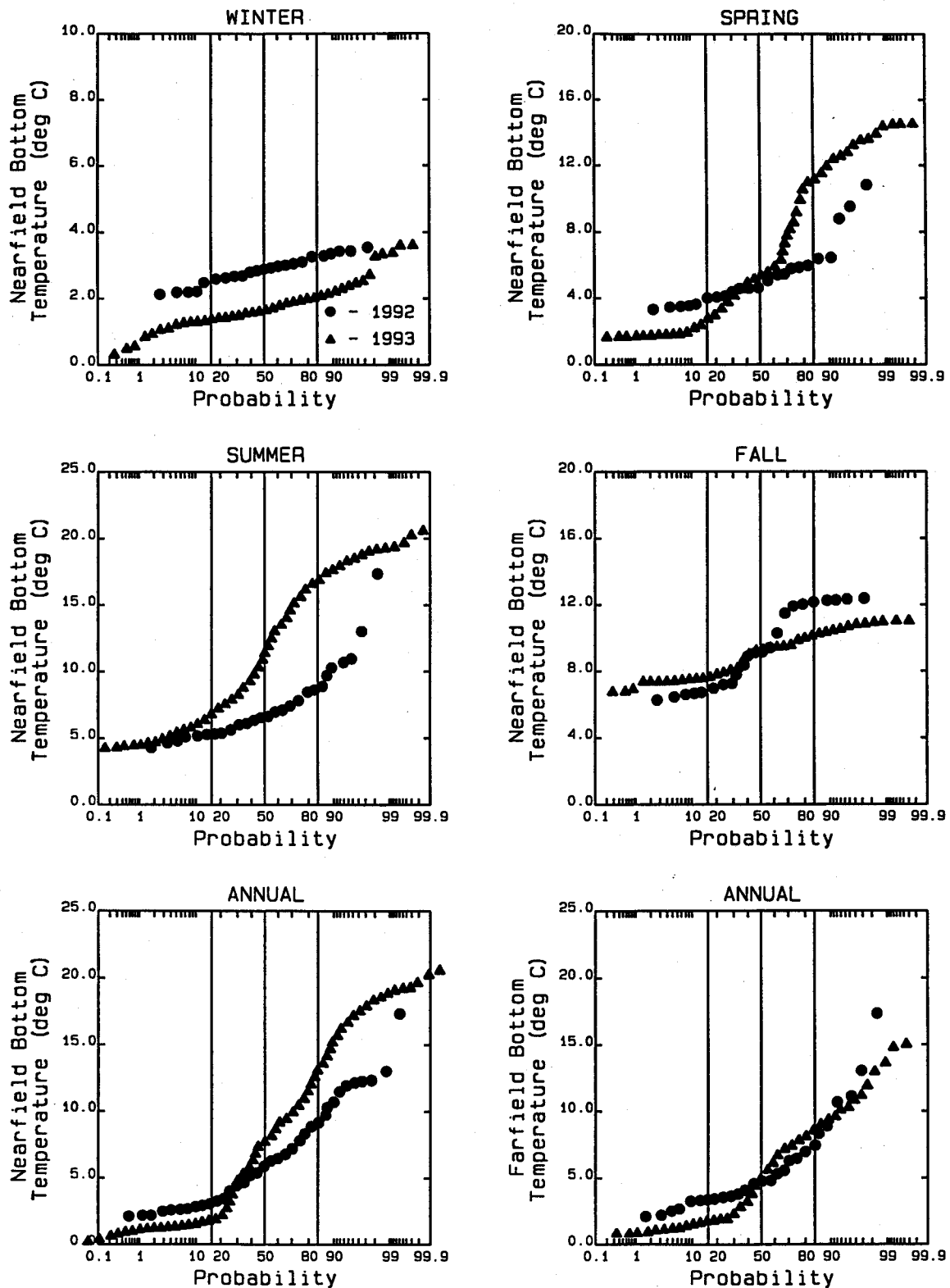
FIGURE 3-19. SEASONAL AND ANNUAL PROBABILITY DISTRIBUTIONS FOR 1992 AND 1993 BOTTOM TEMPERATURE DATA AT NEARFIELD AND FARFIELD STATIONS

The farfield temperature data are quite similar between the two years, although 1993 had slightly lower wintertime temperatures.

3.3.1.2   Salinity

Salinity data for 1992 and 1993 are presented in Figure 3-20. The seasonal cycle of salinity stratification is weaker than that observed in the temperature data. Maximum surface to bottom differences in salinity are on the order of 0.5 ppt during the summer months versus about 10°C for temperature. The relatively small differences in salinity stratification are in part due to the limited freshwater inputs into the Bays. Salinities are highest at the beginning of the year and decrease in the spring and summer in response to the spring freshet. In the fall, the salinities increase towards levels observed at the beginning of the year. Again, the two years show similar patterns, except that the 1993 spring freshet appeared to occur earlier in the year (April versus May) and appeared to be larger in magnitude.

Figures 3-21 and 3-22 present seasonal and annual probability plots of surface and bottom water salinities, respectively, for the nearfield and farfield stations. These figures show that the winter (February/March) salinities were approximately the same in both years. As was noted in the temporal plots the magnitude of the spring freshet appears to have been stronger in 1993 than in 1992, as is evidenced by the 0.5 to 1 ppt difference in spring (April, May, and June) surface salinities between the two years. The summers (July, August, and September) and falls (October, November, and December) are quite similar in terms of surface and bottom salinity, although there appears to be some residual effects of the 1993 spring freshet in the summer bottom waters. On an annual basis the salinities are quite similar in both the nearfield and farfield data in both years. The only difference appears to be related to the magnitude of the 1993 spring freshet which yielded slightly fresher waters in the spring of 1993.
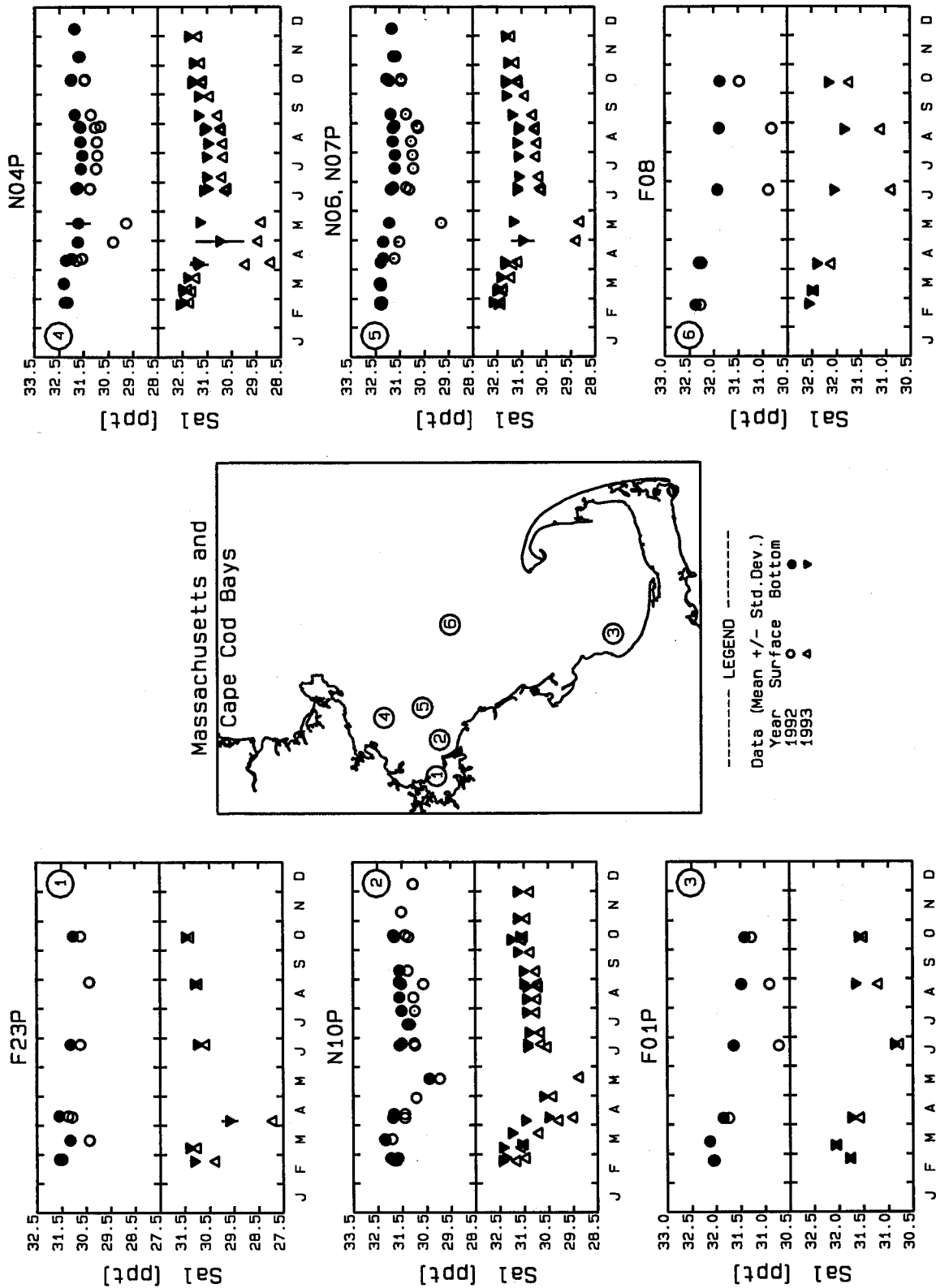
FIGURE 3-20. OBSERVED 1992 AND 1993 SALINITY DATA FOR SELECTED STATIONS
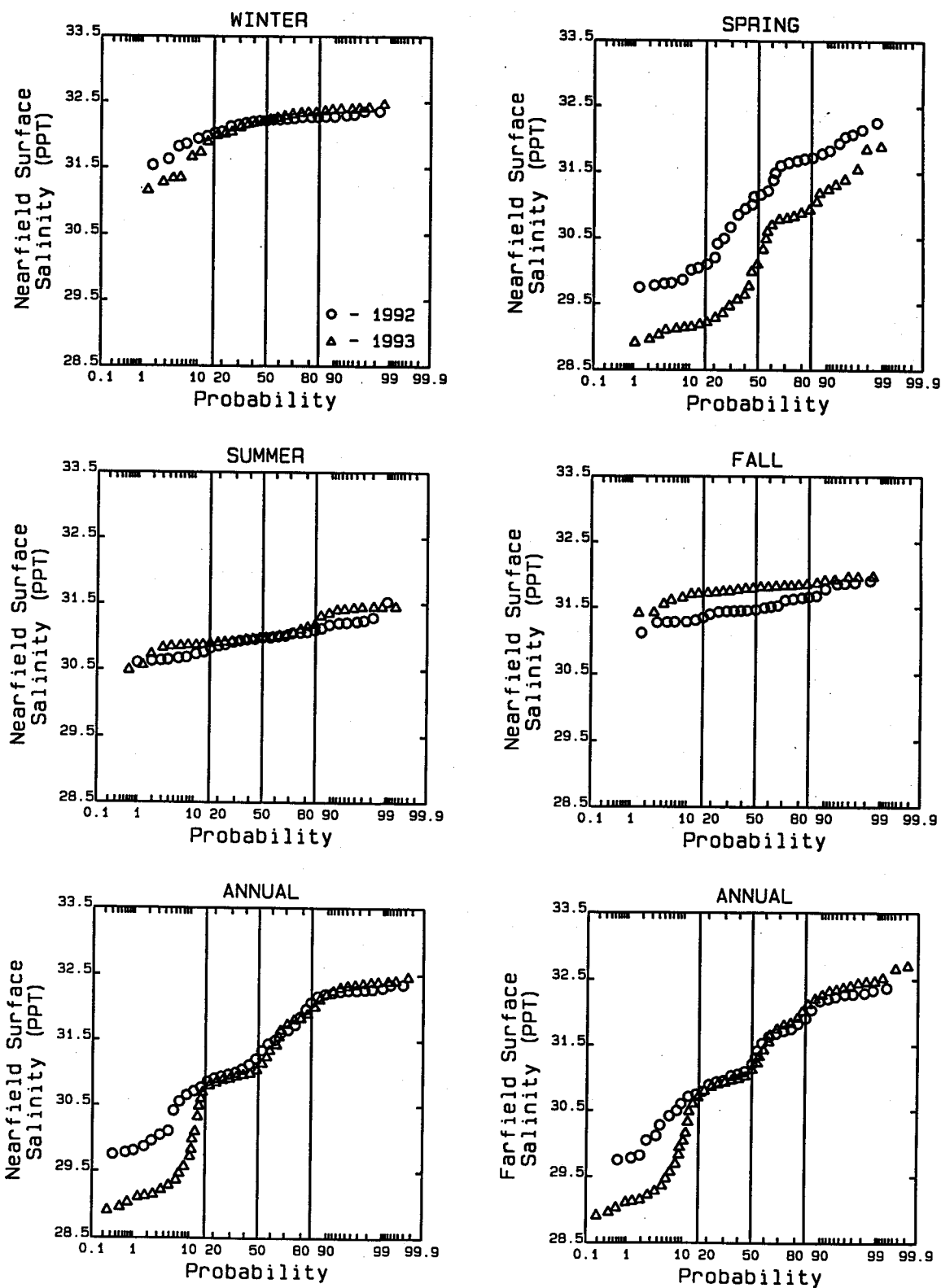
FIGURE 3-21. SEASONAL AND ANNUAL PROBABILITY DISTRIBUTIONS FOR 1992 AND 1993 SURFACE SALINITY DATA AT NEARFIELD AND FARFIELD STATIONS
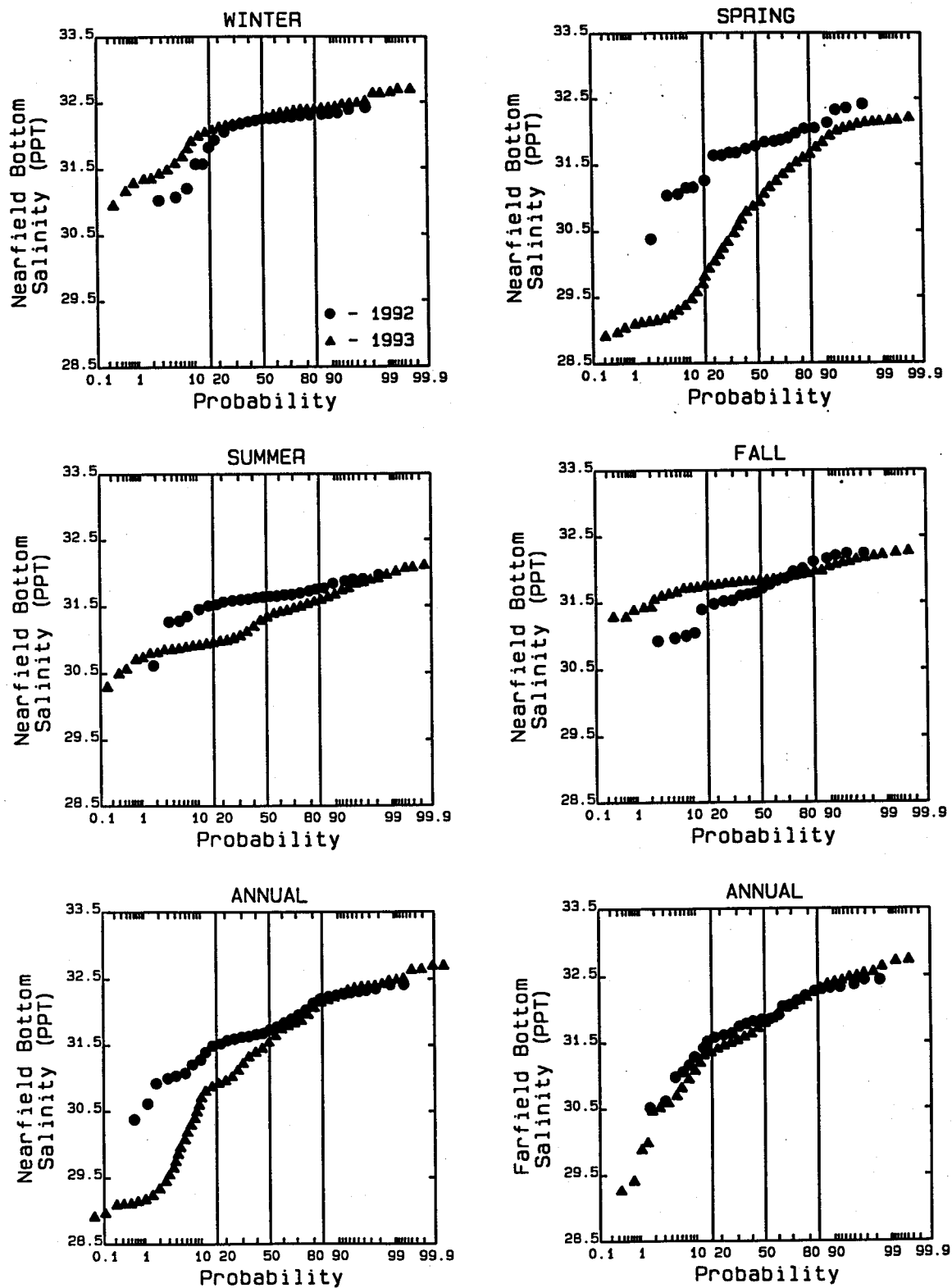
FIGURE 3-22. SEASONAL AND ANNUAL PROBABILITY DISTRIBUTIONS FOR 1992 AND 1993 BOTTOM SALINITY DATA AT NEARFIELD AND FARFIELD STATIONS

3.3.1.3   Extinction Coefficient

Figure 3-23 displays estimates of the vertical light attenuation or extinction coefficients. These values were determined using estimates of the 1 percent surface light level depth and k_e = 4.6/H, where H is the depth of the 1 percent light level. These are the raw in-situ values uncorrected for phytoplankton effects. The k_e observed at station F23P is higher than the rest of the study area indicating that light does not penetrate as deeply into the water column at this location due to algal and inorganic solids effects. Station N10P, which is in the immediate vicinity of the Boston Harbor plume, also has slightly higher, 0.3 to 0.4 m^{-1}, k_e values as compared to the other stations. At station F01P the effect of the late winter/early spring algal bloom can be seen in February and March, when extinction coefficients are between 0.4 and 0.6 m^{-1} versus 0.2 to 0.3 m^{-1} for the rest of the year. In areas of lower algal productivity and away from the effects of coastal runoff, i.e., stations N04P, NO6, NO7P and F08, the extinction coefficients are observed to be lower, about 0.15 to 0.3 m^{-1}.

3.3.2 Chemical and Biological Water Quality Parameters

3.3.2.1   Chlorophyll

Figure 3-24 presents time series plots of surface chlorophyll for 1992 and 1993 at selected locations in the study area. The 1992 data set shows elevated chlorophyll levels, 6 to 9 μg/L, occurring in late February at stations N04P and F01P.   Chlorophyll concentrations then decrease rapidly through April and remain at low levels less than 1 μg/L through the summer, before a moderate increase is observed in October. In 1992 station F23P chlorophyll concentrations increase during the spring, reaching approximately 5 μg/L during the summer months before declining in the fall. Phytoplankton populations in this area are closer to the major sources of nitrogen, phosphorus and silica and as will be shown subsequently do not appear to be nutrient limited. Station N10P has low concentrations of chlorophyll in the late winter/spring before increasing to concentrations of 4 to 7 μg/L in the summer. The other nearfield stations show low concentrations of chlorophyll-a throughout most of the year, save for a moderate bloom in October. The
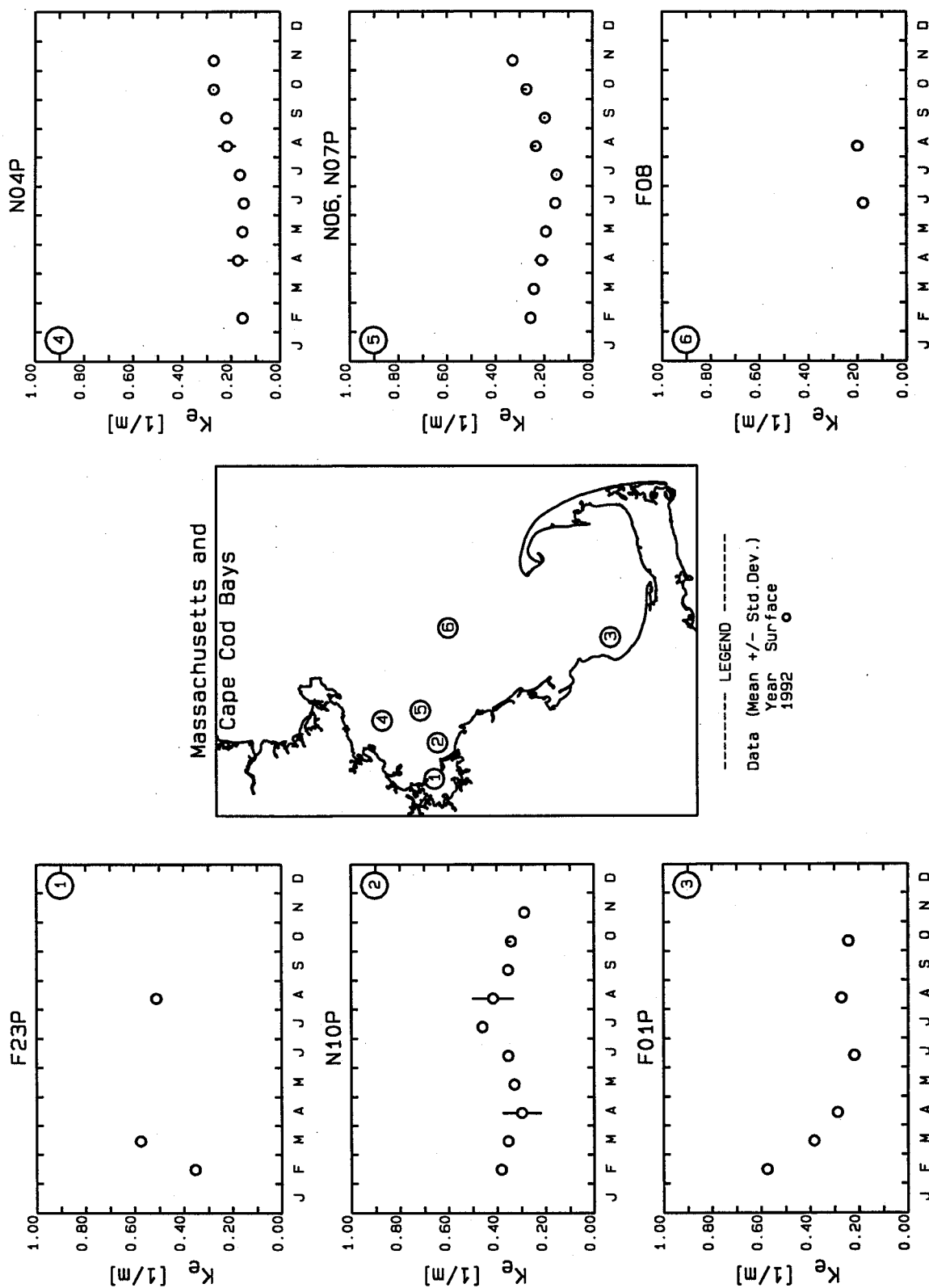
FIGURE 3-23. ESTIMATED 1992 LIGHT EXTINCTION COEFFICIENTS FROM ONE PERCENT LIGHT LEVEL DEPTH FOR SELECTED STATIONS
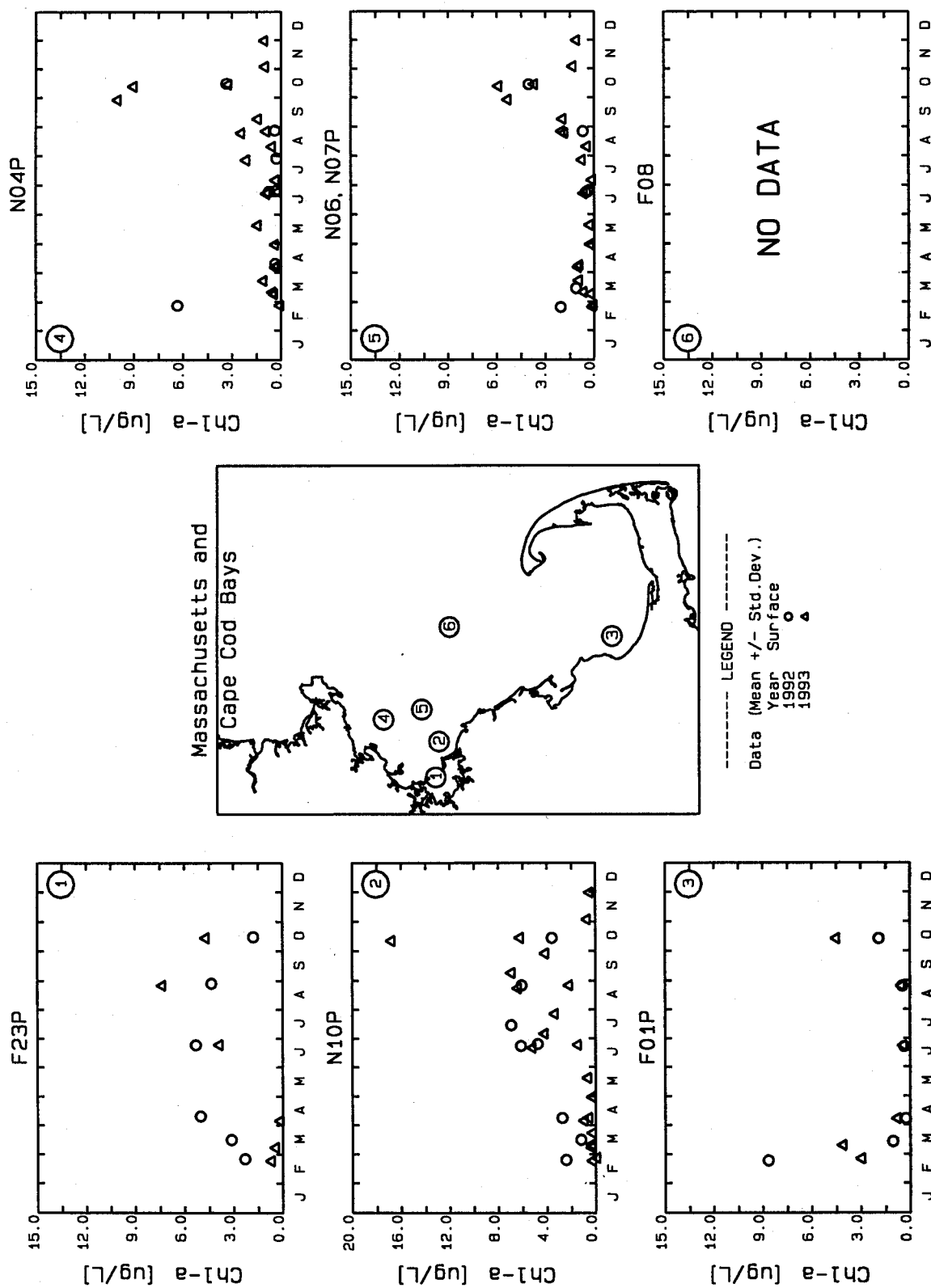
FIGURE 3-24. OBSERVED 1992 AND 1993 SURFACE CHLOROPHYLL DATA FOR SELECTED STATIONS

pattern of chlorophyll concentrations differs in 1993. The spring bloom is much less evident, observed only at Station F01P; summer concentrations are about equal. However, in 1993 there is a larger fall bloom than was observed in 1992. The highest chlorophyll concentrations are observed at stations N10P and N04P with levels reaching 9 to 16 μg/L.

Figure 3-25 presents a series of seasonal and annual probability distributions of nearfield and farfield chlorophyll-a and fluorescence data. These figures show that for the winter period the maximum discrete chlorophyll-a and fluorescence values for 1992 and the maximum discrete chlorophyll-a data for 1993 were about the same, at approximately 3 to 7 μg/L. The majority of the 1992 chlorophyll-a and fluorescence data, however, were greater than the 1993 chlorophyll-a data, 1 to 3 μg/L for 1992 versus 0.5 to 1.5 μg/L for 1993. Chlorophyll distributions for spring and summer of both years appear to be similar. Maximum nearfield surface chlorophyll-a concentrations of approximately 6 μg/L are observed in the spring, while summer maxima are between 12 and 15 μg/L. Median fall concentrations are approximately the same for both years, about 3 μg/L. However, fall maxima in 1993 are near 20 μg/L versus 6 μg/L in 1992. On an annual basis the nearfield chlorophyll-a and fluorescence data are approximately the same for both years. The farfield median chlorophyll levels were slightly higher in 1992 versus 1993; maxima for both years were approximately the same, at about 10 μg/L.

Sporadic mid-depth chlorophyll blooms have been observed during the stratified spring/summer period. These blooms occur near the pycnocline where nutrients are available and light is not limiting. Figure 3-26 presents vertical profiles of chlorophyll-a fluorescence, and discrete chlorophyll data from 1992 for two nearfield stations and a farfield station in Cape Cod Bay for four months of the year. The chlorophyll fluorescence data representing an almost continuous vertical cast were calibrated for each survey by Battelle Ocean Sciences using discrete chlorophyll data (shown as open circles on the plots) and linear regression analysis. The February data show the water column to be well mixed with similar concentrations from the surface to the bottom. The highest chlorophyll concentrations are observed at stations N04P, off Marblehead, and F02P in eastern Cape
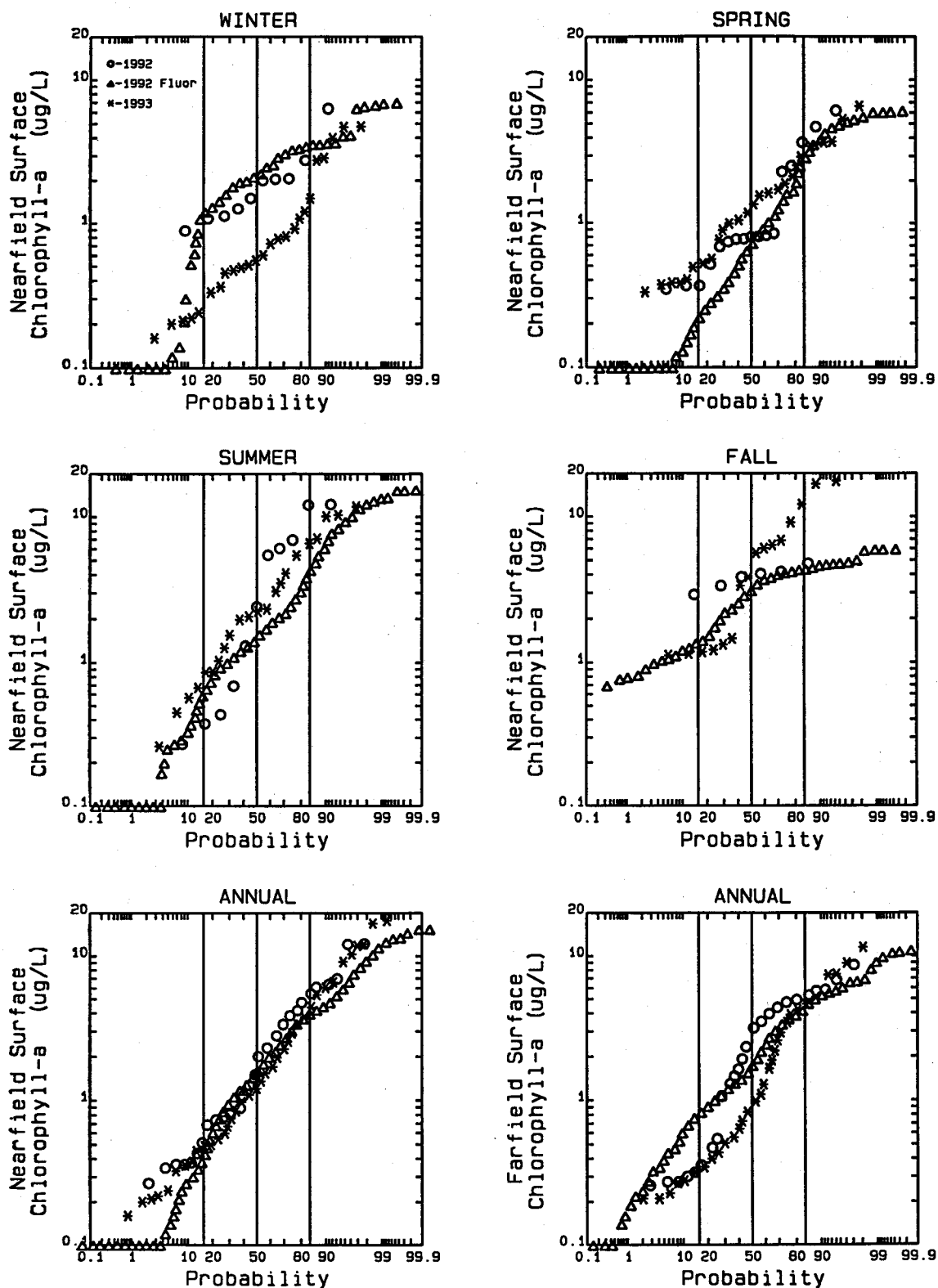
FIGURE 3-25. SEASONAL AND ANNUAL PROBABILITY DISTRIBUTIONS FOR 1992 AND 1993 SURFACE CHLOROPHYLL-A DATA AND 1992 SURFACE FLUORESCENCE DATA AT NEARFIELD AND FARFIELD STATIONS
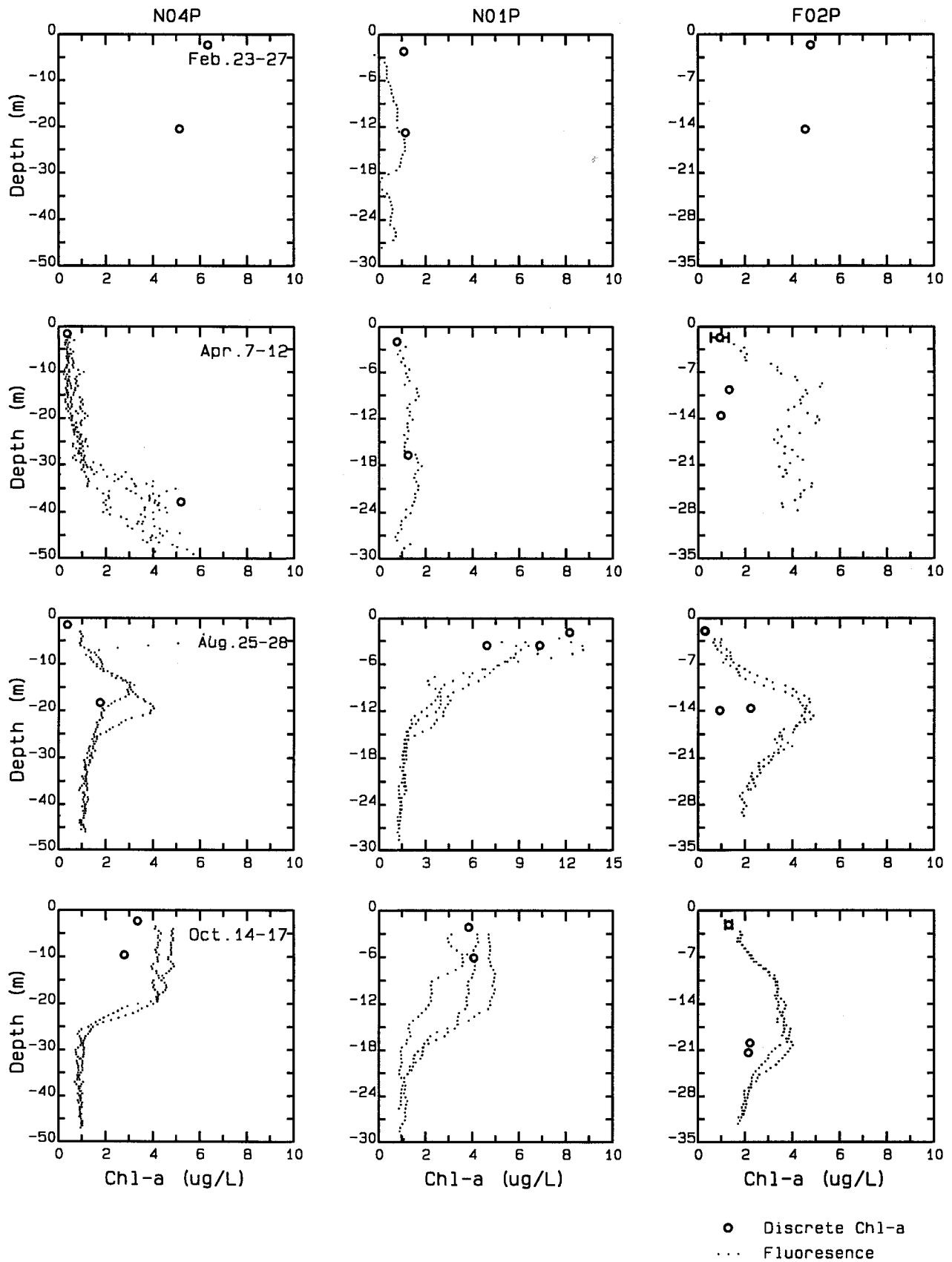
FIGURE 3-26. DEPTH PROFILES FOR 1992 CHLOROPHYLL-A AND FLUORESCENCE
DATA FOR SELECTED STATIONS AND DATES

Cod Bay. In April, sub-surface chlorophyll maximums are observed in the fluorescence data at stations N04P and F02P; the discrete chlorophyll data also show a maximum at depth for station N04P. It should also be noted that three vertical fluorescence profiles obtained over a three day period are presented and all three casts are fairly consistent.

Data from August show the patchiness of algal biomass as the two nearfield stations show slightly different patterns. One of the August vertical casts for station N04P shows both a surface maximum and a subsurface maximum at about 20 m depth, while the second vertical cast taken one day apart shows a fluorescence maximum at about 15 m depth; the discrete chlorophyll-a data also show a maximum at depth. At station N01P maximum fluorescence levels are observed near the surface with high discrete chlorophyll measurements as well. Three vertical fluorescence casts are plotted for N01P and all shown a consistent vertical pattern. The farfield station, F02P, has a maximum fluorescence value at approximately 15 meters. The fluorescence data measured at this depth are about twice as high as the observed discrete chlorophyll-a data. In October, the nearfield stations show higher chlorophyll levels to be found near the water surface, while station F02P shows a sub-surface maximum. The fluorescence data at the 9 to 12m depth at station N01P varied by a factor of two among the three October casts.

Figure 3-27 presents probability plots of seasonal subsurface or "mid-depth" (12.5 to 17.5 m) chlorophyll-a concentrations for the nearfield stations, as well as annual subsurface concentrations for the nearfield and farfield stations during 1992 and 1993; 1992 chlorophyll fluorescence data are also included. The discrete chlorophyll data at this depth are more sparse, therefore limiting the ability to detect meaningful change between the two years. However, the mid-depth data appear to follow trends similar to the surface data in terms of inter-annual variation. The winter (February and March) chlorophyll levels are quite different between 1992 and 1993. The 1992 chlorophyll and fluorescence data indicate a median of between 1.5 and 2 μg/L; in 1993 a median of about 0.5 μg/L is
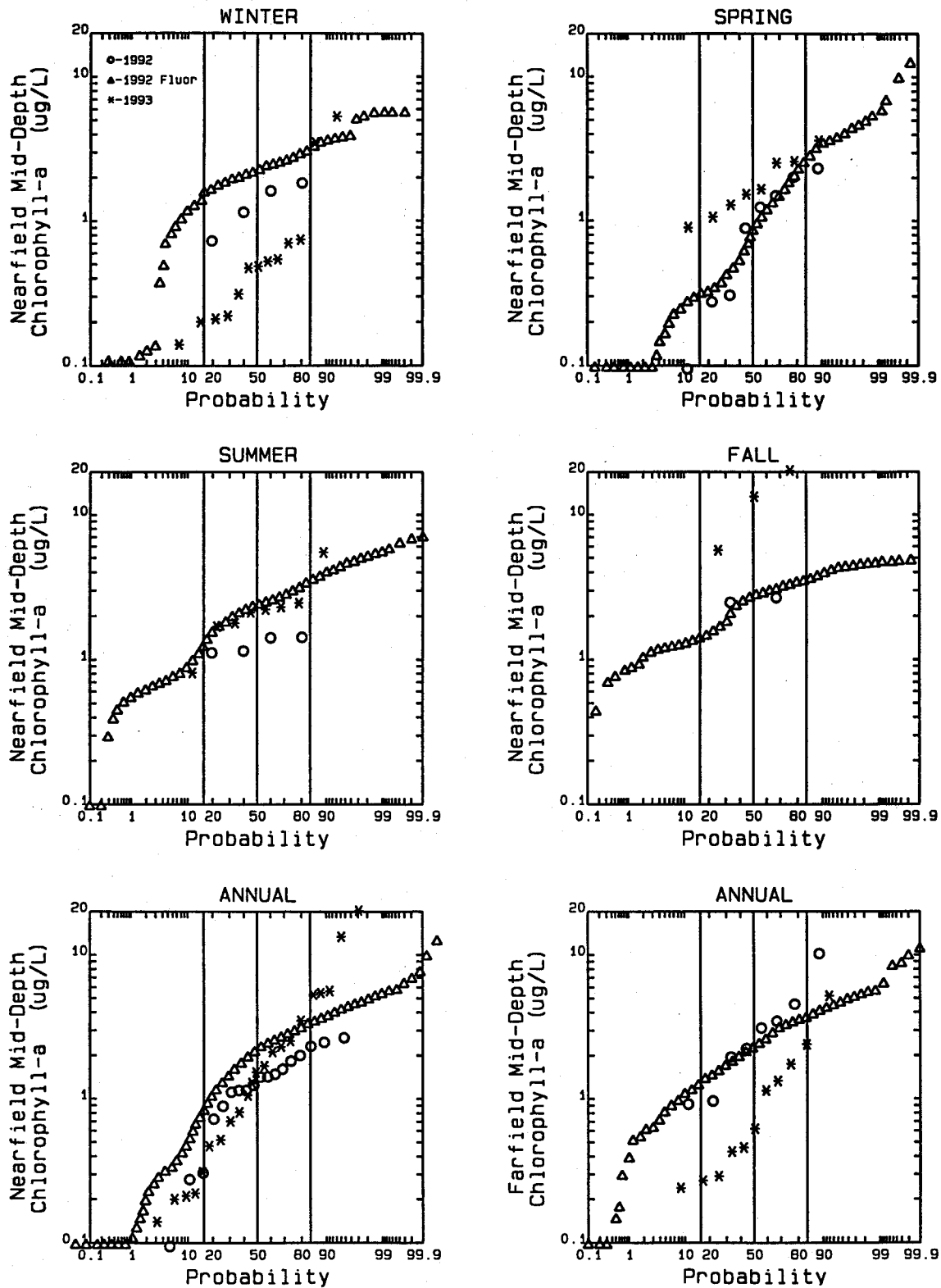
FIGURE 3-27. SEASONAL AND ANNUAL PROBABILITY DISTRIBUTIONS FOR 1992
AND 1993 MID-DEPTH CHLOROPHYLL-A DATA AND 1992 MID-DEPTH
FLUORESCENCE DATA AT NEARFIELD AND FARFIELD STATIONS

observed. The data, however, indicate that maximum chlorophyll levels were approximately the same, between 3 and 6.

The spring (April, May, and June) and summer (July, August, and September) probability figures show similar chlorophyll concentrations for 1992 and 1993. Median spring concentrations are between 1 and 2 μg/L with maxima of 10 to 12 μg/L; summer median chlorophyll concentrations are between 1 and 2 μg/L with maxima of 5 to 7 μg/L. Although there are very few data in the fall of 1993 with which to make comparisons it appears as if the magnitude of the fall 1993 bloom was considerably larger in 1993 versus 1992. The chlorophyll data for the farfield stations suggests that 1992 chlorophyll-a concentrations were 0.5 to 1.5 μg/L higher than 1993 levels. It is also interesting to note that there is slightly more variation in the mid-depth nearfield chlorophyll data than the surface data in the spring; in the summer, however, there is significantly greater variation in the nearfield surface data then is observed in the mid-depth data.

3.3.2.2   Organic Carbon

In areas removed from anthropogenic sources, POC is produced largely as a consequence of algal primary productivity. Therefore, it might be expected that POC and chlorophyll-a would be correlated to some degree. Comparing Figures 3-24 and 3-28 indicates that for 1992 this is generally the case. The Boston Harbor entrance POC data (station F23P), show an increase in concentration from 0.2 mg/L in February to about 0.65 mg/L in April, following a trend similar to that observed in the chlorophyll data. POC concentrations then gradually decrease through October, again similar to the changes observed in chlorophyll concentrations. POC concentrations also follow similar patterns at the other data stations. POC concentrations tend to be slightly higher in the spring and fall at stations N04P, N06, and N07P as compared to the summer levels, similar to the temporal pattern observed in the chlorophyll data. The Cape Cod station (F01P) also shows evidence of the spring bloom, but POC concentrations do not decrease as rapidly as the chlorophyll data do in March and April.
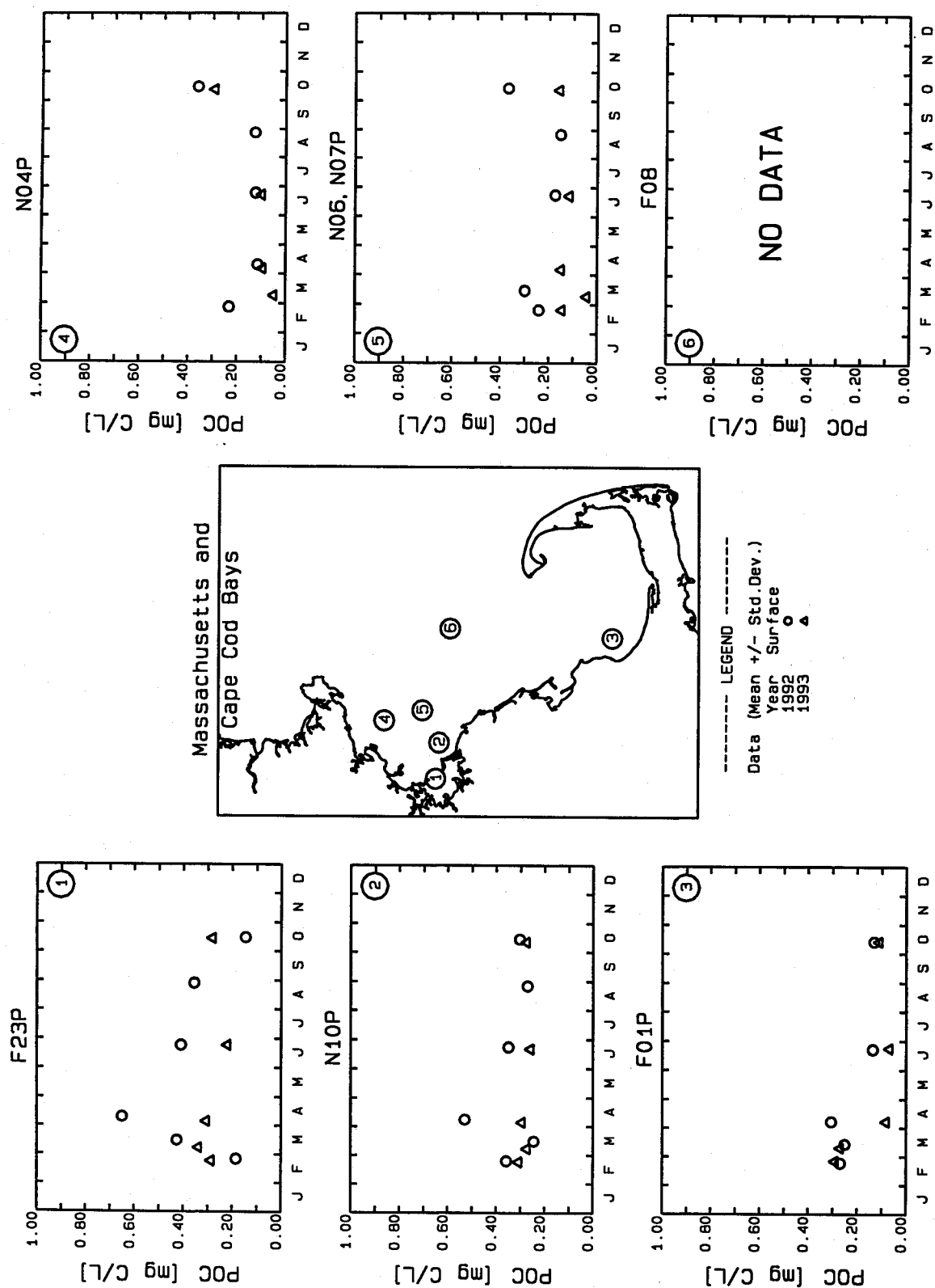
FIGURE 3-28. OBSERVED 1992 AND 1993 SURFACE POC DATA FOR SELECTED STATIONS

Figure 3-29 presents a series of seasonal and annual probability distributions to illustrate the inter-annual variability in POC data. Although there is limited POC data with which to make meaningful comparisons on a seasonal time-scale, on an annual basis the two years do not appear to be markedly different. The degree of variability appears to be the same on an annual basis for both nearfield and farfield stations. Median and maximum nearfield POC concentrations are approximately 0.1 mg/L higher in 1992 versus 1993.

3.3.2.3   Phosphorus

Figure 3-30 presents temporal plots of surface and bottom water inorganic phosphorus (PO_4). The 1992 surface phosphate concentrations show a seasonal cycle affected by phytoplankton levels. The highest surface PO4 concentrations are observed during the winter when uptake by phytoplankton is at a minimum. Surface phosphorus levels decrease rapidly during the spring and remain low during the summer due to algal uptake.   Bottom water phosphorus concentrations also decrease during the late winter/early spring, before stratification develops. This is due to vertical exchange with the surface waters where uptake by phytoplankton occurs. As density stratification occurs no further exchange between surface and bottom waters occurs at the deep water stations (N14P, N06, N07P, and F08) and a vertical gradient in PO_4 develops. This gradient remains until the fall overturn of the Bays system which occurs between mid-October and mid-November.

The 1993 data set shows a similar pattern to the 1992 data set, but concentrations differ from station to station. At Station F23P, with the exception of the beginning of the year, phosphorus levels tend to be lower at both the surface and the bottom. In Cape Cod Bay, at Station F01P, surface phosphorus concentrations tend to be higher in 1993 except during October when a fall algal bloom occurs. At the nearfield stations, during the summer months, surface concentrations of phosphorus are lower in 1993, while bottom water concentrations are generally higher. Station F06 also shows higher bottom water concentrations in 1993.

3-50

FIGURE 3-29. SEASONAL AND ANNUAL PROBABILITY DISTRIBUTIONS FOR 1992 AND 1993 SURFACE POC DATA AT NEARFIELD AND FARFIELD STATIONS

FIGURE 3-30. OBSERVED 1992 AND 1993 PO$_4$ DATA FOR SELECTED STATIONS

Figures 3-31 and 3-32 present seasonal and annual probability distributions for nearfield and farfield stations for surface and mid-depth (12.5-17.5 m) PO4, respectively. The nearfield surface and mid-depth PO4 distributions for winter are virtually the same for both years, with median concentrations of 0.015 mg P/L. The median nearfield surface PO4 concentrations are slightly higher in 1992 as compared to 1993; however, mid-depth concentrations are about the same for both years. It is interesting to note that approximately 10 percent of the surface PO4 concentrations are at levels (0.001 mg/L or 1 μg/L) that are commonly thought to limit phytoplankton growth.

Summer nearfield surface and mid-depth PO4 distributions are similar for both years. Median surface PO4 concentrations average approximately 7 μg/L, while mid-depth median concentrations are about 12 μg/L. The summer surface PO4 data also indicate that only 2 to 3 percent of the observations are at growth limiting concentrations. Nearfield surface PO4 data for the fall of 1993 show greater variability than observed in the fall 1992 data and have a higher median value. On an annual basis both the nearfield and farfield surface and mid-depth data are quite similar, particularly in terms of their median values.

3.3.2.4   Nitrogen

Measurements of NH_4, $NO_2 + NO_3$, PON and total dissolved nitrogen (TDN) are available for the 1992 and 1993 data sets. Since phytoplankton use both NH_4 and $NO_2 + NO_3$ for cell growth, the sum of these two variables, dissolved inorganic nitrogen (DIN) will be presented (Figure 3-33) rather than the individual nitrogen forms. In 1992 and 1993 the highest DIN concentrations in the study area are found in the winter/early spring and the late fall near the present outfall, at stations F23P and N10P. As surface DIN is used by phytoplankton for cell growth, lower DIN concentrations result in the late spring and through the summer. As stratification develops during the spring and continues through the summer months, bottom water DIN concentrations increase slightly over early spring levels. This occurs because of low light availability in the bottom waters of the Bay, which precludes phytoplankton productivity, and because of remineralization of detrital

FIGURE 3-31. SEASONAL AND ANNUAL PROBABILITY DISTRIBUTIONS FOR 1992 AND 1993 SURFACE PO$_4$ DATA AT NEARFIELD AND FARFIELD STATIONS

FIGURE 3-32. SEASONAL AND ANNUAL PROBABILITY DISTRIBUTIONS FOR 1992 AND 1993 MID-DEPTH PO_4 DATA AT NEARFIELD AND FARFIELD STATIONS
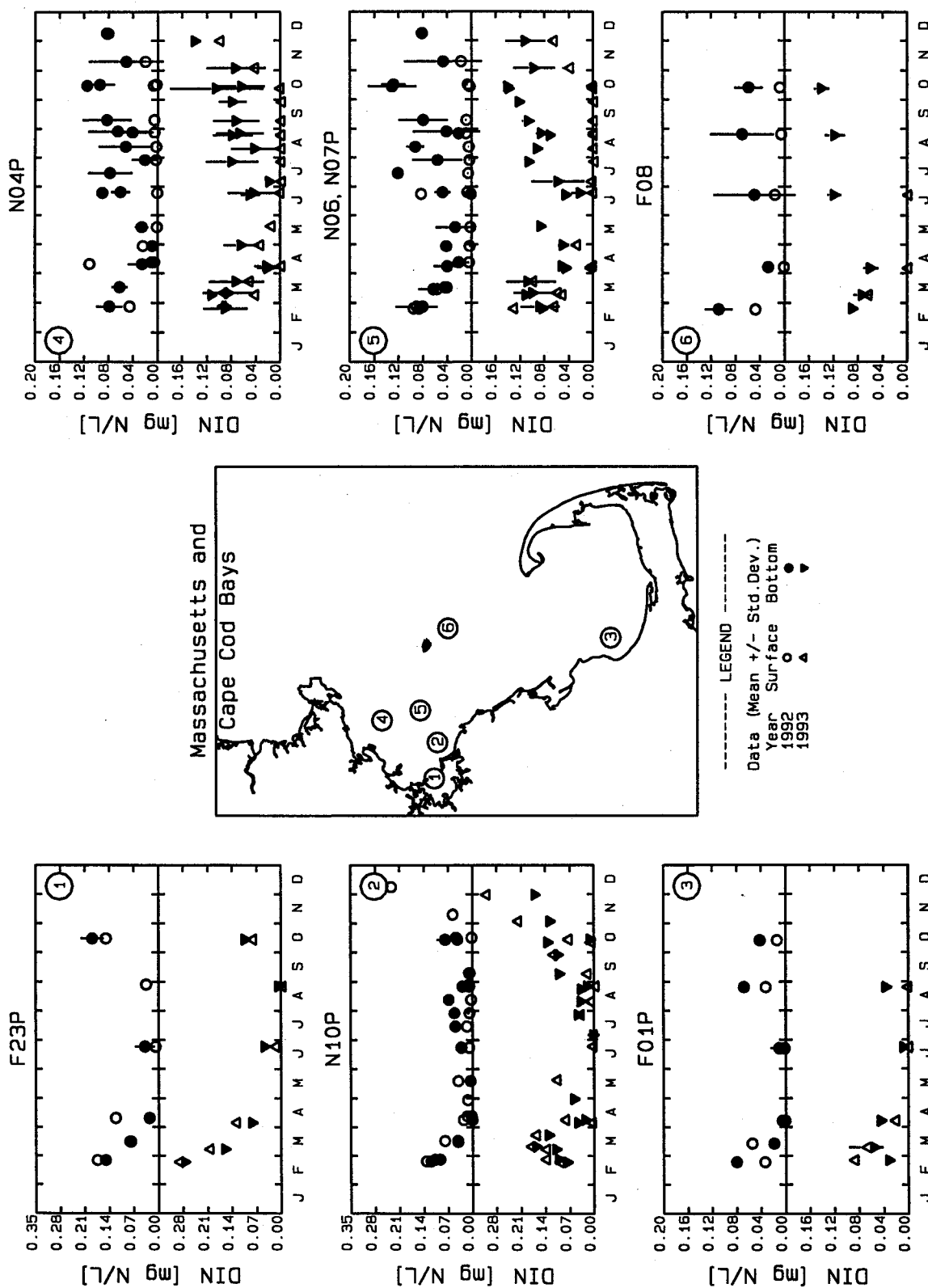
FIGURE 3-33. OBSERVED 1992 AND 1993 DIN DATA FOR SELECTED STATIONS

algae, which settle from the surface layer. One can also note that surface DIN concentrations decrease as a function of distance from Boston Harbor.

Figures 3-34 and 3-35 present seasonal and annual probability distributions of 1992 and 1993 nearfield and farfield DIN data for surface and mid-depth (12.5-17.5 m), respectively. The surface and mid-depth winter data are similar, although the 1993 surface data are slightly higher. There is a significant decline in surface DIN between winter and spring in both 1992 and 1993. Approximately 85 percent of the 1992 surface and mid-depth data and about 50 percent of the 1993 surface DIN concentrations are below 0.01 mg N/L or 10 μg/L, a value commonly thought to limit phytoplankton growth. Spring 1992 mid-depth DIN data are similar to the surface values. However, 1993 mid-depth DIN concentrations are not quite as low as are observed in the surface layer of the water column. By summer approximately 85 percent of the surface DIN concentrations are at or below 10 μg/L in both years. Mid-depth DIN concentrations are also low, but not as low as the surface values. This probably reflects reduced DIN uptake by algae, due to lower light availability, increased mineralization of organic nitrogen and some exchange of DIN across the pcynocline. There is a significant increase in fall DIN levels as primary productivity begins to decline. Median DIN concentrations of 15 to 40 ug N/L are observed in the surface waters and between 20 and 50 ug N/L are observed at mid-depth. Annually the surface DIN data are quite similar for both years, while mid-depth DIN concentrations are slightly higher in 1993. The farfield concentrations of surface and mid-depth DIN are significantly higher in 1993 as compared to 1992.

Observed PON data are presented in Figure 3-36. PON is another measure of the local algal biomass. The 1992 PON data follow a similar trend to that of POC. As the late winter/early spring bloom occurs the PON concentration increases. At stations closer to the Deer and Nut Island outfalls, the PON concentrations drop slightly or level off in the summer and fall. At Station F01P the PON concentrations decline more dramatically as this area of the Bays system becomes strongly nutrient limited. There is also the appearance of a fall algal bloom as PON concentrations increase in October at a number of stations.
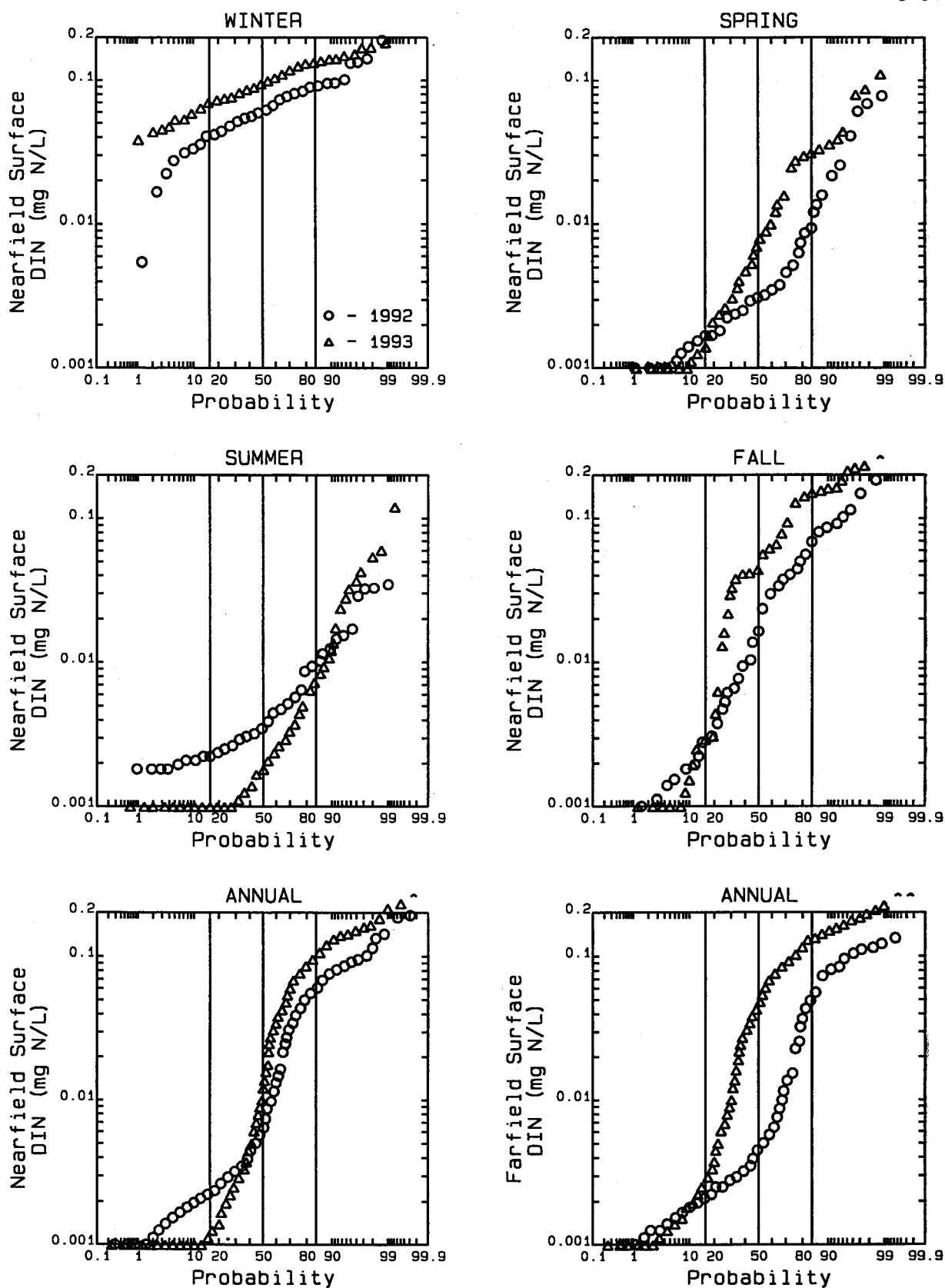
FIGURE 3-34. SEASONAL AND ANNUAL PROBABILITY DISTRIBUTIONS FOR 1992
AND 1993 SURFACE DIN DATA AT NEARFIELD AND FARFIELD STATIONS
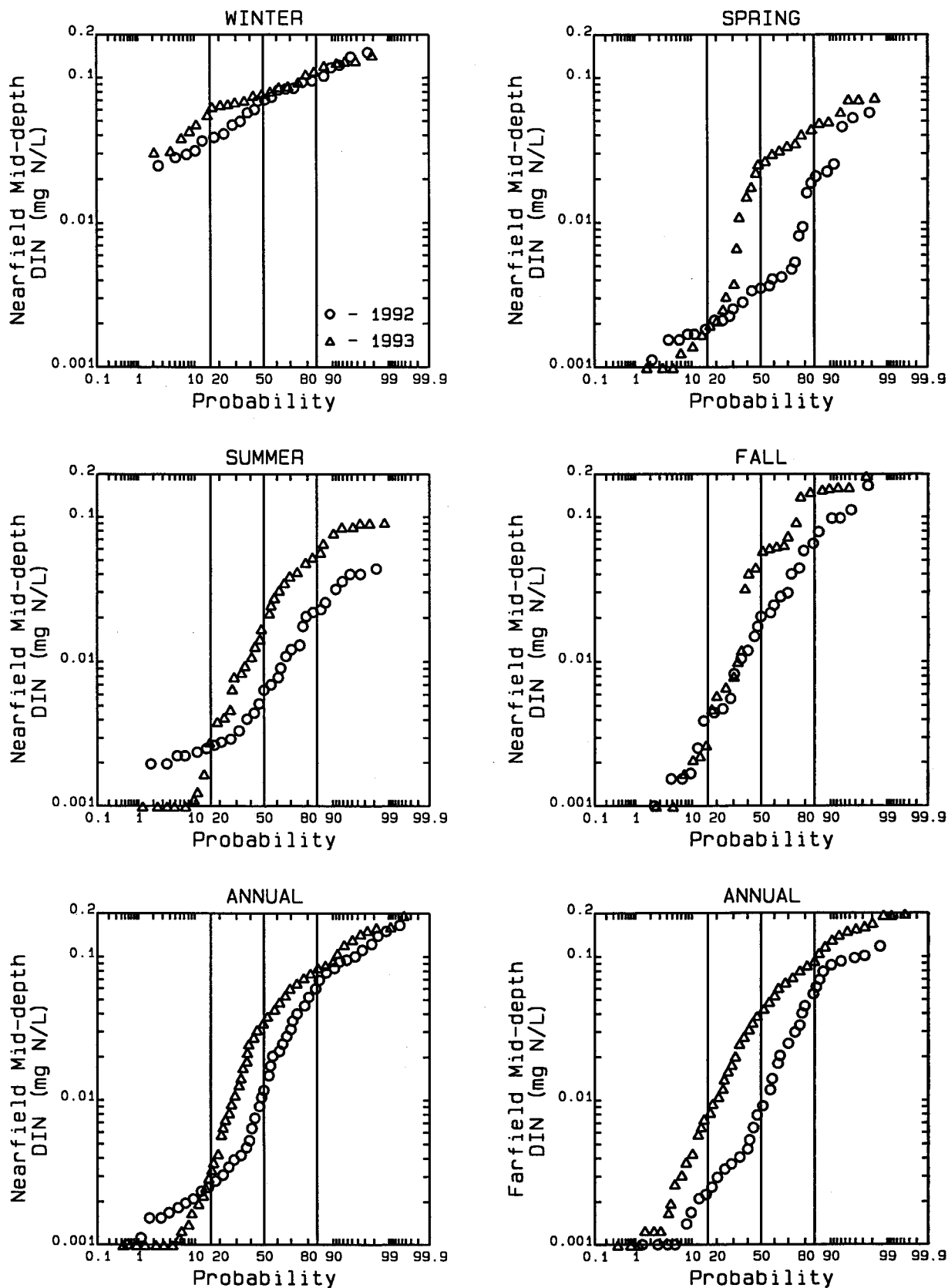
FIGURE 3-35. SEASONAL AND ANNUAL PROBABILITY DISTRIBUTIONS FOR 1992
AND 1993 MID-DEPTH DIN DATA AT NEARFIELD AND FARFIELD STATIONS
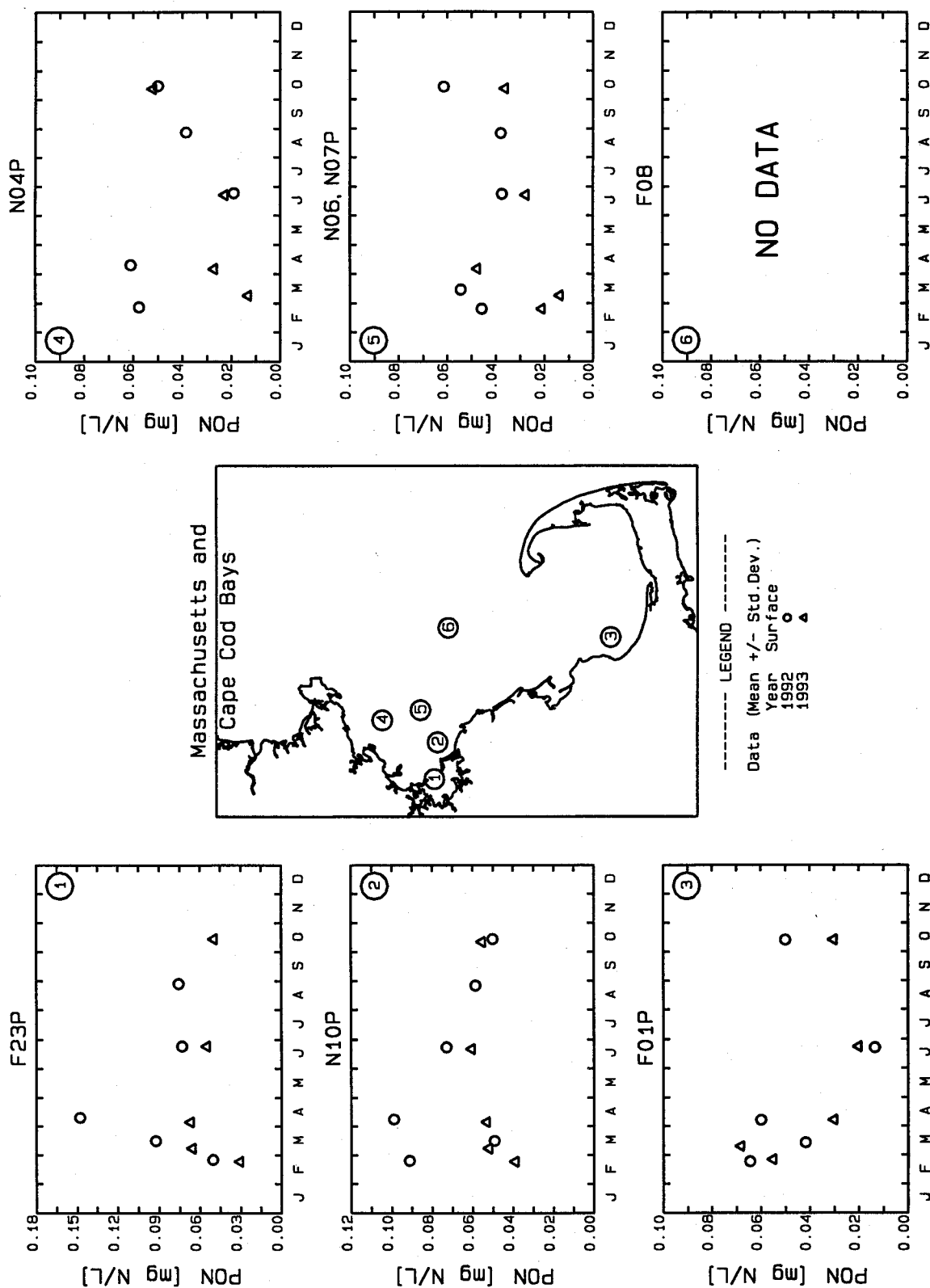
FIGURE 3-36. OBSERVED 1992 AND 1993 SURFACE PON DATA FOR SELECTED STATIONS

The 1993 PON data show seasonal patterns and station to station variability similar to the 1992 data. Near Boston Harbor, there is an initial increase in PON concentrations into March, followed by a gradual decline through the summer and fall. At the nearfield stations, late winter/early spring concentrations of PON are lower than observed in 1992. In Cape Cod, there is a decrease from springtime levels into the summer and an increase in the fall.

3.3.2.5   Silica

The dissolved silica data for 1992 and 1993 are presented in Figure 3-37. The 1992 data show higher concentrations at the beginning and end of the year. Lower surface DSi concentrations during the spring and summer months are a consequence of uptake by diatom phytoplankton. It has generally been observed in Cape Cod (Kelly et al., 1993; Kelly and Turner, 1995) that surface silica becomes the limiting nutrient in the early spring before nitrogen becomes limiting and before the algal population shifts from winter diatoms to a mixed summer assemblage. This phenomenon is observed in April 1992 at Station F01P. Other areas of the Bays show low levels of surface silica in the summer months with a gradual increase into the fall. The bottom water DSi concentrations generally remain higher than the surface concentrations throughout the year.

In the beginning of the year in 1993, silica concentrations are observed to be higher in both the surface and bottom waters, as compared to 1992. By June, the observed concentrations at most of the stations are comparable for 1992 and 1993. In the later portion of the year, surface silica concentrations measured in 1992 appear to be higher than those observed in 1993. This may be related to the larger fall phytoplankton bloom that occurred in 1993.

Seasonal and annual probability distributions of 1992 and 1993 surface and mid-depth DSi are presented on Figures 3-38 and 3-39, respectively, for nearfield and farfield stations. Winter 1992 surface and mid-depth DSi concentrations are lower than observed in 1993, possibly being related to the winter diatom bloom in 1992. Spring
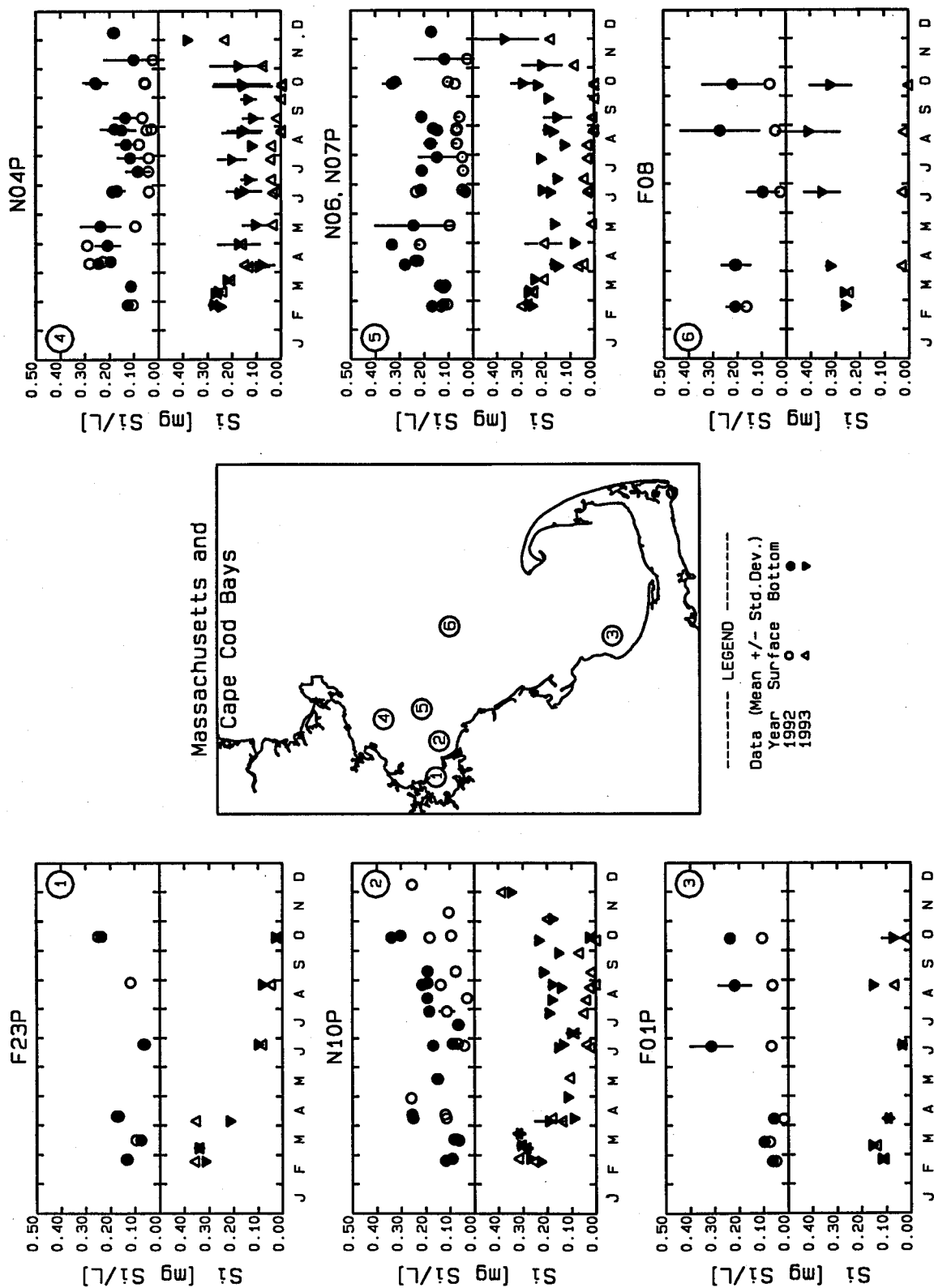
FIGURE 3-37. OBSERVED 1992 AND 1993 DSi DATA FOR SELECTED STATIONS

3-61

3-62
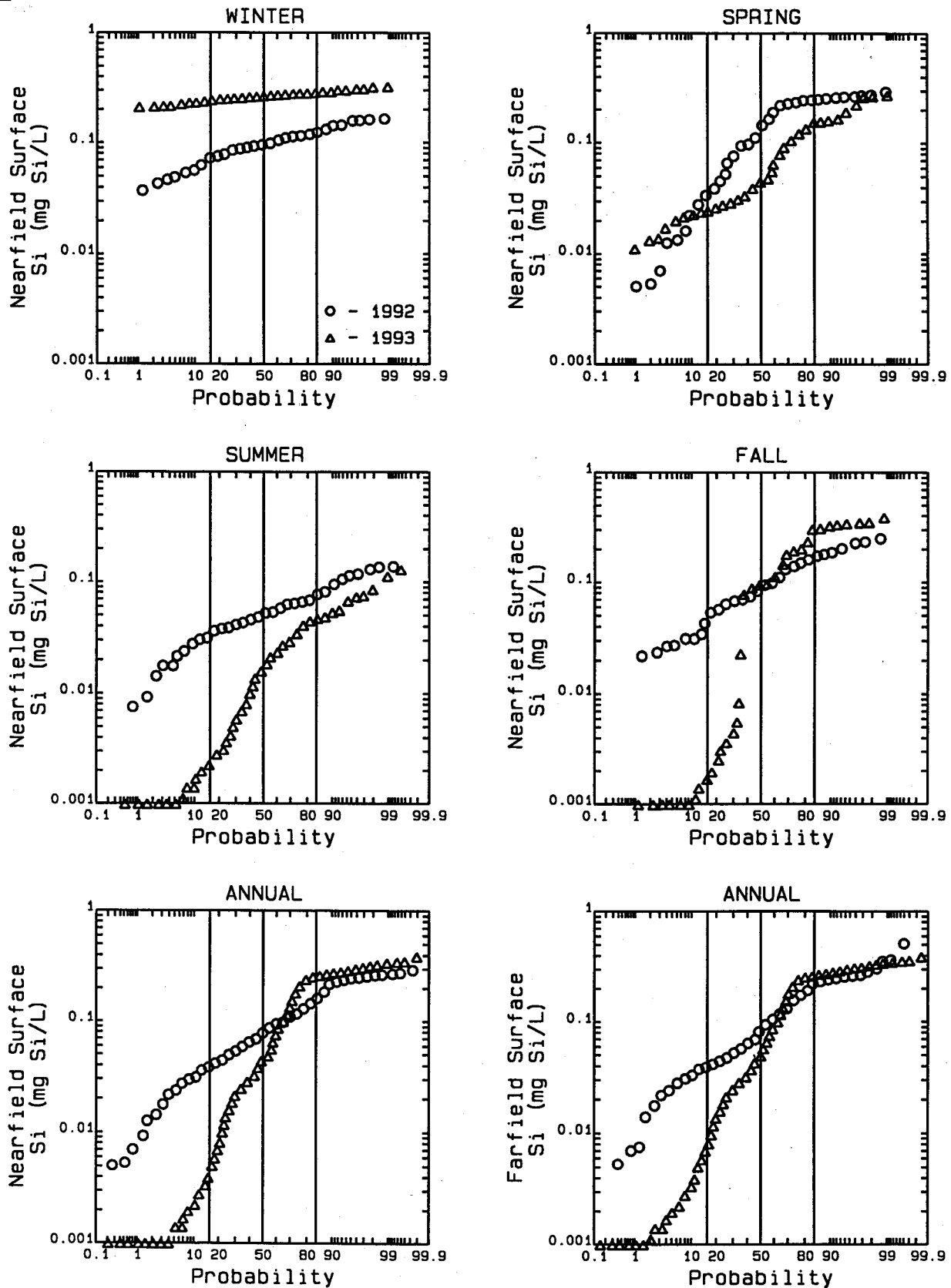
FIGURE 3-38. SEASONAL AND ANNUAL PROBABILITY DISTRIBUTIONS FOR 1992 AND 1993 SURFACE DSi DATA AT NEARFIELD AND FARFIELD STATIONS
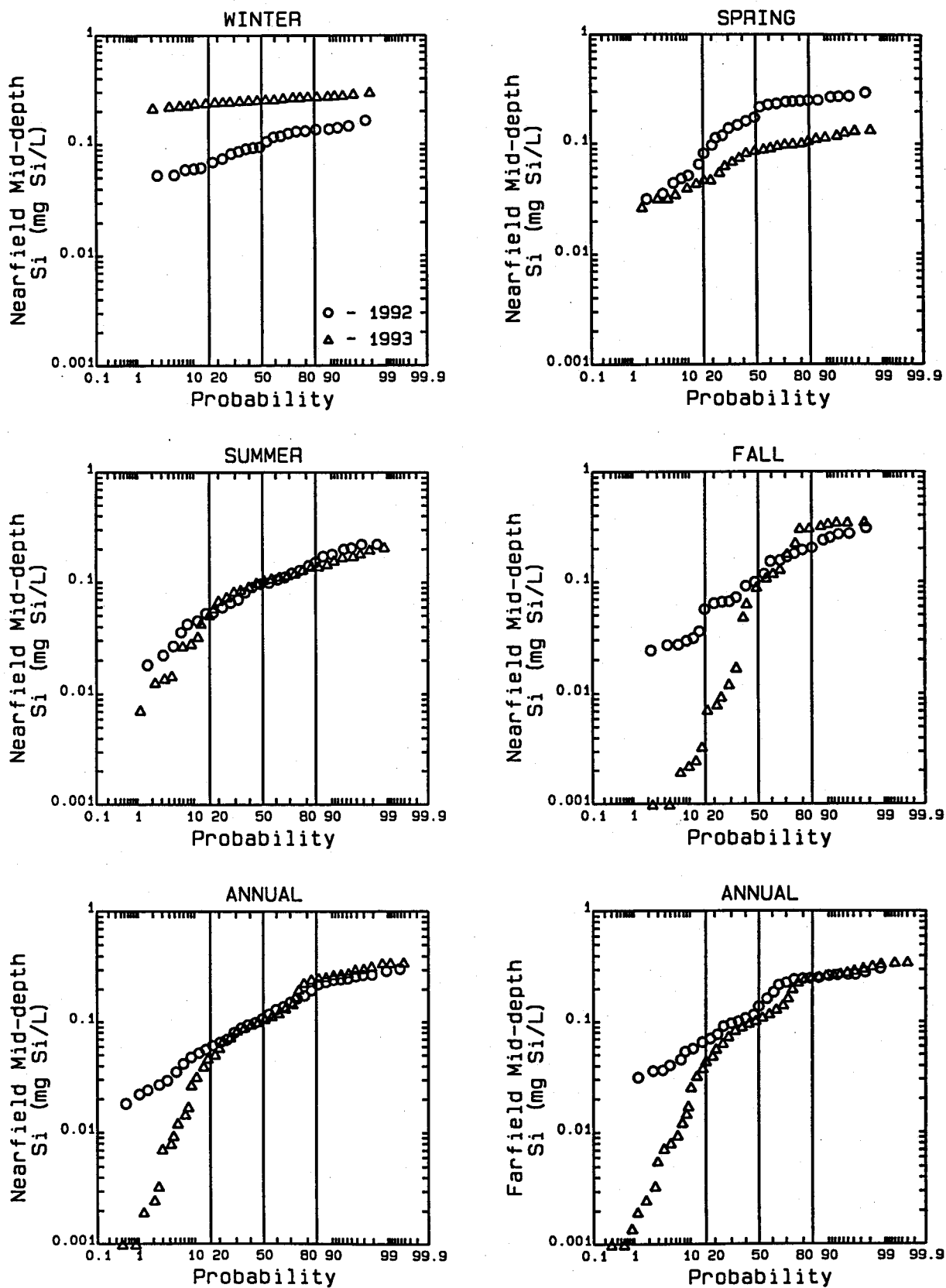
FIGURE 3-39. SEASONAL AND ANNUAL PROBABILITY DISTRIBUTIONS FOR 1992 AND 1993 MID-DEPTH DSi DATA AT NEARFIELD AND FARFIELD STATIONS

median and maxima concentrations of DSi increased by 0.05 to 0.1 mg Si/L over winter values. In contrast spring 1993 surface DSi concentrations showed a marked decrease below winter values. Similar patterns were also observed for mid-depth concentrations. Summer 1992 surface and mid-depth silica concentrations were slightly below spring levels. Summer of 1993 surface DSi concentrations were slightly lower than 1992 concentrations while 1993 summer mid-depth concentrations were virtually the same as observed in 1992. Fall DSi concentrations increased slightly over summer levels in both years. Annually surface and mid-depth silica concentrations were similar in 1992 and 1993 for nearfield and farfield stations, except at the lower concentration levels, where in 1992 was higher than 1993.

3.3.2.6   Dissolved Oxygen

Surface and bottom water dissolved oxygen measurements are shown for six locations for 1992 and 1993 in Figure 3-40. Dissolved oxygen concentrations show a strong seasonal cycle with highest concentrations observed in the winter and early spring, followed by decreasing levels into the summer and fall. This cycle is related to water temperature, primary productivity and community respiration. For the 1992 farfield stations, the highest concentrations of DO are observed in February, with surface and bottom concentrations between 12 and 13 mg O_2/L. For the remainder of the year there is a general downward trend observed in the data with some stations reaching minimum values of 7 mg O_2/L in October. The nearfield stations, where more data were available, show a sharp decline in DO concentrations between February and May, an increase in June, and then a second decreasing trend into October. Dissolved oxygen levels then increase in November and December as the water temperatures decrease, thereby increasing DO saturation and reducing biological processes. It is also worth noting that at the deeper stations in the Bay, bottom water DO is as high or higher than the surface data, suggesting lower levels of community respiration.

The 1993 DO data show a somewhat different pattern than was observed in the 1992 data. The highest DO concentrations in 1993 are observed in April after a slight
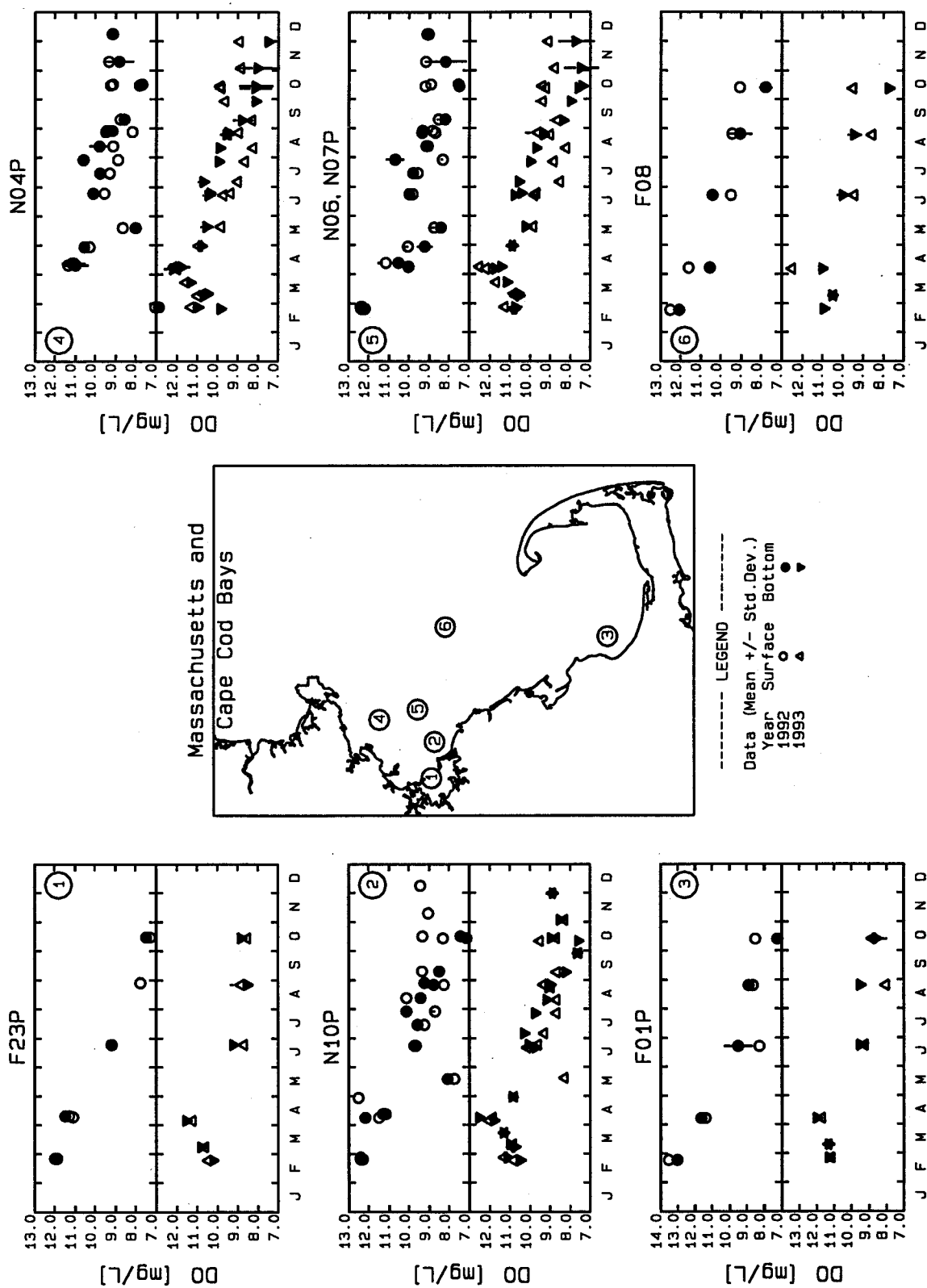
FIGURE 3-40. OBSERVED 1992 AND 1993 DO DATA FOR SELECTED STATIONS

increase above February levels. After April there is a trend of gradually decreasing DO levels which continues into October. The largest decreases are observed to occur between March and June and between August and October with only small decreases in June and July. November and December bottom water DO is also slightly lower in 1993 compared to 1992. The sharp decline in DO concentrations observed in May 1992 is observed in 1993 only at station N10P; the remaining stations show DO concentrations to be 1 to 2 mg G/L higher in 1993 for May.

Figure 3-41 presents a series of probability plots comparing the seasonal differences in bottom water dissolved oxygen between 1992 and 1993 for the nearfield stations and on an annual basis for the nearfield and farfield stations. The 1992 winter DO data (with the exception of one value) are higher by approximately 1 mg G/L than observed in 1993. This may be due in part to the larger algal bloom that occurred in the late winter of 1992. Although phytoplankton would not have been expected to produce oxygen at depth, the fact that the water column was well mixed at this time would have allowed oxygenated water to reach the bottom. In the spring, lower DO values are observed in 1992 with minimum values slightly below 8.0 mg G/L. In the summer, the DO distributions appear quite similar although minimum DO concentrations are slightly lower in 1993. In the fall, the two years appear comparable. The effect of the fall bloom in 1993 is not observed in the bottom water DO data. This may be due to the water column stratification still prevalent at that time. On an annual basis, at the nearfield stations, 1992 and 1993 are very similar. On an annual basis, the 1992 farfield DO data are lower than the 1993 data; the median DO in 1992 is approximately 0.5 mg/L lower than 1993. However, in terms of the minimum DO concentrations there is not a significant difference between the two years.

Figure 3-42, presents comparisons of surface DO concentrations for 1992 and 1993. As was observed in the bottom water dissolved oxygen distributions the winter of 1992 generally had higher oxygen concentrations than 1993. The springtime DO distributions show a reversal; the spring of 1993 had higher DO concentrations than 1992. Dissolved oxygen concentrations in 1993 were on average 0.5 to 1.0 mg G/L higher than
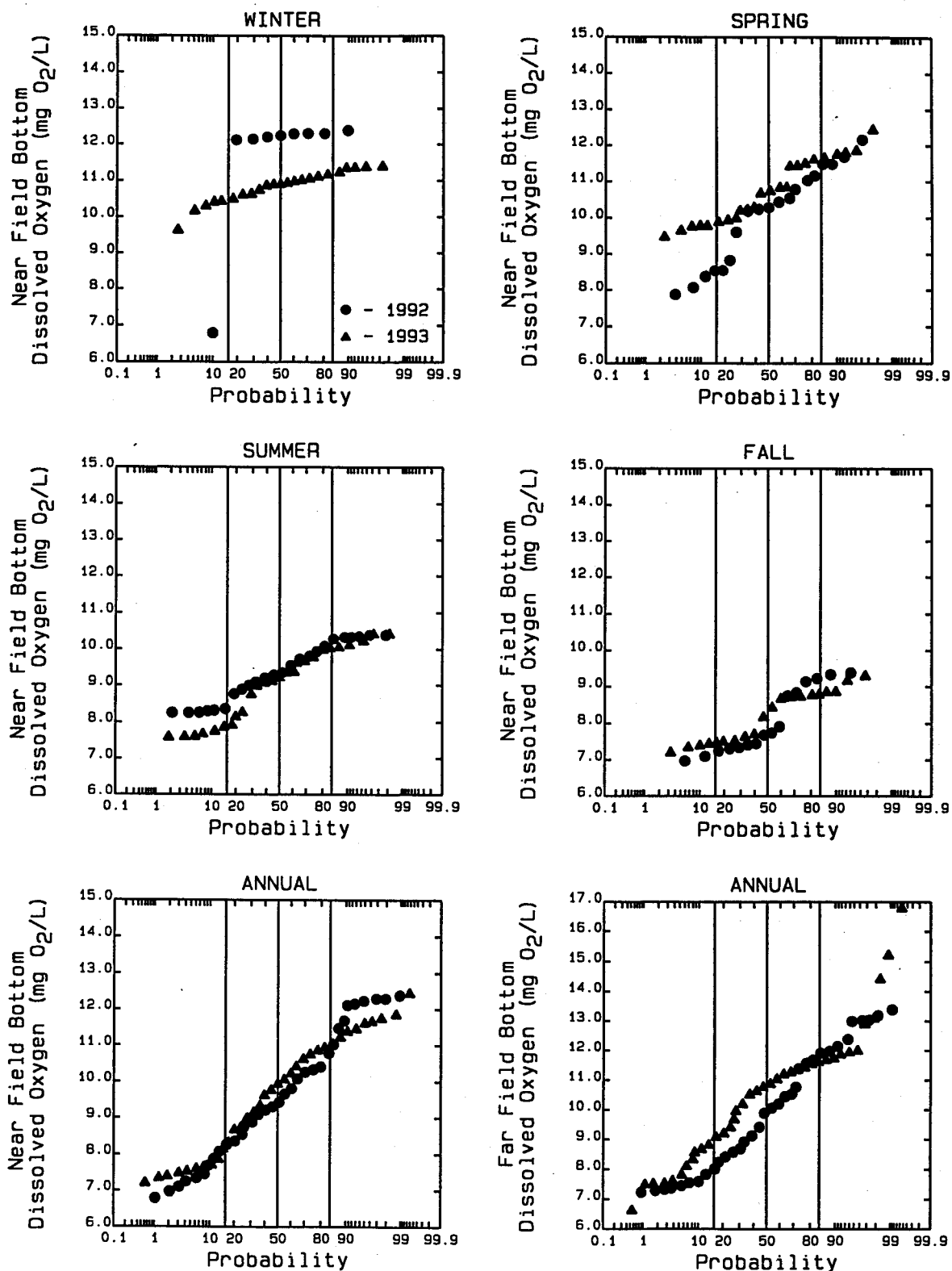
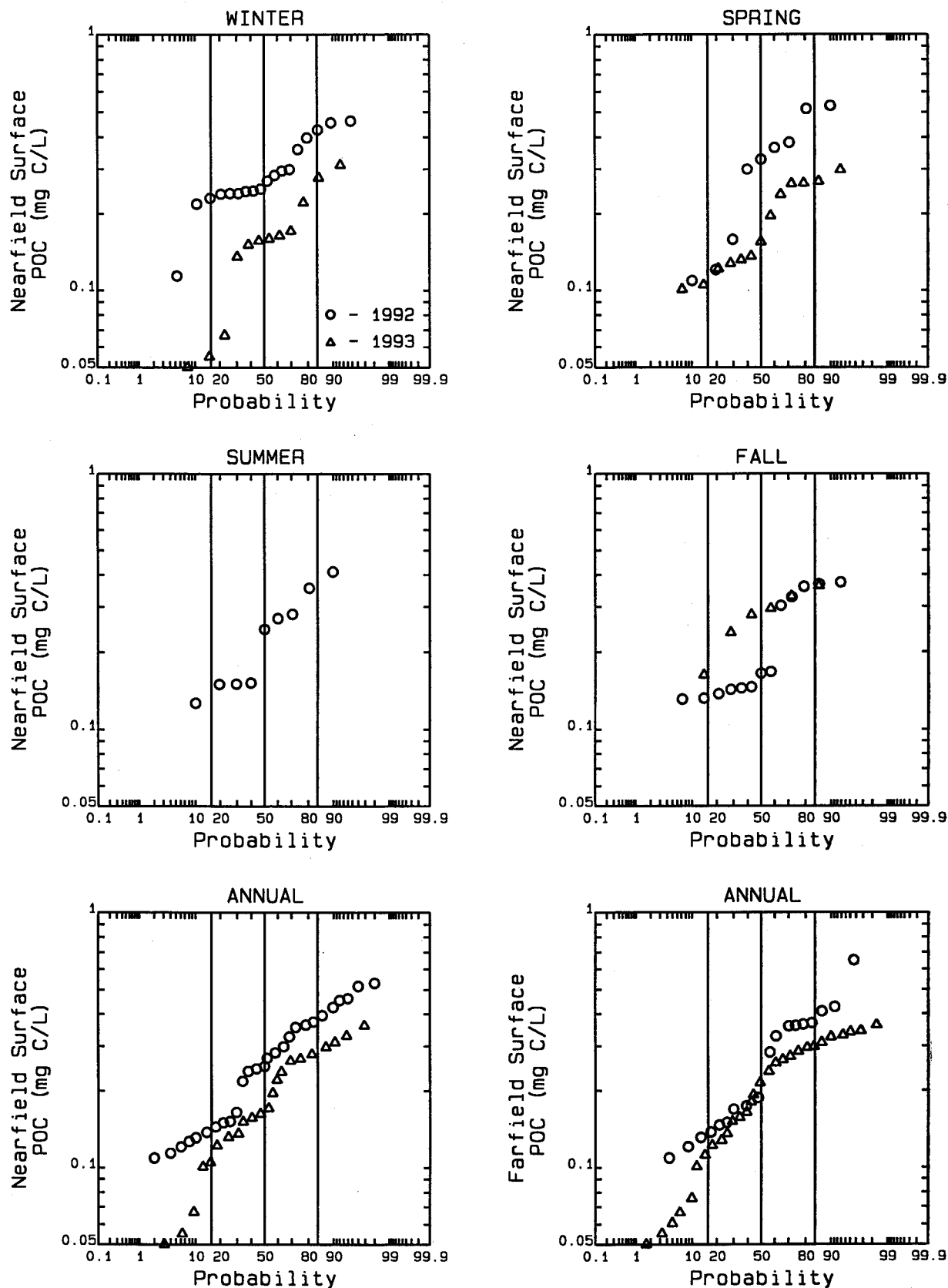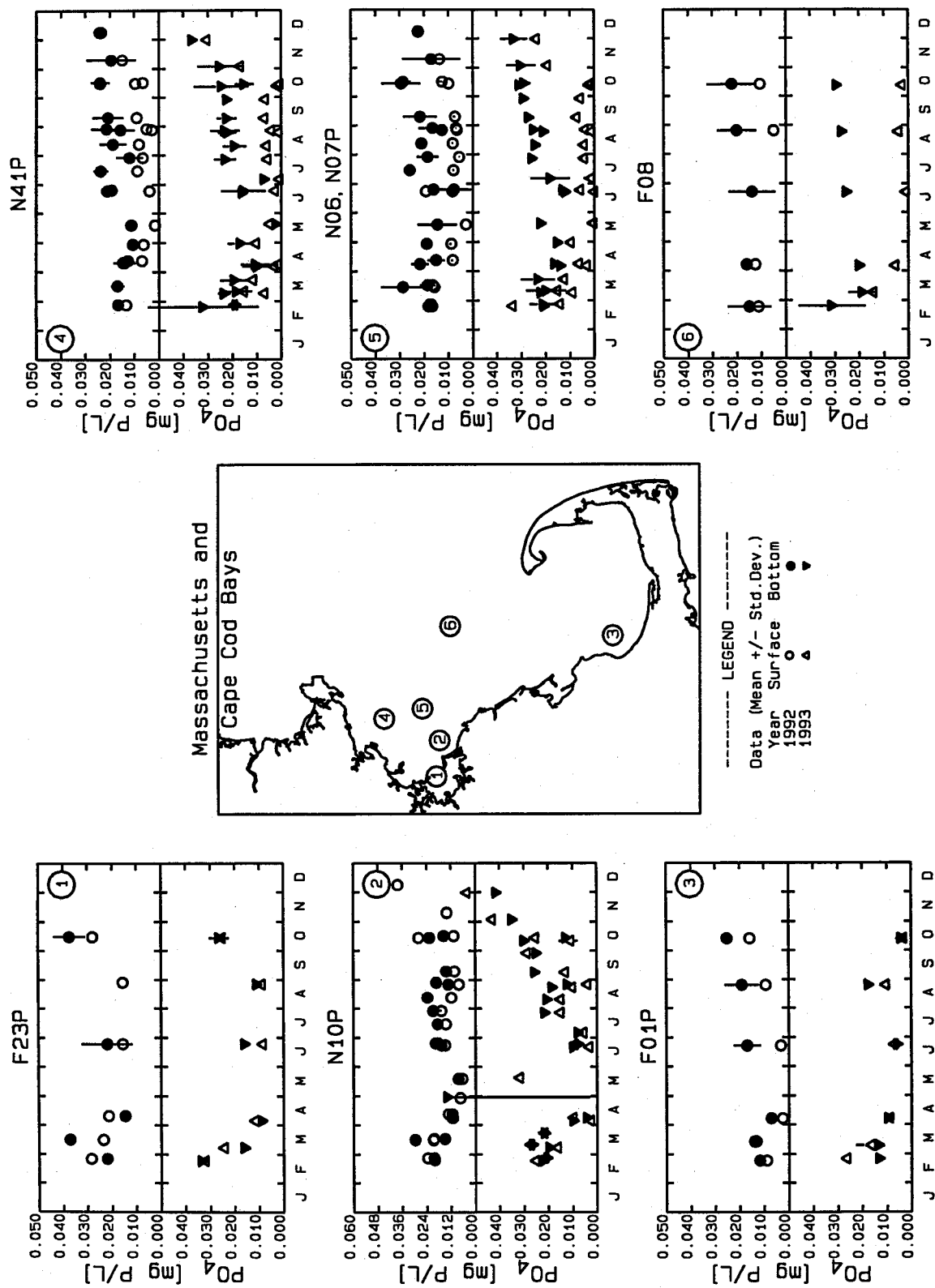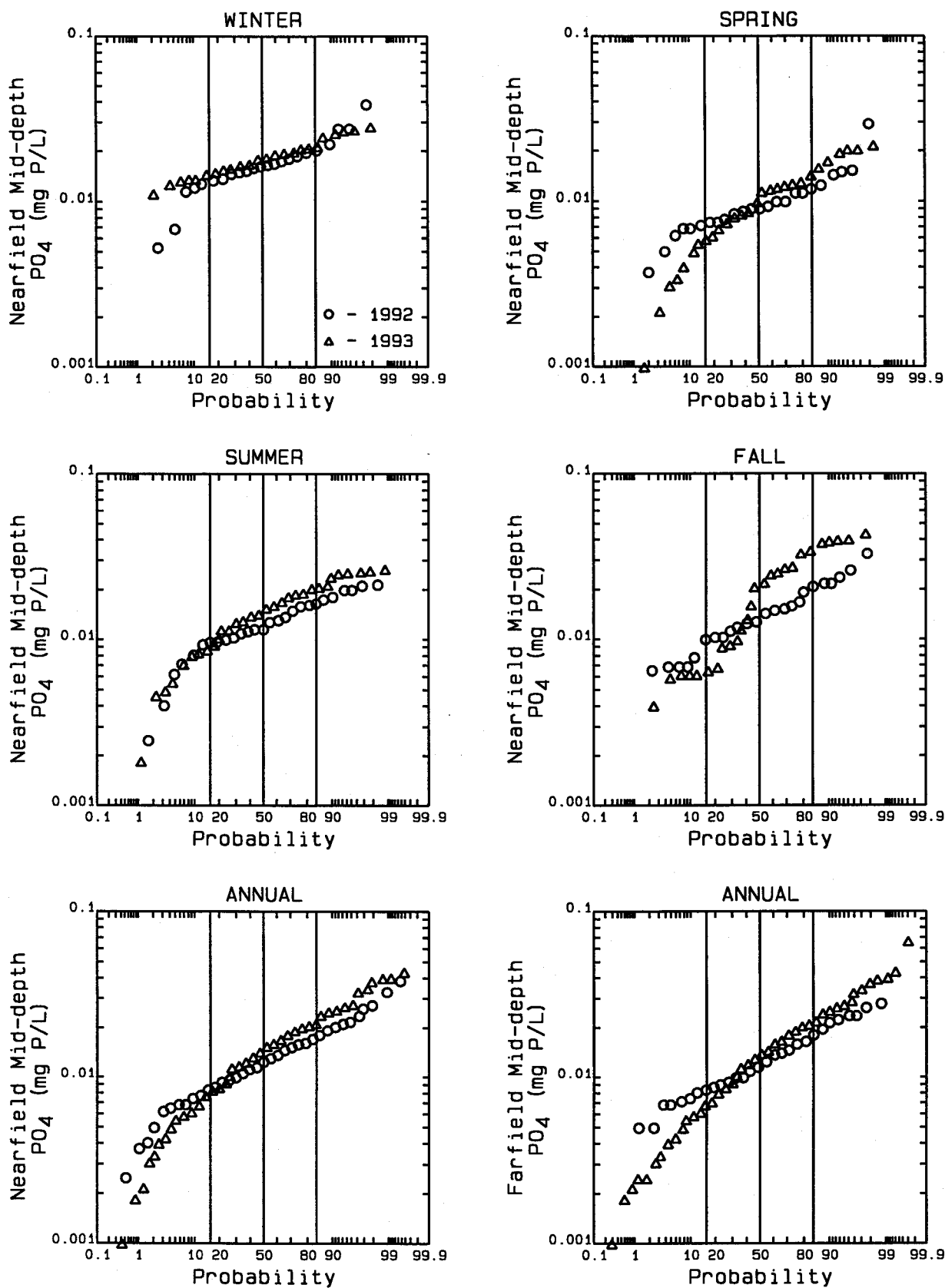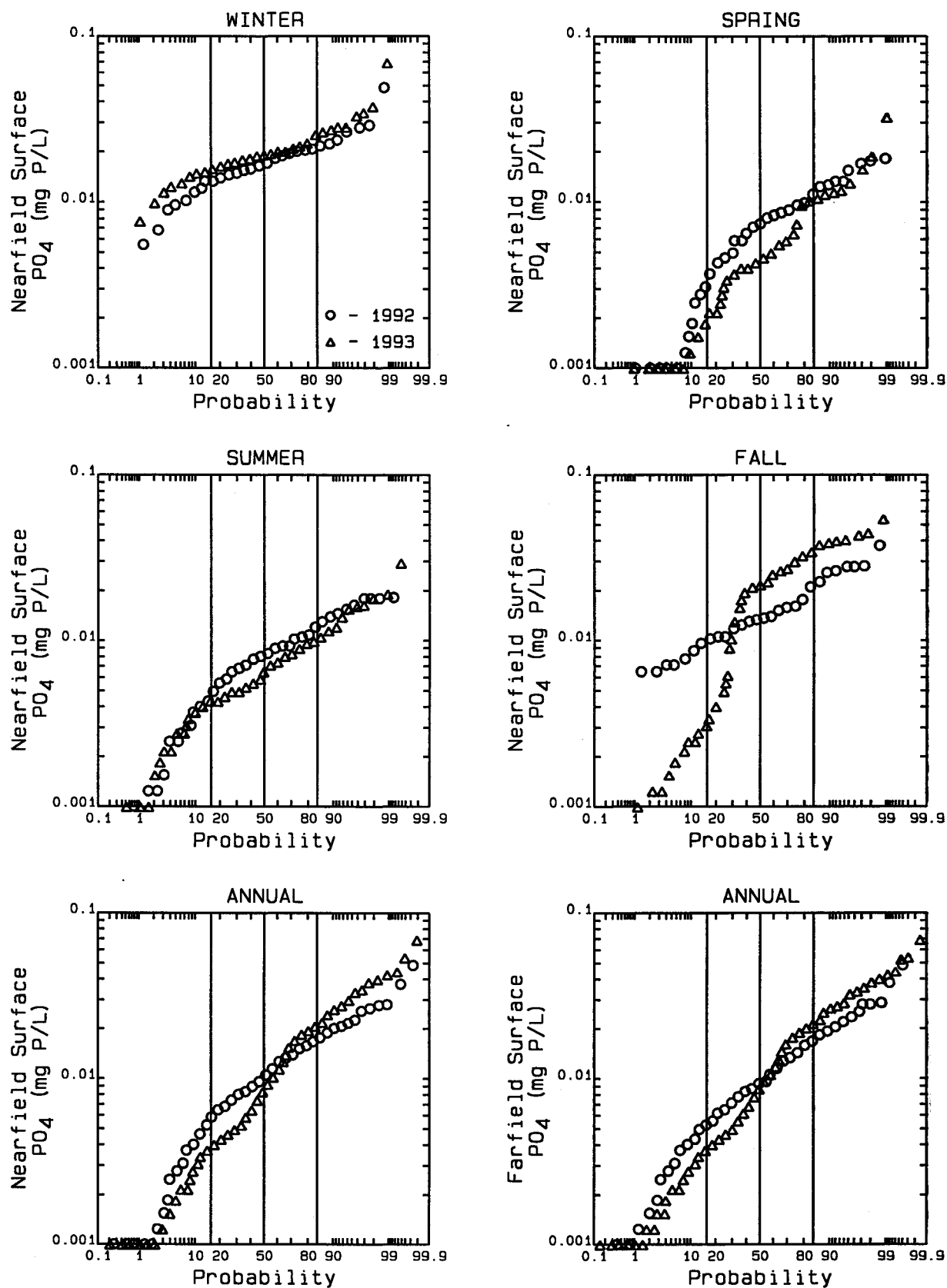FIGURE 3-41. SEASONAL AND ANNUAL PROBABILITY DISTRIBUTIONS FOR 1992 AND 1993 BOTTOM DO DATA AT NEARFIELD AND FARFIELD STATIONS
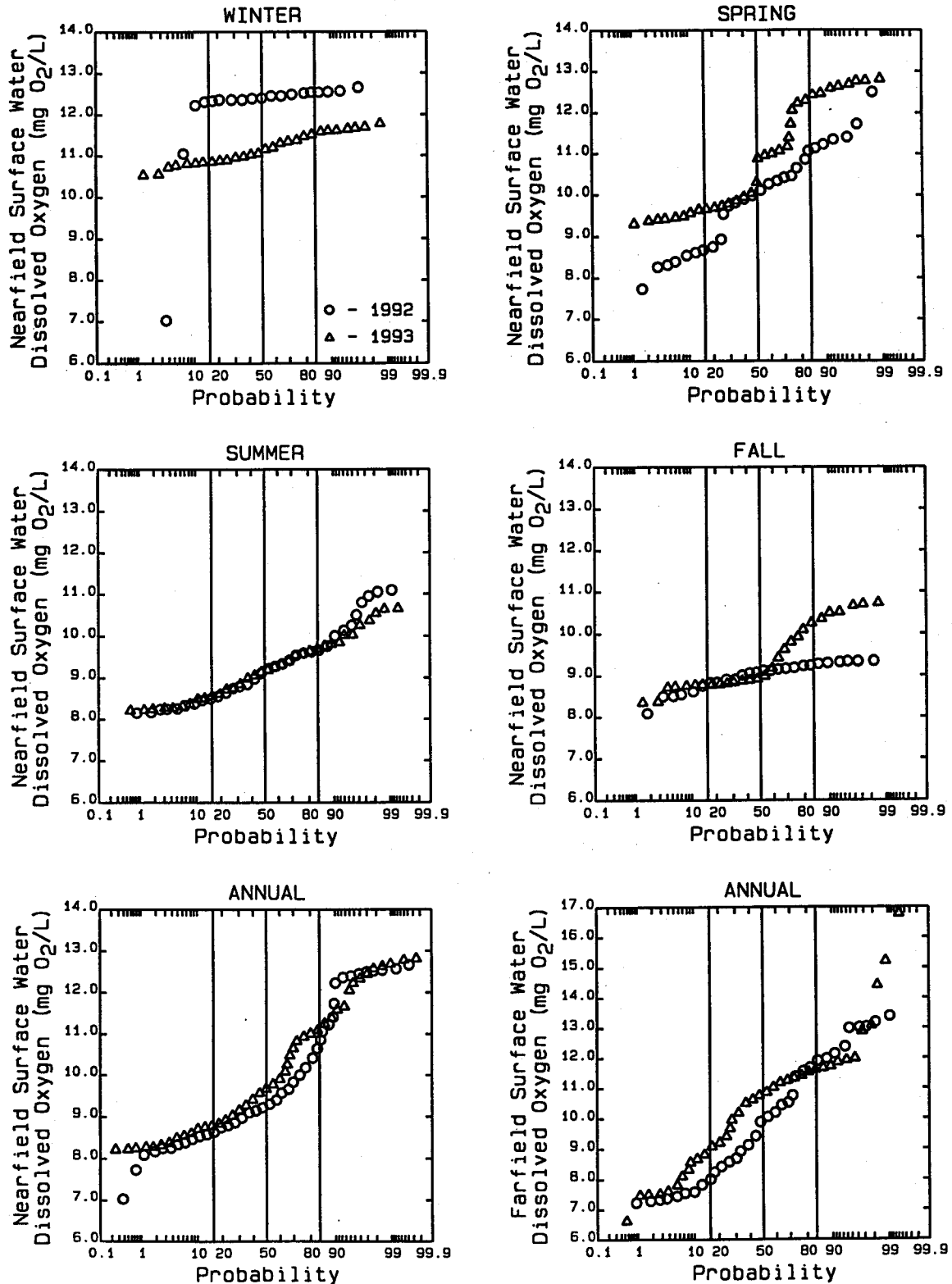
FIGURE 3-42. SEASONAL AND ANNUAL PROBABILITY DISTRIBUTIONS FOR 1992 AND 1993 SURFACE DO DATA OF NEARFIELD AND FARFIELD STATIONS

observed in 1992. Summer surface dissolved oxygen distributions were virtually identical in both years. It is interesting to note that a high percentage (about 60 percent) of the summer bottom water data are higher than the surface data in both years. These data are probably from the deeper nearfield stations, which are likely to have less community respiration due in part to lower water temperatures and the likehood that most of the oxidation of organic carbon is taking place above the pycnocline. Higher concentrations of DO are observed in the fall of 1993, posssibly due to the algal bloom which occurred that year. On an annual basis the nearfield DO distributions are quite similar. The farfield surface DO distributions are similar for both years, although the median and maxima are higher in 1993.

3.4   BOUNDARY CONDITIONS

3.4.1 1990 Boundary Concentration Data

The waters exchanged between the Massachusetts Bays system and the Gulf of Maine carry phytoplankton, nutrients, organic carbon, and dissolved oxygen with them. These mass fluxes may be substantial sources or sinks to the Bays. This is an important consideration in terms of the importance of the present and expected load from MWRA. Based on hydrodynamic model simulations (Signell, 1994) and other data analysis and modeling studies (Geyer et al., 1992) it has been demonstrated that the coastal Gulf of Maine sometimes enters Massachusetts Bay north of Stellwagen Basin and generally exits the Bay south of the Stellwagen Bank, just north of Race Point. This coastal current may bring a large nutrient load with it.

In order to adequately represent the eastern boundary of the model, it was necessary to analyze available data at stations in this portion of the Bay. For 1990, two data sets had station locations that could be utilized for the determination of boundary conditions for that calibration period. The Bigelow Laboratory data set included three stations applicable for specifying boundary conditions. These stations, covering the northern portion of the boundary, were sampled during six cruises between October 1989

and August 1990. The second data set, obtained from WHOI/UMB/UNH included two sets of cruise tracks. The first set included four stations near the boundary and were conducted in April, July, and October of 1990. These stations covered the southern portion of the boundary. The second set of cruises covered nearly the entire edge of the model domain and included 10 or more data stations. These cruises were conducted in February, March, and April of 1991. Figures 3-43 and 3-44 display the location of the stations used to specify boundary conditions for each month of the 1990 calibration period.

Unfortunately, data are available for only 11 of the 19 months in the 1989 through 1991 period. The most noticeable gaps in the data set are for the months of November, December, and January both in 1990 and 1991 when no cruises were conducted. In several of the months where boundary stations were sampled, only a portion of the boundary is described and only some of the water quality parameters used in the model were sampled. Efforts were made to discern if there were spatial patterns to be found between the northern and southern ends of the open water boundary with the Gulf of Maine. However, the lack of comprehensive spatial data precluded this determination. Therefore, the simplifying assumption of spatially constant boundary concentrations from Cape Ann to Race Point on Cape Cod was made, except for February through April 1991 when spatial gradients could be determined from the data. Vertical gradients of water quality constituents in the water column were observed in the data and were included in the specification of the boundary conditions.

Figure 3-45 displays all of the surface and bottom data used to specify the boundary conditions. The symbols, an open triangle for surface data and an inverted filled triangle for bottom data, represent mean monthly values. The lines emanating from the triangles represent the standard deviation of the data. The surface water data show evidence of the annual cycle of phytoplankton chlorophyll-a production. Relatively high concentrations of nutrients and low concentrations of chlorophyll-a and POC are observed in February. These are followed by low nutrient concentrations (DIN, PO_4, and DSi) and higher chlorophyll-a and POC concentrations in the spring. By the early summer there

3-71
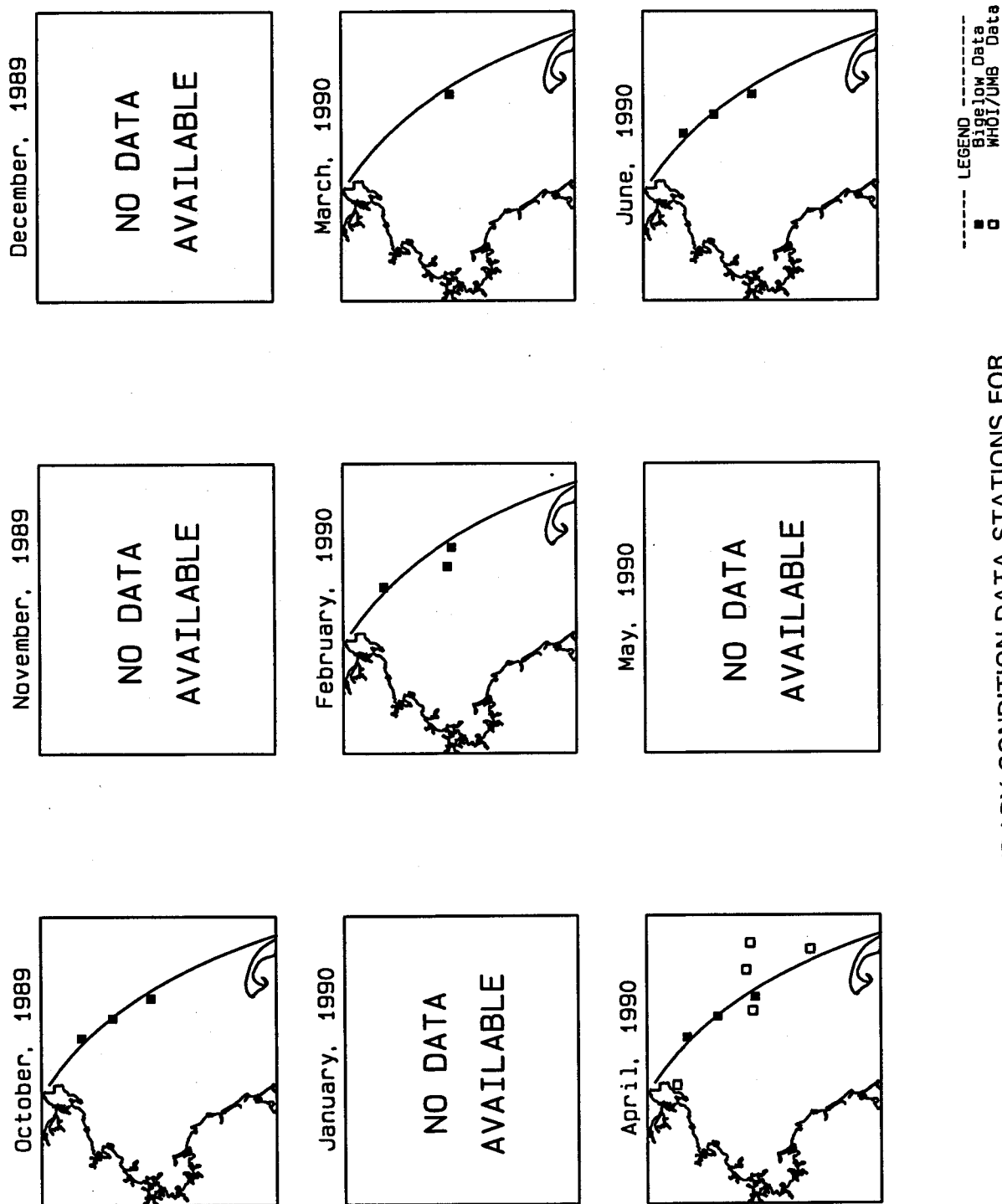
FIGURE 3-43. LOCATIONS OF BOUNDARY CONDITION DATA STATIONS FOR
OCTOBER 1989 THROUGH JUNE 1990

3-72
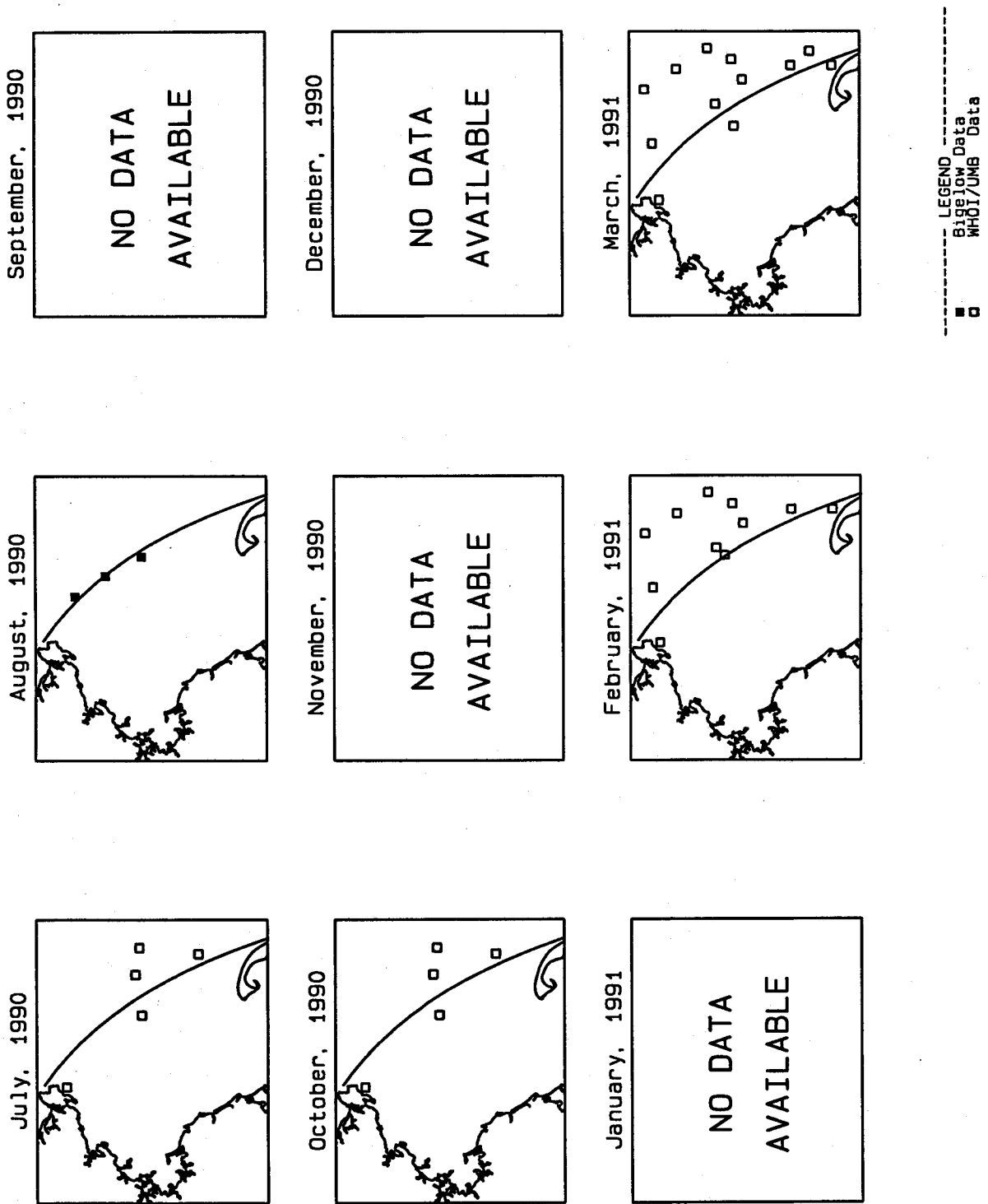
FIGURE 3-44. LOCATIONS OF BOUNDARY CONDITION DATA STATIONS FOR
JULY 1990 THROUGH MARCH 1991
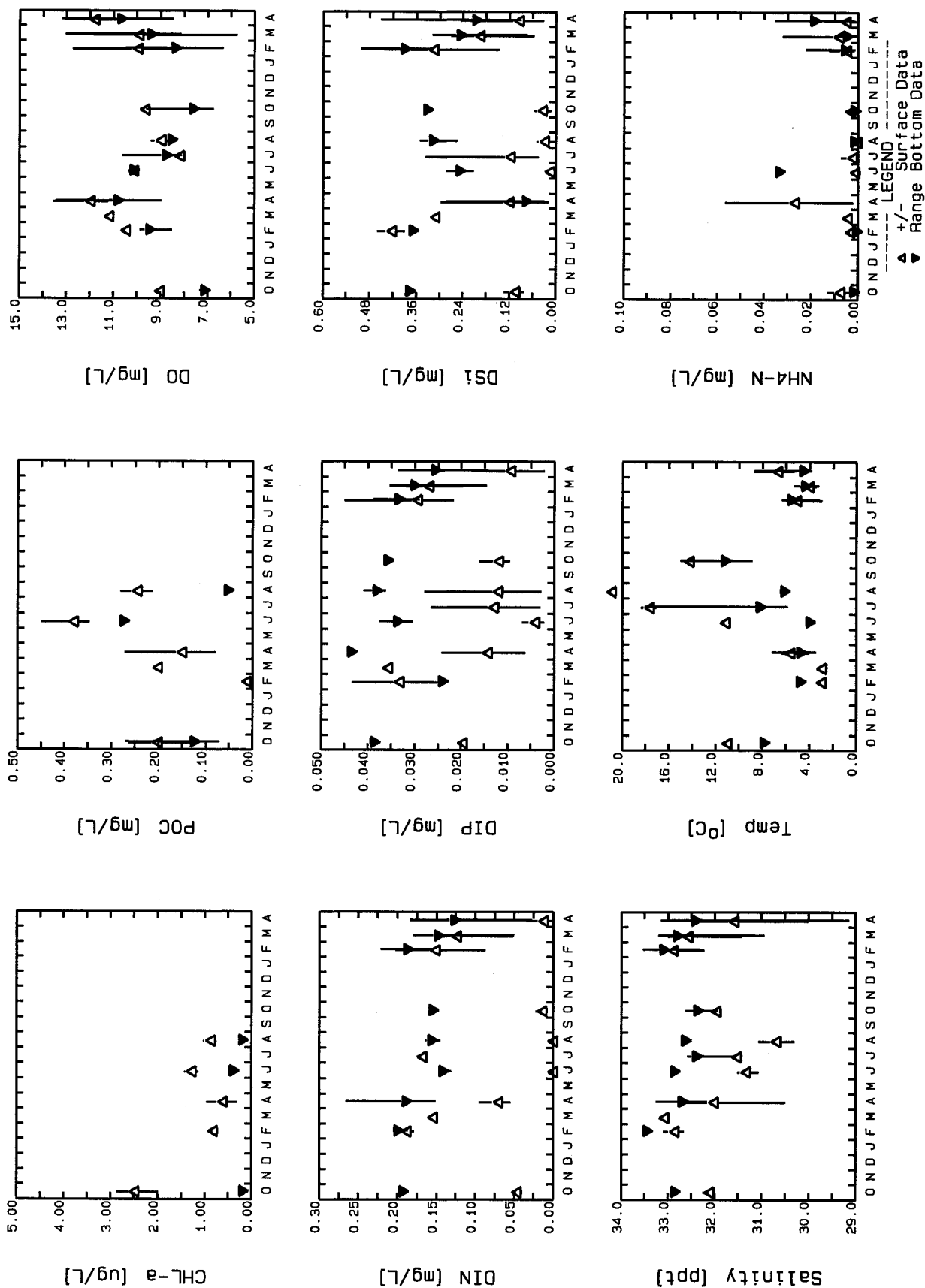
FIGURE 3-45. OCTOBER 1989 THROUGH APRIL 1991 DATA USED TO ASSIGN BOUNDARY CONDITIONS

appears to some nitrogen limitation which reduces chlorophyll-a and POC and also results in an increase in the other dissolved nutrients due to reduced ulitization. With the advent of the fall turnover and decreasing water temperatures and solar radiation, the concentrations of nutrients in the surface waters increase. As has been observed for the stations within Massachusetts and Cape Cod Bay, the boundary stations show a strong annual cycle of surface and bottom water nutrient stratification, with maximum nutrient stratification occurring during the summer months.

There are more data available for the last 3 months of the 1990 period than the previous 16 months. These data indicated a horizontal spatial gradient in various water quality parameters between the northern and southern ends of the model domain boundary. The data indicated lower nutrient concentrations near the southern boundary at the tip of Cape Cod and the boundary conditions were specified accordingly. These lower concentrations may be due to the prevailing current direction within the Bays. As discussed above, it has been observed that fresher nutrient-rich water enters the Bays at the northern boundary near Cape Ann. The water then travels through the Bays system from north to south, permitting the accompanying nutrients to be utilized by phytoplankton. This nutrient-depleted water then exits the system near Race Point located on the northern tip of Cape Cod.

The temperature, salinity, and dissolved oxygen boundary station data also show a seasonal cycle in both the surface and bottom waters. As the water column becomes warmer in the spring the water column becomes stratified, and by late August it is at its most stratified condition. Finally, as air temperature and solar radiation inputs begin to decrease so does the surface water column temperature, until by late fall the water column becomes well mixed. Dissolved oxygen shows a strong seasonal cycle, driven by temperature-mediated DO saturation, water column stratification and primary productivity.

Figures 3-46 and 3-47 present vertical profiles of some of the data used to assign the boundary conditions. These figures show data for the northern portion of the boundary for the first month of the calibration period (October 1989). These figures
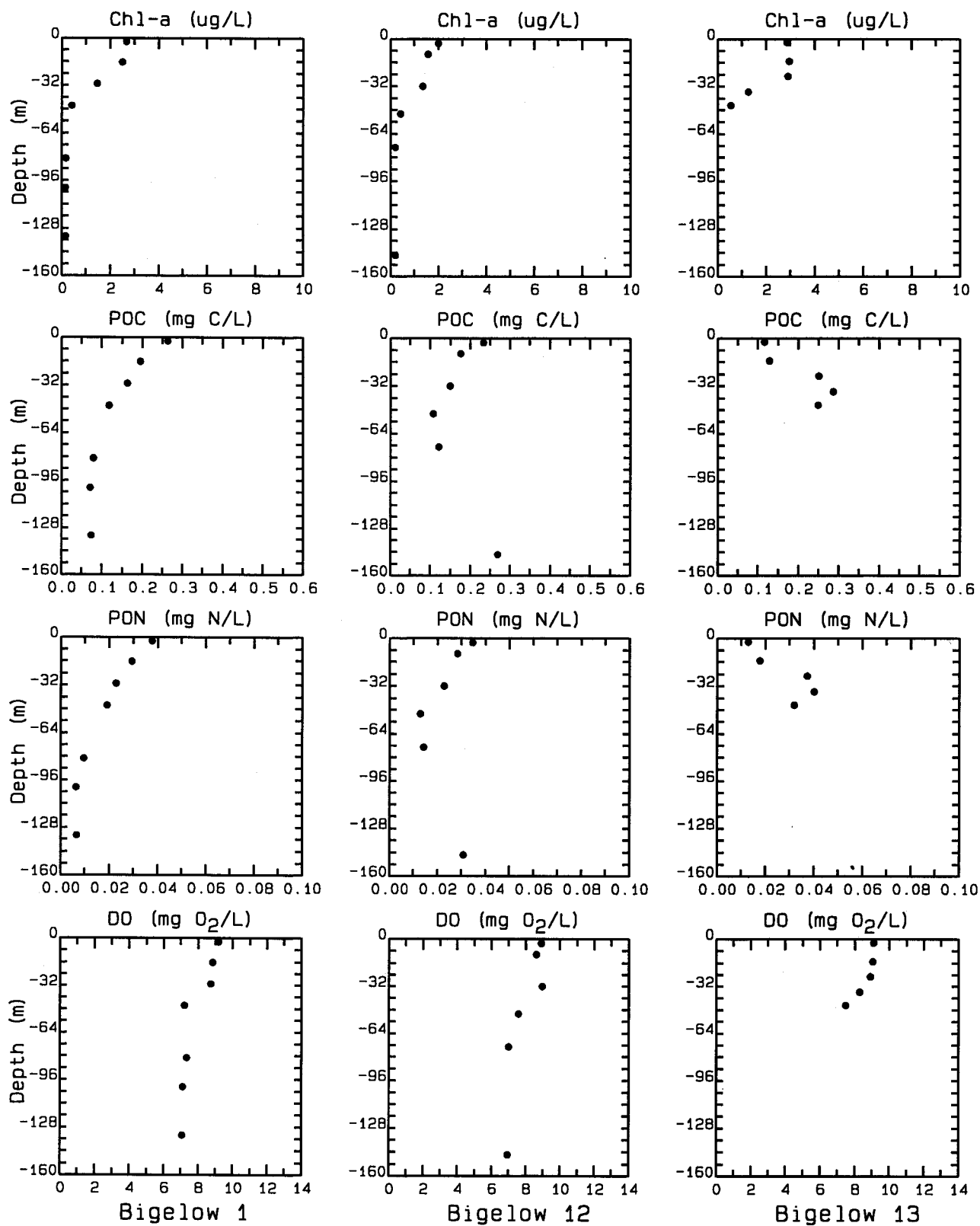
FIGURE 3-46. SAMPLE OF VERTICAL PROFILE DATA USED TO ASSIGN BOUNDARY
CONDITIONS FOR CHL-A, POC, PON AND DO
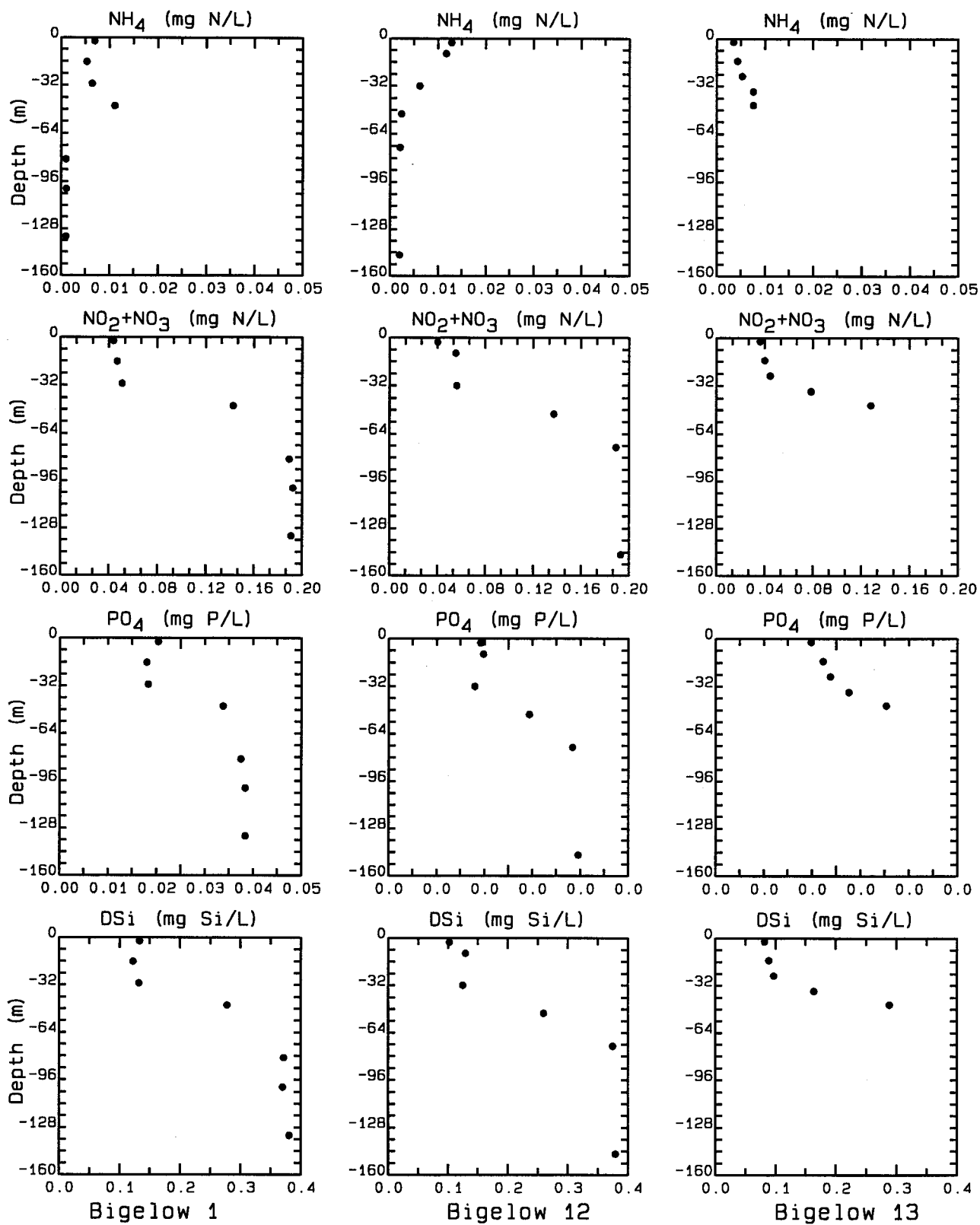
FIGURE 3-47 SAMPLE OF VERTICAL PROFILE DATA USED TO ASSIGN BOUNDARY CONDITIONS FOR NH_4, $NO_2 + NO_3$, PO_4, AND DSi

indicate evidence of phytoplankton growth in the top 30 to 35 meters of the water column. This conclusion is supported by observing (Figure 3-46) elevated concentrations of chlorophyll-a, POC, PON, and DO at the surface of the water column; by observing (Figure 3-47) reduced concentrations of inorganic nutrients in the top 30 to 35 meters of the water column; and by increasing inorganic nutrient ($NO_2 + NO_3$, PO_4, and DSi) concentrations at depth. These types of data were used to estimate the vertical structure in the water column for the open water boundary of the model.

3.4.2 1992 Boundary Concentration Data

The 1992 boundary conditions for January through December 1992 were determined in a different manner than 1990 boundary conditions. Data from 1992 were available from the ongoing outfall relocation water quality monitoring program being conducted by Battelle Ocean Sciences. Farfield surveys were conducted in February, March, April, June, August, and October 1992. Five stations (F21, F22, F12, F08, and F04) were chosen for use in determining boundary conditions, because of their proximity to the boundary of the model domain (Figure 3-48). Unfortunately, these outer most stations are still a distance from the actual model boundary and are on the interior side of the boundary. Furthermore, these stations were sampled for only a few water quality parameters, unlike the biology/productivity stations, which provided a more comprehensive data set. Data were available to determine PO_4, NH_4, $NO_2 + NO_3$, DSi, and, DO boundary conditions. Boundary conditions for the remaining systems in the water quality model were guided by data from 1990 data set and were adjusted during the calibration effort to improve model versus data comparisons at the internal model domain stations as well as the five "boundary" stations.

3.5   SEDIMENT DATA

The physical, chemical, and biological processes that occur in the sediments of coastal environments play an important role in the decomposition of organic matter and the recycling of nutrients. The end-products of these sediment processes can have an
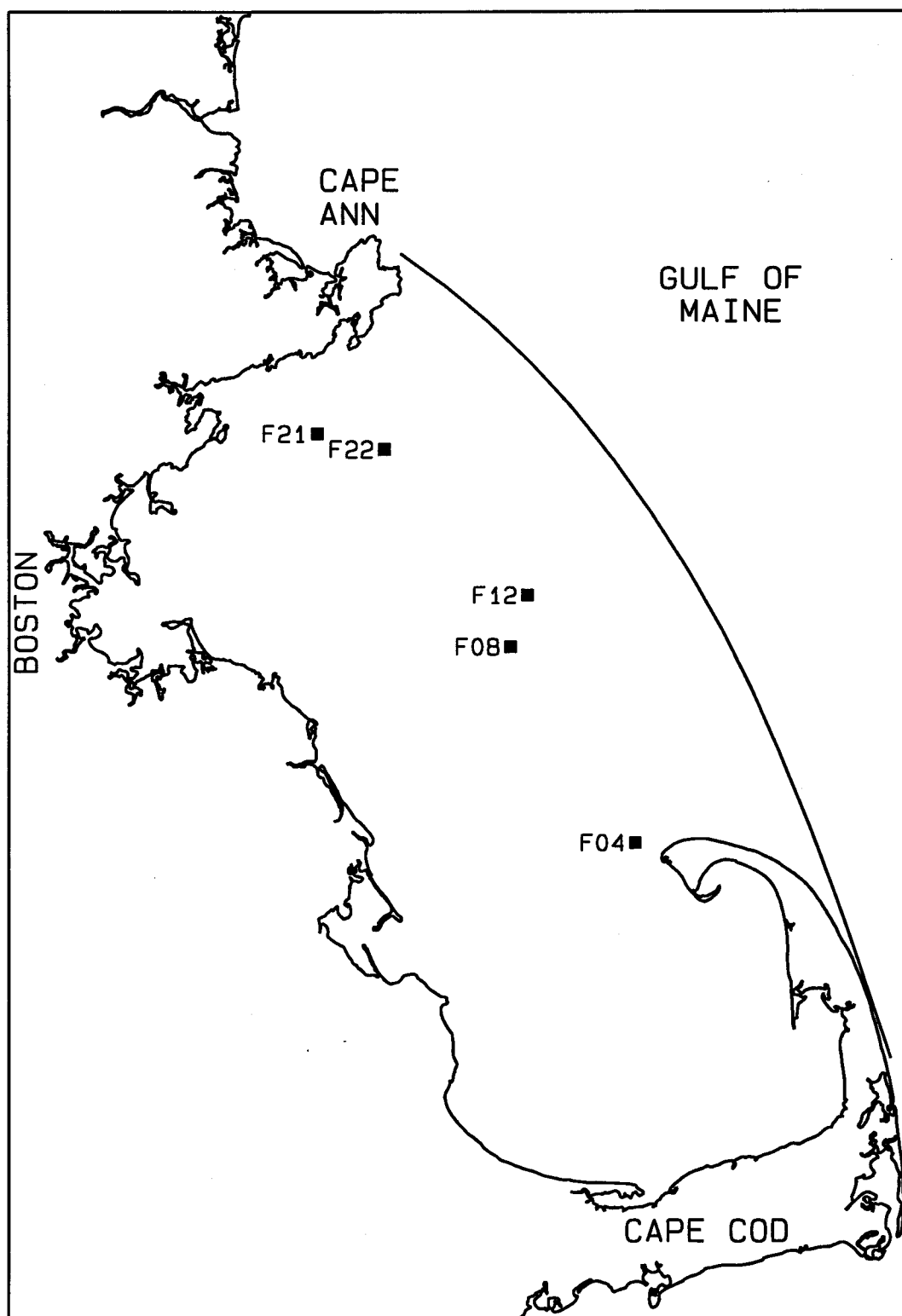
FIGURE 3-48. 1992 SAMPLING STATIONS USED FOR BOUNDARY CONDITIONS

important influence on dissolved oxygen and primary productivity in the overlying water column. During organic matter decomposition in sediments there is considerable oxygen demand which must be supplied from the overlying water column. This sediment oxygen demand (SOD) may comprise a substantial fraction of the total system oxygen consumption. Over lengthy time scales (e.g., years to decades), the sediments can act as an ultimate sink of nutrients and other substances discharged to the water column. Over lesser time scales (e.g., months/seasons to years), however, sediment release of previously-deposited nutrients can be a net source to the water column.

Therefore, in order to gain insight into the potential effects of benthic SOD and nutrient regeneration on the coastal ecosystem caused by the relocation of the MWRA outfall, MWRA funded a series of field and laboratory sampling programs. These studies included measurements of oxygen uptake, nutrient flux and sediment pore water.

Sediment flux and porewater data are available from two sources: the Ecosystems Center of the Marine Biological Laboratory (Giblin et al., 1991, 1993; Tucker et al., 1993) and a program conducted by a joint Battelle Ocean Sciences and University of Rhode Island team (Kelly and Nowicki, 1993). Data were available for 1990 through 1993. Prior to 1993 data were available only for Boston Harbor and the immediate vicinity of Boston Harbor in Broad Sound and Massachusetts Bay. In 1993 some additional nutrient flux measurements were taken in Stellwagen Basin and Cape Cod.

The 1990 study conducted by the Marine Biological Laboratory (MBL) consisted of eight stations: three in the Outer Harbor, two in Broad Sound and three in Massachusetts Bay near the proposed outfall site (see Figure 3-49). Previous studies (SAIC, 1990) suggested that the three Outer Harbor stations (Stations 1, 2, and 3) were being impacted by the Deer Island sewage outfall, as indicated by reducing conditions in the sediments and low abundances of benthic animals. Highly reduced sediments were also present in some areas of Broad Sound (Giblin et al., 1991). Previous investigators have suggested that the presence of these reducing sediments indicated that some material from the Deer Island outfall was being deposited in the areas of Broad Sound. There was no evidence that the
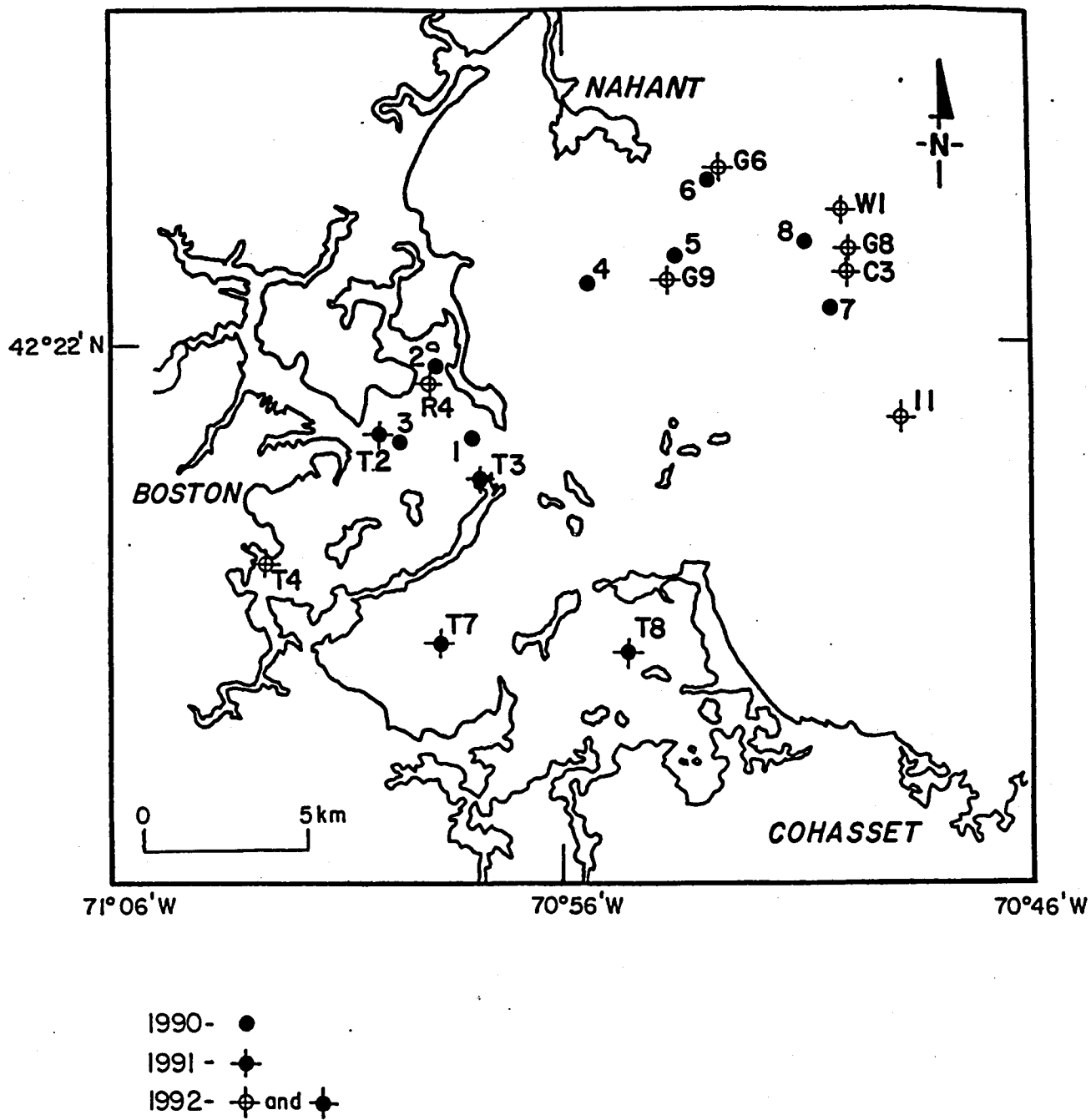
FIGURE 3-49. SEDIMENT FLUX SAMPLING LOCATIONS

other three stations (Stations 6, 7, and 8) received material from the present Deer Island outfall but these stations may receive nutrients and organic matter from the future outfall. Stations 1 through 6 were sampled in September while Stations 7 and 8 were sampled in October. Measurements made for SOD, NH_4 flux, NO_3 flux, and PO_4 flux are shown on Figure 3-50. Stations 1, 2, 3 and 5 appear to be the most impacted by the Deer Island outfall as evidenced by high SOD and NH_4 fluxes from the sediment. The remaining stations located in Massachusetts Bay were found to have relatively low SOD and NH_4 flux rates. Average SOD measurements for the more heavily impacted stations ranged from 0.6 to 2.1 gm O_2/m^2-day while the other stations ranged from 0.25 to 0.35 gm O_2/m^2-day. Average NH_4 fluxes ranged from 106 to 116 mg N/m^2-day at stations 2 and 3 to approximately 60 mg N/m^2-day at stations 1 and 5 to lows of 1-16 mg N/m^2-day at stations 4, 6, 7 and 8. NO_3 flux rates were generally found to be into the sediment at Stations 1, 2, 3, and 5 with site averaged rates from -0.6 to -24.7 mg N/m^2-day (note: negative values denote flux to the sediment). The remaining stations had small net fluxes of NO_3 from the sediment to the overlying water; station averaged NO_3 fluxes ranged from 1 to 2 mg N /m^2-day. Stations 2 and 3 had large PO_4 fluxes out of the sediment with station averages of 52.5 and 200 mg P/m^2-day. Stations 1, 5, 6, 7, and 8 had small PO_4 fluxes out of the sediment with station averages ranging from 0.8 to 5.3 mg P/m^2-day; respectively; station 4 had a small net PO_4 flux into the sediment, with a site average of -0.8 mg P/m^2-day.

In 1991, only four stations (T2, T3, T7 and T8) were sampled by MBL, all in the Outer Harbor region of Boston Harbor, during September. Station locations can be found in Figure 3-49. Measurements were made for SOD as well as NH_4, NO_3 and PO_4 flux rates. Pore water samples were analyzed for DIN, PO_4, alkalinity and sulfide. It has been suggested (Giblin et al., 1992) that the sediments were more oxidized in 1991 than in 1990. This may have been due to Hurricane Bob, which had passed through the region just before the survey. The flux measurements, therefore, may not be typical for Boston Harbor sediments during this time of year. All four stations had similar SOD measurements, as shown on Figure 3-51. Station averaged SOD ranged from 0.69 to 0.93 gm O_2/m^2-day, which are lower than observed for Boston, Harbor stations in 1990.
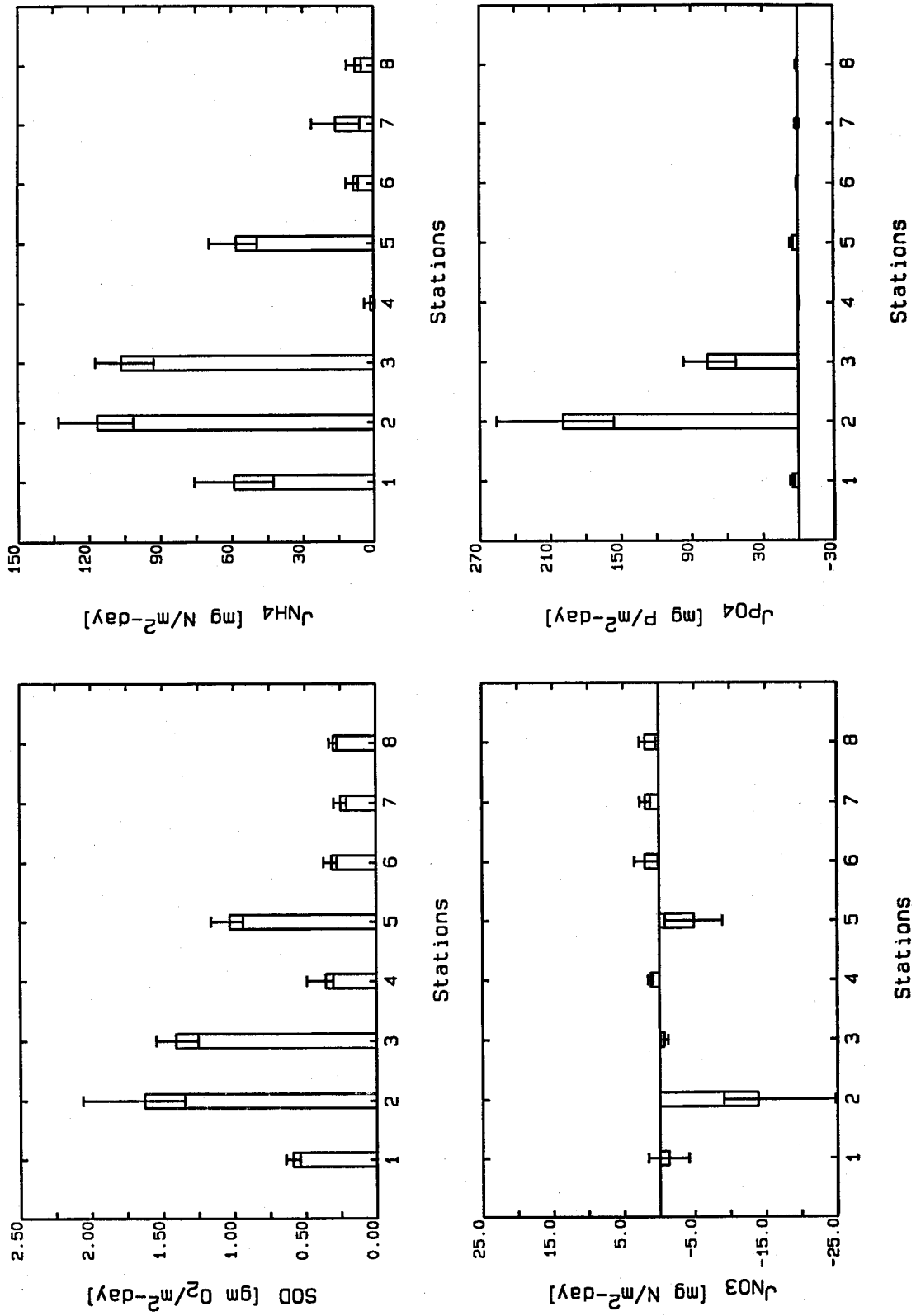
FIGURE 3-50. 1990 SEDIMENT FLUX DATA
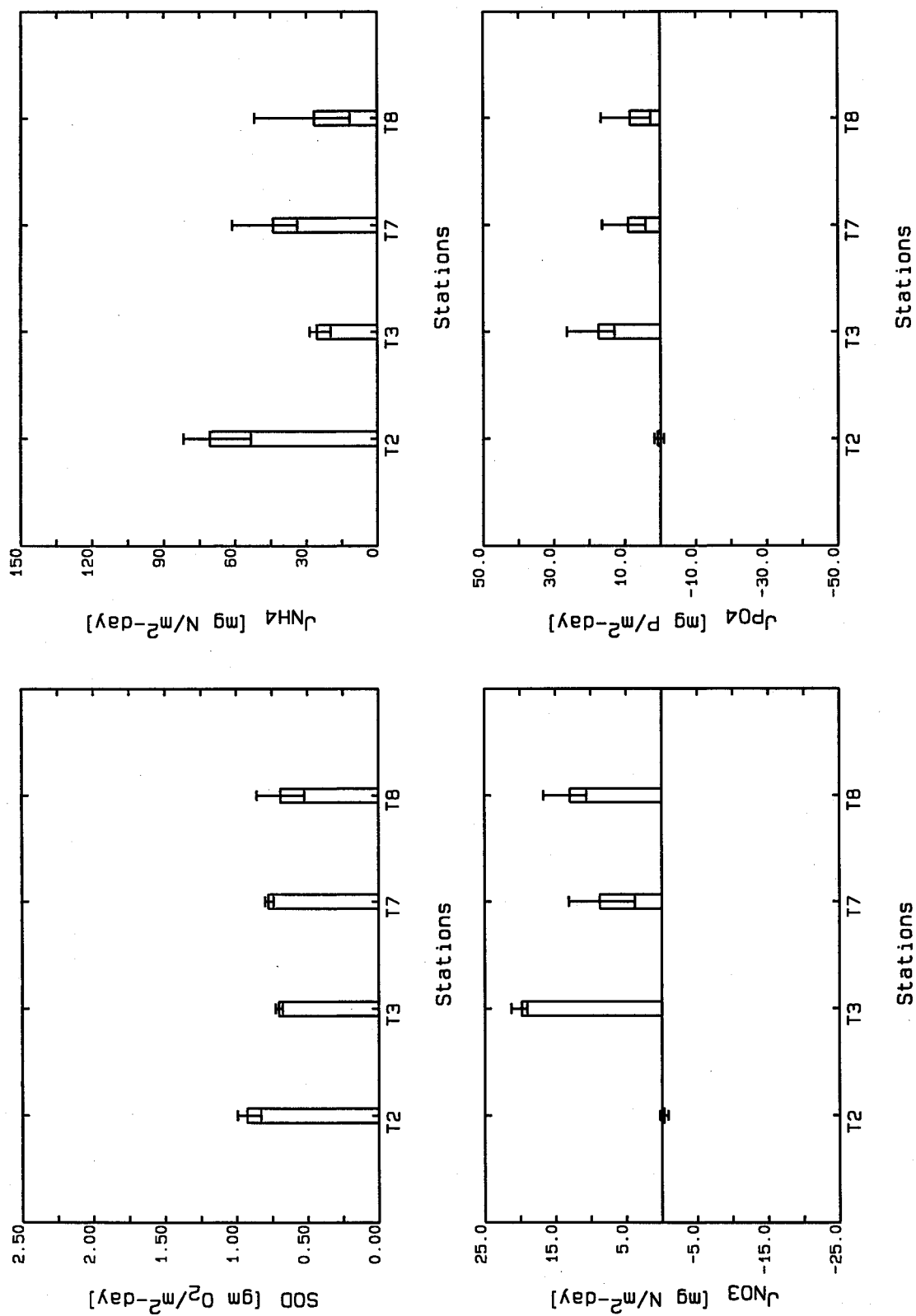
FIGURE 3-51. 1991 SEDIMENT FLUX DATA

NH_4 fluxes varied slightly from station to station, with a low of about 25 mg N/m^2-day at station T3 and a high of 70.8 mg N/m^2-day at station T2. NO_3 fluxes were out of the sediments at three of the four stations in the Harbor in contrast to the 1990 Harbor fluxes which were into the sediment. This suggests that the sediments were more oxidized in 1991 versus 1990. PO_4 fluxes showed a spatial pattern similar to the nitrate fluxes. Stations T3, T7, and T8 had station averaged PO_4 fluxes ranging from 8.5 to 17.4 mg P/m^2-day, while station T2 had a much smaller average PO_4 flux of 0.8 mg P/m^2-day.

During 1992, a more extensive sampling program was conducted. Boston Harbor stations, shown on Figure 3-49, were sampled in April, May, June, August, and November, although not every station was sampled during each survey. Only Station T3 was sampled during each Boston Harbor survey. Stations T2, T7, R4, and T4 were measured only during the August survey. Massachusetts Bay stations (Figure 3-49) were sampled in October and November. Only stations 11, G8, and W1 were sampled in both months. Fluxes were measured for SOD, NH_4, NO_3 and PO_4. Porewater profiles were measured for DIN, PO_4 and sulfide. Sediment denitrification was also estimated using both direct methods (Kelly and Nowicki, 1993 and indirect Giblin et al, 1993) stoichiometric techniques.

Figure 3-52 presents the 1992 sediment flux data grouped by month. Station T3, the site of the former Nut Island sludge discharge continually had the highest rates of SOD observed at any station. SOD flux rates for station T3 averaged about 1.0 gm O_2/m^2-day in April and May and increased in June and August to 1.7 and 2.2 mg O_2/m^2-day. The SOD rate was still high in November, observed at 2.1 mg O_2/m^2-day oxygen uptake at station T8 showed less variation over an annual cycle. In August, when the six Boston Harbor stations were measured, the range in reported SOD, excluding T3, was between 0.7 and 1.41 gm O_2/m^2-day. Measurements of SOD for October and November in Massachusetts Bay ranged from 0.40 to 0.96 gm O_2/m^2-day. The highest values were found at Station W1 and the lowest value at G9.
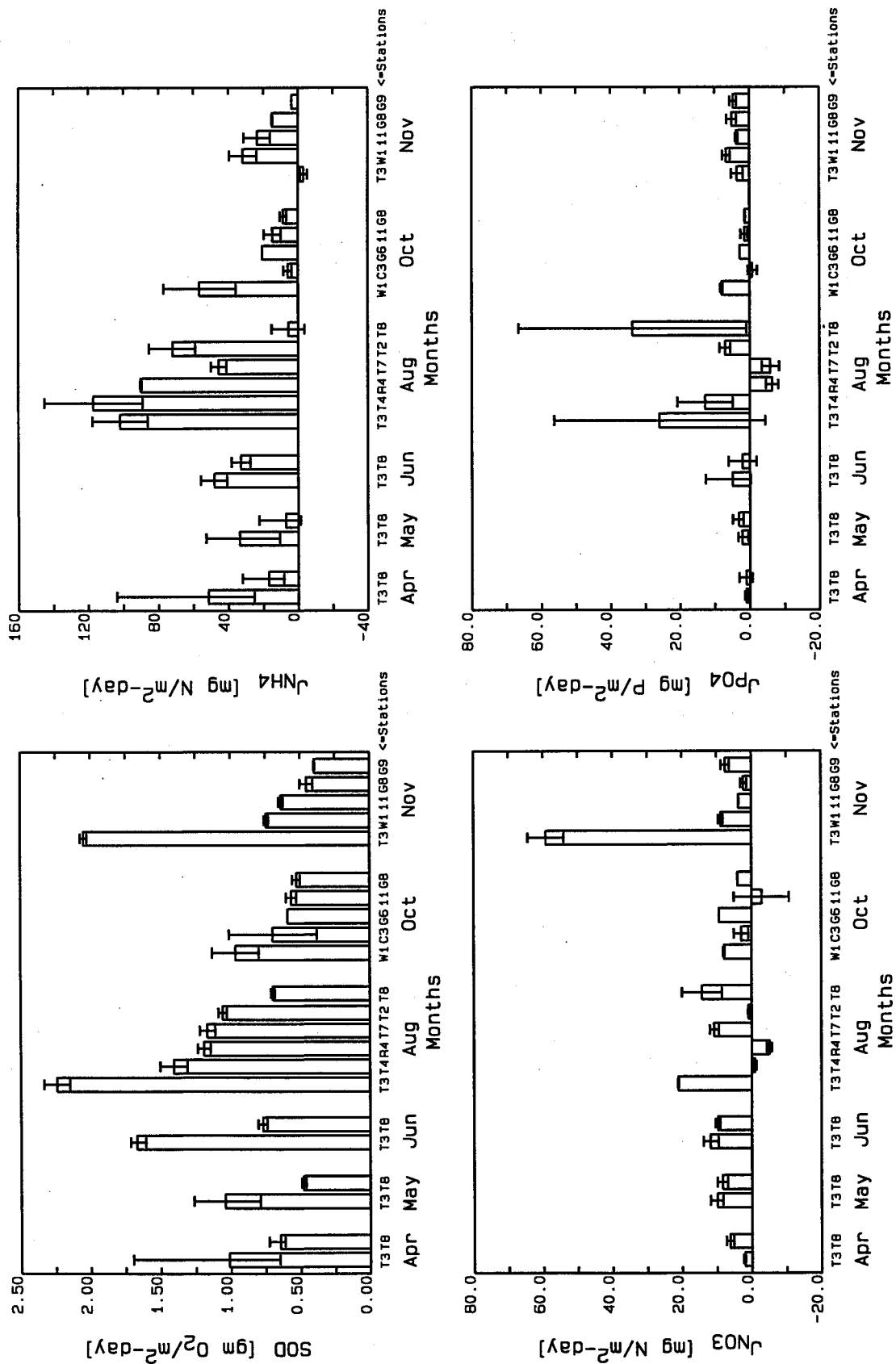
FIGURE 3-52. 1992 SEDIMENT FLUX DATA

NH_4 fluxes showed similar spatial and temporal patterns as the SOD fluxes. Generally station T3 had highest NH_4 fluxes, except for station T4 in August. NH_4 flux rates at station T3 increased between the spring and August from 33.6 - 51.5 mg N/m^2-day to 102 mgN/m^2-day. In November a small NH_4 flux into the sediment (-3.2mg N/m^2-day) was recorded at T3. Station T8 had no temporal pattern for the four months it was sampled. The flux rates at T8 ranged from 5.7 to 32.9 mg N/m^2-day. During August the highest NH_4 flux rate was measured at Station T4 with a value of 117.1 mg N/m^2-day. NH_4 flux rates in Massachusetts Bay during the fall ranged from 3.8 to 56.6 mg N/m^2-day. There was little change between October and November, except for station W1, which had the highest flux rates of those observed in the Bay.

NO_3 flux rates tended to increase during the year at both Stations T3 and T8. Station T3 also had an unusually high nitrate flux of 59.2 mg N/m^2-day in November. This may have been due to a large population of filter feeding amphipods, which were first observed in June at this site (Giblin et al., 1993). In August, flux rates ranged from -5.0 to 21.1 mg N/m^2-day. Fluxes into the sediment were observed at Stations R4 and T4. In Massachusetts Bay, the rates were similar and low at all stations during October and November, ranging from -2.9 to 8.8 mg N/m^2-day. The highest rates were found at W1.

PO_4 fluxes were small during April, May, and June at Stations T3 and T8, with station averages ranging from 1.1 to 5.1 mg P/m^2-day. During August PO_4 flux rates at stations T3 and T8 increased significantly, to 26.0 and 33.8 mg P/m^2-day, respectively. There was also considerable variability in the replicates of these core. Stations T2 and T4 had smaller positive flux rates while stations T7 and R4 had PO_4 fluxes into the sediment. In Massachusetts Bay, the highest PO_4 flux rates were measured at W1 and were higher in October as compared to November. PO_4 flux rates were, in general, small in Massachusetts Bay, with station averages ranging from -0.8 to 8 mg P/m^2-day.

Denitrification in coastal systems may remove a substantial fraction of the nitrogen load delivered to coastal waters (Seitzinger, 1980). The process of denitrification converts dissolved inorganic nitrogen to nitrogen gas. This process, then, removes dissolved

inorganic nitrogen that could become available to phytoplankton for primary production and converts it to a form which is nonnutritive, unutilized and exported from the water to the atmosphere via degassing.

Benthic dentification in Boston Harbor had been a controversial issue before the sediment monitoring program was begun. Christensen (1991) speculated that denitrification might remove at least 25 percent, and perhaps as much as 70 percent, of the nitrogen discharged to the Harbor. Initial dentrification measurements were made in 1991 (Gilblin et al., 1992, Kelly and Nowicki, 1992, Nowicki, 1994) and were followed by a more comprehensive set of measurements in 1992 (Giblin et al., 1993, Kelly and Nowicki, 1993). Additional measurements of denitrification at several Boston Harbor stations, as well as several Massachusetts Bay stations were made in 1993 (Giblin, 19995).

Giblin et al. (1993) estimated 1992 denitrification rates for Boston Harbor to range from 7.8 to 89.3 mg N/m^2-day with an overall mean of 35 mg N/m^2-day. These compared favorably with those estimated by Kelly and Nowicki (1993) which ranged from 8.8 to 113.6 mg N/m^2-day with an average of 33.6 mg N/m^2-day. In Massachusetts Bay the average MBL estimated denitrification rate for October and November was 22.4 mg N/m^2-day. In 1992 Kelly and Nowicki measured denitrification at the same stations and time periods and found an overall mean of 14.9 mg N/m^2-day. Utilizing these newer data Kelly and Nowicki (1993) performed a nitrogen mass balance for Boston Harbor, and estimated that a maximum of 11 to 12 percent of the N input to the Harbor is removed by denitrification in bottom sediments during the warmer part of the year and probably less than 10 percent on an annual cycle.

SECTION 4

WATER QUALITY MODEL

4.1 INTRODUCTION

4.1.1 Conservation of Mass

The modeling framework used in this study and detailed in this report is based upon the principle of conservation of mass. The conservation of mass accounts for all of a material entering or leaving a body of water, transport of the material within the water body, and physical, chemical and biological transformations of the material. For an infinitesimal volume oriented along the axes of a three-dimensional coordinate system, a mathematical formulation of the conservation of mass may be written:

$$\frac{\partial c}{\partial t} = \frac{\partial}{\partial x}(E_x \frac{\partial c}{\partial x}) + \frac{\partial}{\partial y}(E_y \frac{\partial c}{\partial y}) + \frac{\partial}{\partial z}(E_z \frac{\partial c}{\partial z}) - U_x \frac{\partial c}{\partial x} - U_y \frac{\partial c}{\partial y} - U_z \frac{\partial c}{\partial z}$$

dispersive transport   advective transport

$$\pm \; S(x,y,z,t) \quad + \quad W(x,y,z,t) \tag{4-1}$$

sources or sinks   external inputs

where:

c = concentration of the water quality variable $[M/L^3]$,

t = time $[T]$,

E = dispersion (mixing) coefficient due to tides and density and velocity gradients $[L^2/T]$,

U = advective velocity $[L/T]$,

S = sources and sinks of the water quality variable, representing kinetic interactions $[M/L^3\text{-}T]$,

W = external inputs of the variable c $[M/L^3\text{-}T]$,

x,y,z = longitudinal, lateral and vertical coordinates,

M,L,T = units of mass, length and time, respectively.

The modeling framework employed in this study is made up of three components: the transport of water quality variables within the Bay due to density-driven currents and dispersion; the kinetic interactions between variables; and the external inputs of the water quality variables. The transport within the Bay is a complex process and is affected by freshwater inflows, temperature, wind and offshore forcings from the Gulf of Maine. The kinetics control the rates of interactions among the water quality constituents. Ideally, in a modeling effort, they should be independent of location per se, although they may be functions of exogenous variables, such as temperature and light, which may vary with location. External inputs of nutrients and oxygen-demanding material are derived from municipal and industrial discharges, combined sewer overflows (CSOs), natural surface runoff, groundwater, and atmospheric deposition to the water surface of Massachusetts Bay.

The kinetic framework employed in the Massachusetts Bays eutrophication and sediment nutrient flux model (BEM) draws primarily from modeling efforts on the Chesapeake Bay system (Cerco and Cole, 1993; Di Toro and Fitzpatrick, 1993) and Long Island Sound (HydroQual, 1991). These models in turn can trace their ancestry back to the early eutrophication models developed by Di Toro et al. (1971), Thomann et al. (1974), Di Toro and Matystik (1980), Di Toro and Connolly (1980), and Thomann and Fitzpatrick (1982). These early modeling frameworks had gained wide acceptance within the modeling community and in fact the modeling framework used in the Potomac Estuary study (Thomann and Fitzpatrick, 1982) became the basis for the EUTRO-WASP modeling code supported by the US EPA.

The principal differences between early models of the 1970s and 1980s and the Chesapeake Bay and Long Island Sound eutrophication models is the addition of state-variables which distinguish between labile and refractory components of organic matter (carbon, nitrogen, and phosphorus) and the inclusion of a sediment nutrient flux submodel which is key to closing the mass balance between the water column and the

sediment bed. These refinements were made after a preliminary eutrophication model of Chesapeake Bay was developed by HydroQual, Inc. (1987). During the projection phase of that study, it was discovered that model predictions did not show a response to nutrient reductions because the model did not include a direct mass balance based coupling between the water column and the sediment bed. Since there was no direct coupling between the water column and the bed, the sediment oxygen demand and nutrient fluxes did not change in response to nutrient reduction scenarios and therefore there was little change in water column water quality.

In response to this finding the next generation of eutrophication based water quality models developed for Chesapeake Bay and Long Island Sound included the development of a nutrient flux submodel (Di Toro and Fitzpatrick, 1993) and included additional water quality state-variables, which recognized the labile and refractory components of detrital algae and other organic matter. Evidence for the labile and refractory nature of organic matter has long been noted in the literature (Grill and Richards, 1964; Foree and McCarthy, 1970; Otsuki and Hanya, 1972; Garber, 1984; Parsons et al., 1984; Westrich and Berner, 1984; and Pett, 1989).

The modeling framework used in this study utilizes the 24 state-variables shown in Table 4-1. Data are available to make direct comparisons against model computations for six of the state-variables, as noted in Table 4-1. Data are also available by which to calibrate the water quality model by combining pairs or groups of model state-variables as also shown in Table 4-1.

The model framework, discussed below, incorporates these state-variables and is designed to simulate the annual cycle of phytoplankton production, its relation to the supply of nutrients, and its effect on dissolved oxygen. The calculation is based on formulating the kinetics which govern the interactions of the biota and the various nutrient forms, and the application of these kinetics to Massachusetts Bay within the context of mass conservation equations.

TABLE 4-1. STATE-VARIABLES UTILIZED BY THE KINETIC FRAMEWORK

*	1.	- salinity (S)
✓	2.	- phytoplankton carbon - winter diatoms (P_{c1})
✓	3.	- phytoplankton carbon - summer assemblage (P_{c2})
✓	4.	- refractory particulate organic phosphorus (RPOP)
✓	5.	- labile particulate organic phosphorus (LPOP)
✓	6.	- refractory dissolved organic phosphorus (RDOP)
✓	7.	- labile dissolved organic phosphorus (LDOP)
*	8.	- dissolved inorganic phosphorus (PO_4)
✓	9.	- refractory particulate organic nitrogen (RPON)
✓	10.	- labile particulate organic nitrogen (LPON)
✓	11.	- refractory dissolved organic nitrogen (RDON)
✓	12.	- labile dissolved organic nitrogen (LDON)
*	13.	- ammonia nitrogen (NH_3)
*	14.	- nitrite + nitrate nitrogen ($NO_2 + NO_3$)
*	15.	- biogenic silica (BSi)
*	16.	- dissolved available silica (DSi)
✓	17.	- refractory particulate organic carbon (RPOC)
✓	18.	- labile particulate organic carbon (LPOC)
✓	19.	- refractory dissolved organic carbon (RDOC)
✓	20.	- labile dissolved organic carbon (LDOC)
✓	21.	- reactive dissolved organic carbon (ReDOC)
✓	22.	- algal exudate dissolved organic carbon (ExDOC)
	23.	- aqueous sediment oxygen demand (O_2^*)
*	24.	- dissolved oxygen (DO)

FIELD MEASUREMENTS

* < = > Direct Measurements

✓ < = > Indirect Measurements

Chlorophyll-a ⇒ 2 + 3

	Particulate	Dissolved
Carbon	2 + 3 + 17 + 18	19 + 20 + 21 + 22
Nitrogen	9 + 10	11 + 12
Phosphorus	4 + 5	6 + 7

The following section presents the conceptual framework for the water quality kinetics. A full set of the equations used for the water column portion of the model

framework are presented in Appendix A - Water Column Kinetics. A brief overview of the sediment submodel is presented in this section, while a more detailed mathematical presentation of the sediment model is presented in Appendix B - Sediment Flux Submodel. The reader is also referred to Di Toro and Fitzpatrick (1993) for a complete description of the sediment submodel and its calibration to the Chesapeake Bay data set.

4.2 EUTROPHICATION KINETICS

4.2.1 General Structure

Salinity is included in the water quality modeling framework to insure that the water quality model is coupled properly to the hydrodynamic model. If the water quality model is able to reproduce the salinity fields as computed by the hydrodynamic model, this implies that information from the hydrodynamic model has not been lost as a result of the use of grid aggregation and the time-averaging of hydrodynamic transport. Temperature is obtained directly from the hydrodynamic model computations. Temperature is an important variable since the biological and chemical processes that occur within the system are temperature-mediated. In addition, temperature, together with salinity, determines the saturation value for dissolved oxygen within the water column.

For salinity there are no reaction kinetics involved; i.e., salinity is conservative. There are no direct sources or sinks of salinity, other than via exchange with the model boundaries or via freshwater dilution resulting from wastewater treatment plant effluents and from rivers (such as the Neponset, Charles, etc.) draining to the Bays.

Figure 4-1 presents the principal kinetic interactions for the phosphorus and nitrogen nutrient cycles. In the phosphorus system kinetics, PO_4 is utilized by phytoplankton for growth. Phosphorus is returned from the phytoplankton biomass pool to the various dissolved and particulate organic phosphorus pools and to PO_4 as a result of endogenous respiration and zooplankton grazing. The various forms of organic phosphorus undergo hydrolysis and mineralization and are converted to PO_4 at temperature-dependent rates.
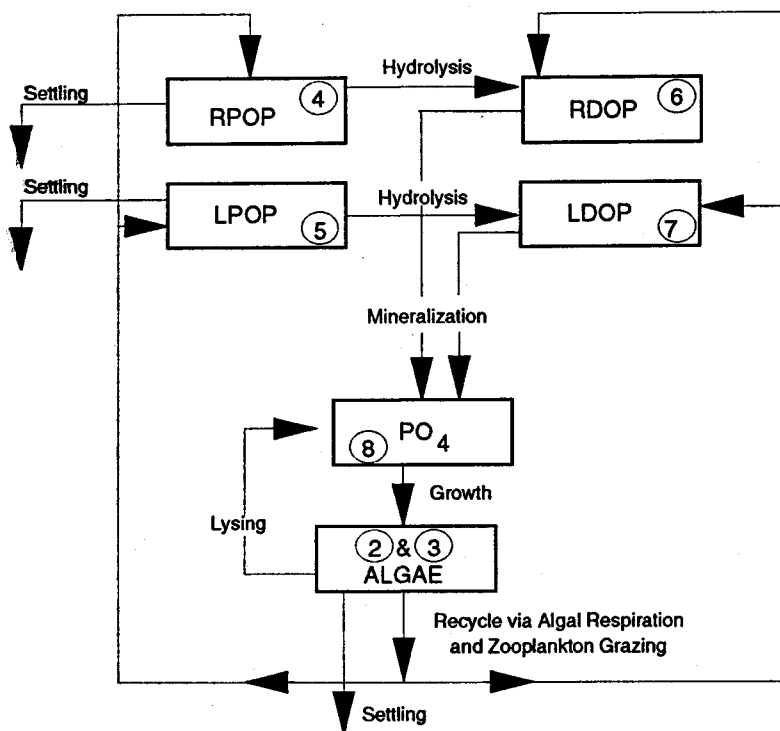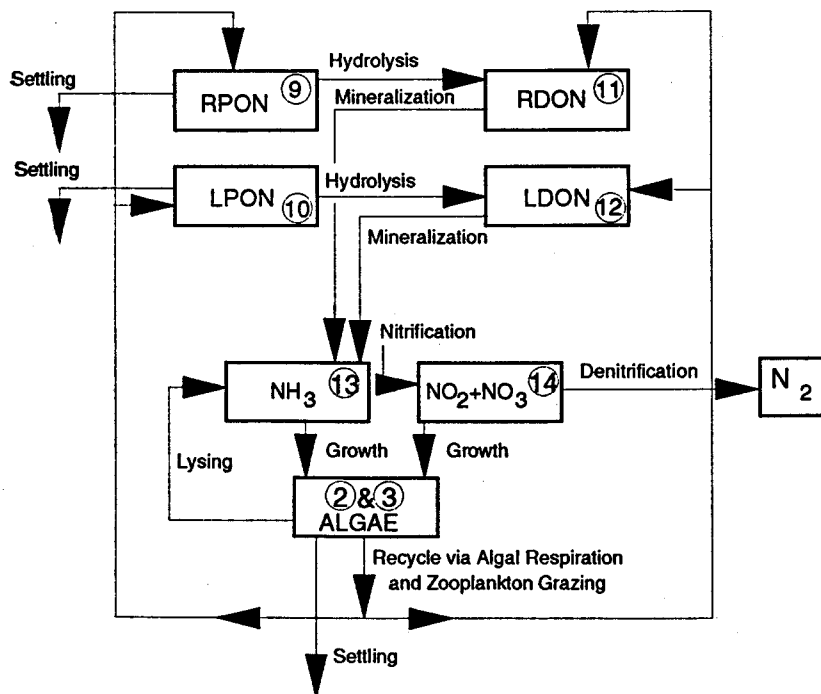
FIGURE 4-1. PRINCIPAL KINETIC INTERACTIONS FOR PHOSPHORUS AND NITROGEN

The kinetics of the nitrogen species (Figure 4-1) are fundamentally the same as the kinetics of the phosphorus system. NH_4 and $NO_2 + NO_3$ are used by phytoplankton for growth. NH_4 is the preferred form of inorganic nitrogen for algal growth, but phytoplankton will utilize $NO_2 + NO_3$ for growth as NH_4 concentrations become depleted. Nitrogen is returned from algal biomass and follows pathways that are similar to those of phosphorus. Organic nitrogen undergoes hydrolysis and mineralization and is converted to NH_4 at a temperature-dependent rate; NH_4 is then converted to NO_3 (nitrification) at a temperature- and oxygen-dependent rate. In the absence of oxygen, NO_3 can be converted to nitrogen gas (denitrification) at a temperature-dependent rate.

The silica cycle is illustrated on Figure 4-2. Inorganic or available silica is utilized by diatomaceous phytoplankton during growth. Silica is returned to the biogenic silica pool as a consequence of algal respiration and zooplankton grazing and must undergo mineralization processes before becoming available for phytoplankton growth.

The transformation processes of organic carbon are also shown on Figure 4-2. Organic carbon sources include anthropogenic inputs and the by-products of primary production and zooplankton grazing. POC undergoes hydrolysis to form DOC. DOC can then undergo bacterially mediated oxidation.

Dissolved oxygen is coupled to the other state-variables, as shown on Figure 4-3. The sources of oxygen included in the model are atmospheric reaeration and algal photosynthesis. The sinks of oxygen include: algal respiration; oxidation of detrital algal carbon and organic carbon discharged from wastewater treatment plant facilities and nonpoint source discharges; nitrification; and sediment oxygen demand.

The water quality model also includes a sediment submodel that is coupled to the water column. This model was originally developed by HydroQual (Di Toro and Fitzpatrick, 1993) for the joint U.S. EPA/U.S. Army Corps of Engineers study of Chesapeake Bay. The framework of the sediment submodel includes three principal processes: the deposition of particulate organic matter (POM) to the sediment from the water column; the decay or
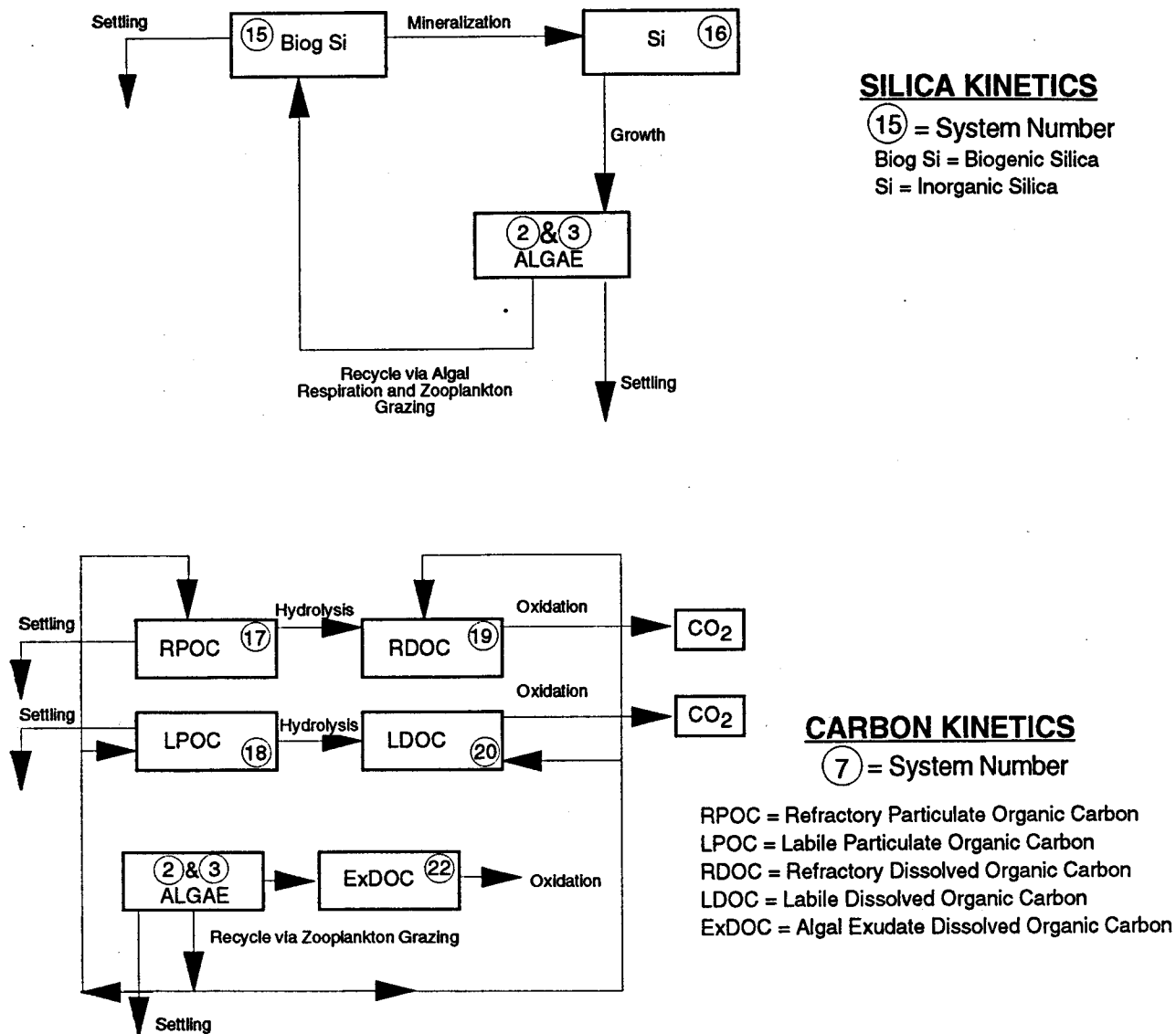
FIGURE 4-2. PRINCIPAL KINETIC INTERACTIONS FOR SILICA AND ORGANIC CARBON
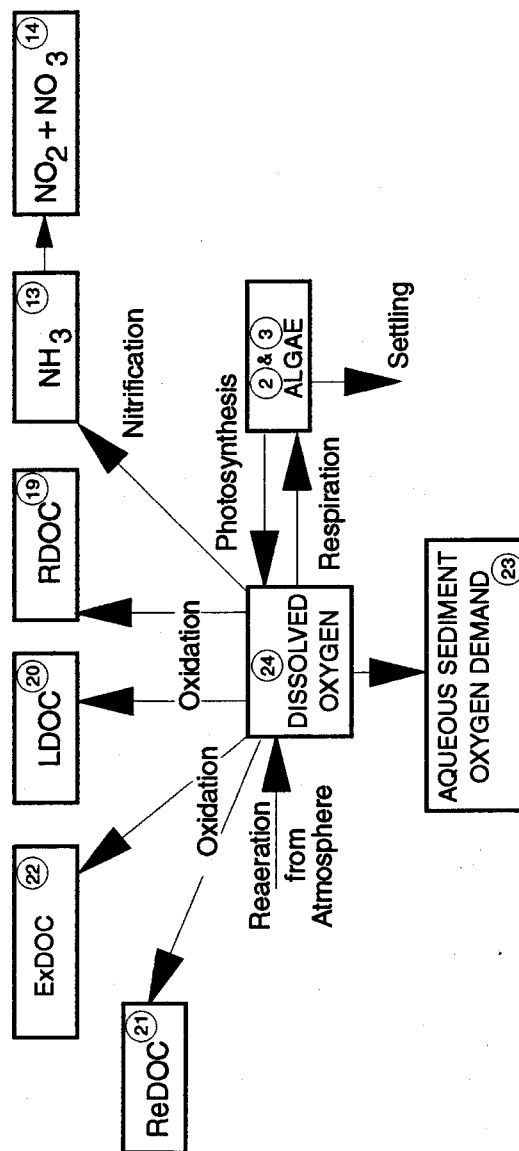
DISSOLVED OXYGEN

(24) = System Number

LDOC = Labile Dissolved Organic Carbon
RDOC = Refractory Dissolved Organic Carbon
NH_3 = Ammonia
$NO_2 + NO_3$ = Nitrite + Nitrate
ReDOC = Reactive Dissolved Organic Carbon

$NO_2 + NO_3$ (14)

NH_3 (13)

RDOC (19)

LDOC (20)

ExDOC (22)

ReDOC (21)

(24) DISSOLVED OXYGEN

(2 & 3) ALGAE

AQUEOUS SEDIMENT OXYGEN DEMAND (23)

Nitrification

Photosynthesis

Respiration

Settling

Oxidation

Oxidation

Oxidation

Reaeration from Atmosphere

FIGURE 4-3. PRINCIPAL KINETIC INTERACTIONS FOR DISSOLVED OXYGEN

diagenesis of the POM in the sediment; and a balance between the flux of resulting dissolved end-products to the overlying water column and the burial of dissolved and particulate end-products via sedimentation.

4.2.2 Phytoplankton

The present version of the water quality model considers two functional phytoplankton groups: winter and summer. These distinctions are made to recognize some of the physiological differences between the phytoplankton species that dominate in each of these seasons in terms of optimal temperature and light conditions and nutrient requirements. The winter functional group is characterized as favoring low temperature and light conditions and as having a high requirement for silica in addition to nitrogen and phosphorus, as a nutrient source. The summer group represents a mixed population of phytoplankton, including greens, blue-greens, dinoflagellates and some diatoms. This group favors higher temperature and light conditions and has lower silica requirements than does the winter group.

The kinetic framework used for both functional algal groups is largely the same. Differences between the groups are expressed by the choice of model coefficients. The growth rate (G_p) in the present model is affected by growth reduction factors for temperature, light and available nutrients, as shown in Equation (4-2):

$$G_P = \mu_{Pmax}(T_{opt}) \quad \bullet \quad G_T(T) \quad \bullet \quad G_I(I) \quad \bullet \quad G_N(N) \qquad (4\text{-}2)$$

$$\text{temperature} \qquad \text{light} \qquad \text{nutrients}$$

where

$$\mu_{Pmax}(T_{opt}) \quad = \text{ nutrient saturated growth rate at the optimal temperature}$$

$$G_T(T) \quad = \text{ the reduction factor caused by temperature}$$

$$G_I(I) \quad = \text{ the reduction factor caused by light attenuation}$$

$G_N(N)$ = the reduction factor caused by nutrient limitation.

The algal growth model used in this study draws directly from Laws and Chalup (1990) and an earlier modeling framework developed by Shuter (1979). The following paragraphs provide an overview of the Laws/Chalup model. In the Laws/Chalup model, the carbon in the phytoplankton cell is considered to be found in one of four compartments: structural carbon (S), reservoir or storage carbon (R), carbon associated with the light reactions (photochemical reactions) of photosynthesis (L), or carbon associated with the dark reactions (carbohydrate production and protein and lipid synthesis) of photosynthesis (D). Hence, total cell carbon, $C = S + R + L + D$. Chlorophyll is assumed to exist only in the L portion of the cell. Nutrients (nitrogen, phosphorus, and silica) are found in the S, L, and D portions of the cell and are assumed to be found in the same ratios in each of these pools. R is assumed to consist entirely of C storage products (carbohydrates and lipids) and hence contains no nutrients. The fraction of C allocated to structural purposes (S/C) is assumed to be constant and independent of growth conditions.

The steady-state gross photosynthetic rate per cell (ρ) is described by

$$\rho = G_{prl} \, L \, I = G_{prd} \, D \qquad (4\text{-}3)$$

where I is the incident irradiance; G_{prd} is the gross photosynthetic rate per unit D and is a constant; and G_{prl} is the gross rate of photosynthesis per unit L per unit light intensity and is a function of environmental conditions. Respiration losses are assumed to be described by

$$k_{PR} = k_{RB} + k_{RG} \, G_{prd} \, D \qquad (4\text{-}4)$$

where k_{RB} is the basal respiration rate per cell, i.e. the rate required to maintain the cell in the absence of growth, and k_{RG} is the growth-rate-dependent respiration coefficient (Laws and Bannister, 1980). The substrate for respiration is assumed to come from the R pool.

From the foregoing assumptions, it follows that the rate of nutrient assimilation f_N is constrained by

$$\frac{d}{dt}(S+L+D) = W_{Nx} \, f_N \tag{4-5}$$

where W_{Nx} is the ratio of C to nutrient x (either nitrogen, phosphorus or silica). It also follows that

$$\frac{dC}{dt} = G_{prd} \, D - k_{RB} - k_{RG} \, G_{prd} \, D \tag{4-6}$$

Under conditions of balanced growth it must be true that for any component X of the cell,

$$\mu = \frac{1}{X} \frac{dX}{dt} \tag{4-7}$$

where μ is the growth rate in units of inverse time. Combining Equations (4-6) and (4-7) yields

$$\mu \, C = G_{prd} \, D - k_{RB} - k_{RG} \, G_{prd} \, D \tag{4-8}$$

Laws and Chalup then go on to define the assumptions and conditions under which a nutrient saturated version of Equation 4-8 can be developed. The nutrient saturated growth rate, μ_{Pmax}, is of the form

$$\mu_{Pmax} = \frac{G_{prd}(1 - k_{RG})(1 - S/C)I}{I + G_{prd}/G_{prls}} - \frac{k_{RB}}{C} \tag{4-9}$$

where G_{prls} is the nutrient-saturated value of G_{prl}. Laws and Chalup then account for the relationship between light and G_{prls} by use of Equation (4-10)

$$G_{prls} = \frac{G_{prlo}}{1 + I/I_s} \qquad (4\text{-}10)$$

where G_{prlo} is the value of G_{prls} when $I = 0$, and I_s is the value of I when $G_{prls} = 0.5G_{prlo}$.

In the natural environment, the light intensity or incident irradiance, I, to which the phytoplankton are exposed is not uniformly at the optimum value. At the surface and near-surface of the air-water interface, photosynthesis occurs at or near maximum rates due to high light intensities, while at depths below the euphotic zone, light is not available for photosynthesis due to attenuation by background and algal related turbidity. During the day the light intensity at the air-water interface varies as a function of the angle of the sun relative to the horizon. Therefore, the BEM framework was designed to account for both of these factors. To account for the effect of variations of available light as a function of depth, the light intensity, I(z), at any depth, z, is related to the incident surface intensity, I_{surf}, via the extinction coefficient, k_e, through the formula $I(z) = I_{surf} \exp(-k_e z)$. The average light intensity to which the phytoplankton are exposed within a water column slice of thickness H may be obtained from the following integral:

$$I_{av} = \frac{1}{H} \int_0^H I(z)\, dz \qquad (4\text{-}11)$$

where:

$I(z)$ $= I_{surf}\, e^{-k_e z}$,

e $= 2.718$,

H $=$ thickness of water column slice (m),

k_e $=$ the total extinction coefficient, computed from the sum of the base (non-algal related) light attenuation, k_{ebase}, and the self-shading attenuation due to the ambient phytoplankton population, $k_c P_{chl\text{-}a}$, (m^{-1}),

k_{ebase} $=$ the base extinction coefficient due to background conditions created by natural turbidity and exogenous suspended solids (m^{-1}),

k_c $=$ the algal related extinction coefficient per unit chlorophyll $(m^2/mg\ chl\text{-}a)$,

$P_{chl\text{-}a}$ $=$ the ambient phytoplankton population as chlorophyll (mg chl-a/L), where $P_{chl\text{-}a} = a_{ChlC}\, P_c$,

P_c = the ambient phytoplankton population as carbon (mg C/L),

a_{ChlC} = the ratio of algal chlorophyll to algal carbon (mg chl-a/mg C),

The result of this integral is:

$$I_{av} = \frac{I_{surf}}{k_e H} \left(1 - e^{-k_e H}\right) \qquad (4\text{-}12)$$

The value of the surface light intensity, I_{surf}, may be evaluated at any time within the day, t, using the following formula:

$$I_{surf}(t) = \frac{I_{tot}}{0.635\, f} \sin\left[\frac{\pi\,(t_d - t_{sunrise})}{f}\right] \qquad (4\text{-}13)$$

where:

I_{tot} = total daily incident solar radiation,

f = fraction of daylight (daylight hours/24),

t_d = time of day,

$t_{sunrise}$ = time of sunrise.

Phytoplankton have been shown to be able to adapt to variations in light intensity (Steemann Nielsen et al., 1962; Steemann Nielsen and Park, 1964; Morel et al., 1987). Experimental data have indicated that phytoplankton take two to four days to adapt to changes in light intensity. Therefore, the value of I_s in Equation 4-10 is permitted to change as a function of the antecedent light history, according to the formula:

$$I_s = \left(I_{tot_{n-3}} + I_{tot_{n-2}} + I_{tot_{n-1}}\right) / 3 \qquad (4\text{-}14)$$

where:

$I_{tot_{n-3}}$ = total solar radiation three days preceding current model day,

$I_{tot_{n-2}}$ = total solar radiation two days preceding current model day,

$I_{tot_{n-1}}$ = total solar radiation one day preceding current model day.

The nutrient saturated growth rate is then temperature-corrected using spatially dependent, values of ambient water column temperature. The temperature-corrected growth rate is computed using the following equation, which relates $\mu_{Pmax}(T)$, the growth rate at ambient temperature, T, to $\mu_{Pmax}(T_{opt})$, the growth rate at the optimal temperature, T_{opt}:

$$\mu_{Pmax}(T) = \mu_{Pmax}(T_{opt}) \ e^{-\beta_1 \ (T-T_{opt})^2} \qquad T \leq T_{opt} \qquad (4\text{-}15a)$$

or

$$\mu_{Pmax}(T) = \mu_{Pmax}(T_{opt}) \ e^{-\beta_2 \ (T_{opt}-T)^2} \qquad T > T_{opt} \qquad (4\text{-}15b)$$

and where β_1 is the effect of temperature below T_{opt} on growth and β_2 is the effect of temperature above T_{opt} on growth. A principal difference between the winter diatom group and the summer assemblage is that the winter group has a much lower T_{opt} than does the summer assemblage. The nutrient saturated, temperature-corrected growth rate is then adjusted to reflect attenuation due to nutrient levels. The effects of various nutrient concentrations on the growth of phytoplankton have been investigated, and the results are quite complex. As a first approximation to the effect of nutrient concentration on the growth rate, it is assumed that the phytoplankton population in question follows Monod growth kinetics with respect to the important nutrients. That is, at an adequate level of substrate concentration, the growth rate proceeds at the saturated rate for the ambient temperature and light conditions. However, at low substrate concentration, the growth rate becomes linearly proportional to substrate concentration. Thus, for a nutrient with concentration N_j in the jth segment, the factor by which the saturated growth rate is reduced in the jth segment is $N_j/(K_m + N_j)$. The constant, K_m, which is called the Michaelis, or half-saturation constant, is the nutrient concentration at which the growth rate is half the saturated growth rate. Since there are three nutrients, nitrogen, phosphorus and silica, considered in this framework, the Michaelis-Menten expression is evaluated for each nutrient and the minimum value is chosen to reduce the saturated growth rate,

$$G_N(N) = \text{Min}\left(\frac{DIN}{K_{mN} + DIN}, \frac{PO_4}{K_{mP} + PO_4}, \frac{DSi}{K_{mSi} + DSi}\right). \tag{4-16}$$

Three terms have been included in the modeling framework to account for the loss of phytoplankton biomass: endogenous respiration, sinking or settling from the water column and zooplankton grazing. Respiration has already been defined via Equation (4-4). The sinking of phytoplankton is an important contribution to the overall mortality of the phytoplankton population. Published values of the sinking velocity of phytoplankton, mostly in quiescent laboratory conditions, range from 0.1 to 18.0 m/day. In some instances, however, the settling velocity is zero or negative. Actual settling rates in natural waters are a complex phenomenon, affected by vertical turbulence, density gradients, and the physiological state of the different species of phytoplankton. An important factor shown to influence the physiological state of the algae is nutrient availability. Work by Bienfang et al. (1982) and Culver and Smith (1989) has shown that the settling rate of marine diatoms is increased primarily by low concentrations of silica, although low concentrations of nitrogen and low light availability were also found to increase diatom sinking rates. Although the net effective settling rate under nutrient stressed conditions is greatly reduced in relatively shallow, well-mixed regions of an estuary, sinking can contribute to the overall mortality of the algal population. In addition, the settling of phytoplankton can be a significant source of nutrients to the sediments and can play an important role in the generation of SOD. For these reasons, a term representing phytoplankton settling has been included in the algal mortality expression, and is determined by:

$$k_{sP} = \frac{v_{sPb}}{H} + \frac{v_{sPn}}{H}(1 - G_N(N)) \tag{4-17}$$

where k_{sP} is the net effective algal loss rate due to settling (day^{-1}), v_{sPb} is the base settling velocity of phytoplankton (m/day), v_{sPn} is the nutrient dependent settling rate (m/day), $G_N(N)$ is defined by Equation (4-16), and H is the depth of the model segment.

Zooplankton grazing may, depending upon the time of year and zooplankton biomass levels, be an important loss rate for phytoplankton. Rather than attempt to model the complex and dynamic processes of zooplankton grazing and growth, a simple first order loss rate representing the effect of zooplankton grazing on algal biomass is included in the model. The loss rate due to grazing is temperature corrected as per Equation (4-18),

$$k_{grz}(T) = k_{grz}(20°C) \; \theta_{grz}^{(T-20)} \tag{4-18}$$

where $k_{grz}(T)$ is the temperature corrected loss rate due to zooplankton grazing, $k_{grz}(20°C)$ is the loss rate at 20°C and θ_{grz} is the temperature correction factor for zooplankton grazing. The units of k_{grz} are day^{-1}.

4.2.3 Algal Stoichiometry and Nutrient Uptake Kinetics

A principal component in the mass balance equation for the nutrient systems in the model eutrophication framework is the nutrient uptake associated with algal growth. In order to quantify the nutrient uptake it is necessary to specify the phytoplankton stoichiometry in units of nutrient uptake per mass of phytoplankton biomass synthesized. For carbon as the unit of phytoplankton biomass, the relevant ratios are the mass of nitrogen, phosphorus, and silica per unit mass of carbon. Lacking extensive measurements of the particulate forms of carbon, nitrogen, phosphorus and biogenic silica, this study assumed that the phytoplankton present in Massachusetts Bay are comprised of carbon and nutrients which approximate Redfield ratios; i.e. 106C:16N:1P (atomic), under nutrient saturated conditions. For silica, it was assumed that at nutrient saturated conditions the winter diatoms had a carbon to silica ratio of 106C:18Si (atomic), while a ratio of 106C:6.5Si (atomic) was used for the summer functional group (recognizing that only a portion of the summer assemblage is comprised of diatoms).

However, while the use of Redfield ratios may be appropriate under nutrient saturated conditions, it has been shown (Anita et al., 1963; Caperon and Meyer, 1972;

Chalup and Laws, 1990) that algae change their cellular composition or stoichiometry as a function of nutrient status. This is accounted for in the Laws/Chalup model via the following equations:

$$N_x:C = \left[QF + (1-QF)\ (\mu/\mu_{Pmax})\right] / W_{Cx} \tag{4-19}$$

$$= 1/W_{Cx} \quad \text{when } \mu = \mu_{Pmax}$$

and

$$Chl:C = \frac{1 - (1-QF)\ (1-\mu/\mu_{Pmax}) - S/C - (\mu+k_{RB}/C) / \left[(1-k_{RG})\ G_{prd}\right]}{W_{chl}} \tag{4-20}$$

$$= \{1 - S/C - (\mu_{Pmax}+k_{RB}C) / [(1-k_{RG})\ G_{prd}]\} / W_{chl} \quad \text{when } \mu = \mu_{Pmax}$$

where:

$N_x:C$ = the ratio of nutrient x (nitrogen, phosphorus or silica) to carbon,

QF = quotient of $N_x:C$ values at relative growth rates of 0 and 1,

μ = the nutrient corrected growth rate ($\mu = \mu_{Pmax}\ G_N(N)$),

W_{Cx} = the ratio of C to nutrient x in S, L, D,

$Chl:C$ = the ratio of chlorophyll-a to C in P,

W_{Chl} = the ratio of C to chlorophyll-a in P.

The latter equation accounts for changes in the chlorophyll to carbon ratio both as a function of nutrient status and light. Equations 4-19 and 4-20 provide the equilibrium carbon to nutrient and carbon to chlorophyll ratios. However, as has been shown from experimental studies, there is a time period over which it takes the phytoplankton to reach new equilibrium conditions in response to changes in nutrient status and/or available light. This is accounted for in BEM by use of the following equations:

$$\frac{dN_x:C^n}{dt} = k_{eq}\ (N_x:C_{eq}^n - N_x:C^n) \tag{4-21}$$

$$N_x:C^{n+1} = N_x:C^n + dt \frac{dN_x:C^n}{dt} \tag{4-22}$$

and

$$\frac{dChl:C^n}{dt} = k_{eq} (Chl:C_{eq}^n - Chl:C^n) \tag{4-23}$$

$$Chl:C^{n+1} = Chl:C^n + dt \frac{dChl:C^n}{dt} \tag{4-24}$$

where:

$N_x:C^n, N_x:C^{n+1}$ = the nutrient to carbon ratios at time step n and n+1, respectively

$N_x:C_{eq}^n$ = the equilibrium nutrient to carbon ratio at time step n, as determined from Equation 4-19

k_{eq} = a constant which determines the time to achieve equilibrium,

$Chl:C^n, Chl:C^{n+1}$ = the chlorophyll to carbon ratios at time step n and n+1, respectively

$Chl:C_{eq}^n$ = the equilibrium chlorophyll to carbon ratio at time step n, as determined from Equation 4-20,

dt = length of time step.

The model evaluates the nutrient to carbon and chlorophyll to carbon ratios to be used for the next time level based on the ratios at the current time level and the equilibrium ratios, determined from Equations 4-19 and 4-20, based upon environmental conditions at the current time level. A value of 1 /day was chosen for k_{eq}, based on the literature (Steeman Nielsen and Park, 1964; Anita et al., 1963; Caperon and Meyer,1972). This corresponds to an equilibrium time of approximately 3 days.

Once the stoichiometric ratios have been determined, the mass balance equations may be written for the nutrients in much the same way as for the phytoplankton biomass. The principal processes determining the distribution of nutrients among the various pools are: uptake of inorganic nutrients by phytoplankton for cell growth, the release of inorganic and organic nutrients algal respiration and predation processes, and the recycling of organic nutrients to inorganic forms via bacterial hydrolysis and mineralization.

Rather than attempt to model bacterial recycling of organic nutrients by including a bacterial system (for which there are little or no data against which to calibrate), a phytoplankton-dependent saturated recycle formulation was used. The assumption is made that bacterial biomass, and hence the recycling rate, is proportional to the phytoplankton biomass. A number of field and laboratory studies (Hendry, 1977; Lowe, 1976, Menon et al., 1972; Jewell and McCarty, 1971) support this hypothesis. The saturated recycling relationship may be written

$$k(T) = k'(20^{\circ}C)\theta^{(T-20)} \frac{P_c}{K_{mPc} + P_c} \qquad (4-25)$$

where $k(T)$ is the temperature corrected recycling rate, $k'(20^{\circ}C)$ is the saturated recycling rate at $20^{\circ}C$, P_c is the phytoplankton biomass, K_{mPc} is the half-saturation constant for recycling, θ is the temperature correction coefficient. Basically, this mechanism employs a quasi-first-order recycle that slows the recycling rate if the algal population is small, yet does not permit the recycling rate to increase in an unlimited fashion as phytoplankton biomass increases. Instead the mechanism permits zero-order recycling when the phytoplankton greatly exceed the half-saturation constant. The latter assumes that at higher population levels, other factors are limiting recycling rates or kinetics, so that it proceeds at its maximum zero-order rate.

4.2.3.1 Organic Carbon

Six organic carbon state variables are considered: reactive dissolved organic carbon (ReDOC), labile dissolved organic carbon (LDOC), refractory dissolved organic carbon

(RDOC), labile particulate organic carbon (LPOC), refractory particulate organic carbon (RPOC) and dissolved algal exudate (ExDOC). Reactive, labile and refractory distinctions are based upon the time scale of oxidation or decomposition. Reactive organic carbon decomposes on a time scale of days to a week or two; labile organic carbon decomposes on the time scale of several weeks to a month or two; refractory organic carbon decomposes on the order of months to a year. Reactive and labile organic carbon decompose primarily in the water column and, in the case of LPOC, rapidly in the sediments. Refractory organic carbon decomposes much more slowly, and for RPOC almost entirely in the sediments.

The principal sources of organic carbon are anthropogenic inputs, natural runoff, and detrital algal carbon, the latter which is produced as a result of zooplankton predation. Zooplankton take up and redistribute algal carbon to the organic carbon pools via grazing, assimilation, respiration and excretion. Since zooplankton are not directly included in the model, the redistribution of algal carbon by zooplankton is simulated by empirical distribution coefficients. An additional term, representing the excretion of DOC by phytoplankton during photosynthesis, is included in the model. This algal exudate is very reactive and has a time constant similar to the reactive DOC. The decomposition of organic carbon is assumed to be temperature and bacterial biomass mediated. Since bacterial biomass is not directly included within the model framework, phytoplankton biomass is used as a surrogate variable as per Equation (4-25).

4.2.3.2 Phosphorus

The Massachusetts Bay eutrophication model includes five principal phosphorus forms: labile and refractory dissolved organic (LDOP and RDOP, respectively), labile and refractory particulate organic (LPOP and RPOP, respectively), and PO_4. Inorganic phosphorus or PO_4 is utilized by phytoplankton for growth and is returned to the various organic and inorganic forms via respiration and predation. A fraction of the phosphorus released during phytoplankton respiration and predation is in the inorganic form and readily available for uptake by other viable algal cells. The remaining fraction released is in the

dissolved and particulate organic forms. The organic phosphorus must undergo a mineralization or bacterial decomposition into inorganic phosphorus before it can be used by phytoplankton.

4.2.3.3 Nitrogen

The kinetic structure for nitrogen is similar to that for the phosphorus system. During algal respiration and death, a fraction of the cellular nitrogen is returned to the inorganic pool in the form of NH_4. The remaining fraction is recycled to the dissolved and particulate organic nitrogen pools. Organic nitrogen undergoes a bacterial decomposition, the end-product of which is NH_4. NH_4 in the presence of nitrifying bacteria and oxygen, is converted to nitrite nitrogen and subsequently nitrate nitrogen (nitrification). Both NH_4 and $NO_2 + NO_3$ are available for uptake and use in cell growth by phytoplankton; however, for physiological reasons, the preferred form is NH_4.

The process of nitrification in natural waters is carried out by aerobic autotrophs, *Nitrosomonas* and *Nitrobacter*, in particular. It is a two-step process with *Nitrosomonas* bacteria responsible for the conversion of ammonia to nitrite (NO_2) and *Nitrobacter* responsible for the subsequent conversion of nitrite to nitrate (NO_3). Aerobic conditions are essential to this reaction process. In order to reduce the number of state variables required in the modeling framework, nitrite and nitrate are incorporated together as a single state variable ($NO_2 + NO_3$). Therefore, the process of nitrification is assumed to be approximated by a first-order (with respect to NH_4) reaction rate that is a function of the water column dissolved oxygen concentration and ambient temperature.

Denitrification refers to the reduction of NO_3 (or NO_2) to N_2 and other gaseous products such as N_2O and NO. This process is carried out by a large number of heterotrophic, facultative anaerobes. Under normal aerobic conditions found in the water column, these organisms utilize oxygen to oxidize organic material. However, under the anaerobic conditions found in the sediment bed or during extremely low oxygen conditions in the water column, these organisms are able to use NO_3 as the electron acceptor. The

process of denitrification is included in the modeling framework simply as a sink of nitrate. This can always occur in the anaerobic sediment layer. In the water column, however, denitrification should only occur under extremely low dissolved oxygen conditions. This is accomplished computationally by modifying the linear first-order (with respect to $NO_2 + NO_3$) denitrification rate by the expression $K_{NO3}/(K_{NO3} + DO)$. This expression is similar to the Michaelis-Menten expression; for K_{NO_3} equal to 1 mg/L and concentrations of dissolved oxygen greater than 1 mg/L, the expression reduces denitrification to near zero, whereas for dissolved oxygen levels less than 0.1 mg/L, this expression permits water column denitrification to occur.

4.2.3.4 Silica

Two silica state-variables are considered: dissolved available (DSi) and particulate biogenic (BSi). DSi is utilized by diatoms during growth for their cell structure. Particulate biogenic silica is produced from diatom losses associated with respiration and grazing by zooplankton. Particulate biogenic silica undergoes mineralization to available silica or settles to the sediment from the water column.

4.2.3.5 Dissolved Oxygen

A by-product of photosynthetic carbon fixation is the production of dissolved oxygen. The rate of oxygen production and nutrient uptake is proportional to the growth of the phytoplankton. An additional source of oxygen from algal growth occurs when the available ammonia nutrient source is exhausted and the phytoplankton begin to utilize the available nitrate. This additional oxygen source can be seen by comparing Equations (4-26a) and (4-26b) (Morel 1983).

$$106\ CO_2 + 16\ NH_4^+ + H_2PO_4^- + 106\ H_2O \tag{4-26a}$$

$$\Rightarrow Protoplasm + 106\ O_2 + 15H^+$$

$$106 \ CO_2 + 16 \ NO_3^- + H_2PO_4^- + 122 \ H_2O + 17 \ H^+ \qquad (4\text{-}26b)$$

$$\Rightarrow \text{Protoplasm} + 138 \ O_2$$
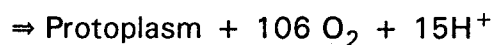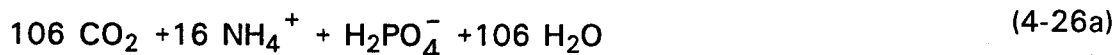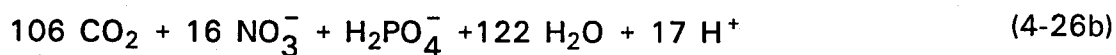
The above equations present the stoichiometric description of the photosynthetic process assuming NH_4 (Equation 4-26a) or $NO_2 + NO_3$ (Equation 4-26b) as the nitrogen source and assuming algal biomass to have Redfield stoichiometry:

$$\text{Biomass} = C_{106} \ H_{263} \ O_{110} \ N_{16} \ P_1 \qquad (4\text{-}27)$$

Oxygen-deficient or under-saturated waters are replenished via atmospheric reaeration. The reaeration coefficient is a function of a mass transfer coefficient, k_L, which is a function of wind velocity, and temperature, and is computed using Equations (4-28a,b, and c) (Banks and Herrera, 1977):

$$k_L = \max \left(1.0, \ 0.728 \ U_W^{0.5} - 0.317 0_W + 0.0372 U_W^2 \right) \qquad (4\text{-}28a)$$

$$k_a \ (20^\circ C) = k_L/H \qquad (4\text{-}28b)$$

$$k_a(T) = k_a(20^\circ C)\theta_a^{(T-20)} \qquad (4\text{-}28c)$$

where

k_L = the surface mass transfer coefficient (m/day),

U_W = wind velocity (m/s),

H = depth (m),

θ_a = temperature coefficient.

Dissolved oxygen saturation is a function of both temperature and salinity and is determined via Equation (4-29) (Hyer et al., 1971):

$$DO_{sat} = 14.6244 - 0.367134\ T + 0.0044972\ T^2 - 0.0966\ S \qquad (4\text{-}29)$$

$$+\ 0.00205\ S\ T + 0.0002739\ S^2$$

where S is salinity in ppt.

Dissolved oxygen is diminished in the water column as a result of algal respiration, which is the reverse process of photosynthesis; as a result of nitrification; and as a result of the oxidation of carbonaceous material (including detrital phytoplankton).

4.2.4 Sediment Submodel

An important component of the water column nutrient and dissolved oxygen mass balance equations is the interaction between the water column and the sediments. In previous water quality modeling studies of coastal eutrophication the SOD and nutrient fluxes were input as distributed loads. However, there was generally no effort to ensure that the SOD and nutrient fluxes bore any relationship to the delivery of organic material to the sediment. The present sediment submodel, which was developed as part of the Chesapeake Bay study (Di Toro and Fitzpatrick, 1993), corrects that modeling deficiency and effectively closes the mass balance between the water column and the sediment.

The sediment submodel, like the water column portion of the integrated water quality model, is based on the principle of mass balance. The sediment receives the fluxes of POC, PON, POP, and BSi, collectively referred to as POM from the overlying water column. Mineralization, which is termed diagenesis, produces soluble end-products. These end-products can react in the aerobic and anaerobic layers of the sediment. The difference between the resulting aerobic layer dissolved concentration and the overlying water concentration determines the flux to or from the sediment. The magnitude of the flux is determined by the surface mass transfer coefficient. The sediment submodel also includes

the burial, via sedimentation, of particulate and dissolved species. These processes are illustrated on Figure 4-4. Details of the sediment mass balance and flux submodel can be found in Appendix B, while a more detailed development of the model and its calibration to the Chesapeake Bay data set is presented in Di Toro and Fitzpatrick, 1993.

4.3   MODEL CALIBRATION PROCEDURE

The overall objective of the model validation procedure is to calibrate the water quality model to the observed data, utilizing a set of model coefficients and parameters that are consistent with the observed data and field studies and are within the general ranges of values reported in the literature and accepted by the modeling community. Coincident with this objective is the goal to utilize a set of model coefficients for model validation that are consistent across spatial segments and consistent in time. One would have a greater degree of confidence in the model's predictive ability if a reasonable calibration to observed data is achieved using a spatially and temporately consistent set of model coefficients rather than if a reasonable calibration was achieved by varying model coefficients on a grid cell to grid cell basis or on a day to day basis. This is because it is expected that biological and chemical processes to be consistent over space and time.

The general calibration procedure followed in this study was to perform a series of iterative runs of the model using estimated values of the various coefficients and parameters. Initial estimates for most of the model coefficients were made by assuming that Massachusetts Bay would have essentially the same chemical and biological dynamics as Chesapeake Bay and Long Island Sound. Therefore, the nutrient recycle rates, organic carbon oxidation rates and recycle fractions calibrated during the Chesapeake Bay (Cerco and Cole, 1993) and Long Island Sound (HydroQual, 1991) were used as a starting point in this study. Initial estimates of the algal growth model coefficients were based on the paper by Laws and Chalup (1990). Comparisons were then made between model output and observed data, using computer generated plots in order to make a qualitative assessment of the model's goodness of fit. This process continued through the adjustment or tuning of the model parameters and boundary conditions until a reasonable

SEDIMENT FLUX MODEL
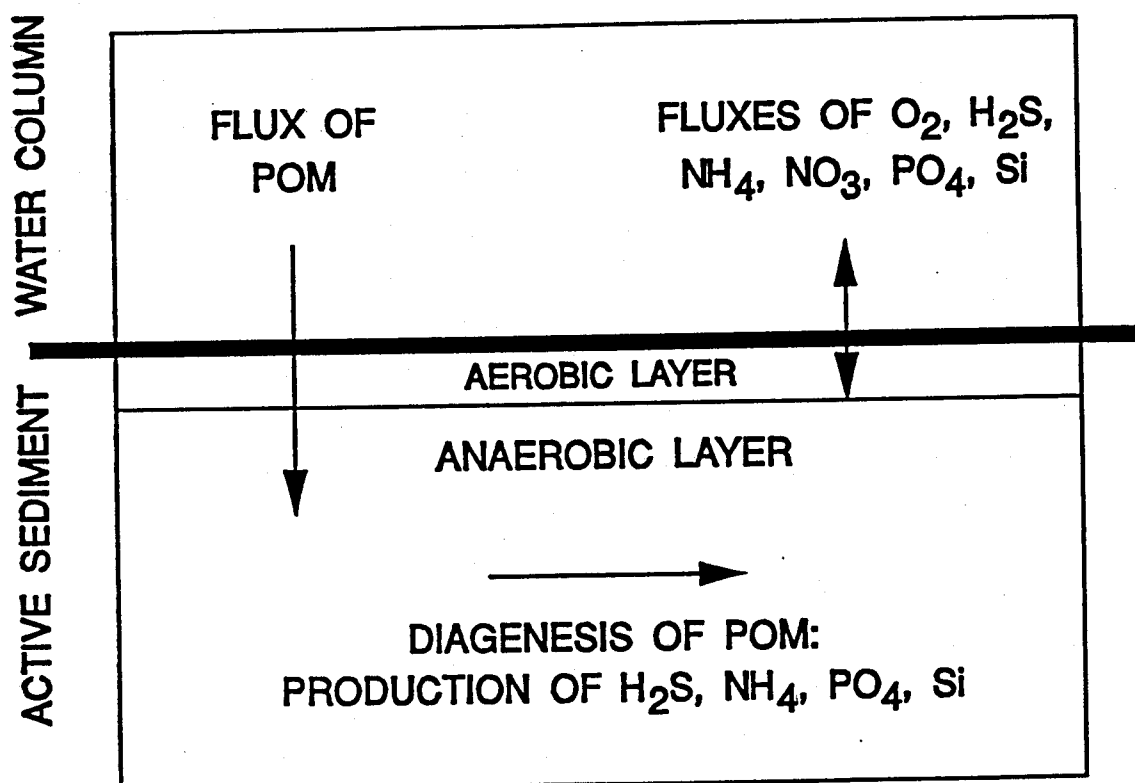
FIGURE 4-4. SEDIMENT FLUX MODEL

reproduction of the observed data was attained or no further improvement was possible. Section 5.0 provides the details of the calibration effort and presents model versus data comparisons for the final calibration run.

SECTION 5

CALIBRATION

5.1   INTRODUCTION

The discussions of the previous sections present the carbon and nutrient inputs to the study area, the available data for model calibration purposes, and the model framework used for the Massachusetts and Cape Cod Bay Eutrophication Model (BEM). This section will integrate those pieces together and discuss the implementation of the model together with results of the calibration effort.

The final calibration is the result of approximately 100 hydrodynamic and water quality model runs, which were made to obtain a consistent set of model coefficients that are reasonable and reproduce the observed data for all the state-variables considered. With the exception of exogenous variables such as solar radiation and extinction coefficients, all model coefficients were spatially and temporally consistent throughout the 1990 and 1992 simulations. The method of determining the values for the modeling coefficients was essentially one of trial and error. The starting point was a set of rate constants and parameter values which had been used in the previous coarse grid analysis of Massachusetts Bay (HydroQual, Inc., 1993) and in the Long Island Sound Study (HydroQual, Inc., 1991).

There are many inputs required by the water quality model, such as the hydrodynamic transport fields, boundary conditions, loadings, extinction coefficients, solar radiation, and fraction of daylight. Depending upon the available data these variables were assigned on either a daily, monthly or annual average basis. These time-variable values were approximated by a series of step functions, consisting of a series of values of the variables and julian dates (or breakpoints) which define when a particular value is to be used.

5.2   MODEL INPUTS

5.2.1 Hydrodynamics

A key factor in determining the effect outfall relocation will have on Massachusetts Bay and Cape Cod Bay is the transport of nutrients within the Bays. In order to simulate these transport processes, a variant of the Blumberg-Mellor (1987) hydrodynamic model was developed and calibrated by the USGS. This time-variable three-dimensional hydrodynamic model is coupled with the water quality model in order to make a complete analysis of the effect of the outfall relocation. The hydrodynamic model provides all of the transport information to the water quality model as well as temperature and salinity information.

The hydrodynamic model, ECOM, solves the primitive equations using finite differences on a curvilinear orthogonal grid in the horizontal plane and discrete sigma levels in the vertical. The curvilinear grid used for the hydrodynamic model is 68x68, resulting in a horizontal spacing ranging from 600 m in the vicinity of Boston Harbor to nearly 6 km along part of the open boundary. There are 12 vertical sigma levels in the model grid. The bottom nine layers are uniform in thickness while the top three layers are 0.1, 0.3, and 0.6 as thick as one of the bottom nine layers, respectively. This results in vertical spacing from 0.3 m in the shallowest water to 14 m in the deepest water. Figure 5-1 presents the hydrodynamic grid. The model domain extends well offshore of Massachusetts Bay, in order that exchange with the Gulf of Maine may be simulated. The domain also extends north to include the Merrimack River which is a major source of freshwater which can influence transport within Massachusetts Bay. ECOM was forced with daily measurements of freshwater inflow at the mouth of the Merrimack, Charles, Mystic and Neponset Rivers, and at the current outfall site; inflows from the Gulf of Maine; atmospheric heating/cooling derived from data supplied at four hour intervals; and, finally, space- and time-variable water level fluctuations specified along the eastern boundary of the domain. These boundary water level fluctuations were specified using a combination of M_2 tides, obtained
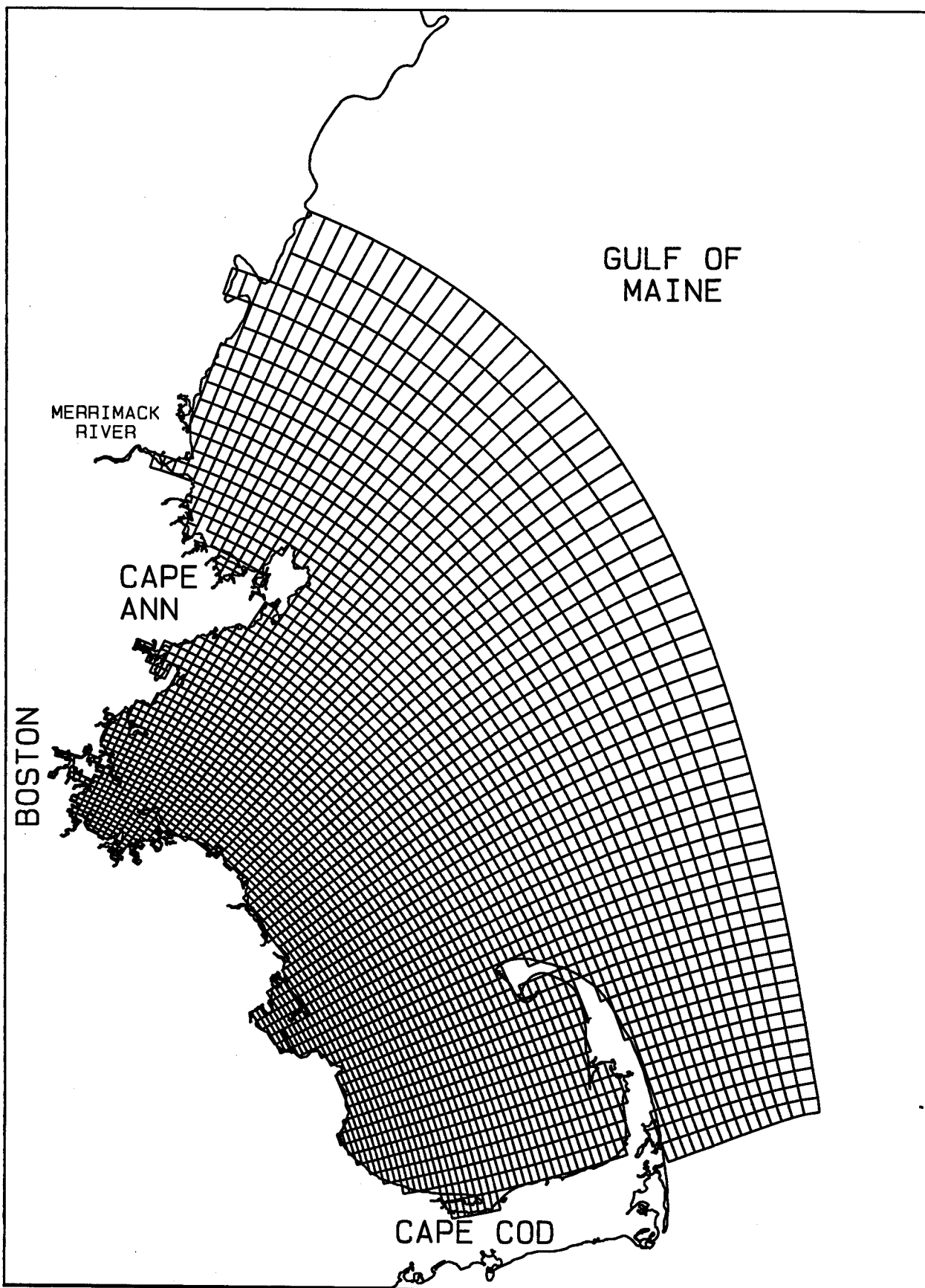
FIGURE 5-1. HYDRODYNAMIC MODEL GRID

from a Gulf of Maine tidal model, and subtidal water level fluctuations obtained from a western Gulf of Maine model.

In order to provide information for the water quality model the hydrodynamic model was run for the period October 1989 through December 1992. The model was calibrated and verified with information from an intensive moored and shipboard data collection program (Geyer, et al., 1992) parts of which encompassed the entire simulation period. Details of the hydrodynamic model calibration may be found in Signell et al. (1993), Blumberg et al. (1993), and Signell (1995). Model calibration/verification analysis included model versus data comparisons of tidal stage, current velocity and direction, and salinity and temperature. An overview of the calibration/verification is presented below.

The hydrodynamic model in general successfully predicted the counterclockwise direction of currents as observed in the seasonal data. ECOM also reproduced the observed vertical stratification of temperature and salinity which occurred between April and October during each year of the calibration/verification period. The degree of stratification and the timing of the onset of stratification and fall overturn also matched fairly well with the data. Seasonal and long term trends were generally reproduced by the model whereas short term events were sometimes missed. The accuracy of the calibration of temperature and salinity can be observed in some of the temporal and vertical profile plots which will be presented later in this section.

In order to reduce the computational burden faced by the water quality model if it were to run on the same grid as the hydrodynamic model, spatial aggregation of the hydrodynamic model was employed. Once the hydrodynamic model was calibrated, the transport, temperature and salinity information was aggregated onto the water quality grid by combining a 3x3 grid of horizontal hydrodynamic cells into one water quality segment. Figure 5-2 presents an example of grid aggregation. The flows, both horizontally and vertically, are summed up to complete a flow balance. The horizontal dispersion is arithematically averaged on each side of the grid box. The vertical dispersion is the reciprocal of the average of the reciprocal sum of the individual dispersions or:
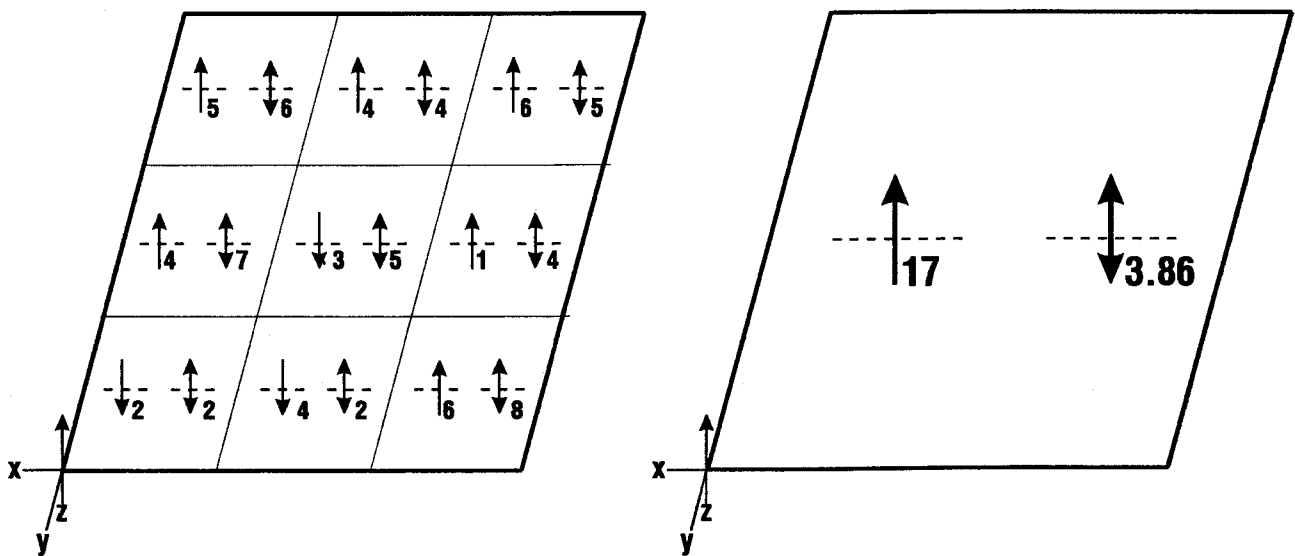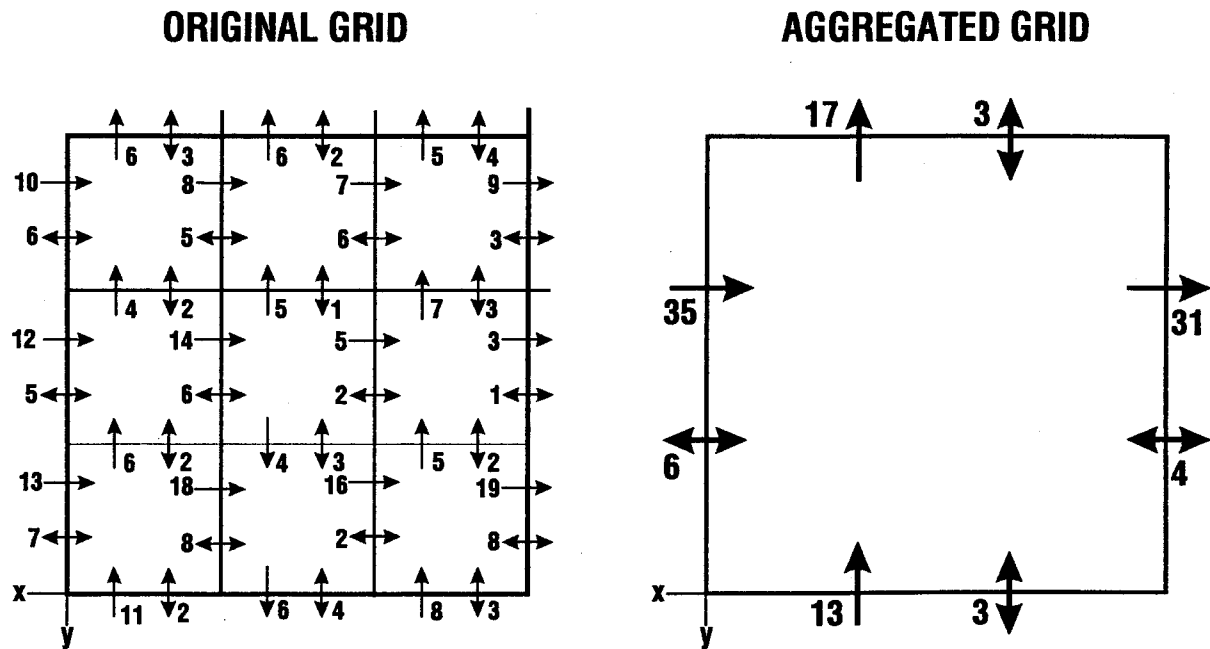
FIGURE 5-2. EXAMPLE OF GRID AGGREGATION

$$\frac{1}{R_A} = \frac{\sum_{i=1,n} \frac{1}{R_i}}{n} \tag{5-1}$$

were R_A is the vertical dispersion coefficient of the appregated grid cell, and R_i are the dispersion coefficients of the individual cells included in the apprepation and n is the number of segments to be aggregated. This gives more weight to the smaller dispersion values which keeps the vertical stratification computed by the hydordynamic model in tact. However, to maintain spatial integrity in the region near Race Point on the northern end of Cape Cod, it was not possible to perform a full 3x3 aggregation; instead a 2x2 aggregation was used. In a further effort to reduce the computational burden and to lessen uncertainties associated with specifying water quality boundary conditions, the boundary of the water quality model was shifted westward to a transect between Cape Ann and Race Point. This location is at the easternmost water quality data stations available to provide boundary conditions in 1990. All freshwater flows included in the hydrodynamic model are included in the water quality model. The resulting water quality grid is presented in Figure 5-3. In addition to horizontal aggregation, a partial vertical aggregation was used wherein the top three sigma levels from the hydrodynamic model were combined into one water quality model segment. The spatial and vertical aggregation was tested and was determined to balance mass and adequately reproduce temperature and salinity gradients calculated by the hydrodynamic model.

Besides employing spatial aggregation, some temporal averaging of the hydrodynamic model output was performed. This was necessary both to reduce the disk storage required to save the hydrodynamic fields (segment volumes, salinities, water temperature and three-dimensional velocities and mixing coefficients) necessary to force the water quality model. The hydrodynamic model time step varied between 1.5 and 6 minutes, depending upon the season. The output from the hydrodynamic model, ECOM, was averaged over one hour intervals for use in the water quality model. Even with this temporal averaging period and the use of spatial grid aggregation, the hydrodynamic output files required between 528 Mbytes (for the 1992 calibration period) and 836 Mbytes (for the 1990 calibration period).
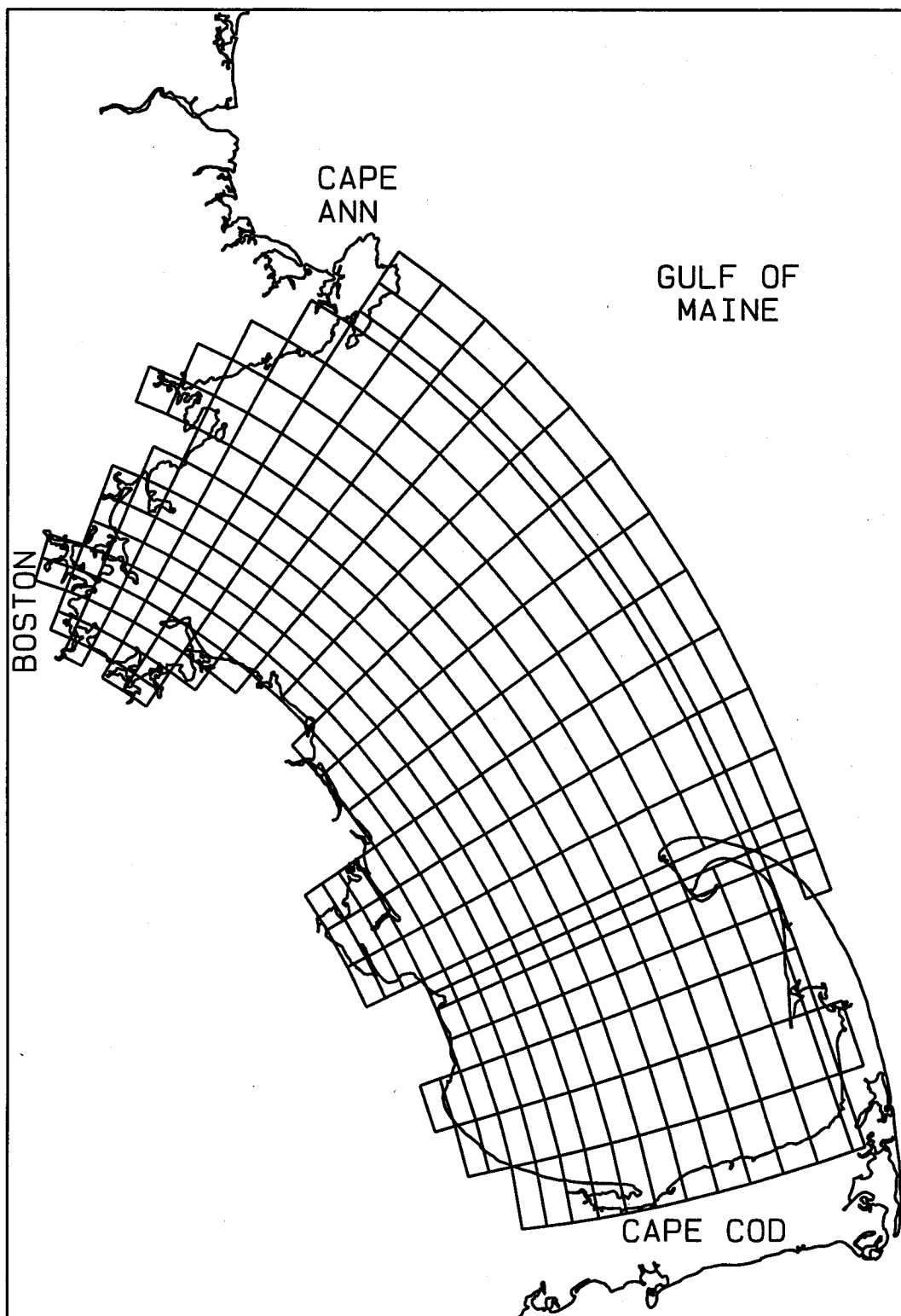
FIGURE 5-3. WATER QUALITY MODEL GRID FOR MASSACHUSETTS BAY

In order to ensure that the spatial aggregation and temporal averaging of the hydrodynamic model computations does not adversely affect the water quality model, salinity is run in the water quality model, BEM, and compared to the hydrodynamic model output. Initial salinity concentrations are obtained from the hydrodynamic model and boundary conditions are updated on an hourly basis again using concentrations determined from hydrodynamic model computations.

Figure 5-4 presents a series of comparisons between hydrodynamic and water quality model computations of surface and bottom water salinity for a number of locations within the model domain. Both the hydrodynamic and water quality salinity concentrations presented have been averaged over five day intervals. The ECOM results are shown using solid lines, while the BEM results are shown using a dotted line. In general, the BEM computations of salinity compare favorably to the ECOM salinity concentrations; BEM tracks the temporal tends in surface and bottom salinity and approximately reproduces the vertical stratification in salinity computed by ECOM. In particular, the BEM vs ECOM comparisons for Boston Harbor (panel/location 1) are very good. The BEM does, however, under-estimate the degree of stratification in southwest Cape Cod Bay (panel/station 3). This may be due to the effects of grid aggregation, time-averaging or differences between the numerical schemes used in the two models. ECOM uses a central-differencing scheme in time and space, while the BEM uses an Smolarkiewicz-corrected upwind spatial scheme and a forward-in-time scheme.

Additional insight into the behavior of the ECOM/BEM interfacing was obtained from an analysis of the advective and tidal exchange between Boston Harbor and Massachusetts Bay, as determined from flushing time calculations. Earlier analyses by Signell and Butman (1992) and Signell (1992), using a vertically-integrated fine-grid representation of the harbor and northwestern Massachusetts Bay, estimated flushing times of approximately 17 days, due to tidal effects only, and between 8 to 12 days based on a combination of wind and tidal effects, respectively. Estimates of flushing time provided by BEM ranged from four to eight days with an average of five days. While these estimates are lower than those made by Signell there are two significant differences
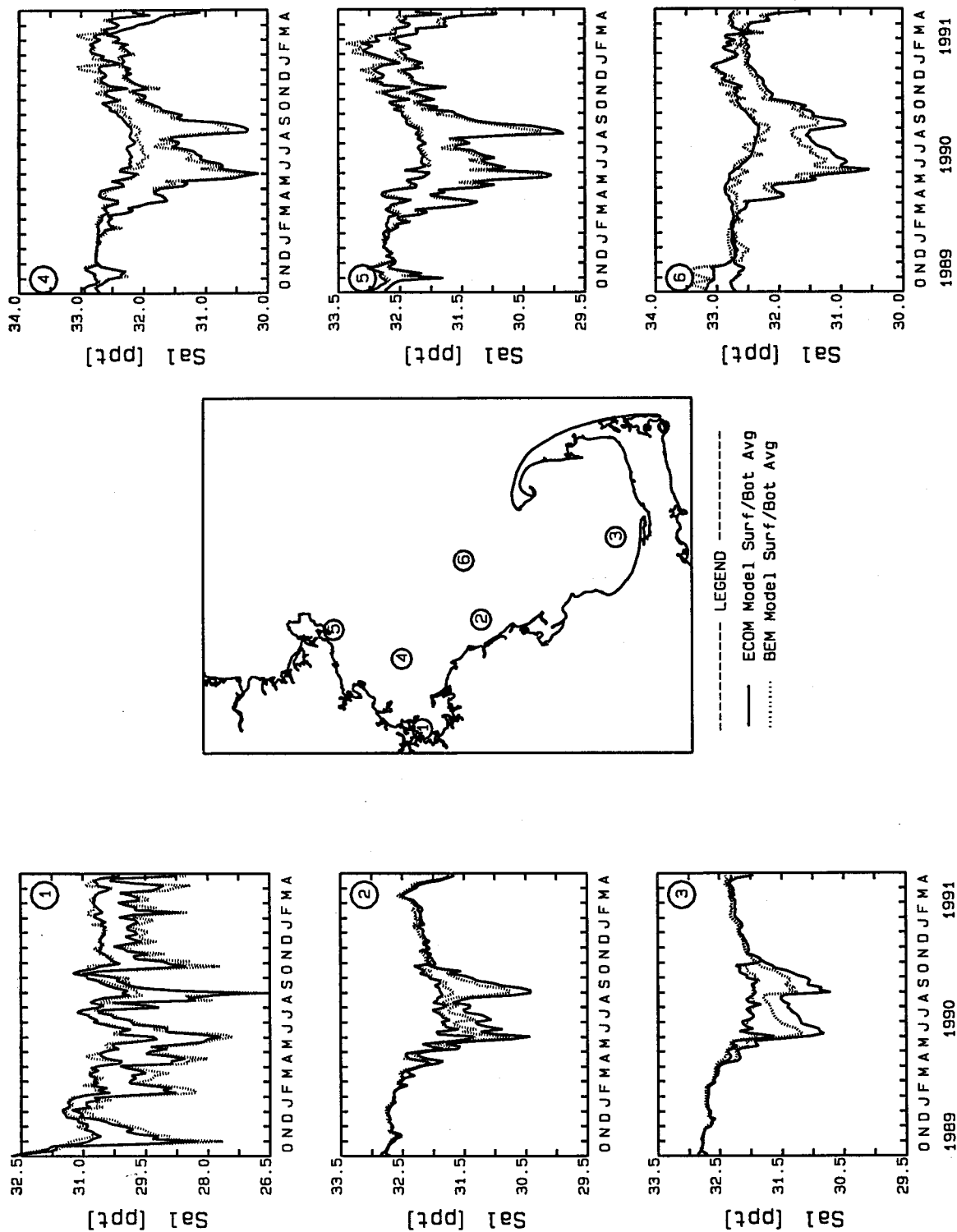
FIGURE 5-4. COMPARISONS OF COMPLETED SALINITY BETWEEN HYDRODYNAMIC AND WATER QUALITY MODELS

between the analyses. First, the earlier analyses performed by Signell and Butman and Signell did not include sources of freshwater inputs to Boston Harbor, such as the MWRA wastewater effluents and the Charles River and Neponset Rivers, which would act to reduce the residence time or increase the flushing time of the harbor. A second difference is that the earlier analyses evaluated the flushing time using a uniformly distributed tracer throughout the harbor, while the present analysis considered only a tracer discharged at the location of the present Deer Island outfall, which is located near the entrance to the harbor. As acknowledged by Signell and Butman their estimate of a single flushing time for the harbor is somewhat of an artificial construct, since the material released in the strong tidal channels near the harbor mouth would be flushed much more rapidly than the harbor as a whole. Therefore, accounting for these differences between the two analyses, it appears as if the BEM is approximately reproducing the correct flushing dynamics of Boston Harbor. The BEM estimates of flushing time also fall within the range of values obtained from numerous experimental and theoretical studies as summarized by Stolzenbach and Adams (1995). These authors reported a range of values from 1.6 to 10.5 days, with a "best estimates" of approximately five days (Adams, 1995). Based on the generally favorable ECOM and BEM salinity comparisons and the Boston Harbor flushing time computations, it appears that the spatial aggregation and temporal averaging of the hydrodynamic model do not affect water quality model computations in such a way as to preclude their use for water quality model computations.

5.2.2 Boundary Conditions

The data available for specifying the boundary conditions have been discussed in Section 3.4. Once the data analysis was completed, monthly values of the various water quality constituents were estimated and incorporated into the model by assigning boundary concentrations at 4 standard levels: 0, 25, 60, and 160 meters. The water quality model then interpolates these data and assigns concentrations to each of the sigma level depths of the model. Since the available data for specifying the boundary conditions was sparse, some calibration of the boundary concentrations was required. This was accomplished by comparing model output to data using both temporal and vertical plots. Since the

boundary conditions were specified as being horizontally constant in the model, a data fit was chosen which best represented the entire data set for a particular month. In areas or months where no data were available, boundary conditions were determined using nearby stations or information other years where data were available. Recent analysis of the 1994 monitoring data, which included stations in close proximity to the boundary of the water quality model, appear to support the use of stations F21, F22, F12, and F08 as suitable for use in developing the 1992 boundary conditions (Kelly, 1995). For months when no data existed, boundary concentrations were estimated by visually interpolating data from months prior to and after the month in question. Salinity and temperature boundary conditions were obtained directly from the hydrodynamic model. Values used for the 1990 boundary conditions are listed in Appendix C. Figures 5-5 and 5-6 present temporal pictures of the boundary conditions used for 1990, together with the available observed data. Values for the 1992 boundary conditions are listed in Appendix D and are shown on Figures 5-7 and 5-8.

It should be noted that the 1992 boundary conditions assigned for the five measured parameters had concentrations somewhat lower than the 1990 values. It is unclear as to the exact reasons for these differences; they may be related to differences in Gulf of Maine nutrient concentrations between the two years, or due to reduced exchange or inflow from the Gulf of Maine between the two years.

The model requires boundary concentrations for all 24 state-variables. For many of these state-variables there were no data, or there were only measurements representing the sum of a number of state-variables. For example, from the Bigelow Laboratory data set there are measurements of particulate organic carbon (POC). The model, however, includes two types of non-living particulate organic carbon, and two functional algal groups, which also contribute to the POC pool. Therefore, it was necessary to estimate the fraction of POC in each of these pools using data from other systems and past modeling experience.
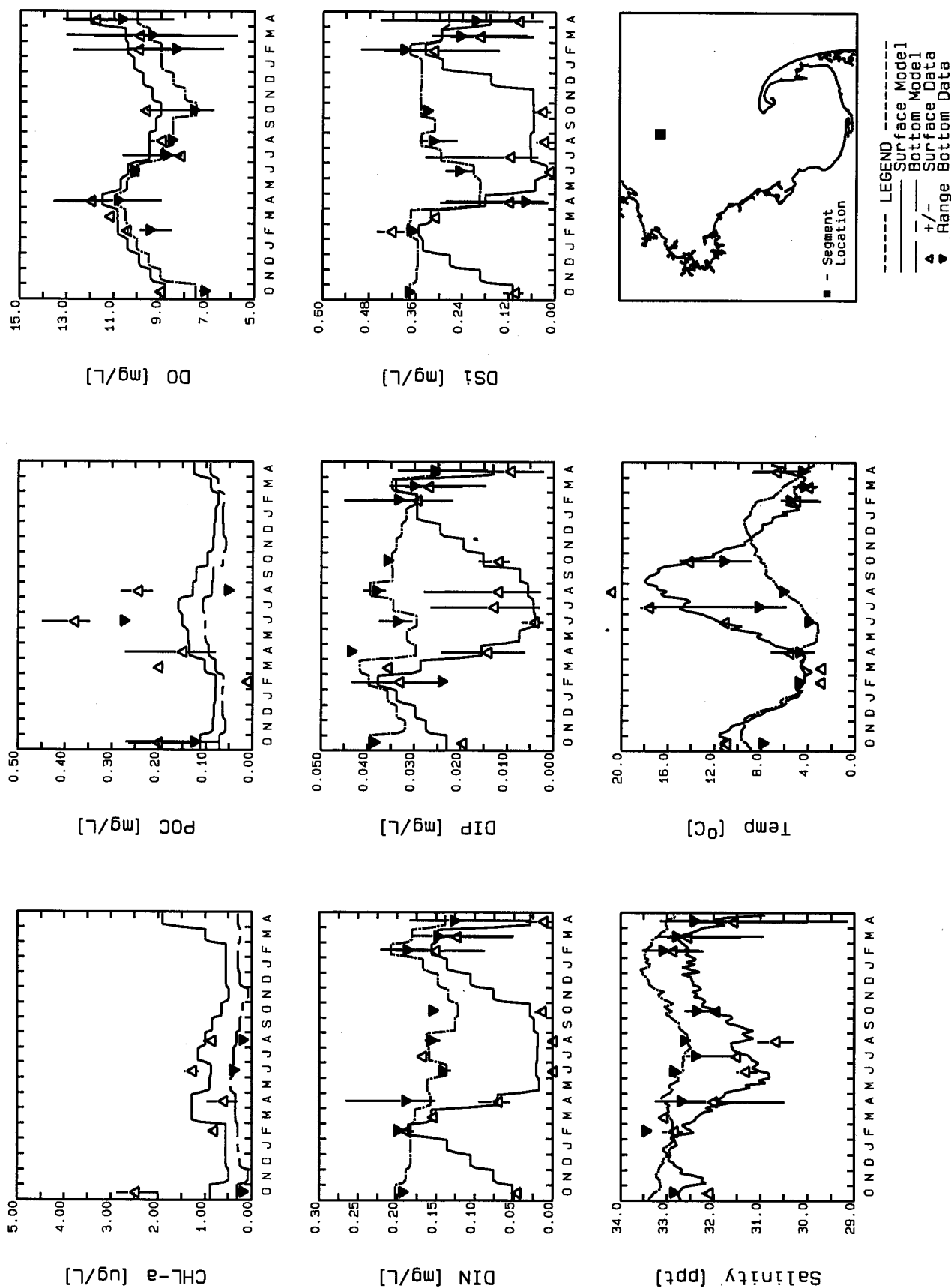
FIGURE 5-5. ASSIGNED BOUNDARY CONDITIONS FOR 1989 THROUGH 1991: CHL-a, POC, DO, DIN, PO$_4$, DSi, SALINITY AND TEMPERATURE
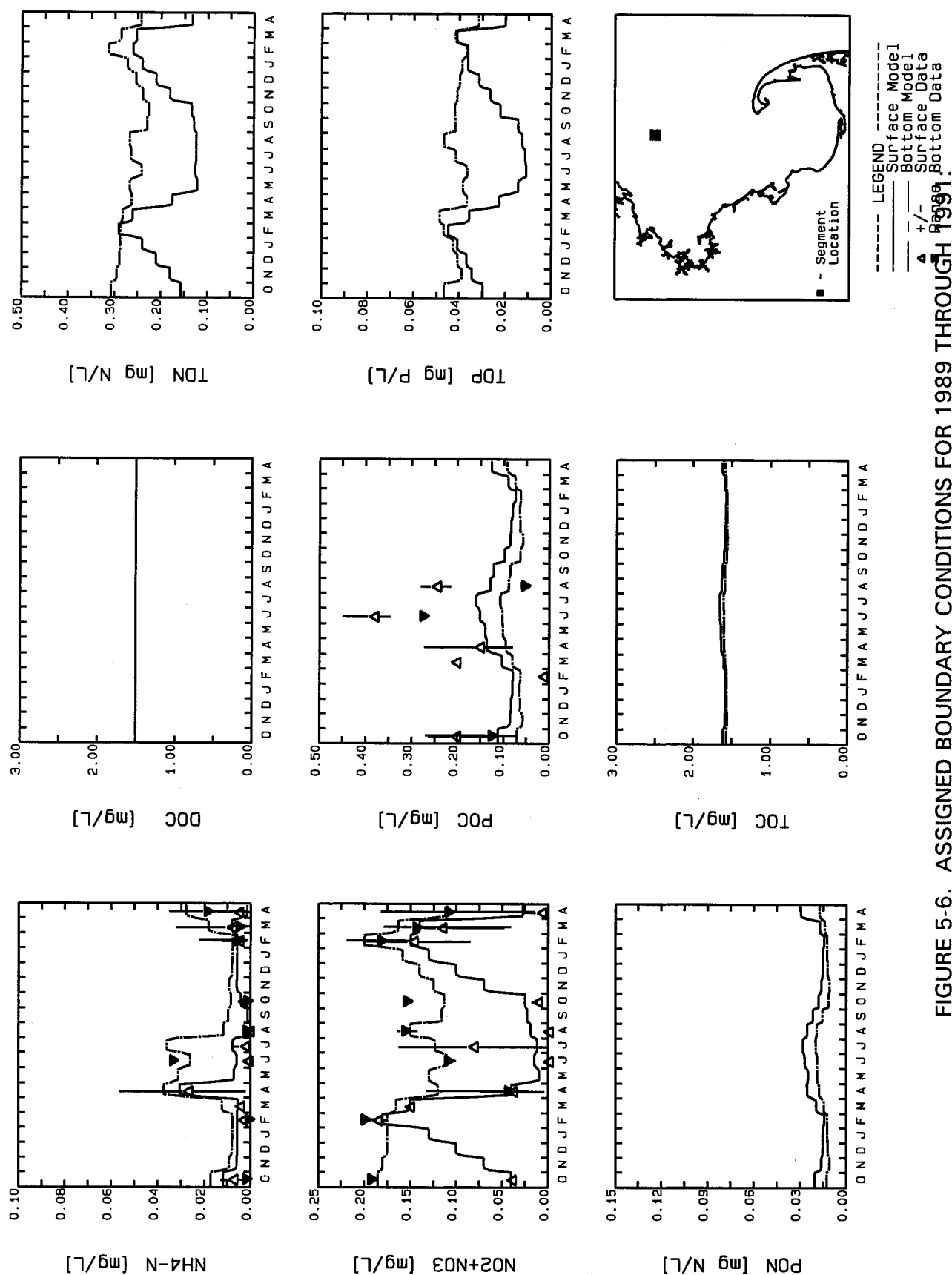
FIGURE 5-6. ASSIGNED BOUNDARY CONDITIONS FOR 1989 THROUGH 1991.
NH_4, DOC, TDN, $NO_2 + NO_3$, POC, TDP, PON, AND TOC
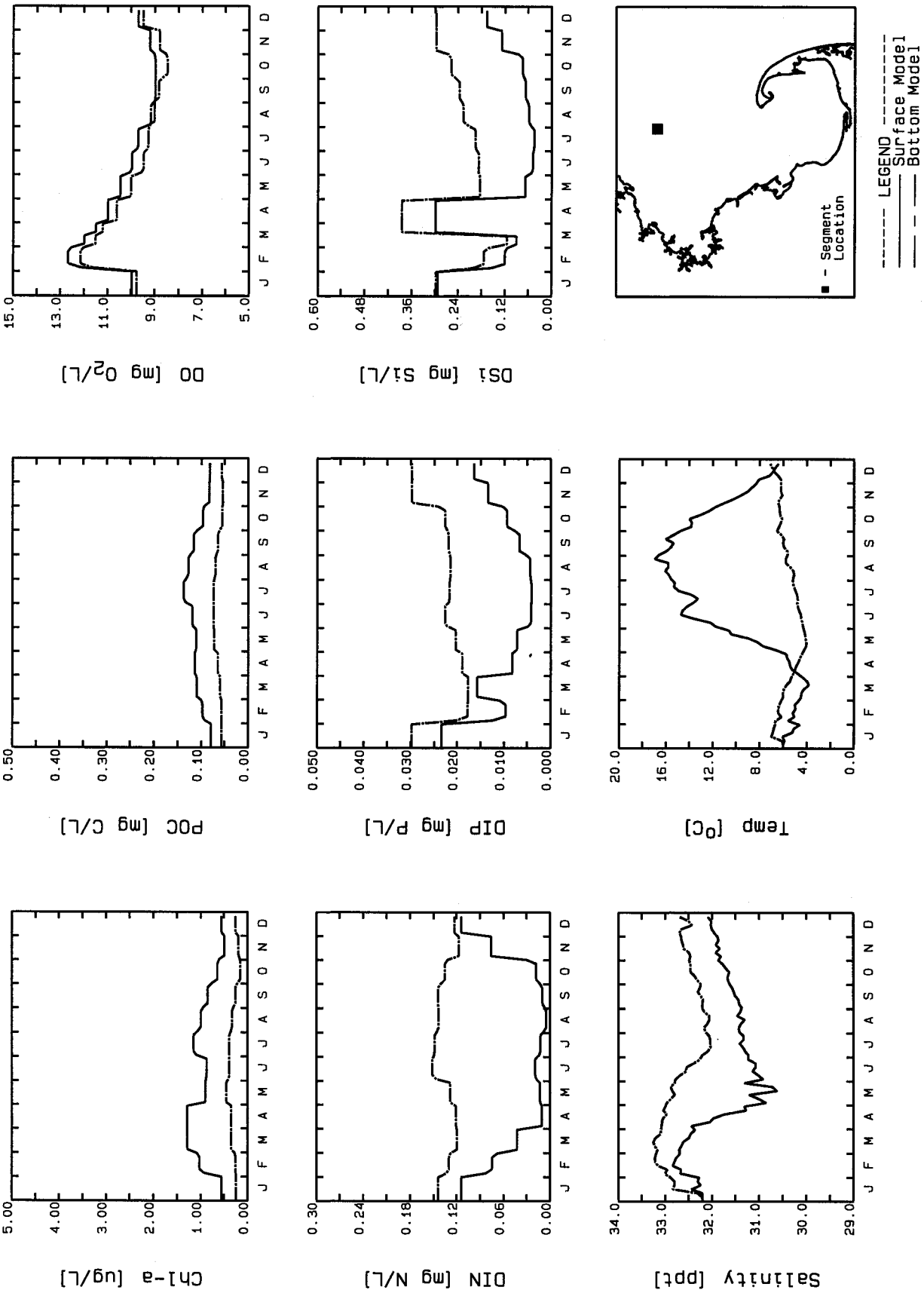
FIGURE 5-7. ASSIGNED BOUNDARY CONDITIONS FOR 1992:
CHL-a, POC, DO, DIN, PO$_4$, DSi, SALINITY AND TEMPERATURE
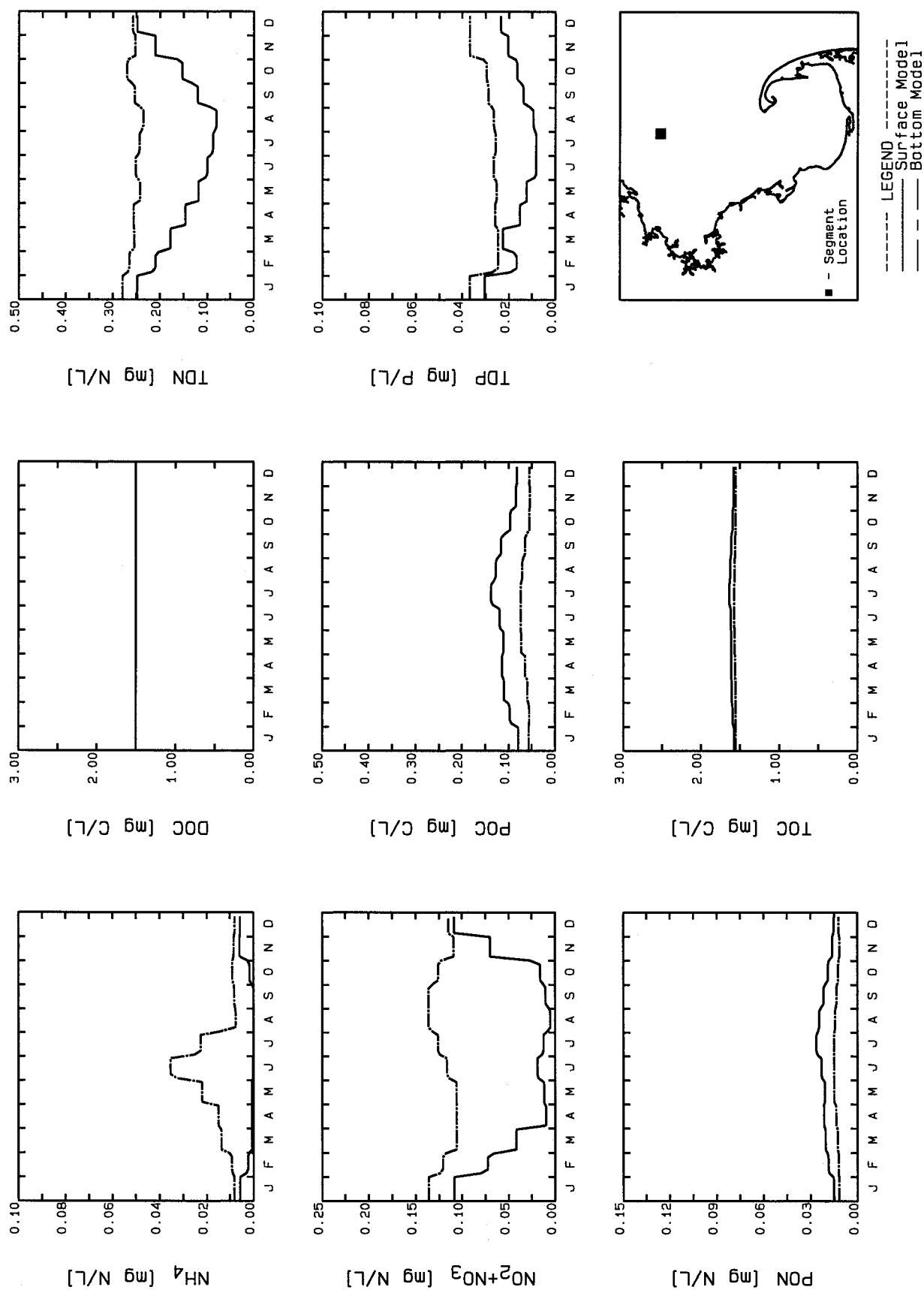
FIGURE 5-8. ASSIGNED BOUNDARY CONDITIONS FOR 1992: NH_4, DOC, TDN, $NO_2\_NO_3$, POC, TDP, PON, AND TOC

5.2.3 Pollutant Loading

Information concerning loading has been presented in Section 2. The information available for the point sources listed in the 1991 Menzie-Cura loading report included only TN, TP, and BOD. The MWRA loading report presented a more detailed breakdown of nutrients including NH_4, $NO_2 + NO_3$, and, in some cases, PO_4. Additional nutrient data, including NH_4, $NO_2 + NO_3$, PO_4, and Si, for the MWRA facilities were made available as a result of special monitoring by Battelle Ocean Sciences. The water quality model, however, requires additional information concerning the various forms of nitrogen, phosphorus and carbon; i.e., organic versus inorganic, and dissolved versus particulate. For nitrogen the model requires estimates for NH_4, $NO_2 + NO_3$, RPON, LPON, RDON, LDON. Similarly, for phosphorus the model requires estimates for PO_4, RPOP, LPOP, RDOP, and LDOP. Carbon is likewise divided into RPOC, LPOC, RDOC, LDOC, and ReDOC. Therefore, it was necessary to estimate the components for each of these pools for input to the model. The choices used to split the organic nitrogen, phosphorus and carbon loads were guided by previous modeling efforts in Chesapeake Bay (Cerco and Cole, 1993) and Long Island Sound (HydroQual, 1991).

Values used for the 1990 and 1992 loads are presented in Appendix E. Tables E-1 and E-2 present the nutrient fractions used to compute the necessary loads for the model's 24 state-variables. Tables E-3 through E-9 present the resulting loadings estimated from these nutrient fractions. The following paragraphs discuss the rationale for choosing these particular splits.

For the MWRA treatment plants, TKN, NH_4, TP, and PO_4 data were available, so it was possible to estimate the concentrations of the total organic nutrients. The resulting values were then split into the appropriate organic pools. Guided by suspended solids data and knowing that the MWRA facilities provide only primary treatment, the majority of the MWRA organic nutrients would be in the particulate form. Nutrient splits for the other facilities outside of Boston differ because they provide secondary treatment. CSOs were assumed to have nutrient splits similar to those used for the MWRA treatment facilities.

For the riverine discharges, the fractional splits used were guided by modeling experience from the Chesapeake Bay and Long Island Sound studies. The lack of reactive dissolved organic carbon in the riverine sources is due to the assumption that all ReDOC undergoes biological oxidation within the river by the time it flows into the Bay system. Non-CSO runoff is assumed to have nutrient splits the same as riverine splits for nitrogen and phosphorus outside of Boston Harbor.

5.2.4 Extinction Coefficients

Water transparency and, therefore, the light extinction coefficient, plays an important role in primary productivity. Phytoplankton productivity is greater in areas of high light penetration than in light limited areas, given the same nutrient availability. The data indicate that higher light extinction coefficients are appropriate in the area around Boston Harbor. This is due to high suspended solids loadings associated with sediment resuspension and transport, riverine inputs and the discharge of sludge and effluent from the Nut and Deer Island wastewater treatment facilities. Extinction coefficients are also higher in regions of high algal biomass. This reflects the effect of algal self-shading. The extinction coefficients used as input to the model were determiend from Battelle's measurements of vertical attenuation of surface light and chlorophyll-a. Estimates of the one percent light level were made from the vertical light profiles and total light extinction coefficients were made using the following equation:

$$k_{e_{obs}} = \frac{4.6}{H} \qquad \text{(Note: } e^{-4.6} \approx .01) \qquad (5\text{-}2)$$

where

$k_{e_{obs}}$ = the total water column extinction coefficient (m^{-1})

H = depth of the 1 percent surface light level (m),

These estimates were then corrected using the averaged vertical chlorophyll-a concentration, between the water surface and the one percent light level depth as per Equation 5-3:

$$k_{e_{base}} = k_{e_{obs}} - k_c \cdot chl\text{-}a_{obs} \qquad (5\text{-}3)$$

where

$k_{e_{base}}$ = the base or background extinction coefficient related to non-algal turbidity (m^{-1}),

$k_{e_{obs}}$ = the total water column extinction coefficient (m^{-1}),

k_c = the extinction coefficient per unit of phytoplankton chl-a $(m^2/mg$ chl-a),

$chl\text{-}a_{obs}$ = the observed chl-a concentration (mg/m^3).

The resulting $k_{e_{base}}$ were plotted as a function of the depth of the model segment in which it was sampled, as shown in Figure 5-9. Two curves were fit through the data so as to be able to estimate $k_{e_{base}}$ for segments for which no light measurements were made. The following empirical equations resulted:

$$k_{e_{base}} = 0.6 \qquad (m^{-1}) \text{ Boston Harbor} \qquad (5\text{-}4)$$

$$= 0.42e^{-0.065H} + 0.16 \quad (m^{-1}) \text{ North of Scituate Harbor}$$

$$= 0.06e^{-0.045H} + 0.16 \quad (m^{-1}) \text{ South of Scituate Harbor}$$

where H represents the depth of the segment. These equations represent the fact that Boston Harbor turbidity is influenced by sediment resuspension and transport, riverine inputs and by solids in the MWRA effluent and that shallow water near-shore areas are impacted by runoff and anthropogenic sources of solids while deeper mid-Bay segments are less impacted by these sources. The Bays system was divided into northern and southern regions, using Scituate as a dividing line, recognizing that there are greater anthropogenic inputs of suspended solids to northern Massachusetts Bay from Boston Harbor and other northern communities than enter the southern portion of the Bays system.
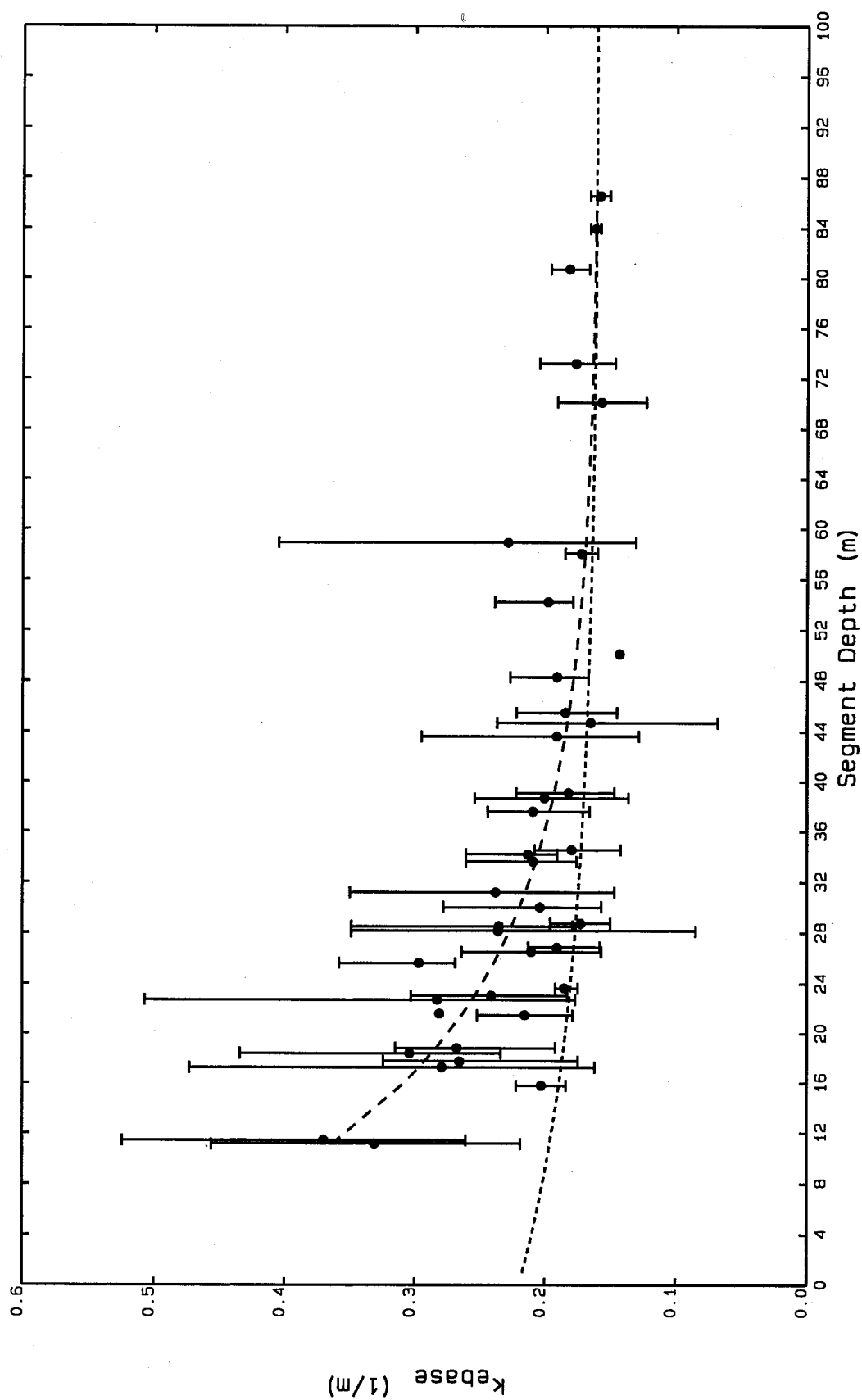
FIGURE 5-9. ANALYSIS OF LIGHT EXTINCTION INFORMATION USED TO ASSIGN SPATIALLY VARIABLE K_{ebase}

5.2.5 Reaeration Coefficients

Reaeration coefficients were determined internally in the water quality model, by providing observations of wind velocity, and using Equations 4-28a, b, and c. Wind velocity data were measured at the Boston Buoy located in northwestern Massachusetts Bay. The wind data used for the calibration periods are shown as five-day moving averages on the top panel of Figure 5-10.

5.2.6 Solar Radiation

Solar radiation is a principal exogenous input that plays a major role in determining phytoplankton growth. Short wave radiation from the sun is used by phytoplankton for photosynthesis. As this radiation passes through the atmosphere, it can be absorbed and scattered by gases in the air and by water vapor, clouds, and dust. As a result of such processes, solar radiation reaching the earth's surface is in two forms, direct and diffuse radiation. Values of daily incident solar radiation, as measured at Seabrook, New Hampshire were used as input to the model. A plot of five-day moving average solar radiation values used in the model is presented in the middle panel of Figure 5-10. As can be seen the annual cycle of solar radiation is similar for the three years of record, with maximum values observed in May, June, and July.

5.2.7 Fraction of Daylight

The growth rate formulation for phytoplankton used in the model, as described in Section 4, depends on the length or fraction of daylight, as photosynthesis takes place only in the presence of sunlight. The fraction of daylight for each day of the year may be calculated using basic trigonometry assuming the earth is a perfect sphere. (Corrections of six to eight minutes per day, which account for atmospheric refraction of the sun's rays at sunrise and sunset are assumed negligible.) Daily fractions of daylight were calculated using a methodology developed by Duffie and Beckman (1970), which depends on the
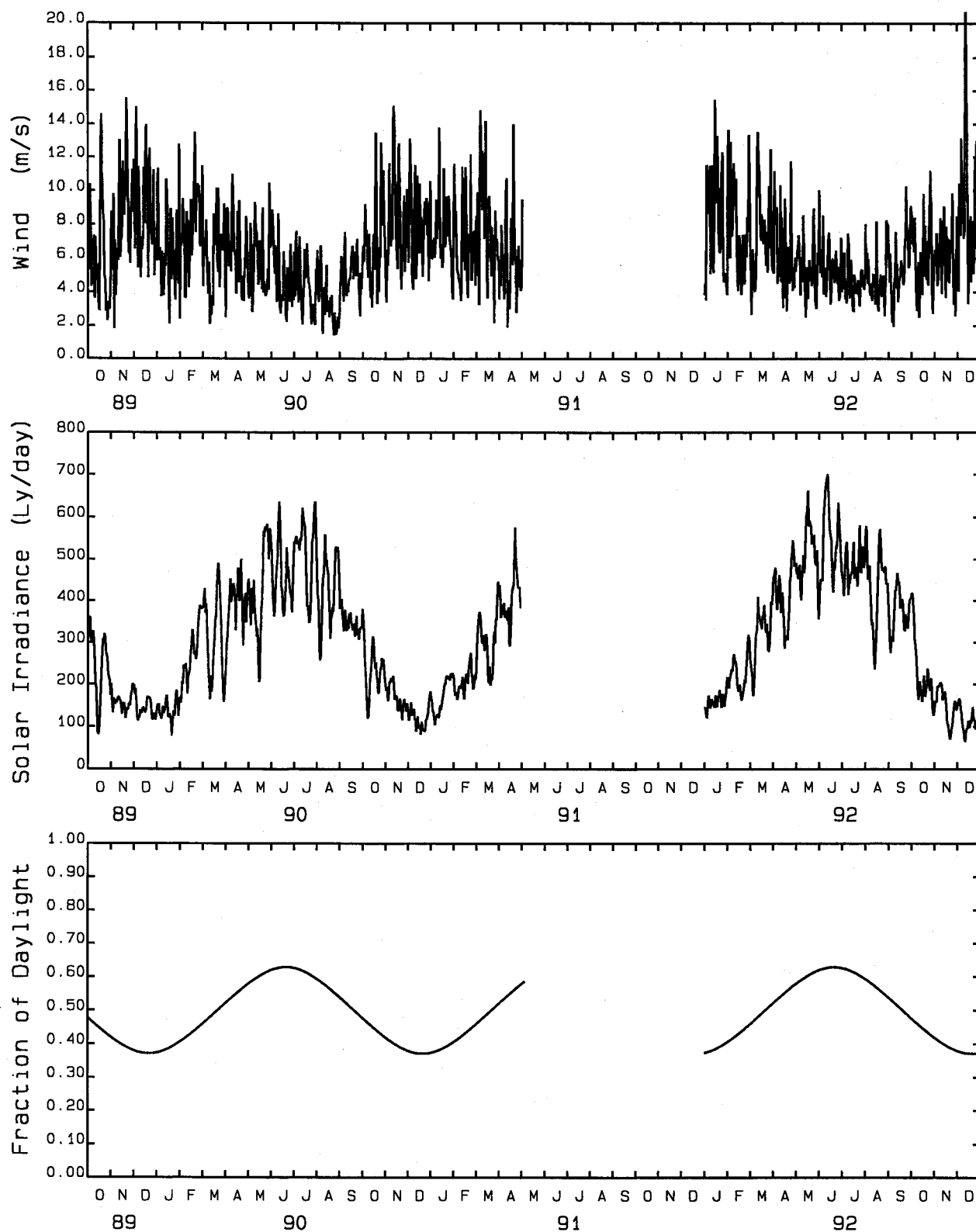
FIGURE 5-10. WIND, SOLAR IRRADIANCE AND FRACTION OF DAYLIGHT USED IN
MODEL CALIBRATION

latitude of the location of interest and the declination of the sun as a function of the time of year. Values used in the model are presented in the lower panel of Figure 5-10.

5.2.8 Particulate Organic Matter Deposition Velocities and Sedimentation Velocities

An important parameter required by the sediment submodel is the net deposition velocity of particulate organic matter settling from the water column to the sediment. Lacking the results of a mechanistic sediment transport modeling (currently under development by the USGS), it was thought that a review of data from side-scan acoustic profiles could be used to determine which regions of the study area were depositional or non-depositional. This determination would in turn would permit the specification of particulate organic matter (POM) deposition velocities. However, an analysis by Knebel (1993) suggests that some regions of the Bay are transitional in nature; i.e., sometimes being depositional and at other times, as forced by storm events, non-depositional. The determination of deposition velocities was further complicated by not having side-scan acoustic data for all regions of the Bay, as well as by having water quality model segments which contained both depositional and non-depositional zones. Therefore, to simplify the analysis it was decided to treat the entire water quality model domain the same and to specify a net POM deposition settling rate of 1 meter/day.

The sedimentation velocity is the rate at which material is buried in the sediment, relative to the surface of the sediment layer. Sedimentation velocities for coastal estuaries have been observed to be on the order of 0.1 to several cm/yr. Sedimentation velocities of from 0.12 to 2.0 cm/yr and from 0.2 to 0.6 cm/yr have been estimated using Pb-210 dating for Boston Harbor and Massachusetts Bay, respectively (Fitzgerald, 1980; Bothner, 1987). Given the variability observed in the data a spatially constant value of 0.25 cm/yr was used in this study.

5.3 CALIBRATION PARAMETERS

Model parameter evaluation is a recursive process. Parameters are selected from a range of feasible values, which are based on the literature and/or previous modeling studies, evaluated in the model, and adjusted until optimal agreement between model computations and observed water quality is achieved. Ideally, the range of feasible values is determined by observation or by laboratory and/or field experiment. For some parameters, however, no observations are available. Then, the feasible range is determined from parameter values reported in the literature or reported in similar modeling studies or by the judgement of the modeler.

Although the set of potentially adjustable model parameters used in this study numbers over one hundred, in reality a much smaller subset of parameters were actually adjusted during this study. The reason for this is that a number of the model coefficients have proved to be "universal" across a number of estuarine and coastal ecosystems similar to the Massachusetts Bays system. This subset of model parameters has been successfully applied to eutrophication models of Chesapeake Bay and Long Island Sound to name two of the current state-of-the-science studies.

The adjustable set of model coefficients may be sub-divided into five principal groupings: algal growth and algal stoichiometry parameters; nutrient recycle parameters; organic carbon oxidation and nitrification parameters; organic matter settling and deposition parameters; and sediment nutrient flux submodel parameters. Initial values for most of the parameters associated with the first three groupings were based on the previously mentioned Chesapeake Bay (Cerco and Cole, 1992) and Long Island Sound (HydroQual, 1991) studies. However, with the incorporation of the new Laws/Chalup algal growth model in the modeling framework, a new set of algal growth and algal stoichiometry parameters were required. Initial values for these coefficients were guided by the values reported in Laws and Chalup (1990) and field observations. Values for the organic matter settling were guided by the literature and previous modeling studies. The model parameters used to specify deposition to the sediment have been described above.

As was reported above, it was initially hoped that spatially dependent deposition velocities could be determined either from direct observation or by indirect methods involving hydrodynamic model computations. However, it was quickly realized that this would not be possible and hence a spatially uniform deposition velocity was chosen. After this decision was made, this model parameter was not adjusted further during the calibration process.

Model parameters associated with the fifth group, the sediment nutrient flux submodel, were as determined from the Chesapeake Bay study (DiToro and Fitzpatrick, 1993). The only adjustments to these coefficients were related to the temperature correction coefficients associated with diagenesis, nitrification and denitrification and to the coefficients which determine phosphorus partitioning in the sediment bed. The changes to the temperature correction and phosphorus partitioning coefficients were determined via calibration of a stand-alone version of the sediment model to the MERL mesocosm studies conducted by Oviatt et al. (1984). These studies were conducted using Narragansett Bay waters and were sampled bi-weekly. The data from this study provided a comprehensive test of the sediment flux submodel for waters with temperatures more similar to those observed in Massachusetts Bay than were observed in Chesapeake Bay. In addition, the coefficients used to determine phosphorus partitioning in the sediments in Chesapeake Bay were driven by sediments which contained high iron content, associated with the discharge of upbasin stormwater runoff and the discharge of steel mill production wastewaters to the northern portion of Chesapeake Bay. The partition coefficients arrived at through calibration to the MERL data set remained constant during the remainder of the calibration process.

Appendix F provides a contrast between the model parameters used in this study and those employed in the Long Island Sound study. As can be seen with the exception of the model parameters associated with the Laws/Chalup algal growth model, the two model parameter data sets are reasonably consistent. This suggests that a fairly robust modeling framework has been developed for the study of estuarine and coastal eutrophication. It also provides a greater degree of confidence that the calibrated model

reproduces the inter- relationships between phytoplankton, nutrients and dissolved oxygen for Massachusetts Bay and that the resulting model can be used with confidence for projection purposes.

5.4   CALIBRATION RESULTS

5.4.1 Introduction

The ultimate goal of this project is to develop a mathematical model which describes the nutrient cycling and oxygen dynamics of Massachusetts Bay. One method for judging the adequacy of the model in describing these processes is to compare the results of model computations to observed data. However, there is inherent variability in the measurements of the concentrations of water quality variables. This variability may be due to natural processes; for example, algal patchiness or the effect of local cloud cover or wind mixing on local phytoplankton primary productivity. There is also spatial variability introduced when one compares the observed data from one or two randomly selected sampling locations to the model output of a segment. Finally, variability may also be due to measurement imprecision or measurement error, although this is probably a small component of the overall variability. Therefore, given this variability, it is unrealistic to expect a model to exactly reproduce all observed water quality. However, the model should reproduce seasonal and spatial trends in the data, as well as the interrelationships between variables.

For example, it is expected that the model reproduce the annual cycle of phytoplankton biomass and primary productivity. For the Bay this should be reflected in high algal biomass during the late spring and early summer, followed by decreasing algal biomass levels in the late summer, with highest primary productivity occurring during the summer months. The model should also be able to reproduce the super-saturated dissolved oxygen concentrations observed in the surface layer of the water column in and around the region of peak phytoplankton biomass.

Some sediment flux data were also available against which to compare model computations. The adequacy of the sediment submodel can be judged by comparing model computations against the observed sediment nutrient and oxygen fluxes. The initial sediment sampling program was more limited in scope than the water column sampling program. Hence, the comparisons of observed and computed fluxes are more limited than the water column comparisons.

5.4.2 1990 Calibration Results

For the 1990 calibration period calibration results are presented using time-series comparisons of model versus data for a number of the key water quality parameters. These include phytoplankton chlorophyll-a, POC, DO, DIN, PO_4, and DSi. Model versus data comparisons are also presented for salinity and temperature, to illustrate the calibration status of the hydrodynamic model. The time-series results cover the period October 1989 through April 1991. The figures present model versus data comparisons for surface and bottom water data and the surface and bottom layers of the water quality model. The observed data are presented using open circles to represent surface measurements and filled circles to represent bottom measurements. Where there is more than one station or measurement within a water quality segment, the standard deviation is also shown with a vertical line about the mean. BEM results are represented using a solid line for the surface layer and a dashed line for the bottom layer. The modeled annual cycle of DO saturation is also included on these figures, as a dotted line, for reference purposes. Model results represent a five day average of model computations.

The 1990 calibration data set is limited by the relative paucity of water quality data. The best data set for water quality model calibration purposes is the Bigelow Laboratory data (Townsend et al., 1991). However, these stations are clustered in the northwestern and north-central portion of Massachusetts Bay. Therefore, the presentation of the water quality model calibration will be limited to this area.

Figure 5-11 presents calibration results using data from Station 10 of the Bigelow Laboratory data set, as well as Stations SA4 and SA5 of the UMB/WHOI/UNH data set (Geyer et al., 1992). In general, the hydrodynamic model compares favorably to the observed salinity and temperature. The hydrodynamic model is able to reproduce the annual cycle of surface and bottom water temperature, including the marked period of stratification observed in the summer months. The hydrodynamic model also tends to reproduce the observed salinity data, including those periods marked by large freshets from the Merrimack River and other Gulf of Maine tributaries. The hydrodynamic model, however, appears to over-estimate the magnitude of the spring freshet in 1990; in June and July the hydrodynamic model under-estimates surface water salinity. The model does, however, reproduce the marked decreases in surface salinities that occur both in August 1990 and between February and April 1991.

Figure 5-11 also presents BEM calibration results for phytoplankton biomass, DO and the key inorganic nutrients. The water quality model appears to compare favorably to the observed surface chlorophyll-a and fluoresence data. The model is able to reproduce the decrease in chlorophyll-a that occurs between October 1989 and February 1990. The model then reproduces the spring bloom which occurs between February and late April, when chlorophyll-a concentrations increase from less than 1 to over 4 μg/L. The model also reproduces the decline in chlorophyll-a that occurs between April and June, as well as the further decline into August. The BEM results for POC are also encouraging. The model reproduces the general trends observed in the surface POC data, decreasing POC concentrations between October 1989 and February 1990, followed by increasing POC concentrations between February and April. The model, however, while maintaining elevated levels of POC during the summer, under-estimates concentrations of POC during July and August.

The BEM also reproduces some of the key features of the observed DO data. While the model does not reproduce the extremely supersaturated DO data observed in June 1990, possibly due to under-estimating the June algal bloom, the results are encouraging for the other months. The BEM does, in general, compute supersaturated surface DO
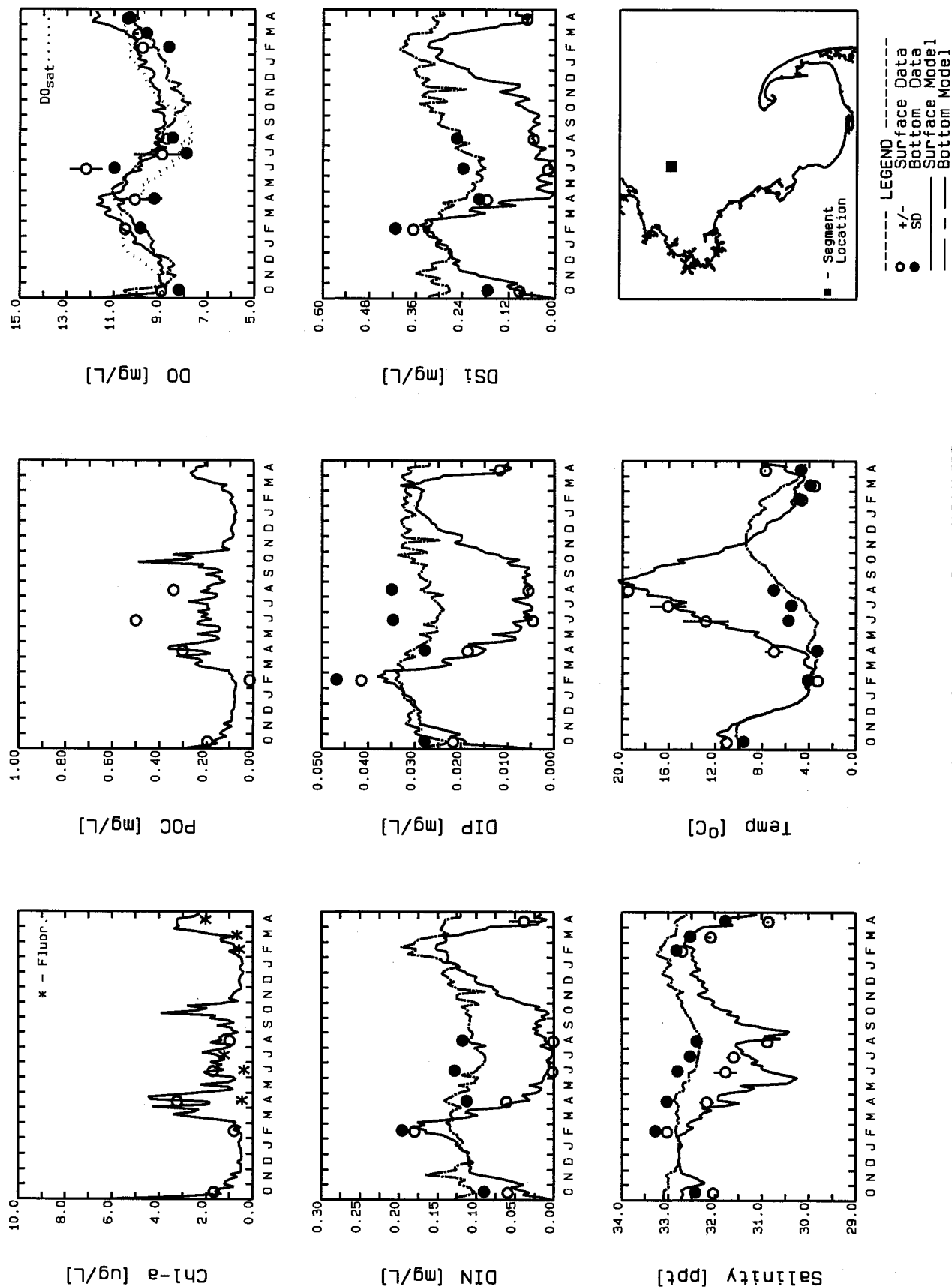
FIGURE 5-11. 1989 THROUGH 1991 TEMPORAL CALIBRATION RESULTS FOR GRID CELL (15,16) VERSUS DATA STATIONS BIGELOW 10, WHOI/UMB/UNH SA4 AND SA5

concentrations between April and October, which is supported by the data. In addition, the model computes surface DO concentrations which are under-saturated between November and March, again which is indicated by the data.

With respect to the inorganic nutrients, the BEM computations are in good agreement with the observed data, particularly the surface data. The model is able to reproduce the marked declines in surface DIN, PO_4 and DSi, that occur between February and June, as the spring phytoplankton bloom takes place. The model also reproduces the timing of the depletion of DSi and DIN, as well as the increasing DSi concentrations by August, as DIN continues to limit phytoplankton biomass. The model also properly computes the low, but non-limiting, concentrations of PO_4 observed during the summer period.

Figure 5-12 presents water quality model calibration results using Station 17 of the Bigelow Laboratory data set. The hydrodynamic model computations of salinity and temperature compare favorably to the observed data, although the model appears to over-estimate surface temperatures in June and July by 1 to 3°C. The BEM reproduces the magnitude of the spring bloom as indicated by chlorophyll-a. The model then correctly computes the decline in chlorophyll-a concentrations observed in April, but fails to reproduce a June bloom, as indicated by chlorophyll-a, POC and supersaturated DO concentrations. The model again provides a favorable comparison for chlorophyll-a, POC and DO in August.

The calibration results for the inorganic nutrients are also favorable. The model again reproduces the annual cycle of reduced concentration levels in the surface waters of Massachusetts Bay observed during the summer months. The model also properly computes the timing of DSi and DIN depletion in the surface waters and the low but non-limiting PO_4 concentrations. The model also approximately reproduces the stratification in inorganic nutrients observed during the summer months.
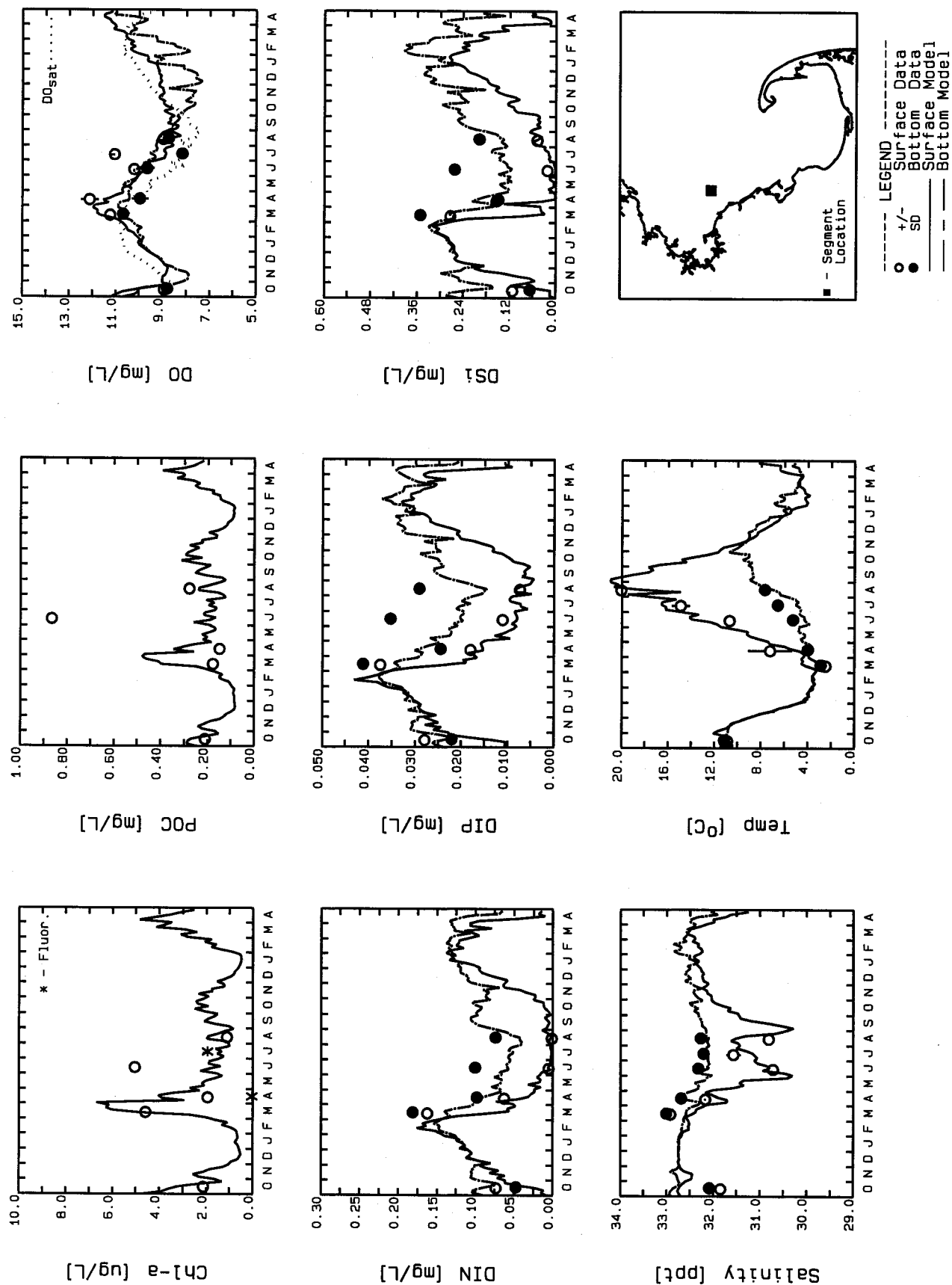
FIGURE 5-12. 1989 THROUGH 1991 TEMPORAL CALIBRATION RESULTS FOR
GRID CELL (10,15) VERSUS DATA STATION BIGELOW 17

5.4.3 1992 Calibration Results

The only changes in model inputs between the 1990 and 1992 calibration periods were new hydrodynamic model transport fields, input loadings (in particular, the reduction of inorganic carbon and nutrients associated with the cessation of the discharge of the wastewater treatment plant sludge) and exogenous inputs such as wind and solar radiation. All other model inputs, in particular the model kinetic coefficients, such as algal growth rates, nutrient recycle rates, etc., were the same as used for the 1990 period.

To demonstrate the model calibration results for this period, a sequence of time-series model versus data plots will be presented. The plotting symbols are as described above. The best data in the 1992 monitoring program data set for calibration purposes are those collected as part of the near field productivity effort. In addition to measuring hydrographic and inorganic nutrient data, Battelle measured discrete chlorophyll-a, chlorophyll fluorescence, POC, PON, and total dissolved nitrogen and phosphorus. Therefore, stations which contain these data provide an excellent basis for evaluating the calibration results for BEM.

Figure 5-13 presents model versus data comparisons for a model cell which encompasses Stations N16P, N17, and N21. The hydrodynamic model is well calibrated as judged by comparisons to observed salinity and temperature. The hydrodynamic model was able to reproduce the timing of the spring freshet from the Gulf of Maine, correctly computing the decrease in surface salinity that occurs between April and May, followed by the return to more saline conditions again in June. The hydrodynamic model also reproduced well the seasonal cycle in surface and bottom water temperatures.

With respect to the biological and chemical parameters the model results are encouraging. The model was able to reproduce some of the features of the annual cycle of primary production in northern Massachusetts Bay. The BEM provided an excellent calibration to the observed inorganic nutrient data, including the following features: the observed summer stratification in DIN, PO_4, and DSi; the depletion in surface DIN during
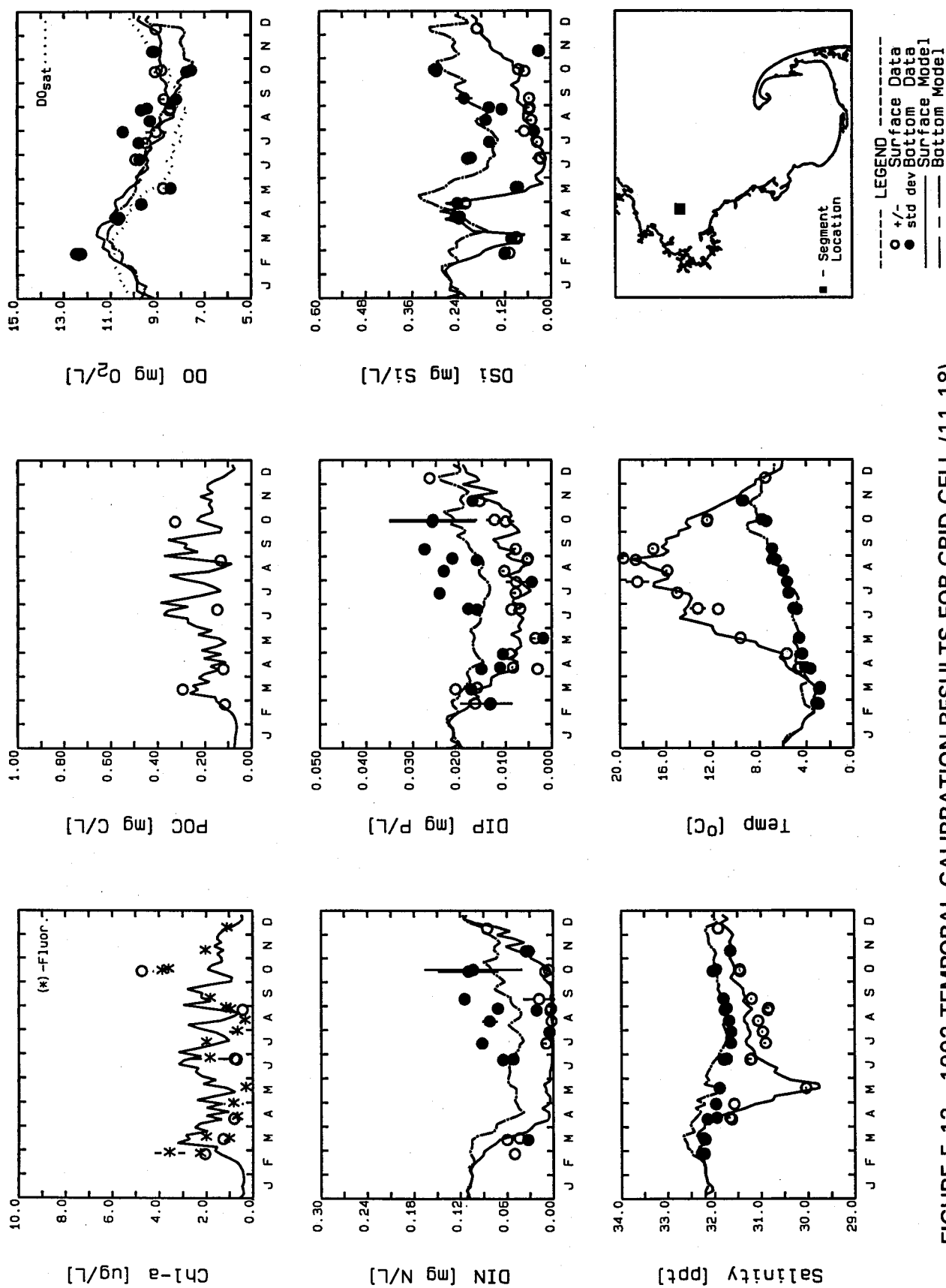
FIGURE 5-13. 1992 TEMPORAL CALIBRATION RESULTS FOR GRID CELL (11,18) VERSUS DATA STATIONS N16P, N17, AND N21

the summer months; the marked decline in surface DSi that occurs between April and June, together with the slow increase in surface DSi that occurs between June and October; the seasonal cycle in surface PO_4. The water quality model also appears to provide a reasonable calibration to the observed chlorophyll-a and fluorescence data, although there is considerable week to week variability that the model only partially reproduced. The BEM also compared favorably to the POC data, although it over-estimates the POC data in June. It is also interesting to note the variability in the model computation of chlorophyll-a and POC and the variability in the observed chlorophyll-a. This may be a result of wind conditions setting up offshore surface layer flows which would carry chlorophyll and nutrient rich waters from Boston Harbor into the region of this station/water quality model segment. This will be discussed latter in this section.

The model results for DO are encouraging. The model reproduced the annual cycle of DO, including the minimum DO concentrations that are observed in the bottom waters in October, and the degree of DO stratification. The model, however, under-estimated the super-saturated conditions observed in February. This suggests that the model may not have reproduced the timing of a winter bloom that occurred that year. The model also over-estimated surface and bottom DO concentrations that were observed in May. This may be the result of under-estimating the decline in the spring algal bloom and the associated bacterial oxidation of detrital algal biomass. However, despite these discrepancies the BEM performs well overall.

Two additional stations are presented for judging the calibration status of the BEM. These two stations will provide some contrasts to the future outfall site (N16P, N17, and N21) station results. The first of these two stations is N10P, located just outside the entrance to Boston Harbor. Figure 5-14 presents the model versus data results for this station. One of the first features to note is that both the data and the model computations indicate a lesser degree of stratification in salinity and temperature during the summer months as compared to stations N16P, N17, and N21. This may be due to the mixing associated with the large tidal currents associated with Boston Harbor, as well as due to the shallower water depth in this region.
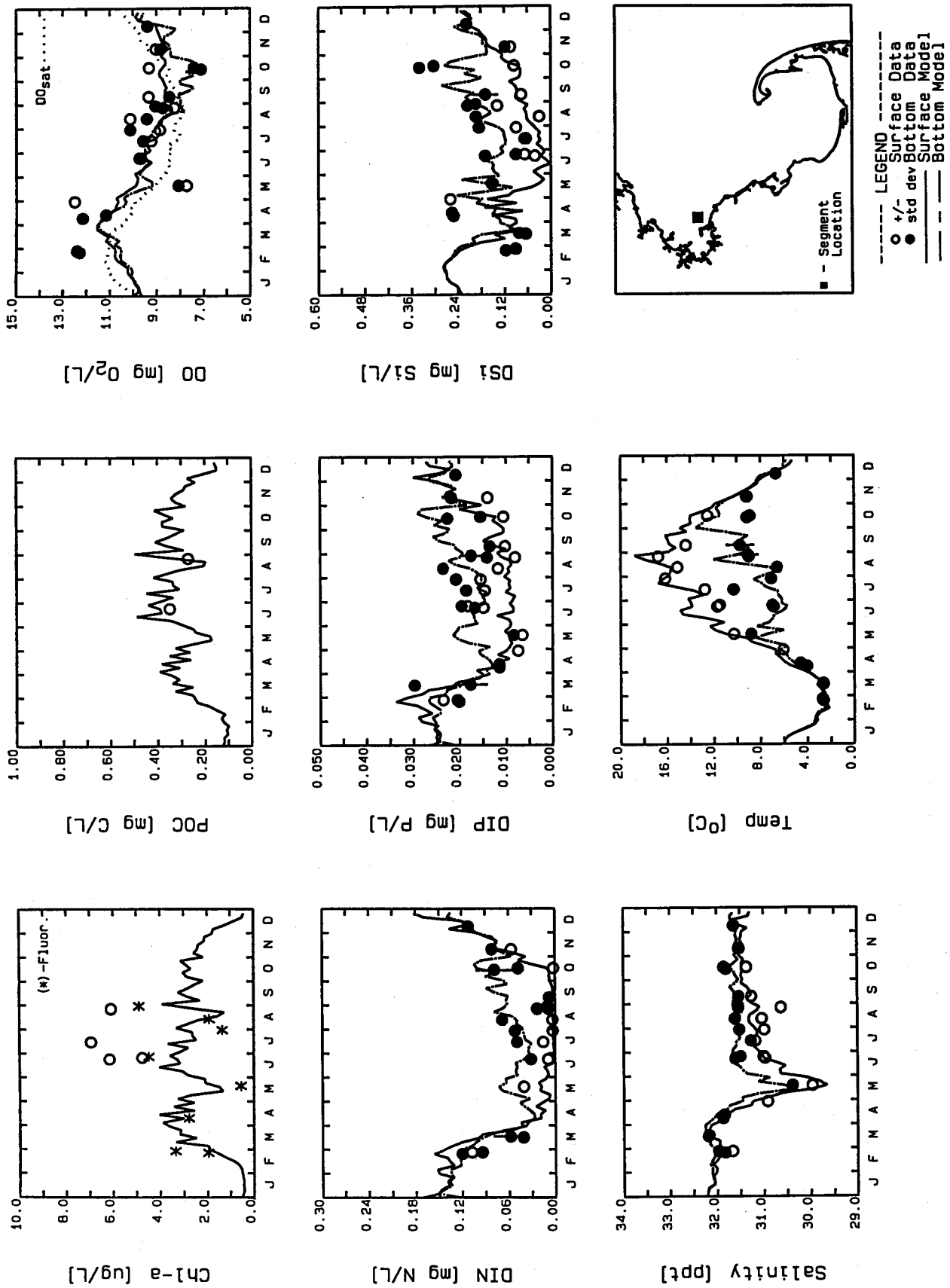
FIGURE 5-14. 1992 TEMPORAL CALIBRATION RESULTS FOR GRID CELL (8,18) VERSUS DATA STATION N1OP

The other features to note are the higher concentrations of chlorophyll-a, fluorescence and POC. This difference in biomass levels between the two stations reflects the fact that the N10P station (and water quality segment) is closer to the Boston Harbor effluent plume and, therefore, not as nutrient limited. This greater availability of nutrients can be seen in the higher concentrations of DIN that were observed in February/March and November/December. The model also provided a favorable comparisons to the observed nutrients, including differances in the seasonal cycle between surface and bottom waters due to density stratification and primary productivity. The model did, however, over-estimate bottom water nutrients (DIN and DIP) in August and early September. The reasons for this discrepancy are not known.

The final station for which this series of temporal results are presented is F01P (Figure 5-15). This station is located in the southwest corner of Cape Cod Bay. Although the data base for calibration analysis is not as extensive for this station compared to stations in Massachusetts Bay, the available data are sufficient to get a sense of the calibration and to contrast this region of the study area against the Massachusetts Bay stations. First to note is the fact that the hydrodynamic model calibration results are favorable. Although the hydrodynamic model over-estimated the surface salinity in late August, the remaining model versus data comparisons for salinity and temperature were favorable.

Although the data are sparse, it appears as if the BEM is providing a favorable calibration for the Cape Cod Bay portion of the study area. The model approximately reproduced the winter/early spring bloom as indicated by chlorophyll-a, POC and DO, as well as surface water nutrient depletion. The model, however, appeared to be a week or two late in the timing of the bloom, as can be seen in the model's under-estimation of February POC and DO.

Of particular note, the model was able to compute the fact that the winter/spring bloom became silica limited in late March, just before DIN became limiting. This is in
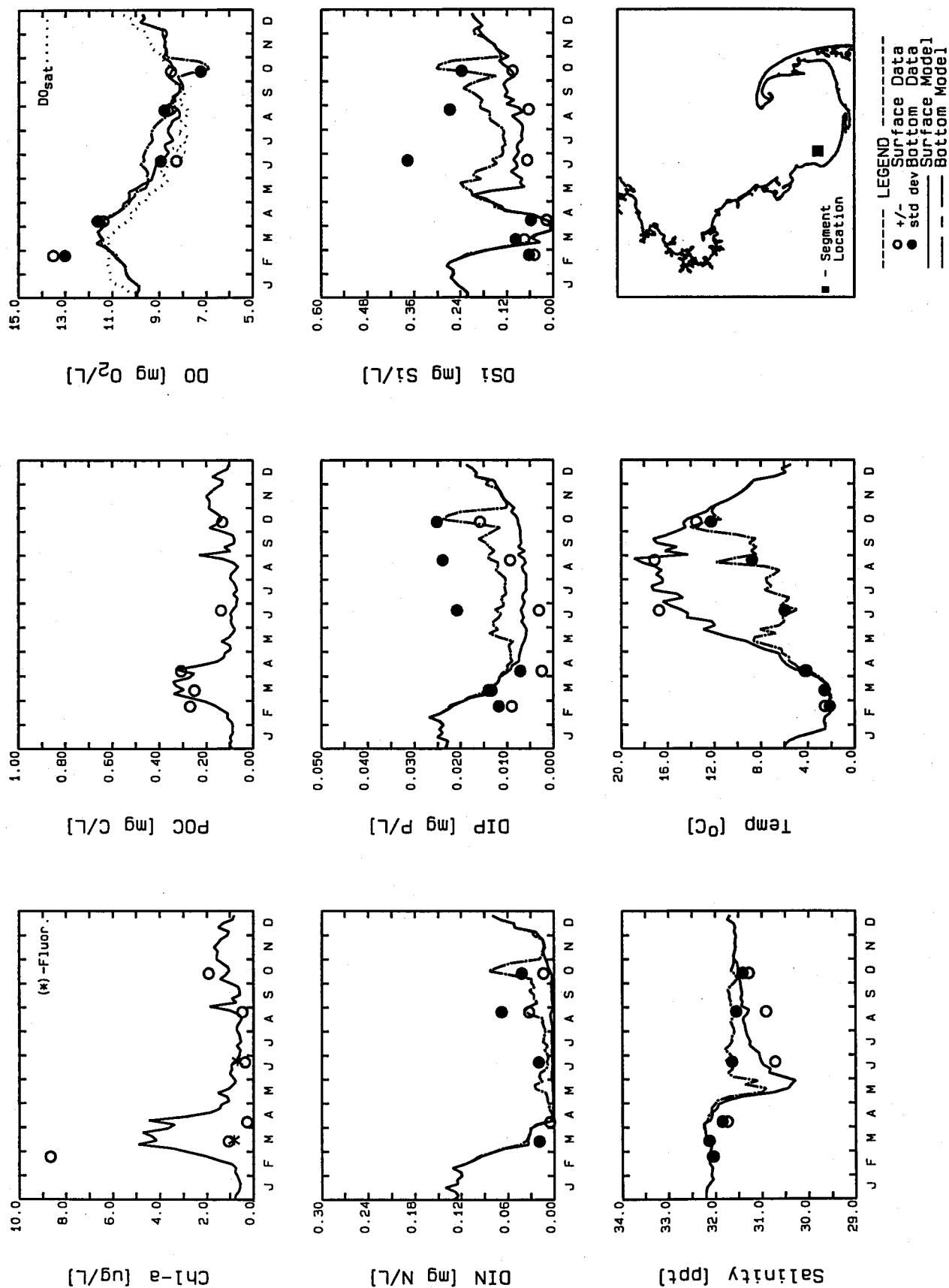
FIGURE 5-15. 1992 TEMPORAL CALIBRATION RESULTS FOR GRID CELL (6,4) VERSUS DATA STATION F01P

marked contrast to the northern Massachusetts Bay stations, which do not give evidence of possible silica limitation until late May or early June.

The model provided a favorable calibration to the observed DO data. The model computations, although missing the super-saturated February values, were generally within 0.5 mg/L of the observed data. It is also interesting to note, that the DO concentrations in Cape Cod Bay were not as supersaturated as those observed in Massachusetts Bay, indicating perhaps a greater degree of nutrient limitation.

Another way of viewing the model calibration results is to present a series of temporal plots for one state-variable or water quality constituent at a time for a number of stations located in various regions of the study area. In this way it is possible to judge whether the model can reproduce the differences in water quality that may be observed in each region. Figure 5-16 presents comparisons between model computations and observed data for chlorophyll-a and fluorescence. Model computations are shown as five-day averages (solid line) and range (shading). Two stations, F23P and N10P are located near Boston Harbor. Except for the February bloom observed at stations F01P and N04P and one survey in late August at station N04P, chlorophyll-a and fluorescence concentrations at F23P and N10P are higher than those observed at the other stations shown on this figure. Model computations of chlorophyll-a are also greatest at these at these two stations. Overall, the model can reproduce the spatial gradient in chlorophyll-a and fluorescence observed within the Bays' system, which show a gradient of decreasing chlorophyll concentration with distance away from the Harbor into Massachusetts Bay. Other researchers have noted this feature (Townsend et al., 1991; Kelly, 1993).

Another feature of the Bays' system that the model can reproduce is presented in Figure 5-17. This figure presents comparisons of model computed DSi versus observed data. A number of researchers have noted (Becker, 1992; Kelly, 1993) that the late winter/early spring diatom bloom virtually depletes silica in Cape Cod Bay; this phenomenon is generally not observed in Massachusetts Bay. Figure 5-17 shows that station F01P is virtually deplete of DSi in April, as opposed to the other Massachusetts Bay
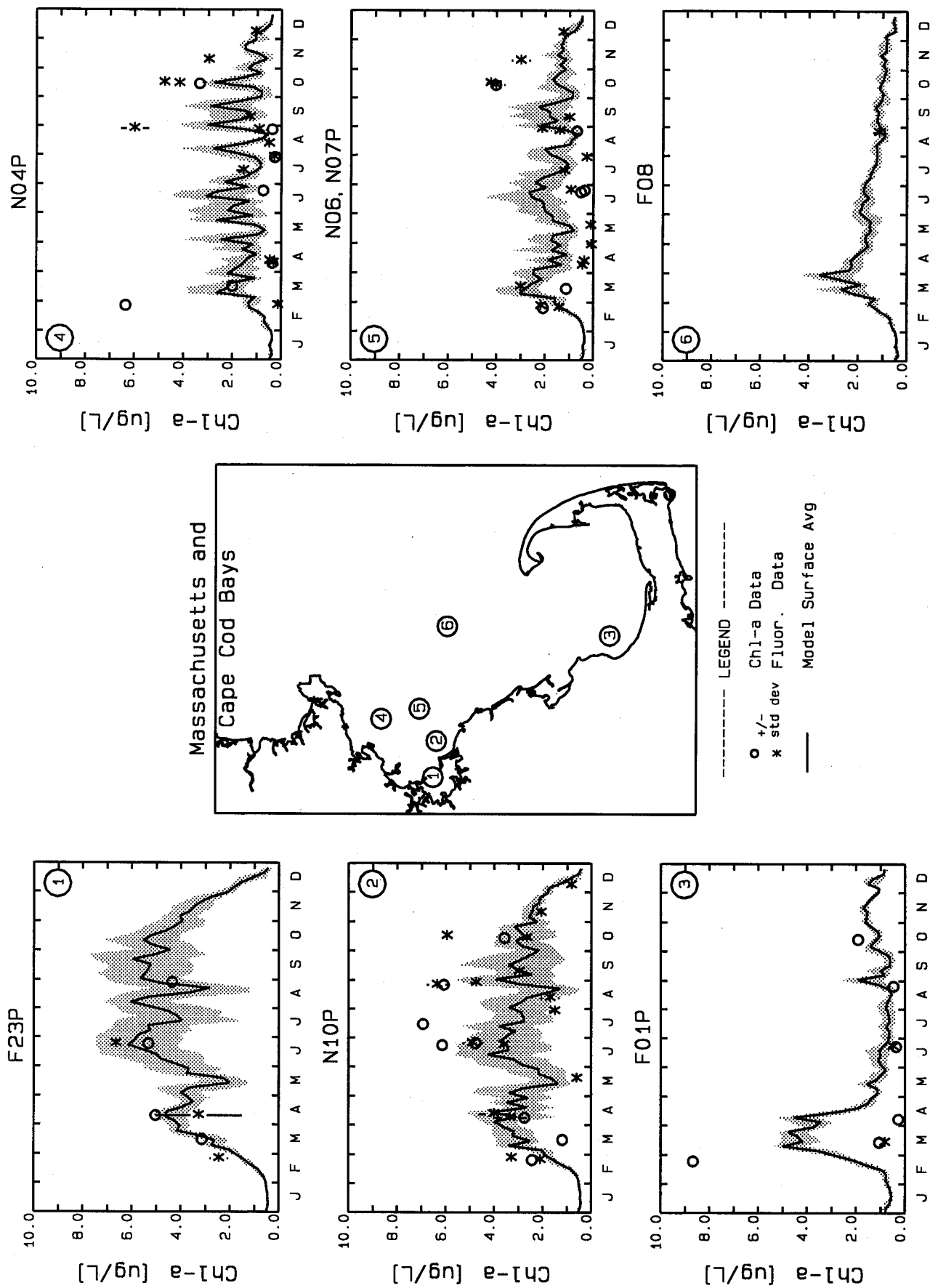
FIGURE 5-16. 1992 CHLOROPHYLL-a CALIBRATION FOR SELECTED STATIONS
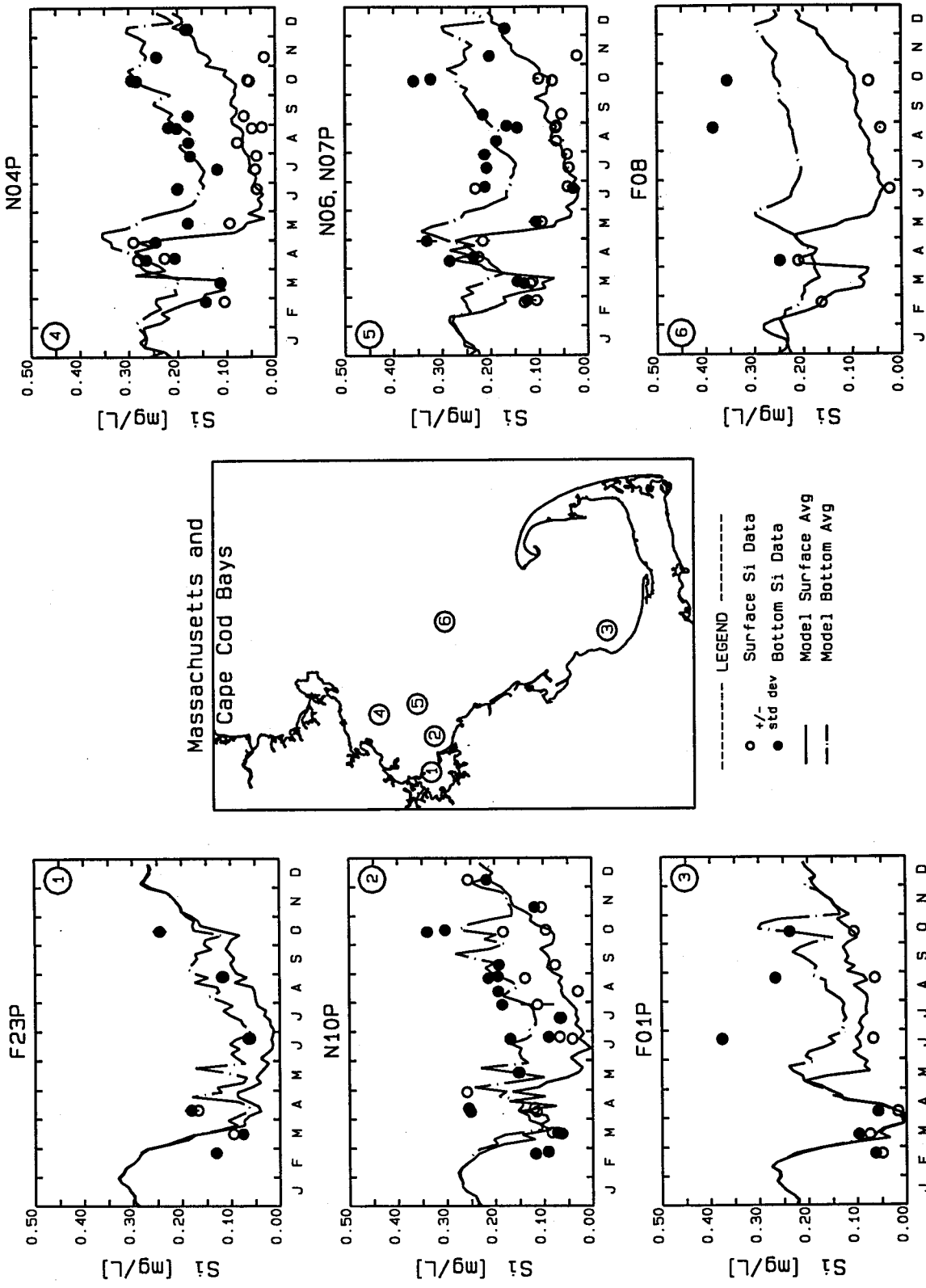
FIGURE 5-17. 1992 DSi CALIBRATION FOR SELECTED STATIONS

stations that still have significant DSi levels in April. This may due, in part, to the influx of DSi into Massachusetts Bay that accompanies the spring freshet.

Figure 5-18 presents model calibration results for light extinction, k_e, for a number of stations within the study area. The model reproduces the observed spatial gradient in k_e, which shows decreasing light extinction as a function of distance from Boston Harbor. This is in part due to the base light extinction coefficients used as input to the model. The model fails to reproduce the high values of light extinction observed at station F01P in February and March. This is in part because the model failed to reproduce the late winter diatom bloom in this region. A series of model versus data comparisons is presented for dissolved oxygen on Figure 5-19. Model computations are shown for the surface and bottom waters using five-day averages. In addition, the maximum surface and minimum bottom DO concentrations are also illustrated. One feature of the observed data that the model is partially able to reproduce is that for a number of stations the bottom waters DO concentrations are higher than the surface water concentrations during the summer months. The model is also able to reproduce the yearly DO minimums observed in October/November, and the stratification in DO that occurs at that time. The model, as was noted earlier, overestimates surface and bottom water DO concentrations that are observed in May. Overall, though, the model provides a favorable comparison to the annual cycle of dissolved oxygen observed within the Bays system.

Figures 5-20 through 5-23 present depth profiles of observed data versus model computations for Station F01P located in western Cape Cod. These figures provide comparisons for February, March, June, and October 1992. These figures illustrate the ability of the hydrodynamic and water quality models to reproduce the observed vertical gradients in water quality. The data points, shown as circles, were sampled on the day indicated in the figure title. These binned points have been plotted at the mid-depth of the sigma layer in which they are found. The model computations are plotted as a solid line for a five day average in which the data sampling was completed. The dashed lines represent the maximum and minimum concentrations computed within the five day period. Plotted on each figure are salinity, temperature and sigma-t (a measure of the density), in
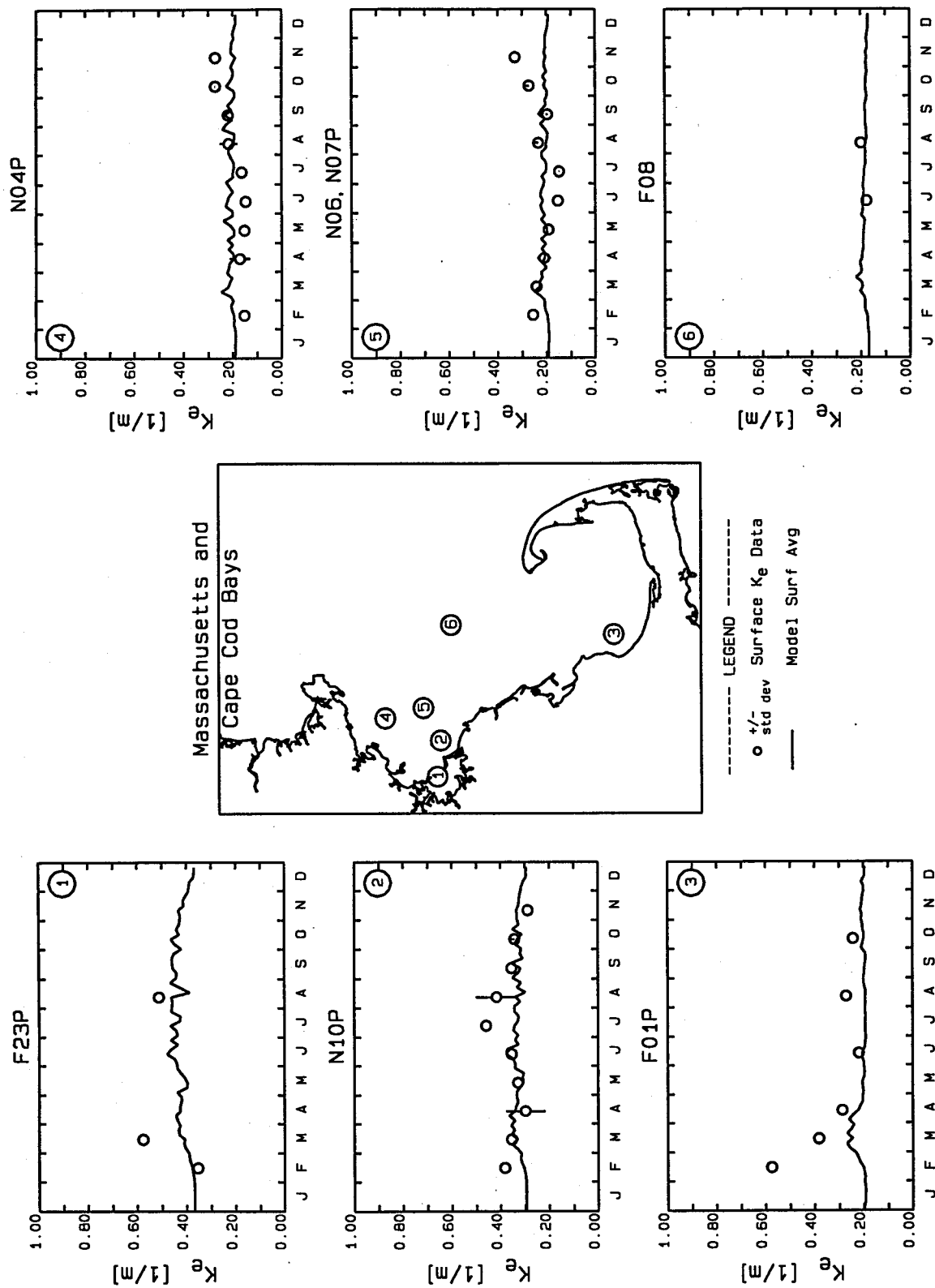
FIGURE 5-18. K_e CALIBRATION FOR SELECTED STATIONS
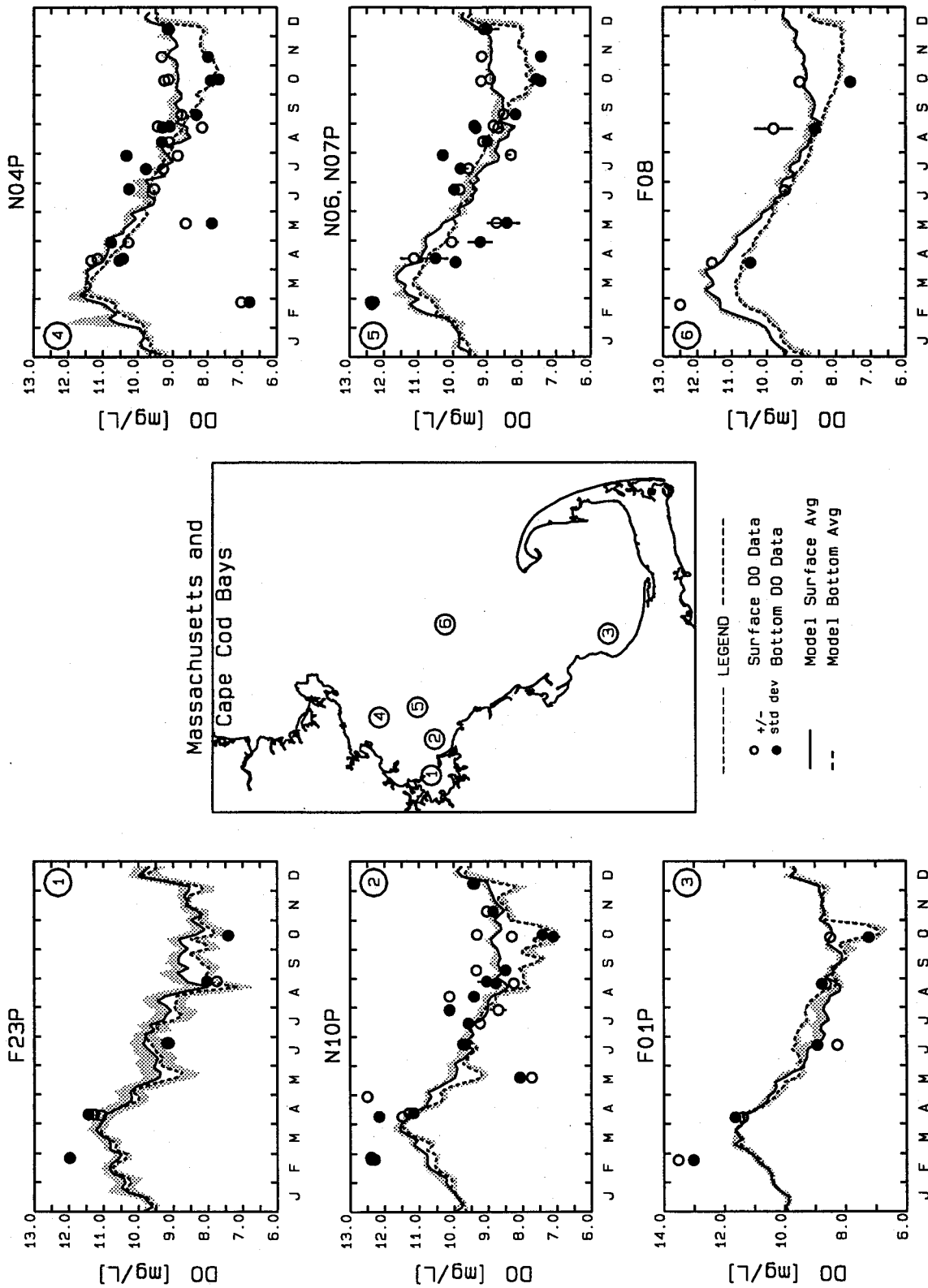
FIGURE 5-19. 1992 DO CALIBRATION FOR SELECTED STATIONS
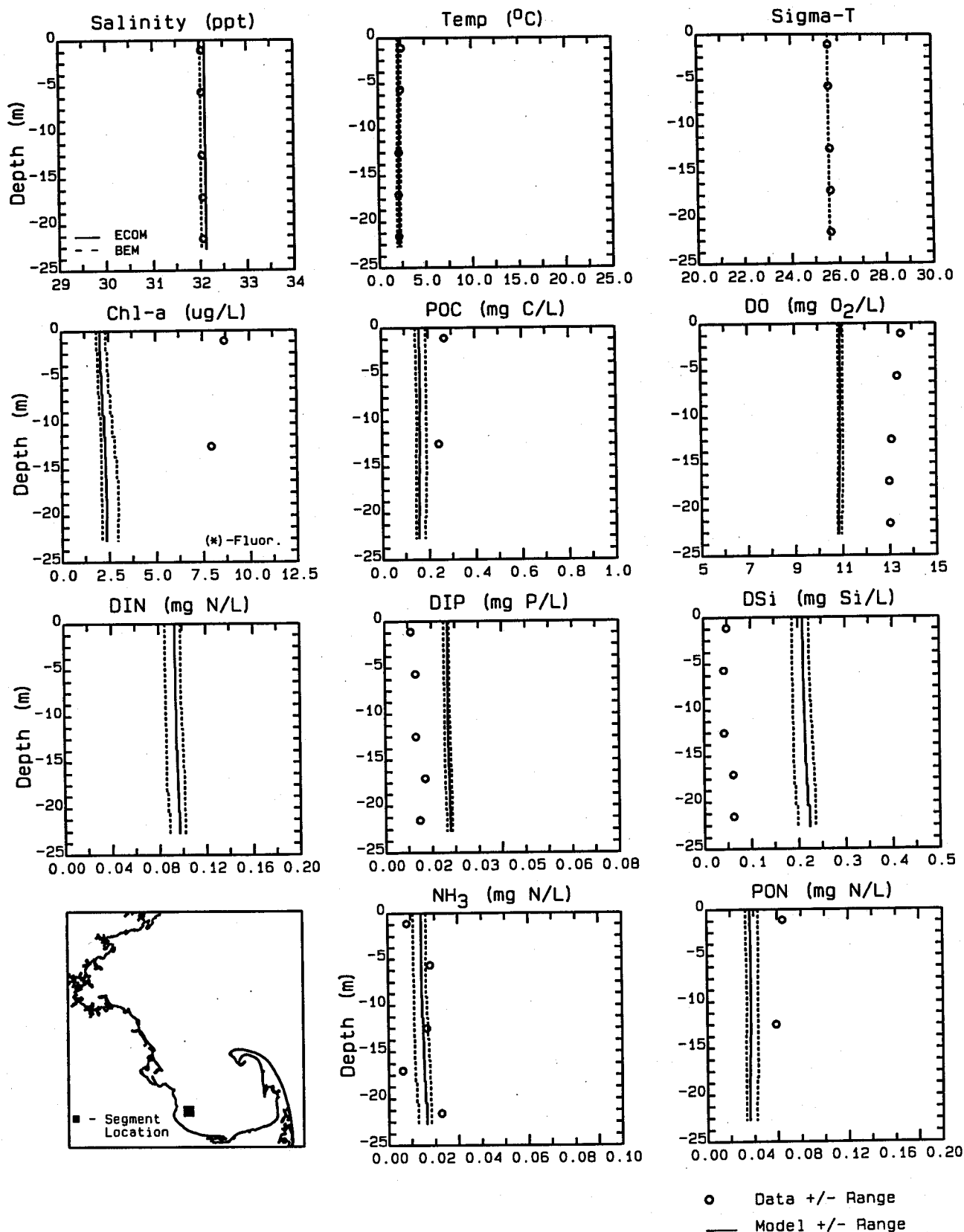
FIGURE 5-20. CALIBRATION RESULTS FOR GRID CELL (6,4) VERSUS DATA STATION
F01P FOR FEBRUARY 23, 1992
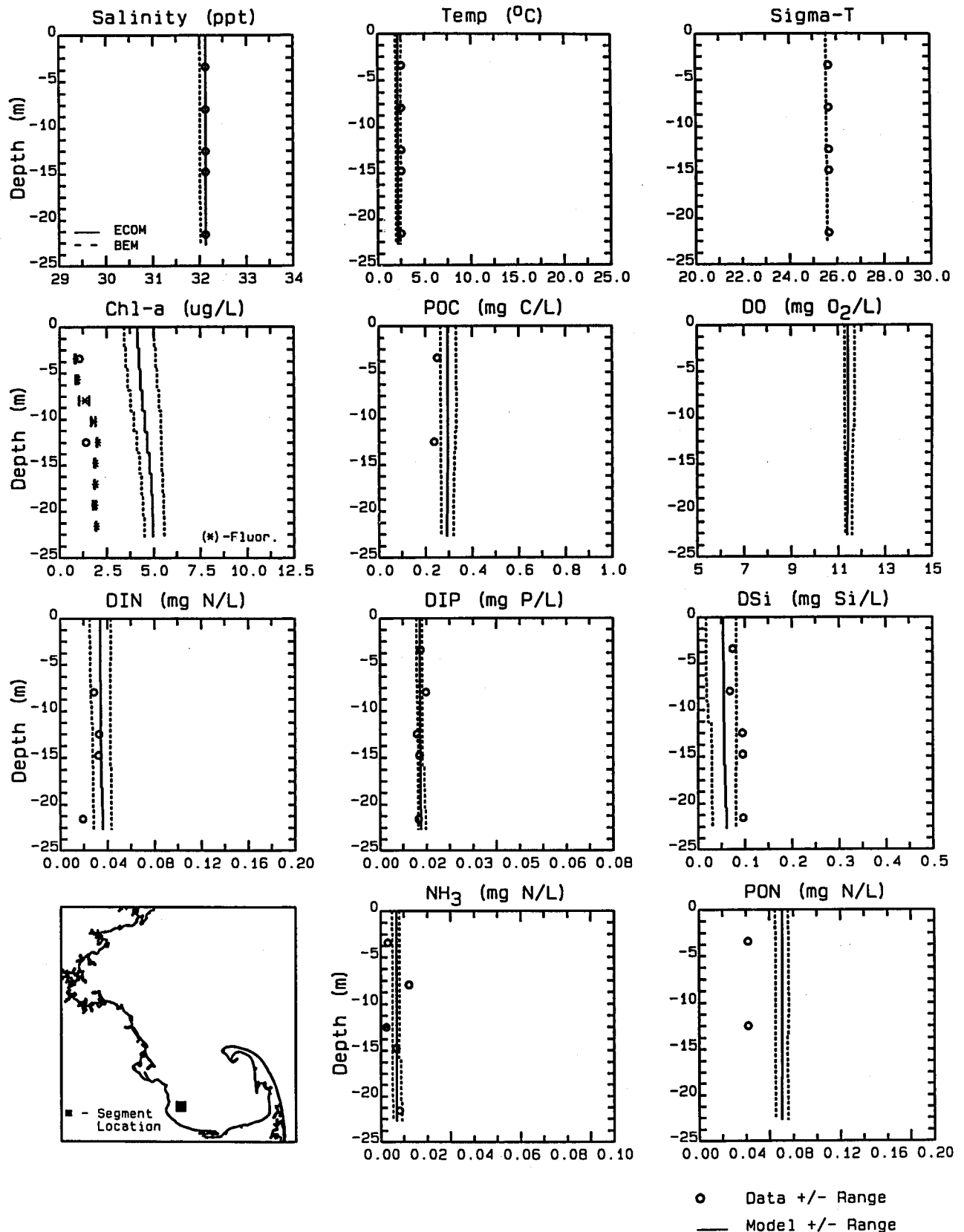
FIGURE 5-21. CALIBRATION RESULTS FOR GRID CELL (6,4) VERSUS DATA STATION
F01P FOR MARCH 14, 1992
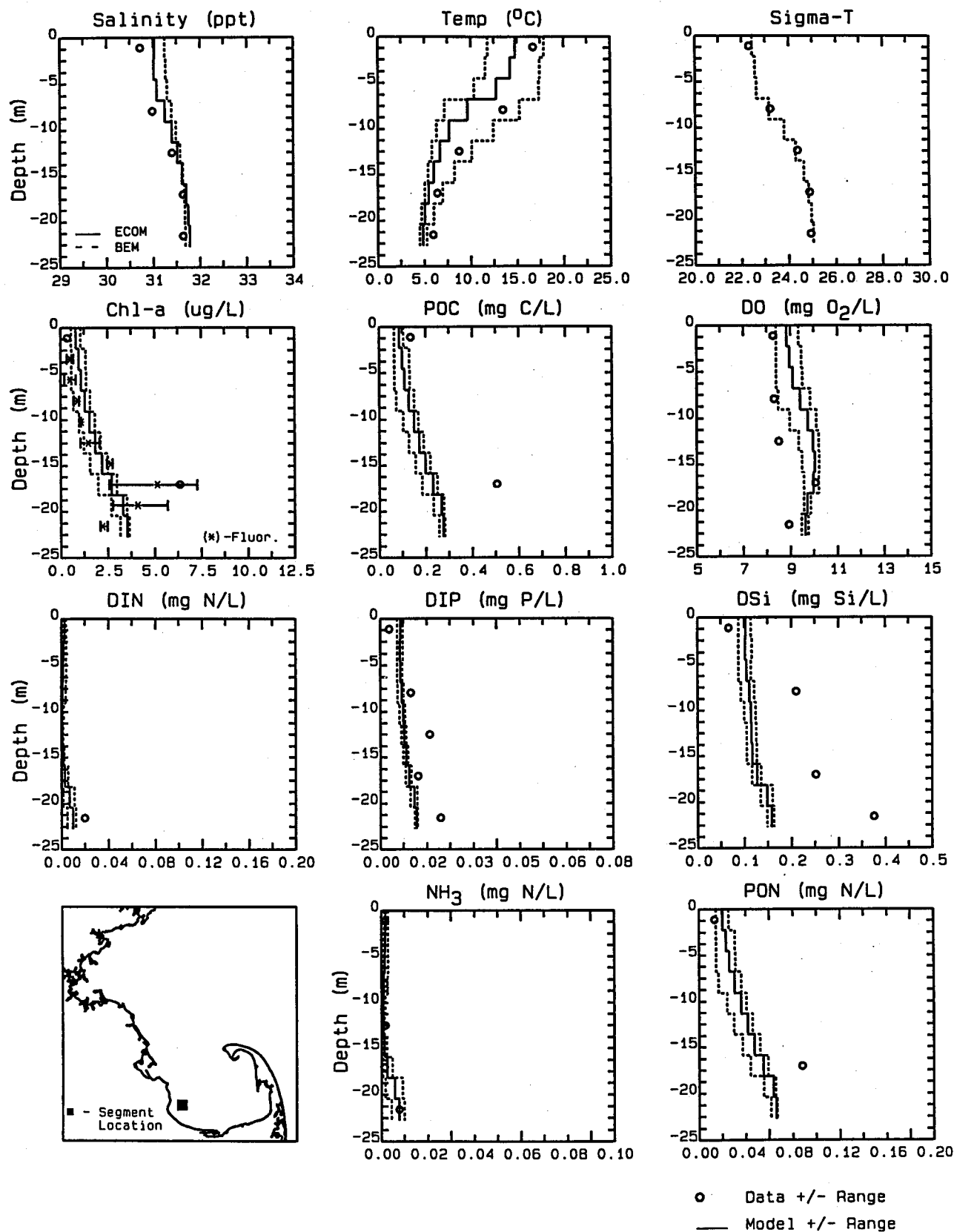
FIGURE 5-22. CALIBRATION RESULTS FOR GRID CELL (6,4) VERSUS DATA STATION F01P FOR JUNE 22, 1992
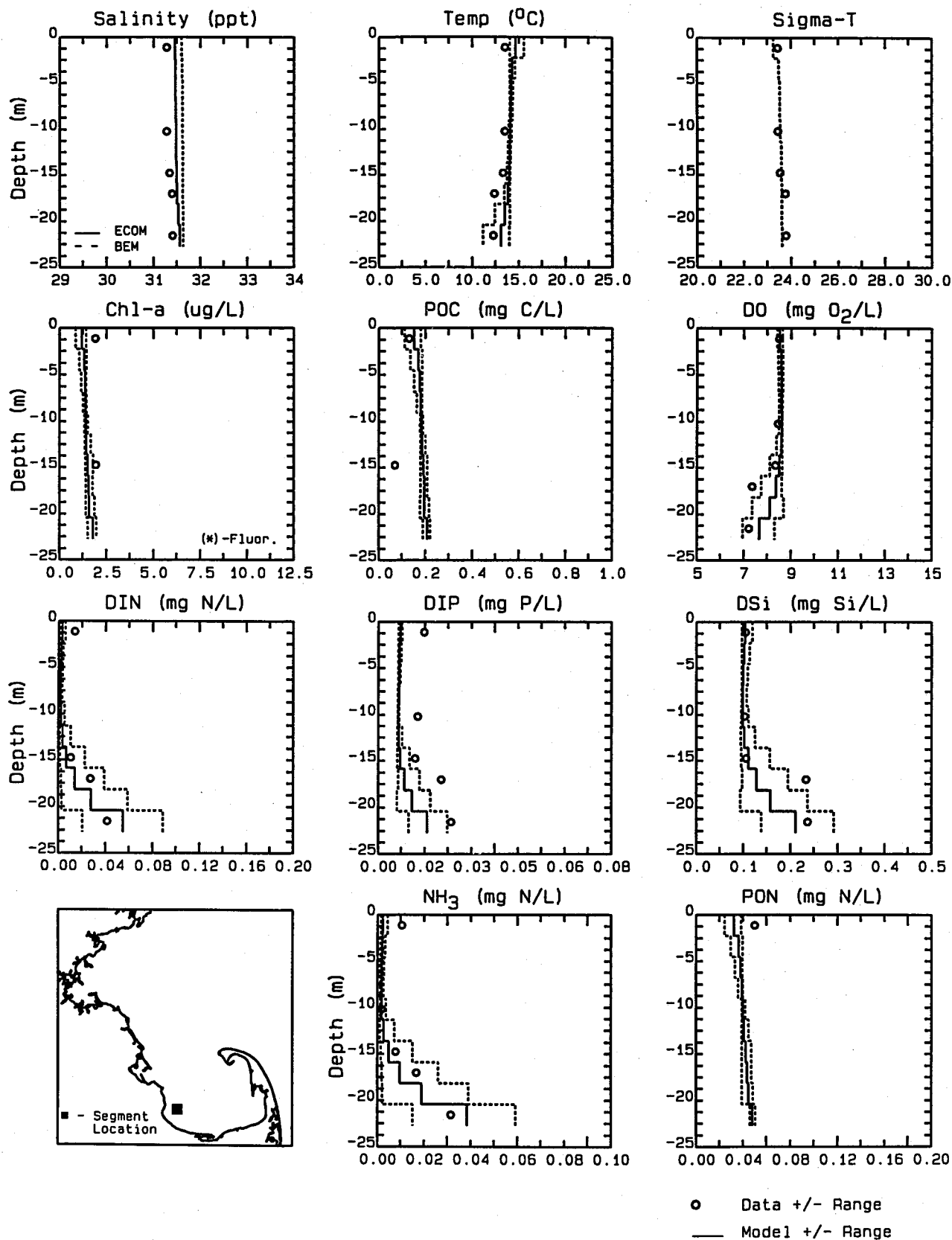
FIGURE 5-23. CALIBRATION RESULTS FOR GRID CELL (6,4) VERSUS DATA STATION
F01P FOR OCTOBER 13, 1992

order to determine the performance of the hydrodynamic model. Chl-a, POC and DO are plotted to determine the water quality model's ability to reproduce algal productivity. DIN, DIP, and DSi reveal the model's ability to successfully determine nutrient concentrations during phytoplankton growth. The difference between the DIN and NH_3 figures indicates the $NO_2 + NO_3$ concentration. PON is another measurement of the phytoplankton population.

The vertical profile comparison between the model and data for February is shown in Figure 5-20. The data and model indicate this to be a vertically well-mixed period. The salinity, temperature, and sigma-t are constant from top to bottom, and the hydrodynamic model succeeds in reproducing this feature. As was observed in Figure 5-16, the model does not have the correct timing for the early spring bloom. The chlorophyll-a panel shows the model under-estimates the phytoplankton population during this time. As a consequence, the model also under-estimates the DO, and over-estimates the nutrients (DIP and DSi) because there is no nutrient uptake by the phytoplankton.

Salinity, temperature and sigma-T data indicate that in March (Figure 5-21) the water column is still vertically mixed and that the hydrodynamic model is well calibrated during this time. The model now predicts an algal bloom. However, as the data indicate, the actual phytoplankton population has decreased since February. As a consequence of the development of the bloom, computed nutrient levels now compare favorably to the data. It appears as if the model is able to reproduce the processes of phytoplankton productivity and nutrient cycling that occur in Cape Cod Bay, however, the timing of these processes is off.

In Figure 5-22 it can be observed that by June the water column had become stratified, as indicated by salinity, temperature and sigma-t gradients. The hydrodynamic model compares favorably with the salinity, temperature, and sigma-t data. The water quality model is able to reproduce many features of the observed data. These include the generation of a sub-surface chlorophyll-a maximum between 15 and 20 meters. Higher concentrations of POC and PON also show sub-surface phytoplankton productivity at

depth. The model also reproduces, in part, the sub-surface DO maximum. Finally, the model also approximately reproduces the observed gradients in NH_4, DIP and DSi.

Figure 5-23 displays calibration results for the fall by comparing data and model results for October. During the fall overturn the water column becomes well mixed again. The data indicates the water column is well mixed down to approximately 15 meters. For this period the hydrodynamic model reproduces the vertical gradients observed in salinity, temperature and sigma-t column. Phytoplankton productivity is low and the model does a reasonable job of predicting concentrations of chlorophyll-a and POC. Dissolved oxygen in the bottom water is at a yearly minimum, and the model compares favorably to the data. The model approximately reproduces the observed nutrient gradients, especially between the 15 and 20 m depths.

5.4.4 Primary Productivity and Community Respiration

Another measure of the water quality model calibration can be determined by comparing model computations of system metabolism (the production and consumption of organic matter) versus observed data. Two measures of metabolism which can be made from field data are primary productivity and community respiration.

Figure 5-24 presents model versus data comparisons of integrated water column production. The upper panel (from Kelly, 1993) draws on data collected as part of the outfall monitoring program and shows estimates of integrated water column production. These estimates were derived from oxygen changes across a light-dark gradient for the six nearfield biology/productivity stations. Also plotted on this panel are: 1973/1974 in situ measurements of primary productivity, as reported by Parker (1974), taken a few kilometers south of the proposed outfall diffuser; and a 1987/1988 data set derived from incubator measurements of water from three stations located in the vicinity of the current nearfield stations, in western Massachusetts Bay, as reported by MWRA (1988, 1990). The data presented on this panel show a marked variability not only between data sets but
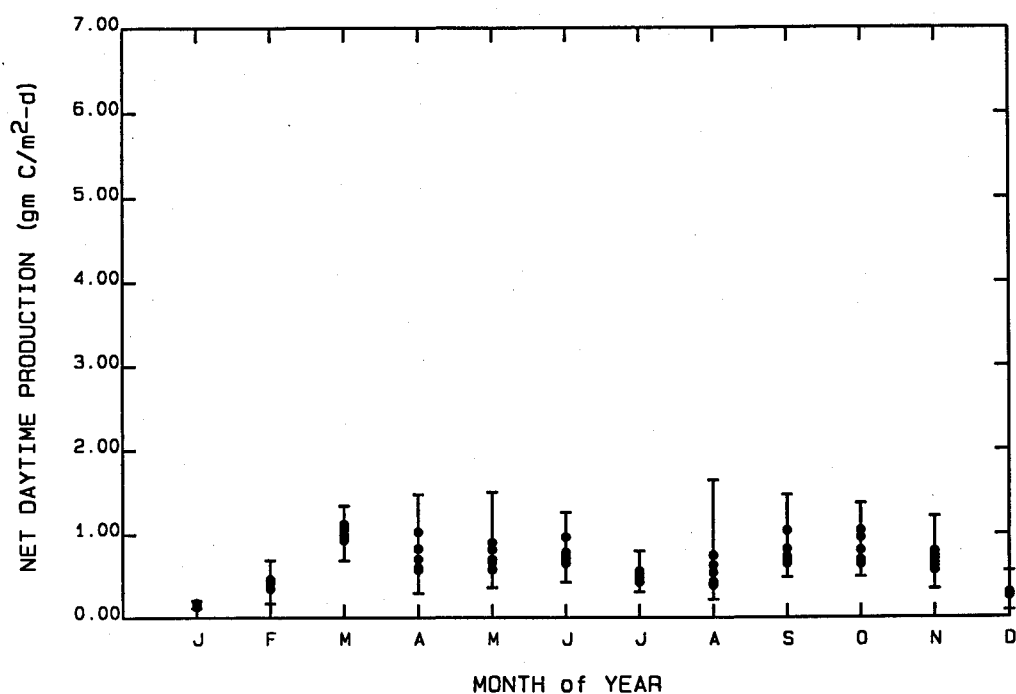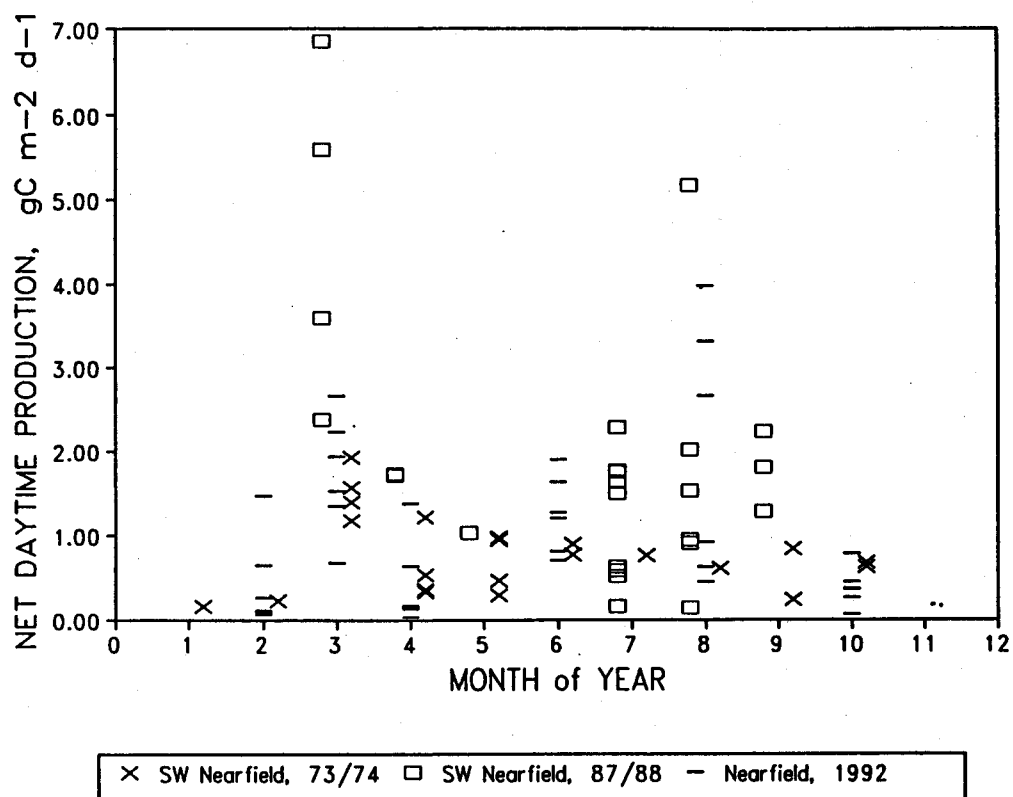
FIGURE 5-24. COMPARISONS OF OBSERVED AND MODEL COMPUTED NEARFIELD PRIMARY PRODUCTIVITY

also within individual studies. Maximum rates of productivity are observed in March, June, and August; low rates of productivity are found during the winter months.

In the lower panel of Figure 5-24, model output, from the same six locations as the Battelle biology/productivity stations, is plotted to provide a comparison against the data from these previous field studies. The model computes maximum rates of productivity in March, June, and September. This closely mirrors the timing of the peak observed values in the data. While the magnitude of the productivity computed by the model falls within the range of measured observations, the model computations tend to be low. In addition, the model shows less variability than is observed in the data.

The current monitoring program attempted to measure bottom water respiration rates using dark BOD bottles and incubations times of about six hours. However, as noted by Kelly (1993), it appears that respiration rates in Massachusetts Bay are low enough that this short incubation time is inadequate for direct measurements of water column respiration. Kelly (1993) proposed an alternate means of estimating bottom water respiration via looking at long-term changes in bottom water dissolved oxygen.

Figure 5-25 presents model versus data comparisons for bottom water DO at nearfield stations and farfield stations located in Stellwagen Basin. The top two panels represent DO measurements taken at depths below 20 meters at the nearfield stations (Panel A) and below 50 meters in Stellwagen Basin (Panel C). The lower two panels (B and D) represent model computed five-day averaged DO at the same locations and depths at which the data were taken.

For the nearfield stations, the model (Panel B) reproduces the general trend observed in the data (Panel A); i.e., highest DO concentrations in late February and early March and lowest DO concentrations observed in October followed by increasing DO in November and December. The model does not, however, reproduce the magnitude of the DO decrease that is observed to occur between April and May although it does show some decline. The cause for the observed DO decline that occurs between April and May is
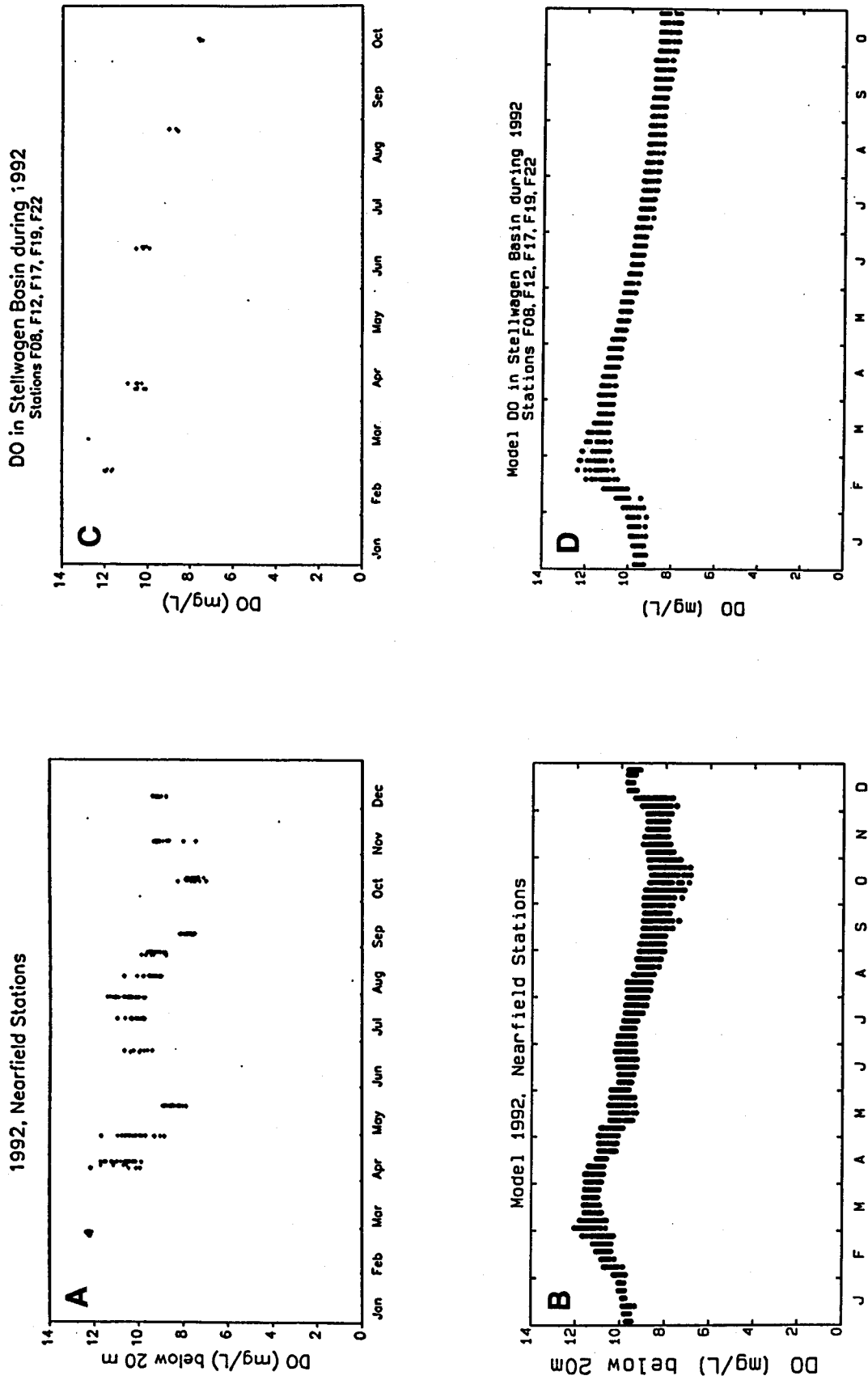
FIGURE 5-25. COMPARISONS OF OBSERVED VERSUS COMPUTED BOTTOM WATER DO CONCENTRATIONS AT NEARFIELD AND STELLWAGEN BASIN STATIONS

unclear. Kelly (1993) attributed the sharp decline to respiration processes associated with the die-off of the winter/spring diatom bloom. However, the possiblity does exist that it could be advective transport of low DO waters from the Gulf of Maine. The observed decline in DO concentrations coincides with the freshet that occurs in late April/May. Unfortunately, there are no boundary DO data to confirm or refute this alternate hypothesis.

The model also does not compute the increase in DO that occurs between the end of May and late July. Again this process is not fully understood. Kelly (1993) offered two possible mechanisms. First, primary production at low light levels within the pycnocline may contribute. Second, the variability in the density structure of many nearfield stations suggests that physical stratification may, on occasion, be partially disrupted, thus permitting the addition of oxygen to the bottom depths of the water column. The model does, however, seem to compute the approximate range of DO concentrations observed in the field from month to month, and does reproduce the long-term decline in DO concentrations observed to occur between February and October.

In Stellwagen Basin, the model performs more favorably when compared to the observed DO data. The model computes the high values in late February and early March and follows the slow downward trend in DO concentrations until October. Both the data and the model show less variability in DO concentrations for the Stellwagen Basin stations than is observed at the nearfield stations.

Panels A and C of Figures 5-24 were developed by Kelly (1993) to make estimates of the community respiration that occurs at these stations, which could account for the decline in bottom water DO. By community respiration we mean the sink of DO due to algal respiration, oxidation of organic carbon, nitrification, and SOD. Kelly used linear regression analysis on the changes in DO to estimate respiration rates. A linear regression of nearfield data for April through October yielded a respiration rate of 0.0136 mg O_2/L-day. However, using shorter time periods for the regression analysis, the data for April to May and July to October yielded higher estimates of respiration rates of 0.037 to

0.060 mg O_2/L-day, respectively. For the Stellwagen Basin stations, a linear regression for April to October yielded an estimated respiration rate of 0.015 mg O_2/L-day, while the period from June to October was estimated to be 0.023 mg O_2/L-day. As noted by Kelly, these estimates of respiration rates must be viewed with some caution since the analysis which attempts to estimate the net community respiration may be influenced by advective/dispersive processes not yet fully understood.

Model rates of community respiration were calculated by summing the oxygen consumption from algal respiration, oxidation of organic carbon, nitrification, and SOD. Respiration rates were calculated for each month. Computed rates ranged from 0.0083 to 0.0212 mg O_2/L-day at the nearfield stations and from 0.0057 to 0.0096 mg O_2/L-day in Stellwagen Basin. While these rates are lower than those estimated by Kelly they are generally within a factor of two and reproduce the observation that Stellwagen Basin respiration is lower than the nearfield rates. It should also be noted that the model values are directly computated and are not influenced by advective and dispersive transport, unlike Kelly's estimates which may be affected by transport processes.

5.4.5 Model Versus Data Probability Distributions

Figures 5-11 through 5-25 present an overview of the model calibration by presenting temporal and vertical model versus data comparisons. The results are encouraging. The model appears to reproduce or partially reproduce the principal temporal and vertical features of the water quality within the Bays. These include:

- the onset of the winter/spring phytoplankton bloom earlier in Cape Cod Bay than the rest of the Massachusetts Bay system

- the decrease in phytoplankton biomass, as indicated by chlorophyll-a and fluorescence, in Massachusetts Bay as one moves further away from Boston Harbor

- the limitation of the winter/spring phytoplankton bloom in Cape Cod Bay by silica

- the non-limiting concentrations of inorganic phosphorus

- the limitation of summer primary productivity by inorganic nitrogen

- the observed vertical gradients in the inorganic nutrients with low levels in the surface (due to algal uptake) and higher levels in the bottom waters of the Bays (due to remineralization of detrital algal biomass and less algal uptake)

- the annual cycle of dissolved oxygen, with super-saturated conditions occuring between late winter/early spring and late summer and with minimum levels occuring in late September and October.

- the annual cycle of primary productivity in northwest Massachusetts Bay.

These comparisons, however, tend to be rather exacting tests of the model since the data represent grab samples at a fixed point in time and space. Kelly (1992,1993) has shown that there is considerable variability in both space and time in the observed data using tow-yo measurements. These data show high frequency variability, which suggest that a grab sample may not always be representative of the water quality conditions of a large spatial area such as would be encompassed in a model segment that is 4-9 km^2. Therefore, in order to evaluate the model calibration on another level, i.e., the degree to which the model reproduces the variability observed in the field data, model output is compared to field data using probability distribution plots. These comparisons utilize data and model computations for 1992, since the 1992 data set is more comprehensive in time and space.

The model versus data comparisons are separated into nearfield and farfield analyses. The nearfield data (as defined in Figure 3-16) are divided seasonally as follows: winter (February and March), spring (April through June), summer (July through September), fall (October through December), and on an annual basis (February through December). No data were collected in January. The model output is separated in the same manner. Since temporal sampling was conducted less frequently for the farfield stations, the farfield analysis was performed only on an annual basis.

Figure 5-26 presents model versus data comparisons for surface chlorophyll-a. The filled circles represent the discrete chlorophyll-a data while the asterisks represent chlorophyll fluorescence data. The model computations are plotted as a solid line and represent the range in chlorophyll-a concentration computed in five day averages. During the winter (Panel A), the model reproduces the majority of the range observed in the chlorophyll-a and fluorescence data, failing only at the extreme maximum and minimum values. In the spring (Panel B), the model tends to overpredict both the chlorophyll-a and fluorescence, matching only the higher values. These results suggest that the model has a phasing problem in computing winter and spring algal blooms for the nearfield stations. Panel C shows that while the model calculates the median summer chlorophyll-a, it cannot reproduce the high degree of chlorophyll and fluorescence variability which occurs during these months. During the fall (Panel D), the model consistently underpredicts the chlorophyll-a and fluorescence concentrations by 1 to 3 μg/L. On an annual basis (Panel E), the model performs well, reproducing the chlorophyll-a and fluorescence data within a standard deviation on both sides of the median. The model, however, is not as dynamic as the field data as it does not compute the extreme high and low values.

The model appears to reproduce a major portion of the observed chlorophyll and fluorescence data variability, as shown on Panel F. Differences between maximum observed chlorophyll-a and fluorescence and model computed chlorophyll are generally less than 1μg/L. Differences between minimum observed chlorophyll/fluorescence and model chlorophyll are generally less than 0.2 μg/L. The model does not, however, reproduce the S-shaped curve observed in the chlorophyll-a data as plotted on a logarithmic scale.
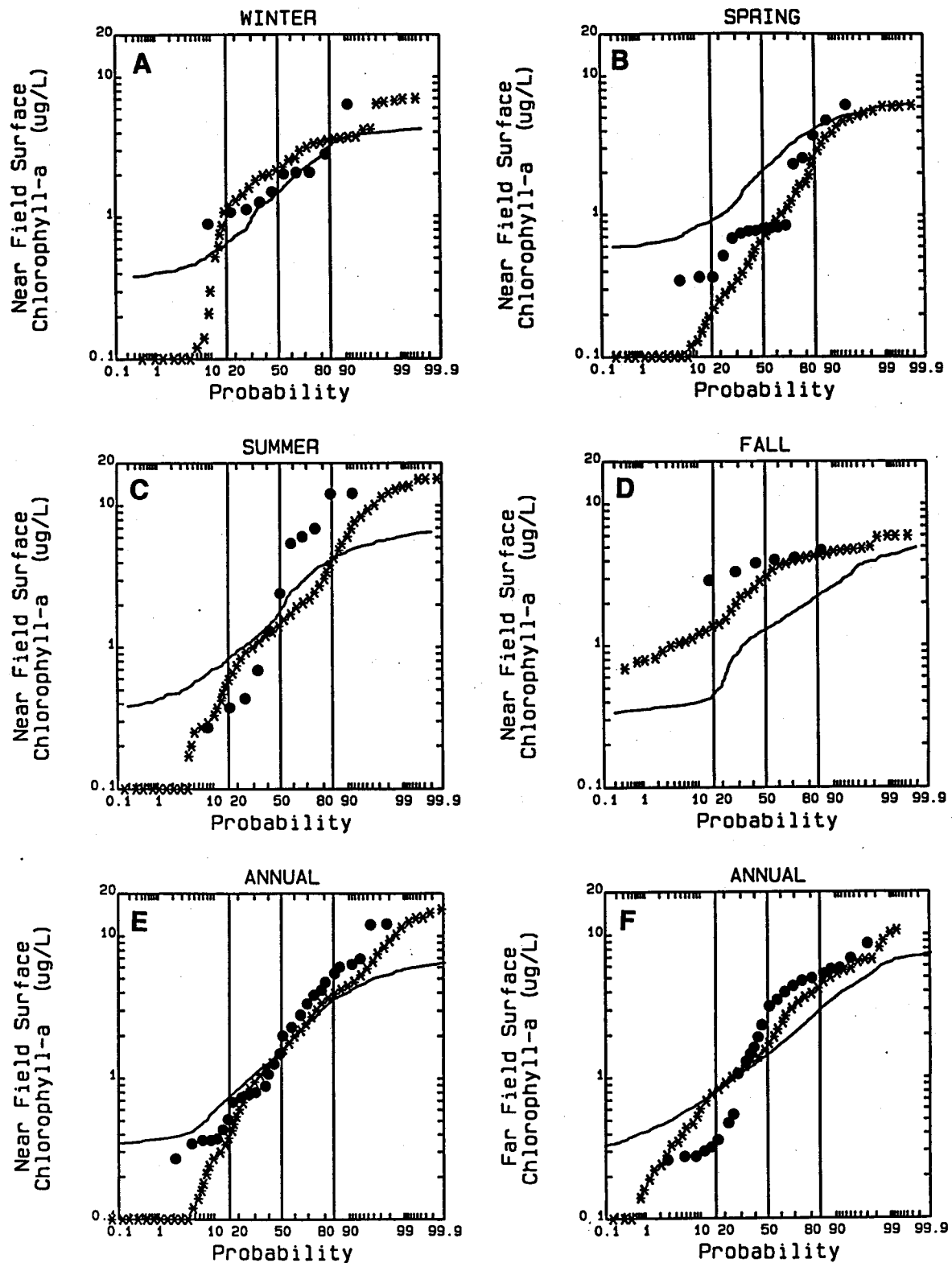
FIGURE 5-26. PROBABILITY DISTRIBUTIONS OF DATA AND MODEL SURFACE
CHLOROPHYLL-a CONCENTRATIONS

Figure 5-27 presents a similar analysis to Figure 5-26 for mid-depth (12.5-17.5 m) chlorophyll concentrations. For the winter period, the model computations compare favorably to the observed data, except for the approximately 5 percent of the data, which fall below 0.5 μg/L. In the spring the model overestimates chlorophyll and fluorescence data by 1 μg/L . The model does an excellent job in reproducing the size and variability of the fluorescence data for the nearfield summer data. In the fall, the model underestimates the observed data by 1 μg/L, although it does approximately reproduce the observed variability. On an annual basis the model does an excellent job of reproducing the observed fluorescence data, except for the lower 5 percent of the data, which is 0.5 μg/L or less. The model also compares favorably to the observed chlorophyll-a data. Model versus data comparisons are also very good for the annual distribution of chlorophyll and fluorescence at the farfield stations.

Model versus data comparisons for the nearfield bottom dissolved oxygen are presented in Figure 5-28. The model and data are presented in the same manner as for chlorophyll-a above. In the winter (Panel A), the model fails to compute the high dissolved oxygen concentrations observed in the data. The reasons for this discrepancy are not clear since the winter chlorophyll (Figure 5-26, Panel A) comparisons are favorable. During the spring (Panel B), the model reproduces the majority of the DO data distribution quite well, but is unable to match the extreme high and low measurements. Summertime DO concentrations (Panel C) are consistently underpredicted by the model by approximately 0.5 to 1.0 mg/L. The general slope of the data and model match quite well, however. The model reproduces the observed fall DO concentrations very well (Panel D). This is very important because it has been observed that the lowest DO concentrations occur during this time. On an annual basis (Panel E), the model does a good job reproducing the observed data failing only for the highest observed DO concentrations. For the farfield bottom DO (Panel F) the model reproduces the low to median concentrations very well. However, the model consistently underpredicts the higher DO concentrations observed in the data. In general, the model reproduces most of the observed variability observed in
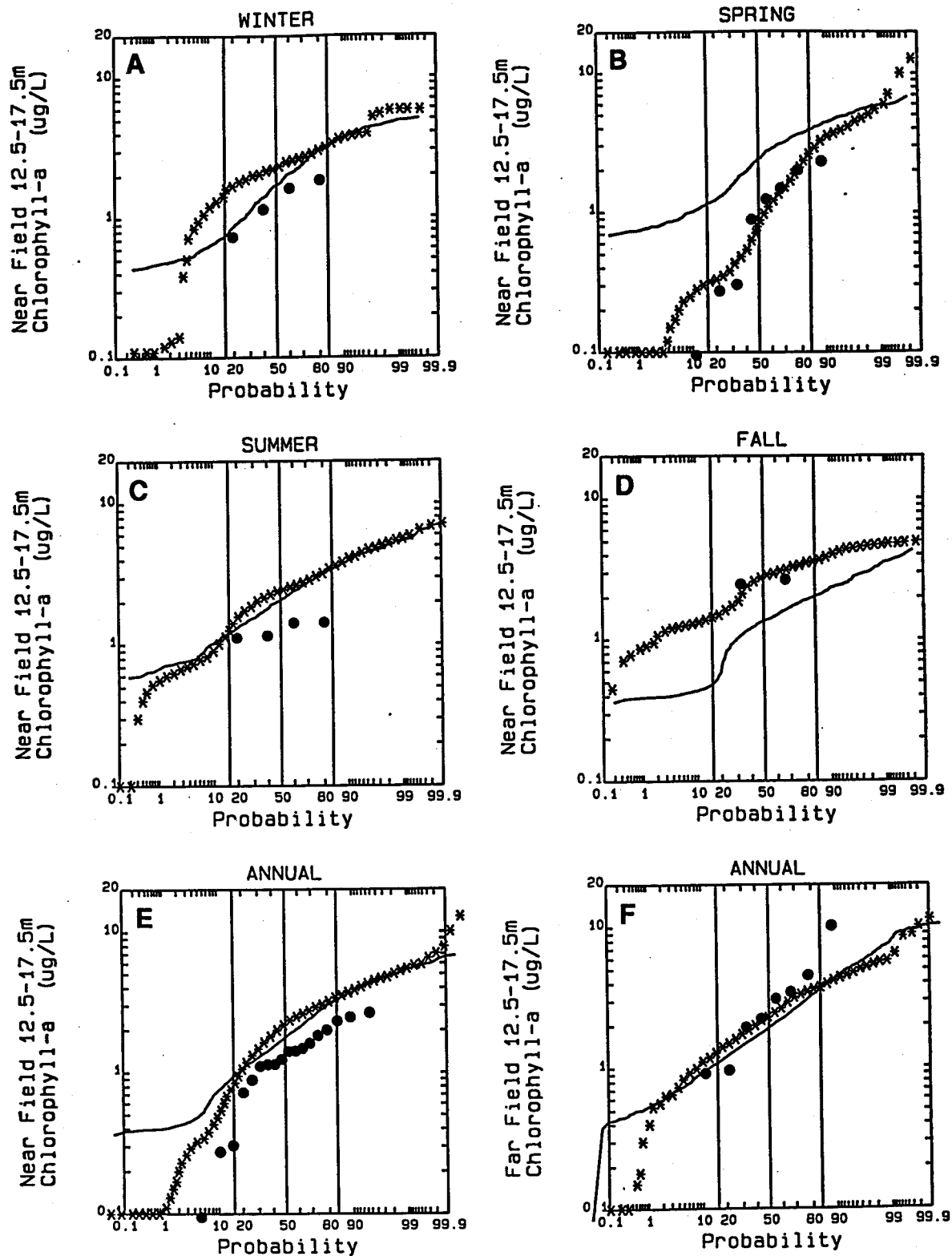
FIGURE 5-27. PROBABILITY DISTRIBUTIONS OF DATA AND MODEL MID-DEPTH CHLOROPHYLL-a CONCENTRATIONS
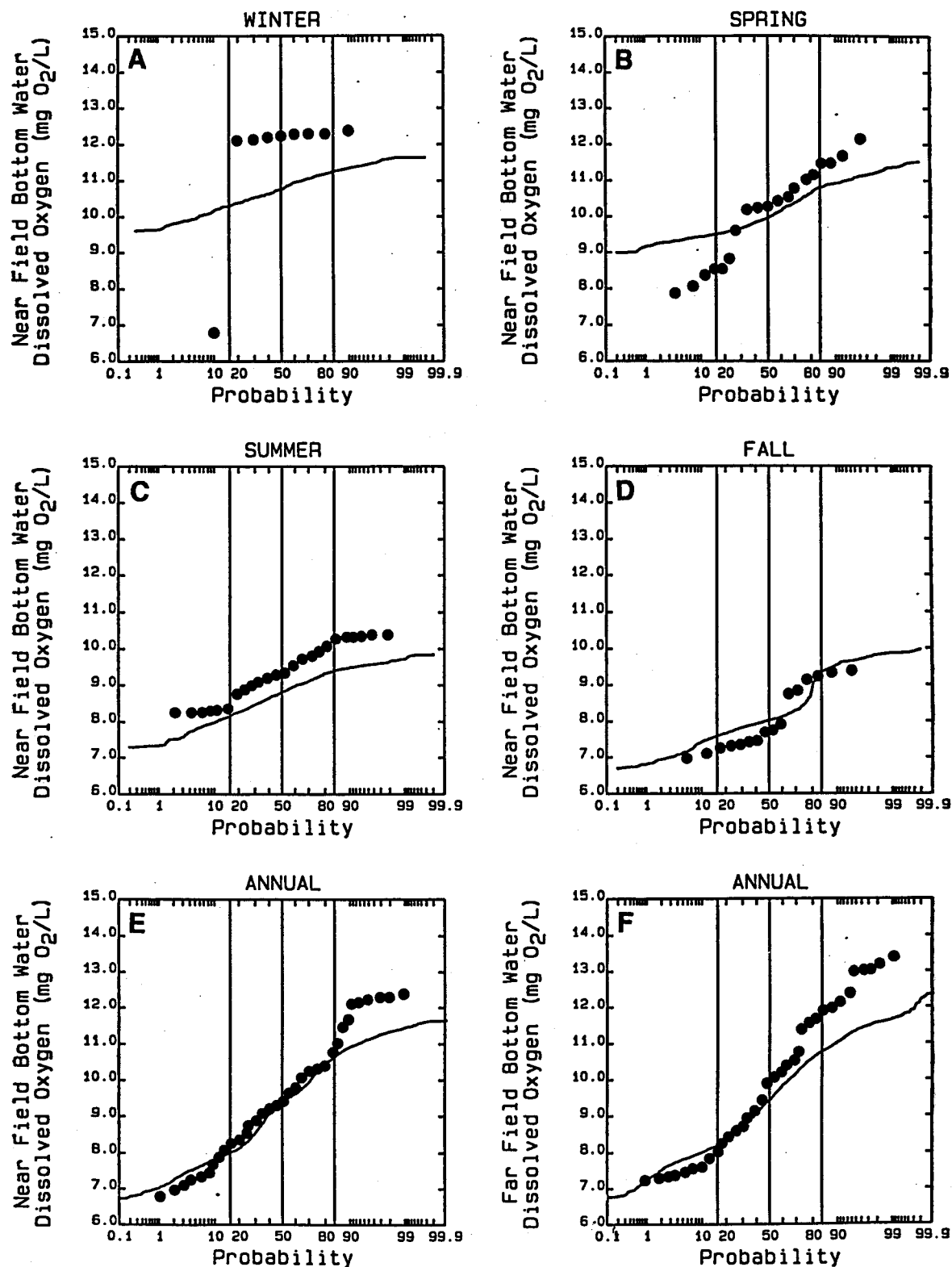
FIGURE 5-28. PROBABILITY DISTRIBUTIONS OF MODEL AND DATA BOTTOM DO CONCENTRATIONS

the DO data and in particular performs well for the more critical period of the year when DO levels are at a minimum.

5.4.6 Model Computed Phytoplankton Variability

One feature of the BEM computations shown in Figures 5-11 through 5-16 is the variability in chlorophyll-a and POC computed by the model, particularly in some stations removed from Boston Harbor. One hypothesis offered earlier in this section suggested the export of algal biomass and/or nutrients from Boston Harbor to the stations in question under the proper wind conditions. Another hypothesis is that these variations may vary with the incident solar radiation. To decide whether either or both hypotheses are feasible, a non-conservative tracer was discharged at the location of the current MWRA outfall. This tracer had a decay rate of 0.1 /day to insure no long term build up of concentration. Figures 5-29 and 5-30 present model computations, for the months of May through September 1990 and 1992, respectively. Plotted on these figures are surface chlorophyll-a, total nitrogen, and surface and bottom water tracer concentrations. In addition, the figures also show five-day averaged solar irradiance, wind velocity and direction and freshwater flow discharged to Boston Harbor.

Comparing the temporal profiles for solar-radiation and chlorophyll-a at model segment 1, indicates that there is little correlation between incident solar radiation and surface chlorophyll. For example, during the third 10-day interval in May 1990 there is a rapid increase in solar radiation. During this same interval there is a sharp decline in chlorophyll-a. There is, however, a very strong correlation between chlorophyll-a and the tracer, which emanates from Boston Harbor. Virtually each peak and valley in the chlorophyll time-series has a corresponding peak and valley in the tracer time-series for this segment. Less pronounced peaks in total nitrogen (TN) also correspond to the timing of the chlorophyll and tracer peaks.

What process, then, determines the deliverly of Boston Harbor chlorophyll and nitrogen (and tracer) into this portion of Massachusetts Bay during the summer months?
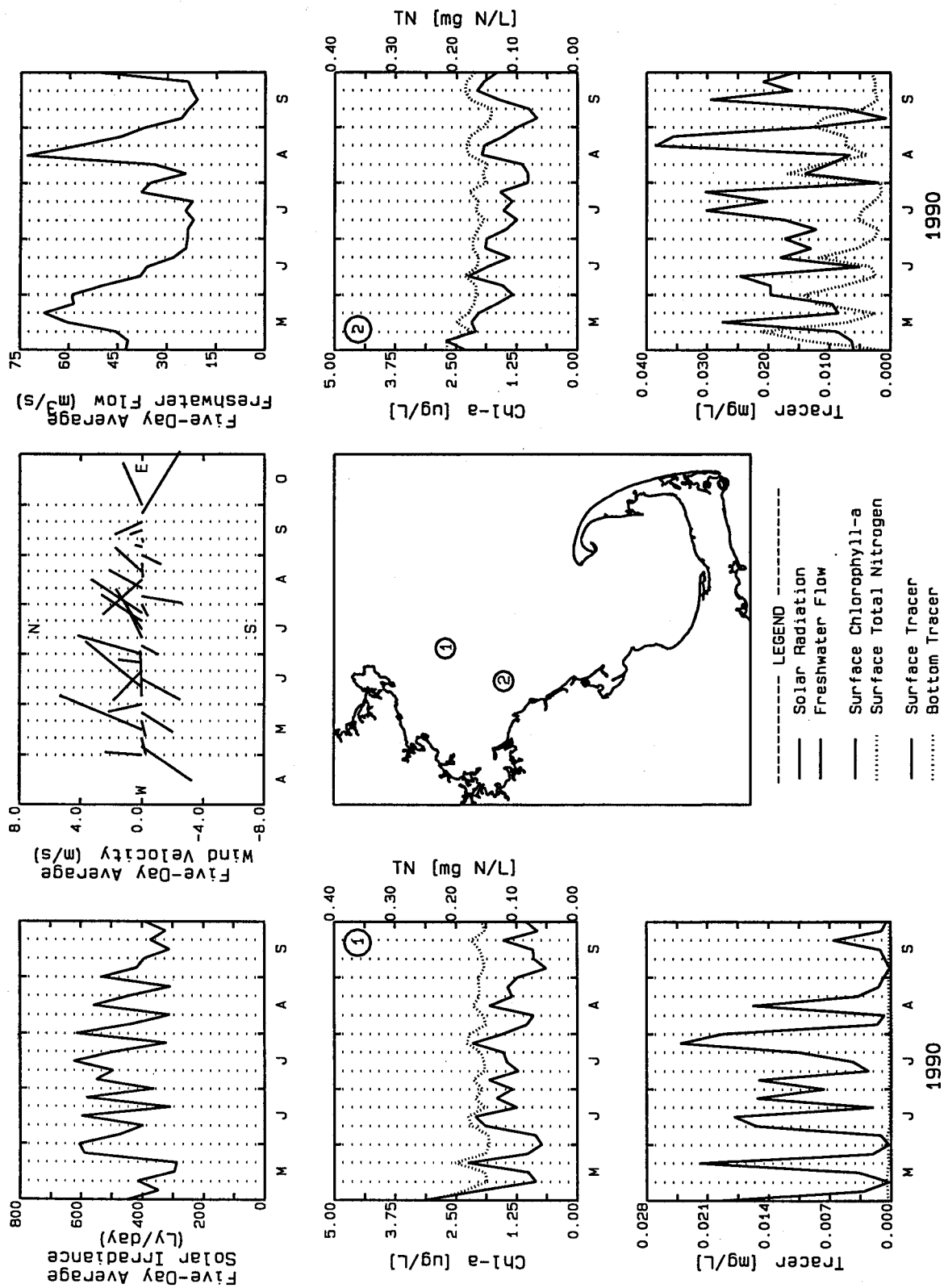
FIGURE 5-29. ANALYSIS OF VARIABILITY IN 1990 MODEL OUTPUT
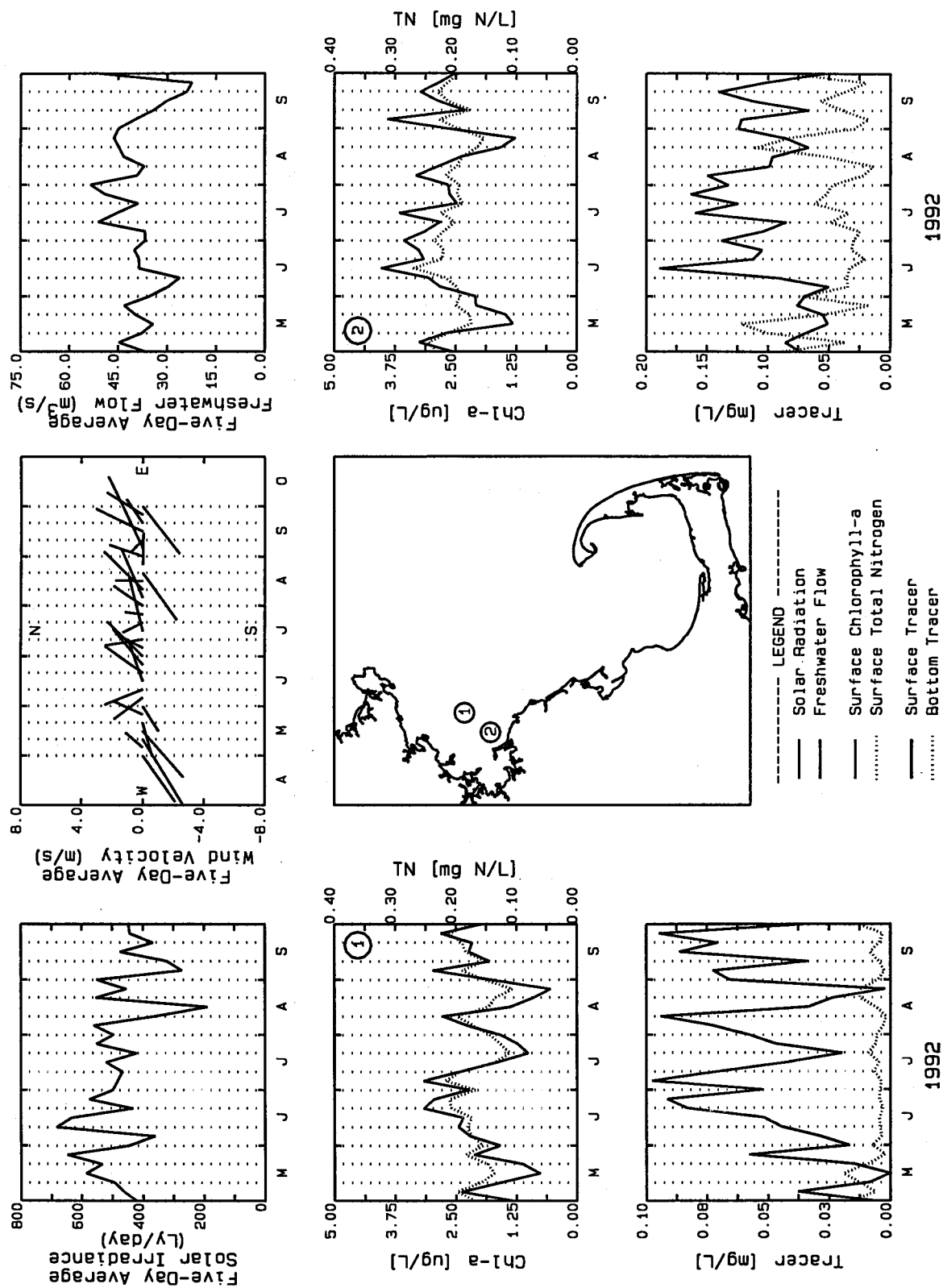
FIGURE 5-30. ANALYSIS OF VARIABILITY IN 1992 MODEL OUTPUT

If one closely examines the wind speed and direction, one can see a pattern in which winds which blow to the east appear to carry Boston Harbor waters into this portion of Massachusetts Bay. For example, winds during the 5-day interval just prior to the first chlorophyll peak on day May 20, are strongly towards the northeast. Over the next three 5-day intervals winds change direction and are blowing in a westward direction toward shore. Winds during the first two 5-day intervals in June are blowing directly east or to the northeast. This results in the next increase in chlorophyll-a and tracer concentrations. This pattern of eastward winds and corresponding increases in chlorophyll and tracer concentrations appear to be a consistent feature for this segment.

The effects of wind on water motion and hence chlorophyll-a appear to be different at segment 2. This model segment is located nearer to shore and is shallower (about 34 m) than segment 1. It can be observed that the peaks in chlorophyll and the surface tracer concentrations do not always coincide. For, example, the mid-August chlorophyll peak develops during a period of decline in tracer concentration. Analysis of the chlorophyll and surface and bottom tracer time-series indicates that declines in chlorophyll-a often coincide with short term mixing or downwelling events, wherein surface and bottom water concentrations of the tracer are approximately equal. These mixing or downwelling events appear to be correlated with winds blowing to the southwest. Figure 5-29 presents a similar analysis for two model segments located closer to Boston Harbor for 1992. Segment 1 is located in the vicinity of the future outfall and has a depth of about 39 m. One can see that there is a fairly good correlation between peaks in chlorophyll concentrations and peaks in tracer concentrations. There is still correlation between wind direction and chlorophyll and tracer peaks and valleys, but there one or two instances where the wind direction/chlorophyll/tracer correlation does not work. For example, there is marked decline in chlorophyll and tracer concentrations between the first 5-day interval and the fourth 5-day interval in July even though a strong eastward wind occurs on the third 5-day interval. However, two of the other significant declines in chlorophyll and tracer concentrations that occur in mid-March and at the end of August do coincide with strong southwestward wind events.

Model segment 2 which is located just offshore just north of Cohasset and has a water depth of 18 m. This station is strongly affected by southwestward and westward winds. The downwelling or mixing events observed in mid-May, the end of May and mid-August correspond to southwestward wind events. Some of the temporal behavior of chlorophyll in this segment may be attributed to its close proximity to Boston Harbor. Evidence for this is provided by the higher levels of chlorophyll and total nitrogen (as well as tracer concentrations) relative to those model segments present in Figure 5-28.

5.4.7 Sediment Model Calibration

As discussed in Section 3.5, a limited data set was available with which to evaluate the performance of the sediment model. Toward the end of this study, Dr. Anne Giblin (Marine Biological Laboratory) provided 1993 sediment nutrient flux data. These data included new station locations in Stellwagen Basin and in Cape Cod Bay. Although the 1993 data were not described in Section 3.5, they are included on the model calibration figures to follow.

Due to the limited sediment flux data collected in each year, it was decided to pool all of the flux data together and compare the pooled data set against 1992 model computations. The data for 1990 through 1992 are grouped together and plotted using an asterisk to represent the segment average of the replicate cores. The range of the 1990 through 1992 data is also shown and indicates that, in general, the reproducibility of the replicate cores was quite good. The 1993 data are plotted separately using open circles for station and replicate averages. Also plotted are the standard errors of the replicate cores. Silica and denitrification fluxes are presented compared to 1993 data only.

Figure 5-31 presents model versus data comparisons of SOD for two model segments in Boston Harbor; a model segment located near the future outfall site; a segment located in Stellwagen Basin; and a model segment in northeastern Cape Cod Bay. The locations of these stations are shown in the lower right hand panel of the Figure 5-31. Panel (1) shows the SOD calibration results for a segment near the mouth of the Inner
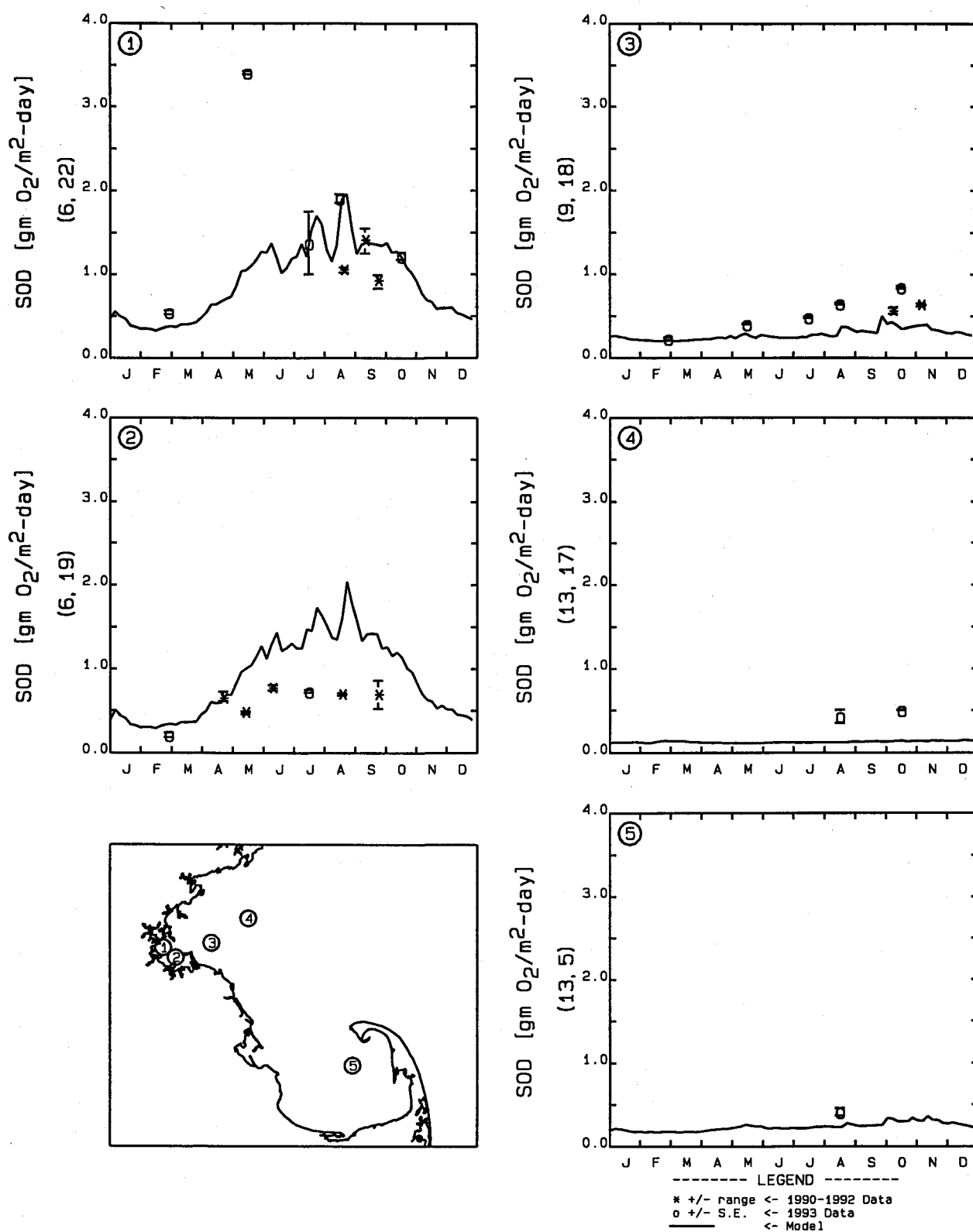
FIGURE 5-31. 1992 SEDIMENT FLUX SUBMODEL CALIBRATION RESULTS FOR SOD

Harbor. Except for a high SOD recorded in May of 1993, which may be suspect since Giblin (1995) reported that a much lower rate was observed in May 1994, the model provides a favorable calibration to the observed data. During the winter, when water temperatures are at their lowest, biological activity in the sediment bed is also at its lowest level. Consequently, sediment oxygen demand is low, 0.5 gm O_2/m^2-day, during this time. As the water column warms, primary productivity increases and organic carbon deposition increases. In addition, biological activity in the sediment increases. These processes contribute to increased SOD. The model computes maximum rates of SOD in August of approximately 2.0 gm O_2/m^2-day. This compares favorably to the August 1993 SOD measurement. As the water temperature begins to decrease, both the model and data show a decrease in SOD. Panel (2) show sediment calibration results for a station located in Hingham Bay, in the southern portion of Boston Harbor. The calibration is not as favorable for this model segment. The model and data show evidence of a seasonal cycle but the model overpredicts the SOD by 0.5 to 1.0 gm O_2/m^2-day during the summer. Panel (3) presents calibration results for a station located near the future outfall site. The SOD measurements at this station are slightly lower than observed in Hingham Bay, during May through August, averaging about 0.5 gm O_2/m^2-day. The model computes slightly lower SOD rates than are observed. One explanation for this discrepancy may be related to the variability in organic matter deposition in this area of Massachusetts Bay. Giblin (1995) has indicated that all of the sites in Massachusetts Bay selected for nutrient flux sampling were depositional and were probably accumulating and concentrating organic material. There were other locations in the immediate vicinity of these stations, however, which were found to be non-depositional. This spatial pattern of depositional and non-depositional sedimentary environments in this region is also consistent with the analysis of Knebel (1993). The model segments, which are a number of square kilometers in size, encompass both depositional and non-depositional bottom sediments. Therefore, since the model spreads the organic matter deposition over the entire area of the sediment bed contained within the model cell, it is not surprising that the observations of SOD are slightly under-estimated. What is encouraging, however, is that the model does reproduce the marked differences in SOD between Boston Harbor and this portion of Massachusetts Bay.

Calibration results for the Stellwagen Basin segment are presented in panel (4). At this station the observed SOD is even lower than at the future outfall site. This is in part due to the fact that this station is located in deep waters. Therefore it is likely that a greater portion of the particulate organic carbon will be oxidized in the water column. In addition, since this portion of the bay is more nutrient limited, there is less production of organic matter in the surface waters. The observed data average about 0.5 gm O_2/m^2-day, while the model computes an SOD rate of approximately 0.12 gm O_2/m^2-day. The under-estimation by the model is consistent with the comments offered above for the future outfall location. In Cape Cod Bay, panel (5), the single measurement of SOD is about 0.45 gm O_2/m^2-day, while the model computes a value of 0.25 gm O_2/m^2-day.

Computed and observed ammonium fluxes (J_{NH_4}) are presented in Figure 5-32 for the same five model segments. Comparisons between observed and computed NH_4 fluxes show almost the same spatial pattern as was observed for SOD. The model provides a favorable comparison for the Inner Harbor segment; over-estimates NH_4 flux in Hingham Bay. The model provides a better calibration to the observed flux rates near the future outfall site, in Stellwagen Basin, and in Cape Cod Bay. The model is generally able to reproduce the relatively high NH_4 flux rates (150 mg N/m^2-day) in Boston Harbor, as well as the relatively lower NH_4 flux rates (0 to 25 mg N/m^2-day) observed outside of the harbor.

Computed and observed nitrate fluxes are presented in Figure 5-33. The two model segments shown for Boston Harbor provide an inteesting contrast to the SOD and J_{NH_4} data. The Inner Harbor segment over-estimates J_{NO_3}, while the model versus data comparison for Hingham Bay is quite favorable. It should be noted that the nitrate fluxes computed and observed for the Inner Harbor station are low (generally less than 15 mg N/m2-day) relative to the ammonium flux rates (75 to 125 mg N/m^2-day). It is also interesting to note the differences between the 1993 data and the earlier data for the August to September time period. Calibration results for the segment near the future outfall site and Cape Cod Bay are encouraging. The model under-estimates J_{NO_3} flux in
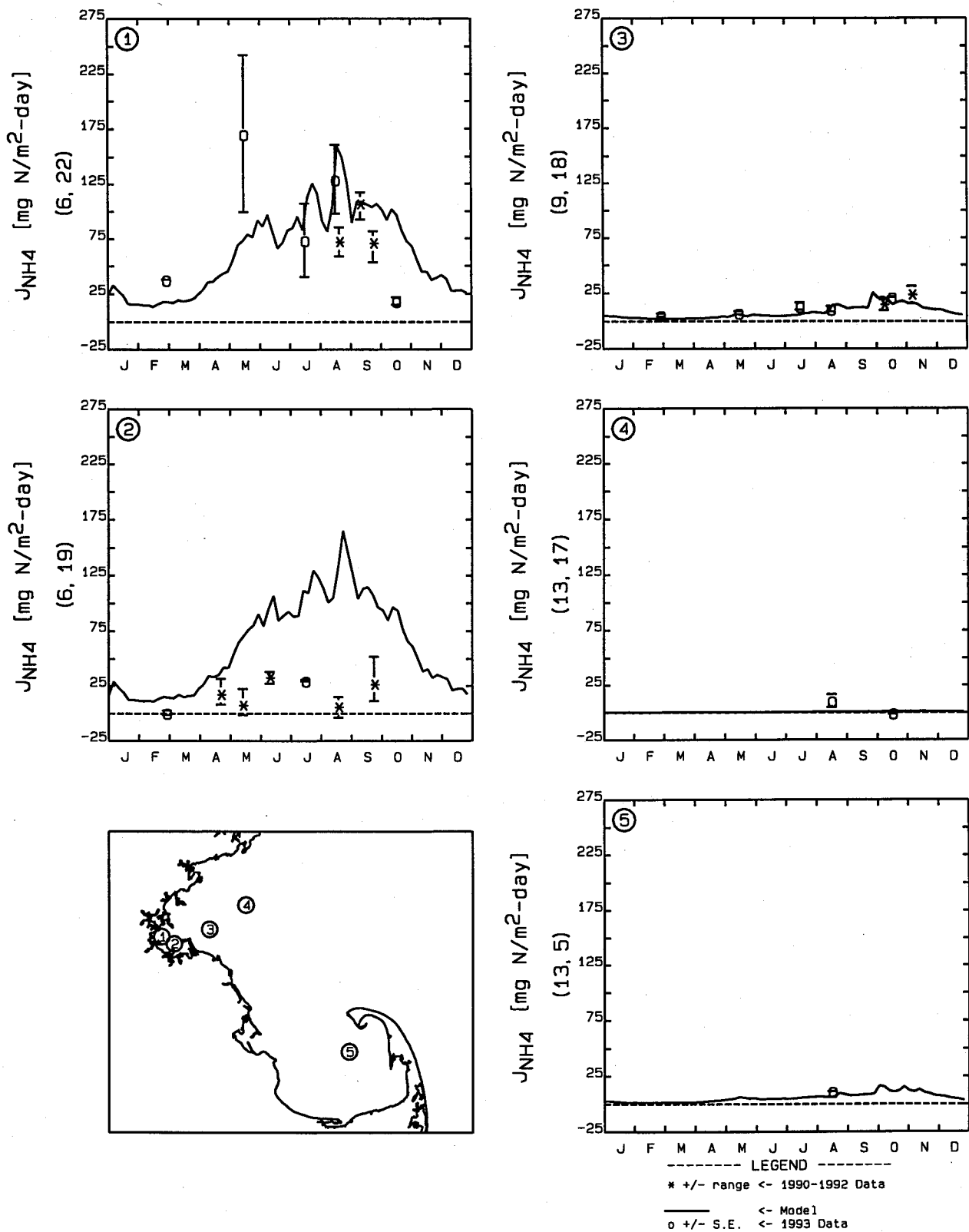
FIGURE 5-32. 1992 SEDIMENT FLUX SUBMODEL CALIBRATION RESULTS FOR J_{NH4}
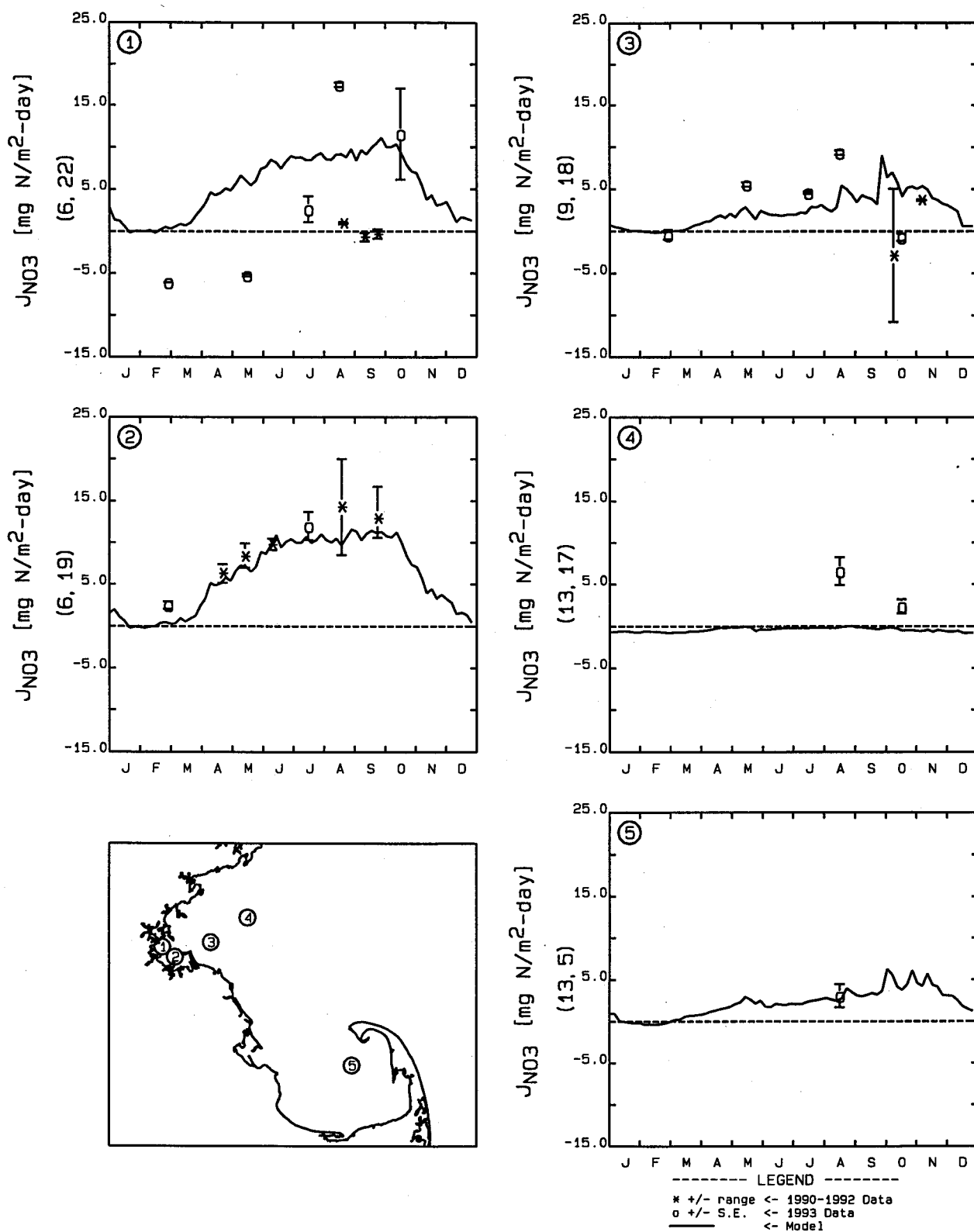
FIGURE 5-33. 1992 SEDIMENT FLUX SUBMODEL CALIBRATIONS RESULTS FOR J_{NO3}

Stellwagen Basin. Again it should be noted that these flux measurements were taken from depositional sediment locations.

Figure 5-34 presents the model versus data comparisons for rates of sediment denitrification. As has been described in Section 3.5, denitrification is the conversion of nitrate into nitrogen gas (N_2) and is one method by which nitrogen can be removed from the Bays system. With the exception of the Inner Harbor segment, the model estimates of sediment denitrification compare favorably to the observed data. In the model segments of the Bays, the model computes an average denitrification rate of 15 mg N/m^2-day. The model computes lower rates at both the Inner Harbor and Hingham Bay segments. The greatest discrepancy between model and data is in the Inner Harbor segment. It is worth noting the considerable variability between the denitrification rate estimates obtained from Nowicki and Giblin. The model compares more favorably to the Nowicki data set, but does not match the summertime observations. At the remaining sites, the two methods for estimating denitrification compare well and the model reasonable calibration to the data.

Using the results of the sediment model computations of sediment denitrification rates and nitrogen burial, together with estimated nitrogen mass loadings to Boston Harbor, indicates that only 2 to 4 percent of the total nitrogen loading to the harbor is lost to the sediment via denitrification or burial. This implies that greater than 95 percent is exported to Massachusetts Bay. Our estimates of denitrification and burial are lower than those estimated by Giblin et al. (1993) and Kelly (1993). Their estimates of loss via denitrification and burial were approximately 10 percent. The reason for this discrepancy is that the model's annually averaged denitrification rate is 6.6 mg N/m^2-day versus an estimated annual average rate of 36 mg N/m^2-day, based on measurements. However, the sediment denitrification rates were measured from sediment cores taken in depositional areas of the Harbor. Considering the analysis of Knebel (1993) it is possible that between 25 to 40 percent of Boston Harbor can be considered to be non-depositional or to be areas of transitory deposition. Therefore, the estimates of nitrogen loss via denitrification made by Giblin et al. and Kelly may be 25 to 40 percent too high. This would reduce the
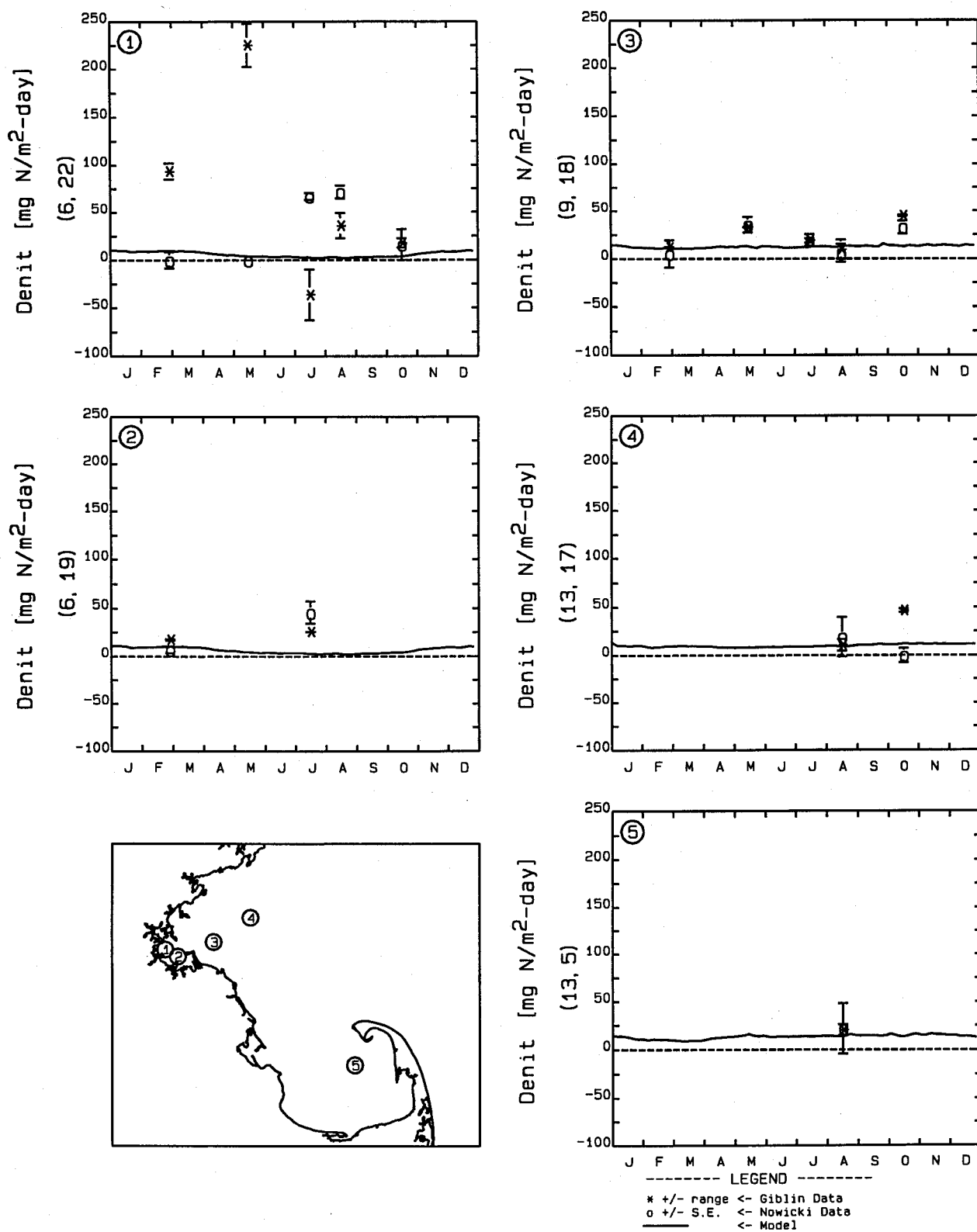
FIGURE 5-34. 1992 SEDIMENT FLUX SUBMODEL CALIBRATIONS RESULTS FOR DENITRIFICATION

differences between the model estimates of nitrogen loss and those based on the field data.

Calibration results for inorganic phosphorus fluxes (J_{PO_4}) are presented in Figure 5-35. The model approximately reproduces the PO_4 fluxes for the two Boston Harbor segments. The model provides a favorable comparison to the observed data for the model segments located outside of Boston Harbor: the computed and observed PO4 fluxes are small, generally less than 5 mg P/m^2-day.

Comparisons of model versus data for silica fluxes are displayed in Figure 5-36. For the Charles River segment, the model compares favorably to the fluxes measured in February, July and October, but underpredicts fluxes measured in May and August. The model overestimates Si fluxes observed in Hingham Bay by 25 to 40 mg Si/m^2-day in July. Outside of Boston Harbor, however, the model significantly underpredicts the silica fluxes. Giblin (1995) measured similar flux rates for the Bays in 1995 and, therefore, has confidence in the data. As of the preparation of this report, we have not been able to reconcile these differences. However, the under-estimation of silica flux does not appear to have had a significant adverse impact on the overall water quality model calibration.

5.5 INTERANNUAL MODEL VARIABILITY

The Massachusetts Bay/Cape Cod Bay estuary is a dynamic system subject to year-to-year variability. This variability is primarily due to changes in weather, circulation patterns, and changes in pollutant loadings. For the water quality model to be an effective predictive tool it must be able to reproduce some of the major features of system variability that can be observed in the data. While some of this variability can be imposed on the water quality model by using hydrodynamic model circulation transport regimes, observed changes in boundary conditions, and appropriate changes in pollutant loadings, it remains to be seen if the imposition of these forcings affect water quality within the model domain. The following series of figures present comparisons of model computations between February-December 1990 and February-December 1992. These comparisons will
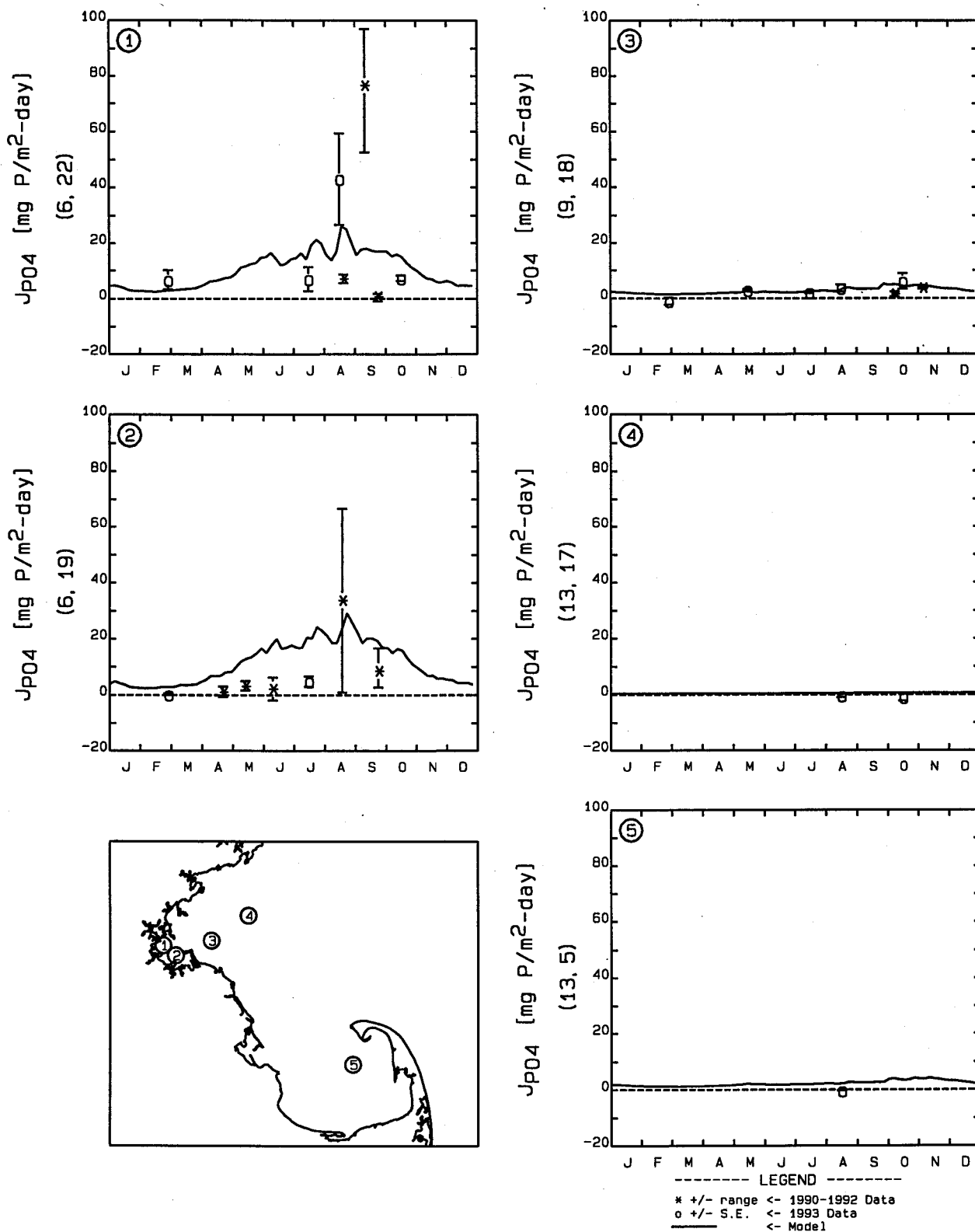
FIGURE 5-35. 1992 SEDIMENT FLUX SUBMODEL CALIBRATION RESULTS FOR J_{PO4}
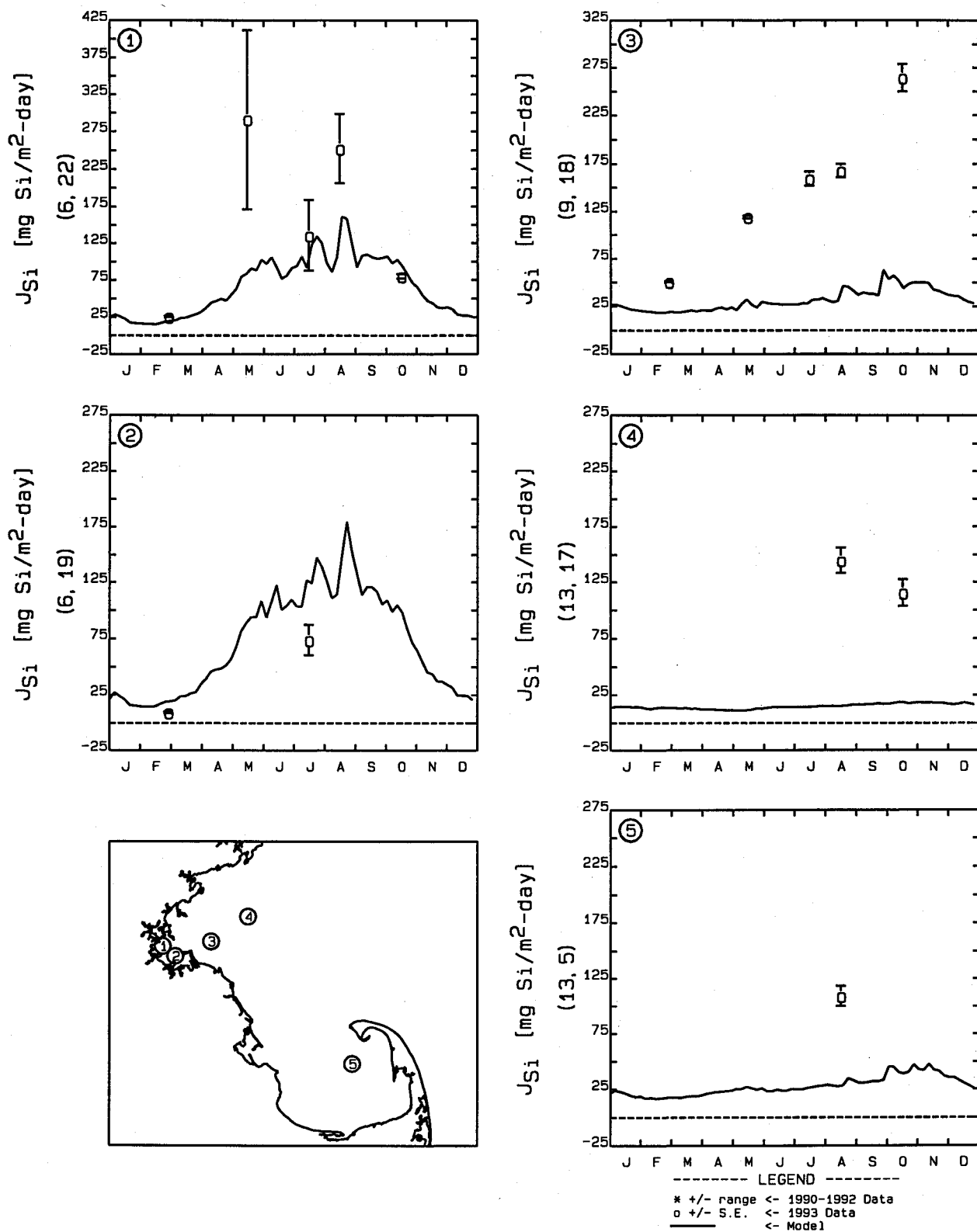
FIGURE 5-36. 1992 SEDIMENT FLUX SUBMODEL CALIBRATION RESULTS FOR J_{Si}

provide some insight into the year-to-year variability which the model was able to compute. Differences in the inputs to the water quality model between the two years include: hydrodynamics, boundary conditions, rainfall (which effects atmospheric loads), river loadings for the Charles, Mystic and Neponset Rivers, and sludge discharge from the Nut Island and Deer Island treatment plants (sludge discharge was discontinued in December 1991).

Figures 5-37 and 5-38 present probability plots of computed chlorophyll distributions for nearfield and farfield surface and mid-depth model segments, respectively. The 1990 model results are presented using a solid line, while 1992 model output is presented using a dotted line. The median chlorophyll-a concentrations are similar in the surface layer of the nearfield stations, for each season of the year. However, the maximum chlorophyll levels were higher in 1990. This is most evident for the winter period when the maximum 1990 chlorophyll-a concentrations are approximately 7 ug/L versus approximately 3 ug/L in 1992. On an annual basis for the farfield stations, 1990 chlorophyll concentrations are slightly higher than the concentrations computed in 1992. Mid-depth comparisons between the two years show a similar pattern to the surface computations. It is interesting to note is that during the spring and summer, chlorophyll-a concentrations at mid-depth are higher than at the surface. This may be due to surface nutrient limitation, whereas phytoplankton at depth may be able to utilize nutrients that "leak" across the pycnocline.

Figures 5-39 and 5-40 display model output of DIN at the surface layer and mid-depth respectively. Except for the fall, the 1990 model computations show higher concentrations than those computed for 1992. This is due, in part, to higher DIN boundary concentrations which were specified for 1990. The effect of these higher DIN concentrations is to produce higher chlorophyll-a concentrations as seen in Figures 5-37 and 5-38. During the spring and summer when DIN concentrations are reduced at the surface due to algal uptake, higher DIN concentrations are still available at the mid-depth, which permit higher chlorophyll concentrations to develop at mid-depth. On an annual basis the 1990 DIN levels are also higher than those computed for 1992.

FIGURE 5-37. PROBABILITY DISTRIBUTIONS OF 1990 AND 1992 MODEL SURFACE CHLOROPHYLL-a CONCENTRATIONS

FIGURE 5-38. PROBABILITY DISTRIBUTIONS OF 1990 AND 1992 MODEL MID-DEPTH
CHLOROPHYLL-a CONCENTRATIONS
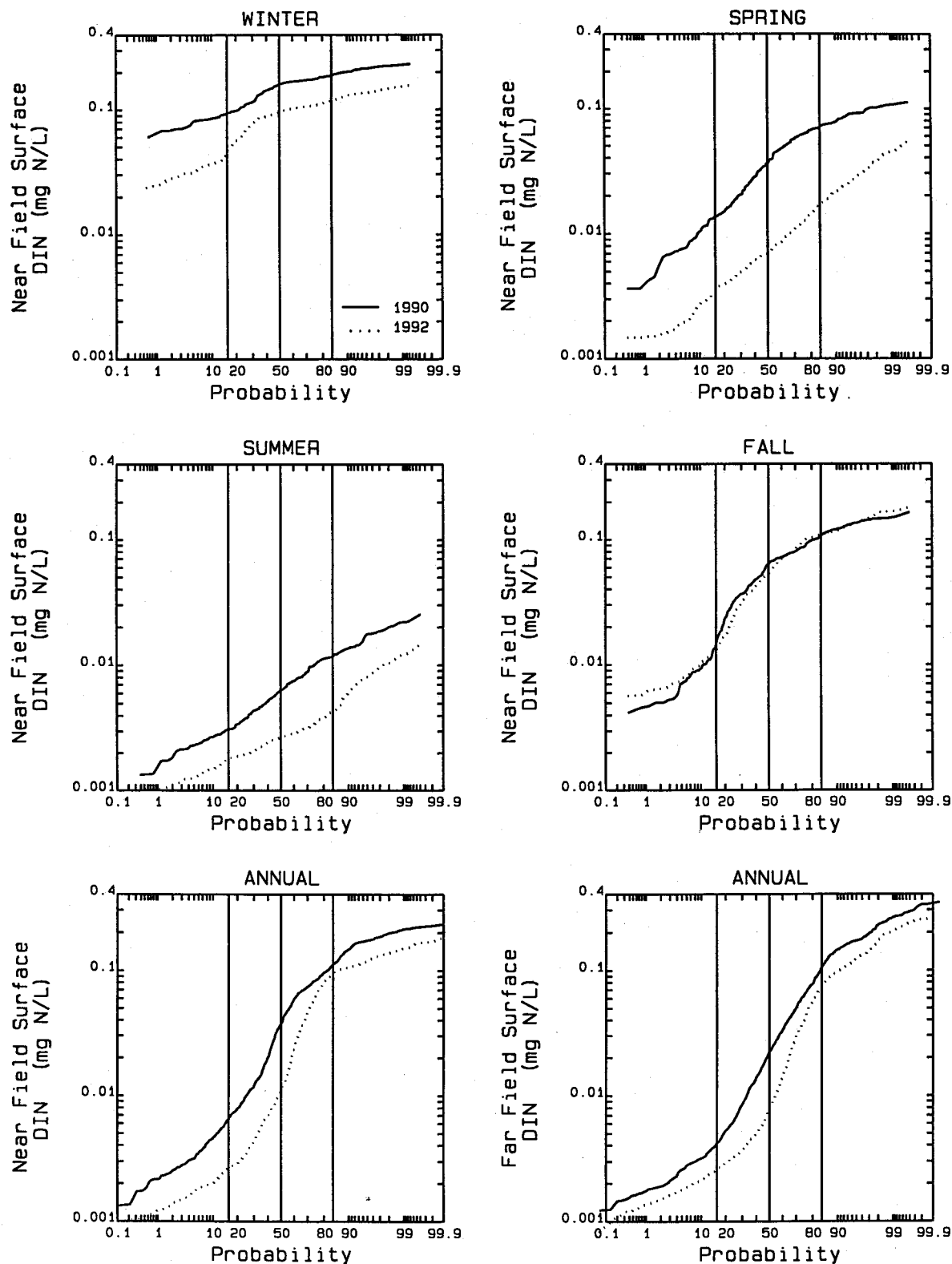
FIGURE 5-39. PROBABILITY DISTRIBUTIONS OF 1990 AND 1992 MODEL SURFACE DIN CONCENTRATIONS
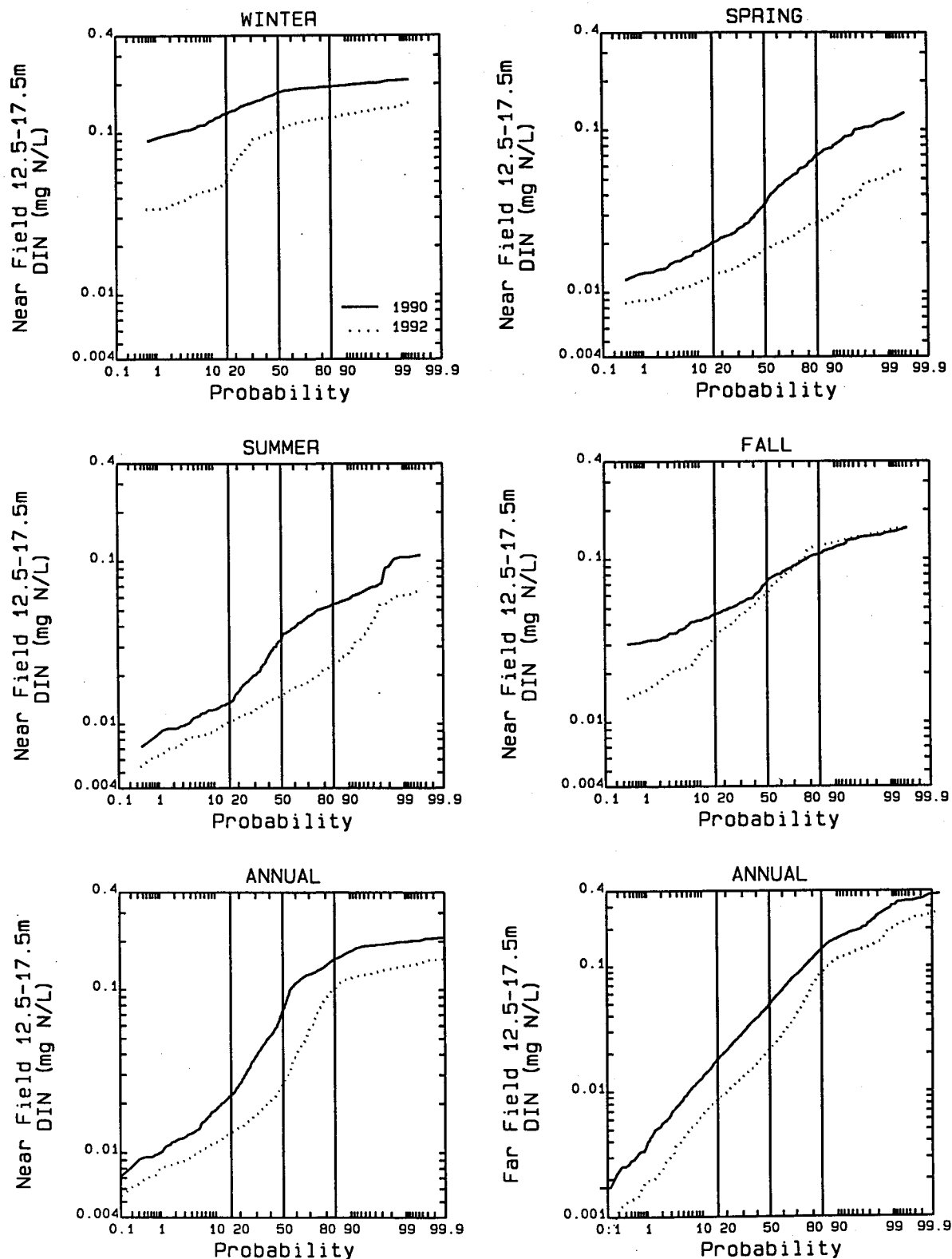
FIGURE 5-40. PROBABILITY DISTRIBUTIONS OF 1990 AND 1992 MODEL MID-DEPTH DIN CONCENTRATIONS

Another nutrient in Massachusetts Bay, which is sometimes found to be limiting, is silica. Model distributions for silica are shown in Figures 5-41 and 5-42 for the surface and mid-depth, respectively. Again boundary conditions are a primary factor in determining the differences between the two years. Higher boundary conditions were assigned for the winter of 1990 then were imposed for the winter of 1992. This results in the higher concentrations observed in the nearfield segments for the winter of 1990. In the spring of 1992, a large pulse of silica was input at the boundary. As a consequence silica concentrations are higher in the the spring of 1992 versus 1990.

A comparison of 1990 and 1992 model output for dissolved oxygen is presented for the bottom waters and the mid-depth in Figures 5-43 and 5-44, respectively. On an annual basis the two years are similar. Seasonally, however, higher DO concentrations of approximately 0.5 mg/L were computed for 1992 in the winter. Boundary conditions account for most of this difference between the two years. Spring concentrations of DO are similar for both the bottom and mid-depth waters. Summer bottom water DO was lower in 1990 as compared to 1992. This may be in part due to stronger vertical stratification in the water column. Evidence for this is present in Figure 5-45, which shows differences in surface and bottom water salinities. As can be seen there are greater differences between surface and bottom salinities in the summer of 1990, suggesting stronger vertical stratification. Dissolved oxygen concentrations are higher at the bottom and mid-depths of the water column in 1992. This phenomenon may also be related to differences in density stratification bewtween the two years. As can be seen of Figure 5-45, salinity gradients are weaker in the fall of 1992. This may permit the fall turnover of the water body to occur earlier, thereby re-aerating the bottom and mid-depth portions of the water column.
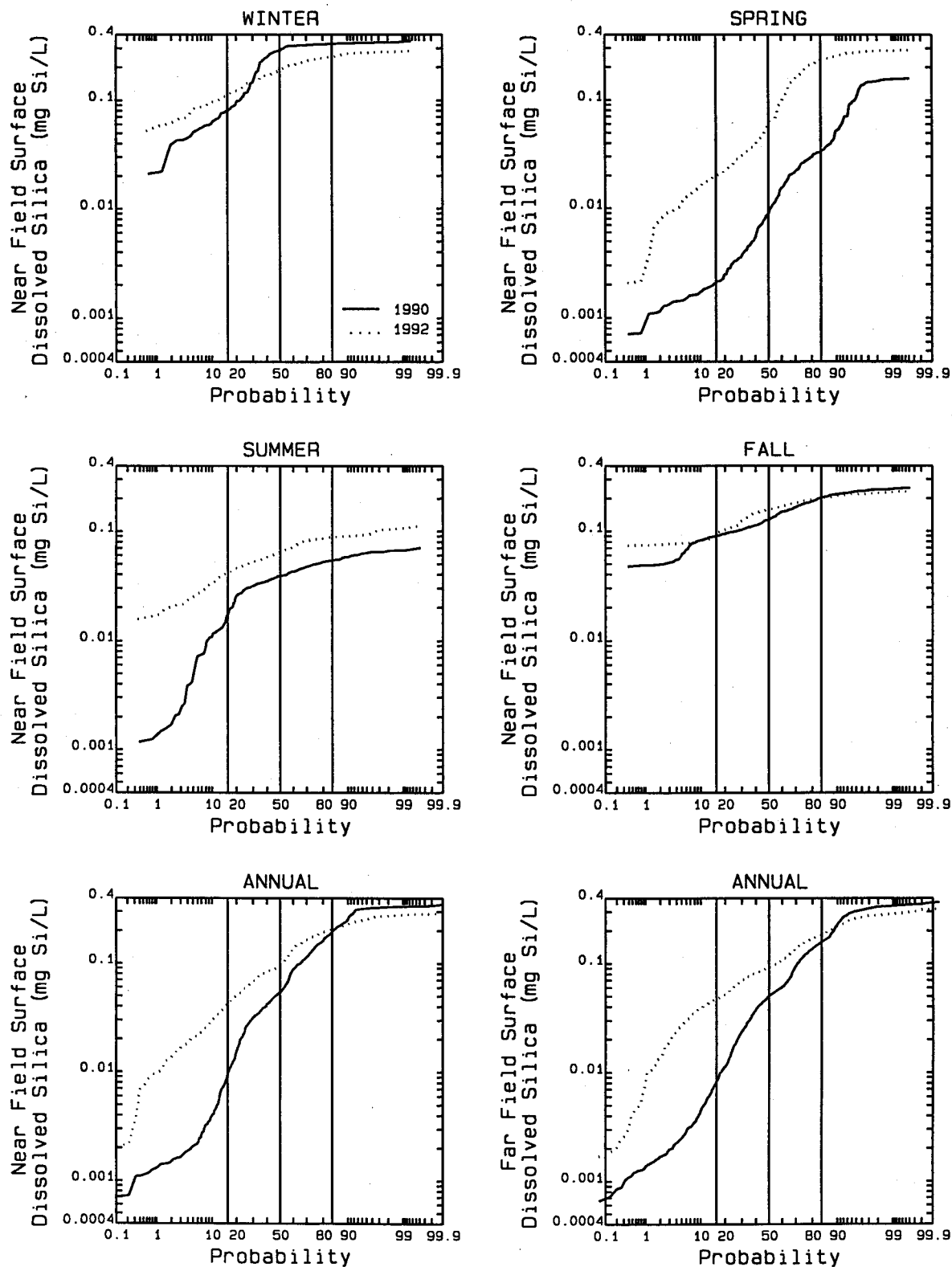
FIGURE 5-41. PROBABILITY DISTRIBUTIONS OF 1990 AND 1992 MODEL SURFACE Si CONCENTRATIONS
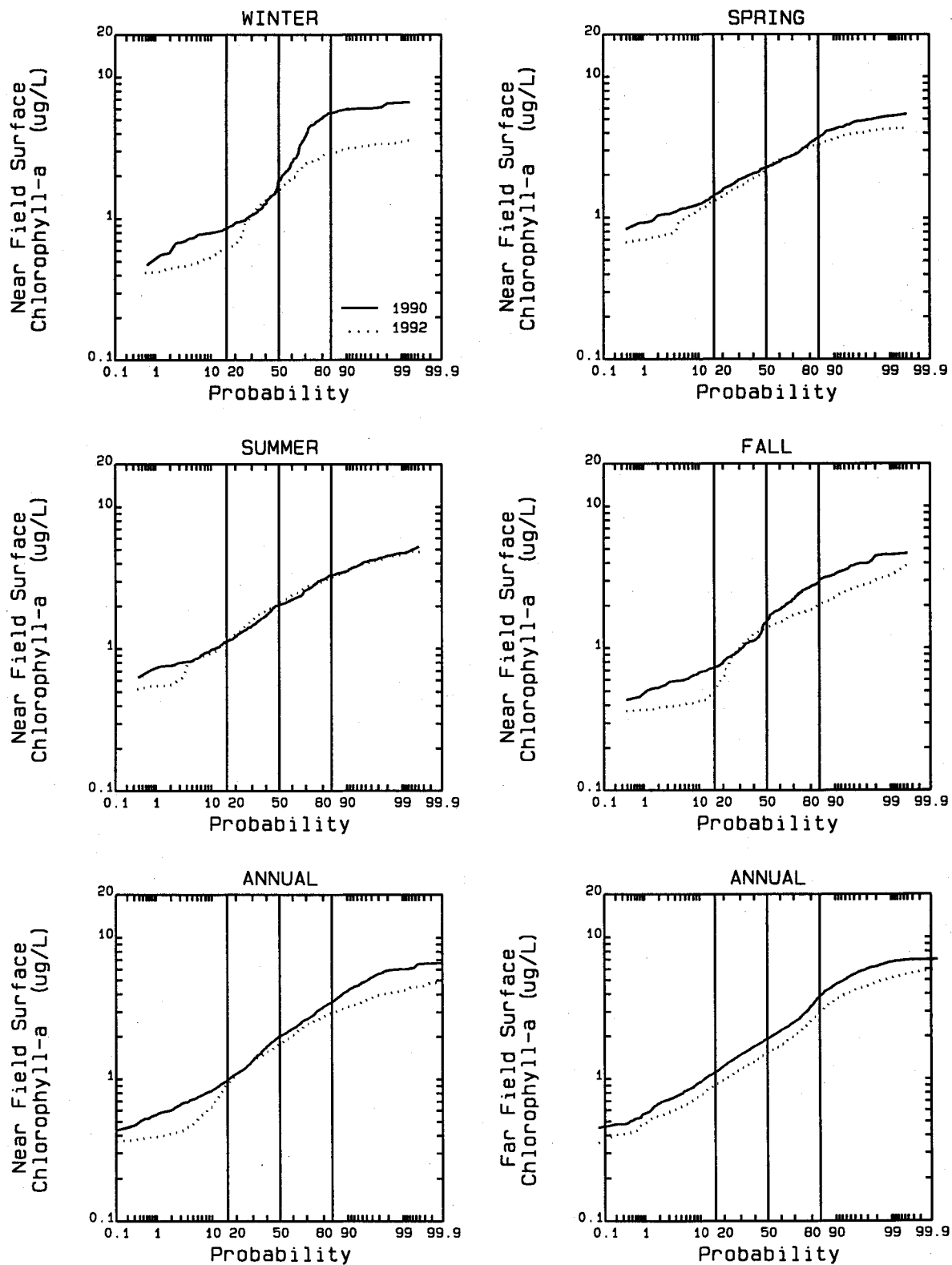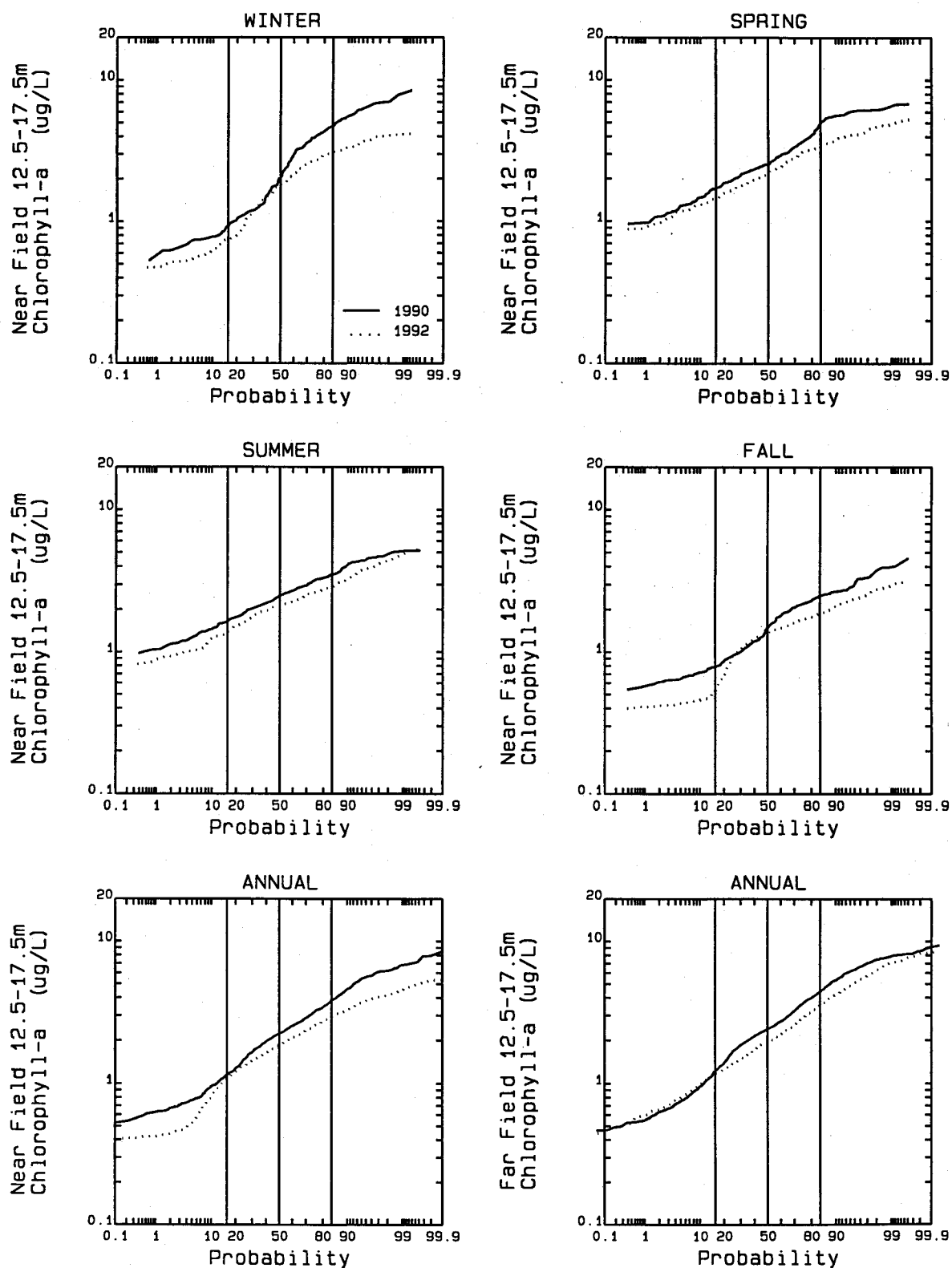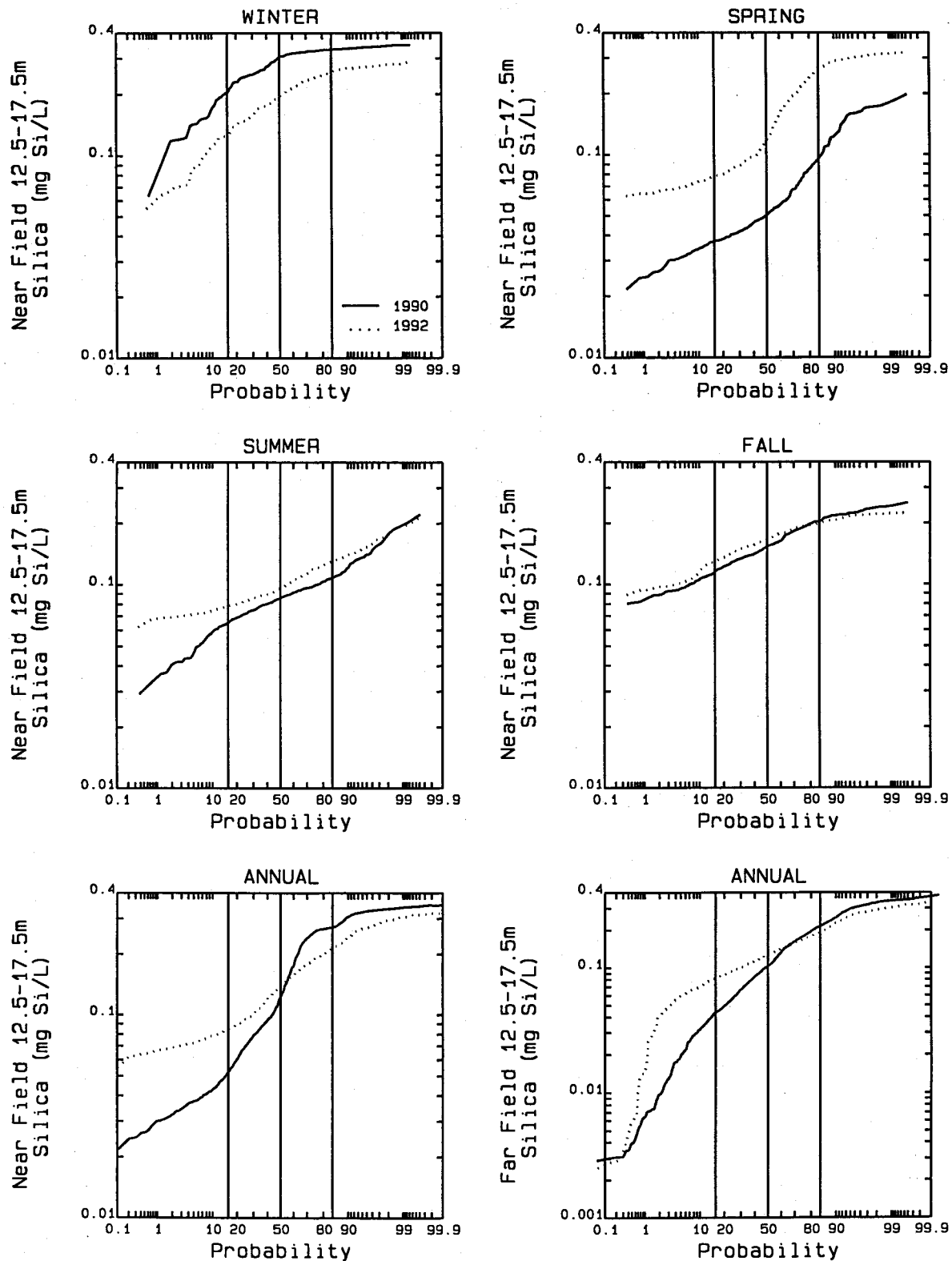
FIGURE 5-42. PROBABILITY DISTRIBUTIONS OF 1990 AND 1992 MODEL MID-DEPTH
Si CONCENTRATIONS
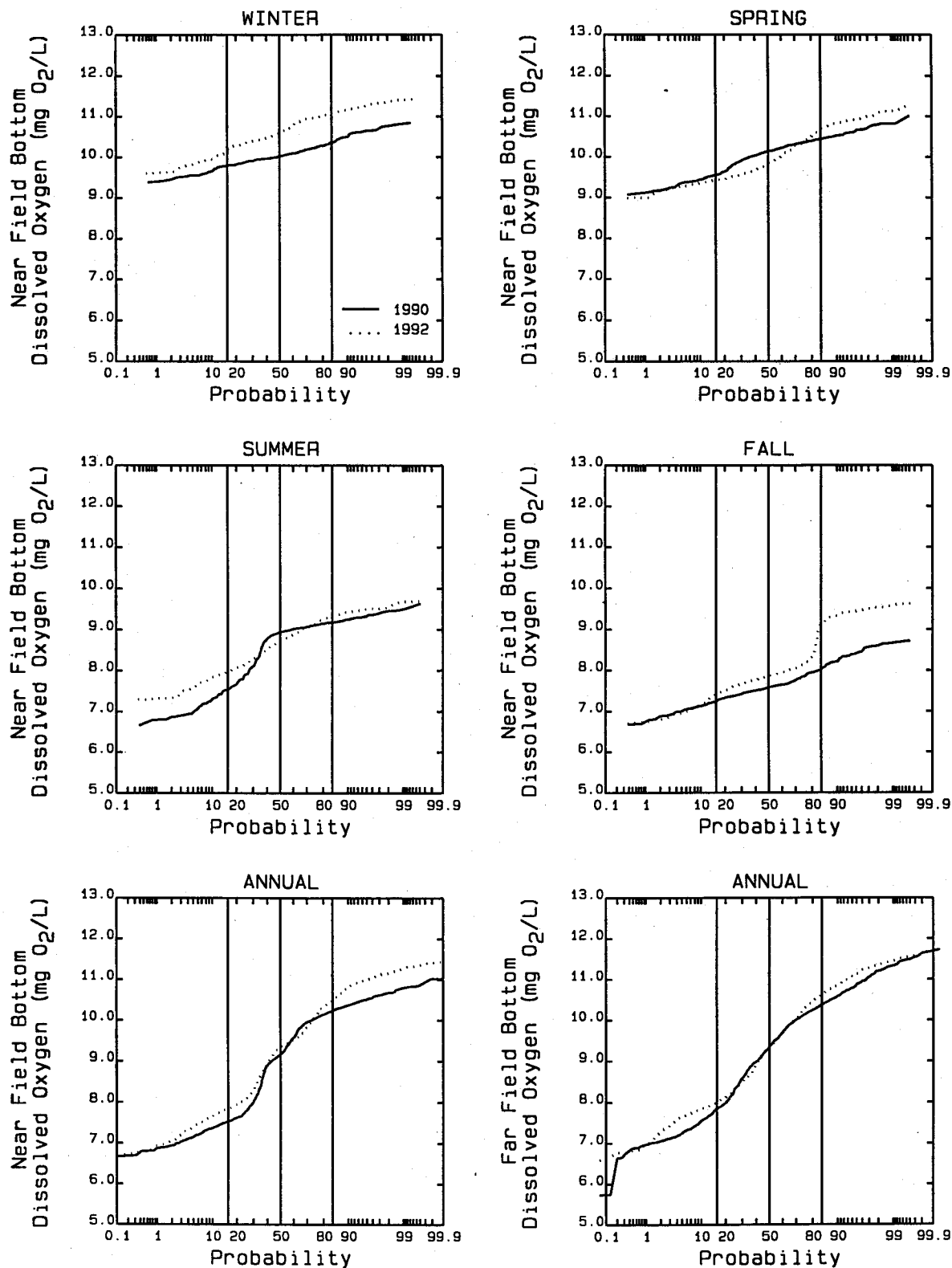
FIGURE 5-43. PROBABILITY DISTRIBUTIONS OF 1990 AND 1992 MODEL MINIMUM
BOTTOM DO CONCENTRATIONS
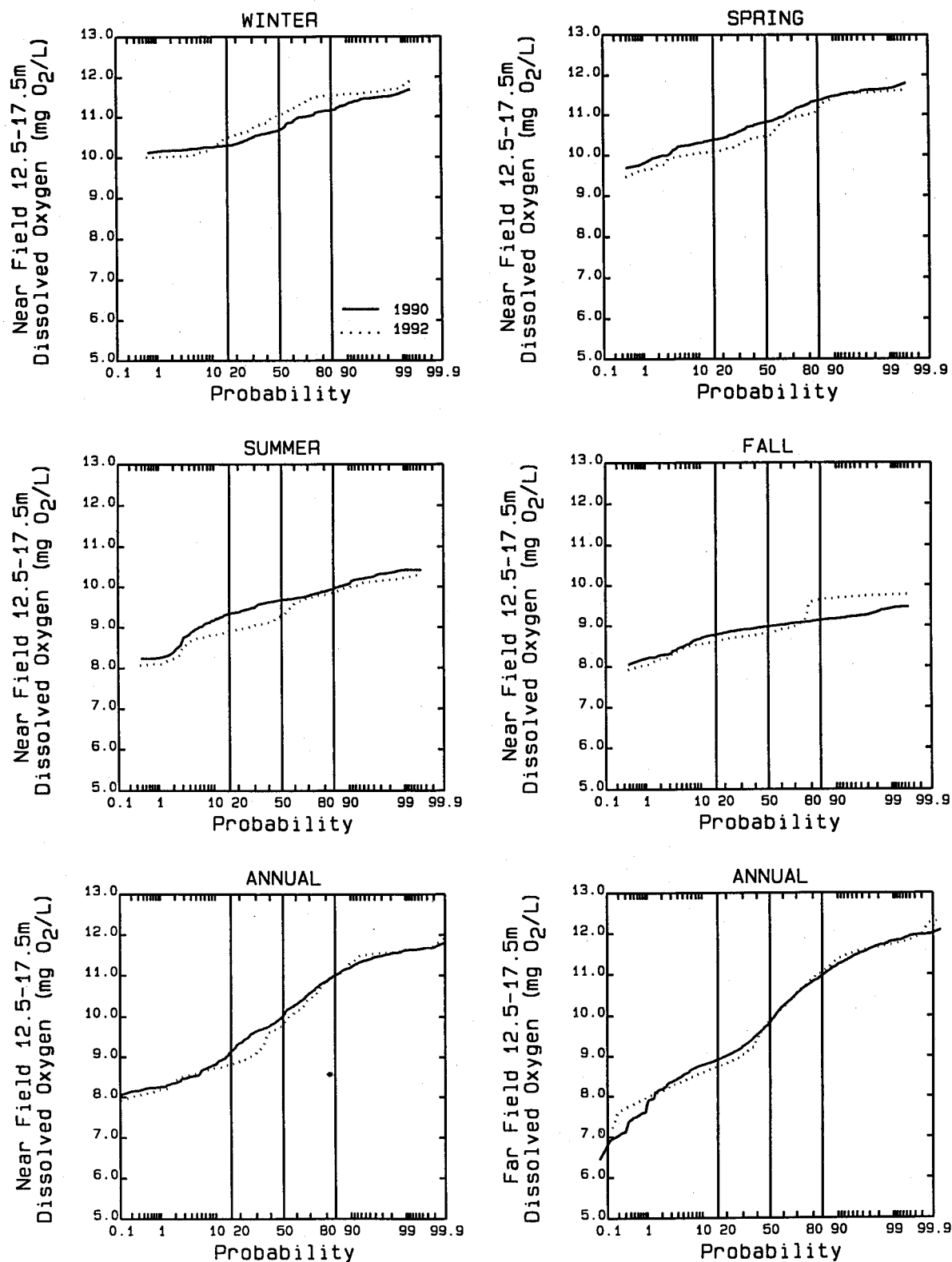
FIGURE 5-44. PROBABILITY DISTRIBUTIONS OF 1990 AND 1992 MODEL MID-DEPTH DO CONCENTRATIONS
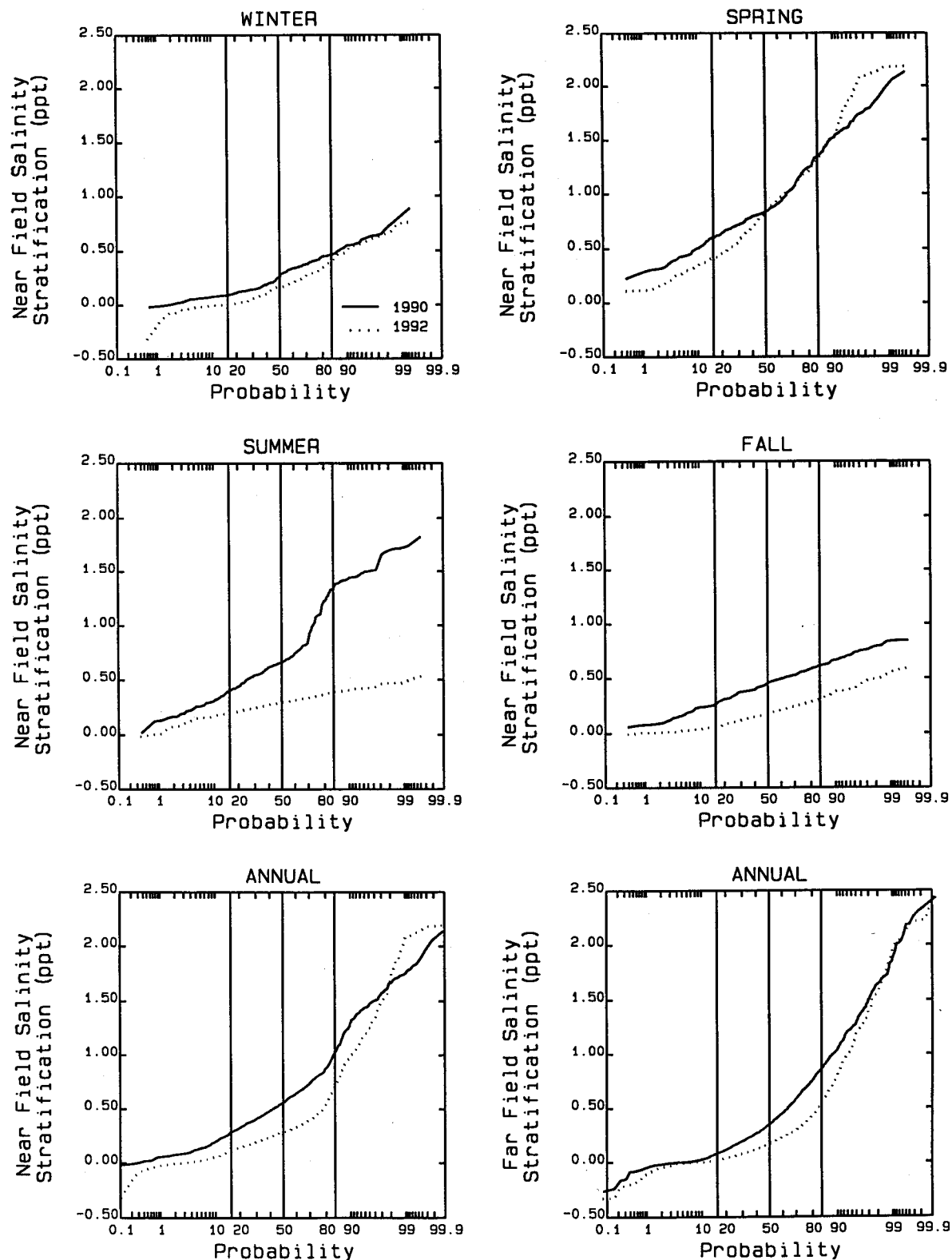
FIGURE 5-45. PROBABILITY DISTRIBUTIONS OF 1990 AND 1992 MODEL SALINITY STRATIFICATION

SECTION 6

SENSITIVITY ANALYSIS

At the request of the Model Evaluation Group (a peer review committee of scientists and water quality managers familiar with water quality modeling and/or the Massachusetts Bays system) a number of model sensitivity runs were performed using the calibrated water quality model developed during this study. The purpose of these runs was to attempt to ascertain the importance of the various sources of nutrients being delivered to the Bays system. Therefore, three sensitivity runs were conducted: (1) a 25 percent reduction in the boundary nitrogen concentrations, (2) eliminating atmospheric inputs, and (3) zeroing out all internal sources (point, nonpoint and atmospheric inputs); i.e., consider only the boundary input of nutrients.

These runs were conducted using the 1992 calibration as the base line condition. The appropriate loads and/or boundary conditions were changed and the model was run for a period of one year. It should be noted that the output from these runs yields only a partial water quality response to the conditions being imposed on the model, since the model runs were not cycled for multiple years. This is an important consideration, since the sediment layer of the coupled water column/sediment nutrient flux submodel would not have achieved a new equilibrium in response to the revised loading conditions. This consideration is particularly true for the portion of the model domain located in and around Boston Harbor. This region of the model would be expected to require three to five years to reach a new equilibrium in response to the removal of point and nonpoint source loadings. These sensitivity runs are also subject to some carry-over from the January initial conditions under which the model is run. This is not as serious a concern as is the time to reach sediment equilibrium, since the initial conditions should be flushed out of the Bays system within a relatively short period of time. Geyer et al. (1992) have made estimates of residence time within the Bays system which range from 15 to 100 days. The lower values are typical of the residence time for the upper portion of the water column in late winter/spring period, while the higher values are more typical of estimated summer bottom water residence times. While the output from these runs should be

viewed under the light of the above constraints, they, nevertheless, provide some insights into the behavior of the model in response to major changes in nitrogen loading to the system.

The sensitivity results to be presented below will presents a series of comparisons between the calibration model results (i.e., the base case) and the sensitivity run results. Generally, comparisons will be presented for the months of March, August, and October. March and August were chosen for comparison purposes because these months have some of the highest recorded measurements of primary productivity (Figure 5-17). October was chosen because it is the month with the lowest reported concentrations of bottom water dissolved oxygen (Figure 5-18).

6.1 NITROGEN RESPONSE

The first set of sensitivity analysis results will present concentrations of total nitrogen (TN) in Boston Harbor and the Massachusetts and Cape Cod Bays system. Figure 6-1 presents a comparison of March and August surface TN concentrations for the base calibration versus a 25 percent reduction in boundary nitrogen concentrations. These surface contour plots represent a five-day averaged value from the middle of each month (i.e., approximately March 15 and August 15). The first point to note on this figure is the marked difference between nitrogen levels for the base calibration in March and August in Massachusetts and Cape Cod Bays. In March TN concentrations are approximately 0.35 mg N/L, while by August they have decreased to between 0.1 and 0.2 mg N/L. As can also be seen the concentrations of TN are considerably higher in Boston Harbor, about 0.6 to 0.7 mg N/L, as compared to the rest of the Bays system. One can also note a slight TN plume from Boston Harbor that appears to hug the coastline of Massachusetts Bay, extending down towards Plymouth in March and extending out into northern Massachusetts Bay in August.

Comparing the 25% boundary reduction to the calibration indicates only fairly small changes in TN concentrations between the two runs. The most noticeable differences that

Surface Total Nitrogen

March TN (Calibration)

August TN (Calibration)

March TN (Projection)

August TN (Projection)

25% Reduction of N BC

(mg/L) 0.7 0
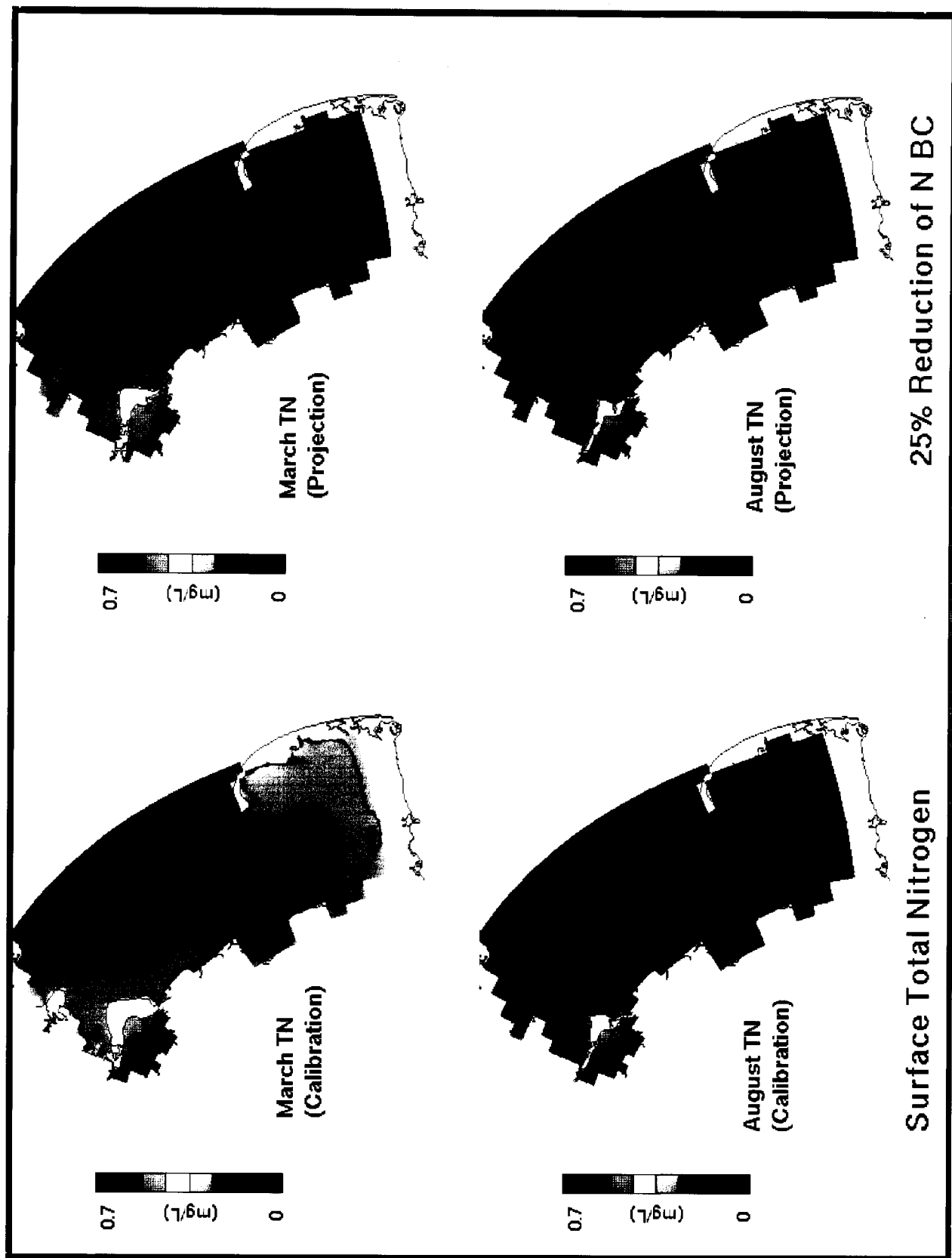
FIGURE 6-1. COMPARISONS OF SURFACE TN FOR MARCH AND AUGUST BETWEEN MODEL CALIBRATION RESULTS AND MODEL SENSITIVITY RESULTS FOR A 25 PERCENT REDUCTION OF TN BOUNDARY CONCENTRATIONS

can be discerned are in northeastern Massachusetts Bay in March, where the change in boundary concentrations results in about a 0.1 mg N/L reduction in this region of Massachusetts Bay, and a slight decline in TN concentrations in northern Cape Cod Bay in August. The latter change probably results from the reduced influx of TN into the Bays during the spring rather than a reduced flux of TN during the summer months.

Figure 6-2 presents a comparison of March surface TN for the calibration (designated as No Action on this figure), 25% reduction in boundary nitrogen, zero atmospheric deposition, and zero internal loading (boundary inputs only). The comparison between the calibration (or no action) and 25% boundary reduction run has been described above. With respect to the no atmospheric deposition run, one can detect only slight reductions in surface TN in the nearshore regions of the system, in particular near Plymouth and southwestern Cape Cod Bay. The impact of removing all internal loadings is most notable in Boston Harbor and those regions influenced by the Boston Harbor effluent plume.

Another way in which to view the sensitivity outputs is presented in Figure 6-3. In this figure the output computations of the sensitivity run are subtracted from the base case (no action) calibration and the results are then presented using contour plots. The no action panel is, of course, a plot of zero change in concentration. As has been described earlier the major changes in surface TN in response to a 25% reduction in boundary nitrogen are confined to northern eastern Massachusetts Bay, although some small differences can also be seen throughout the Bays system. The no atmospheric deposition sensitivity run shows virtually no change from the calibration or no action run as might be expected since the atmospheric loads are distributed over a wide area. The difference plot for the no internal loading sensitivity run shows the most dramatic differences in and around Boston Harbor. TN concentrations are shown to decrease by 0.2 mg N/L or greater in Boston Harbor and by approximately 0.1 mg N/L in those nearfield areas influenced by the Boston Harbor plume. One can also note a reduction in TN on the northern shoreline of Massachusetts Bay in response to the removal of TN associated with the other North Shore treatment facilities.

No Action

25% Nitrogen Reduction of BC

No Atmospheric Deposition

No Loads Only BC

0.7 (mg/L) 0

Effect of Sensitivity Analyses on Surface Total Nitrogen (March)

FIGURE 6-2. COMPARISON OF MARCH SURFACE TN BETWEEN MODEL CALIBRATION RESULTS AND MODEL SENSITIVITY RESULTS FOR A 25 PERCENT REDUCTION OF BOUNDARY NITROGEN, NO ATMOSPHERIC DEPOSITION AND NO INTERNAL LOADINGS

No Action

25% Nitrogen Reduction of BC

No Atmospheric Deposition

No Loads Only BC

Effect of Sensitivity Analyses on Surface Total Nitrogen (March)

FIGURE 6-3.   COMPUTED CHANGES IN MARCH SURFACE TN BETWEEN MODEL CALIBRATION RESULTS AND MODEL SENSITIVITY RESULTS FOR A 25 PERCENT REDUCTION OF BOUNDARY NITROGEN, NO ATMOSPHERIC DEPOSITION AND NO INTERNAL LOADINGS

Figure 6-4 presents a sensitivity difference plot, similar to Figure 6-3, but for the bottom waters of the system. The results for each of the sensitivity runs are similar to those observed for the surface layer results, but a few differences are worth noting. First, for the 25% reduction in boundary nitrogen, it can be seen that there is a greater reduction in bottom water TN at the northeast boundary than is computed in the surface waters. However, the reduction in boundary nitrogen has a greater spatial extent in the surface waters than is observed in the bottom waters. This is probably due to the fact that most of the waters being imported into the bay with the spring freshet are confined to the surface layers of the system. Second, with respect to the no internal load sensitivity run, it can be seen that a larger portion of the nitrogen export from Boston Harbor is confined to the surface water of northwest Massachusetts Bay, even during this period of time, when the bay is fairly well-mixed vertically.

Figures 6-5 and 6-6 present the sensitivity difference contour plots for August surface TN and bottom TN, respectively. Compared to Figure 6-3, the 25% reduction in boundary nitrogen does not show as large an impact in the surface waters of the bay. This is probably due to two factors: (1) reduced influx of Gulf of Maine waters into the northern boundary and (2) the fact that surface boundary nitrogen is already at low concentrations. The August surface layer results for the no atmospheric deposition run are similar to those observed in March, virtually no change in TN concentrations. The magnitude of change for the August no internal load sensitivity is similar to that computed in March. The major reductions in surface TN occur in Boston Harbor and northwest Massachusetts Bay. It is interesting to note that for this particular 5-day period in August the Boston Harbor plume extends further into Massachusetts Bay than it does in March.

Results for the August bottom water are presented on Figure 6-6. The 25% reduction in boundary nitrogen sensitivity results for August provide an interesting contrast to the March model computations. While the reduction in bottom water TN does not appear to be as great for the northeastern boundary in August as are computed in March, the remaining portions of the system appear to be more significantly affected. The reason for this difference may be due to the residual effects of the model initial conditions, which
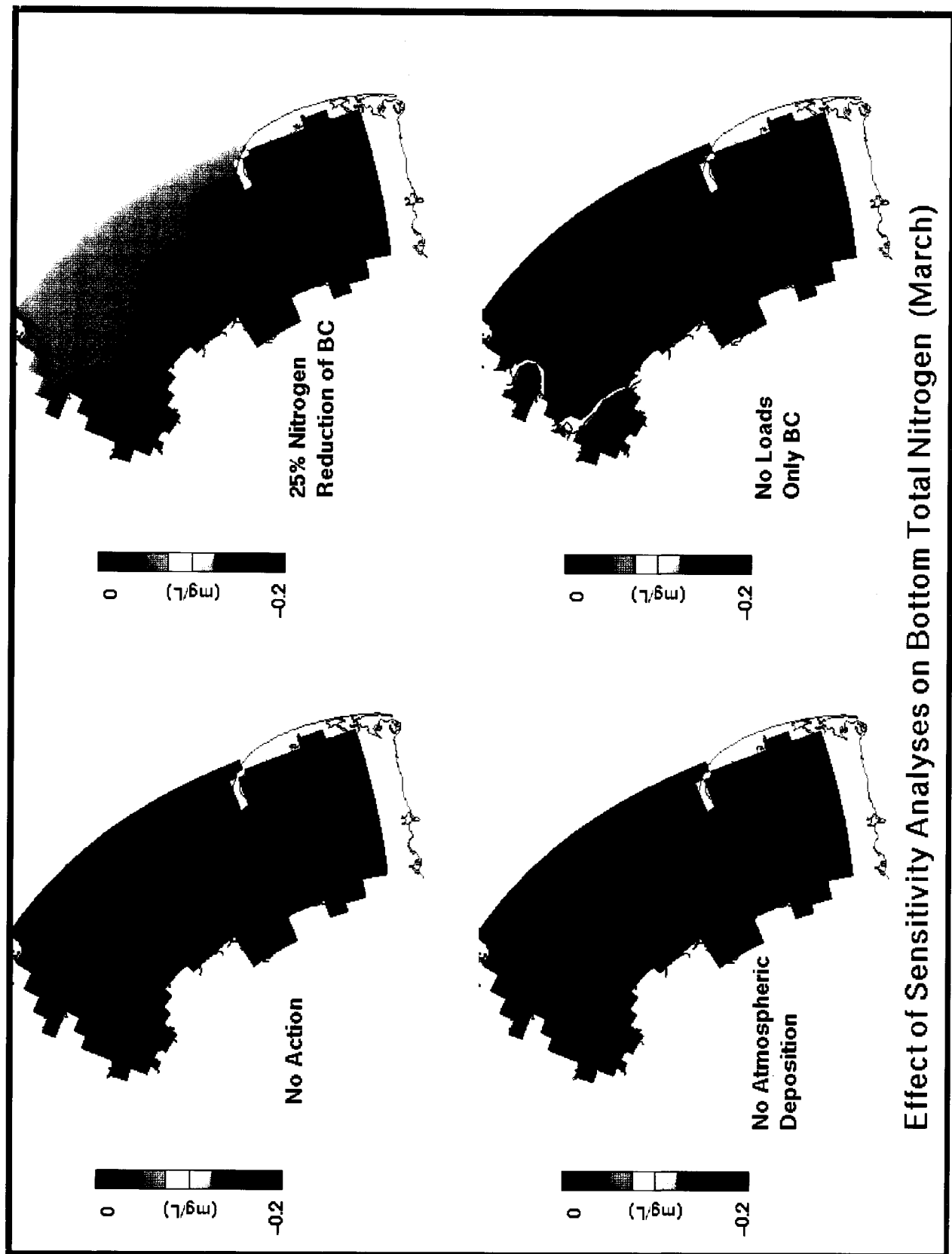
FIGURE 6-4. COMPUTED CHANGES IN MARCH BOTTOM TN BETWEEN MODEL CALIBRATION RESULTS AND MODEL SENSITIVITY RESULTS FOR A 25 PERCENT REDUCTION OF BOUNDARY, NITROGEN, NO ATMOSPHERIC DEPOSITION, AND NO INTERNAL LOADINGS

25% Nitrogen Reduction of BC

No Loads Only BC

No Action

No Atmospheric Deposition

Effect of Sensitivity Analyses on Surface Total Nitrogen (August)

FIGURE 6-5. COMPUTED CHANGES IN AUGUST SURFACE TN BETWEEN MODEL CALIBRATION RESULTS AND MODEL SENSITIVITY RESULTS FOR A 25 PERCENT REDUCTION OF BOUNDARY NITROGEN, NO ATMOSPHERIC DEPOSITION AND NO INTERNAL LOADINGS

25% Nitrogen
Reduction of BC

No Loads
Only BC

No Action

No Atmospheric
Deposition

Effect of Sensitivity Analyses on Bottom Total Nitrogen (August)

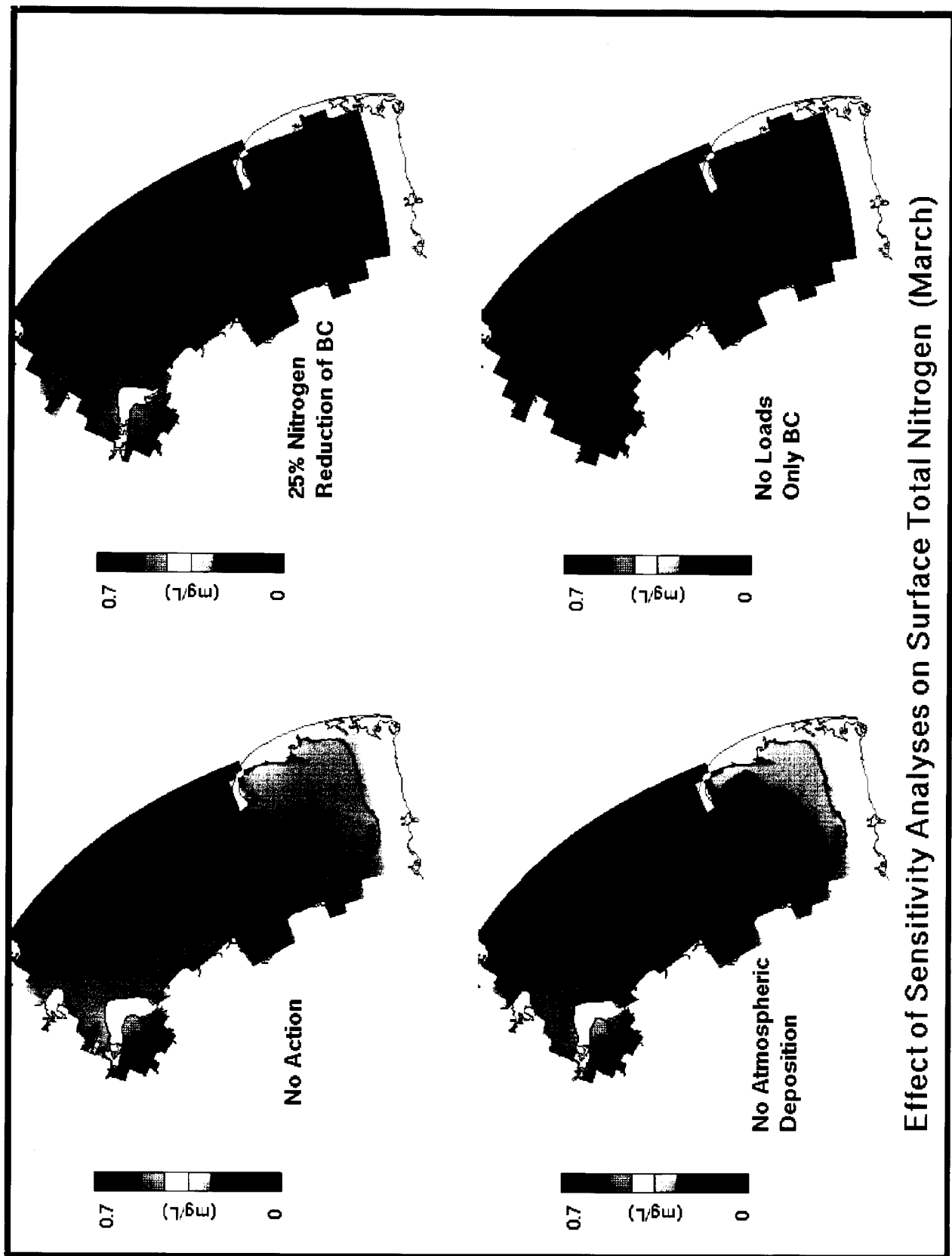FIGURE 6-6. COMPUTED CHANGES IN AUGUST BOTTOM TN BETWEEN MODEL CALIBRATION RESULTS AND MODEL SENSITIVITY RESULTS FOR AT 25 PERCENT REDUCTION OF BOUNDARY NITROGEN, NO ATMOSPHERIC DEPOSITION AND NO INTERNAL LOADINGS
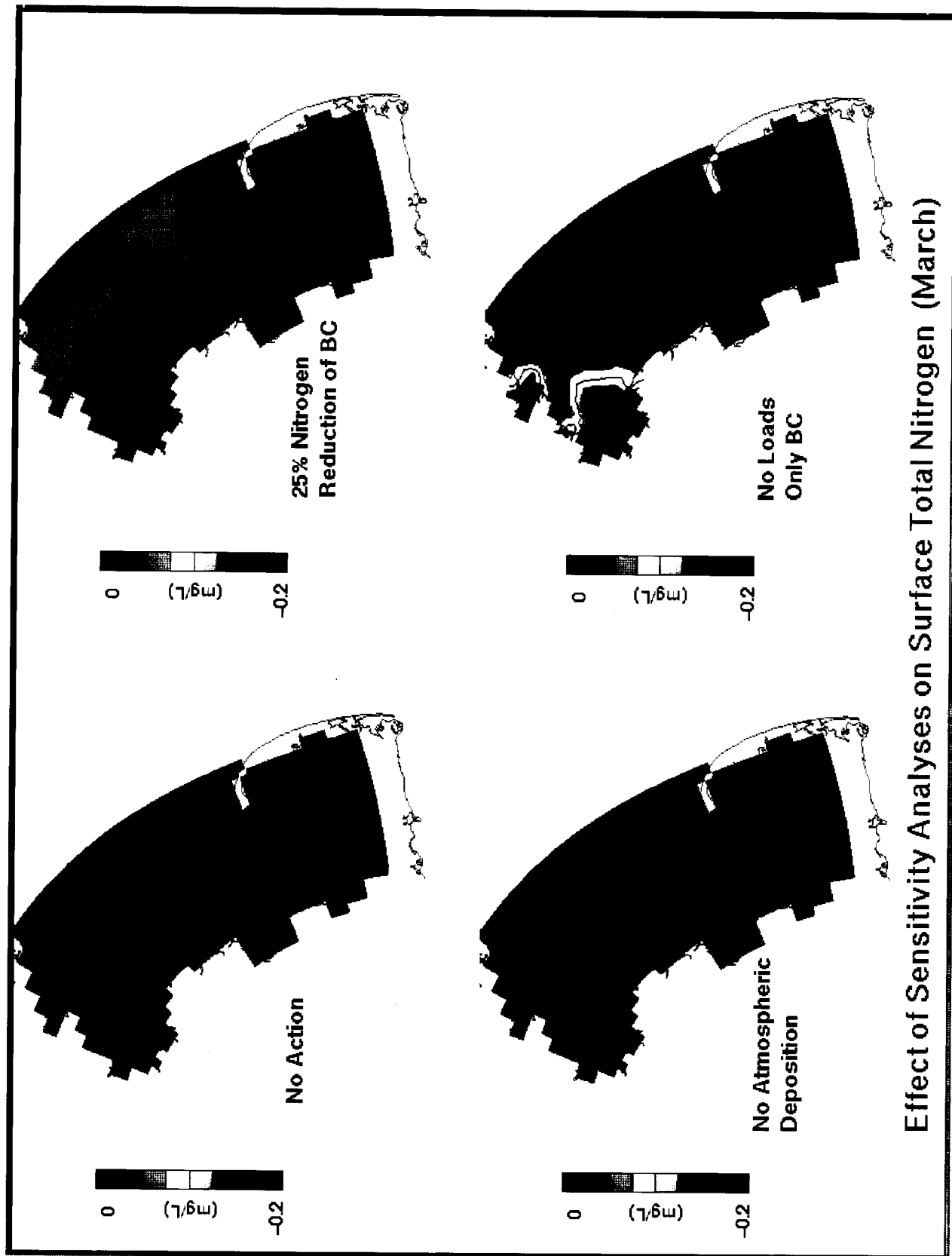
may be affecting the March bottom water results. Evidence for this hypothesis may also be seen in the lowered levels of bottom water August TN for the no internal load sensitivity run. It is also interesting to note that the southern portion of Cape Cod Bay appears to be more impacted by the 25% reduction in boundary nitrogen concentrations than it does by the elimination of all internal loadings to the system.

6.2   CHLOROPHYLL RESPONSE

Figure 6-7 presents comparison of surface contours of chlorophyll-a for the months of March and August as computed for the calibration and the 25% reduction in boundary nitrogen concentrations. As can be seen for the calibration, there is a marked difference in the distributions of chlorophyll-a within the Bays for the months of March and August. As can be seen in March the chlorophyll-a concentrations are generally higher throughout the Bays as compared to August. There is a fairly large bloom in Cape Cod Bay that is virtually absent in August. By August, with the exception of Boston Harbor, inorganic nitrogen levels have decreased throughout the bays and have limited phytoplankton growth. However, since there is a source of inorganic nitrogen from the MWRA outfalls located in Boston Harbor, chlorophyll-a levels in Boston Harbor and its plume are at concentrations of 3 μg/L or greater. (Note, for visualization purposes an upper limit of 5 μg/L was used for the August contours. Concentrations of chlorophyll-a in Boston Harbor are actually on the order of 5 to 15 μg/L.) As can be seen on this figure there is virtually no difference between the March chlorophyll-a concentrations computed for the calibration case and the 25% reduction in boundary nitrogen concentrations. This may be due to two factors: (1) the possibility that residual nitrogen initial conditions are still influencing March growth, and (2) the fact that despite the reduction in boundary nitrogen, dissolved inorganic nitrogen concentrations have not as yet reached growth limiting conditions.

By August it is known that inorganic nitrogen levels have reached growth limiting conditions. It is further expected that the effects of the initial conditions should have been flushed from the bays. Therefore, it is interesting to note that there is not a significant

March Chl–a
(Projection)

(ug/L)

8   0

August Chl–a
(Projection)

(ug/L)

5   0

March Chl–a
(Calibration)

(ug/L)

8   0

August Chl–a
(Calibration)

(ug/L)

5   0

Surface Chlorophyll–a

25% Reduction of N BC

FIGURE 6-7. COMPARISON OF SURFACE CHLOROPHYLL-A FOR MARCH AND AUGUST BETWEEN MODEL
CALIBRATION RESULTS AND MODEL SENSITIVITY RESULTS FOR A 25 PERCENT REDUCTION OF TN BOUNDARY
CONCENTRATIONS

difference between the August contours. Virtually the only discernible differences between the base calibration chlorophyll-a and the 25% reduction in boundary nitrogen can be seen in the east-central portion of Massachusetts Bay. The reduction in chlorophyll-a concentrations in this region is on the order of 0.5 to 1 μg/L.

Figure 6-8 presents a comparison between the various sensitivity runs for surface August chlorophyll-a. As has been noted above the differences in chlorophyll-a between the calibration (no action) and the 25% reduction in boundary nitrogen are small. This is also true for the no atmospheric deposition sensitivity run. In contrast there is a marked difference between the base case calibration and the no internal load sensitivity run. As can be seen concentrations of chlorophyll-a have been significantly reduced in Boston Harbor, generally to less than 5 μg/L. The plume of chlorophyll-a that is associated with Boston Harbor nutrients is also largely eliminated. Figure 6-9, presents the same results as Figure 6-8, but instead subtracts the sensitivity run from the base case run to accentuate the differences between model runs. As can be seen elimination of all internal loads would reduce chlorophyll-a concentrations between 0.5 to greater than 2.5 μg/L in northwestern Massachusetts Bay.

6.3 DISSOLVED OXYGEN RESPONSE

A critical variable to the health of the Bays' ecosystem is dissolved oxygen (DO). Therefore, as part of the sensitivity analysis plots of model computed minimum DO response to changes in loadings to the system were generated. Figure 6-10 presents contour plots of the bottom water minimum DO concentrations for a five-day in mid-March and for a five-day period at the end of October for the calibration and for the 25% reduction in boundary nitrogen concentrations. As can be seen for March there is virtually no difference between the baywide concentrations of DO as computed by the base calibration and the reduced boundary nitrogen runs. Although minimum DO concentrations are usually observed in Boston Harbor during the summer months, October was chosen for plotting purposes because this is usually the month wherein lowest levels of bottom water DO are observed in Massachusetts and Cape Cod Bays. As was observed for the

25% Nitrogen Reduction of BC

No Loads Only BC

No Action

No Atmospheric Deposition

Effect of Sensitivity Analyses on Surface Chlorophyll–a (August)
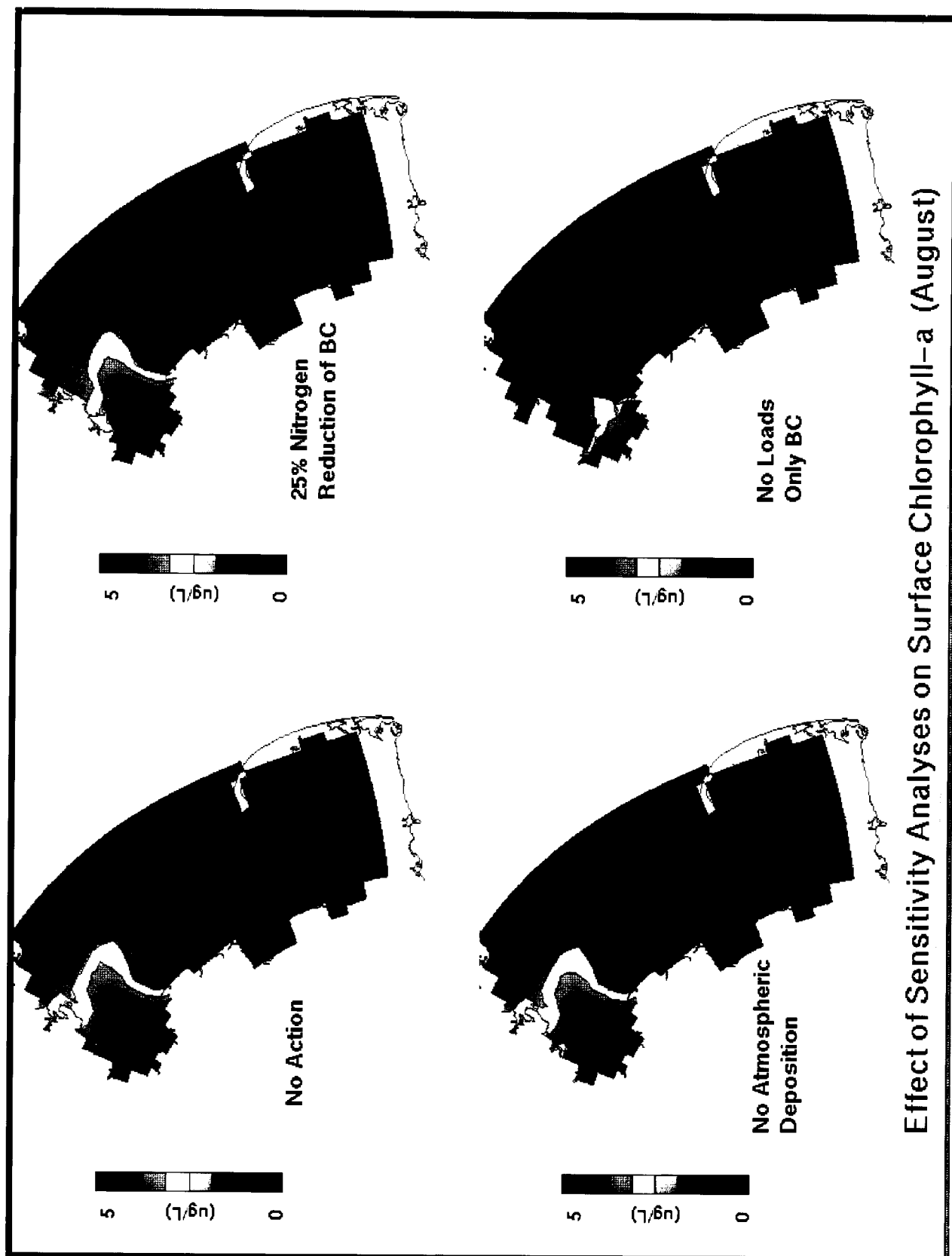
FIGURE 6-8. COMPARISON OF AUGUST SURFACE CHLOROPHYLL-A BETWEEN MODEL CALIBRATION RESULTS AND MODEL SENSITIVITY RESULTS FOR A 25 PERCENT REDUCTION OF BOUNDARY NITROGEN, NO ATMOSPHERIC DEPOSITION AND NO INTERNAL LOADINGS
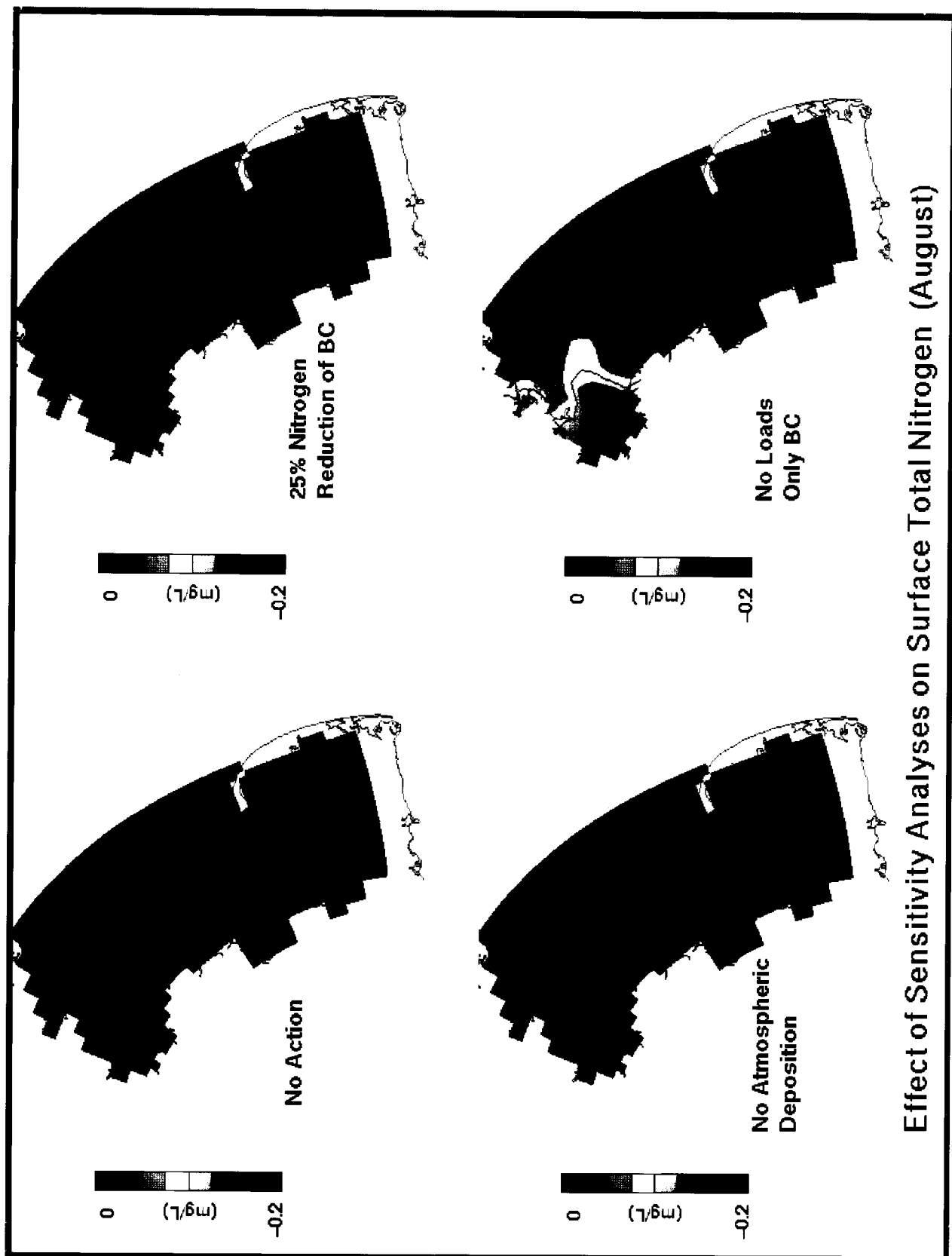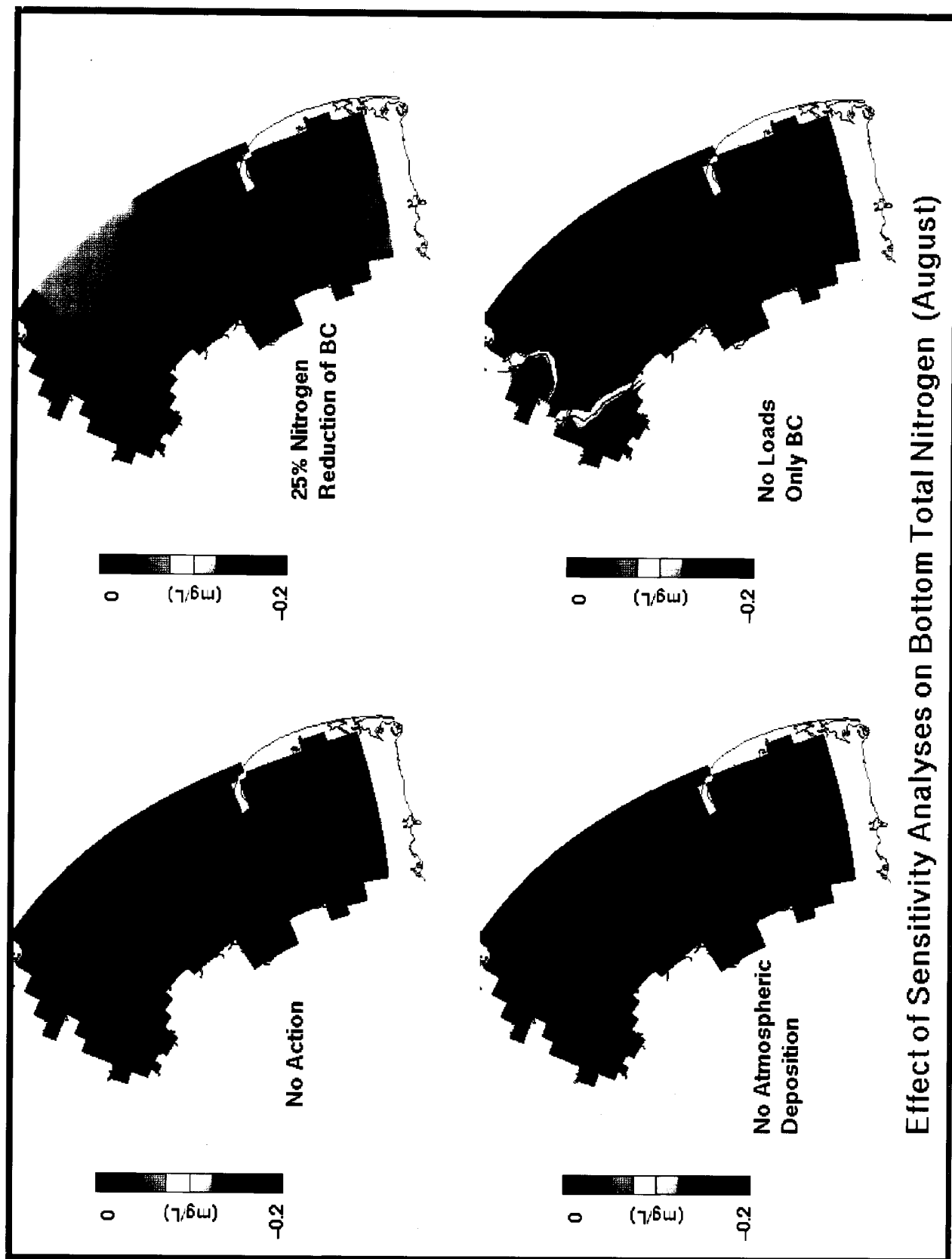
25% Nitrogen Reduction of BC

0 — (ug/L) — -2.5

No Loads Only BC

0 — (ug/L) — -2.5

No Action

0 — (ug/L) — -2.5

No Atmospheric Deposition

0 — (ug/L) — -2.5

Effect of Sensitivity Analyses on Surface Chlorophyll–a (August)

FIGURE 6-9. COMPUTED CHANGES IN AUGUST SURFACE CHLOROPHYLL-A BETWEEN MODEL CALIBRATION RESULTS AND MODEL SENSITIVITY RESULTS FOR AT 25 PERCENT REDUCTION OF BOUNDARY NITROGEN, NO ATMOSPHERIC DEPOSITION AND NO INTERNAL LOADINGS
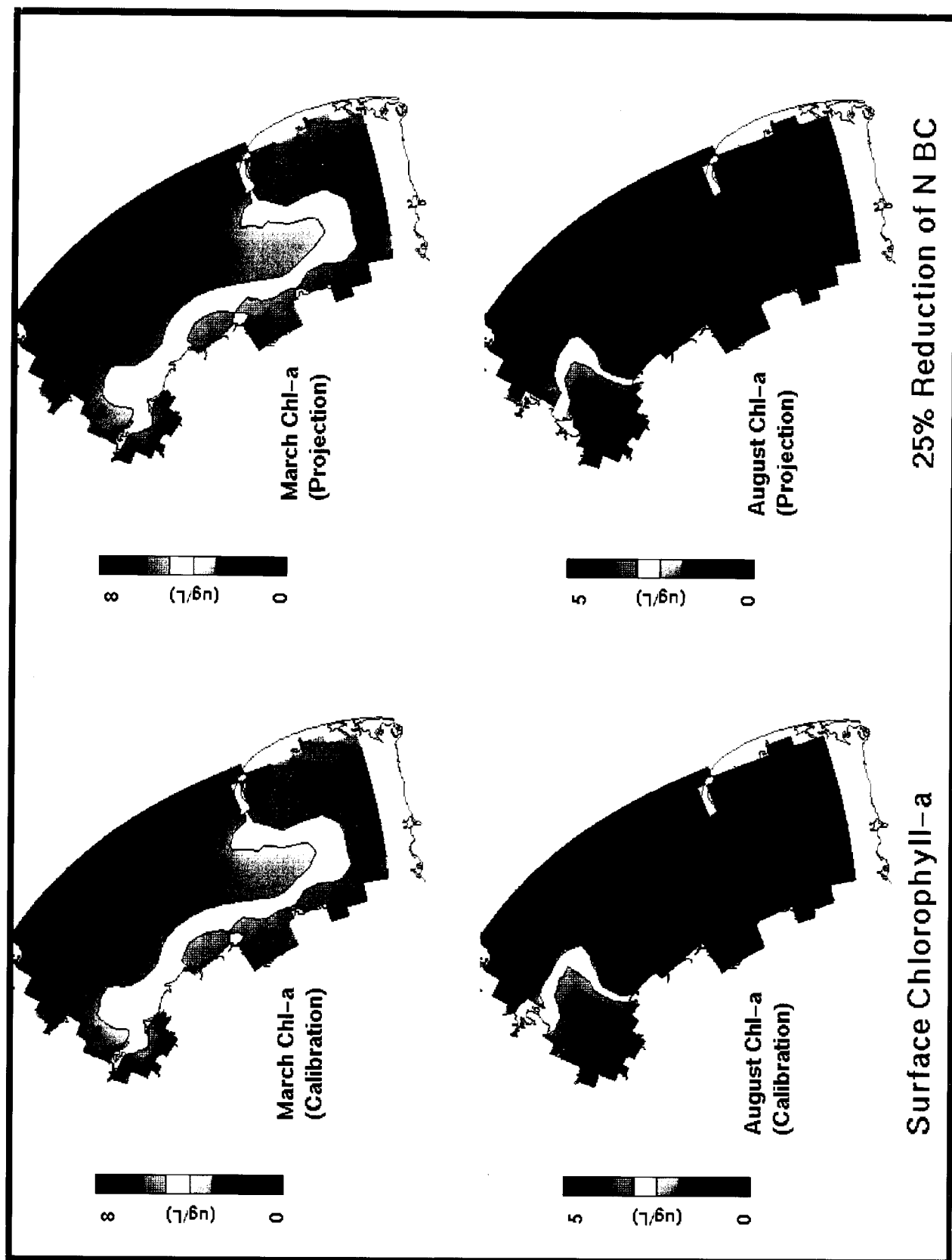
Bottom Dissolved Oxygen
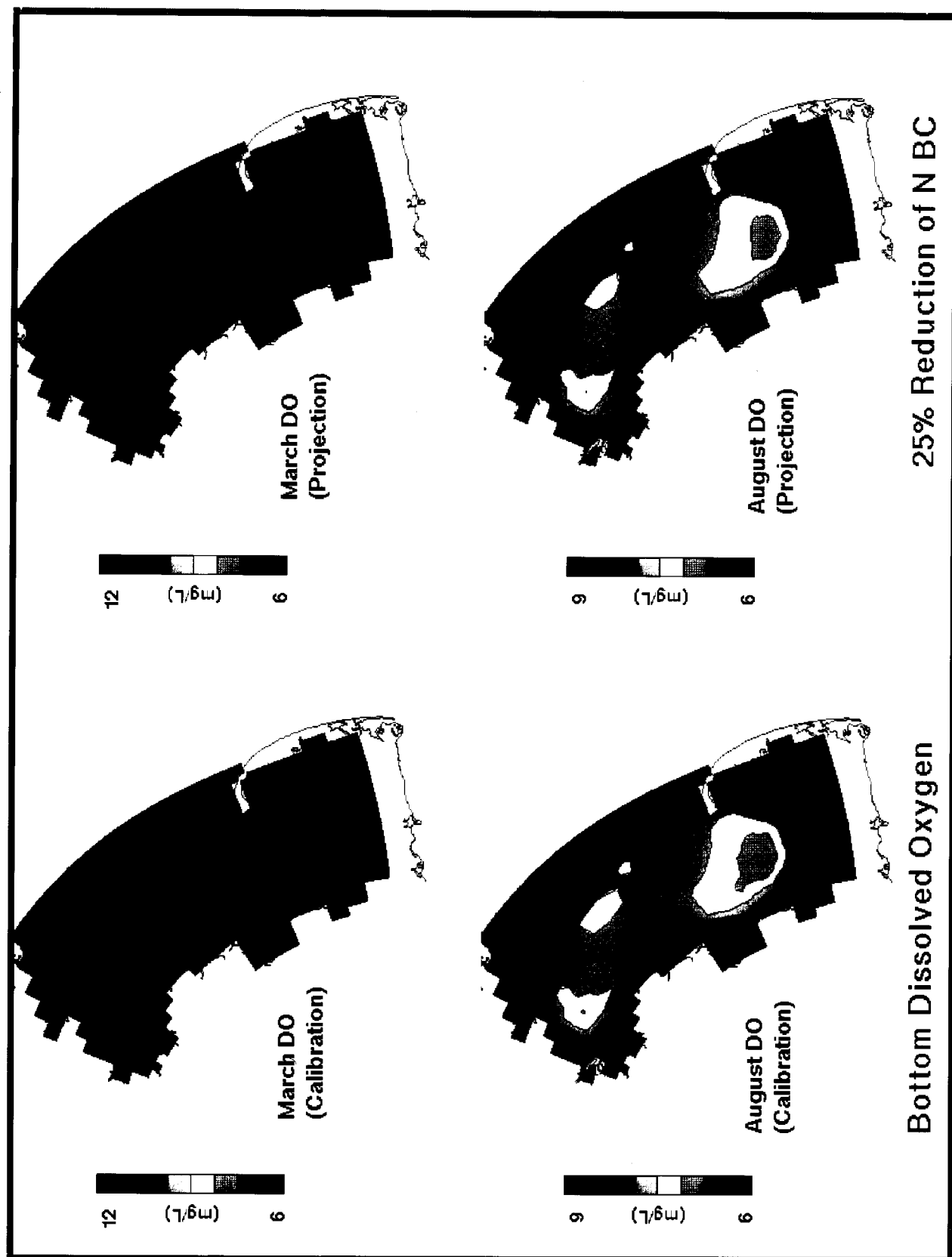
25% Reduction of N BC

FIGURE 6-10. COMPARISON OF MINIMUM BOTTOM DO FOR MARCH AND OCTOBER BETWEEN MODEL CALIBRATION RESULTS AND MODEL SENSITIVITY RESULTS FOR A 25 PERCENT REDUCTION OF NITROGEN BOUNDARY CONCENTRATIONS

March comparisons, there is virtually no difference between the October minimum DO concentrations computed by the model for the calibration (no action) and the reduced boundary nitrogen runs. The only discernible change occurs in the north central portion of Cape Cod Bay, where the 25% reduction in boundary nitrogen concentrations results in an increase of bottom layer DO concentrations of a few tenths of a mg/L.

Figure 6-11 presents contour plots of model computed minimum DO for October for the base calibration (no action) and the three sensitivity runs. As has been noted above there is virtually no difference between the calibration or no action run and the 25% reduction in boundary nitrogen run, except in Cape Cod Bay. A similar result can be observed for the no atmospheric deposition run. The no internal load run, however, shows an increase in DO concentrations in Boston Harbor and northwest Massachusetts Bay. This result can be better shown using a difference contour plot (Figure 6-12) of the change in DO deficit. This plot is made by subtracting the results of the sensitivity run from the results of the calibration run. As can be seen for the no internal load run, the DO deficit has decreased (i.e., an increase in DO) in Boston Harbor and northwest Massachusetts Bay between 0.25 and 0.5 mg/L. It can also be noted for the no internal load sensitivity run, that there is a small decrease in DO levels (shown as a small increase in the "DO deficit") in southeast Cape Cod Bay. This is the result of a reduction in algal biomass for the no internal load run, which results in a decrease in super-saturated DO concentrations in this region of the model domain. In this figure one can also discern a small increase in DO levels (a decrease in DO deficit) in a large portion of Massachusetts and Cape Cod Bays. This may occur as a consequence of a decrease in oxygen consumption associated with reduced bottom water nitrification and reduced oxidation of detrital algal carbon.

6.4 PARTICULATE ORGANIC CARBON DEPOSITION RESPONSE

The final variable for which sensitivity results will be presented is the flux of particulate organic carbon (POC). The flux of POC is an important variable because the deposition of POC to the sediment is an important food source for the benthic community and because it is key to determining the sediment oxygen demand (SOD). An

25% Nitrogen Reduction of BC

No Loads Only BC

No Action

No Atmospheric Deposition

Effect of Sensitivity Analyses on Minimum Bottom DO (October)

FIGURE 6-11. COMPARISON OF MINIMUM OCTOBER BOTTOM DO BETWEEN MODEL CALIBRATION RESULTS AND MODEL SENSITIVITY RESULTS FOR A 25 PERCENT REDUCTION OF BOUNDARY NITROGEN, NO ATMOSPHERIC DEPOSITION AND NO INTERNAL LOADINGS

No Action

25% Nitrogen Reduction of BC

No Atmospheric Deposition

No Loads Only BC

0.5
(mg/L)
-0.5

Effect of Sensitivity Analyses on Minimum Bottom DO (October)

FIGURE 6-12. COMPUTED CHANGES IN MINIMUM OCTOBER BOTTOM DO BETWEEN MODEL CALIBRATION RESULTS AND MODEL SENSITIVITY RESULTS FOR A 25 PERCENT REDUCTION OF BOUNDARY NITROGEN, NO ATMOSPHERIC DEPOSITION, AND NO INTERNAL LOADINGS
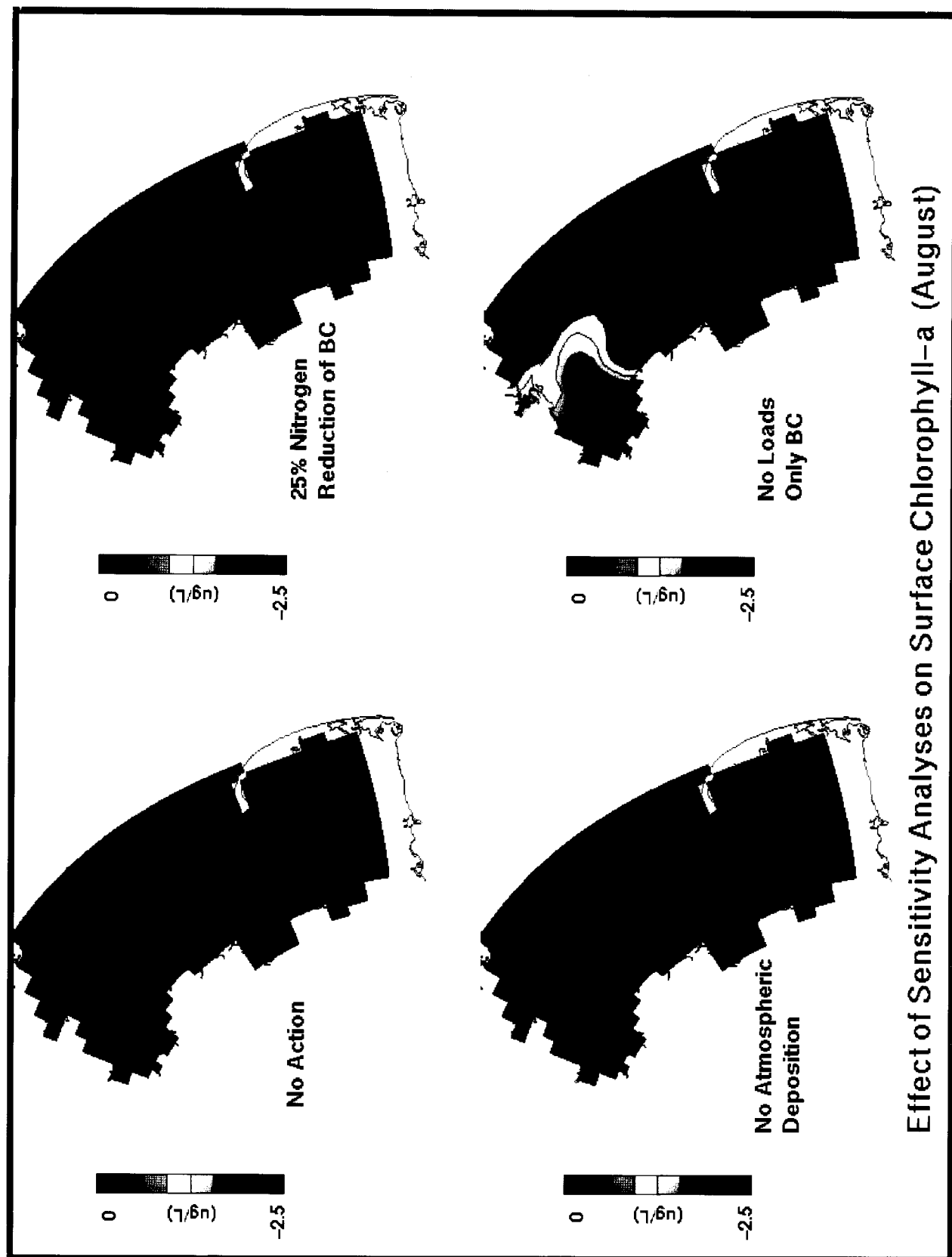
over-enrichment of POC deposition can adversely impact a benthic community and, when accompanied by high SOD rates, can result in waters low in dissolved oxygen. With the exception of Boston Harbor and other regions of the bay which receive POC from sewage treatment plant effluents, most POC deposition flux is associated with detrital algal biomass. As can be seen in Figure 6-13, the calibration results indicate that the flux of POC to the sediments is highest in Boston Harbor and the nearshore shallow regions of Massachusetts and Cape Cod Bays. It can also be seen that by far the highest POC flux rates are in Boston Harbor, with rates of 800 to 1,000 mg C/m^2-day or greater. As can also be seen on this figure, there is virtually no difference between the calibration (no action) and the 25% reduction in boundary nitrogen run.

Figure 6-14 presents contour plots of POC sediment flux for the calibration and the three sensitivity runs. As can be seen, only the no internal load run shows any significant change in depositional flux. Figure 6-15 presents the difference contour plots, which better illustrate the relative change in flux rates. Boston Harbor and Salem Sound show significant reductions (>250 mg C/m^2-day) in POC flux rates for the no internal load run. This run also indicates reductions in POC flux in Plymouth Bay and the southeast corner of Cape Cod Bay, but these reductions are generally less than 75 mg C/m^2-day. One can also detect small reductions (< 40 mg C/m^2-day) in POC flux in the southern portion of Cape Cod Bay for the 25 percent reduction in boundary nitrogen run and in southeastern Cape Cod Bay for the 25 percent reduction in boundary nitrogen and no atmospheric deposition runs.

March Flux POC
(Projection)

1000 (mg/m2-d) 0

August Flux POC
(Projection)

1000 (mg/m2-d) 0

25% Reduction of N BC

March Flux POC
(Calibration)

1000 (mg/m2-d) 0

August Flux POC
(Calibration)

1000 (mg/m2-d) 0

Flux POC
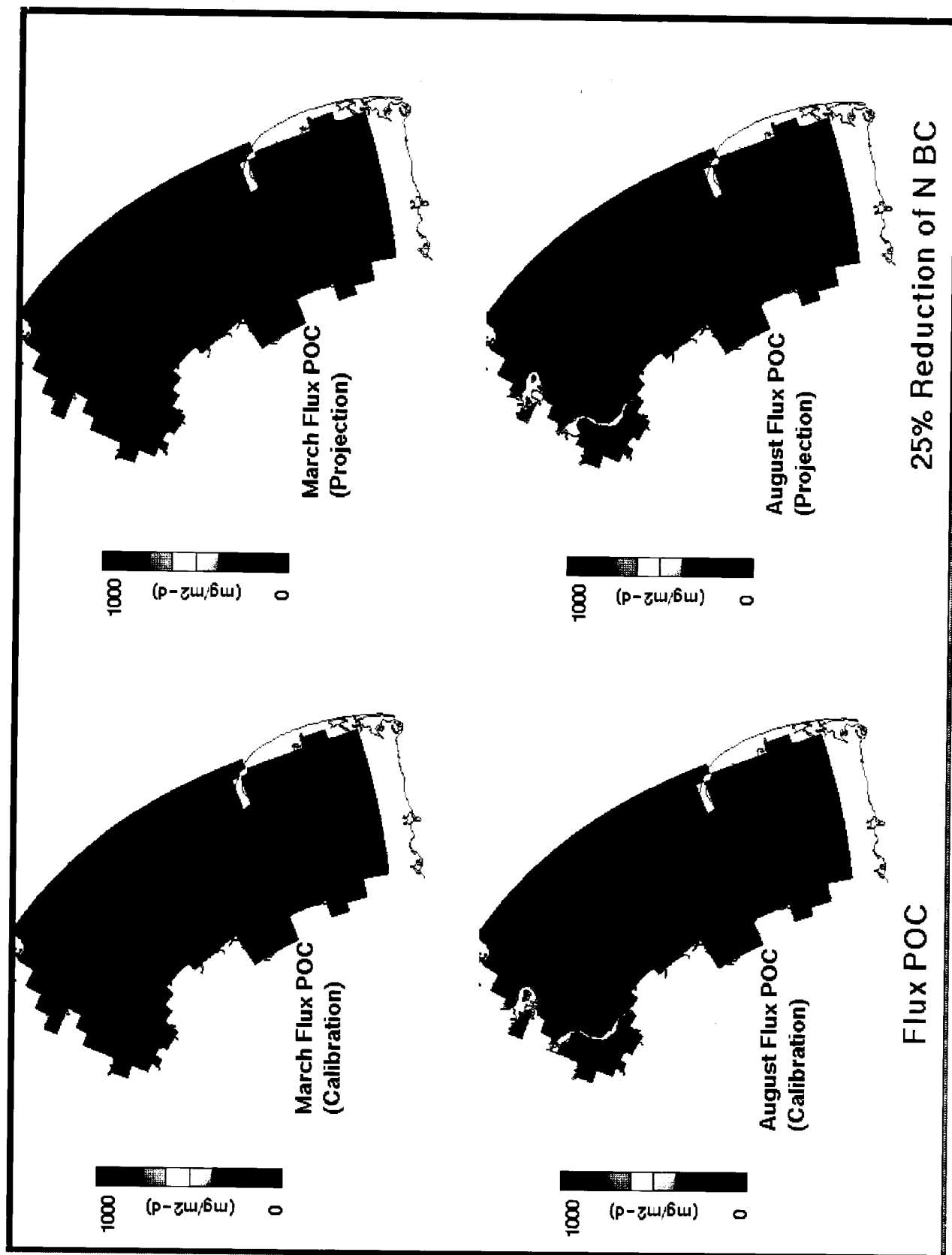
FIGURE 6-13. COMPARISONS OF POC FLUX FOR MARCH AND AUGUST BETWEEN MODEL CALIBRATION RESULTS AND MODEL SENSITIVITY RESULTS FOR A 25 PERCENT REDUCTION OF TN BOUNDARY CONCENTRATIONS
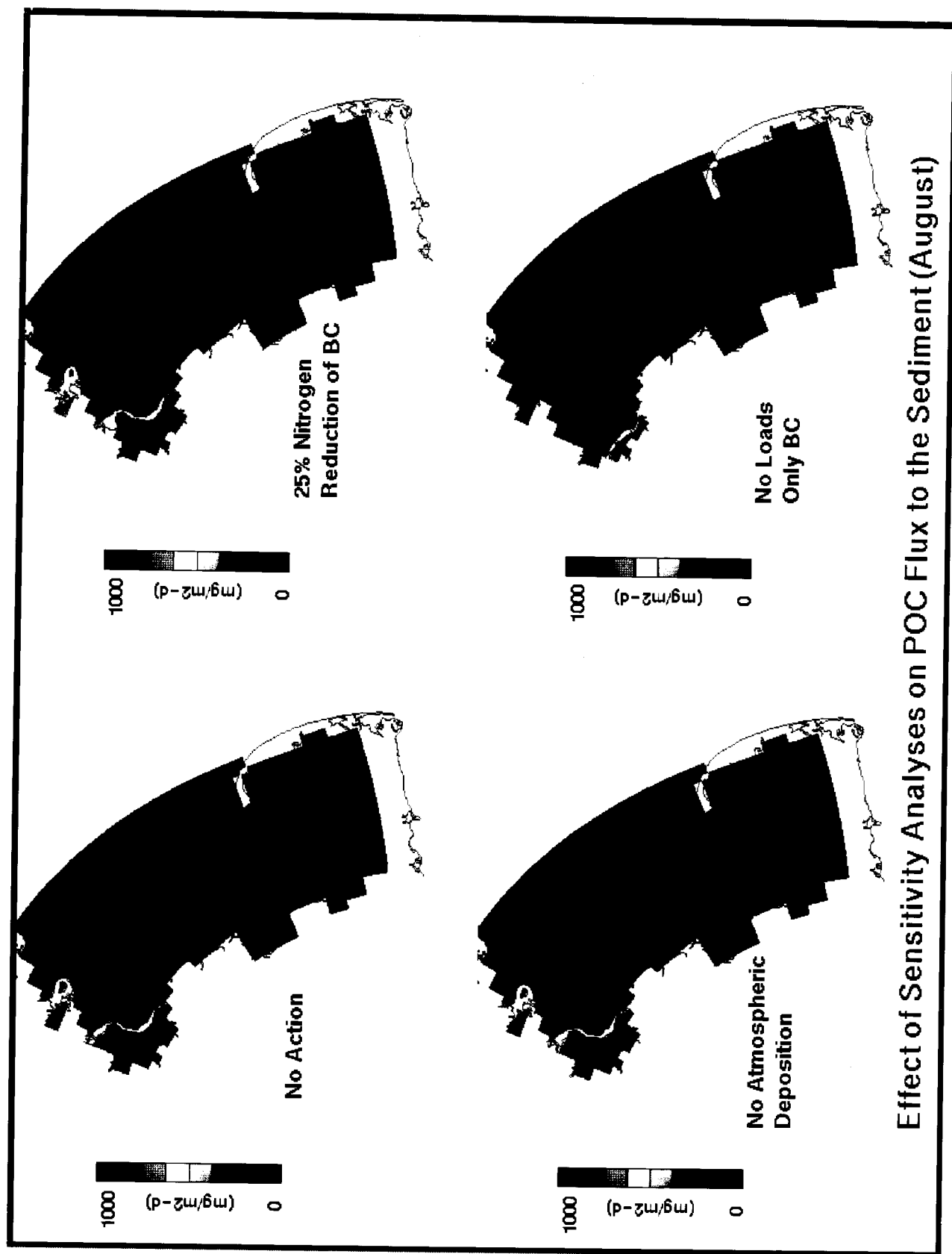
FIGURE 6-14. COMPARISON OF AUGUST POC FLUX BETWEEN MODEL CALIBRATION RESULTS AND MODEL SENSITIVITY RESULTS FOR A 25 PERCENT REDUCTION OF BOUNDARY NITROGEN, NO ATMOSPHERIC DEPOSITION AND NO INTERNAL LOADINGS
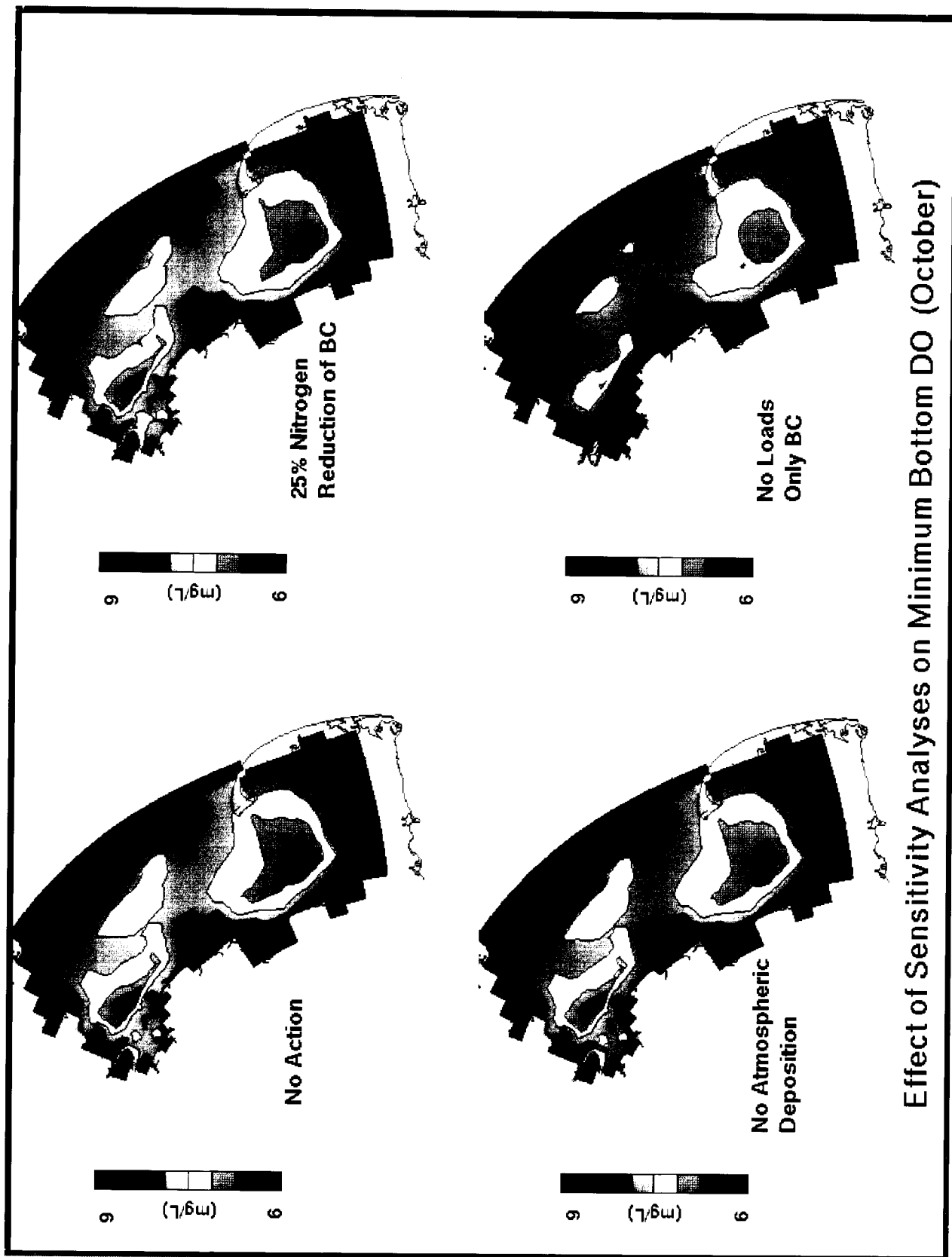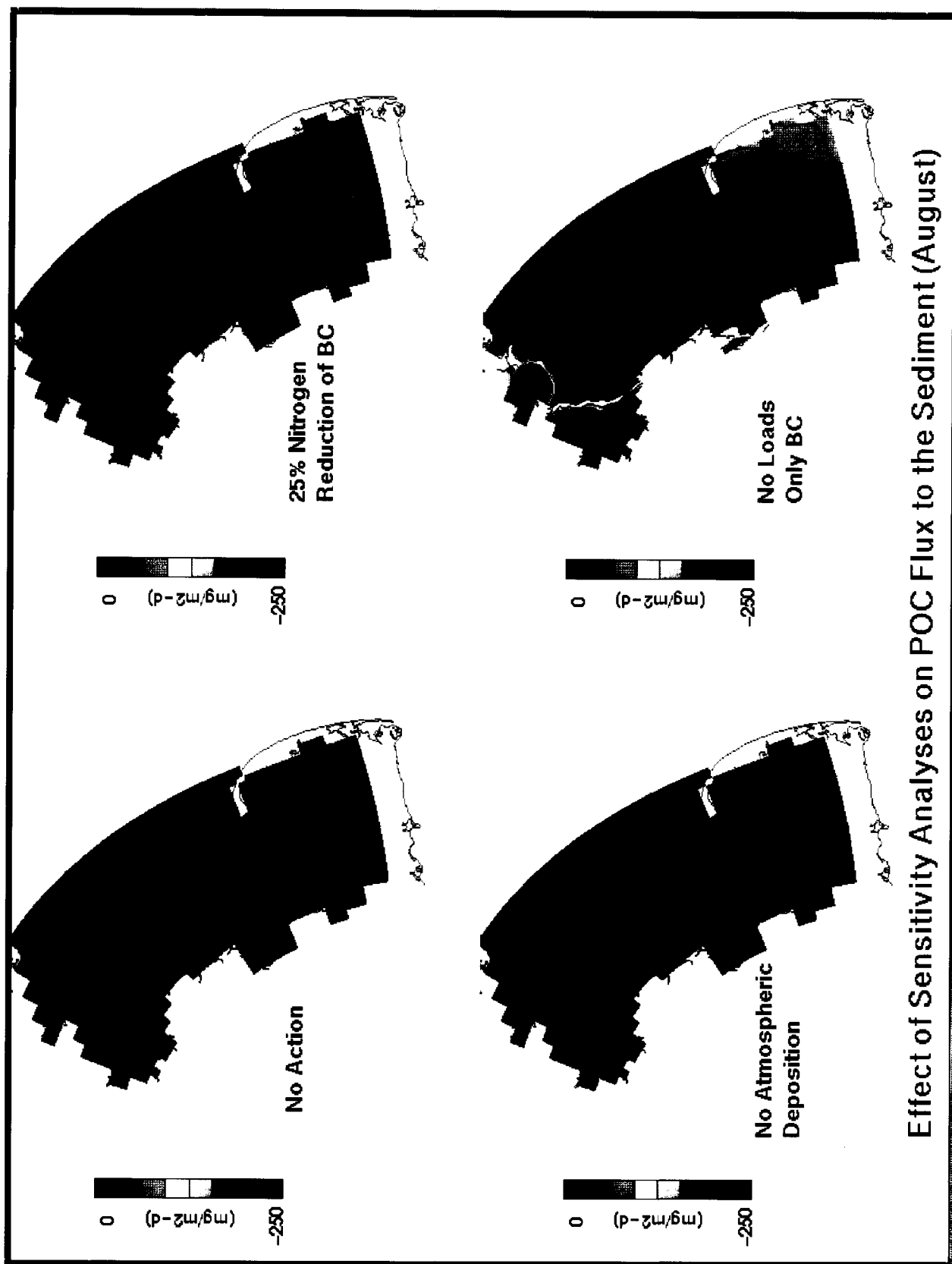
Effect of Sensitivity Analyses on POC Flux to the Sediment (August)

FIGURE 6-15. COMPUTED CHANGES IN POC FLUX BETWEEN MODEL CALIBRATION RESULTS AND MODEL SENSITIVITY RESULTS FOR A 25 PERCENT REDUCTION OF BOUNDARY NITROGEN, NO ATMOSPHERIC DEPOSITION, AND NO INTERNAL LOADINGS
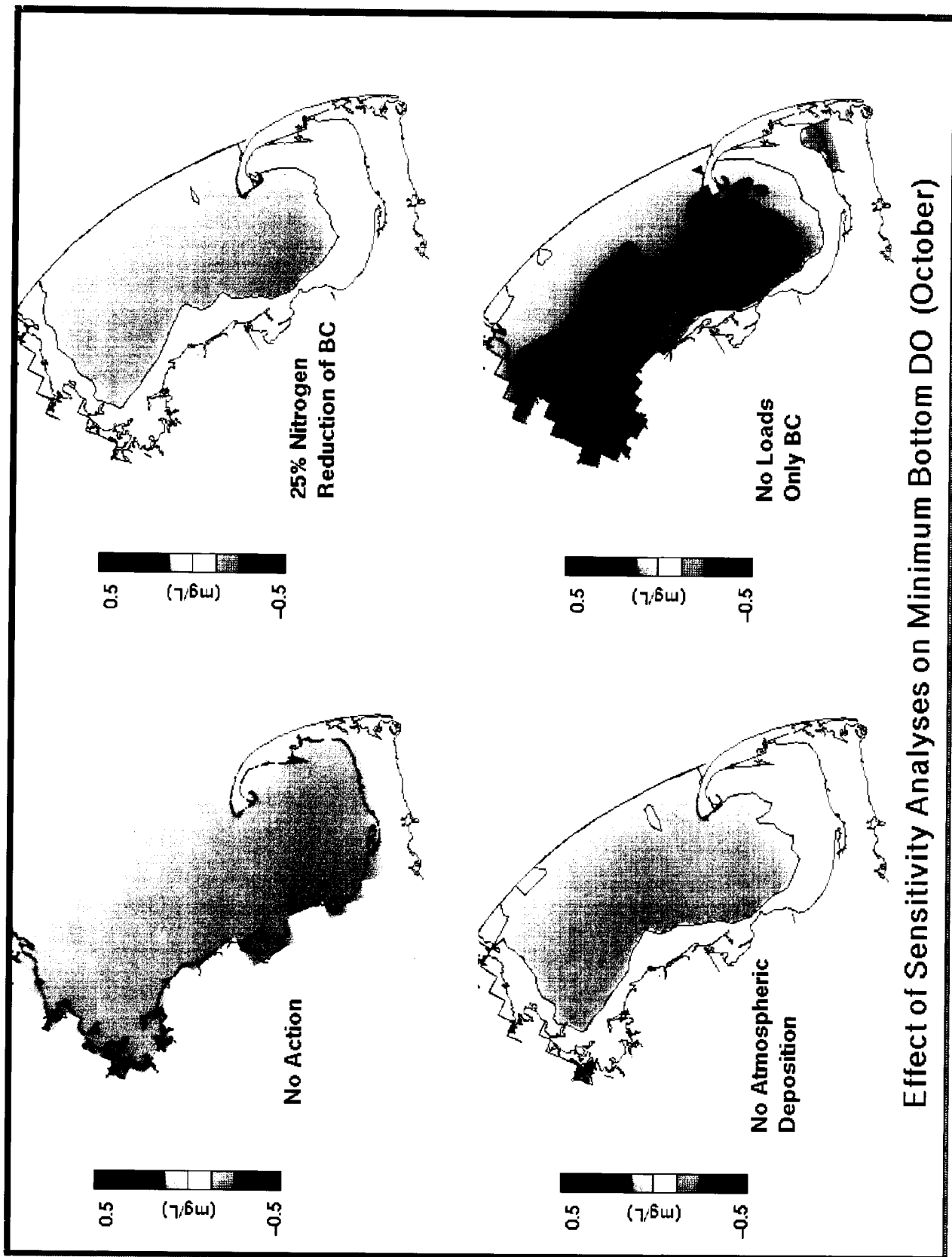
SECTION 7

PROJECTIONS

7.1   INTRODUCTION

The Bays Eutrophication Model (BEM) has been calibrated and appears to adequately reproduce the major processes that affect water quality and eutrophication, in particular, in the Massachusetts Bay/Cape Cod Bay system. With the calibration completed, the model can now be used as an aid in the decision making for those managers involved with maintaining or improving water quality in the Bays. Therefore, several projections were made to compute the effectiveness of various remediation alternatives on the Bays' water quality. This section details three of these projections: 1) relocation of the Deer Island and Nut Island treatment plant outfalls into Massachusetts Bay, about 15 km from their current locations, 2) outfall relocation and upgrading of the treatment facilities to secondary treatment, and 3) upgrading MWRA facilities to secondary treatment and continued discharge at the current outfall locations.

The projections were run using the 1992 calibration as the base run. For the projection runs all of the boundary conditions, model coefficients and loadings, except for the MWRA treatment plant loads, were the same as those used for the base calibration. Table 7-1 presents a comparison of the base organic carbon and nutrient loadings used for the projections versus those used for the calibration. Secondary treated effluent nutrient loads are based on concentrations measured in trailer secondary treatment pilot plant experiments. Recent results from a one million gallon per day secondary treatment pilot plant (Hunt et al, 1995) show a wide range in nutrient removals. Assumed phosphorus and nutrient removals are consistent with those observed in this larger pilot plant.

Since the MWRA outfall is being relocated from Boston Harbor into Massachusetts Bay, it was necessary to rerun the hydrodynamic model to account for the effects of flow relocation on the circulation in Boston Harbor and the Bays. As part of the projection analysis an evaluation of the ability of the fine-grid hydrodynamic model to reproduce the

proper plume dynamics in the vicinity of the future outfall was performed (HydroQual, 1995). The results and conclusions of this analysis are presented in Appendix F.

Running the projections for a period of five years was also necessary, cycling the hydrodynamic and water quality forcings (i.e., water temperatures, winds, solar radiation, boundary conditions, and nutrient loadings) to assure that the model computations achieved a new equilibrium response. This was necessary due to the relatively long time constants for the decay of particulate organic matter delivered to the sediments in previous years. Therefore, these projections are meant to reflect long term conditions (assuming loadings do not vary significantly) rather than conditions that might be observed immediately after a change has been made.

TABLE 7-1. DAILY AVERAGE MWRA ORGANIC CARBON AND NUTRIENT LOADINGS (KG/DAY) FOR THE 1992 BASE CALIBRATION AND THE PROJECTION RUNS		
	Calibration (Primary Treatment)	Projection (Secondary Treatment)
Total organic phosphorus (TOP)	2,073	533
PO_4	2,930	1,993
Total organic nitrogen (TON)	13,042	4,212
NH_4	16,514	16,848
$NO_2 + NO_3$	911	1,264
Dissolved Silica (DSi)	5,614	5,614
Total Organic Carbon (TOC)	150,225	51,950
Dissolved Oxygen (DO)	2,805	2,805

7.2 REVISED WATER QUALITY GRID

During the projection analysis, it was determined that the grid aggregation used in the water quality model resulted in an inability of the water quality model to reproduce the

effluent plume dynamics of the future outfall properly. In particular, it was found that grid aggregation caused the plume to be trapped at depth throughout the year, even during the winter time when the water column is well-mixed. This was due to the fact that grid aggregation averaged the vertical velocities in the immediate vicinity of the outfall, where the horizontal variation in vertical velocity is very large due to the buoyant plume. As a result the vertical rise velocity of the effluent was understated. To correct this problem the grid was modified to include finer segmentation around the location of the future outfall. This was accomplished by not aggregating the hydrodynamic grid in the area of the future outfall. The new grid aggregation resulted in a 23x28 segment grid as compared to the original 20x25 segment grid. Figure 7-1 presents a comparison of the two grids.

To be assured that the new grid reproduced the effluent plume dynamics properly, the following computer simulations were performed. First, a two-system model, containing conservative particulate and dissolved tracers, was run using the unaggregated or uncollapsed hydrodynamic grid. Then, parallel runs were performed using the original water quality model grid and the new aggregated water quality grid. These runs were performed for the months of March, an unstratified period, and August, a stratified period. The tracers were discharged into the bottom two segments of the future outfall location. Figure 7-2 presents the results of the model runs. The solid line represents the results from the uncollapsed hydrodynamic grid; a dashed-dotted-dashed line is used to represent the original aggregated water quality grid; and a dashed line is used to represent the results from the new water quality grid used for projections.

The water quality model, run when using the unaggregated or uncollapsed hydrodynamic model, shows that during March the effluent plume reaches the surface layer of the model for both the dissolved and particulate tracers. The water quality model, run when using the original grid aggregation scheme (shown on the left panel of Figure 7-1), fails to reproduce the plume hydrodynamics properly. The model computations show that the tracers are effectively trapped below the model surface at approximately mid-depth, between layers six and seven of the model. Concentrations of the tracers
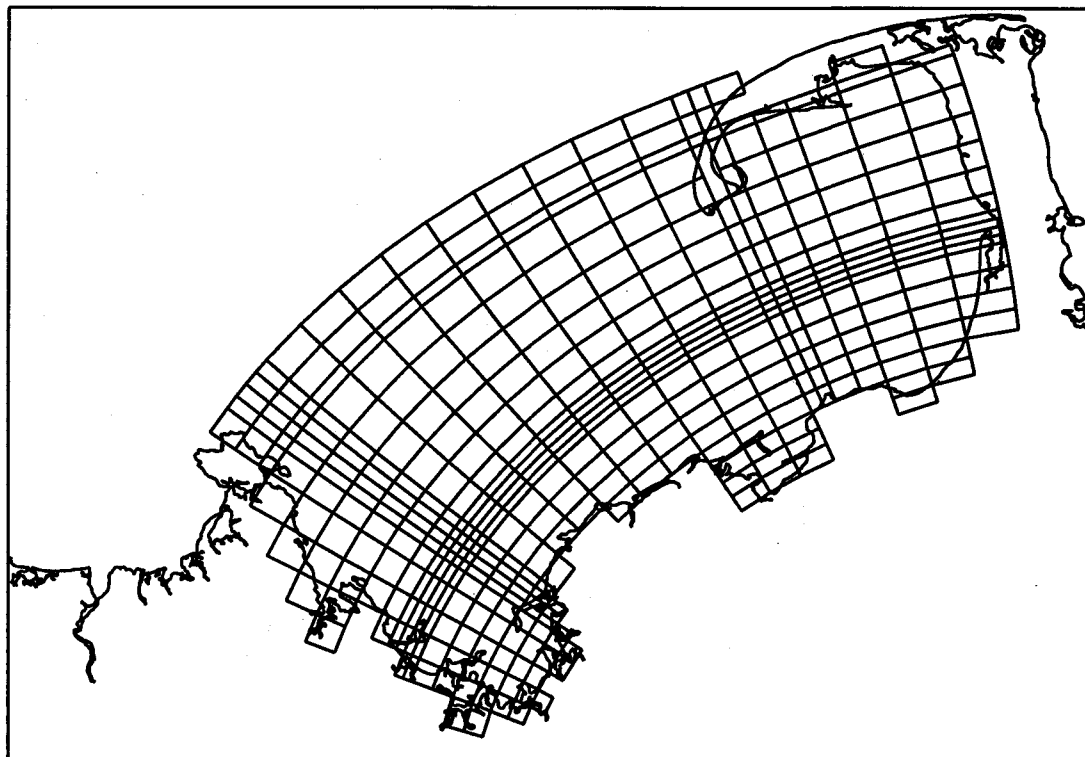
Modified Water Quality Model Grid
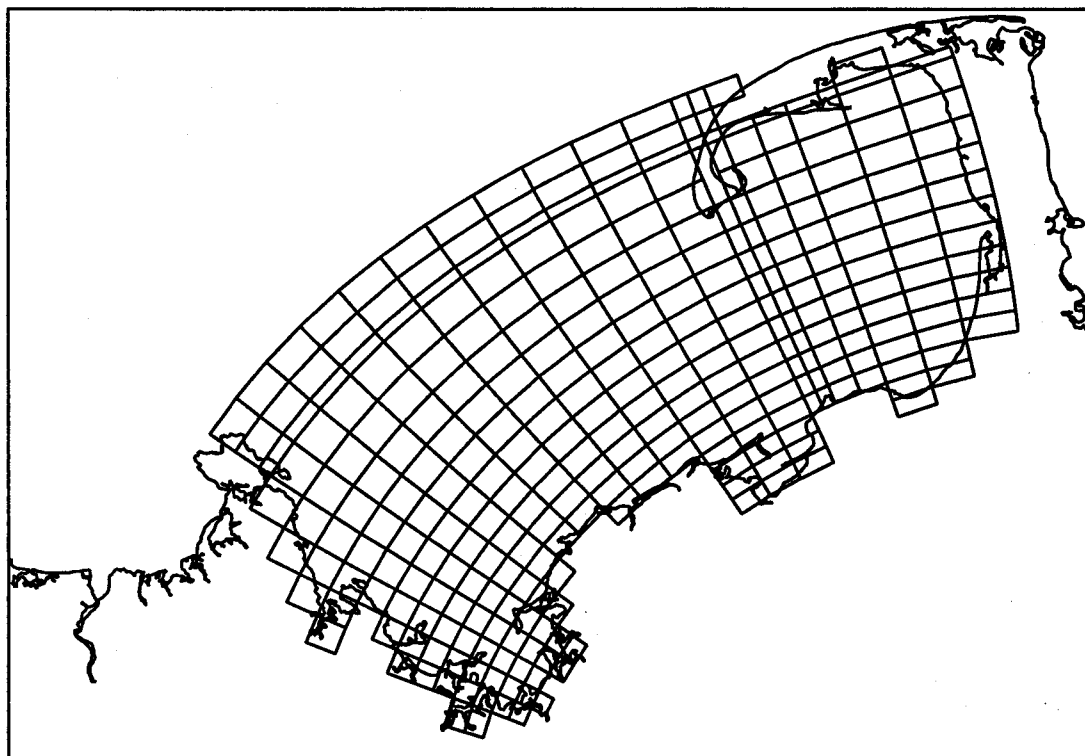
Original Water Quality Model Grid

FIGURE 7-1. ORIGINAL AND MODIFIED WATER QUALITY MODEL GRIDS
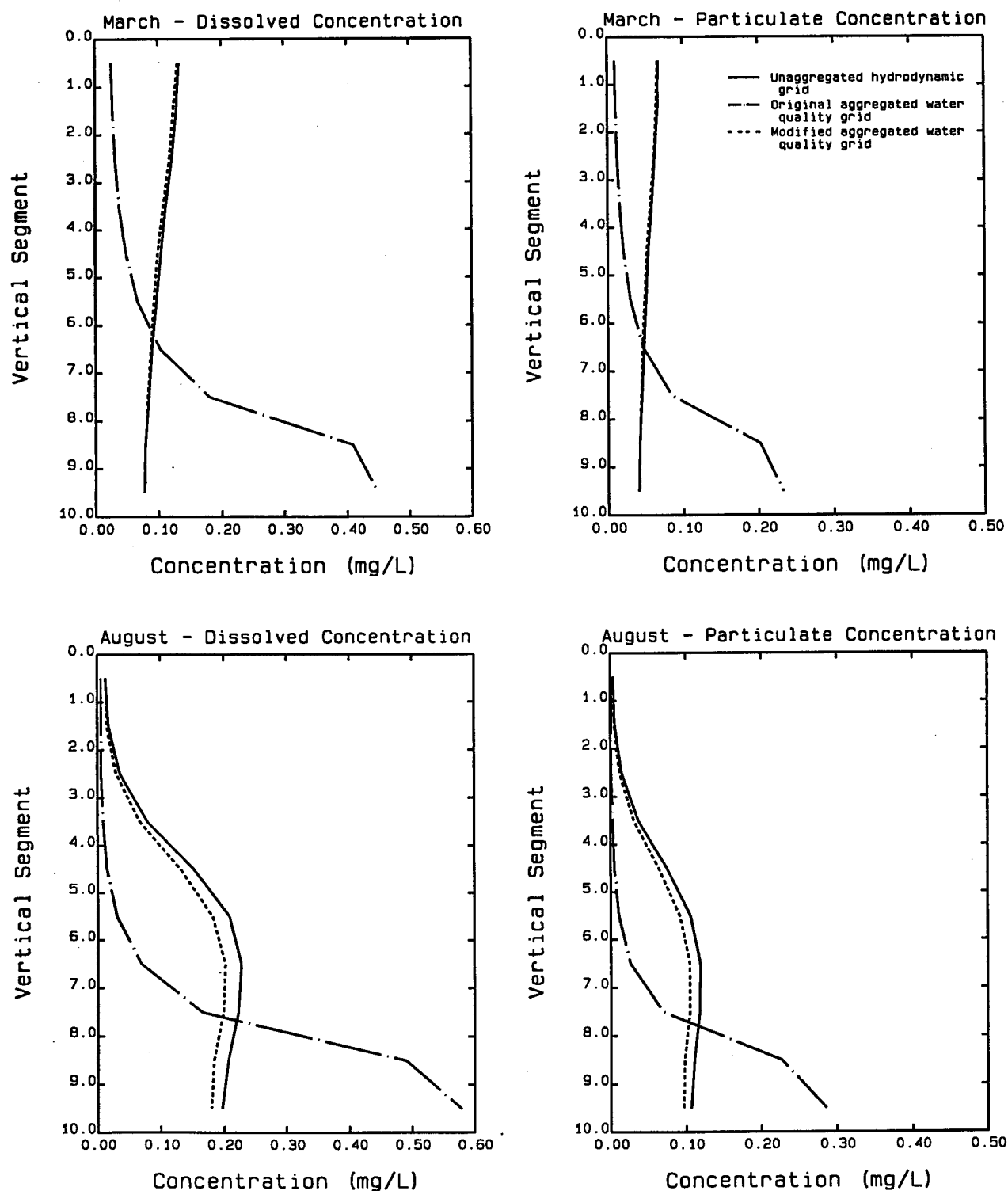
FIGURE 7-2. COMPARISON OF CONSERVATIVE TRACER CONCENTRATION OUTPUT FOR THE UNAGGREGATED HYDRODYNAMIC GRID, ORIGINAL AGGREGATED AND MODIFIED AGGREGATED WATER QUALITY MODEL GRIDS

computed using the modified water quality grid (the right panel of Figure 7-1) agree almost exactly with the unaggregated model concentrations for both the dissolved and the particulate tracers. During August the unaggregated model computations show that the tracers are for the most part trapped below the model surface. The effluent plume appears to be trapped between layers four and five of the model. Tracer concentrations, as computed using the original water quality grid, are in sharp disagreement with the results of the unaggregated grid. Tracer concentrations computed using the revised grid show significant improvement over those obtained from the original water quality grid. Although the model computations obtained using the revised grid are not in exact agreement with the unaggregated grid, the differences between the two model computations are generally less than 10 to 12 percent.

The revised grid aggregation was used for projection runs. It was not necessary to re-run the calibration because during the calibration period, there was no discharge through the new MWRA Massachusetts Bay outfall and hence no buoyant plume to cause sharp horizontal gradients in vertical velocity. The existing discharges near the mouth of Boston Harbor are rapidly mixed vertically and horizontally by tidal currents.

7.3   PROJECTION RESULTS

7.3.1 Dissolved Inorganic Nitrogen

Figure 7-3 shows a comparison of surface DIN concentrations, for a five-day period in early March, between the 1992 calibration and the three projections. It is important to note that for the calibration and future outfall location runs, the actual measured concentrations and flows were used to compute the loadings; loadings for runs with secondary treatment were computed using constant effluent concentrations and measured flows from 1992. It was found that on occasion the measured 1992 nutrient (N and P) concentrations were lower than those estimated to be achieved under secondary treatment. Consequently, there are some months when the N and P loadings, and in particular NH_4, and $NO_2 + NO_3$ (cf. Table 7-1), for the secondary treatment runs are higher

Current Outfall Location w/Primary

0.4 (mg/L) 0

Current Outfall Location w/Secondary

0.4 (mg/L) 0

Future Outfall Location w/Primary

0.4 (mg/L) 0

Future Outfall Location w/Secondary

0.4 (mg/L) 0
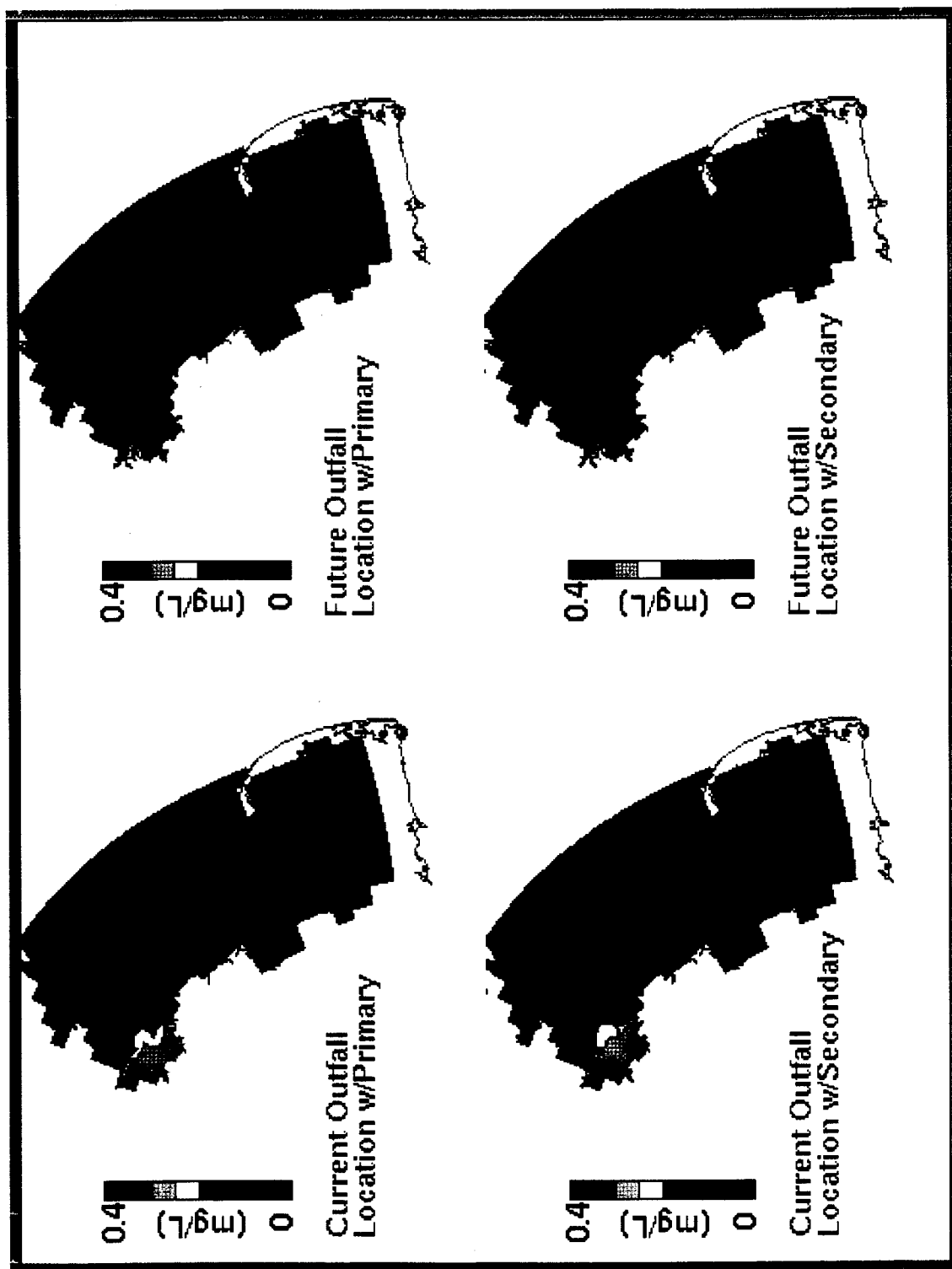
FIGURE 7-3. CALIBRATION AND PROJECTION RESULTS FOR MARCH SURFACE DIN

than the base case calibration loads. The latter is to be expected, since secondary treatment usually results in some conversion of DON to NH_4 and $NO_2 + NO_3$. For the base case calibration run, model computations show (upper left panel of Figure 7-3) the highest concentrations of DIN in Boston Harbor, with concentrations of approximately 0.25 mg N/L. DIN concentrations decrease with distance from Boston Harbor. Another area containing higher DIN concentrations is located in the northern part of Massachusetts Bay near the South Essex and Lynn Water and Sewer treatment plants. The projection run for secondary treatment at the current outfall location (lower left panel of Figure 7-3) shows similar concentration isopleths to the base calibration run. Concentrations in the immediate vicinity of the current outfalls, however, are slightly higher, due to higher effluent DIN loads.

When the outfall is relocated (upper right panel of Figure 7-3), the model computes greatly reduced concentrations of DIN in Boston Harbor. However, nitrogen loadings from CSOs and tributaries discharging to Boston Harbor still result in DIN concentrations reaching approximately 0.1 mg N/L. At the future outfall site the effluent plume reaches the surface, during this unstratified period, and affects a small area around the outfall site. Concentrations in this area reach approximately 0.2 mg N/L. Areas far removed from the future outfall do not appear to be affected by the outfall relocation. In fact, there appears to be a slight reduction in surface DIN at some locations, most notably around Plymouth Harbor. The secondary treatment projection for the future outfall case (lower right panel of Figure 7-3) shows similar results.

The calibration and projection results for March bottom DIN are presented on Figure 7-4. The results are similar to those observed for surface DIN except that bottom concentrations are higher due to reduced algal uptake in light limited conditions. Under the calibration conditions the highest concentrations are observed in Boston Harbor, with levels near 0.25 mg N/L, and near the South Essex and Lynn Water and Sewer treatment plants, with concentrations approaching 0.2 mg N/L. A broad area of slightly elevated DIN concentrations is observed in the northeastern portion of Massachusetts Bay. This feature is observed in the projection runs as well. With the outfall relocation, the area in the

**Current Outfall
Location w/Primary**

**Current Outfall
Location w/Secondary**

**Future Outfall
Location w/Primary**

**Future Outfall
Location w/Secondary**

0.4

(mg/L)

0
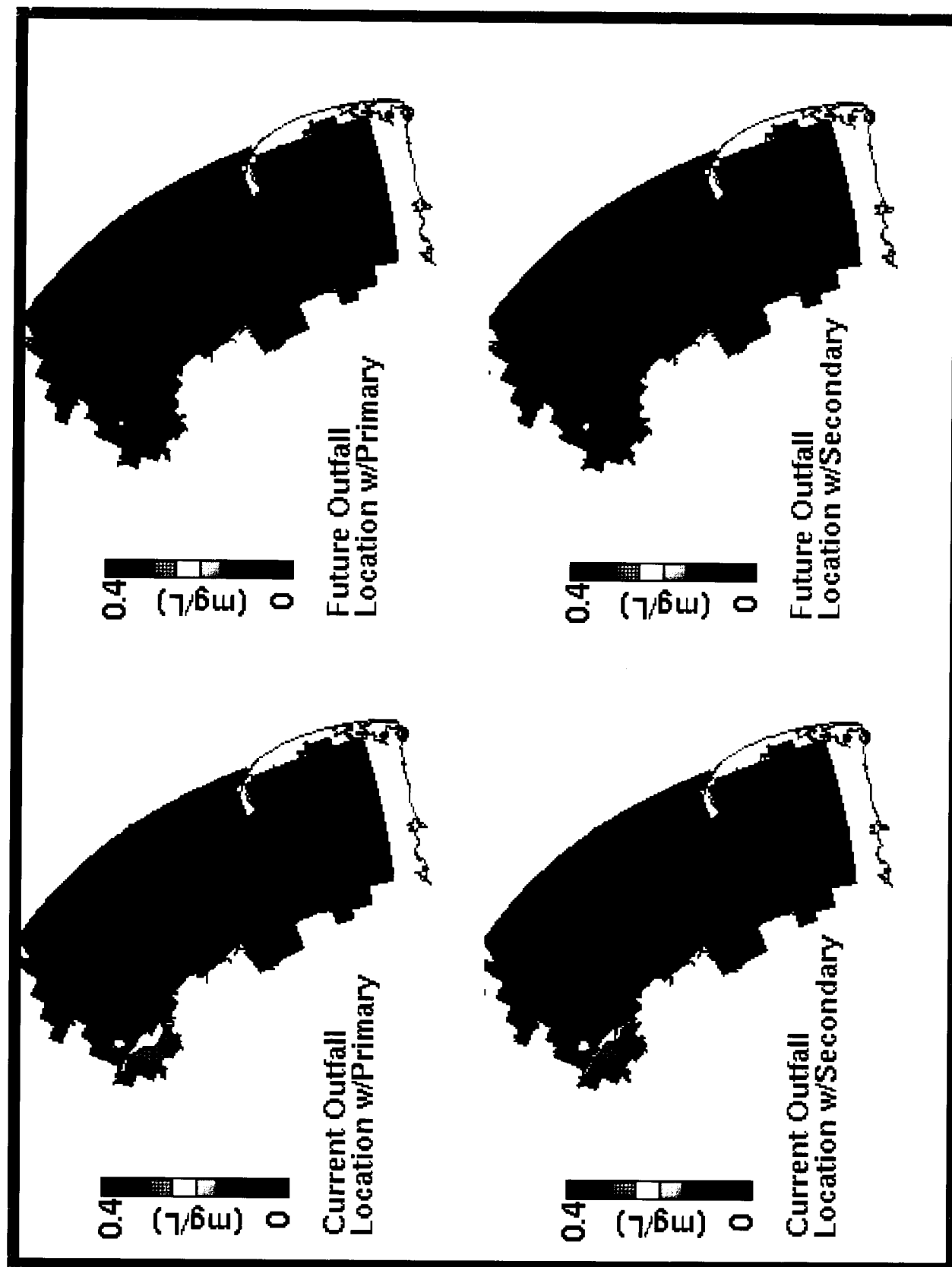
FIGURE 7-4.   CALIBRATION AND PROJECTION RESULTS FOR MARCH BOTTOM DIN

immediate vicinity of the outfall is observed to increase slightly in DIN concentration. Boston Harbor, however, shows significant reductions in the concentrations of DIN.

During August, concentrations of DIN are low in Massachusetts and Cape Cod Bays, due to algal primary productivity. Figure 7-5, which illustrates surface DIN in Boston Harbor and the northwestern portion of Massachusetts Bay, shows that for the base calibration run the concentrations of DIN are low everywhere, except in the immediate vicinity of the current outfall sites in Boston Harbor and in some near shore regions along the North Shore which receive wastewater inputs. The results of the outfall relocation show reduced concentrations of DIN in Boston Harbor. Furthermore, one does not see elevated concentrations of DIN in the surface waters near the future outfall site because water column stratification traps the plume below the pycnocline.

Figure 7-6 displays the results for August bottom DIN. Although DIN concentrations are virtually depleted in the surface layer of the water column during this time, moderate DIN levels can be observed at depth. Results from the calibration run show high levels of DIN in Boston Harbor (in particular in the Inner Harbor Charles River), near the South Essex and Lynn treatment plants and in the deeper waters along the eastern boundary of the model. Under the future outfall scenario the concentrations of DIN decrease in outer Boston Harbor and in the Inner Harbor. In addition, the immediate area around the future outfall shows elevated DIN concentrations. One can also note that the 0.05 to 0.10 mg N/L concentration isopleth extends further southward toward Cape Cod Bay, but does not in fact enter the Bay.

Figure 7-7 presents a plot of Boston Harbor and nearfield DIN concentrations for a depth of 15m. Concerns have been raised that the introduction of the outfall may stimulate phytoplankton productivity at mid-depth because the effluent plume may rise to this depth. As can be seen, DIN concentrations are projected to increase slightly at this depth with the introduction of the plume.

Future Outfall
Location w/Primary

Future Outfall
Location w/Secondary

Current Outfall
Location w/Primary

Current Outfall
Location w/Secondary

0.1 (mg/L) 0
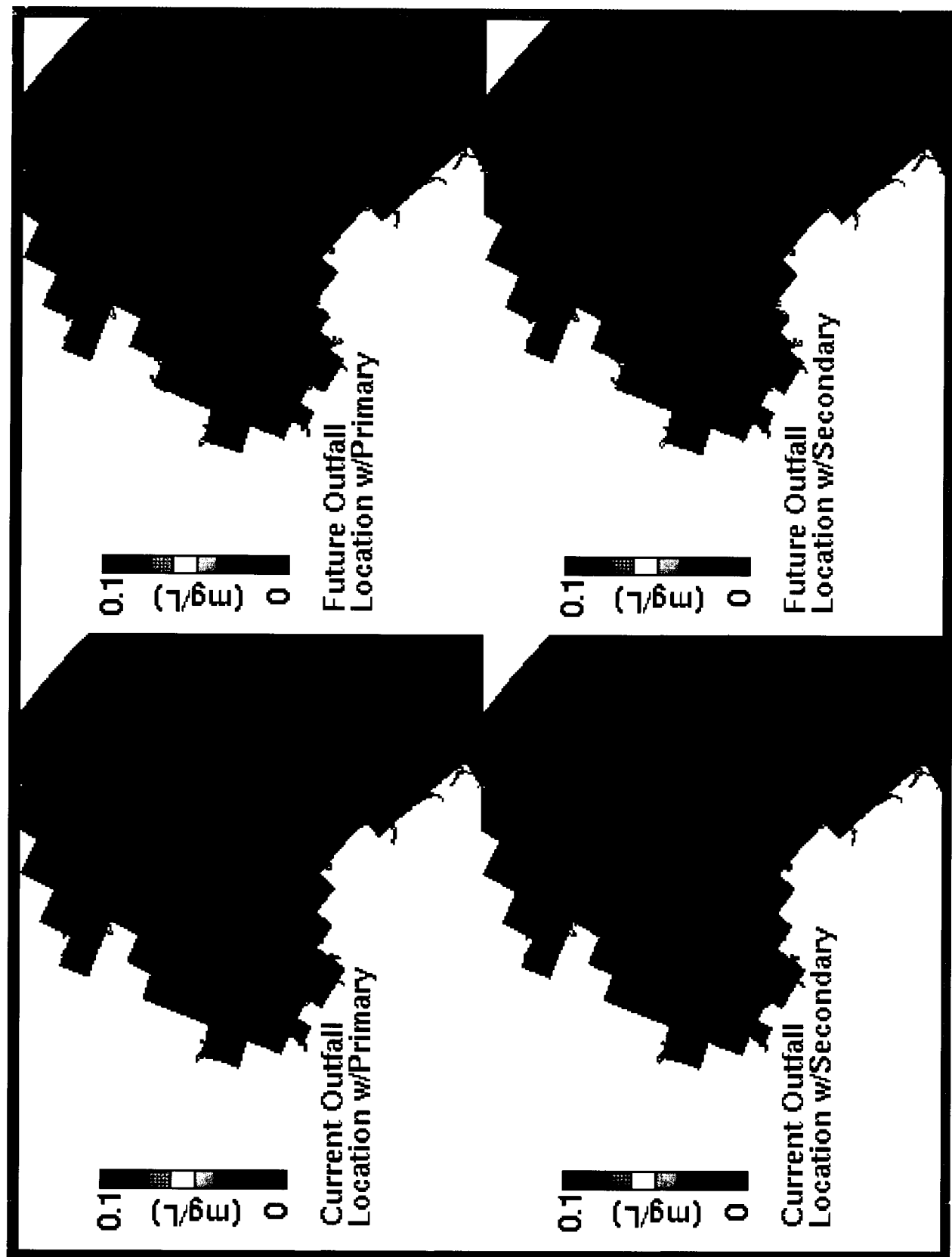
FIGURE 7-5. CALIBRATION AND PROJECTION RESULTS FOR AUGUST SURFACE DIN

Future Outfall Location w/Primary

0.4 (mg/L) 0

Future Outfall Location w/Secondary

0.4 (mg/L) 0

Current Outfall Location w/Primary

0.4 (mg/L) 0

Current Outfall Location w/Secondary

0.4 (mg/L) 0
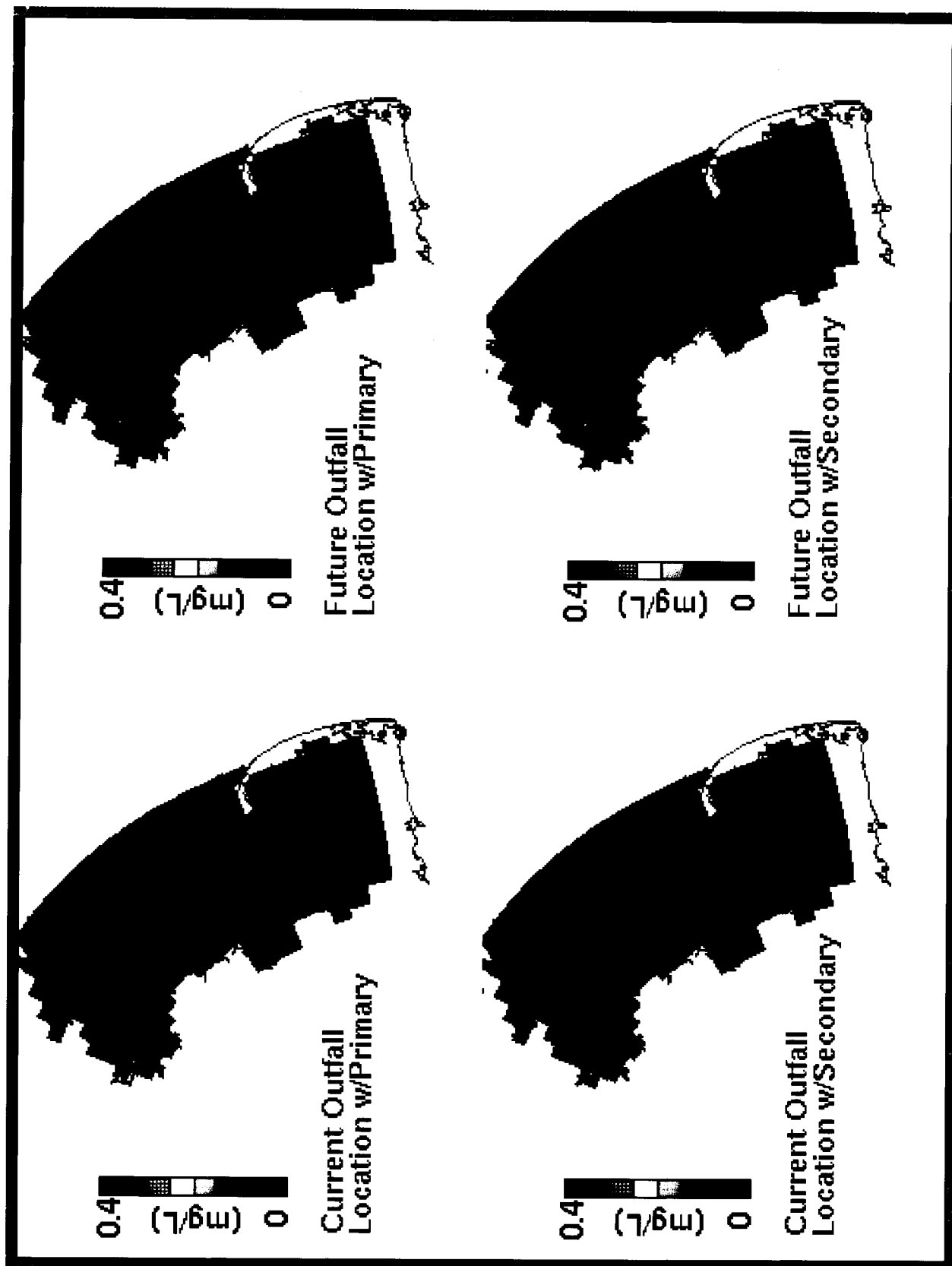
FIGURE 7-6. CALIBRATION AND PROJECTION RESULTS FOR AUGUST BOTTOM DIN

Current Outfall Location w/Primary

0.2 (mg/L) 0

Current Outfall Location w/Secondary

0.2 (mg/L) 0

Future Outfall Location w/Primary

0.2 (mg/L) 0

Future Outfall Location w/Secondary

0.2 (mg/L) 0
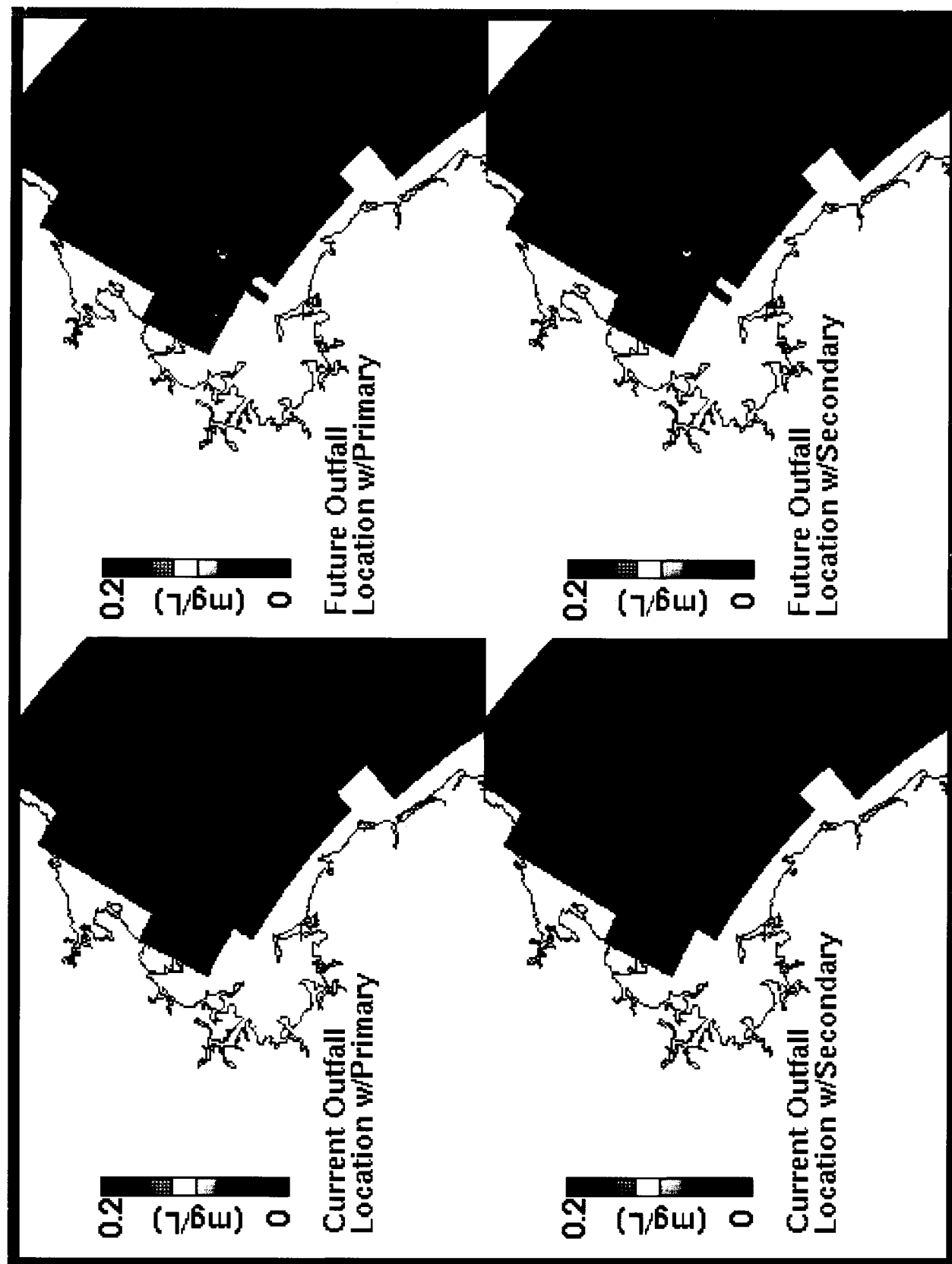
FIGURE 7-7. CALIBRATION AND PROJECTION RESULTS FOR AUGUST MID-DEPTH DIN

Figures 7-3 through 7-7 present spatial profiles of surface and bottom water DIN concentrations for the calibration and projections. These profiles represent five-day averages for fixed periods in March and August. While providing some idea of the spatial differences in DIN concentrations to be expected between current and projection scenarios, one does not get a true sense of the differences to be expected over an annual cycle. Therefore, Figures 7-8 and 7-9 present time-series plots of DIN concentrations at the water surface and the approximate mid-depth (12.5 to 17.5 m) or chlorophyll-maximum for a number of stations within the study area. These figures present comparisons between the base case calibration and the future outfall with secondary treatment. Figure 7-8 focuses on locations within Boston Harbor and in northwestern Massachusetts Bay, in the vicinity of the future outfall. Figure 7-9 presents model results for other regions of Massachusetts Bay and Cape Cod Bay.

The first location shown on figure 7-8 is located in the Inner Harbor section of Boston Harbor. Since this is a relatively shallow location, the bottom of the water column is plotted rather than the mid-depth. This location shows the greatest impact from the outfall relocation. Concentrations of DIN are reduced by as much as 50 percent during the winter months in both the surface and bottom waters. During the summer months, the surface layer becomes depleted in nitrogen for both the calibration and projection runs. The bottom waters still show elevated levels of DIN for both the calibration and projection runs. The projection run, however, shows about a 50 percent decrease in DIN below the calibration results.

The second location is in the vicinity of the present Deer Island outfall. This is also a shallow model segment and again the bottom water segment is plotted, The calibration shows elevated surface concentrations of DIN in the winter, early spring and fall months. Concentrations decrease during the summer months, but do not reach nutrient limiting conditions. The projection run shows a significant decrease in surface layer DIN concentrations for this station. In particular, surface DIN appears to reach nutrient limiting concentrations as early as mid-April and remain at low levels through out the summer.
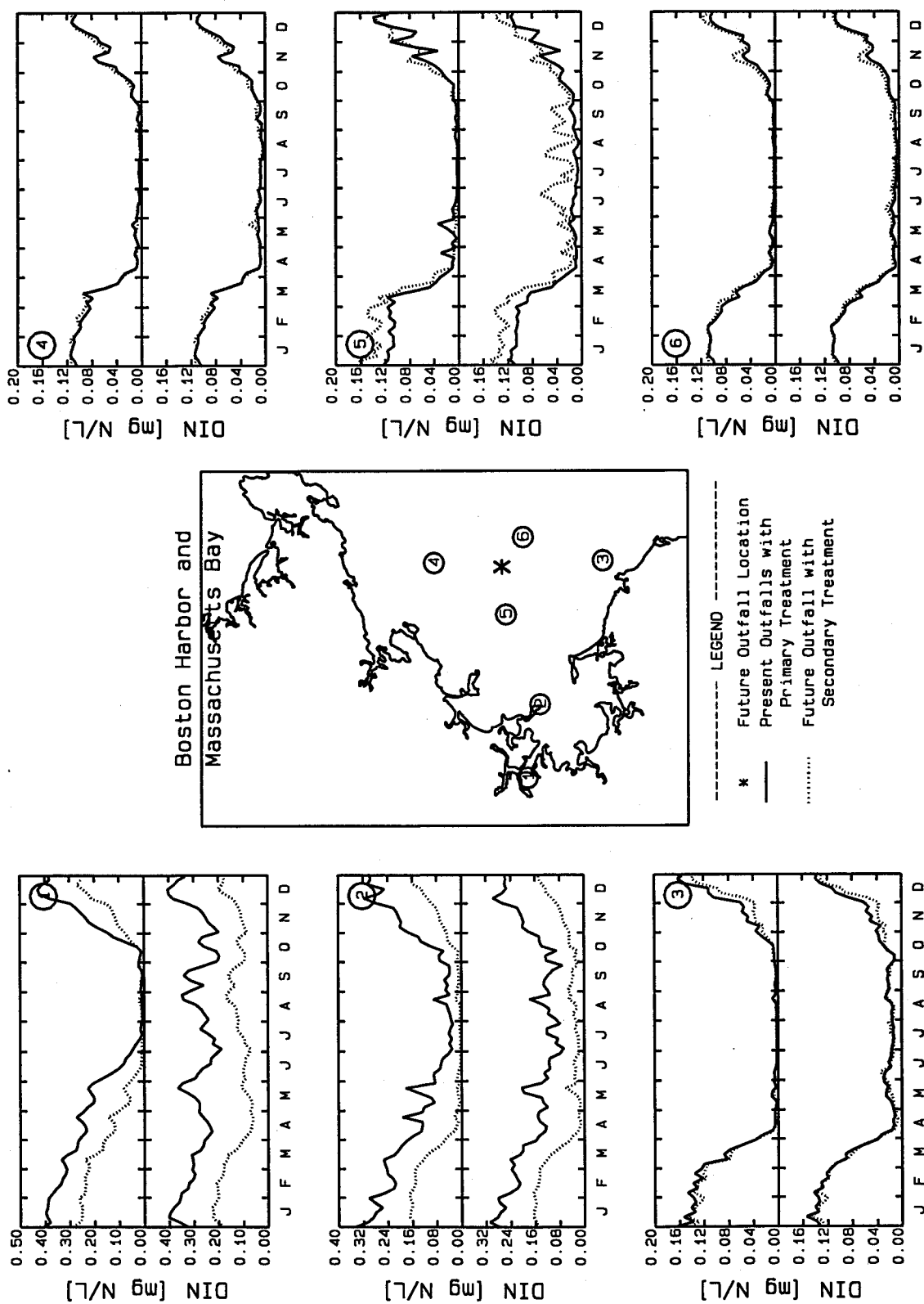
FIGURE 7-8. COMPARISONS OF NEARFIELD CALIBRATION AND PROJECTION RESULTS FOR SURFACE AND MID-DEPTH DIN
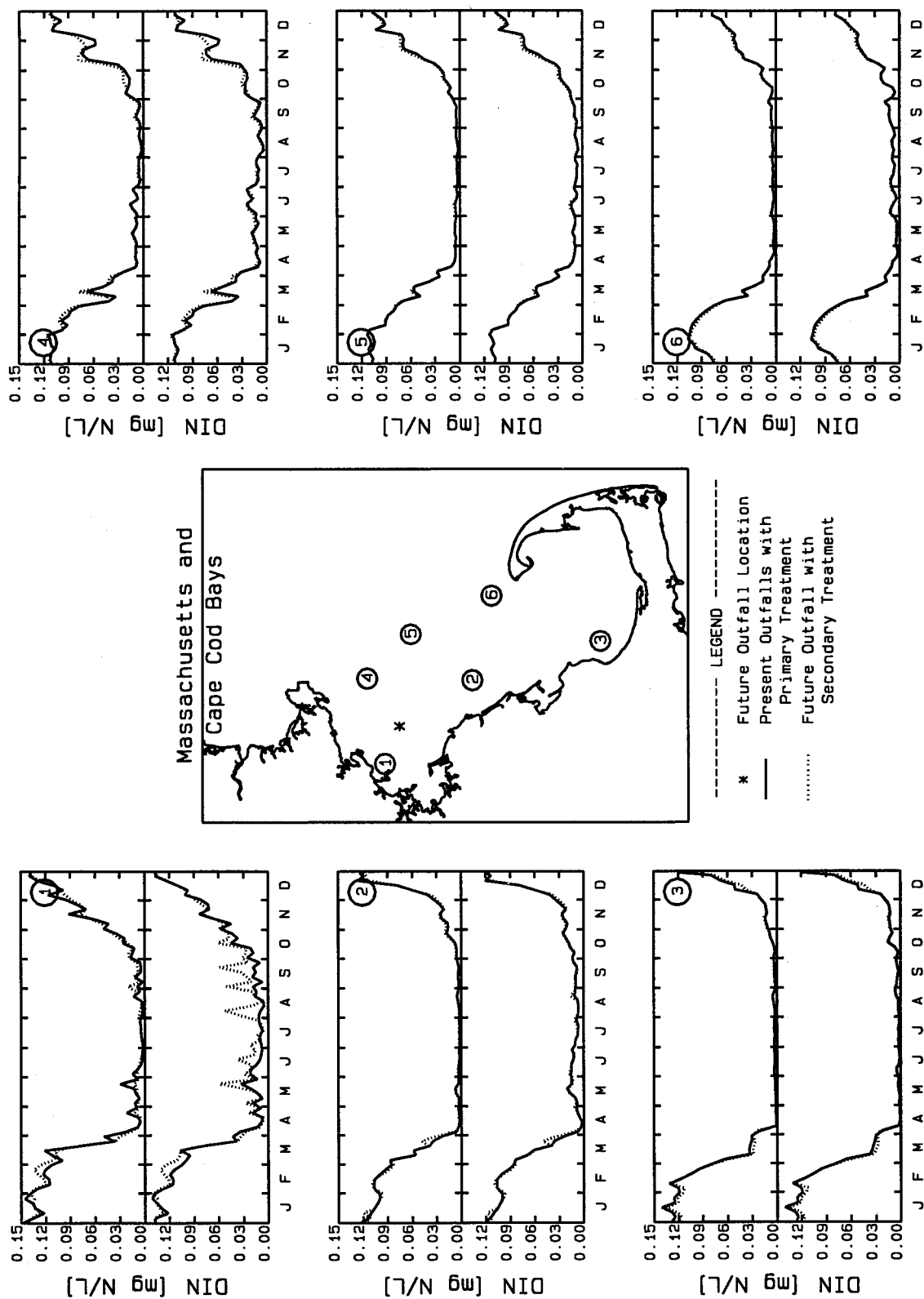
FIGURE 7-9. COMPARISONS OF FARFIELD TEMPORAL CALIBRATION AND PROJECTION RESULTS FOR SURFACE AND MID-DEPTH DIN

Bottom water concentrations for the projection run are approximately 0.1 mg N/L below those computed for the calibration run.

A grid cell located in the near shore region just off Cohasset was chosen as the third location for comparing calibration and projection results. As can be seen the temporal profiles for both the calibration and projection runs are quite similar. Generally, the projection shows slightly lower DIN concentrations in both the surface and mid-depth. There are, however, periods during the summer when the projection run shows slightly higher DIN concentrations at mid-depth.

The remaining three locations chosen to compare calibration and projection results are in close proximity to the future outfall. In general, these locations show that the outfall relocation results in slightly elevated concentrations of DIN in both the surface and mid-depth waters during the winter months, when the water column is well-mixed. During the summer months, the projection run shows slightly reduced surface concentrations of DIN. This is due to the trapping of the effluent plume below the pycnocline. Results for the mid-depth portion of the water column are variable; in some months the calibration results are slightly greater, in some months the projection run show slightly greater DIN concentrations.

Figure 7-9 presents model computations for a number of model segments more distant from the future outfall location. These stations are located (1) just offshore near Nahant; (2) in relatively shallow water near Humarock; (3) in southwest Cape Cod Bay near Sandwich; (4/5) in Stellwagen Basin; and (6) in southeastern Massachusetts Bay, just north of Race Point. In general, the model computations of DIN in the surface waters and at depths near the chlorophyll maxima (12.5 to 17.5 m) are virtually the same at all locations for both the calibration and projection runs. It appears from the results presented in this figure (as well as Figure 7-8) that, with the exception of Boston Harbor, the effects of the outfall relocation are very small and localized.

7.3.2 Chlorophyll-a

The results for the calibration and projection runs for March surface chlorophyll-a are presented in Figure 7-10. The calibration shows that during this period the highest concentrations are found in the southwest portion of the Bays and Boston Harbor. The average chlorophyll-a concentrations in these regions are between 4 and 5 μg/L. Chlorophyll concentrations are observed to decrease with distance from the shoreline and Boston Harbor toward the boundary. Chlorophyll concentrations do not appear to change significantly with the outfall relocation, although a small change can be observed in north-central Cape Cod Bay. One can also note a small depression or hole in chlorophyll concentration in the immediate vicinity of the future outfall. This is shown more clearly in Figure 7-11, which focuses on the nearfield region of the future outfall and Boston Harbor. Since the MWRA effluent contains no chlorophyll and because the effluent plume rises to the water surface during March, a depression in chlorophyll concentration occurs in the region where the effluent plume breaches the surface. With the finer resolution provided from Figure 7-11, one can also note a small reduction in chlorophyll in the Inner Harbor region of Boston Harbor.

Since secondary treatment does not significantly reduce nutrient concentrations in the effluent, it would be expected that the chlorophyll-a levels would not differ significantly with the addition of secondary treatment. Comparing the upper and lower panels of Figure 7-11 shows this to be true.

Nearfield surface chlorophyll-a concentrations for August are shown in Figure 7-12. With the exception of Boston Harbor and its immediate vicinity, phytoplankton during this period have become nitrogen limited. Consequently, chlorophyll-a concentrations around the Bays are lower than those computed in March. For the calibration, the highest concentrations are observed in Boston Harbor; in the western portion of the Harbor, chlorophyll-a concentrations reach 10 μg/L. Chlorophyll-a levels decrease rapidly with distance from Boston Harbor. As a result of moving the MWRA discharge, chlorophyll-a levels in Boston Harbor are significantly reduced. However, a small increase in chlorophyll

Current Outfall Location w/Primary

10 (ug/L) 0

Future Outfall Location w/Primary

10 (ug/L) 0

Current Outfall Location w/Secondary

10 (ug/L) 0

Future Outfall Location w/Secondary

10 (ug/L) 0

FIGURE 7-10. CALIBRATION AND PROJECTION RESULTS FOR MARCH FARFIELD SURFACE CHLOROPHYLL-a

10 (ug/L) 0
Future Outfall
Location w/Primary

10 (ug/L) 0
Future Outfall
Location w/Secondary

10 (ug/L) 0
Current Outfall
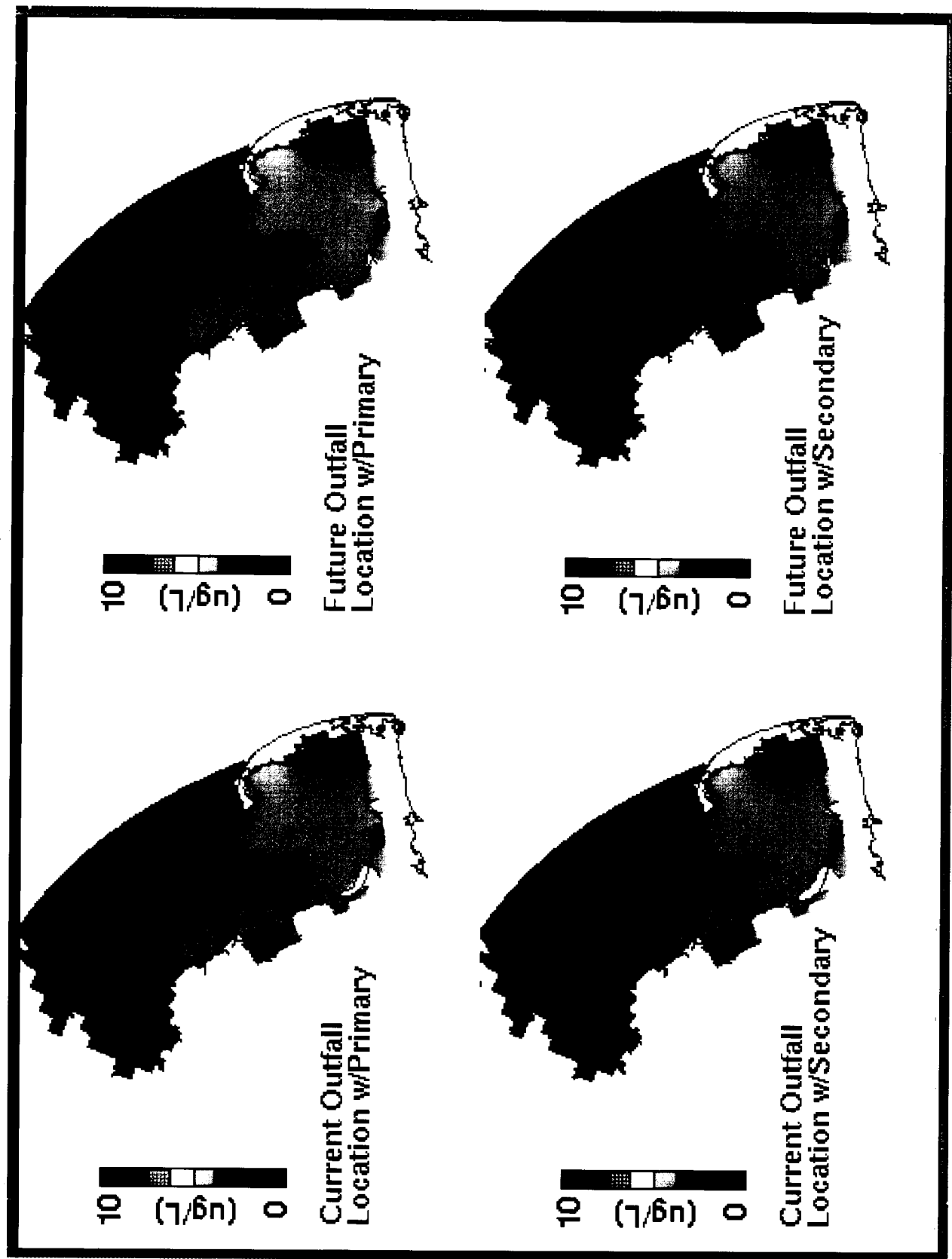Location w/Primary

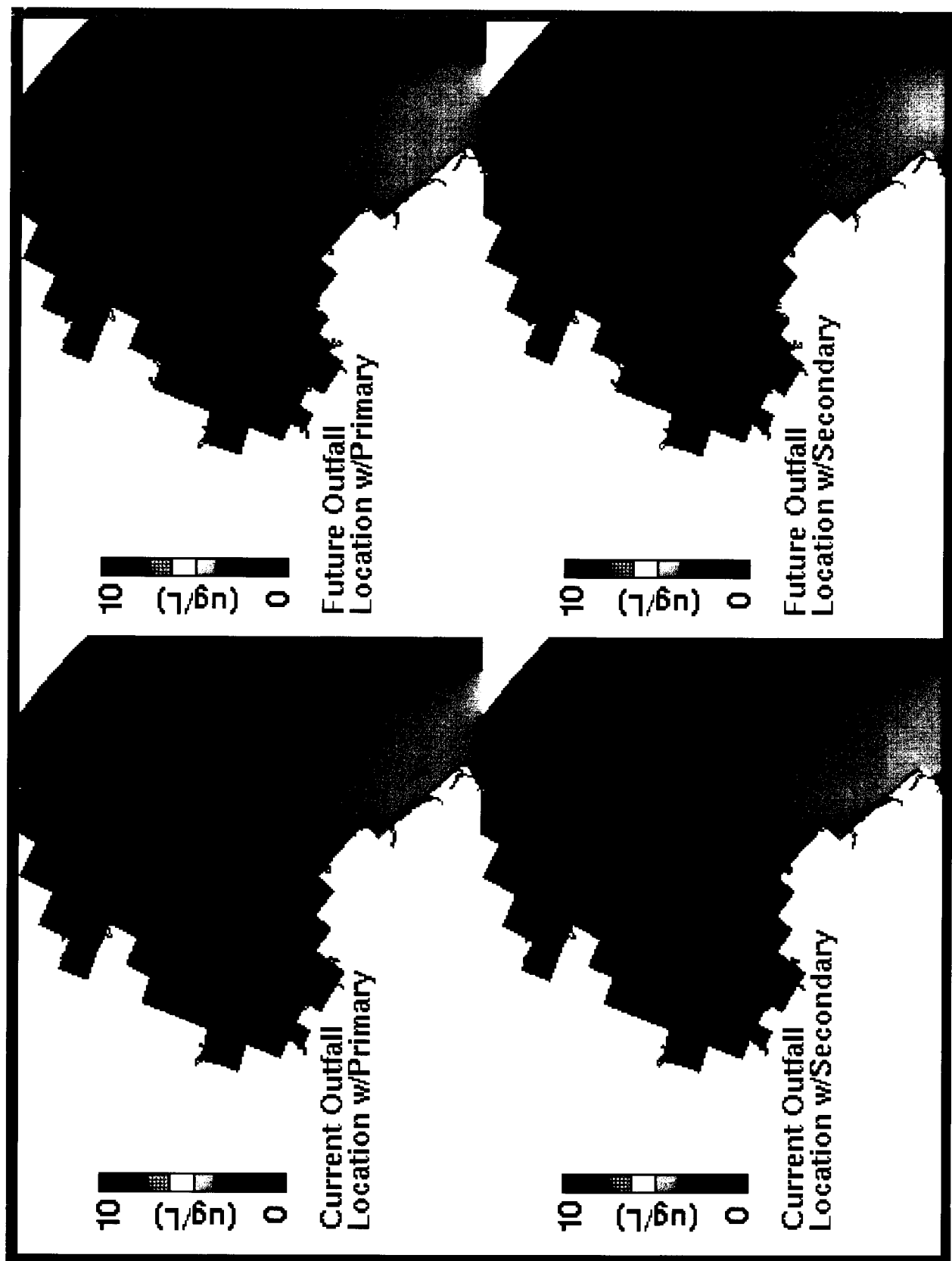10 (ug/L) 0
Current Outfall
Location w/Secondary

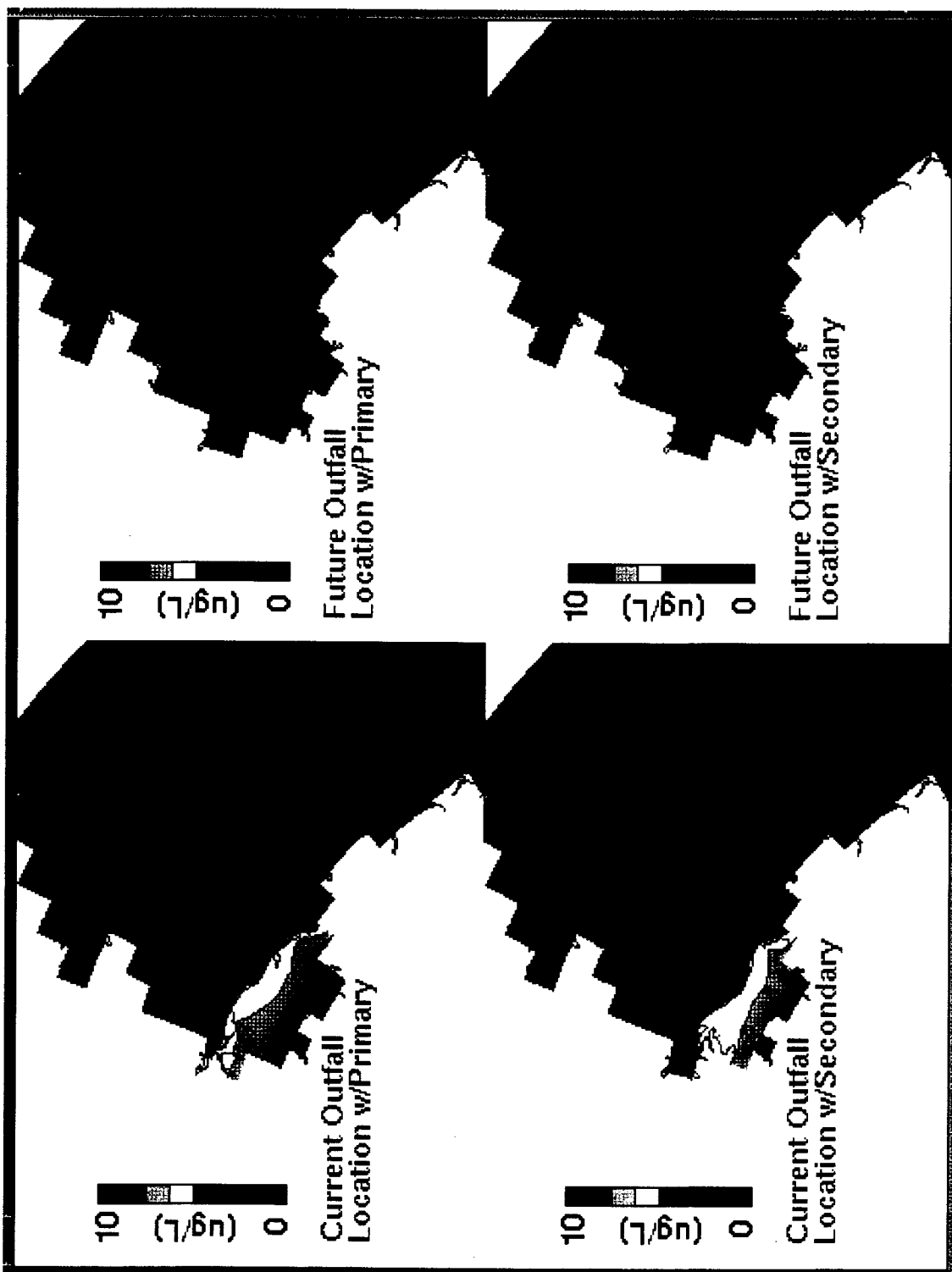FIGURE 7-11. CALIBRATION AND PROJECTION RESULTS FOR MARCH NEARFIELD SURFACE CHLOROPHYLL-a

FIGURE 7-12. CALIBRATION AND PROJECTION RESULTS FOR AUGUST SURFACE CHLOROPHYLL-a

is computed along the coast near Plymouth Harbor. The upgrade of the MWRA facilities to secondary treatment appears to have a small effect on chlorophyll-a levels. Chlorophyll concentrations are the 15 m depth are presented on Figure 7-13. As can be seen the outfall relocation has only a small effect on mid-depth chlorophyll levels in the nearfield. Concentrations are shown to decrease slightly north of the outfall, while increasing slightly southwest of the future outfall.

Figure 7-14 presents a time-series comparisons of surface and mid-depth (or depth of the chlorophyll maxima) for a number of model segments located in Boston Harbor and in the vicinity of the future outfall. Due to their relatively shallow water depths, the bottom layer is plotted for segments (1) and (2). Segments (1) and (2) show the greatest impact from the outfall relocation. Maximum chlorophyll concentrations are reduced by approximately 3 μg/L in the summer and fall months at both station locations. Segment (3) located near Cohasset, shows reduced levels of chlorophyll in the surface layer, beginning in April and continuing through the summer and fall period of stratification. Mid-depth chlorophyll levels computed for the projection run at this station are either the same or slightly lower than those computed for the calibration run.

Surface chlorophyll concentrations at segment (5) are generally 1 to 1.5 μg/L lower for the projection run during the months of July through September. There are short periods, which usually occur during marked declines, when the surface concentrations are the same for both the calibration and the projection. Mid-depth (or depth of the chlorophyll maxima) chlorophyll concentrations are quite similar for this station. There are times when the calibration computes higher chlorophyll concentrations at mid-depth and other times when the projection computes slightly higher concentrations. The remaining two nearfield stations show similar temporal patterns. In general, the projection run shows slightly lower surface chlorophyll concentrations. Results at the depth of the chlorophyll maximum are varied; generally the temporal profiles are quite similar but there are also brief periods when the projection computes slightly lower or slightly higher chlorophyll concentrations compared with the calibration run.

Current Outfall
Location w/Primary

Current Outfall
Location w/Secondary

Future Outfall
Location w/Primary

Future Outfall
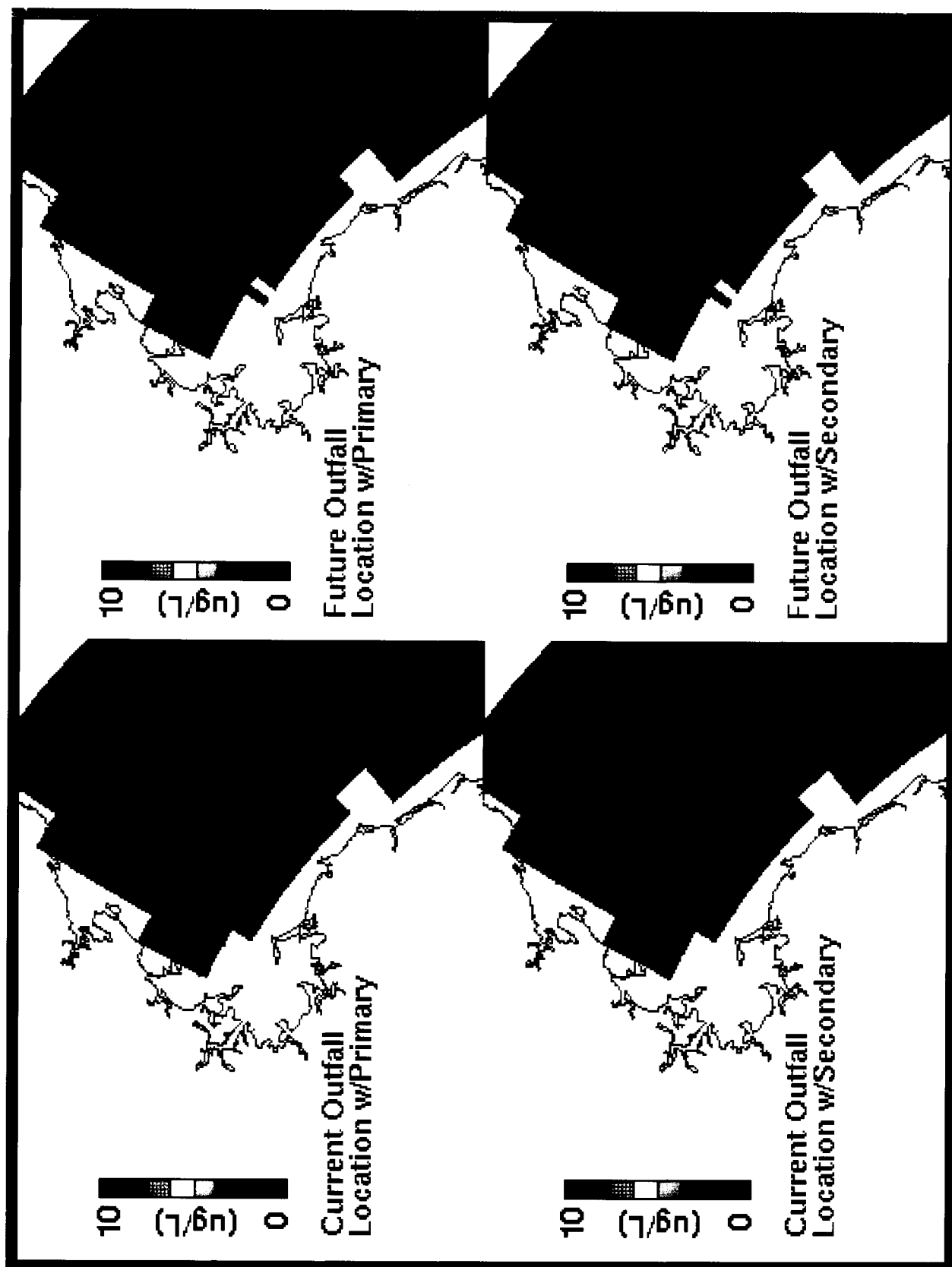Location w/Secondary

10 (ug/L) 0

FIGURE 7-13. CALIBRATION AND PROJECTION RESULTS FOR AUGUST MID-DEPTH CHLOROPHYLL-a
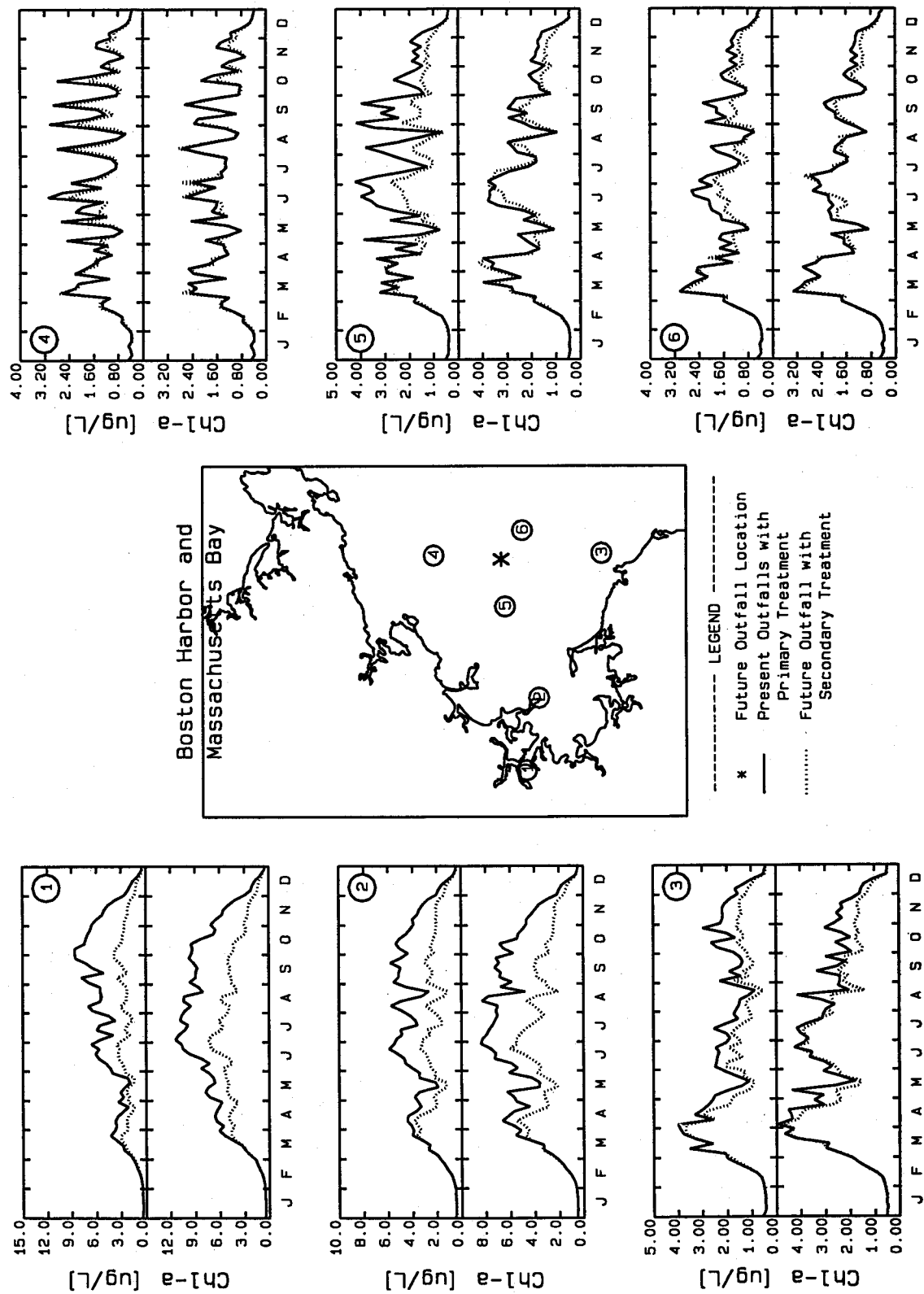
FIGURE 7-14. COMPARISONS OF NEARFIELD TEMPORAL CALIBRATION AND PROJECTION RESULTS FOR SURFACE AND MID-DEPTH CHLOROPHYLL-a

Calibration and projection results for surface and mid-depth (or depth of the chlorophyll maximum) are presented for a number of farfield stations in Figure 7-15. Except for the Nahant and Humarock segments, the model computations for both the surface and depth of chlorophyll maximum layers are virtually indistinguishable. The projection run computes slightly lower surface chlorophyll concentrations near Nahant, while computing slightly higher mid-depth concentrations in March, June, and early August. For the remaining periods of time, the mid-depth concentrations are either the same or slightly lower than the calibration run. As was observed for dissolved inorganic nitrogen, the outfall relocation does not have a significant affect on chlorophyll-a concentrations except in Boston Harbor and its immediate vicinity.

7.3.3 Dissolved Oxygen

Figure 7-16 displays the comparison of the calibration and three projections for minimum bottom DO in March. DO concentrations are relatively high everywhere, ranging from 9 mg O_2/L in the Inner Harbor to greater than 12 mg O_2/L near the boundary. The calibration figure shows an area of lower DO along the western coastline of Massachusetts and Cape Cod Bays, extending from Boston Harbor down into western Cape Cod Bay. Higher concentrations of DO are computed for the eastern portions of Massachusetts Bay. Results for all three projection scenarios are similar. All three projection runs show higher DO concentrations in Boston Harbor, while showing minimal changes in DO elsewhere in the model domain. The combination of outfall relocation and secondary treatment creates a larger area of DO improvement near the entrance of Boston Harbor.

In August minimum bottom dissolved oxygen concentrations have decreased below March levels. Dissolved oxygen concentrations for the calibration run (Figure 7-16), now range from less than 5 mg O_2/L in the Inner Harbor to approximately 9 mg O_2/L in the eastern portion of Massachusetts Bay. These lower DO levels are due to a number of factors, including: higher water temperatures, which lower DO saturation and which increase biological oxidation rates; increased rates of sediment oxygen demand; and increased stratification of the water column, which prevents exchange with more highly

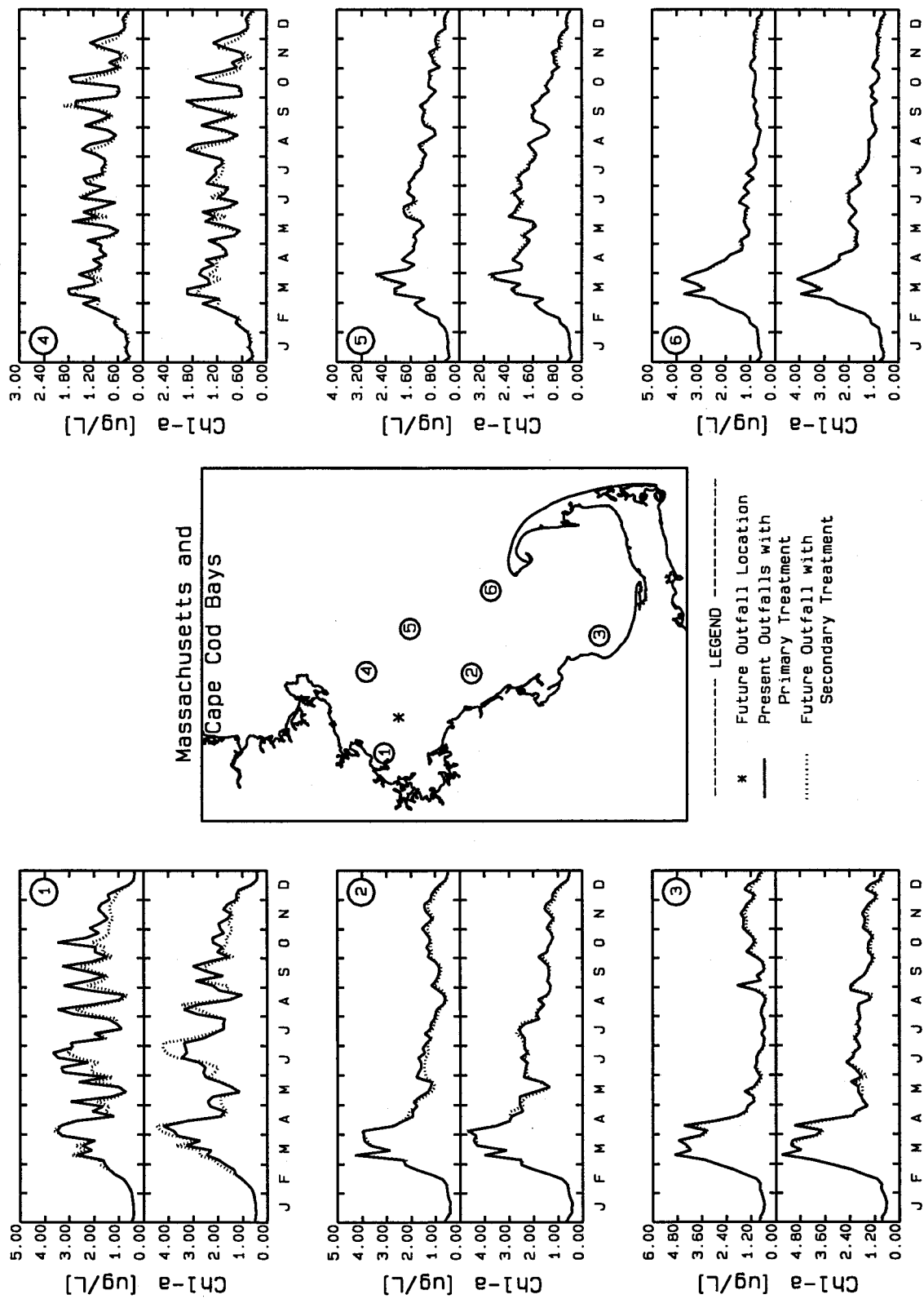FIGURE 7-15. COMPARISONS OF FARFIELD TEMPORAL CALIBRATION AND PROJECTION RESULTS FOR SURFACE AND MID-DEPTH CHLOROPHYLL-a

Legend (mg/L): 12 — 8

Future Outfall Location w/Primary

Future Outfall Location w/Secondary

Current Outfall Location w/Primary
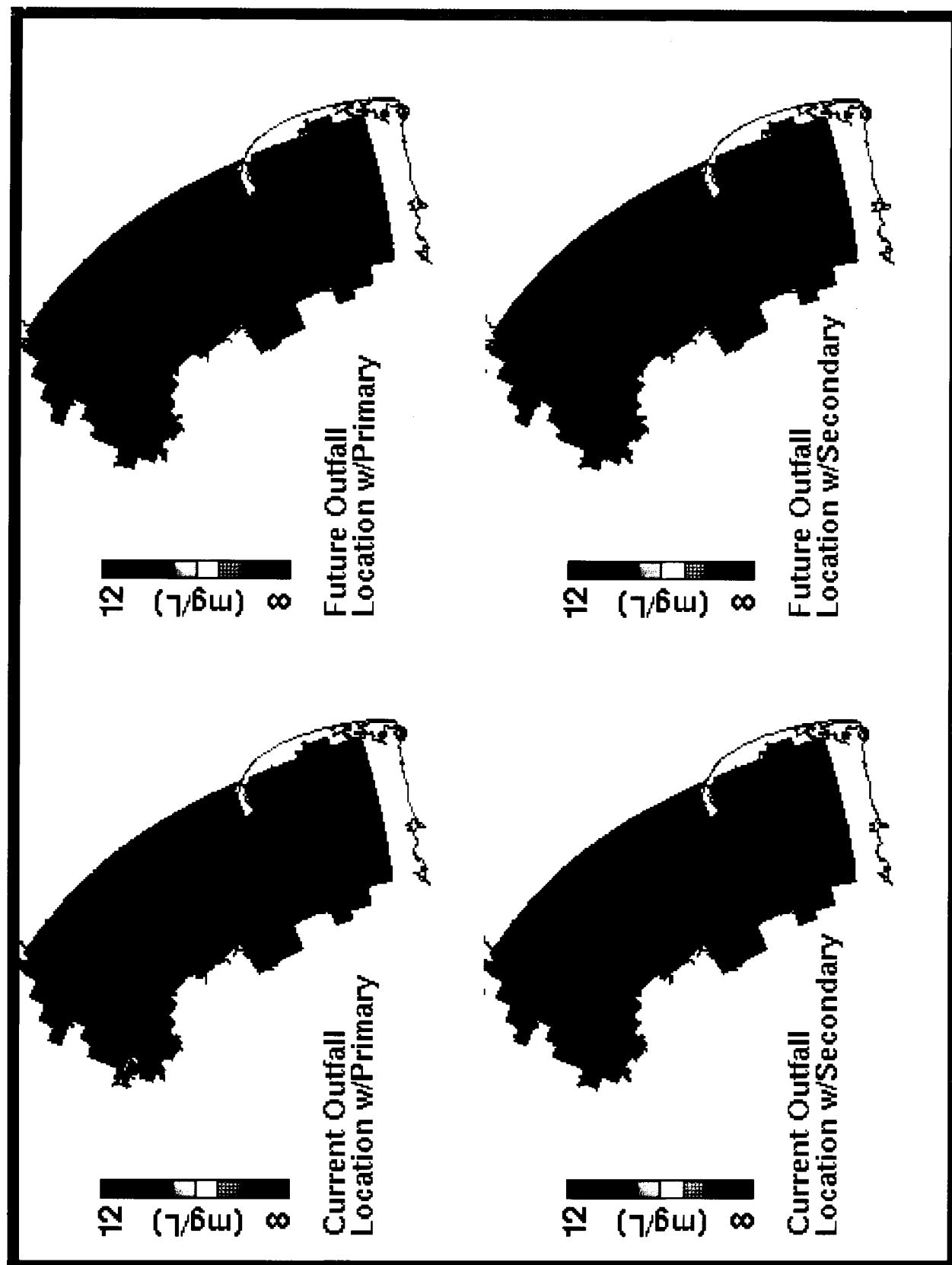
Current Outfall Location w/Secondary

FIGURE 7-16. CALIBRATION AND PROJECTION RESULTS FOR MARCH MINIMUM BOTTOM DO

oxygenated surface waters. When the outfall is relocated (upper right panel of Figure 7-15), DO levels improve in Boston Harbor, particularly in the Inner Harbor. However, there is also a small decrease in the DO concentration in an area around the outfall and to the north of the outfall. Upgrade of the MWRA facilities to secondary treatment and continued discharge at the current outfall locations (lower left panel of Figure 7-17) also shows improvement in DO levels in Boston Harbor and its immediate vicinity. Dissolved oxygen concentrations are no longer below 5 mg/L in the Inner Harbor. Upgrading to secondary treatment and outfall relocation increases DO concentrations in Boston Harbor. Interestingly, upgrading to secondary treatment while continuing to discharge at the current outfall location appears to provide a greater level of improvement in August minimum DO in the Harbor, than does upgrade to secondary treatment and outfall relocation. This may be an artifact of the changes in harbor circulation that result from outfall relocation.

As has been noted earlier in this report, the minimum DO concentrations are usually observed during the month of October. Figures 7-18 and 7-19, then, present the results of the calibration and three projections of minimum dissolved oxygen for a five-day period in October. By October the water column has been stratified since April and the bottom waters have had limited exchange with more oxygenated surface waters during this time. Figure 7-18 presents results for Massachusetts and Cape Cod Bays, while Figure 7-19 provides comparisons for Boston Harbor and the nearfield to the future outfall. Calibration results show the lowest oxygen levels in the Inner Harbor area. Another area of low dissolved oxygen can be observed in western Cape Cod Bay. However, the DO concentration does not fall below 6.0 mg O_2/L in Cape Cod Bay; the lowest computed values are approximately 6.6 mg O_2/L. Outfall relocation results in an increase in DO concentrations in Boston Harbor. Outfall relocation does not appear to have a significant impact on bottom water dissolved oxygen concentrations in the nearfield region of the future outfall. For this five-day period, it appears as if the bottom currents are heading northward towards Nahant, resulting in a small tongue of lower DO extending northward from the future outfall location. Both projection scenarios which consider secondary treatment show higher levels of DO in Boston Harbor and northeast Massachusetts Bay.

10 (mg/L) 5

Current Outfall
Location w/Primary

10 (mg/L) 5

Current Outfall
Location w/Secondary

10 (mg/L) 5

Future Outfall
Location w/Primary

10 (mg/L) 5

Future Outfall
Location w/Secondary

FIGURE 7-17. CALIBRATION AND PROJECTION RESULTS FOR AUGUST MINIMUM BOTTOM DO

Current Outfall
Location w/Primary

10 (mg/L) 5

Future Outfall
Location w/Primary

10 (mg/L) 5

Current Outfall
Location w/Secondary

10 (mg/L) 5

Future Outfall
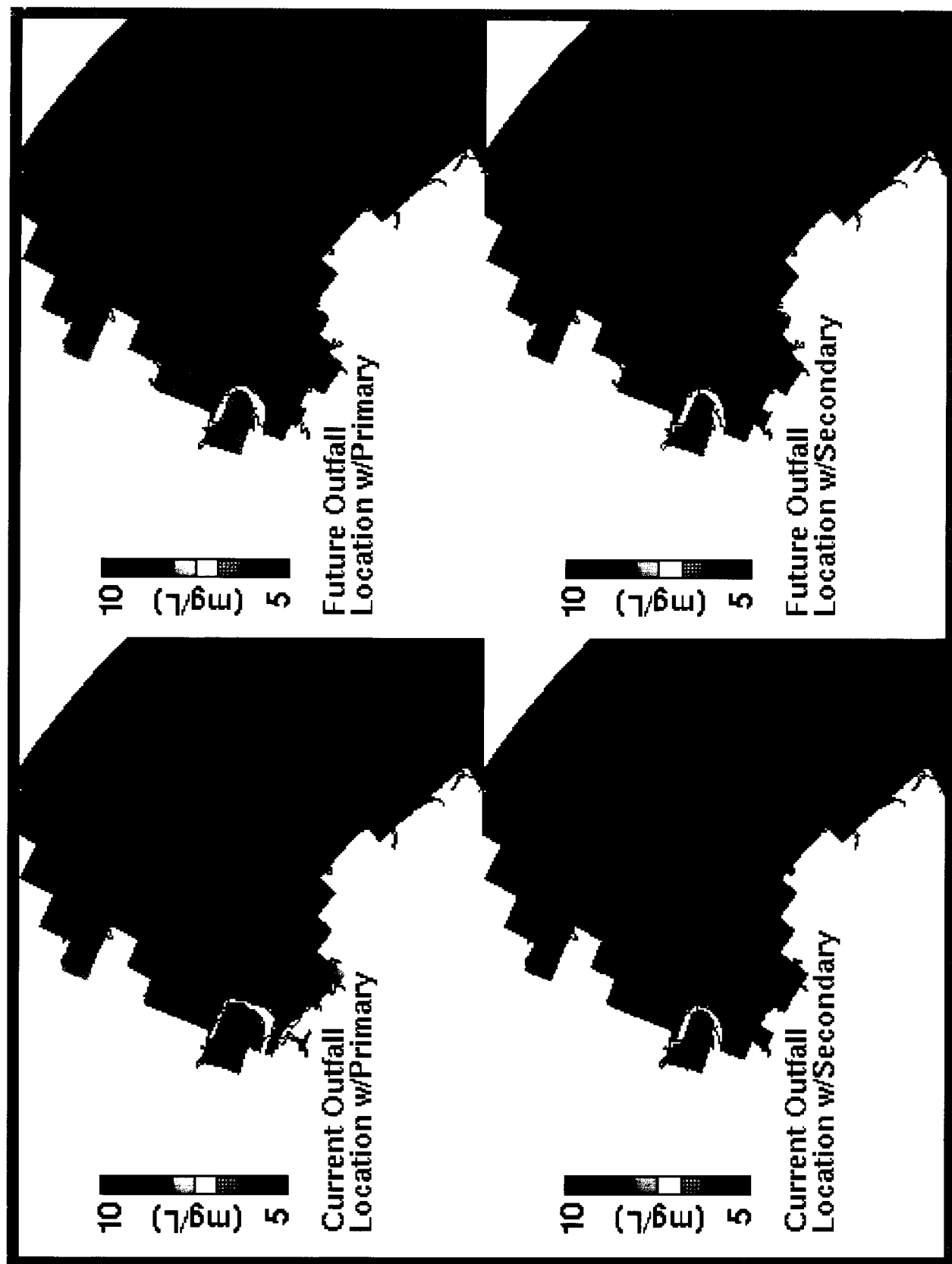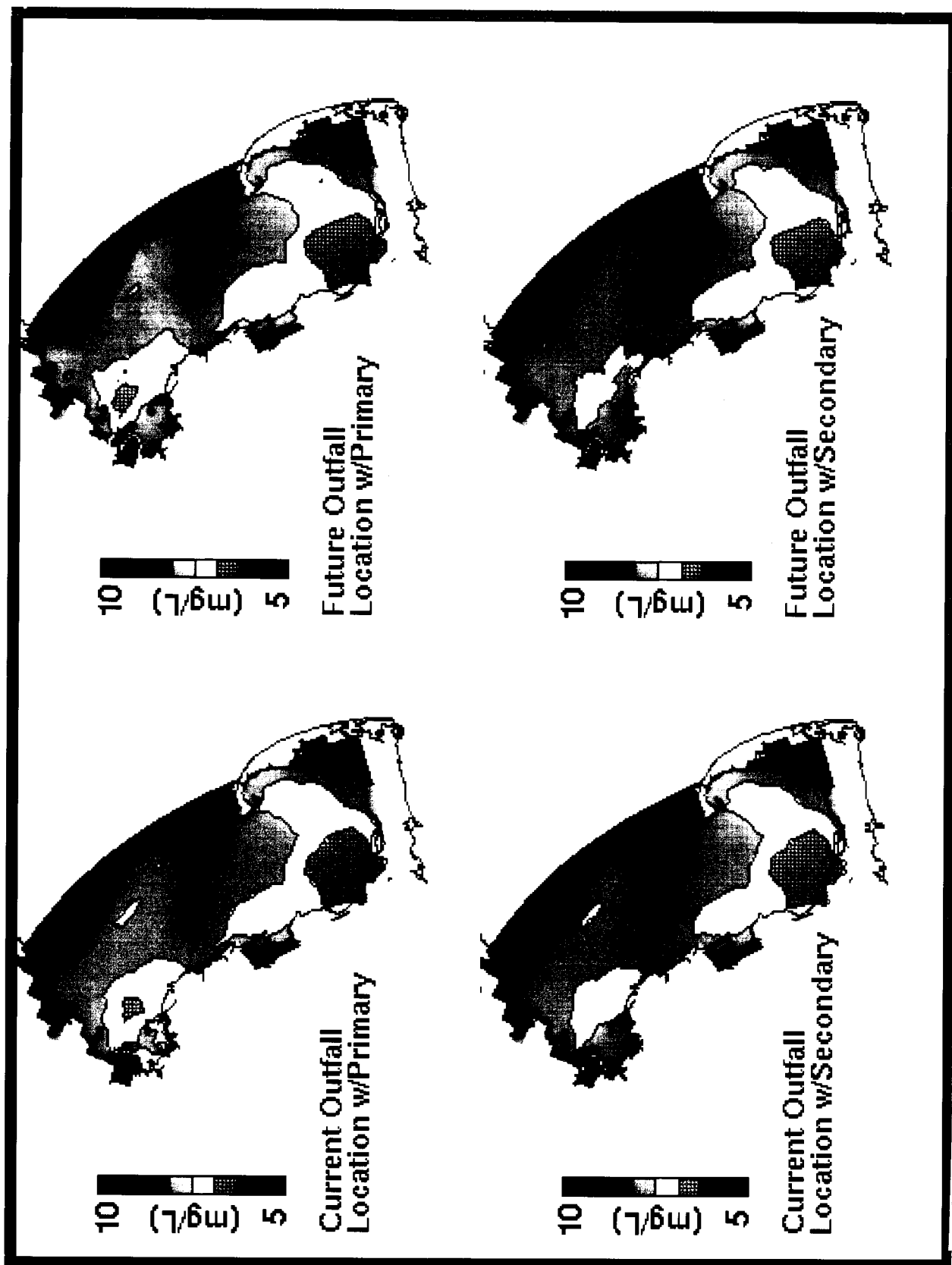**Location w/Secondary**

10 (mg/L) 5

FIGURE 7-18. CALIBRATION AND PROJECTION RESULTS FOR FARFIELD OCTOBER MINIMUM BOTTOM DO
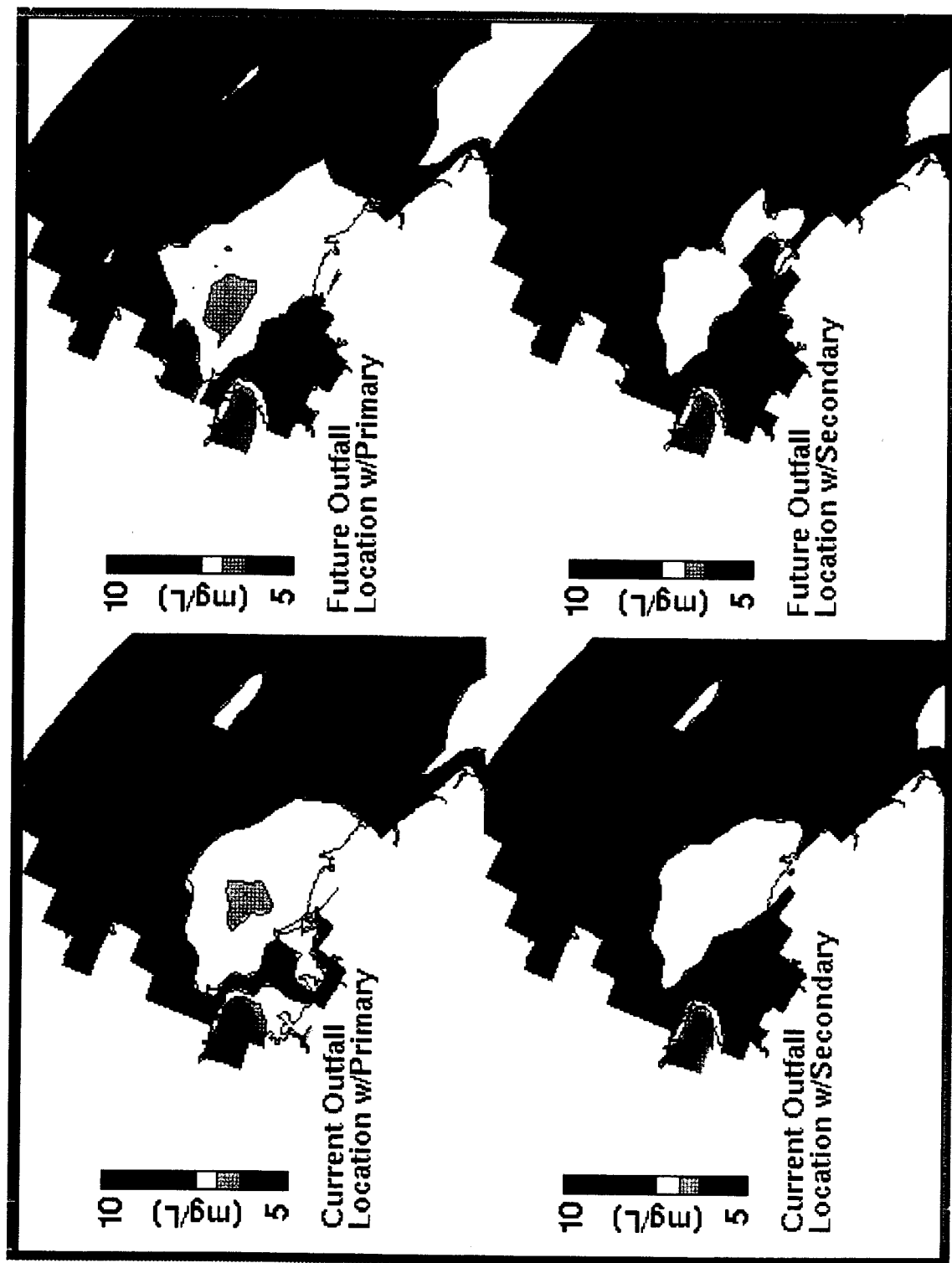
FIGURE 7-19. CALIBRATION AND PROJECTION RESULTS FOR NEARFIELD OCTOBER MINIMUM BOTTOM DO

Upgrading to secondary treatment does not affect bottom water DO concentrations in more farfield regions such as Cape Cod Bay.

Figures 7-20 and 7-21 present comparisons of mid-depth (or depth of chlorophyll-maxima) and bottom water minimum DO between the base calibration and the outfall relocation with secondary treatment runs. These comparisons are presented for a number of segments in Boston Harbor, the nearfield and the farfield. Unlike Massachusetts and Cape Cod Bays, minimum DO concentrations in Boston Harbor are observed in the summer months rather than October. The upgrade to secondary treatment and outfall relocation improves DO concentrations in the Inner Harbor region of Boston Harbor by approximately 2 mg/L during the critical summer months. This improvement is significant in that DO concentrations in this model segment are no longer in violation of Massachusetts State standards. This projection run also shows increases in DO concentrations at the mouth of the Harbor, near the current outfall. Projection results for the remaining nearfield and farfield model segments show either small increases in bottom water DO in the critical fall months or are virtually the same as the base calibration run.

In summary, the three projections show varying degrees of improvement in dissolved oxygen in Boston Harbor. Outfall relocation alone improves minimum DO concentrations between 0.19 and 1.84 mg O_2/L. Upgrading the treatment plants to secondary treatment and moving the outfall location improves the DO minimum by another 0.02 to 0.20 mg O_2/L in Boston Harbor. Interestingly, just upgrading the MWRA treatment facilities to secondary treatment and maintaining the current discharge locations improves the minimum DO concentrations in Boston Harbor by 0.42 to 1.33 mg O_2/L. With outfall relocation only and no upgrade in wastewater treatment the model projects that the minimum DO at the outfall location will decrease from 7.16 to 6.81 mg O_2/L. The lowest DO, however, will be found in a segment to the northwest of the outfall. The model indicates that the DO in this segment will decrease from 6.80 to 6.60 mg O_2/L. The model also predicts that the minimum DO at the future outfall site will improve to 7.29 mg O_2/L with secondary treatment and outfall relocation. The model also indicates that secondary treatment alone would provide a greater benefit in dissolved oxygen
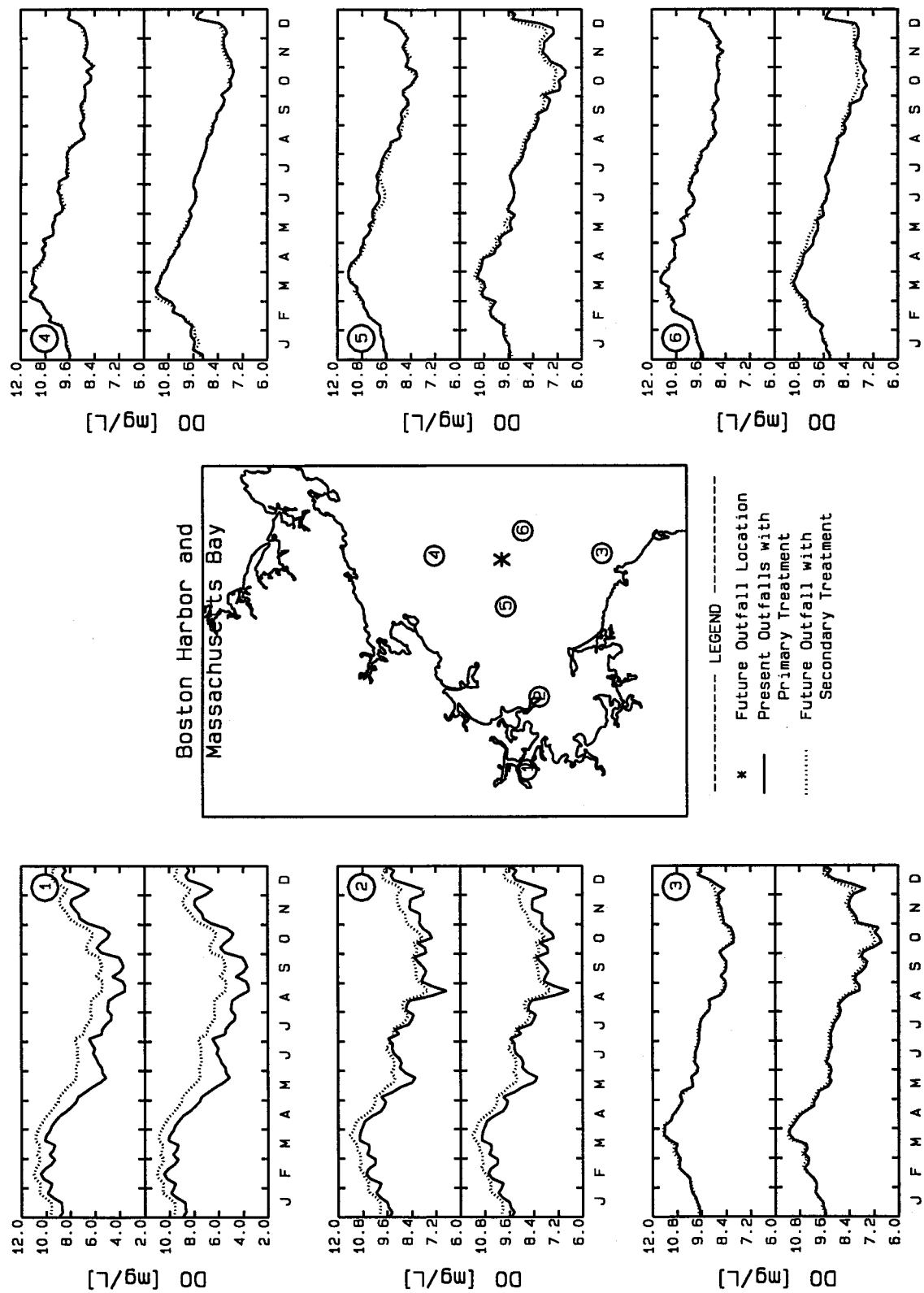
FIGURE 7-20. COMPARISONS OF NEARFIELD TEMPORAL CALIBRATION AND PROJECTION RESULTS FOR MID-DEPTH AND BOTTOM MINIMUM DO
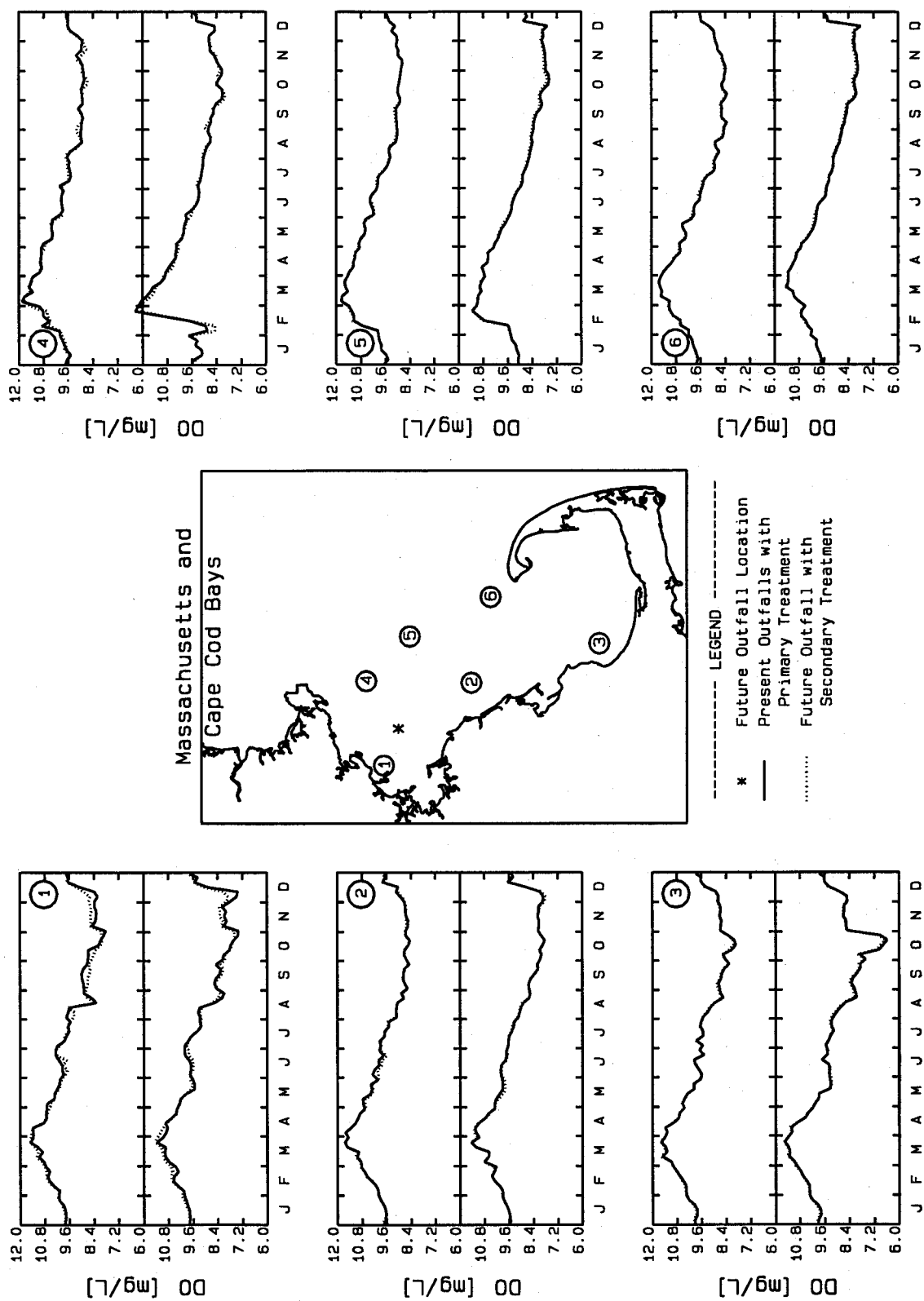
FIGURE 7-21. COMPARISONS OF FARFIELD TEMPORAL CALIBRATION AND PROJECTION RESULTS FOR MID-DEPTH AND BOTTOM MINIMUM DO

concentrations than could be achieved by outfall relocation alone. Secondary treatment and outfall relocation provides an even greater measure of protection for Boston Harbor and the Bays' ecosystem.

7.3.4 Particulate Organic Carbon (POC) Flux

As has been described earlier, the flux of POC is an important variable because it acts as a food source to the benthic community. However, an excess of POC deposition can result in high sediment oxygen demand and have an adverse impact on the benthic community. Figures 7-22 and 7-23 present model computations of POC flux (J_{POC}) to the sediment for a five-day period in August for Massachusetts and Cape Cod Bays and for Boston Harbor and northeast Massachusetts Bay, respectively. These figures indicate that the highest fluxes of POC to the sediments are computed in Boston Harbor and the nearshore areas of Massachusetts Bay and western Cape Cod Bay. Within Boston Harbor the highest fluxes are computed in the western portions of the harbor, near the Neponset River. Model computations show the flux of particulate organic carbon to the sediment to be reduced in Boston Harbor under all three projection scenarios. However, the greatest reductions are found for those projections that involve outfall relocation. This is due to the fact that outfall relocation reduces DIN concentrations in the harbor and, therefore, reduces the production (and subsequent deposition) of algal biomass.

Outfall relocation without secondary treatment (upper right panel of Figure 7-23) results in an increase in POC deposition in the vicinity of the future outfall. Upgrading treatment of the MWRA effluent reduces the magnitude of the POC depositional flux at the future outfall site. This result occurs due to reduced levels of POC in the MWRA effluent that could be achieved under secondary treatment.

Figures 7-24 and 7-25 present temporal comparisons of J_{POC} for Boston Harbor and a number of nearfield and farfield stations in Massachusetts and Cape Cod Bays for the calibration and future outfall with secondary runs. Segment (6), in Figure 7-24, represents the actual outfall segment. As can be seen, the projection runs show significant

Calibration

Future Outfall
Location

Current Outfall
Location w/Secondary

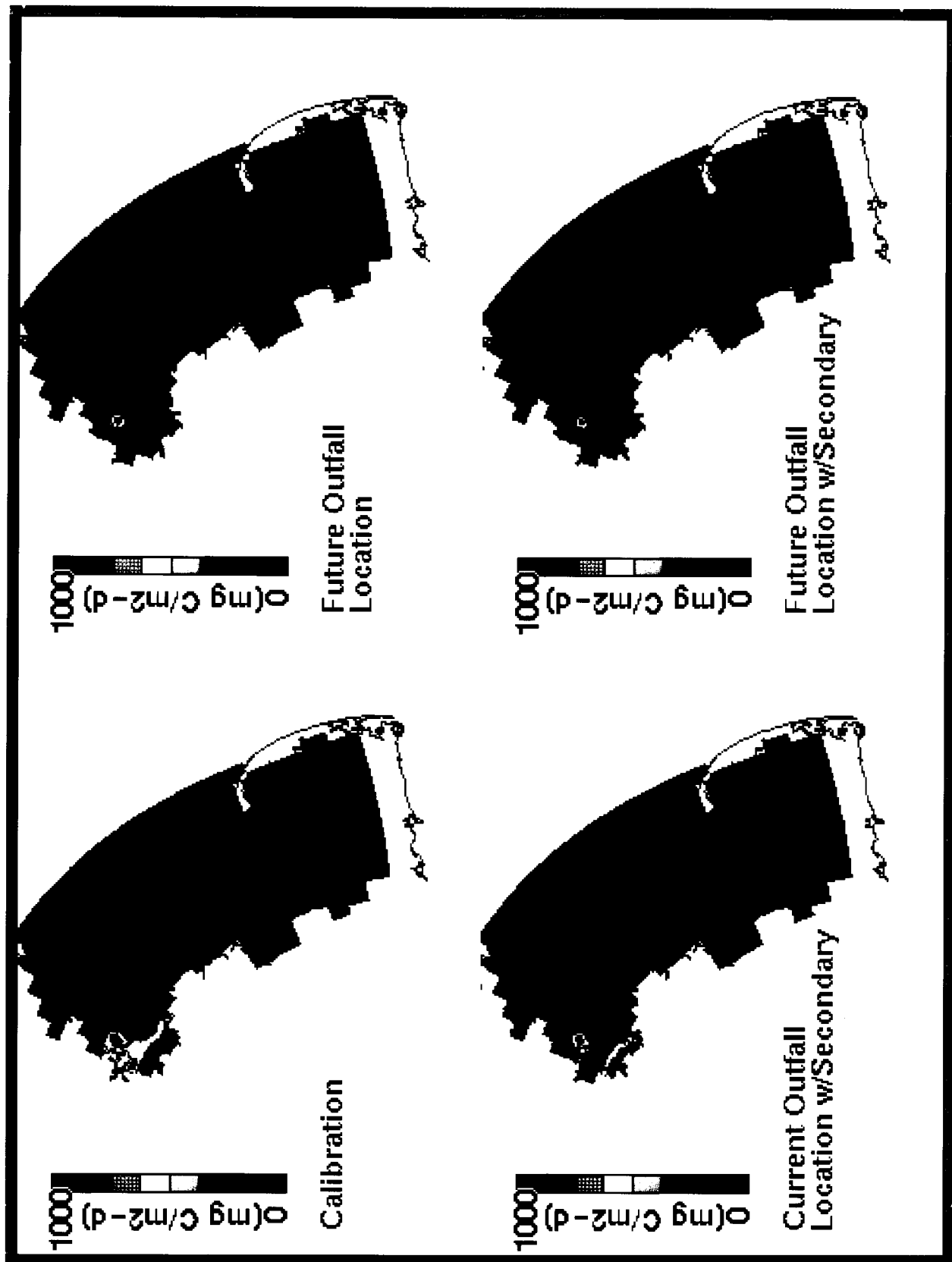Future Outfall
Location w/Secondary

0 (mg C/m2-d) 1000

FIGURE 7-22. CALIBRATION AND PROJECTION RESULTS FOR FARFIELD AUGUST POC FLUX
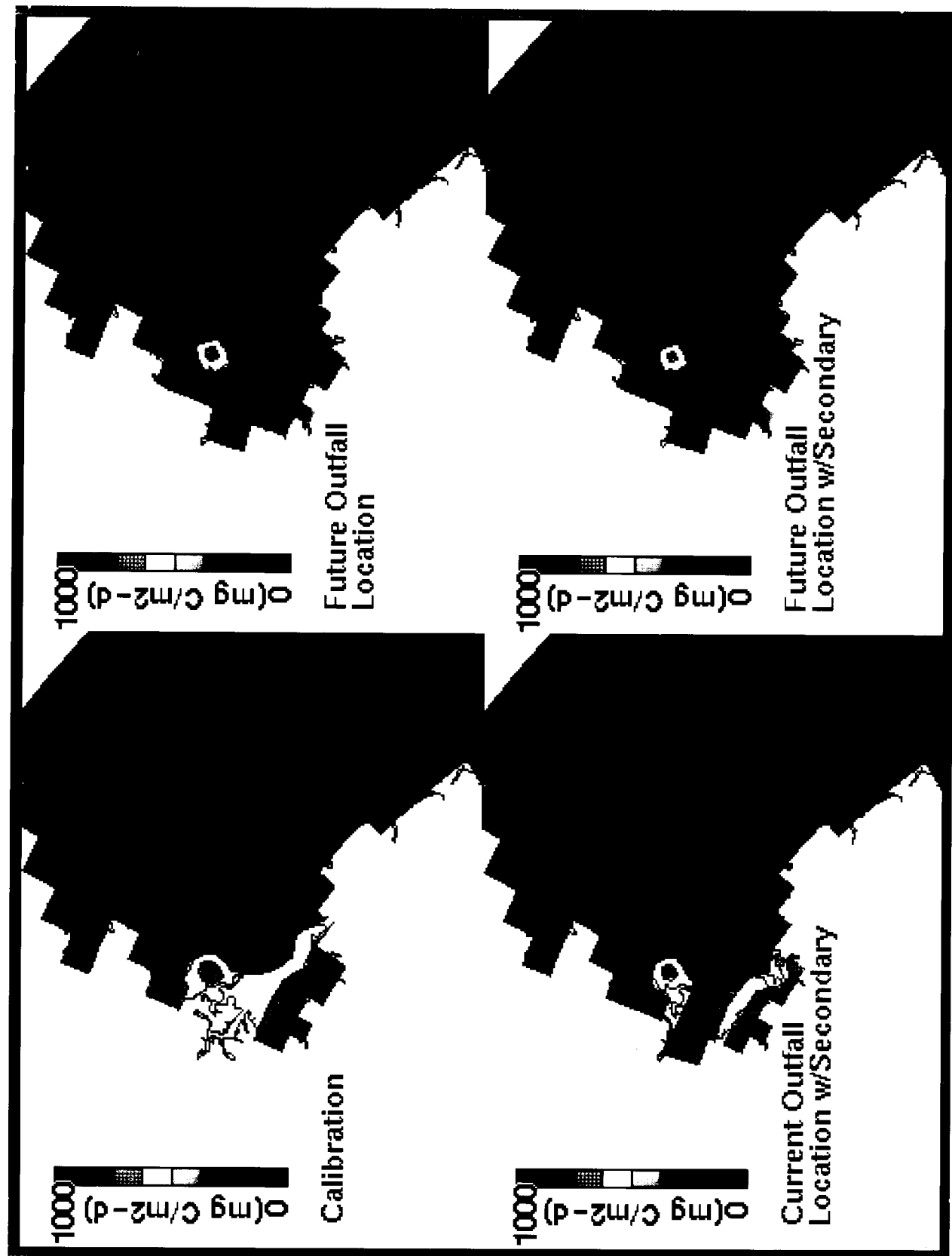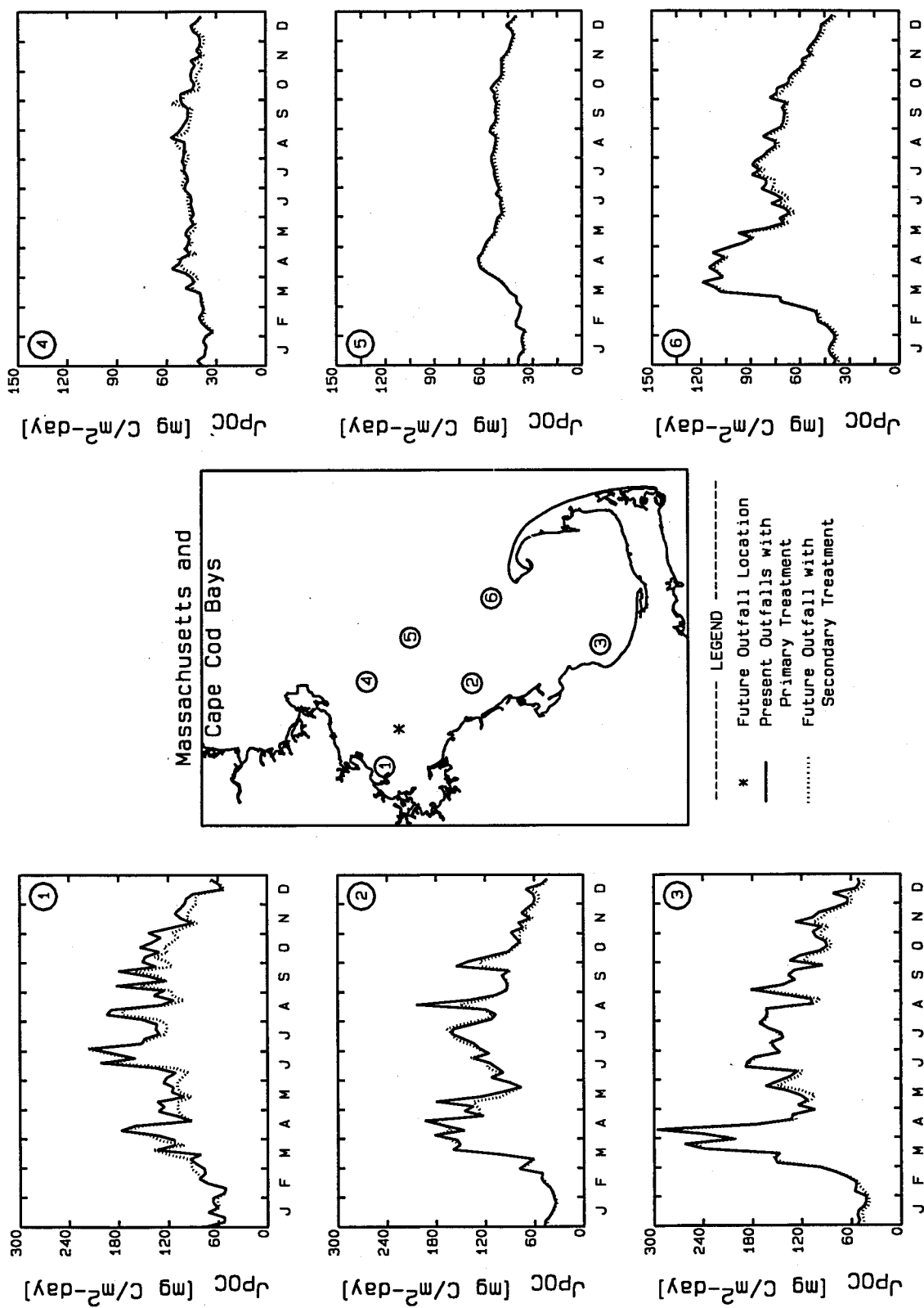
FIGURE 7-23. CALIBRATION AND PROJECTION RESULTS FOR NEARFIELD AUGUST POC FLUX

FIGURE 7-25. COMPARISONS OF FARFIELD TEMPORAL CALIBRATION AND PROJECTION RESULTS FOR J_{POC} FLUX

reductions in POC deposition in the two Boston Harbor segments. POC depositional flux is also reduced at segment (3). Segments (4) and (5) show little change in J_{poc}. Segment (6), the future outfall location, shows an increase in POC deposition. As has been observed for DIN, chlorophyll and DO, stations farfield from the present outfall show little change as a result of the outfall relocation.

To summarize, the projection results shows that relocating the present MWRA outfall alone reduces the maximum computed POC flux at the current outfall location from 591.6 to 352.0 gm C/m^2-day and reduces the annual mean flux from 374.3 to 180.8 g C/m^2-day. In the western portions of Boston Harbor, the model computes a reduction in the maximum carbon flux of over 450 gm C/m^2-day and a reduction of the mean by over 240 gm C/m^2-day. However, under this scenario the future outfall location will show an increase in maximum POC flux from 191.2 gm C/m^2-day to 639.9 gm C/m^2-day. This increase is very localized, however. The annual mean POC flux is projected to increase from 91.7 gm C/m^2-day to 334.2 gm C/m^2-day.

Upgrading to secondary treatment and relocating the outfall results in only a minor additional reduction in POC flux in Boston Harbor as compared to just relocating the outfall alone. Maximum annual POC fluxes are reduced by only an additional 20 to 30 gm C/m^2-day, while the mean annual POC flux decreases by approximately 10 gm C/m^2-day. However, a significant reduction of POC flux is achieved at the future outfall site when the treatment plant is upgraded to secondary treatment. Compared with outfall relocation alone, the yearly maximum is decreased by approximately 360 gm C/m^2-day to a flux rate of 277.4 gm C/m^2-day. The annual mean POC flux is also reduced to 167.0 gm C/m^2-day.

The model projection associated with upgrading the treatment plant to secondary treatment and discharging at the current outfall location showed a moderate reduction of the flux of POC throughout Boston Harbor. The maximum POC flux decreased by 150 to 442 gm C/m^2-day when compared with the 1992 calibration results. The annual mean POC flux is reduced from 374.3 gm C/m^2-day to 254.4 gm C/m^2-day in Boston Harbor.

7.3.5 Sensitivity of Future Outfall with Secondary Treatment to Changes in Light Extinction

Currently light attenuation or extinction coefficients are relatively high in Boston Harbor compared to other regions of the study area. This is in part due to high solids concentrations in the MWRA effluent; solids introduced to the system form riverine, CSO and storm water inputs; and solids resuspension during tidal flooding and ebbing and wave action. Without having a detailed suspended solids model it is difficult to project the change in background light extinction that would occur as a result of the outfall relocation. However, based on the suspended solids loading estimates for Boston Harbor developed by Menzie-Cura (1991), we estimated that MWRA could contribute as much as 50 percent of the solids loading to the Harbor and as a very conservative estimate up to 50 percent of the light extinction above levels observed in unimpacted portions of Massachusetts Bay. As a sensitivity, the base extinction coefficients were reduced in Boston Harbor and the future outfall with secondary treatment projection was rerun. Figures 7-26 through 7-28 present the results of this projection run compared to the base calibration run.

Figure 7-26 presents results for chlorophyll-a. The new projection indicates that for the Inner Harbor segment the winter bloom begins to develop a few weeks earlier, due to increased light availability. The surface layer shows reductions in chlorophyll similar to that observed in Figure 7-14. However, the bottom layer shows an increase in chlorophyll relative to the projection results in Figure 7-14 and in fact generates concentrations similar to the base calibration. These results suggest that light limitation is very important in this area of the Harbor, which still receives nutrient inputs from riverine and CSO inputs.

Results for the other model segments are not significantly different for the two runs, save for the late winter bloom beginning to develop a little earlier.

As a consequence of the changes in chlorophyll biomass resulting from the change in light extinction organic carbon deposition increases (Figure 7-27) relative to the future outfall/with secondary treatment run shown in Figure 7-14. POC flux in the Inner Harbor
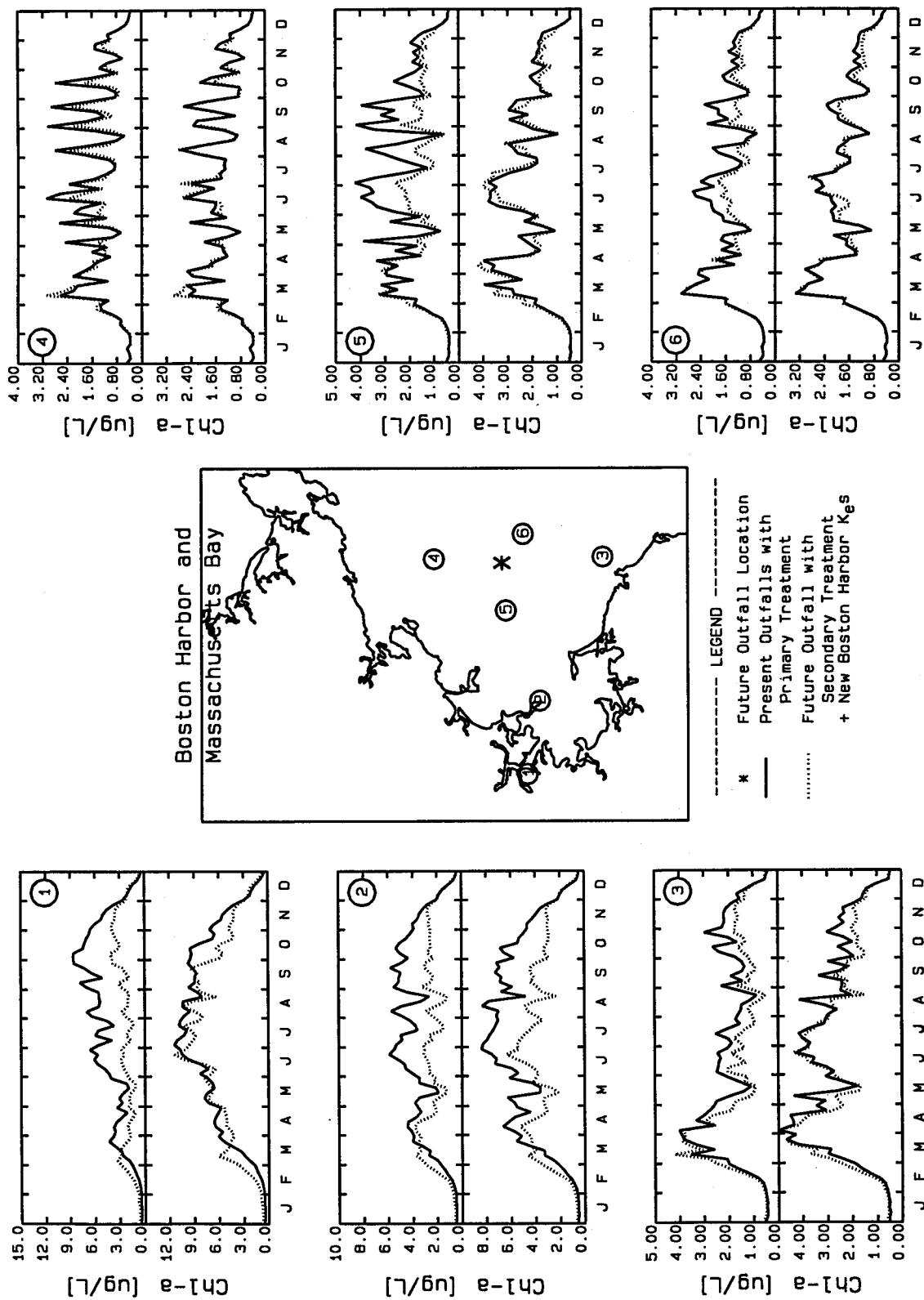
FIGURE 7-26. COMPARISONS OF NEARFIELD TEMPORAL CALIBRATION AND REDUCED K_e PROJECTION RESULTS FOR SURFACE AND MID-DEPTH CHLOROPHYLL-a
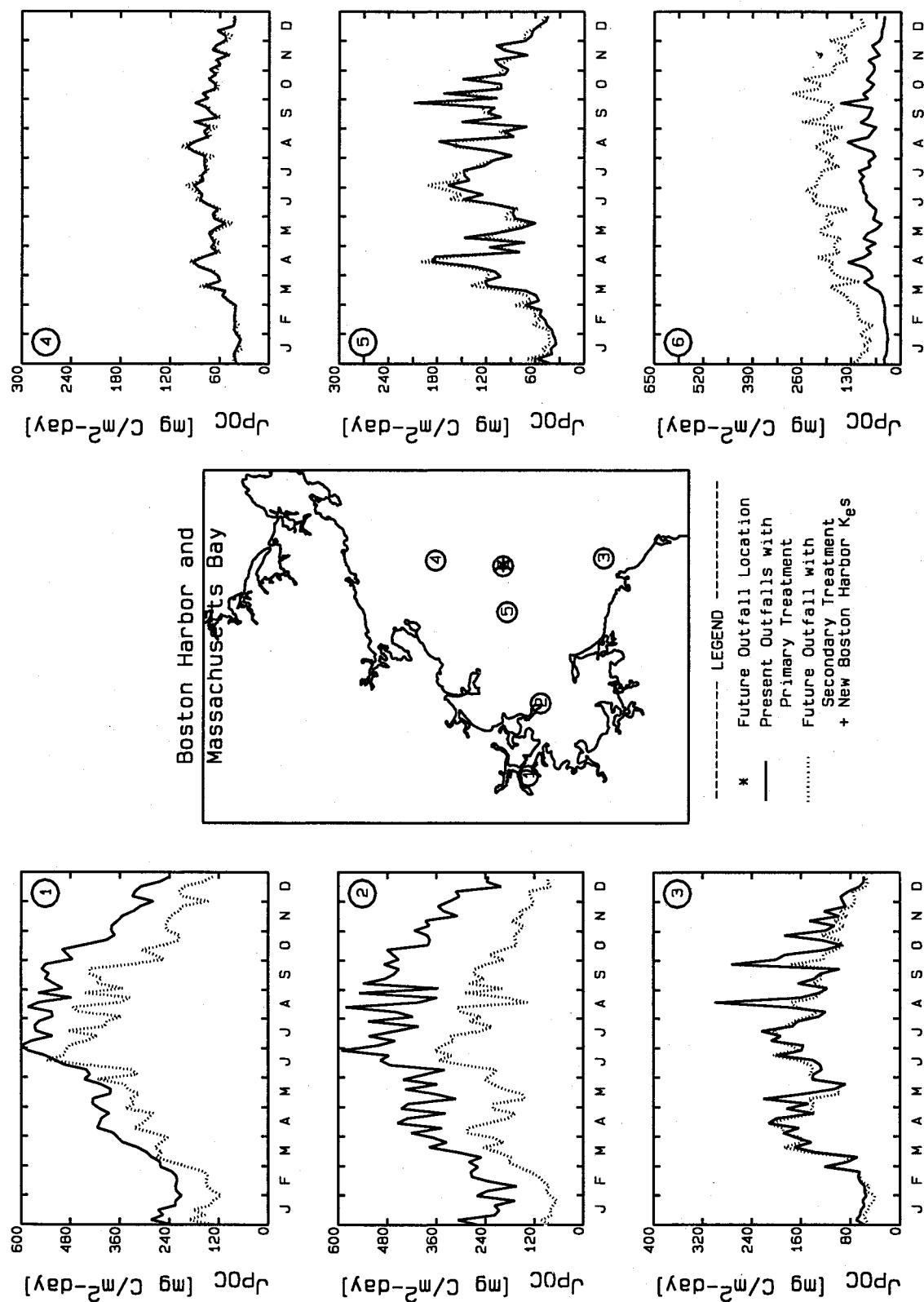
FIGURE 7-27. COMPARISONS OF NEARFIELD TEMPORAL CALIBRATION AND REDUCED K_e PROJECTION RESULTS FOR POC FLUX
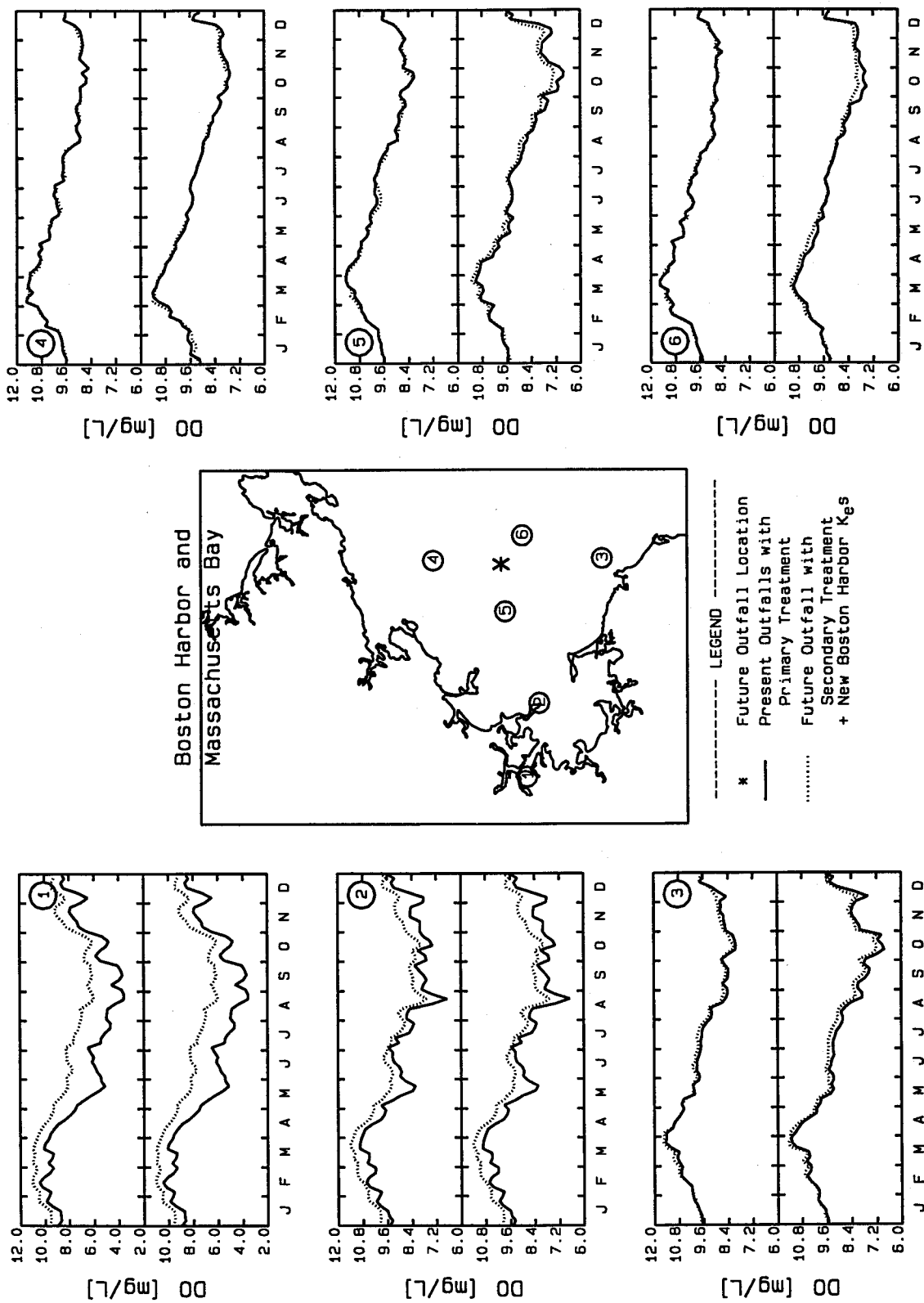
FIGURE 7-28. COMPARISONS OF NEARFIELD TEMPORAL CALIBRATION AND REDUCED K_e PROJECTION RESULTS FOR MID-DEPTH AND BOTTOM DO

increases to levels almost equal to the base calibration run. POC flux also increases slightly at the other segments relative to the projection results shown on Figure 7-22.

Interestingly, bottom water DO concentrations are shown to improve (Figure 7-26) in the Inner Harbor for this projection run relative to those results shown on Figure 7-20. This is due to increased productivity in the bottom water of this relatively shallow segment. Small increases in minimum bottom water are also computed for segments 2 and 3. The remaining model segments show almost no change in DO levels.

7.4   SUMMARY

All three remediation alternatives presented above show improvements in water quality in Boston Harbor. Relocating the outfall will reduce chlorophyll-a levels and the POC flux to the sediment in Boston Harbor. Dissolved oxygen levels will improve in the Harbor as well. Model computations also indicate that most effects from outfall relocation appear to be very localized to the outfall location. Upgrading the MWRA treatment plants to secondary treatment and discharging at the current outfall location will also improve the concentrations of dissolved oxygen in Boston Harbor and reduce the flux of POC to the sediment. However, secondary treatment without outfall relocation will do little to change chlorophyll-a levels. However, there is no regulatory standard for chlorophyll-a and current levels do not appear to pose a problem. Relocating the outfall and updating to secondary treatment will provide the greatest improvement in water quality for Boston Harbor and the Massachusetts Bay and Cape Cod Bay ecosystem.

SECTION 8

REFERENCES

Adams, E.Eric, 1995. Personal communication.

Alber, M. and A.B. Chan, 1994. Sources of contaminants to Boston Harbor: revised loading estimates. MWRA Environmental Quality Department Technical Report No. 94-1. Boston, MA.

Anita, N.J., C.D. McAllister, T.R. Parsons, K. Stephens, and J.D.H. Strickland, 1963. Further measurments of primary production using a large-volume phastic sphere. Limnol.Oceanogr. 8:166-183.

Banks, and Herrera, 1977. The effect of wind and rain on surface reaeration. J. Envir. Engr. Div., ASCE. 103:489-504.

Becker, S.M., 1992. The seasonal distribution of nutrients in Massachusetts and Cape Cod Bays. Masters Thesis. University of New Hampshire.

Beeton, A.M., 1958. Relationship Between Secchi Disk Readings and Light Penetration in Lake Huron. American Fisheries Society Trans. 87:73-79.

Bienfang, P.K., P.J. Harrison and L.M. Quarmby, 1982. Sinking Rate Response to Depletion of Nitrate, Phosphate and Silicate in Four Marine Diatoms, Marine Biology, 67, 295-302.

Blumberg, A.F. and G.L. Mellor, 1987. A Description of a Three-Dimensional Coastal Model, pp. 1-16. Coastal and Estuarine Sciences, Vol. 4. AGU, Washington, D.C.

Blumberg, A.F., R.P. Signell and H.L. Jenter, 1993. Modeling Transport Processes in the Coastal Ocean. J. Marine Env. Engg. 1:31-52.

Bothner, M.H., 1987. Geochemical and Geological Studies of Sediments in Boston Harbor and Massachusetts Bay (abs.) in Program, Science and Policy of Boston Harbor and Massachusetts Bay; Planning for the Twenty-First Century. Annual Boston Harbor/Massachusetts Bay Symposium of the Massachusetts Bay Marine Studies Consortium, Boston, Massachusetts, November 12 & 13, 1987.

Caperon, J. and J. Meyer, 1972. Nitrogen-limited growth of marine phytoplankton - I, Changes in population characteristics with steady-state growth rate. Deep- Sea Research, 19:501-618.

Cerco, C.F. and T. Cole, 1993. Application of the 3-D Eutrophication Model CD-QUAL-ICM to Chesapeake Bay, Draft Report to the U.S. EPA Chesapeake Bay Program. Prepared by U.S. Army Corps of Engineers, WES, Vicksburg, Mississippi.

Chalup, M.S., and E.A. Laws, 1990. A test of the assumptions and predictions of recent microalgal growth models with the marine phytoplankter *Pavlova lutheri*. Limnol. Oceanogr. 35:583-596.

Christensen, J.P., 1991. Nitrogen loading to Boston Harbor and export to Massachusetts Bay. Report No. 91-125. Oceanic Associates, Brunswick, Maine.

Coupe, R.H. Jr., and W.E. Webb, 1984. Water Quality of the Tidal Potomac River and Estuary: Hydrologic Data Report Supplement; 1979 through 1981 water years, U.S. Geological Survey Open-File Report 84-132.

Culver, M.E. and W.O. Smith, Jr., 1989. Effects of Environmental Variation on Sinking Rates of Marine Phytoplankton, J. Phycol. 25, 262-270.

Di Toro, D.M., and J.J. Fitzpatrick, 1993. Chesapeake Bay Sediment Flux Model. Prepared for the U.S. Environmental Protection Agency and U.S. Army Engineer District, Baltimore. HydroQual, Inc., Mahwah, New Jersey.

Di Toro, D.M., D.J. O'Connor, and R.V. Thomann, 1971. A dynamic model of the phytoplankton population in the Sacramento-San Joaquin Delta. In Nonequilibrium Systems in Natural Water Chemistry, Adv. Chem. Ser. 106. American Chemical Society, Washington, D.C. pp. 131-180.

Di Toro, D.M. and J.P. Connolly, 1980. Mathematical models of water quality in large lakes, Part 2: Lake Erie. EPA-600/3-80-065.

Di Toro, D.M. and W.F. Matystik, 1980. Mathematical models of water quality in large lakes, Part 1: Lake Huron and Saginaw Bay. EPA-600/3-80-056. HydroQual, 1987. A steady-state coupled hydrodynamic/water quality model of the eutrophication and anoxia process in Chesapeake Bay. Prepared for the U.S. EPA Chesapeake Bay Program. Mahwah, New Jersey.

Duffie, J.A. and W.A. Beckman, 1974. Solar Radiation Thermal Processes. John Wiley and Sons, New York, New York.

Fitzgerald, M.G., 1980. Anthropogenic Influence of the Sedimentary Regime of an Urban Estuary - Boston Harbor, Woods Hole Oceanographic Institution Report WHOI-80-38, Woods Hole, Massachusetts.

Garber, J. 1984. Laboratory study of nitrogen and phosphorus remineralization during decomposition of coastal plankton and seston. Estuarine, Coastal and Shelf Science, 18:685-702.

Geyer, W., G.B. Gardner, W.S. Brown, J. Irish, B. Butman, T. Loder and R. Signell, 1992. Physical Oceanographic Investigation of Massachusetts and Cape Cod Bays, Technical Report MBP-92-03, Massachusetts Bays Program, U.S. EPA Region I/Massachusetts Coastal Zone Management Office, Boston, Massachusetts, 497 pp.

Giblin, A.E., 1995. Personal Communication.

Giblin,A.E., J. Tucker and C. Hopkinson, 1991. Sediment oxygen demand and nitrogen flux in Massachusetts Bay. MWRA Environmental Quality Department Technical Report No. 91-5.

Giblin, A.E., C. Hopkinson, J. Tucker, 1993. Metabolism, nutrient cycling and denitrification in Boston Harbor and Massachusetts Bay sediments. MWRA Environmental Quality Department Technical Report No. 93-2.

Grill, E. and F. Richards, 1964. Nutrient regeneration from phytoplankton decomposing in seawater. J.Mar.Res. 22:51-69.

Hendry, G.S., 1977. Relationships Between Bacterial Levels and Other Characteristics of Recreational lakes in the District of Muskoka, Interim Microbiology Report, Laboratory Service Branch, Ontario Ministry of the Environment.

Hunt, C.D., D.E. West and C.S. Peven, 1995. Deer Island Effluent Characterization and Pilot Treatment Plant Studies, June 1993 - November, 1994. MWRA Environmental Quality Department Technical Report 95-7.

HydroQual, Inc., 1987. A Steady-State Coupled Hydrodynamic/Water Quality Model of the Eutrophication and Anoxia Process in Chesapeake Bay, Prepared for the U.S. EPA Chesapeake Bay Program, Mahwah, New Jersey.

HydroQual, Inc., 1989. Development and Calibration of a Coupled Hydrodynamic/Water Quality/Sediment Model of Chesapeake Bay, prepared for the U.S. EPA Chesapeake Bay Program, Mahwah, New Jersey.

HydroQual, Inc., 1991. Water Quality Modeling Analysis of Hypoxia in Long Island Sound, Prepared for Management Committee Long Island Sound Estuary Study and New England Interstate Water Pollution Control Commission.

HydroQual, Inc., 1993. A Water Quality Model for Massachusetts Bay and Cape Cod Bay: Model Design and Initial Calibration. MWRA Environmental Quality Department. Technical Report No. 93-5.

HydroQual, Inc., 1993. Chesapeake Bay Sediment Flux Model. Prepared for U.S. Corps of Engineers. Waterways Experiment Station, Environmental Laboratory.

Hyer, P.V., C.S. Fang, E.P. Ruzeck, and W.J. Hargis, 1971. Hydrography and Hydrodynamics of Virginia Estuaries, Studies of the Distribution of Salinity and Dissolved Oxygen in the Upper York System, Virginia Institute of Marine Science.

Jewell, W.J. and P.L. McCarty, 1971. Aerobic Decomposition of Algae. Environ. Sci. Technol. 1971, 5(10), p. 1023.

Kelly, J.R., 1993. Nutrients and Massachusetts Bay: An Update of Eutrophication Issues. MWRA Environmental Quality Department Technical Report No. 93-17.

Kelly, J.R. and B.L. Nowicki, 1992. Sediment denitrification in Boston Harbor. MWRA Environmental Quality Department Technical Report Series No. 92-2. Massachusetts Water Resources Authority.

Kelly, J.R., and B.L. Nowicki, 1993. Direct mesurements of denitrification in Boston Harbor and Massachusetts Bay sediments. MWRA Environmental Quality Department Technical Report No. 93-3.

Kelly, J.R. and J. Turner, 1995. Water column monitoring in Massachusetts and Cape Cod Bays: Annual Report for 1993. Draft report to MWRA.

Knebel, H.J., 1993. Sedimentary environments within a glaciated estuarine-inner shelf system: Boston Harbor and Massachusetts Bay. Maine Geology, 110:7-30.

Laws, E.A., and T.T. Bannister, 1980. Nutrient and light-limited growth of *Thalassissira fluviatilis* in continuous culture, with implications for phytoplankton growth in the oceans. Limnol. Oceanogr. 25:457-473.

Laws, E.A., and M.S., Chalup, 1990. A microalgal growth model. Limnol. Oceanogr. 35:597-608.

Lowe, W.E., 1976. Personal Communication. Canada Centre for Inland Waters, Burlington, Canada.

Massachusetts Port Authority, 1992. Application pursuant to the National Pollutant Discharge Elimination System: Individual stormwater discharge permit associated with industrial activities for Logan International Airport, Boston, Massachusetts. Prepared by Rizzo Associates, Inc. Submitted to Region I, Environmental Protection Agency, October 1992.

Menon, A.S., W.A. Gloschenko and N.M. Burns, 1972. Bacteria-Phytoplankton Relationships in Lake Erie, Proc. 15th Conf. Great Lakes Res., 94, Inter. Assoc. Great Lakes Res., 101.

Menzie-Cura & Associates, 1991. Sources and Loadings of Pollutants to Massachusetts Bays Program Task 1 of the Massachusetts Bays Programs. Prepared for the Massachusetts Bay Program, Massachusetts Coastal Zone Management/U.S. EPA. Technical Report No. MBP-91-01.

Metcalf and Eddy, 1990. Boston Harbor Project - Deer Island Related Facilities: Trailer Pilot Plant Report. Submitted to MWRA, Program Management Div., Boston, Massachusetts.

Morel, A., L. Lazzara, and J. Gostan, 1987. Growth rate and quantum yield time response for a diatom to changing irradiances (energy and color). Limnol. Oceanogr. 32:1066-1084.

Morel, F.M., 1983. Principles of Aquatic Chemistry, John Wiley and Sons, New York, New York.

MWRA, 1988. Secondary treatment facilities plan. Vol. 5, Appendix 7: Nutrient Analysis, Massachusetts Water Resources Authority, Boston, Massachusetts.

MWRA, 1990. Marine resources extended monitoring program. Vol. 2. Massachusetts Water Resources Authority, Boston, Massachusetts.

MWRA, 1991. Combined sewer overflow monitoring: Boston Harbor and its tributary rivers, June 1989 - October 1990. WRAA Environmental Quality Department Technical Report No. 91-2.

MWRA, 1993. Interim CSO Report. Prepared by Metcalf and Eddy for MWRA.

MWRA, 1994. Combined Sewer Overflow Conceptual Plan/System Master Plan. Prepared by Metcalf and Eddy for MWRA.

MWRA, 1995. Personal communication.

Norwicki, B.L., 1994. The effect of temperature, oxygen, salinity, and nutrient enrichment or estuarine denitrification rates measured with a modified gas flux technique. Est. Coast. Sci. 38:137-156

Otsuki, A. and T. Hanya, 1972. Production of dissolved organic matter from dead green algal cells. Limnol.Oceanogr.17:248-257.

Oviatt, C.A., M.E.Q. Pilson, S.W. Nixon, J.B. Frithsen, D.T. Rudnick, J.R. Kelly, J.F. Grassle, and J.P. Grassle, 1984. Recovery of a polluted estuarine system: a mesocosm experiment. Mar.Ecol.Prog.Ser. 16:203-217.

Parker, J.I., 1974. Phytoplankton Primary Productivity in Massachusetts Bay. Ph.D. Dissertation. University of New Hampshire.

Parsons, T., M.Takahashi, and B. Hargrave, 1984. Biological oceanographic processes. 3rd ed. Pergamon Press, Oxford.

Pett, R., 1989. Kinetics of microbial mineralization of organic carbon from detrital Skeletonema Costatum cells. Mar.Ecol.Prog.Ser.52:123-128.

Rex, A., 1993. Combined sewer overflow receiving water monitoring: Boston Harbor and its tributary rivers. MWRA Environmental Quality Department Technical Report No. 93-4.

Riley, G.A., H. Stommel and D.F. Bumpus, 1949. Quantitative Ecology of the Plankton of the Western North Atlantic, Bull. Bingham Oceangr. Coll., 12(3), 1-169.

Robinson, W.E., T.J. Coffey and P.A. Sullivan, 1990. New England Aquarium's Ten Year Boston Harbor Monitoring Program: First Report (March 1987-July 1989). New England Aquarium Edgerton Research Laboratory, Boston, Massachusetts.

Science Application International Corp., 1987. REMOTS Survey of Broad Sound, Massachusetts Bay. Report # SAIC-8717511 & 141. Submitted to Stone and Webster, April 1987.

Seitzinger, S., 1988. Denitrification in freshwater and coastal marine ecosystems: Ecologiccal and geochemical significance. Limol. Oceanogr. 33:702-724.

Shuter, B., 1979. A model of physiological adaptation in unicellular algae. J. Theor.Biol. 78:519-552.

Signell, R.P., H.L. Jenter and A.F. Blumberg, 1993. Modeling the Seasonal Circulation in Massachusetts Bay Estuarine and Coastal Modeling III. Proceedings of the Third International Conference , sponsored by the Waterway, Port, Coastal, and Ocean Div./ASCE.

Signell, R.P. and B. Butman, 1992. Model Tidal Exchange and Dispersion in Boston Harbor, Journal of Geophysical Research, Vol. 97, No. C10, pp. 15, 591-15, 606.

Signell, R.P., 1992. Wind- and tide-induced flushing of Boston Harbor, Massachusetts. In Estuarine and Coastal Modeling, proceedings of the 2nd International Conference, edited by M.Spaulding, pp.594-506, ASCE, New York.

Smayda, T.J., 1992. Phytoplankton of Massachusetts Bay and Modification of nutrient supply. MCA Report 92-1, prepared for S.T.O.P. 51 pp.

Steele, J.M., 1962. Environmental Control of Photosynthesis in the Sea, Limnol. Oceanogr., 7, 137-150.

Steeman Nielsen, E., V.K. Hansen, and E.G. Jorgensen, 1962. The adaptation to different light intensities in Chorella vulgaris and the time dependence on transfer to a new light intensity. Physid. Plant. 15:505-517.

Steeman Nielsen, E., and T.S. Park, 1964. On the time course in adapting to low light intensities in marine phytoplankton. J. Cons. Int. Explor. Mer. 29:19-24.

Stenstrom, M.K., G.S. Silverman and T.A. Bursztynaky, 1984. Oil and Grease in Urban Stormwaters. ASCE J. Environmental Engineering 110:58-72.

Stolzenbach, K.D. and E.E. Adams, 1995. Contaminated sediments in Boston Harbor. Draft Report. Marine Center on Coastal Water Quality. MIT Sea Grant College Program, Cambridge, Massachusetts.

Sverdrup, H.U., M.W. Johnson, and R.H. Fleming, 1942. The Oceans. Prentice-Hall, Englewood Cliffs, New Jersey, 1087pp.

Thomann, R.V., D.M. DiToro, and D.J. O'Connor, 1974. Preliminary model of Potomac Estuary phytoplankton. J. Env. Engr. Div. ASCE 100:699-708. Foree, E. and P. McCarty, 1970. Anaerobic decomposition of algae. Env.Sci.&Tech.4:842-849.

Townsend, D.W., L.M. Cammen, J.P. Christensen, S.G. Ackleson, M.D. Keller, E.M. Haugen, S. Corwin, W.J. Bellows, and J.F. Brown, 1990a. Oceanographic Conditions in Massachusetts Bay: 24 October 1989 Cruise Results. Bigelow Laboratory for Ocean Sciences. Report to MWRA.

Townsend, D.W., L.M. Cammen, J.P. Christensen, S.G. Ackleson, M.D. Keller, E.M. Haugen, S. Corwin, W.J. Bellows, and J.F. Brown, 1990b. Cruise Results of 6 February, 6 March and 10 Arpil, 1990. Bigelow Laboratory for Ocean Sciences. Report to MWRA.

Townsend, D.W., L.M. Cammen, J.P. Christensen, S.G. Ackleson, M.D. Keller, E.M. Haugen, S. Corwin, W.J. Bellows, and J.F. Brown, 1990c. Cruise results from 5 June and 14 August, 1990. Bigelow Laboratory for Ocean Sciences. Report to MWRA.

Townsend, D.W., L.M. Cammen, J.P. Christensen, S.G. Ackleson, M.D. Keller, E.M. Haugen, S. Corwin, W.J. Bellows, and J.F. Brown, 1991. Final Report Seasonality of Oceanographic Conditions in Massachusetts Bay. Report to MWRA.

Tucker, J., A.E. Giblin, C. Hopkinson, 1993. Porewater profiles from Boston Harbor and Massachusetts Bay sediments. Prepared for Massachusetts Water Resources Authority.

U.S. EPA, 1983. Results of the National Urban Runoff Program Executive Summary and 2 Volumes. U.S. Environmental Protection Agency. Monitoring and Data Support Division, NTIS Nos. PB84-185545, PB84-185552, PB84-185560.

U.S. EPA, 1988. "Boston Harbor Wastewater Conveyance System" Vols I & II, Draft Supplemental Environmental Impact Statement.

Veliela, I., J. Costa, J.M. Teal, B. Howes, and D. Aubrey, 1990. Transport of groundwater-borne nutrients from watersheds and their effects on coastal waters. Biogeochemistry 10:177-198.

WEF and ASCE, 1991. Design of Municipal Wastewater Treatment Plants Volume I. WEF Manual of Practice No. 8, ASCE Manual and Report on Engineering Practice No. 76.

Westrich, J. and R. Berner, 1984. The role of sedimentary organic matter in bacterial sulfate reduction: the G model tested. Limnol.Oceanogr.29:236-249.

Zemba, S.G., 1993. Atmospheric Deposition of Nitrogen Compounds to the Massachusetts Bays, Draft Report.

Appendices

in

N - 165